

PROTECTING NEW ORLEANS:

REVISION OF THE HURRICANE PROTECTION SYSTEM IN ORDER TO PREVENT LAKE BORGNE INDUCED FLOODING DURING HURRICANES



E.A. van Vugt

23/05/2008

PROTECTING NEW ORLEANS:

***REVISION OF THE HURRICANE PROTECTION SYSTEM IN ORDER TO
PREVENT LAKE BORGNE INDUCED FLOODING DURING HURRICANES***

EVERT ABRAHAM VAN VUGT

Master Thesis

Faculty Of Civil Engineering And Geosciences

Delft University Of Technology

Section Of Hydraulic Engineering

Thesis Committee:

Prof.drs.ir. J.K. Vrijling
Ir. A. van der Toorn
Ing. H.J. Everts
Dr.ir. H.G. Voortman

Delft University Of Technology [Hydraulic Engineering]
Delft University Of Technology [Hydraulic Engineering]
Delft University Of Technology [Geo-Engineering]
ARCADIS Nederland BV

Student Information:

Evert van Vugt
St. no. 1143727
M: +31 (0)6 301 693 46
@: evertvanvugt@hotmail.com

23/05/2008

FINAL VERSION



Preface

This present thesis has been executed as the final stage of the study Civil Engineering and Geosciences at Delft University of Technology in order to achieve the degree of Master of Science in Civil Engineering. It focuses on the revision of the current protection system of New Orleans and is part of the specialization Hydraulic Structures.

In this thesis, the performance of the current hurricane protection system of New Orleans has been analyzed. Revisions are proposed for the part of the system adjacent to Lake Borgne, after which one of the projected defence structures is quantified into a preliminary design. For a proper reading of this thesis, it is advised to note these different scales within it. This division in scales is represented in the chapters of this thesis:

1. Introduction: New Orleans and Hurricane Katrina – *Macro scale* – Analysis of what happened in New Orleans during Hurricane Katrina;
2. The Hurricane Protection System of New Orleans compared to flood protection in the Netherlands – *Macro scale* – Review on flood protection development in the Netherlands and future considerations;
3. Master plan of the New Orleans region – *Macro to meso scale* – Analysis of flood protection concepts within Lake Borgne as part of a comprehensive master plan for southern Louisiana;
4. Evaluation of barrier concepts within this master plan – *Meso to micro scale* – *2 barriers* – Evaluation of possible concepts within both the Gulf Intracoastal Waterway and the Mississippi River Gulf Outlet;
5. Overview of navigable floodgate structures for the Gulf Intracoastal Waterway – *Micro scale* – *1 barrier* – Determination of the favorable navigable floodgate structures for this location;
6. Quantified program of requirements of the projected storm surge barrier within the Gulf Intracoastal Waterway – *Micro scale* – *1 barrier* – Specification of boundary conditions and requirements;
7. & 8. Preliminary design of the projected storm surge barrier within the Gulf Intracoastal Waterway – *Micro scale* – *1 barrier* – Elaboration of the boundary conditions and requirements into a preliminary design;
9. Review on degradations: maintenance and analysis on vibrations – *Micro scale* – *1 barrier* – Brief review on the structure after realization.

As a final remark regarding the content of this thesis, it should be noted that it describes the design process quite roughly. Revision of the current defence system is such a comprehensive and debated issue that multiple design teams spanning a wide range of disciplines and knowledge should attend in the process. The results presented in this thesis should therefore be handled with care and not be directly used for design input. Reevaluation of the results is advised in the future as only minimum information was available during the execution of this thesis.

The research presented in this thesis has been performed in cooperation with Delft University of Technology and ARCADIS Nederland BV. ARCADIS provided me with a place to work and put at my disposal the required resources to carry out this thesis, for which I am thankful. I would like to thank my colleagues at ARCADIS Rotterdam for supporting me throughout the period of this graduation project, but I would especially like to thank Hessel Voortman for his helpful support and guidance throughout this period.

The research has been carried out under the supervision of Prof. drs. ir. J.K Vrijling. I would like thank him and the other members of my graduation committee ir. A van der Toorn and ing. H.J. Everts for their kind cooperation, advice and feed-back in their different areas of expertise.

At last, I would like to thanks my family and friends for being there and helping me during my years in Delft in order to bring this study to a good end.

Evert van Vugt

Rotterdam, May 2008

Executive Summary

On the morning of August 29, 2005, Hurricane Katrina, one of the strongest storms ever to hit the coast of the United States, brought intense winds, high rainfall, waves and storm surge to the Gulf of Mexico shores of Louisiana, Mississippi and Alabama. Communities in all three states suffered damage, but this thesis focuses on the devastation to city of New Orleans and also partly on the southeast of Louisiana. During and after Hurricane Katrina, many levees and floodwalls were overtopped and several were breached. This allowed water from Lake Pontchartrain and Lake Borgne to flow into major portions of New Orleans. A storm of Hurricane Katrina's strength and intensity is expected to cause major flooding and damage. However, the main portion of the destruction was caused not only by the storm itself but by the storm's exposure to engineering and related policy failures. The levees and floodwalls breached because of a combination of unfortunate decisions, made over many years and at almost all levels of responsibility. As lives and public safety are to be protected, significant changes are required in the way flood protection systems are funded, designed, managed and maintained.

Immediately after Hurricane Katrina flooded New Orleans, President George W. Bush and the U.S. Department of Homeland Security declared that no one could have predicted such devastation. Yet engineers had warned for years that a major hurricane crossing the Gulf of Mexico could drown the region. Documents indicate that various gates had been recommended as far back as 1968 and in each decade since, but none of the designs has ever been funded. In Katrina's wake, the blueprints for these structures are rapidly being dusted off and integrated into a Grand Plan for Louisiana by the Louisiana State University, engineering companies and the U.S. Army Corps of Engineers (USACE). The idea that improving only existing projects would not provide protection to communities outside the existing levee system was the basis for this Grand Plan, which serves as the basis of this thesis. In the part adjacent to Lake Borgne, the Grand Plan projects gates in the Chef Menteur Pass and Rigolets Pass and in the confluence of the Mississippi River Gulf Outlet (MRGO) and Gulf Intracoastal Waterway (GIWW). This Hurricane Barrier Plan (HBP) is favorable as it provides high protection levels for all parishes in the Lake Pontchartrain basin. It enhances the system's reliability because it implements a secondary levee protection system. In addition, it is expected to be less expensive than raising existing levee systems and can be constructed in a much shorter time. It is recommended to implement two flood protection structures in combination with a new, straight levee alignment between them. This alternative has the best high water safety and the most positive ecological influence. It is intended to close off the IHNC, forming a first line of man-made defences against storm surges from Lake Borgne to the east. This line of defense would substantially reduce high water and wave action against the interior levees and floodwalls, potentially reducing the costs of future upgrades, maintenance and associated repairs to the system. In addition it accommodates large retention area, favorable for the discharge of excess rainfall water. The alternative requires one floodgate in the GIWW and possibly another one in the MRGO. It is possible to close off the MRGO, to allow only shallow draft shipping vessels or to sustain the channel's deep draft dimensions, all requiring a different connection at this certain point.



The GIWW forms a protected navigable waterway running approximately 1,050 miles (1,700 km) along the Gulf Coast between Texas and Florida. It links all of the Gulf Coast ports and enables these ports to access the inland waterway system. About 38,000 vessels pass along the stretch of the GIWW around New Orleans, making it a highly navigated waterway. It should therefore remain open for navigation, which requires that a protection barrier in the form of a navigable floodgate structure is built.

Although the MRGO provides a second route to the Port of New Orleans of about 40 miles (64 km) shorter than primary route via the Mississippi River, the use and benefits of it are under heavy debate. Since the channel's opening in 1963, its usage by the shipping industry has been less than anticipated and traffic has been well below original projections. Maintenance expenditure has risen over time and it appeared instructive to determine whether these investments are legitimate. In this thesis, the permanent closure of the MRGO is discussed by focusing on its main issues: storm propagation and the preservation of (deep draft) navigation. It is concluded that closing the MRGO is the best option for the future and can be provided by either constructing a total closure across the MRGO or by ceasing all operation maintenance activities. The latter has fewer environmental benefits but yields the greatest average annual net economic benefits. It is recommended not to allow the permanent closure of the MRGO without coupling its timing to correspond to the completion of the IHNC Lock Replacement Project, which is projected to be completed in 2013. This provides an interesting option of combining both stated alternatives. The permanent closure of the MRGO is the most beneficial and should be implemented. Ceasing all maintenance activities affects the shallow draft navigation that uses the MRGO as an alternative route when the IHNC is congested or unexpectedly closed. It is estimated that this navigation could no longer do so after about 2014. This corresponds with the moment of completion of the IHNC Lock Replacement Project, making that it is possible for shallow draft navigation to use the MRGO up to the moment of permanent closure. This results in maximum economical benefit. Depending on the construction time of the chosen master plan, it could be optimal to first build the flood protection structure within the GIWW and adjacent levee sections including the new alignment. After completion of the IHNC Lock Replacement Project, construction works on the closure of the MRGO will be started. Although this will leave the MRGO open for a longer period of time, storm surge propagation studies have shown that there is no noticeable effect of the MRGO for large storm surge events.

The comparison of navigable floodgate types for the GIWW is divided into two parts. First the killer requirements regarding the proposed hurricane protection barrier are stated and evaluated per floodgate types in order to eliminate those floodgate types that do not conform with these main requirements at an early stage. Secondly, the remaining floodgate types are evaluated on the basis of typical structural concerns.

	VLG	PFG	HFG	SIG	STG	FSTG	SMG	RG
Killer requirement 1: Fully controllable at all design flow and wave conditions, including reverse differential head conditions.	Yes	No	Yes	No	Yes	No	Yes	Yes
Killer requirement 2: Able to withstand some degree of siltation as scouring could occur during the discharge of water	Yes		No		Yes		No	Yes
Killer requirement 3: Navigation requirements should impose limited design consequences	Yes				Yes			No
Floodgate types that require further investigation regarding their structural concerns	Yes	No	No	No	Yes	No	No	No

VLG = vertical lifting gate, PFG = pneumatic flap gate, HFG = hydraulic flap gate, SIG = slide gate, STG = sector gate, FSTG = floating sector gate, SMG = segment gate, RG = radial gate

The vertical lifting gate is chosen as the optimal flood protection structure for several main reasons. The required clearance height, generally the only limitation of this gate, is relatively small and applicable. Its hoisting system is complex but well known, providing a highly reliable closure system, and its maintenance is relatively easy. Finally, it has the ability to safely discharge excess water from the retention area, which represents one of the main functions of the gate. The only concern is flow-induced vibrations for which the structure should be checked.

Ideally, comprehensive modeling should be performed in order to determine the level of protection required in the study area. Hydrodynamic modeling of storm surge and waves has been conducted by the USACE. The storm selected for the rough order of magnitude estimations is based on the Probable Maximum Hurricane (PMH), which describes a Category 5 intensity storm on the Saffir-Simpson Scale. The return period of the central pressure associated with this PMH is calculated for a certain coastal stretch of the Gulf of Mexico. This leads to a return period of PMH in vicinity of New Orleans area equal to 2,000 years. The probability that this PMH strength hurricane making landfall in the particular coastal stretch causes the worst case possible further depends on the exact location of landfall, its path and forward speed. This indicates that the return period for this leading scenario results in an even larger value than 2,000 years. The level of protection of 1/2,000 [1/year] is used in this thesis.

For the preliminary design of the flood protection structure, Dutch standards are followed. The primary design requirements are stated for the probability of exceedance of the allowable volume of water. This volume could enter the retention area either over the closed structure (overflow and/or overtopping), through the open structure (failure of closure elements) or over the outer levee alignment (overtopping). The variation of the surge level is modeled lightly related to Hurricane Katrina.

It appears that the offset of the surge takes a longer time than the rise of it. This is used in the model by stating the water offset 2 times longer than rise of the water level. In the design of the gate a slow moving hurricane is modeled, opposite to the fast moving Hurricane Katrina. The slower hurricane prolongs the surge elevation and represents a more severe situation. In order to determine the most optimal retaining height of the lifting gate, the following parameters are determined:

- Maximum allowable surface elevation in the retention area at the time of a maximum surge event = 0.73 m;
- Minimum required crest height of the outer levee and associated overtopping discharge over the total event:

<i>Outer levee alignment - requirement: maximum overtopping discharge ≈ 100 (l/s)/m</i>					
tan α = incline of the outer slope of the levee		1/4 [-]			
h _c = crest level		47 ft MSL			
combined reduction factor		0,7 [-]			
<i>crest height outer levee: + 47 ft MSL</i>	surge level [ft]	overtopping discharge [(l/s)/m]	duration		overtopping volume [m ³ /m]
			[hour, <-- l]	[hour, l -->]	
<i>slow moving (PMH, max)</i>	6	0,06	24	x (no diff. head)	5,2
	9	0,13	12	24	16,8
	12	0,30	6	12	19,4
	15	0,69	4	8	29,8
	18	1,56	4	8	67,4
	21	3,55	2	4	76,7
	24	8,06	2	4	174,1
	27	18,33	2	4	395,9
	30	41,68	1	2	450,1
	33	94,78	1		341,2
	total overtopping volume		1576,7		[m ³ /m]
length levee alignment		18		[km]	
surface area retention basin		90		[km ²]	
surface elevation retention basin		0,32		[m]	

- The overtopping and/or overflow allowed over the lifting gate, as direct consequence of the difference between the maximum allowed surface elevation and the share of the elevation caused by overtopping of the levee alignment. This latter parameter iteratively determines the minimum required height of the lifting gate:

<i>Vertical lifting gate - requirement: maximum allowed surface elevation retention basin = 0,73 - 0,32 = 0,41 m</i>					
<i>vertical lifting gate: + 22 ft MSL</i>	surge level [ft]	overtopping discharge [(m ³ /s)/m]	duration		overtopping volume [m ³ /m]
			[hour, <-- l]	[hour, l -->]	
<i>slow moving (PMH, max)</i>	6	0,05	24	x (no diff. head)	4493
	9	0,11	12	24	14256
	12	0,23	6	12	15163
	15	0,50	4	8	21384
	18	1,05	4	8	45274
	21	2,22	3	4	55894
	24	3,75	3	4	94475
	27	6,41	2	4	138499
	30	10,06 < max = 10.0	1	2	108670
	33	14,48 < max = 10.0	1		52124
	total overtopping volume		550231		[m ³ /m]
width structure		64		[m]	
surface area retention basin		90		[km ²]	
surface elevation retention basin		0,39		[m]	

- Optimize the height of the lifting gate with introduction of allowed leakage:

<i>Requirement: maximum surface elevation retention basin due to leakage + overtopping / overflow ≤ 0.41 m</i>				
<i>Combination 1</i>	leakage width:	total leakage volume	163397	[m ³ /m]
	0.05 m at sides and bottom	surface elevation retention basin	0,12	[m]
	Required height lifting gate:	maximum discharge over the gate	11,46	[(m ³ /s)/m]
	+ 24 ft MSL	total overtopping volume	371711	[m ³ /m]
		surface elevation retention basin	0,26	[m]
<i>Combination 2</i>	leakage width:	total leakage volume	333385	[m ³ /m]
	0.10 m at sides and bottom	surface elevation retention basin	0,24	[m]
	Required height lifting gate:	maximum discharge over the gate	7,53	[(m ³ /s)/m]
	+ 27 ft MSL	total overtopping volume	208926	[m ³ /m]
		surface elevation retention basin	0,15	[m]
<i>Combination 3</i>	leakage width:	total leakage volume	454720	[m ³ /m]
	0.05 m at sides, 0.15 m at bottom	surface elevation retention basin	0,32	[m]
	Required height lifting gate:	maximum discharge over the gate	4,50	[(m ³ /s)/m]
	+ 30 ft MSL	total overtopping volume	113289	[m ³ /m]
		surface elevation retention basin	0,08	[m ³ /m]

It can be concluded that the minimum leakage width of 0.05 m at all sides is not desirable. The associated required gate height of +24 ft (7.3 m, MSL) still results in a maximum combined overtopping discharge larger than the prescribed maximum of 10 m³/s per meter width. Time dependent processes are not included at this point. Quantifying the time dependent processes of seal level rise and subsidence leads to conclude that the optimal combination of allowed leakage and minimum required gate height is combination 3. The sum of both processes predicts a relative maximum surge elevation rise of 3 + 1.5 = 4.5 ft per 100 year. Computing the maximum overflow discharge results in: $h_{kr} = 30$ ft (projected gate height) – (max. surge level + 4.5 ft) = -7.5 ft, which gives $q = 9.4$ (m³/s)/m. This projected gate height has the additional benefit that no perfect closure is needed at the bottom during a storm event. A space of 0.15 m can be allowed between the gate and the top of the sill, which reduces the need for maintenance of the sill and increases the reliability of the closing process.

The safety of the closing process is reviewed in this thesis and proven sufficient, although requiring more detailed hydrological information. Evaluation of the largest contributing probabilities of failure of the process results in:

- An additional measuring device system decreases the probability of non-availability with an order 10⁻²;
- Human induced failures are still relatively high. Additional expertise and/or training are required in order to decrease the probability of human induced failures;
- The probability of failure of the electro-hydraulic system is high as the failure of one hydraulic system leads to failure of the overall closure process. This should be decreased by designing an alternative back-up operation system or manual system. It is also advised to investigate the design of a system which allows the gate to be lowered under its own weight.
- The non-availability due to ship collision can be decreased by designing a fender wall within the prone substructure of the lifting gate. The probability of a ship collision remains the same, but would not immediately lead to failure of the substructure and/or steel gate. The failure frequency decreases.

In the preliminary design presented in this thesis, two main parts of the barrier will be reviewed. The barrier can roughly be divided in the concrete civil works, forming the substructure of the barrier, and the steel lifting gate. In this thesis, an indicative order of magnitude calculation is presented in order to determine a first estimation of the needed concrete civil works. For this calculation, the stability of the structure and the potential of shearing are reviewed. The calculation results lead to conclude that the loading under maximum surge level and significant wind offset in the retention area is the critical loading scenario. The checks on shearing and maximum granular stresses are both critical in this event. The concrete substructure needs to be sufficiently large to create enough down force and to prevent shearing. This is a direct result of the high differential head and associated high resultant horizontal force. The most significant contribution of this method is that it provides insight in the relative criticalness of each scenario. It appears that the occurrence of a wave low during extreme conditions is not critical and the influence of the representative wind load on the gate in lifted position can be neglected.

In the design of the steel lifting gate reference is made to the Hartel Canal Barrier, a proven protection scheme in the Netherlands consisting of a lifting gate. Typical for this barrier are the lens-shaped barrier section. This shape has been chosen in order to place their centers of gravity close to the plane of suspension. The overturning moment atop the towers as result of the eccentric suspension can in this way been kept small. The hydraulic load is transferred to the supports in the gate recesses of the towers. The lens-shaped retaining wall is less easy to manufacture than a flat wall, but it enables to use the material strength in a more economical manner. In the design of this particular section of the lifting gate, several conclusions can be made:

- During the design it appeared favorable to introduce an additional lens-shaped section. The addition of an extra support halves the leading field length. This reduces the maximum moment with a factor of about 4 and halves the maximum shear force. As a result, the cross-beam can be constructed much finer.
- From the investigated development of member forces it can be concluded that a parabolic gate curvature is favorable over a circular curvature. The maximum moment and shear force is smaller and also the range of these forces is smaller. This allows for a finer design, which means that the gate can be lighter. It also allows for a more optimal use of the steel as the loading is more uniformly distributed over the length of the chord. In this thesis, the front and rear chord are taken at similar cross-sectional dimensions. The reduction in steel volume for the leading lens-shaped cross-section caused by the use of clamped joints over hinged joints results in: $\Delta V_{\text{steel;joints}} = 16 \cdot 10^3 \text{ mm}^2/\text{m} \cdot (69.8 + 65.5) = 2.17 \text{ m}^3$ per leading lens-shaped section. With the given unit weight of steel ($\rho_{\text{rep}} = 7850 \text{ kg/m}^3$), this volume is equal to $2.17 \cdot 7850 = 17.0 \cdot 10^3 \text{ kg} = 17.0$ tonnes per leading lens-shaped barrier section.
- A lens-shaped barrier section as calculated in this thesis is more critical with purely hinged joints than with clamped joints. The hinged joints model results in stresses of about 10% higher than the model with clamped joints. The clamped joints model presents a more uniform distribution of the bending moment, which is partly transmitted to the rear chord. Changes in normal and shear force can be neglected. The realization of hinged joints is more difficult and labor-intensive. This extra effort is not even beneficial and therefore not advised.
- The upper lens-shaped barrier section can be designed much finer, thus reducing the overall weight and resulting in more optimum use of steel. The reduction in weight is significant and reduces the costs of the steel. More importantly, it reduces the forces on the hydraulic cylinders and moving parts of the barrier.
- Designing the retaining wall with the method of equivalent cross-section is favorable over the method of the separation of components. The difference in weight for both calculation methods is equal to 19.7 tonnes.

The total mass of the gate can be determined by the summation of the five main structural parts, which results in:

$$m_{\text{gate}} = 7850 * (55.2 + 11.5 + 44.3 + 6.0 + 17.6) = 7850 * 134.6 = 1060 * 10^3 \text{ kg} = 1060 \text{ tonnes}$$

The main contributors to this total mass are the bottom and center lens-shaped barrier sections. The front plate forms the largest single contributor at 20% of the total mass of the gate. In the detailed design stage, efforts should be made to investigate any possible reduction of the front plate thickness. This would significantly decrease the mass of the gate. The upper lens-shaped barrier section requires only $11.5 / 27.6 = 40\%$ of the steel volume needed for the leading lens-shaped sections. This results in a weight reduction of $(27.6 - 11.5) * 7850 = 126 \text{ tonnes}$, which is equal to about 12% of the current total weight of the gate.

	Cross-sectional dimensions (height, flange thickness)	Cross-sectional area component	Component main length	Number of components	Required steel volume component
	[mm]	[mm ²]	[m]	[-]	[m ³]
Leading lens-shaped barrier section					
- Front chord	a = 1250 mm, t = 40 mm	193600	65.5	2	25.4
- Rear chord	a = 1250 mm, t = 40 mm	193600	69.8	2	27.2
- Transverse girders (table 8.10 and 8.11)					
A	a = 500 mm, t = 20 mm	38400	18.0	2	1.4
B	a = 450 mm, t = 20 mm	34400	16.9	2	1.2
C	a = 400 mm, t = 20 mm	30400	13.5	2	0.82
D	a = 350 mm, t = 20 mm	26400	7.9	2	0.42
				subtotal	55.2
Upper lens-shaped barrier section					
- Front chord	a = 650 mm, t = 30 mm	74400	65.5	1	4.9
- Rear chord	a = 650 mm, t = 30 mm	74400	69.8	1	5.2
- Transverse girders (table 8.12: t = 20 mm)					
A	a = 350 mm, t = 20 mm	26400	18.0	1	0.48
B	a = 350 mm, t = 20 mm	26400	16.9	1	0.45
C	a = 300 mm, t = 20 mm	22400	13.5	1	0.30
D	a = 250 mm, t = 20 mm	18400	7.9	1	0.15
				subtotal	11.5
Retaining wall					
- Front plate	h = 14650 mm, t = 30 mm	439500	65.5	1	28.6
- Longitudinal stiffener	IPE 240	3910	2.0	14 x 33	3.6
- Cross beam	HE 700 A	26000	14.5	32	12.1
				subtotal	44.3
x-type bracing system					
- Transverse girders					
A	a = 250 mm, t = 10 mm	9600	8.5	12	0.98
B	a = 250 mm, t = 10 mm	9600	10.3	8	0.79
C	a = 250 mm, t = 10 mm	9600	9.0	8	0.69
D	a = 250 mm, t = 10 mm	9600	9.9	4	0.38
- Rear chord	a = 250 mm, t = 10 mm	9600	10.0	32	3.2
				subtotal	6.0
Guide posts					
	h = 14650 mm, t = 200 mm (t is eq. plate thickness)	2930000	3.0	2	17.6

An estimation of the balance of components determines whether the center of gravity of the lens-shaped section is close to the plane of suspension. The pitch ratio between the parabolic front and rear gate curvature is 2, which implies that the weight of the front chords and retaining wall may only be two times larger than the weight of the rear chords and x-type bracing systems. Calculation of the front arch mass including the retaining wall and rear arch mass including the bracing systems results in a mass of 588 tonnes and 280 tonnes respectively.

It can be concluded that the overturning moment is sufficiently small. The mass of the rear arch multiplied by two nearly equals the mass of the front arch. In addition, the center of gravity of the transverse girders and associated x-type bracing systems is located in the rear arch. This means that the overturning moment is even smaller.

Finally, vibrations of the gate in vertical direction are reviewed as it is one of the possible modes of degradation. The main causes of vibration concern the gate lip and the bottom and/or side seals designs. Fluttering of rubber seals can generate vibrations of the gate. Vibration tendencies could be reduced if a rubber seal is not used. This leads to leakage when the gate is closed. The gate is designed to allow a leakage width of 50 mm at both sides of the gate and a bottom leakage opening of 150 mm. Rubber seals are therefore not advised in the design.

Based on the calculation results of the main parameters pertaining to the lifting gate vibration in vertical direction, major problem should not be expected. The system is positively damped and the excitation frequency is sufficiently small compared to the first eigenfrequency. There might be some problems with higher eigenfrequency modes. During the detailed design stage, the situation regarding vertical vibration should be kept in close watch. From literature, some remarks can be made at this point. Researchers have focused on vertical lifting gates and findings of these efforts have shown that flat-bottomed gates have to be avoided. The inclination of the lip should be 45 degrees and the skin plate should be at the upstream side of the gate. Another structural feature to reduce vibrations is the design of proper hinges between the cylinder arms and the gate lugs. These are projected to be Cardan joints, which is a joint in a rigid rod that allows the rod to bend in any direction. In choosing this joint, all possible movements of the gates can be tolerated including an unequal lifting movement.

List Of Figures And Tables (Report)

Figures:

- Fig. 1.1: Major hydrological features in the vicinity of New Orleans
Fig. 1.2: Main parishes and neighborhoods of New Orleans
Fig. 1.3: Main waterways of New Orleans
Fig. 1.4: Hurricane Katrina – path and intensity history
Fig. 1.5: Wind vectors / storm surge elevation just after landfall at Buras
Fig. 1.6: Left – Hurricane Katrina: maximum sustained wind field, Right – Hurricane Katrina: rainfall estimates
Fig. 1.7: Three USACE Hurricane Protection Projects in Southern Louisiana
Fig. 1.8: Overview of the failures of several floodwalls and levees along the canals into New Orleans
Fig. 1.9: Comparison actual storm surge with design
Fig. 1.10: Comparison actual wave conditions with design
- Fig. 2.1: The Netherlands without flood protection
Fig. 2.2: Overview of both the Haarlemmermeer and the IJ bay
Fig. 2.3: The Zuiderzee Works
Fig. 2.4: The Delta Project
Fig. 2.5: Dike ring areas in the Netherlands – safety standard per dike ring area
Fig. 2.6: Dutch Flood Defence Act
Fig. 2.7: Mississippi River Delta and Dutch Delta
Fig. 2.8: The dike ring areas of New Orleans, in combination with their direct water threat
Fig. 2.9: Direct water threats regarding the Netherlands
Fig. 2.10: Location of the cities of New Orleans (left) and Amsterdam (right), presented with their main waterways
Fig. 2.11: Cross section of the central part of Amsterdam (upper) and New Orleans (lower)
Fig. 2.12: Southeast Louisiana – multiple lines of defence
- Fig. 3.1: Grand Plan of southern Louisiana as provided by the LSU, engineering companies and USACE
Fig. 3.2: Schematized water movement for two hurricane winds field passing New Orleans
Fig. 3.3: Overview of the storm surge generation process
Fig. 3.4: Deltaic cycle - evolution of depositional systems in the Mississippi River Deltaic Plain
Fig. 3.5: Distribution of hurricanes and tropical storms along the Louisiana coast from 1901–1996
Fig. 3.6: Projected coastal land loss by 2050
Fig. 3.7: Examples of levee breach along the GIWW (left) and the MRGO (right)
Fig. 3.8: Levees along the GIWW / MRGO – correlation between erosion and types of material used
Fig. 3.9: Hurricane Barrier Plan
Fig. 3.10: Pre-Katrina levee conditions in the study area
Fig. 3.11: Coastal defensive zone system of both the St. Bernard and Orleans Parish
Fig. 3.12: Time series of water surface elevation along the MRGO
Fig. 3.13: Zero alternative
Fig. 3.14: Zero (-) alternative
Fig. 3.15: Land reclamation alternative
Fig. 3.16: The process of wind setup over vegetated wetlands
Fig. 3.17: Breakwater alternative
Fig. 3.18: Floodgate(s) alternative, alignment I
Fig. 3.19: Floodgate(s) alternative, alignment II
Fig. 3.20: Floodgate(s) alternative, alignment III
- Fig. 4.1: Projected location of both flood protection structures in combination with the local bathymetry of Lake Borgne
Fig. 4.2: Orleans East Parish: comparison of wave maxima (left) and water level maxima (right) with design values
Fig. 4.3: St. Bernard Parish: comparison of wave maxima (left) and water level maxima (right) with design values
Fig. 4.4: Near shore wave conditions – basin scale WAM model
Fig. 4.5: Main navigation options around New Orleans
Fig. 4.6: Characteristics of the bridges spanning the Rigolets
Fig. 4.7: Retention area for flood protection, retention of rainfall runoff and preservation of wetlands
Fig. 4.8: Mississippi River Gulf Outlet – overview and mileage
Fig. 4.9: Freshwater diversion at Violet Canal, St. Bernard Parish
- Fig. 5.1: Minimum width of a navigable waterway
Fig. 5.2: Options for navigable floodgate structures
- Fig. 6.1: Vertical lifting gate – site selection
Fig. 6.2: Prevailing winds at Lake Borgne and main wind fetches
Fig. 6.3: Geological complexity of the New Orleans region
Fig. 6.4: Geological cross section
Fig. 6.5: Zone B Gulf of Mexico Hurricanes – central pressure return periods
Fig. 6.6: Modeled levee alignment presenting maximum hydraulic conditions
Fig. 6.7: Main standards regarding a flood protection structure
Fig. 6.8: Modeled variation of the surge level in time
Fig. 6.9: Overview of the projected defence system – characteristics of the retention area

- Fig. 6.10: Cross-section 1-1' – retention area and associated design conditions
 Fig. 6.11: Cross-section 2-2' – lifting gate and conditions
 Fig. 6.12: Mobilization of personnel – the accessibility of the projected site
 Fig. 6.13: Event tree describing the probability of failure of the closing process of the lifting gate
- Fig. 7.1: Schematization loading of the concrete substructure
 Fig. 7.2: Front view of main types of foundation configurations: combined concrete walls / floor (left) and separate piers (right)
 Fig. 7.3: Indication of the wave pressure distribution according the linear wave theorem
 Fig. 7.4: Modified model of Goda
 Fig. 7.5: Modified model of Goda – wave pressures
 Fig. 7.6: Modified model of Goda – resulting wave forces
 Fig. 7.7: Maximum surge level and wave conditions under maximum differential head – influence (im)permeable layer
 Fig. 7.8: Maximum surge level and wave conditions under maximum differential head – loading scheme used for calculations
 Fig. 7.9: Maximum surge level and wave conditions under maximum differential – influence pile plan
 Fig. 7.10: Maximum negative differential head
 Fig. 7.11: Maximum surge level and maximum wave conditions in combination with the occurrence of a wave low
 Fig. 7.12: Representative wind load on the gate in lifted position
 Fig. 7.13: Severe conditions during temporary closure of the substructure for maintenance
- Fig. 8.1: Hartel Canal Barrier – overview of the barrier and introducing its main component
 Fig. 8.2: Stress-strain curve of steel
 Fig. 8.3: First impression of the calculation model, in which the transverse girders are set at a constant 8.0 m interval
 Fig. 8.4: Leading loading scenario for the design of the lifting gate
 Fig. 8.5: Initial analysis of the lens-shaped barrier section
 Fig. 8.6: Schematization to determine the coordinates needed to describe the circular gate curvature
 Fig. 8.7: Bending moment development for variable arch pitches
 Fig. 8.8: Normal force development for variable arch pitches
 Fig. 8.9: Schematization of the center frame
 Fig. 8.10: Center frame – development of normal forces, hinged joint model
 Fig. 8.11: Introducing the own weight of the x-type bracing system of the rear chord
 Fig. 8.12: Schematization of the retaining wall – front plate, longitudinal stiffeners and cross beams
 Fig. 8.13: Model front plate and schematized loading
 Fig. 8.14: Front plate – development of member forces: moment (upper) and shear force (lower)
 Fig. 8.15: Cross beam – model and member forces for a mutual distance of 2.0 m: moment (center) and shear force (lower)
 Fig. 8.16: Equivalent cross-section
- Fig. 9.1: Schematization of an almost closed gate
 Fig. 9.2: Graphical presentation of the added mass coefficient
 Fig. 9.3: Graphical presentation of the development of energy head
 Fig. 9.4: Transmission coefficients
 Fig. 9.5: Hartel Canal Barrier – global view of projected cylinders and detail of the cylinder joint to one of the gates

Tables:

- Table 1.1: Saffir-Simpson Hurricane Scale
 Table 1.2: Hurricane Katrina characteristics
- Table 2.1: General distinction in direct loading of the dike rings areas of New Orleans
- Table 3.1: Rough estimation of required crest heights under Hurricane Katrina induced wave conditions
 Table 3.2: Mutual importance of the stated criteria
 Table 3.3: Master plan concepts on meso scale – multi criteria evaluation
- Table 4.1: Classification of waterways and associated design vessels
 Table 4.2: Vessel traffic on the Gulf Intracoastal Waterway for the section New Orleans to Mobile Bay
 Table 4.3: Vessel traffic on the Mississippi River Gulf Outlet
 Table 4.4: Main economics concerning the closure of the Mississippi River Gulf Outlet
- Table 5.1: Design vessels regarding the flood protection structure
 Table 5.2: Characteristics for determining the minimum width of a navigable waterway
 Table 5.3: Results for the limitation speed of vessel passing the floodgate structure
 Table 5.4: Favorable and unfavorable aspects of vertical lifting gates
 Table 5.5: Vertical lifting gates – proven flood protection schemes
 Table 5.6: Favorable and unfavorable aspects of flap gates
 Table 5.7: Flap gates – proven flood protection schemes
 Table 5.8: Favorable and unfavorable aspects of horizontally moving or rotating gates
 Table 5.9: Horizontally moving or rotating gates – proven flood protection schemes
 Table 5.10: Favorable and unfavorable aspects of floating sector gates
 Table 5.11: Floating sector gates – proven flood protection schemes
 Table 5.12: Favorable and unfavorable aspects of vertically rotating gates
 Table 5.13: Vertically rotating gates – proven flood protection schemes
 Table 5.14: Application of killer requirements
 Table 5.15: Structural characteristics of both vertical lifting gate and sector gate
 Table 5.16: An overview of the main structural concerns for both vertical lifting gate and sector gate
 Table 5.17: Gate selection rationale – evaluation of the vertical lifting gate and sector gate

Table 6.1:	Normal wind speeds
Table 6.2:	Normal conditions – wave height, wave period and wind setup at location of the structure
Table 6.3:	Soil characteristics according to Dutch standards
Table 6.4:	Boundary conditions divided per design requirement
Table 6.5:	Surface elevation of the retention area as a result of overtopping of the outer levee
Table 6.6:	Minimum required gate height as direct result of overtopping and/or overflow allowed over the lifting gate
Table 6.7:	Calculated combinations of leakage width and required gate height
Table 6.8:	Calculation overview of the leading combination of allowed leakage volume and minimum required gate height
Table 6.9:	Dependency of the frequency of exceedence of open retaining level
Table 6.10:	Safety of closure elements – hydraulical components of moving locking devices [9]
Table 7.1:	Modified model of Goda – overview of results
Table 7.2:	Calculation results for maximum surge level and wave conditions under maximum differential head
Table 7.3:	Calculation results for variations on the calculation method: impermeable layer and assumed influence pile plan
Table 7.4:	Calculation results for the maximum negative differential head
Table 7.5:	Calculation results for maximum surge level and wave conditions in combination with the occurrence of a wave low
Table 7.6:	Calculation results for the representative wind load on the gate in lifted position
Table 7.7:	Calculation results for severe conditions during temporary closure of the substructure for maintenance
Table 8.1:	Dimensions of the projected lifting gate compared to the Hartel Canal Barrier
Table 8.2:	Overview of construction steel qualities – strength and stiffness
Table 8.3:	Cross beam – overview of support reactions and leading member forces, all per meter structural width
Table 8.4:	Overview of coordinates to describe variable arch pitches
Table 8.5:	Bottom / center lens-shaped section – design transverse girder, hinged joint model – constant flange thickness
Table 8.6:	Bottom / center lens-shaped section – design transverse girder, hinged joint model – constant outer dimension
Table 8.7:	Upper lens-shaped section – design transverse girder, hinged joint model
Table 8.8:	X-type bracing system – design center frame, hinged joint model – first guess
Table 8.9:	X-type bracing system – design center frame, hinged joint model – preliminary design
Table 8.10:	Bottom / center lens-shaped section – design transverse girder, clamped joint model - constant flange thickness
Table 8.11:	Bottom / center lens-shaped section – check designed transverse girder on equivalent stress < yield point
Table 8.12:	Upper lens-shaped section – check designed transverse girder on equivalent stress < yield point
Table 8.13:	X-type bracing system – design center frame, clamped joint model – preliminary design
Table 8.14:	Upper lens-shaped section – check designed x-type bracing system on equivalent stress < yield point
Table 8.15:	Method of the separation of components – required longitudinal stiffener for variable field width
Table 8.16:	Overview of available HEA-profiles
Table 8.17:	Method of the separation of components – required cross beam for variable mutual distance
Table 8.18:	Method of the separation of components – required volume of steel for longitudinal stiffeners and cross beams
Table 8.19:	Method of the equivalent cross-section – required longitudinal stiffener for variable field width
Table 8.20:	Method of the equivalent cross-section – longitudinal stiffener – additional cross-sectional parameters
Table 8.21:	Method of the equivalent cross-section – required cross beam for mutual distance
Table 8.22:	Method of the equivalent cross-section – cross beam – additional cross-sectional parameters
Table 8.23:	Method of the equivalent cross-section – required volume of steel for longitudinal stiffeners and cross beams
Table 8.24:	Required volumes of steel for both calculation methods and for a variable mutual distance for the cross beams
Table 8.25:	Overview of structural components – determination of the mass distribution over the steel lifting gate

Table Of Content

Preface	I
Executive Summary	II
List Of Figures And Tables (Report)	VII
1. Introduction: New Orleans And Hurricane Katrina	01
1.1 New Orleans	01
1.2 What happened? – Hurricane Katrina	03
1.2.1 Hurricane Katrina – characteristics and development in time	03
1.2.2 Hurricane Katrina – modeled storm parameters	05
1.3 The performance of the Hurricane Protection System of New Orleans	05
1.3.1 General overview of the Hurricane Protection System of New Orleans	05
1.3.2 Failure of the Hurricane Protection System	06
1.3.3 Direct causes of failure	07
1.3.4 Contributing factors of failure	08
1.3.5 Consequences of failure	08
1.4 Principal conclusions and thesis content	08
1.4.1 Principal conclusions and recommendations	08
1.4.2 Thesis content	10
2. The Hurricane Protection System Of New Orleans Compared To The Development Of Flood Protection In The Netherlands	11
2.1 The Dutch flood protection in a historical perspective	11
2.1.1 Land reclamation	11
2.1.2 Improved water management technologies: the Zuiderzee Works	12
2.1.3 Response programs to flooding disasters: legislation and frequent safety assessment	13
2.2 Comparison of New Orleans and Amsterdam	15
2.2.1 New Orleans compared to the Netherlands – historical development and hydraulic boundaries	15
2.2.2 New Orleans compared to Amsterdam – location: important junction for navigation	18
2.2.3 New Orleans compared to Amsterdam – surface level: major cities below mean sea level	18
2.2.4 Principal conclusions	19
2.3 New way of thinking: 'ComCoast'	20
2.3.1 ComCoast – functions, components and general solutions	20
2.3.2 ComCoast – application: multiple lines of defence in the New Orleans region	21
3. Master Plan Of The New Orleans Region: Macro To Meso Scale	23
3.1 Introduction of the study area	23
3.1.1 Grand plan of southern Louisiana	23
3.1.2 Rationale for closing off Lake Pontchartrain	24
3.1.3 Study area – Lake Borgne, Mississippi River Gulf Outlet and Gulf Intracoastal Waterway	25
3.2 Primary contributors to storm water levels in the New Orleans region	26
3.3 Present situation of the New Orleans region	27
3.3.1 Macro scale – Louisiana's changing coastal landscape	27
3.3.2 Macro scale – characteristics of the waterways intersecting the study area	30
3.3.3 Meso scale – levee status pre-Katrina and performance during Katrina	30

3.4	Master plan concepts on <i>macro scale</i>	32
3.4.1	Planning constraints	32
3.4.2	No-action alternative	32
3.4.3	Non-structural alternative	33
3.4.4	Improvement of existing hurricane protection projects	33
3.4.5	Outlined part of the Grand Plan for southern Louisiana – Hurricane Barrier Plan	34
3.5	Outlined part of the Hurricane Barrier Plan – Master plan concepts on <i>meso scale</i>	35
3.5.1	Introduction	35
3.5.2	Design conditions and assumptions	36
3.5.3	'ComCoast' principle – generation of meso-scaled plan concepts	37
3.5.4	Evaluation of plan concepts	48
3.6	Principal conclusions	49
4.	Evaluation Of Barrier Concepts Within Master Plan: <i>Meso To Micro Scale</i>	50
4.1	Location of the flood protection barriers and general site parameters	50
4.2	Boundary conditions, assumptions and constraints	51
4.2.1	Hydraulic conditions – analytical validation of the hydrodynamic modeling for Hurricane Katrina	51
4.2.2	Navigation considerations	53
4.2.3	Environmental considerations	56
4.3	Functional program of requirements on barrier concept level	57
4.4	Barrier concepts at the Gulf Intracoastal Waterway and Mississippi River Gulf Outlet	58
4.4.1	Gulf Intracoastal Waterway – navigable storm surge barrier	58
4.4.2	Mississippi River Gulf Outlet – permanent closure for all navigation	58
4.4.3	Advised moment of implementation of the barrier concepts	62
5.	Overview Of Navigable Flood Protection Structures For The Gulf Intracoastal Waterway	63
5.1	Qualitative technical program of requirements	63
5.2	Options for navigable flood protection structures	66
5.2.1	Vertical lifting gate	67
5.2.2	Flap gate s – pneumatic flap gate and hydraulic flap gate	68
5.2.3	Horizontally moving or rotating gates – slide gate, sector gate and floating sector gate	69
5.2.4	Vertically rotating gates – segment gate and radial gate	71
5.3	Comparison of gate types	72
5.3.1	Killer requirements	72
5.3.2	Structural considerations and concerns	73
5.4	Gate selection rationale and conclusion	75
6.	Quantified Program Of Requirements Of The Navigable Storm Surge Barrier Within The Gulf Intracoastal Waterway	76
6.1	Site selection	76
6.2	Geotechnical design conditions	78
6.2.1	General description, assumptions and constraints	78
6.2.2	Geotechnical analysis	78
6.3	Hydraulic design conditions	80
6.3.1	General description, assumptions and constraints	80
6.3.2	Hydraulic analysis of the Probable Maximum Hurricane – required level of protection	80

6.4	Appliance and quantification of Dutch standards	82
6.4.1	Overview of main design standards	82
6.4.2	Quantification of required boundary conditions	83
6.4.3	Retaining height of the lifting gate – maximum incoming volume of water over the closed structure	86
6.4.4	Safety of the closure elements – maximum incoming volume of water through the open structure	91
7.	Preliminary Design Of The Navigable Storm Surge Barrier Within The Gulf Intracoastal Waterway – Design Of The Concrete Civil Works	98
7.1	Calculation method, assumptions and constraints	98
7.1.1	Introduction to the general calculation method	98
7.1.2	Resultant horizontal wave force on the vertical lifting gate – modified model of Goda	100
7.2	Determination of the critical loading scenario and associated substructure	103
7.2.1	Maximum surge level and wave conditions under maximum differential head	103
7.2.2	Maximum negative differential head – malfunction of the lifting gate after closure	105
7.2.3	Maximum surge level and wave conditions in combination with the occurrence of a wave low	106
7.2.4	Representative wind load on the gate in lifted position	107
7.2.5	Severe conditions during a temporary closure of the substructure for maintenance	109
7.2.6	Ship collision – indicative calculation to estimate order of magnitude and expected influence	110
7.3	Potential of failure due to piping	110
7.4	Principal conclusions – review on the calculation method and results	111
8.	Preliminary Design Of The Navigable Storm Surge Barrier Within The Gulf Intracoastal Waterway – Design Of The Steel Lifting Gate	112
8.1	Introduction of the reference project, calculation method and assumptions	112
8.1.1	Reference project for the gate design – Hartel Canal Barrier	113
8.1.2	Calculation method and assumptions	114
8.2	Design of the barrier cross-section	117
8.2.1	Determination leading reaction forces of the cross beam on the front chord	117
8.2.2	Configuration of the lens-shaped barrier sections	118
8.2.3	Iterative design calculations to find optimal steel cross-sections – chords and transverse girders	123
8.3	Design of the composite retaining wall – plate thickness, stiffeners and cross beams	131
8.3.1	Method of the separation of components	131
8.3.2	Method of the equivalent cross-section	132
8.4	Overview of structure components and optimizations in the steel gate design	139
8.4.1	Quantifying optimizations in the steel gate design	139
8.4.2	Overview of structural components – determination of the mass distribution over the steel lifting gate	142
8.5	Principal conclusions – review on the calculation method and results	143
9.	Review On Degradations – General Maintenance And Analysis On Vibrations	144
9.1	Main modes of degradations and general maintenance approach	144
9.2	Analysis on vibrations	144
9.2.1	Schematization and principal data	145
9.2.2	Calculation of all main parameters pertaining to the vertical lifting gate vibration	146
9.2.3	Conclusion on the lifting gate vibration in vertical direction	151
10.	Principal Conclusions And Recommendations	152
	References	154

APPENDIX A – Hydrodynamic Modeling: General Overview (Including PMH) And Results For Hurricane Katrina	156
A.1 General overview and introduction of the Probable Maximum Hurricane (PMH)	156
A.2 Southern Louisiana – storm peak water levels for <i>Hurricane Katrina</i> using the ARCDIC model	160
A.3 Southern Louisiana – maximum wave conditions for <i>Hurricane Katrina</i> using the STWAVE model	161
A.4 <i>Hurricane Katrina</i> – comparison of wave maxima and water level maxima with design values	163
APPENDIX B – Analytical Validation Of The Hydrodynamic Modeling Results For Hurricane Katrina	165
B.1 Wave conditions offshore and near shore	165
B.2 Wind setup offshore and near shore	169
B.3 Sensitivity analysis of the analytical models	171
APPENDIX C – Hurricane Protection System and its flooding characteristics	174
C.1 Lake Pontchartrain and Vicinity Hurricane Protection Project - finalized reaches divided in parishes	174
C.2 Technical background on the causes of failure for the main levee and floodwall breaches	177
APPENDIX D – Navigable Flood Protection Structures: Examples Of Proven Protection Schemes	181
D.1 Vertical lifting gate	181
D.2 Flap gate: pneumatic flap gate and hydraulic flap gate	182
D.3 Horizontally moving or rotating gate: slide gate, sector gate and floating sector gate	183
D.4 Vertically rotating gate: segment gate and radial gate	185
APPENDIX E – General Design Requirements	187
E.1 Geotechnical Design Requirements	187
E.2 Safety of closure elements – general failure frequencies per structural component	188
APPENDIX F – Water Movement Around Moving Vessels: Theorem Of Schijf [1949]	190
APPENDIX G – Excel Results	193
G.1 Overtopping discharge at the outer levee under variable surge level	193
G.2 Vertical lifting gate – minimum required retaining height at moment of installation	194
G.3 Vertical lifting gate – iterative calculation to determine optimum combination for leakage width and gate height	195
APPENDIX H – MathCAD Results	198
H.1 Maximum water level allowed in the retention area and minimum required crest height of the outer levee	198
H.2 Retaining height of the vertical lifting gate and allowed leakage	199
H.3 Modified model of Goda – wave forces on a vertical wall	200
H.4 Check on shearing and stability of the required concrete civil works – multiple loading scenarios	203
H.5 Retaining wall – optimum front plate thickness, stiffeners and cross beams	219
APPENDIX I – MatrixFrame Results	226
I.1 Cross beam – optimum number of supports	226
I.2 Lens-shaped barrier section, <i>hinged joints</i> – optimum gate curvature and optimum pitch ratio	229
I.3 Lens-shaped barrier section with <i>clamped joints</i> – optimum development of member forces	234
I.4 Upper lens-shaped barrier section with <i>clamped joints</i> – optimum layout for reducing weight	239
I.5 Retaining wall – optimum front plate thickness – longitudinal stiffeners and cross beams	240

“The excuse we have heard from some government officials throughout this investigation, that Katrina was an unforeseeable ultra-catastrophe, has not only been demonstrated to have been mistaken but also misses the point that we need to be ready for the worst that nature can throw at us. Powerful though it was, the most extraordinary thing about Katrina was our lack of preparedness for a disaster so long predicted.

This is not the first time the devastation of a natural disaster brought about demands for a better, more coordinated government response. In fact, this process truly began after a series of natural disasters in the 1960s and into the 1970s. One of those disasters was Hurricane Betsy, which hit New Orleans in 1965. The similarities with Katrina are striking: levees overtopped and breached, severe flooding, communities destroyed, thousands rescued from rooftops by helicopters, thousands more by boat and too many lives lost.

Katrina revealed that this kaleidoscope of reorganizations has not improved our disaster management capability during these critical years. Our purpose and our obligation now is to move forward to create a structure that brings immediate improvement and guarantees continual progress. This will not be done by simply renaming agencies or drawing new organizational charts. We are not here to rearrange the deck chairs on a ship that, while perhaps not sinking, certainly is adrift.”

*Senator Susan Collins
Opening Statement
Committee on Homeland Security and Government Affairs [2006]*

1. Introduction: New Orleans And Hurricane Katrina

On the morning of August 29, 2005, Hurricane Katrina struck southeast Louisiana and triggered what would become one of the worst disasters ever to befall an American city. This introductory chapter provides a review of the performance of the Hurricane Protection System (HPS) of New Orleans existing at the time Hurricane Katrina struck. Section 1.1 introduces the city of New Orleans, section 1.2 describes the main characteristics of Hurricane Katrina and section 1.3 discusses the actual performance of the HPS. It outlines the direct causes and contributing factors that led to the failure of the protective system. Section 1.4 contains the principal conclusions on the review of this current and consequently results in the content of this thesis.

1.1 New Orleans

The city of New Orleans is located in southeastern Louisiana near the points where the Mississippi River flows into the Gulf of Mexico. The city was established in the early 1700s on the high grounds adjacent to the Mississippi River. Over the centuries, New Orleans grew into a mayor city with a population of over a million people. The city's location is the central point of focus. Its strategic location has resulted in prosperity but at the same time New Orleans has to be aware of its prone location since it is situated in tidal lowlands, it is surrounded by water and its defensive wetlands are decaying.

The hydrology of southeast Louisiana is dominated by several major features including the Mississippi River, Lake Borgne, Lake Pontchartrain and the Gulf of Mexico. An overview of these major hydrological features is given in figure 1.1. To the southeast of New Orleans, the Mississippi River bends to the south and flows out through its delta in the Gulf of Mexico. Lake Borgne is directly connected to the waters of the Gulf of Mexico. Lake Pontchartrain is an estuary which connects with the Gulf of Mexico via Mississippi Sound and Lake Borgne.



Fig. 1.1: Major hydrological features in the vicinity of New Orleans

The city of New Orleans has struggled against annual flooding of the Mississippi River and occasional storm surge flooding brought by hurricanes ever since her founding. Once protected from the seasonal floods of the Mississippi River, attention shifted to building levees along Lake Pontchartrain to the north and also Lake Borgne to the east of the city. As both population and infrastructure expanded, the protective levee systems needed to expand drastically to include protection for the growing national economic assets. However, while the new levees provided protection from rising storm surges, they also hydraulically isolated the urban and industrialized areas. This isolation becomes visible when reviewing the composition of these urban areas of New Orleans. Figure 1.2 presents the city's metropolitan area, which is composed of Jefferson Parish, Orleans Parish and St. Bernard Parish. The borders between these parishes generally coincide with the main protective levee systems. It should be noted that the State of Louisiana is divided into parishes, rather than counties like most other U.S. States.

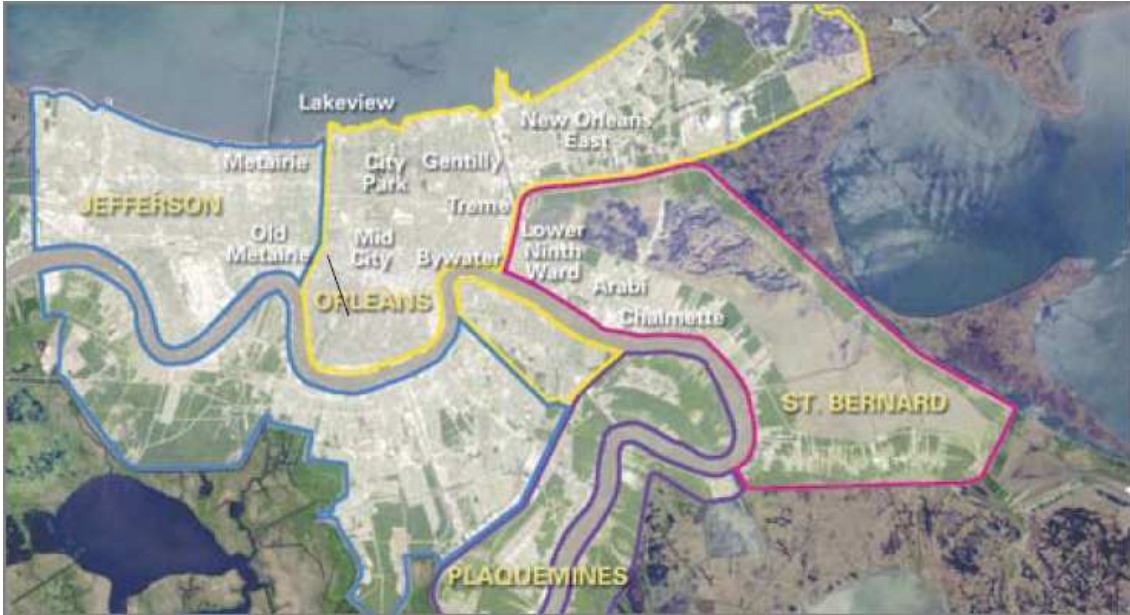


Fig. 1.2: Main parishes and neighborhoods of New Orleans [1]

Large portions of the metropolitan area are currently below mean sea level and continue to sink as New Orleans is built on thousands of feet of highly compressible materials. In the past, flooding and deposition of sediments from the Mississippi River counterbalanced natural subsidence, leaving southeast Louisiana at or above mean sea level. However, due to major flood control structures being built upstream on the Mississippi River and levees being built around New Orleans, fresh layers of sediment are not replenishing surface areas lost by subsidence. In addition to the low elevation of the populated parishes, rainfall runoff can be significant in New Orleans. Nearly runoff must be pumped out of these protected areas to prevent flooding. This is achieved via various outlet channels, which extent into the urban areas as part of the HPS of New Orleans. Main features of this HPS are the levees and floodwalls built along the main waterways and outlet channels. Waterways of significance with respect to the HPS are shown in figure 1.3 and include:

- Mississippi River;
- Outfall canals (17th Street Canal, Orleans Canal and London Avenue Canal);
- Inner Harbor Navigation Canal (IHNC), commonly referred to as the Industrial Canal;
- Gulf Intracoastal Waterway (GIWW) and Mississippi River Gulf Outlet (MRGO).



Fig. 1.3: Main waterways of New Orleans [1]

1.2 What happened? – Hurricane Katrina

Hurricane Katrina was one of the strongest storms ever to hit the coast of the United States and New Orleans was directly in the hurricane's path. As a result, Hurricane Katrina produced unparalleled wave and storm surge conditions for the New Orleans vicinity. This section presents a brief overview of Hurricane Katrina. Section 1.2.1 presents a qualitative description of Hurricane Katrina by outlining its characteristics and development in time. Section 1.1.2 presents a quantitative description of Hurricane Katrina by referring to various models.

1.2.1 Hurricane Katrina – characteristics and development in time

Hurricanes are generally categorized based on maximum wind speed according to the Saffir-Simpson Hurricane Scale, as given in table 2.1

Scale [category]	Pressure [mbar]	Wind Speed [mph]	Wind Speed [m/s]	Surge level [m]	Wave height [m]	Damage [-]
1	> 980	74 – 95	33 – 42	4 to 5	4 – 8	Minimal
2	965 – 979	96 – 110	43 – 49	6 to 8	6 – 10	Moderate
3	945 – 964	111 – 130	50 – 58	9 to 12	8 – 12	Extensive
4	920 – 944	131 – 155	59 - 69	13 to 18	10 – 14	Extreme
5	< 919	> 155	> 70	> 18	12 – 17	Catastrophic

Table 1.1: Saffir-Simpson Hurricane Scale [16]

Hurricane Katrina was a very large Category 3 storm when it passed the New Orleans area on the morning of 29 August 2005. Twenty hours earlier, this storm had been the largest Category 5 and most intense storm on record within the northern Gulf of Mexico. East of the Mississippi River delta, a deep water buoy recorded a significant wave height of 55 ft (16.7 m), the highest ever measured in the Gulf of Mexico. The large size of Katrina throughout its history, combined with the extreme waves generated during its most intense phase, enabled this storm to produce storm surges up to 28 ft (8.5 m). The previous highest high water mark from Hurricane Camille was 24.6 ft (7.5 m) and Camille is the only Category 5 storm to make landfall in the Gulf of Mexico in the interval that records have been kept. In other words, a Category 3 storm like Katrina generated substantially higher surges at landfall than a Category 5 storm like Camille in the area where they both made a direct hit. This means that whereas the Saffir-Simpson characterization scale is a good predictor of wind damage from hurricanes, it is not a particularly good predictor of the storm surge level and wave generation potential for these storms.

The path and intensity history of Hurricane Katrina are shown in figure 1.4. The storm started as a tropical depression in the Bahamas on August 23, 2005. It crossed south Florida as a Category 1 hurricane and then entered the Gulf of Mexico. The storm intensified as it tracked westward. Katrina struck New Orleans early on the morning of 29 August 2005, after building up water levels to the east of New Orleans for several days. Table 1.2 shows the coordinates for the storm center and various storm characteristics for every 3 hour between the 0000 UTC on August 26 and 0000 UTC on August 28. Included is the maximum sustained surface wind speed in relation to the Saffir-Simpson characterization scale.

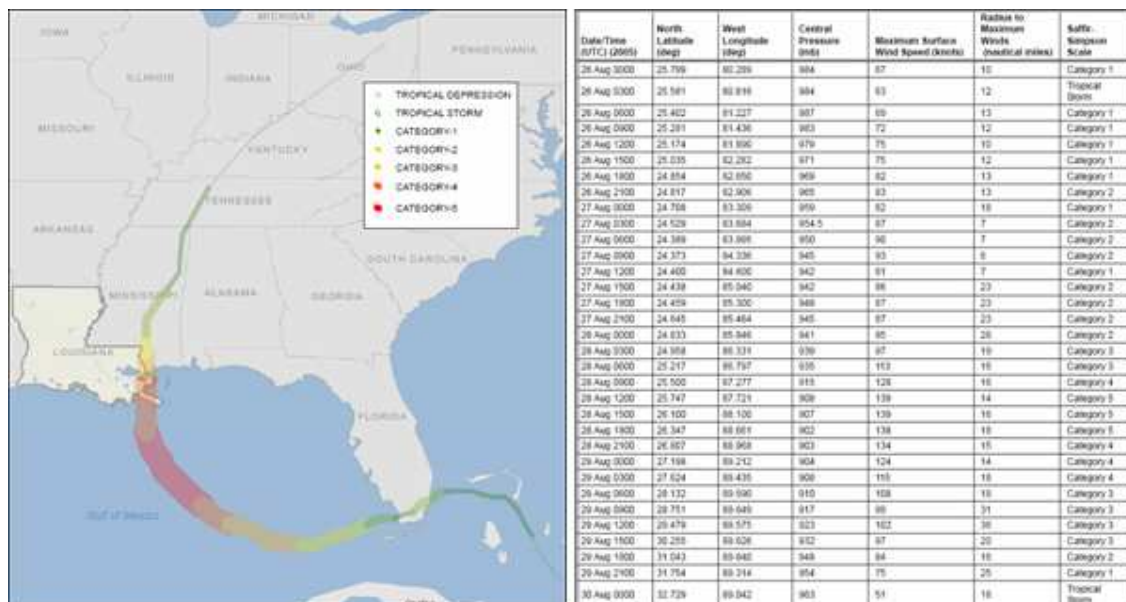


Fig. 1.4: Hurricane Katrina – path and intensity history [15]

Table 1.2: Hurricane Katrina characteristics [31]

On August 28 the storm turned toward the northwest and experienced rapid intensification. It evolved from an upper Category 2 intensity storm to a Category 5 storm in only 12 hours. Katrina attained its peak intensity at around 1200 UTC, when the maximum sustained surface wind speed reached 139 knots (72 m/s). While the storm was tracking to the northwest and approached land, the energy that Hurricane Katrina could draw from the Gulf of Mexico decreased. Water levels in Lake Borgne continued to rise, reaching levels that were 5.5 ft (1.7 m) above normal, high enough to inundate much of the wetland system east of the Mississippi River levees.

Hurricane Katrina made landfall near Buras at 1100 UTC on August 29. At landfall, the maximum sustained surface wind speed was about 100 knots (52 m/s). Figure 1.5 presents wind vectors and storm surge elevation just after this first landfall. At that moment in time, a storm surge from the Gulf of Mexico had built up in Lake Borgne. The Mississippi River delta created a barrier of land just to the west of the hurricane's center against which the massive storm surge piled up. In south Plaquemines Parish, peak water levels reached 20 ft (6.1 m) above mean sea level along its levees.

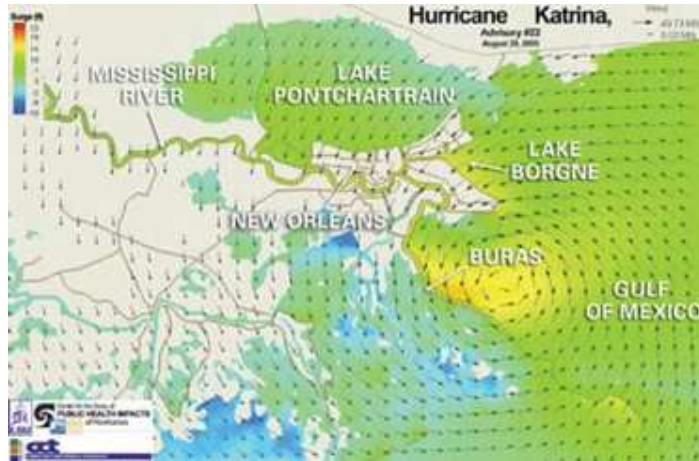


Fig. 1.5: Wind vectors / storm surge elevation just after landfall at Buras [1]

High water levels in Lake Borgne acted to drive water into Lake Pontchartrain, due to the water level difference between the two lakes. In addition to this, locally high winds in Lake Pontchartrain acted to tilt the water surface in the lake. These same winds created high wave conditions on the downwind side of the lake. Peak water levels at the entrances to canal along the lakeshore of New Orleans were nearly 12 ft (3.6 m) above mean sea level. The storm retained its large spatial extent, even as it weakened after landfall. Hurricane Katrina continued to weaken to a Category 2 storm at 1800 UTC on August 29, at which time it had moved well inland.

Rainfall amounts for Hurricane Katrina, though considerable in many places, were not the primary impact of the storm. Figure 1.6 illustrates the preliminary rainfall totals for the period attributed to Katrina (August 28-30, 2005), for locations with at least two inches of rain. The average rainfall during Katrina was measured to be 12 inches [National Oceanic and Atmospheric Administration (NOAA), 2005], equal to 1 ft (0.30 m). Note that the presented rainfall totals are incomplete due to storm damage experienced at many stations along the immediate Gulf coast.

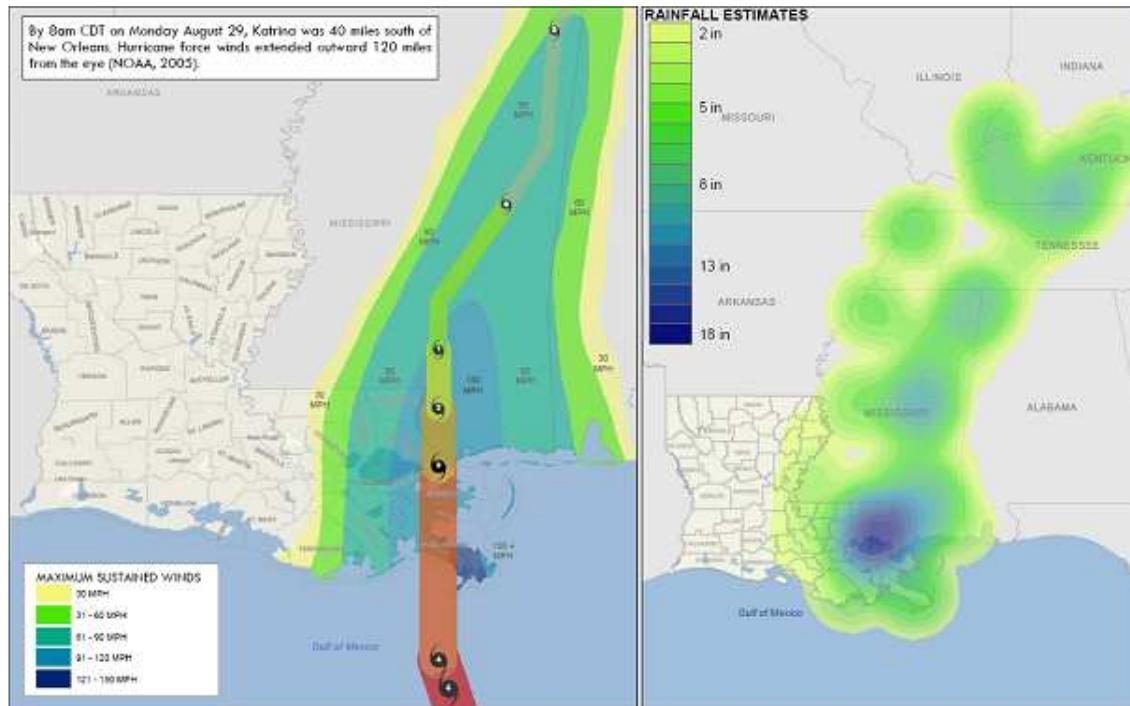


Fig. 1.6: Left – Hurricane Katrina: maximum sustained wind field [15]
Right – Hurricane Katrina: rainfall estimates [15]

1.2.2 Hurricane Katrina – modeled storm parameters

Literally all of the gauging instruments to measure water conditions were destroyed by Hurricane Katrina. Other than high water marks and the amount of devastation, there were few measurements to confirm the actual water level time-histories resulting from the storm. A combination of numerical model results and measured data was introduced by the U.S. Army Corps of Engineers' Interagency Performance Evaluation Task Force [USACE–IPET, 2006] to assess the wave and water level conditions along the entire periphery of the HPS. The WAM-model and STWAVE-model, for the description of offshore and near shore wave conditions respectively, and the ADCIRC storm surge model were used to characterize the wave and storm surge climate produced by the hurricane. A description of each model is given in Appendix A.1. Appendix A.2 provides the maximum surge levels predicted for Katrina using the ARCDIC-model. Appendix A.3 provides the maximum wave height and peak wave period using the STWAVE model. High water marks were used by IPET to confirm the accuracy of the model results. In most cases, the results agree within small range as can be extracted from Appendix A.4.

1.3 The performance of the Hurricane Protection System of New Orleans

Although Hurricane Katrina led to wind damage in New Orleans, most of the devastation was caused by flooding as the levee systems systematically failed. The wind driven storm surge moved into Lake Pontchartrain from the Gulf of Mexico, backing up water into the outlet and navigation canals serving New Orleans. The storm surge overwhelmed levees surrounding engineered works, flooding approximately 80% of New Orleans. Although several floodwalls were overtopped by the storm surge, the London Avenue and 17th Street Canal walls were not overtopped but suffered foundation failures at water level of no higher than about 5 ft (1.5 m) *below* the crest of the floodwalls. Looking at the extent of damage to the HPS of New Orleans and the consequences of subsequent flooding, it is imperative to understand what happened and why.

1.3.1 General overview of the Hurricane Protection System of New Orleans

The United States Army Corps of Engineers (USACE) is responsible for the design and construction of most of the flood protection levees along the Mississippi River and in the New Orleans metropolitan area. The overall strategy of the USACE for the protection of New Orleans was to built levees and floodwalls around segments of the city. The USACE projects are generally grouped into three main units, as shown in figure 1.7:

- The Lake Pontchartrain and Vicinity Hurricane Protection Project;
- The West Bank and Vicinity Hurricane Protection Project;
- New Orleans to Venice Hurricane Protection Project.

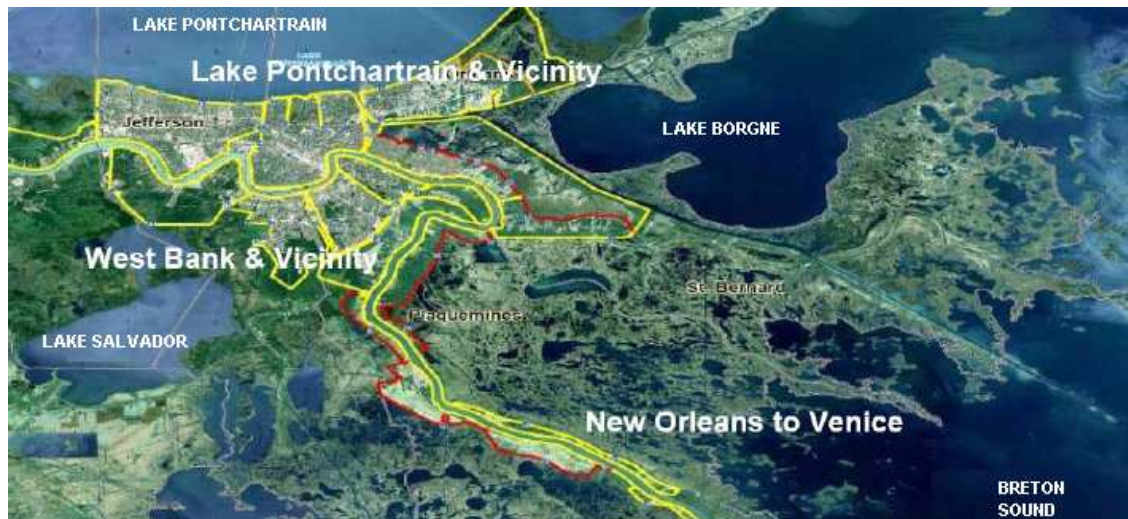


Fig. 1.7: Three USACE Hurricane Protection Projects in southern Louisiana [29]

The main characteristics of the HPS of New Orleans existing at the time Hurricane Katrina struck:

- The HPS includes nearly 350 miles (560 km) of protective structures. Earthen levees comprise the majority of them. When an earthen levee is raised with additional earth fill, it can typically only be heightened by increasing the width at the base. In most urban areas of New Orleans, the land has been developed right up to the base of the levee. Where an existing levee was located adjacent to buildings or other structures, the USACE often resorted to using floodwalls to avoid impacting adjacent development. Maps showing the location of specific types of structures are provided in Appendix C.1.

- The United States Congress directed the USACE to design the HPS for the most severe combination of meteorological conditions considered reasonably characteristic of the region. The approach historically taken by the USACE for design of Gulf Coast structures employs the concept of the Standard Project Hurricane (SPH). The SPH parameters were based on historic hurricanes spanning the period 1900-1956. In 1979, the National Oceanic and Atmospheric Administration (NOAA) issued a report that significantly revised the SPH criteria. This became the basis for the design of the West Bank and Vicinity Project. All activities with respect to the Lake Pontchartrain and Vicinity Hurricane Protection Project continued to use the original SPH criteria until the time of Hurricane Katrina. The selected SPH for this populated region corresponds to a storm surge and rainfall associated with a hurricane that would be roughly the same as what is today classified by the Saffir-Simpson Scale as a fast moving Category 3 hurricane.
- An important part of the protection of New Orleans is its interior drainage system. The average annual rainfall for the New Orleans area is 60 inches (1.5 m). Since much of New Orleans is below sea level, nearly all runoff must be pumped out to prevent flooding. The interior drainage system is designed for removing storm water from rainfall events, not removing water that enters the area from levee or floodwall overtopping or breaches. Pumping of groundwater from underneath the city has accelerated the subsidence of that the area was already prone to because of its natural geology. This subsidence increases the flood risk, should the levees be breached or precipitation exceeds pumping capacity.

1.3.2 Failure of the Hurricane Protection System

Hurricane Katrina was a large hurricane but the disaster of its arrival at New Orleans grew to a full blown catastrophe principally due to the massive and repeated failure of the HPS and the consequent flooding of the urban areas of New Orleans. An overview of the main breaches in the HPS during Katrina is given in figure 1.8.

Timeline of the failures during Hurricane Katrina:

- The storm surge and waves first hit Plaquemines Parish well before Katrina's landfall. The levees along the Mississippi River Gulf Outlet (MRGO) were soon hit with similar conditions. Eventually, the levees of both Plaquemines and St. Bernard Parish were severely overtopped by high surge and high, long period waves. The persistent winds had also built up a significant surge level at the convergence of the GIWW and IHNC. Wind generated waves reached 4 ft (1.2 m) in the IHNC, contributing to high dynamic loading on structures.
- During Hurricane Katrina's landfall, breaches in four floodwalls developed *before* water levels in the adjacent outlet canals overtopped the structures. Information on the causes of each of these failures is presented in Appendix C.2. Within a few hours of the initial breach at the IHNC, rising water in the canal overtopped and eroded levees. On both east and west side of the IHNC, additional floodwall failures allowed water to flood into the adjacent neighborhoods.
- By the time the most significant floodwall failures had occurred, the peak of the surge levels was over. Though surge levels in the Gulf of Mexico and in Lake Pontchartrain dropped, water continued to pour through the many damaged levees and floodwalls. This flooding continued until the water level in the city's bowl shaped landscape equalized with the water level in Lake Pontchartrain.



Fig. 1.8: Overview of the failures of several floodwalls and levees along the canals into New Orleans [1]

With regard to the massive failure of the HPS, it is instructive to examine the surge and wave environment created by Hurricane Katrina with respect to that assumed for the SPH from which the existing structures were designed. In spite of the fact that Hurricane Katrina exceeded the design storm, water levels and waves roughly corresponded to design conditions in some parts of the New Orleans area:

- Figure 1.9 presents a comparison of the surge generated by Hurricane Katrina with that used for the HPS design. Note that the surge level in Lake Pontchartrain was roughly the same as the design level. On the east side of New Orleans, generated surge levels were significantly greater than the design criteria, ranging from 17 to 20 ft (5.2 to 6.1 m) compared to the 12 to 14 ft (3.6 to 4.3 m) assumed in the design.
- Figure 1.10 presents a comparison of the wave conditions generated by Hurricane Katrina with the wave conditions used for the HPS design. With the exception of Plaquemines Parish, the wave heights generated by Hurricane Katrina were not much different from the design conditions. However, the wave periods are a different story. At the shores of Lake Pontchartrain, the wave periods generated were similar to the design assumptions. Along the St. Bernard and Plaquemines levees Hurricane Katrina generated wave periods in the range of 14 to 16 seconds, which were about three times the design wave periods. It is important to note that these longer period waves have much greater potential for run-up and overtopping of HPS structures.



Fig. 1.9: Comparison actual storm surge with design [29]



Fig. 1.10: Comparison actual wave conditions with design [29]

1.3.3 Direct causes of failure

A storm of Hurricane Katrina's strength and intensity is expected to cause major flooding and damage. However, a large portion of the destruction from Hurricane Katrina was caused not only by the storm, but also by the storm's exposure to engineering and policy failures. Levees and floodwalls breached because of a combination of unfortunate decisions made over many years, at almost all levels of responsibility. In general, the HPS was under-designed. A pattern of optimistic engineering assessment with regard to potential risks and potential modes of failure was the basis of a number of major system elements:

- The risks associated with under seepage flows were underestimated. This led to the use of sheet pile foundations that were extended to inadequate depths at several locations, resulting in a number of failures and breaches during Hurricane Katrina.
- Some overtopping of levees is to be expected in a major hurricane like Katrina. However, the levees were not armored against erosion but designed to perform at water elevations up to overtopping. This would become an engineering choice of catastrophic consequences. It allowed the levees, some constructed of highly erodible soil, to be scoured away. To gain protection from overtopping would have required such measures as armoring the back sides of levees or using the more expensive T-walls.
- Design procedures did not include consideration of the potential failure mode that involves formation of a water filled gap at the outboard side of the floodwalls. Formation of such gaps occurred at a number of locations as pressure increased on the outboard sides of the floodwalls, increasing the lateral push of the storm surge against the floodwall and thus resulting in failure. Appendix C.2 describes this failure mechanism in detail. In addition, the margin of safety used in the design process was too low, especially when considering that the hurricane protection system was a critical life-safety structure.
- The USACE defines the SPH as a hypothetical hurricane intended to represent the most severe combination of hurricane parameters that is reasonably characteristic of a specified region. The definition 'reasonably characteristic' implies that the SPH is not an extreme hurricane event. However, the USACE chose SPH meteorological parameters issued in 1959 as representative maximum wind speeds for a hurricane striking New Orleans and did not update them when revised numbers were issued in 1979. Using the SPH and associated meteorological conditions ultimately resulted in HPS being under-designed right from the start.

1.3.4 Contributing factors of failure

In addition to the direct causes of levee breaches, a number of other factors also contributed to the catastrophe:

- The risk to the people of New Orleans, thus probability of failure combined with consequences to human health and safety if that failure would occur, was much higher than people are generally willing to accept. The risks associated with the HPS of New Orleans had never been quantified prior to Hurricane Katrina. As a result, the residents of New Orleans could not have known the actual risks with which they were living. Risk quantification could have raised the awareness of policy-makers and make them understand that this system might have been massively under-designed relative to the standards for other critical life-safety infrastructure. As these risks were not well understood and/or communicated to the public, the importance of evacuating people and protecting property was underestimated.
- The HPS was funded and constructed as individual pieces, not as a system. Each of the hurricane protection projects was designed and constructed on a project-by-project basis over the course of many years as funding became available. At the time of Katrina, some segments of the levee system were not yet complete or the top elevations had not been raised to the authorized protective levels. As a result, the system had strong portions built adjacent to weak portions, pump stations that could not withstand the hurricane forces and many penetrations through the levees for roads and utilities. In addition, there were pressures for tradeoffs and low cost solutions that had inevitably compromised quality, safety and reliability.
- Levee builders used an incorrect datum to measure levee elevations, resulting in many levees not being built high enough. Some levees were built 1 to 2 feet (0.3 to 0.6 m) lower than the intended design elevation. Furthermore, despite the acknowledged fact that New Orleans is subsiding, no measures were taken into account in the design to compensate for the subsidence.
- The management of the HPS was chaotic and dysfunctional. No single agency was in charge of hurricane protection in New Orleans. Responsibility for the maintenance and operation of levees and pump stations was spread over many federal, state, parish and local agencies.

1.3.5 Consequences of failure

The consequences of the flooding of major portions of all four levee-protected areas of New Orleans were catastrophic. The extensive flooding and resultant prolonged loss of services caused what became more of a migration than an evacuation. The flooding caused a breakdown in the area's social and cultural structure, significantly complicating recovery and redevelopment.

Direct damages to residential and non-residential capital reached approximately \$21 billion. Losses to public structures and damages to infrastructure reached \$7 billion. Residential property losses were a staggering 78% of the total. Commercial property losses were 11% of the total, while industrial losses were under 2% [USACE–IPET]. The people of New Orleans suffered the most direct losses of the disaster, which present perhaps the greatest challenge to recovery. Thousands of homes were destroyed. Damages and loss of life were both directly tied to the depth of flooding, which in turn is inversely tied to the elevation of the location.

Two years after the disaster, nearly 1,200 people were confirmed dead in Louisiana as direct result of Hurricane Katrina. Over 100 people are still missing and presumed dead. Loss of life was highly correlated with evacuation. In fact, the flooding in general was disproportionately cruel to the poor, elderly and disabled, groups least likely to be able to care for themselves.

For a storm the size of Hurricane Katrina, loss of life and property is expected. A modeling conducted by the USACE compared expected deaths from the HPS failure with scenarios in which the system did not fail. Results indicate that had the levees and floodwalls not failed and had the pump stations operated properly, nearly 70 % of the deaths would not have occurred. Even without levee breaching, Hurricane Katrina's rainfall and levee overtopping would have caused the worst property loss ever experienced by New Orleans. However, less than half the actual property losses would have occurred. While the pumping assumption of this scenario is not realistic for the time of Katrina, it is a testimony to the value of having a resilient HPS.

1.4 Principal conclusions and thesis content

The catastrophic failure of the HPS of New Orleans represents one of the nation's worst disasters ever. As lives and public safety are to be protected, significant changes will be required in the way hurricane flood protection systems are funded, designed, managed and maintained.

1.4.1 Principal conclusions and recommendations

The principal conclusions and recommendations can best be outline following each reviewed aspect presented in the previous section in this chapter.

Hurricane Katrina

Hurricane Katrina generated a storm surge and wave environment unparalleled in the history of New Orleans, generating water levels that exceeded the design criteria at several locations. It leads to conclude that storm surge and waves are the hazard, not the storm. Meteorological designations such as the Saffir-Simpson Scale by themselves are not adequate to characterize the distributed surge and wave conditions that a HPS will face. These traditional methods of assessing the frequency of occurrence of hurricanes, which depend primarily on historical data, are too simplistic to capture important characteristics of the hurricane hazard such as time- and space-dependent storm intensity and track patterns. Wave and storm surge modeling provides insight into how water surrounding a complex physical system responds to an also complex hurricane wind system.

The Hurricane Protection System of New Orleans

The HPS did not perform as a system. Subsidence, changing population demographics and patterns of hurricane intensity and frequency are examples of time-dependent challenges hurricane protection systems face. All components that contribute to the performance of the overall system must be treated as an integral part of the system. Most important of all, the design methods need frequent review to determine whether they represent best practice and knowledge. An example of this lack of review is the use of the SPH, which has been the heart of most Corps of Engineers hurricane protection projects since the 1960s.

The following quotations indicate the interpretations that developed through the history of development of the protective system of New Orleans regarding what the system's SPH represented:

1. *"The Standard Protection Hurricane wind field and parameters represent a 'standard' against which the degree of protection finally selected for a hurricane protection project may be judged and compared with protection provided at projects in other localities."* [Graham and Nunn, 1959].
2. *"The project is designed to protect against the Standard Project Hurricane moving on the most critical track. Only a combination of hydrologic and meteorological circumstances anomalous to the region could produce higher stages. The probability of such a combination of occurring is, for all practical purposes, nil."* [U.S. Army Corps of Engineers, 1974].
3. *"The Standard Protection Hurricane is a steady state hurricane having a severe combination of values of meteorological parameters that will give high sustained wind speeds reasonably characteristic of a specified coastal location. By reasonably characteristic is meant that only few hurricanes of record over a large region have had more extreme values of the meteorological parameters."* [National Weather Service, 1979].
4. *"The Standard Protection Hurricane was expected to have a frequency of occurrence of once in about 200 years, and represented the most severe combination of meteorological conditions considered reasonably characteristic for the region."* [Government Accountability Office, 2005].

As can be seen, over time the SPH went from being a general indicator of threat levels to a guarantee of safety. The methods used to define the SPH were forgotten, along with their potential flaws and questionable assumptions. For a variety of reasons, the concept of storms much more intense than the SPH was not allowed to explicitly enter the engineering process, even though the development of the SPH also involved a Probable Maximum Hurricane (PMH) [National Weather Service, 1979]:

"The PMH is a hypothetical steady state hurricane having a combination of values of meteorological parameters that will give the highest sustained wind speed that can probably occur at a specified coastal location. One of several possible uses of the values of meteorological parameters is to compute maximum storm surge at coastal points when the hurricane approaches along the most critical track."

It can be concluded that it was clearly recognized that the SPH did not represent a maximum set of conditions for design against hurricane conditions. It is also clear that the general public was not informed about the flooding risks that the selection of the SPH as a basis for design implied.

The important element of the SPH was that it was not revised as knowledge improved after the 1960s. Tremendous strides in the meteorology and oceanography of hurricanes were made during the 1970's and these improvements in technology continue to evolve to the present time. However, the SPH remains essentially the same as it was when it was initially defined in the 1950s.

The performance of the Hurricane Protection System of New Orleans

The design approaches taken were not conservative enough to deal with the unknowns and need to consider a broader spectrum of possible behaviors. These behaviors can be outlined in two terms:

- **Resilience** to catastrophic breaching can provide huge benefits in reduced loss of life and property. It should be considered as a fundamental performance characteristic. A resilient HPS can provide advantages since it has an ability to withstand forces and conditions beyond those intended or assumed in the design without catastrophic failure. The need for it can be outlined by the fact that approximately 70 % of the flooding and half of the losses were the result of breaching. While overtopping alone from Katrina would have created dramatic flooding and losses, the difference would have been staggering in many regards. Reductions in losses of life, property and infrastructure would have a dramatic impact on the ability of a community and region to recover. Added to this can be the savings of the time and funding needed to rebuild the damaged protection system itself, which would accelerate the pace of recovery.

- The HPS lacked redundancy, which is defined as components of the system backing each other up so that failure of one component does not cause the whole system to fail. Essentially, the HPS had only a single line of defence. Failure of a particular structure or levee section directly resulted into massive flooding. Given the extensive flooding of New Orleans, revision of its HPS calls for a strategy of multiple lines of defence. This thesis will introduce and follow this strategy in application of its stated concepts.

The *pumping stations* throughout the New Orleans area should have been an integral part of the overall HPS. Most hurricanes bring heavy rainfall, but the pump stations were designed only to remove storm water runoff and routine seepage water from the interior drainage system in order to pump it into Lake Pontchartrain or other nearby bodies of water. During Hurricane Katrina, pump stations played no significant role in the reduction of flooding because of their inoperability due to a number of reasons, including the necessary evacuation of pump station operators, loss of power and flooding of the pump stations themselves. In addition, most pump stations were not located in the areas of worst flooding and the location of the pump stations at the end of the outfall canals made them vulnerable to reverse flow. Situated behind the canal breaches, the pumps drained water from the city area back in the breached canal, starting a never-ending process of water displacement. Methods were available to prevent reverse flow, but depended on human operators and electrical power neither of which was present at the time. Adding a structure at the mouth of each canal is the key to a better protection. These structures will keep storm surge out, shorten the primary floodwall length and permit existing pump stations to continue operation.

Even if the pumping system had survived the hurricane, it simply would not have been able to pump the huge amount of water that flooded into New Orleans because of overtopping and breaches. In general, hurricane protection systems should be designed and built as integrated systems to enhance reliability and provide consistency in levels of protection. Interior drainage needs to be an integral part of the system because of the important role they can play in limiting the amount and duration of flooding.

1.4.2 Thesis content

Problem description

Hurricane Katrina made landfall in southern Louisiana as a Category 4 storm but at the time it passed New Orleans it already decreased to Category 3. At this moment, it is highly unlikely that New Orleans will be hit by a full Category 5 storm as the city is still surrounded by large quantities of wetland which the storm has to cross before it can hit the populated areas. However, these wetlands are disappearing at an enormous rate, loosing their protective capability. This leads to conclude that the strength of Hurricane Katrina is could have been even higher, a scenario waiting to happen in the future if no major improvements are made soon.

More specifically, southern Louisiana's ongoing peril is the continued overlap of weakened protection with more frequent and intense hurricanes. During these hurricanes, surge waters can enter the IHNC from Lake Borgne to the east and from Lake Pontchartrain to the north. Preventing storm surges from entering the IHNC would protect the vital residential and commercial areas of New Orleans.

The problem description will be specified for one distinctive part of the HPS. In order to make this distinction, the flooding of New Orleans is divided in flooding induced by Lake Borgne (GIWW/MRGO), flooding induced by Lake Pontchartrain (outlet canals and IHNC) and flooding of Plaquemines Parish. This thesis focuses on Lake Borgne induced flooding, especially on the matter whether the implantation of navigable floodgates is the optimal solution for the revision of this part of the HPS of New Orleans. If so, what is the optimal combination of type and location for a floodgate in this part of the HPS?

Objectives and research approach

This thesis will have its focus on the flooding induced by Lake Borgne. The main objectives of this thesis can be outlined on three scales:

- Macro Scale – Introduction on performance of the Hurricane Protection System of New Orleans
What happened during Hurricane Katrina and why? What were the causes and consequences of this natural event? What are the lessons that can be learned and what is needed for the future?
- Meso Scale – Master plan of the New Orleans region
Determine the current situation and what is needed for the future. Determine the best solution to improve this part of the HPS by developing and evaluating several master plans for the area.
- Micro Scale – Preliminary design of a flood protection structure
Further investigate a master plan concept with one or more floodgates by providing a preliminary design of a flood protection structure in either the Gulf Intracoastal Waterway or Mississippi River Gulf Outlet. Analyze the hydraulic boundary conditions by a critical evaluation of the model results on wave characteristics and water level provided by local investigation teams. Objective is to provide a preliminary design of the main structural parts of the barrier.

2. The Hurricane Protection System Of New Orleans Compared To The Development Of Flood Protection In The Netherlands

From almost the first day of the tragedy of Hurricane Katrina, the U.S. hurricane risk reduction system has been compared with the storm and flood risk reduction efforts of the Netherlands. To many, the so-called 'Dutch Approach' has been held as the gold standard for storm risk reduction. The history of the Netherlands is based on a society learning to live in a flood prone area.

The history of flood protection in the Netherlands is outlined section 2.1. A comparison of the Hurricane Protection System (HPS) of New Orleans to the main flood protection strategies of the Netherlands is presented in section 2.2. The historical and flood protection characteristics of the city of Amsterdam are briefly outlined, which have some remarkable resemblances to New Orleans. Finally, section 2.3 provides the new strategy in flood protection of coastal areas currently considered in Europe.

2.1 The Dutch flood protection in a historical perspective

The coastline of the Netherlands is approximately 350 kilometers long. The country is densely populated with more than 15 million people and an average population density of more than 400 people per km². About a quarter of the Netherlands is currently below mean sea level. Protection against flooding is thus an important task and is provided by an extensive, linked system of flood protection structures.

Areas protected by a linked system of flood protection structures are called dike ring areas. The flood protection structures around a dike ring area can be divided into sections, in which load and strength characteristics are generally comparable. Together these sections ensure the safety of the area, both at coastal and inland regions. This complex system is necessary in the Netherlands for multiple reasons:

- Almost 60% of the country is threatened by water due to storm surges at the North Sea and/or high discharges in the main rivers. Figure 2.1 presents the floodable land if there would be no defences.
- In these prone areas, over 70% of the nations gross national product is earned;
- Large cities like Amsterdam and the industrial city of Rotterdam with its important harbor are located below mean sea level.



Fig. 2.1: The Netherlands without flood protection [12]

Flood protection has always received much attention in the Netherlands, but the protective strategy has changed significantly over time. The country and its population have developed to its present state through the reclamation of marsh lands, improved water management technologies and their innovative response programs to flooding disasters. Each of these main characteristics is discussed in the subsequent sections, thereby forming a historical timeline of the flood protection development in the Netherlands.

2.1.1 Land reclamation

In the period 1000 to 1600 AD, the coastal areas of the Netherlands were under significant influence of the sea. The primitive dikes provided poor protection against the sea. Each century had its floods which claimed many lives and large areas of land. These processes essentially shaped the contours of the country. In the south-western part of the country, large inlets made it possible for the sea to enter and damage coastal lands. In the northwestern part, a single large and shallow inlet of the North Sea existed which is known as the Zuiderzee. ('Southern Sea'). Even without inflow from the North Sea, local wind setup on the relatively large Zuideree resulted in high water levels. In reducing the treat to the populated areas around the city of Amsterdam, extensive hydrological measures were needed. Of significant importance was the intermission of the direct connections between the inland lakes around Amsterdam and the Zuiderzee by the construction of dams. This paved the way for a general reshaping of the area during the next centuries.

The 17th and 18th century was characterized by a more dynamic and offensive approach in the battle against the sea. Near the end of this period, large areas of water were converted into productive agricultural areas. This change in approach can best be expressed by the reclamation of the Haarlemmermeer. Interesting in this case is the reasoning behind the reclamation of it. Up until the first quarter of the 19th century, the cities of Haarlem, Leiden and Amsterdam were against the plans for reclamation of the lake. The cities feared their inner canals could not be flushed out sufficiently, directly influencing their supply of drinking water. In addition, Amsterdam feared silting up of the IJ bay and the three cities were eager to preserve their connection for mutual navigation.

At the time, the IJ bay was a long and narrow brackish bay that connected to the Zuiderzee and stretched from Amsterdam inland towards the west. At its west end, only the natural dune ridge across the North Sea coast prevented the IJ bay from directly connecting to it, turning the northern part of the country into an island. The IJ bay provided Amsterdam with access to the sea through the Zuiderzee.

By the 17th century, access to the IJ bay became troublesome due to sand bars across its mouth and increasing ships sizes. It became nearly impossible for seagoing vessels to reach the city. At the same time, the IJ bay gnawed away at the surrounding farmlands, almost connecting with the Haarlemmermeer and seriously threatening the cities of Haarlem and Amsterdam. Figure 2.2 presents an overview of the situation.



Fig. 2.2: Overview of both the Haarlemmermeer and the IJ bay [22]

The opposition would change instantly as the heavy storms of 1836 made the Haarlemmermeer overflow its banks, resulting in extensive flooding of the cities of Amsterdam and Leiden. The main reason for this sudden change in position was the destruction of connecting roads and the belief that in a modern civilianization such situations should not be allowed. Plans were put forth to reclaim both the Haarlemmermeer and the IJ bay and turn them into polders. The Haarlemmermeer was first, falling dry in 1852. The largest part of the IJ bay followed suit in 1876, with only a small lake remaining at Amsterdam that was closed off from the Zuiderzee by locks. At the same time, the North Sea Canal was constructed in the former IJ bay to provide Amsterdam with access to the sea again and revive its ailing port. It cut through the land to connect to the North Sea.

2.1.2 Improved water management technologies: the Zuiderzee Works

A significant step forward in flood protection for the northern part of the Netherlands, including the increasingly populated city of Amsterdam, was the implementation of the Zuiderzee Works. The Zuiderzee Works are a human-made system of dams, land reclamation and water drainage works. The project involved damming off of the Zuiderzee and large scale reclamation of land in the newly enclosed water body by means of polders. Triggered by a major flood in 1916, the closure of the Zuiderzee protects the central part of the Netherlands against flooding. It enabled the reclamation of large formerly tidal areas for agriculture and the construction of a large freshwater basin for both drinking water supply and to flush out salt water in the bordering provinces.

The single biggest structure in the project was a long dam (the Afsluitdijk) protecting the Dutch from the North Sea by taming the Zuiderzee. The dam runs over a length of 20 miles (32 km) and it has a width of about 300 ft (90 m), an initial height of 24 ft (7.3 m) above mean sea level at an incline of 1:4. Previous experiences had demonstrated that till, a term for coarsely graded, heterogeneous sediments of glacial origin, should be primary material for the structure rather than just sand or clay. It had the added benefit that it was easily available as it could be retrieved in large quantities by simply dredging it from the bottom of the Zuiderzee. In 1932, two years earlier than initially forecast, the Zuiderzee ceased to be as the last tidal trench was closed. The IJsselmeer was born, even though it was still salty at the time. Periodically discharging is necessary since it is continually fed by rivers, stream and polders.

Figure 2.3 presents an overview of the Zuiderzee Works. Interesting to note is the originally planned fifth polder, which does not yet exist and may never be completed. It had been the intention to start building a southwestern polder at several points during the project but other polders took precedence. A minor flood near Amsterdam in 1960 had demonstrated the danger a large IJsselmeer still presented. One planned element of the new polder was subsequently executed: a 28 km dike between Lelystad and Enkhuizen, including two complexes of locks and discharge sluices at either end, was to split the IJsselmeer in two. The largest portion (1250 km²) would continue as the IJsselmeer and the smaller lake (700 km²) as the Markermeer. Construction of this dike, known later as the Houtribdijk, lasted from 1963 to 1975, after which it also served as an important road connection. However, it did not result in the construction of the rest of the polder.

The debate on whether to build the fifth polder continued for many years. The need for new agricultural land had mostly disappeared by that time and extra space for housing was not necessary in this region. Existing ecological and recreational values of the Markermeer were considered by many to be equal or superior to any potential such value the new polder would offer. Doubts began to surface about the effectiveness of the polder. In 1986 it was decided to indefinitely postpone the project.

In conclusion, the Zuiderzee Works successfully transformed the heart of the Netherlands into fertile agricultural land with many new communities combined with an extensive fresh water supply and, although not originally envisioned, a collection of valuable ecological and recreational areas. The main characteristics of the Zuiderzee Works are summarized in table 2.1. The shift in design goals is visible in the changes of land usage over time. The need for agricultural land decreased significantly, whereas housing and nature increased. The land used for infrastructure maintained at a constant percentage. It is interesting to note again that many considered ecological and recreational values to be equal or superior to any potential other use.



Fig. 2.3: The Zuiderzee Works [22]

Project	Length /Size	Start	Closure	Drained	Agriculture	Housing	Nature	Infrastructure
Afsluitdijk	32 km	1927	1932	—	—	—	—	—
Wieringermeer	200 km ²	1927	1929	1930	87 %	1 %	3 %	9 %
Noordoostpolder	480 km ²	1936	1940	1942	87 %	1 %	5 %	7 %
East Flevoland	540 km ²	1950	1956	1957	75 %	8 %	11 %	6 %
South Flevoland	430 km ²	1959	1967	1968	50 %	18 %	25 %	7 %
Houtribdijk	28 km	1963	1975	—	—	—	—	—

Table 2.1: Characteristics of the Zuiderzee Works

2.1.3 Response programs to flooding disasters: legislation and frequent safety assessment

Delta Act

In the night of 31 January to 1 February 1953, massive failure of the existing dike system occurred with devastating consequences. An extreme storm hit the North Sea causing the highest water levels observed to date. Especially in the southeastern part of the North Sea large flooding took place. In Britain and Belgium, several hundred people lost their lives. In the Netherlands over 1800 people perished. The large scale of the disaster triggered a large scale reaction. This time the land claimed by the sea was not abandoned. Reconstruction works began immediately as dikes were sealed and polders drained.

Following the disaster, the Delta Committee was installed to advise the government on protection against flooding and to investigate the possibilities for a new safety approach. The most recognizable result of the Committee's work is the implementation of the Delta Project which is presented in figure 2.4. This massive project led to significant strengthening of existing flood defences and to the construction of dams to close off several estuaries from the North Sea, cutting the coastline by about 450 miles (720 km). The basis of this action was the fact that the shorter the coastline, the easier it would be to protect. This idea was not new. In 1932, the earlier mentioned Afsluitdijk was constructed to cut the Zuiderzee off from the North Sea. In the Delta Project, the New Waterway and Western Scheldt would remain open to shipping, given the economic interests of the ports of Rotterdam and Antwerp. The dikes along these waterways would be raised to provide the needed level of protection.

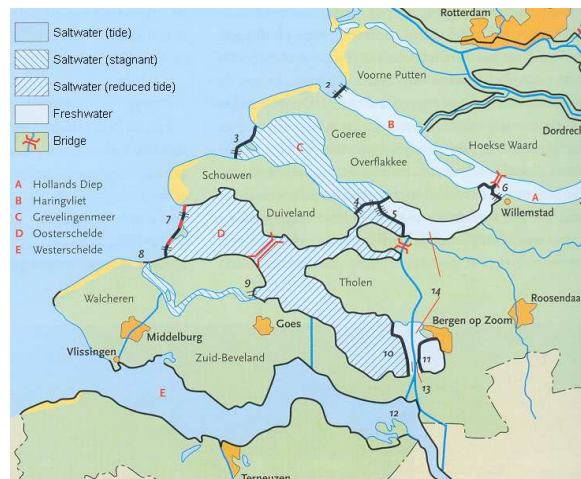


Fig. 2.4: The Delta Project [22]

In conclusion, besides providing protection against the sea, the Delta Project improves water management in many parts of the country, reduces salination, produces freshwater reservoirs and creates recreational areas. In addition, the new dams also greatly improved access to the southwestern part of the Netherlands. This system developed in response to the catastrophic flooding of 1953 is still a model of advanced engineering and water resource management. The organization is a centralized Rijkswaterstaat, which is the national public works department in charge of all flood defense works. This department has direct ties with local agencies responsible for continued development, maintenance and improvement of flood defense works. The *Delta Act*, based on the plans put forward by the Committee, was finally approved by Parliament in 1957.

The scale of the Delta Project enforced the development of new design methods. Therefore, the Delta Committee advised to implement a new system of protection that was based on probabilities, thereby initiating the use of risk assessment methods in civil engineering. The starting point was to establish a desired safety level for each dike ring area or polder. This safety level would be based on the costs of dike construction and on possible damage which could be caused by flooding. This economic analysis led to an optimum safety level expressed as the probability of failure for dikes. In practice the safety level was expressed as the return period of the water level as this was the most dominant hydraulic load.

The safety levels for the various dike ring areas in the Netherlands are shown in figure 2.5. This standard is expressed as the mean annual probability that the prescribed flood level will be exceeded. At present the safety standards depend on the area's economic activities, population size and the nature of the direct threat:

- In the central coastal areas a safety level of 1/10,000 [1/year] is used. This area is the most densely populated area of the Dutch delta and accommodates the largest economic activities;
- Other coastal areas accommodate less economic activities which led to a safety level of 1/4,000 [1/year];
- In the Dutch river areas a safety level of 1/1,250 [1/year] is used. This lower safety level in the river areas gives sufficient protection because extreme river discharges have a relatively large warning time, less economic activities are taking place than in the central part of the Netherlands and the fresh river water leads to a smaller impact of a dike breach.

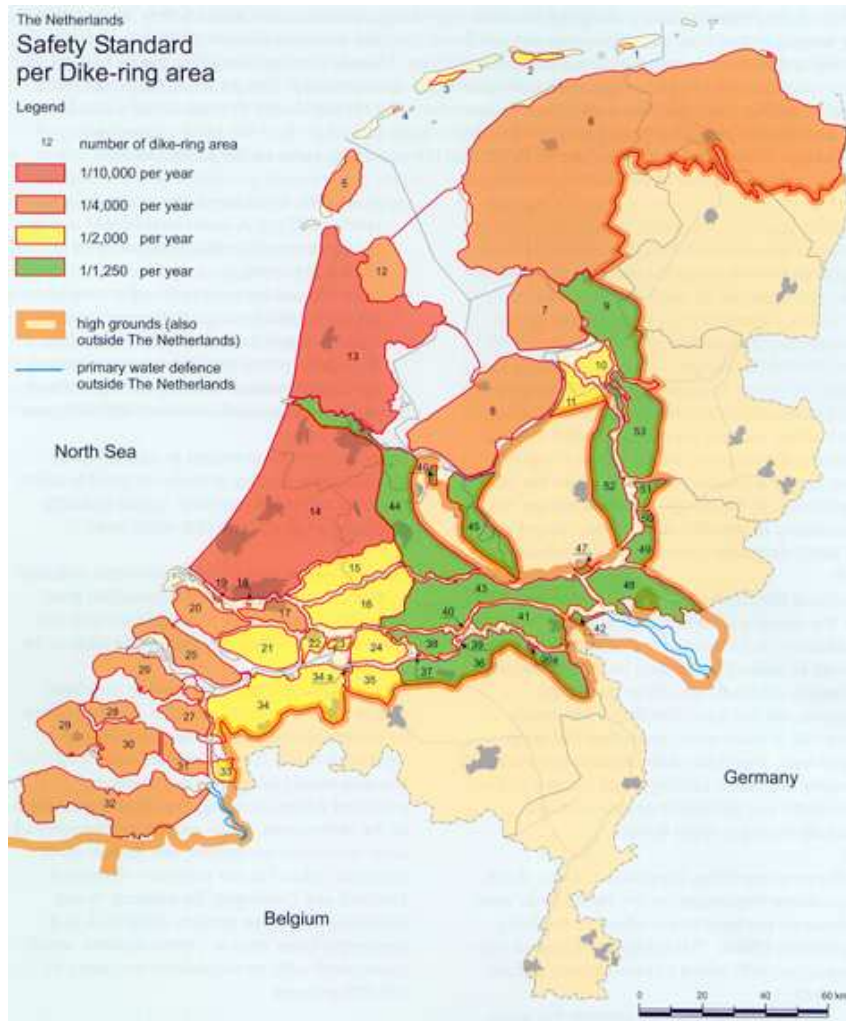


Fig. 2.5: Dike ring areas in the Netherlands – safety standard per dike ring area [12]

The Flood Defence Act

Life in the delta of the Rhine River and Meuse River involves risks, but has also enabled the Netherlands to develop into one of the main gates of Europe. As welfare increased and population density grew, more and better protection systems were built to prevent flooding. Since the danger of flooding is difficult to determine in advance, politics and society usually adopted a reactive position until recently. Until far in the 20th century, dikes were constructed to withhold the highest known water level. Design crest levels of the flood defences were established by requiring an extra height above this observed maximum water level, generally based on experience. The necessity of dike reinforcement usually was only recognized if the water level exceeded the known maximum or failure of the dike system occurred. In order to prevent flooding, weakened points in the dike systems needed to be recognized in time. The process of maintaining the water defences applied in the Netherlands is presented in the figure 2.6.

In the Netherlands safety standards per dike ring area are laid down in the Flood Defence Act, issued in 1996. With this legislation it became compulsory to test the flood defences every five years for going hydraulic conditions. According to this *Flood Defence Act*, local water boards have to carry out a full safety assessment of their defences every 5 years, presented in the lower circle of figure 2.6.

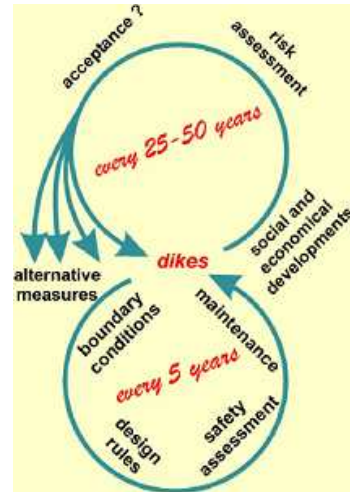


Fig. 2.6: Dutch Flood Defence Act [12]

Responsibility for flood defence and coastal protection is divided among three forms of government: the Ministry of Transport, Public Works and Water Management, provinces and water boards. A water board is a functional form of government, oriented to water management and flood protection structures. The Ministry plays a central role in setting coastal protection policy. Implementation is carried out by water boards. The provinces supervise the water boards and play a key role in the interaction between water management and spatial planning.

The assessments are carried out with hydraulic boundary conditions and technical design rules, which are set and provided by the central government. If the safety standards according to the Flood Defence Act are not met, immediate reinforcement or maintenance of the water defences has to be carried out. The upper circle of figure 2.6 presents the evaluation of the safety standards as such. Until 2001 the main safety policy was based on the probability of exceeding of the normative conditions and was only focusing on physical circumstances. This approach was seen as insufficient because it did not take the economic and population growth into account. This resulted in an updated version of the Flood Protection Act which is now operational. It states that the efficiency and effects of the imposed safety levels have to be reported every ten years. With these periodical checks every five and ten years, both physical and economical changes are incorporated in the Dutch safety policy.

While damage protection in the Netherlands traditionally aimed at reduction through improved dike construction, nowadays new political movement can be seen that searches for measures to prevent flooding without raising the dikes along the rivers. More attention can be found for evacuation planning, early warning systems, insurance of flood damage and for the link with spatial planning. The expected developments of the rise of the sea level, higher river discharges and soil subsidence require a pro-active policy, in which the increase of the interests and investments to be protected will have to be taken into consideration. The new approach to flood protection in the coastal areas can best be outlined by the ComCoast strategy, which is presented in section 2.3.

2.2 Comparison of New Orleans and the Netherlands (Amsterdam)

2.2.1 New Orleans compared to the Netherlands – historical development and hydraulic boundaries

Looking back in history, it can be concluded that the present state of both the Mississippi Delta and Dutch Delta have been shaped by human intervention. Figure 2.7 presents both deltas on similar scale. There are significant differences as to geology, scale and type of interventions and land use, but it is obvious that both deltas are beyond a free natural state. Both deltas have adapted and are still adapting to man-made conditions. In the Netherlands, these interventions span ages dating back to roughly the 10th century. Significant interventions in the Mississippi Delta date back some two centuries.

The search for solutions for flooding at a certain point of time is dominated by the opinions and interests of landowners, business leaders and public leadership. History shows that besides providing flood protection, the development of the Dutch Delta has been dominated by agriculture, in the form of marshland cultivation and fresh water economy, as the most important economic factor besides trade. Keeping out salt water was and continues to be the mainstream thinking in the low lying western part of the Netherlands. This eventually led to the cultivation of nearly all marshlands and closure of many estuaries, the latter mainly triggered by flooding disasters. It was also a guiding principle in finding the response to the flood disaster of 1953. The response to this disaster was based on centuries of thinking and cultivation of the delta, to store fresh water and to keep salt water out. The Dutch find themselves in a safe and green, yet completely man-made and managed environment.



Fig. 2.7: Mississippi River Delta and Dutch Delta at a similar scale (image of the Netherlands is orientated upside down)

As stated before, in the Netherlands flood protection is an important task and provided by an extensive system of primary flood protection structures. The linked systems of primary flood protection structures form dike ring areas. An instructive first step in this comparison is to draw up the existing system of levees surrounding the city of New Orleans. Immediately it becomes clear that in the New Orleans metropolitan area several dike ring areas have been created over time. This leads to conclude that the dike ring area principle appears to originate naturally, independent of hydraulic and social conditions. Confronted with repeated flooding of land, people tend to construct their housing on higher ground and areas protected by simple dikes. Although building efforts begin local, it becomes clear that local protection is not useful if water could still enter the area from other sides. Gradually, locally constructed flood defences are extended until closed dike rings come into being. Figure 2.8 presents the dike ring areas of New Orleans.



Fig. 2.8: The dike ring areas of New Orleans, in combination with their direct water threat

As can be seen in figure 2.8, in the metropolitan area of New Orleans four dike ring areas can be distinguished:

- The green dike ring area presents the western part of Orleans Parish and the northern part of Jefferson Parish. This protected area contains the downtown district. The northern edge of this area is fronted by Lake Pontchartrain and the Mississippi River passes along its southern edge. The Inner Harbor Navigation Canal (IHNC) passes along the east flank. Three drainage canals extend into the area from the north in order to drain the New Orleans of excess rainfall water.

- The yellow dike ring area protects the eastern part of Orleans Parish, commonly referred to as the New Orleans East protected area. This area fronts Lake Pontchartrain along its northern edge and the IHNC along its west flank. The east flank of this polder is fronted by additional wetland. The southern edge is fronted by Lake Borgne and the Gulf Intracoastal Waterway (GIWW).
- The blue dike ring area contains St. Bernard Parish. This area is fronted by the IHNC and has the GIWW channel along its northern edge. At the northeastern corner, the Mississippi River Gulf Outlet (MRGO) bends to the south and forms the boundary on the northeastern edge. Lake Borgne fronts it to the east. The main urban areas occur within the southern and western portions of this area. The densely populated Lower Ninth Ward is located at the west end. A secondary levee separates the undeveloped wetlands of the northeastern portion from the main urban areas.
- The orange dike ring area contains the southern part of Jefferson Parish. It also contains the northern part of the Plaquemines Parish, a narrow protected strip along the Mississippi River heading south from St. Bernard Parish to the mouth of the river at the Gulf of Mexico. This protected strip, with levees fronting the river and a second side of levees facing away from the river forming a protected strip less than a mile wide, serves to protect a number of small communities as well as utilities and pipelines.

The dike ring area principle, in combination with different levels of protection, is still the basis of the Dutch flood protection policy existing today. Although this policy is not present in New Orleans yet, the presence of dike ring areas in this region is remarkable and emphasizes the fact that the dike ring area principle do originate naturally over time. At first glance, the dike ring areas have a distinction in direct loading, which can be summarized as:

Color	Parish	Direct Threat
Green	Jefferson, Orleans	Lake Pontchartrain
Yellow	Orleans (East)	Lake Borgne, Lake Pontchartrain
Blue	St. Bernard	Lake Borgne, Mississippi River
Orange	Jefferson, Orleans, Plaquemines	Mississippi River

Table 2.1: General distinction in direct loading of the dike rings areas of New Orleans

This distinction in load would make the dike ring areas of New Orleans suitable for the Dutch approach of division in compartments with different levels of protection. On the other hand, since the dike ring areas are all relatively small scale and highly populated, the distinction in level of protection of the areas should be small. Further investigation on this matter is recommended.

From this distinction in loading, it can be concluded that water threatens New Orleans in a similar way as it did the Netherlands. Note the word 'did' in this sentence, because the Netherlands have changed. However, before the Afsluitdijk was constructed, the shallow Zuiderzee had an open connection to the North Sea and was a major threat for inland communities. At the time, the Netherlands were closed in by the North Sea from the east and the Zuiderzee from the north. The Zuiderzee is comparable to shallow Lake Borgne and shallow Lake Pontchartrain which close in the city of New Orleans from the north and east respectively. The Netherlands reduced the threat of flooding induced by the Zuiderzee by closing off its direct connection to the North Sea.

In general, the threat of water is still comparable for both areas. Both river and sea, although indirectly for New Orleans, can be responsible for massive flooding. The Netherlands is still under constant threat from both the Meuse River and Rhine River, two major European rivers. Figure 2.9 presents an overview of the direct water threat in the Netherlands. For New Orleans, the southern part of the city is intersected by the final stage of the Mississippi River, as can be seen in figure 2.8.



Fig. 2.9: Direct water threats regarding the Netherlands

One important point of difference should be made, as the hydrological boundary conditions for both locations are not similar. The record surge that prompted the Netherlands to erect barriers was 15 ft (4.6 m), whereas Katrina peaked at 28 ft (8.5 m). This difference has consequences for the design of a protection system. In the Netherlands, different safety levels are used per dike ring area depending on population density and economic value. In the central coastal area a safety level of 1/10,000 [1/year] is used. Although not further investigated, applying this level of safety within the protection system of New Orleans is not expected to be economical.

For a more detailed comparison of New Orleans with the situation in the Netherlands it is particularly interesting to look at the historical development of the city of Amsterdam.

2.2.2 New Orleans compared to Amsterdam – location: important junction for navigation

In reducing the water treat for the city of Amsterdam, plans were put forth in the 19th century to reclaim both the Haarlemmermeer and the IJ bay, turning them into polders. The largest part of the IJ bay was reclaimed leaving only a small lake open around Amsterdam. It was closed off from the Zuiderzee by locks. The Zuiderzee itself, losing its direct connection to the North Sea due to the construction of the Afsluitdijk [1932], was hardly any threat for Amsterdam anymore. Only local winds could raise water levels near the city. However, the Zuiderzee Works [Houtribdijk, 1975] separated Lake IJssel (IJsselmeer) and Lake Marken (Markermeer) which significantly reduces the available wind fetch. A decreasing wind fetch decreases the wind induced setup of the water level. The reclamation of land further reduces the risk of high water levels by limiting fetch directions.

With respect to New Orleans, the situation is quite different. No closure has been made yet. The rising water of the Gulf of Mexico could easily penetrate into Lake Borgne via its open connection. Water levels in Lake Pontchartrain also raise as a result it. Local winds could provide wind setup at Lake Pontchartrain, causing high water levels at its shorelines.

Figure 2.10 presents the location of both Amsterdam and New Orleans in combination with their main waterways. Yellow lines present the navigable waterways for shallow draft vessel (draft ≤ 14 ft = 4.2 m) and the blue lines present the navigable waterways for deep draft (draft > 14 ft). The figure outlines the need for the North Sea Canal connecting Amsterdam to the North Sea as this is the only way deep draft vessel could reach the city. At the end of the 19th century, the North Sea Canal was constructed in a former part of the IJ bay to provide Amsterdam with access to the sea again, allowing seagoing vessels to reach the city to revive its ailing port. It cut through the land to connect to the North Sea. With respect to New Orleans, deep draft vessels could use either the Mississippi River or the MRGO. The MRGO is a man-made navigational channel connecting the Gulf of Mexico to the city of New Orleans. It is also cut through land to allow seagoing vessel to reach the city and its port. Rationale for construction of the MRGO was also primarily economic, because the 40 miles (64 km) shorter route through St. Bernard promised a safer and more efficient passage than the Mississippi River.

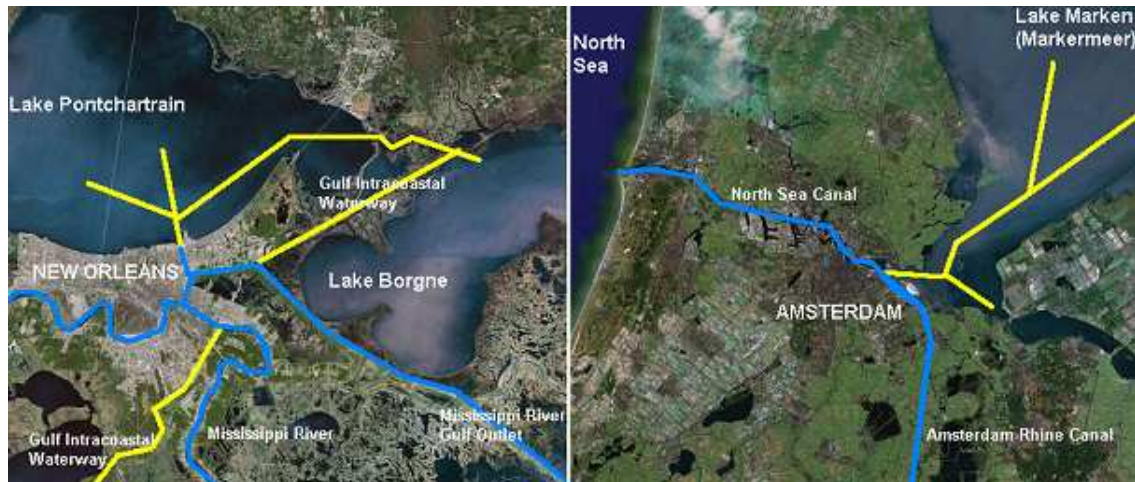


Fig. 2.10: Location of the cities of New Orleans (left) and Amsterdam (right), presented with their main waterways

2.2.3 New Orleans compared to Amsterdam – surface level: major cities below mean sea level

Large portions of the New Orleans metropolitan area are currently below mean sea level. This is consistent with most parts of the Netherlands, including the greater Amsterdam area. The former marshlands in both locations are subjected to a high rate of subsidence, which occurs both naturally and due to man's activities. Over time, levees were constructed to protect the low lying lands and cities against flooding. Drainage systems were constructed in both cities to gain land with low elevation, making it possible to expand human and economical activities to the lower parts. Gradually, this created a landscape in New Orleans that is consistent with that of Amsterdam. Figure 2.11 present a cross section of the central part of both cities in the present situation. It shows that by increasing human and economical assets in the low lands protected by levees, the consequences of flooding increase to higher level. When flooded, water levels in both cities can reach up to 20 ft (6.1 m).

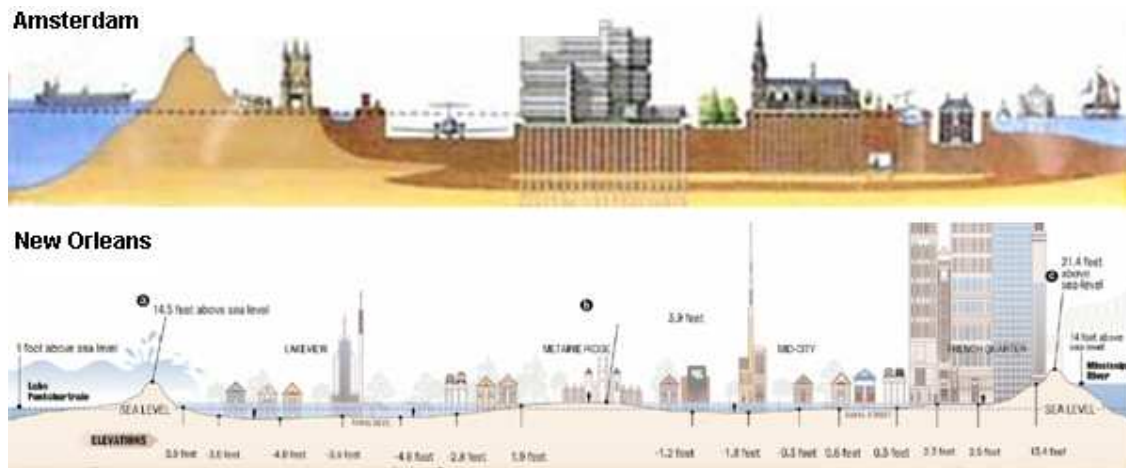


Fig. 2.11: Cross section of the central part of Amsterdam (upper) and New Orleans (lower)

2.2.4 Principal conclusions

Critical areas of the Netherlands are provided with extremely high levels of risk reduction and protected by a cohesive coastal management and flood risk reduction policy based on rational standards and an unwavering financial, engineering and social commitment. There is nothing technologically unique or exceptional about the barrier systems protecting the Netherlands. What makes the 'Dutch Approach' successful is the absolute national support of the flood risk reduction program. The very survival of their nation has moved the Dutch to implement a multi-decade, multi-billion dollar solution with support of their government backed in laws and budgets. The Dutch began with an unambiguous commitment to solving their flooding problem, made bold decisions and then properly funded these solutions. With a similar commitment, boldness and funding the U.S. should try to implement a similar level of hurricane risk reduction for coastal Louisiana.

As described earlier, the standards used in the Netherlands are accepted risks related to the design criteria of the dikes. These standards were developed after the Netherlands suffered catastrophic flooding in the disaster of 1953. This flooding is comparable to the flooding of the greater New Orleans area in the wake of hurricane Katrina in the fact that it was preceded by a history that included poor organization, bad maintenance, warnings not heeded, poor communications, lack of preparedness and an overall underestimation of danger. Sadly, it points out that the city of New Orleans has an even deeper rooted resemblance to the Netherlands in the fact that it adopted a reactive position until disaster struck. New Orleans needed its own massive flooding and the question is whether this will drive the policy to change to a pro-active basis. As stated before, the expected developments of the rise of the sea level, higher river discharges and soil subsidence require this pro-active policy to protect New Orleans in the near future.

At a cost of about \$18 billion and over some 40 years, the Dutch completed the first rounds of the Delta Project and haven't flooded since. At the same time, the Dutch moved aggressively to fill lands behind their coastal barriers, created literally from the sea. Then another bill came in. Over half the estuaries disappeared and those remaining were in trouble. Perhaps the most important lesson that can be learned from this experience is how it has evolved. As a matter of engineering strategy, the Netherlands have now rejected large scale levee and drainage solutions as unworkable and have instead come to rely on the *multiple lines of defence strategy*. This strategy is redundant in the safety it provides and none of the defensive lines need to be designed to provide full protection on their own. Most significantly, the Netherlands have changed their philosophy from 'flood control' to 'water management' and are heading towards the next step: people management. This introduces a *question of commitment*. The Netherlands is a small country and it has dedicated itself to fighting the sea. It can not afford not to as almost 60% of its land is below mean sea level. The State of Louisiana, as valuable as it is to the nation and to those of who live there, is only one small piece of the U.S. The attention span for the regional problems throughout the nation is limited, so will be federal funding. Unless Louisiana goes in a direction that is more self-sustaining over the long term, it could end up short.

It is interesting to note that the overall principle of the both the Zuiderzee Works and the Delta Project is to shorten the first line of defence. Also the reclamation of land played a role in both projects, predominantly in the Zuiderzee Works. It is interesting to determine whether this is a suitable basis for the protection of New Orleans by preventing Lake Borgne induced flooding during hurricanes. Section 3.5 analyses this subject in detail.

2.3 New way of thinking: 'ComCoast'

Another way to implement the pro-active policy needed to protect New Orleans with respect to future natural developments has its roots in a new way of thinking: ComCoast. This section introduces this strategy and determines its application.

2.3.1 ComCoast – functions, components and general solutions

ComCoast is the abbreviation of 'COMbined functions in COASTal defence zones' and is a European project, which develops alternative solutions for flood protection in coastal areas by trying to address new functions to those areas. Rijkswaterstaat, a part of the Dutch Ministry of Public Works and Water Management, is the leading partner. Other participating countries besides are Belgium, Denmark, Germany and Great Britain.

In the coming years climate change will increase the physical loads on coastal defences all over the world. Although dikes have been the traditional weapon against floods for centuries, they might not always offer a long-term solution. ComCoast is looking for a more gradual transition from sea to land, instead of a traditional single line of defence. The project is developing innovative flood risk management strategies to include wider social and environmental functions. Its focus is to find a concept in which safety is not looked at separately from ways in which natural processes and the problem of the usage of space can be integrated. The ComCoast concept can be formulated as a 'coastal defence zone', which contains two principles for this spatial water defence:

1. Load reduction → foreshore sea defence zone → reduction wave attack
2. Load admitting → landward sea defence zone → management of water behind the dike

The ComCoast project searches for alternative coastal defensive solutions using a multiple line of defence strategy. In comparison with a single line defence, a coastal defence zone has a range of components (lines) each with its own function. First these technical functions and its components are formulated from which the main ComCoast solutions can be derived.

- Water retaining
The primary dike retains high water levels and wave run-up. It should retain them up to the design level. The inner slope can have an overtopping-resistant revetment, which permits a greater overtopping discharge.
- Water storage
The area behind the primary dike is a transitional area able to store the overtopping seawater. A secondary dike or higher grounds, encircles the transitional area. The water can be managed by pumping stations.
- Water control / management
In normal weather conditions and during storms the coastal defence zone should be able to drain off water when necessary. First, a drainage system facilitates water control in the transitional area. For larger quantities of water, a pump installation and/or outlet structure can be installed to support the discharge of water by the drainage system. If desired, it can also be used to drain off excessive salt water after a storm.
- Wave reduction
Several elements in front of a dike result in wave reduction. A shallow foreshore creates a moderate wave climate in front of the dike. In addition, wave reduction can also be achieved when there is a previously constructed lower dike or a breakwater.
- Multifunctional use of area
The transitional area can be used for several purposes, including the development of aquatic areas and to enhance environmental values. This is only the case when the area is flooded regularly.

Overview of the main ComCoast solutions:

1. Load reduction → foreshore sea defence zone → reduction wave attack



- Foreland protection

Description: To build a sustainable defence in front of the primary defence to provide a brackish area between the defences for habitat or farming practices.

Required action: To build a soft embankment to act as a buffer for the primary defence.



- Foreshore recharge

Description: Eroded sediments are replaced by pumping dredged materials on top of the eroded foreshore. The dredging would otherwise be dumped at sea and lost. The new sediments reinforce the natural flood defence and also help to restore habitats for wildlife.

Required action: Replenishing the foreland with environmentally safe dredged sediments.

2. Load admitting → landward sea defence zone → management of water behind the dike



– Overtopping defence

Description: Making the defence resistant to wave overtopping and ensuring that any water that is washed over the top can be temporarily stored and drained away.

Required action: Replace the top of the defence and its inner slope with a revetment that will not wear away by severe overtopping.



– Managed realignment

Description: Allow tidal water to flow onto the coastal floodplain to reduce surge tide levels. The inter-tidal zone may silt up keeping (more or less) pace with sea-level rise and land subsidence.

Required action: Partial or full removal of a flood bank to allow managed tidal inundation of the floodplain creating a dynamic inter-tidal zone with considerable natural and recreational value.



– Regulated tidal exchange

Description: Allow tidal inundation of the coastal floodplain in a controlled manner. This creates a transitional zone where the land can evolve over time into a more saline environment. The transitional zone may silt up keeping more or less pace with sea-level rise and land subsidence.

Required action: Regulation of tidal waters through a system of sluices pipes and/or pumps. Low-lying land may require a secondary line of defence.

2.3.2 ComCoast – application: multiple lines of defence in the New Orleans region

New Orleans is separated from the Gulf of Mexico by more than 75 miles (120 km) of marshland and shallow seas. This means that a hurricane and its storm surge approaching from the Gulf of Mexico will have to cross these areas before it hits the protective levee systems. The configuration of this long stretch of coastal land will largely affect the hurricane's wind, waves and surge. This is the reason why it is often said that New Orleans is protected by multiple lines of defence. This naturally existing protection system makes it interesting to implement the ComCoast strategy in funding ways to improve it. The application is further analyzed in section 3.5.

In a paper presented by J.A. Lopez [17, 2006], coastal Louisiana is depicted as a multiple lines of defence system. In this paper, 11 lines of defence are distinguished which can be divided in natural defences (1-5), man-made defences (6-9) and damage control (10, 11). Figure 2.12 presents an overview of these lines of defence.

- 1st: Continental shelf:
The primary benefit of this shallow shelf is to dramatically reduce wave height and wave energy from an approaching hurricane. A negative aspect of the shelf is that it will promote higher storm surges inland.
- 2nd: Barrier islands:
The Louisiana shoreline is characterized by fragmented barriers or shoals with low vertical profiles and low sand content. Barrier islands provide an important wave barrier for interior sounds and coastal marsh. The primary benefits of barrier islands are the near-complete reduction in wave height and the slight reduction in storm surge further inland.
- 3rd: Sounds:
The primary benefit of the Sounds is to provide a relatively shallow water buffer to deep water currents. Negative aspects are the regeneration of waves on the sound side of barrier islands and wave erosion on the back side.
- 4th: Marshland bridges:
Marshland bridges are areas of marsh with relative continuity compared to adjacent areas of significant loss, which reduce fetch, storm surges movement and shoreline erosion of interior marshes and lagoons.
- 5th: Natural ridges:
Natural ridges will impede overland flow across the ridge and potentially reduce storm surge. Natural ridges are economic corridors across the coast, including coastal communities and state highways which are likely to perform as evacuation routes.
- 6th: Man-made soil foundations:
Man-made foundations for transportation may provide incidental benefit to storm surges. Railroads, highways and spoil banks may run parallel to the coast and provide a ridge with a height of several feet.

- **7th: Flood gates:**
Flood gates are typically designed to withhold flood water and to remain open under normal conditions in order not to impede navigation. The effectiveness of flood gates depends on the nearby topography and constructed features such as levees.
- **8th: Flood protection levees:**
Flood protection levees are generally designed to be an absolute barrier defining a protected side and a flood side. The intent is to have no flooding on the protected side as levees in the region are not designed to be overtopped or withstand wave erosion.
- **9th: Flood protection pumping:**
Pumping stations are only used to reduce flood risk from rainfall and not designed to pump out flood water in the case of a significant levee breach.
- **10th: Elevated homes and businesses:**
All homes and businesses in south Louisiana are subject to being flooded if they are not elevated above the normal land elevation. As there will always be potential of a storm exceeding the limits of protection from storm surges, immovable assets should be elevated to the appropriate flood elevation risk. This is the last line of defense for immovable assets.
- **11th: Evacuation:**
Evacuation routes are typically highways, but could include other means of transportation. It is the last line of defence for people and movable assets. Evacuation routes and procedures should always be established for coastal areas and may also serve as re-entry routes.

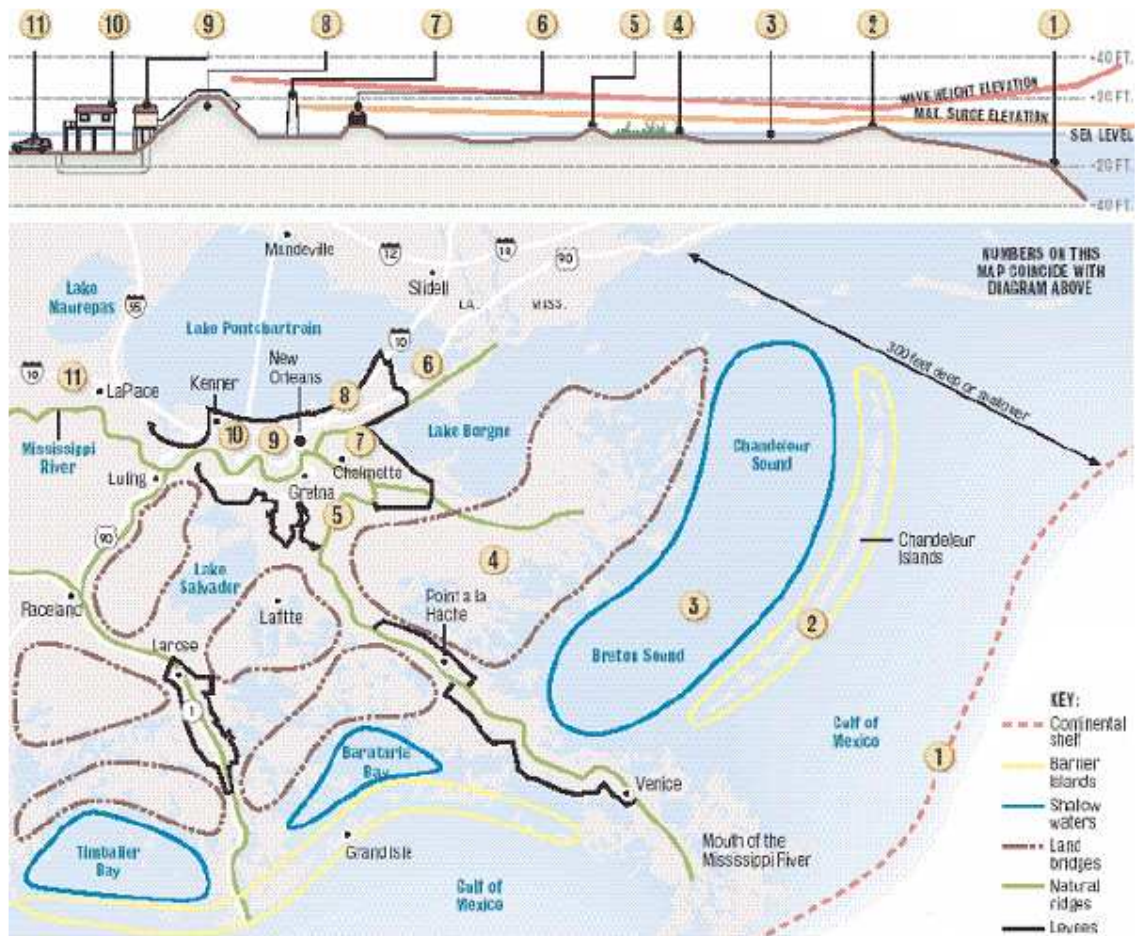


Fig. 2.12: Southeast Louisiana – multiple lines of defence [17]

3. Master Plan Of The New Orleans Region: *Macro To Meso Scale*

This chapter introduces the study area, extracted as part of a given Grand Plan for southern Louisiana. The subsequent sections provide information on the physical process and present situation of this region. Section 3.4 presents alternative master plan concepts on macro scale in order to evaluate the implementation of the mainly structural Grand Plan. Section 3.5 presents plan concepts on meso scale for the area adjacent to Lake Borgne.

3.1 Introduction of the study area

Immediately after Hurricane Katrina flooded New Orleans, President George W. Bush and the U.S. Department of Homeland Security declared that no one could have predicted such devastation. Yet scientists, engineers and Louisiana state politicians had warned for years that a Category 4 or 5 hurricane crossing the Gulf of Mexico from a certain direction would drown the region. Engineering firms and the U.S. Army Corps of Engineers (USACE), which is largely responsible for flood protection, proposed constructing higher earthen levees as well as huge gates that could have prevented storm surges from pouring into inner city canals and bursting their concrete flood walls. Indeed, documents show that various gates had been recommended as far back as 1968 and in each decade since. However, none of these designs has ever been funded. In the meantime, countries such as the Netherlands and Great Britain have erected effective surge barriers that the U.S. has ignored.

3.1.1 Grand plan of southern Louisiana

In Hurricane Katrina's wake, the blueprints for all these structures are rapidly being dusted off, augmented and integrated into a Grand Plan for Southern Louisiana by the Louisiana State University (LSU), engineering companies and the USACE. The idea that improving only the existing project would not provide protection to communities outside the existing levee system was the basis for the Grand Plan presented in figure 3.1.



Fig. 3.1: Grand Plan of southern Louisiana as provided by the LSU, engineering companies and USACE [14]

Three main protection schemes are being proposed to hold back the floodwaters from Category 5 hurricanes:

- The inner ring (red) would extend and add height and width to current levees and canal walls throughout New Orleans. It would connect to existing Mississippi River levees. This option can be seen as a variation of the alternative of improving existing hurricane protection projects, which will be discussed in section 3.4.5.
- A comprehensive levee plan (yellow) would continue the line to the Mississippi state border and west beyond Morgan City to protect more communities and industry. The 440 miles (700 km) of levee would loosely track the Gulf Intracoastal Waterway to the west. It lies only partway to the shoreline, leaving parts of the coast to be lost. In the overall levee system, diverting sluices within Mississippi River levees would open at certain times of the year to allow freshwater, nutrients and sediment to wash down into the marshes, reviving vegetation and building up land to counteract subsidence and sea level rise.
- A third option consists of a chain of dams and long stretches of gates that would connect the barrier islands, forming an outer shield. The basic idea is similar to in place in the Netherlands that was constructed under the Delta Project. At first glance, the comprehensive plan may seem more feasible than the total shield, but the outer shield preserves a significant area of marsh that the other plan would leave exposed. In addition, an outer shield around the region's perimeter would spare every locale, whereas the inner ring and comprehensive plans would inevitably leave some people outside the protection system. Diversions should still be installed to restore wetlands. Along with any plan, a new shipping entry point is recommended partway up the Mississippi, which would require dredged channels but shorten travel times and end dredging of the river tips. These river tips would now fill, sending sediment to the barrier islands and marshes to replace sand eroded by wave action.

In each scheme, numerous gates of different styles would be erected. This is visible in the extracted part of figure 3.1. Gates are proposed at the entries to the outlet channels and the Inner Harbor Navigation Canal (IHNC). In the part adjacent to Lake Borgne, gates are project in the Chef Menteur Pass and Rigolets Pass. These gates should stay open for shipping and for maintaining the natural mixing of freshwater and saltwater but close when needed to prevent storm surges from entering Lake Pontchartrain. This part of the Grand Plan is named the Hurricane Barrier Plan and will be further discussed in section 3.4.6. The main rationale for it is presented in the next section in order to introduce the study area of this thesis.

3.1.2 Rationale for closing off Lake Pontchartrain

Section 1.2 introduced Hurricane Katrina as a very large Category 3 storm when it passed the New Orleans area on the morning of 29 August 2005. It concluded that the Saffir-Simpson Scale used for the characterization of hurricanes is not a particularly good predictor of the associated storm surge level and wave generation potential. These hydrological conditions induced by a hurricane are a function of many factors, including wind speed, translation speed, landfall location, orientation of the storm track at landfall to the shoreline and storm size. These factors can be divided into two main groups:

- Path: landfall location and orientation of the storm track at landfall;
- Intensity: wind speed, translation speed and storm size.

Hurricanes are intense low pressure areas that form over warm ocean waters in the summer and early fall. As warm, moist air rises from the ocean surface into cooler air above, the water vapor condenses to form droplets and clouds. This condensation releases heat, boosting the rise of the air and lowering the central pressure. This process draws warmer air into the storm. In this manner, the energy builds up and the wind speed increases. The low pressure causes wind to spiral inward toward the center of the low pressure area, creating the hurricane. The hurricane winds are the highest at the center and decrease over its spatial extent. On the Northern Hemisphere, the hurricane wind rotation around the center is counterclockwise.

To get a first insight in the hydrological consequences for a hurricane sticking New Orleans, it is instructive to determine the consequences of its landfall location and orientation of the storm track at landfall to the shoreline:

- For a major hurricane passing on a path to the east of New Orleans, like Hurricane Katrina did, the water movement generally follows the pattern shown in white in figure 3.2. Storm surges will built up on the broad continental shelf and the counterclockwise hurricane winds will push the water towards the Mississippi River Delta and into Lake Borgne. High water levels in Lake Borgne act to drive water into Lake Pontchartrain, due to the water level difference between the two lakes. In addition to this, locally high winds in Lake Pontchartrain act to tilt the water surface. The hurricane induced winds create high wave conditions on the downwind side of the lake. Peak water levels at the entrances to the outlet canals along the lakeshore of New Orleans can reach significant heights above normal levels.
- For a major hurricane passing on a path to the west of New Orleans, the water movement generally follows the pattern shown in yellow in figure 3.2. Again, storm surges will built up on the broad continental shelf and the counterclockwise hurricane winds will push the water towards the Mississippi River Delta and into Lake Borgne and Lake Pontchartrain. Locally high winds in Lake Pontchartrain act to tilt the water surface, but in a different manner. These hurricane winds create high wave conditions on the upwind side of the lake. Peak water levels at the entrances to the outlet canals along the lakeshore of New Orleans will be low and water levels at the northern shore can reach significant heights above normal levels. Therefore, although this situation is favorable for New Orleans, it puts communities at the north shore of Lake Pontchartrain at harm.

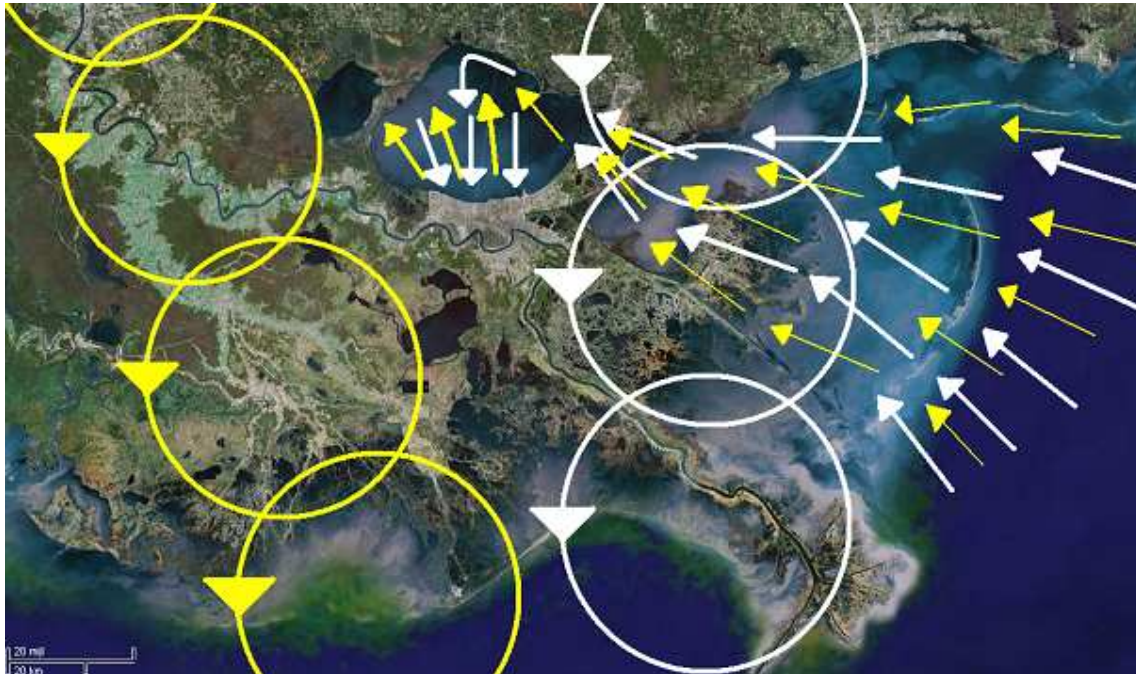


Fig. 3.2: Schematized water movement for two hurricane winds field passing New Orleans

To minimize the influence of locally generated hydrological conditions on the shores of Lake Pontchartrain, it seems reasonable to investigate an alternative for closing it off. This can be achieved by designing structures to close off the Chef Menteur Pass and Rigolets Pass, as is proposed in the presented Grand Plan for southern Louisiana. Closing both of them would prohibit storm surges to enter Lake Pontchartrain and therefore lower the hurricane threat to New Orleans and surrounding communities.

3.1.3 Study area – Lake Borgne, Mississippi River Gulf Outlet and Gulf Intracoastal Waterway

Closing the Chef Menteur Pass and Rigolets Pass is not enough as this still leaves the open connection provided by the IHNC and Gulf Intracoastal Waterway (GIWW) / Mississippi River Gulf Outlet (MRGO). Storm surge waters can still enter the IHNC from Lake Borgne to the east, making it the critical point of both hurricane path options. The severity of the entry of surge water is determined by the hydrological conditions in Lake Borgne. By preventing storm surge water from entering the IHNC, protection of vital residential and commercial areas of New Orleans would be realized. To prevent the entering of local storm surges from Lake Pontchartrain, a gate is proposed at the entrance to the IHNC. This is commonly referred to as the Seabrook location. The IHNC can be closed off from Lake Borgne induced surges by constructing a floodgate at the GIWW/MRGO location. These locations are visible in the extracted part of figure 3.1. The Seabrook location is more or less a fixed location as little to none margins are possible in the highly populated area. On the other hand, the location and design alternative of the GIWW/MRGO location is open for interpretation.

In conclusion, the GIWW/MRGO location needs attention in any scenario. Lake Borgne is in direct contact with the Gulf of Mexico and its area comprises an array of unique characteristics, including the MRGO and the decaying marshes bordering it. The combination of these characteristics and immediate need for improving this part of the protection system makes this the study area of this thesis.

To limit the extent of this thesis, the situation regarding the Mississippi River is briefly mentioned. Lake Borgne and Lake Pontchartrain close in New Orleans from the east and north respectively, whereas the southern part of the city is intersected by the Mississippi River. As this thesis focuses on the direct threats regarding a hurricane driven disaster, the Mississippi River is expelled at this early stage. In the metropolitan area of New Orleans, the levee sections bordering the Mississippi River are generally up to 25 ft (7.6 m) in height. It has proven to provide sufficient protection in the case of Hurricane Katrina. The highly meandering character of the deltaic section of the Mississippi River is expected to limit the influence of hurricane winds as no significant fetch is available. This said, it should be noted that this conclusion is not verified in any way. Since hurricanes can occur on an infinite number of distinctive paths, it should be further investigated whether a critical hurricane path can be determined in regard to the Mississippi River and to what river surges a major hurricane at this critical path would lead.

3.2 Primary contributors to storm water levels in the New Orleans region

As stated in the problem description, southern Louisiana's ongoing peril is the continued overlap of a weakened hurricane protection with more frequent and intense hurricanes. During these hurricanes, storm surges built up in the waters around New Orleans. Primary contributors to storm water levels in order of descending importance for southeastern Louisiana:

- *Wind induced motion of water.* High water levels and wave conditions observed during hurricanes are created by a number of processes. Both waves and water level changes are primarily forced by the wind. Winds change the water level in a process called storm surge generation. Storm surge is defined here as the high still-water levels attributable to the presence of the storm itself. The water level experienced during a storm is dictated not only by the storm surge but also by the astronomical tidal variations that normally occur without the presence of a storm. The word 'still' is intended to differentiate between the slower rise and fall of the water surface due to the storm surge that occurs over time scales of hours and the changes in water surface that occur at much higher frequencies over time scales of seconds. The height of a storm surge depends strongly on the bathymetry of the shoreline. If the hurricane is still above deep water, the surge is not able to develop as the water can be dispersed away from the hurricane as a return flow. If the hurricane passes over a long, shallow shelf before it reaches the shore, the water can not escape downwards anymore and the surge grows. This process is outlined in figure 3.3.

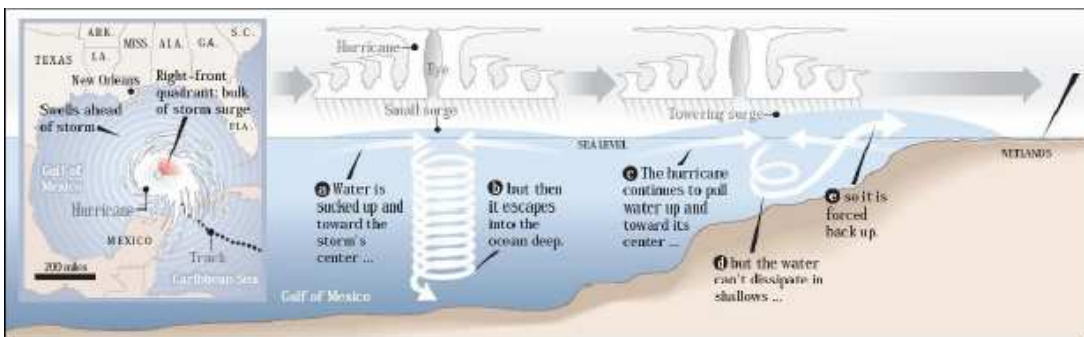


Fig. 3.3: Overview of the storm surge generation process [7]

- *Geographic controls.* Broad, shallow continental shelf regions are the most effective areas for generating storm surge. As winds push, the water moves until it encounters a coastal land mass or other obstruction where it then begins to accumulate. Indentations and irregularities are particularly prone to catching water pushed toward these geographic features by the wind. The Mississippi River Delta is a coastal land feature that acts to catch water being pushed toward it along the continental shelf. Hurricanes in the Northern Hemisphere rotate in counterclockwise direction. Therefore, hurricanes in the northern Gulf of Mexico tend to create winds that blow from the east in the northern section of the Gulf. These winds from the east act to push water toward southeast Louisiana, toward the Mississippi River Delta and Lake Borgne.
- *Breaking wind waves.* The highest significant wave height that can exist locally in shallow water is about 0.6 times the local water depth. When waves propagate into an area in which the significant wave height reaches this fraction of the water depth, significant wave breaking is induced. The change in momentum in breaking waves results in a thrust or force on the water column, which acts to raise the local water level. When waves break and run-up a smooth levee slope, the additional elevation above the mean water level reached by the wave up-rush can be as much as 2 to 3 times the incident wave height.
- *Reduced atmospheric pressure from the storm.* At the center of hurricanes, atmospheric pressure is much lower than at the periphery of the storm. This means the weight of air pushing down on the water column is greater at the edges of the storm than it is at the storm's center. Consequently, an increase in the water surface occurs at the center of the storm. The magnitude of this atmospheric pressure effect can be as much as 1 to 2 ft (0.3 to 0.6 m) in the center of the bulge for a severe hurricane.
- *Favorable or unfavorable timing with high and low tides.* The worst combination is when a hurricane induced storm surge occurs during high tide. Although the storm surge of Katrina did occur during high tide, for southeastern Louisiana the effects was rather small. Reason for this minimal effect is the small astronomical tide range in the area. Section 3.1.1 quantifies this tidal range.
- *Precipitation.* Precipitation can increase the storm induced water level, either by falling directly on the local water bodies or by falling on adjacent watershed and then running off into the water bodies. Figure 1.6 presented the rainfall characteristic for Hurricane Katrina. The contribution of direct precipitation to the peak storm surge for this hurricane is set to be 1 ft (0.3 m). Typically, effects of precipitation in the form of runoff will be experienced after the peak storm water level due to a longer concentration time.

The wind and geographic controls are dominant over the other factors. For major hurricanes impacting southeast Louisiana, it is commonly assumed that these two factors exceed the combined effects of all the other factors.

3.3 Present situation of the New Orleans region

The present situation of the study area can be best described by dividing the selected area into three main parts. These parts include a review on macro scale of Louisiana's changing coastal landscape, on meso scale of the protection levee status pre-Katrina and performance during Hurricane Katrina and also on a hydrological basis by presenting the main characteristics of the waterways intersecting the area. These main parts are presented in this section respectively.

3.3.1 Macro scale – Louisiana's changing coastal landscape

The northern central part of the Gulf of Mexico basin has been site of deposition by large fluvial systems for thousands of years. During the Holocene period, the Mississippi River delta has shifted laterally across the upper continental shelf, creating a large deltaic plain. Each time the Mississippi River had built a large delta lobe seaward at the front of a seaward advancing distributary network (regressive deposition), it subsequently had been abandoned in favor of a shorter, more direct route to the sea. After a delta lobe is abandoned, inundation and reworking of the delta (transgression) begins. This is the result of a decreased sediment supply and of subsidence. The alternating cycles of regression and transgression have been termed the delta cycle [Scruton, 1960], which is presented in figure 3.4. This delta cycle has been of fundamental importance to the construction of the southern Louisiana deltaic barrier shoreline environment and landscape.

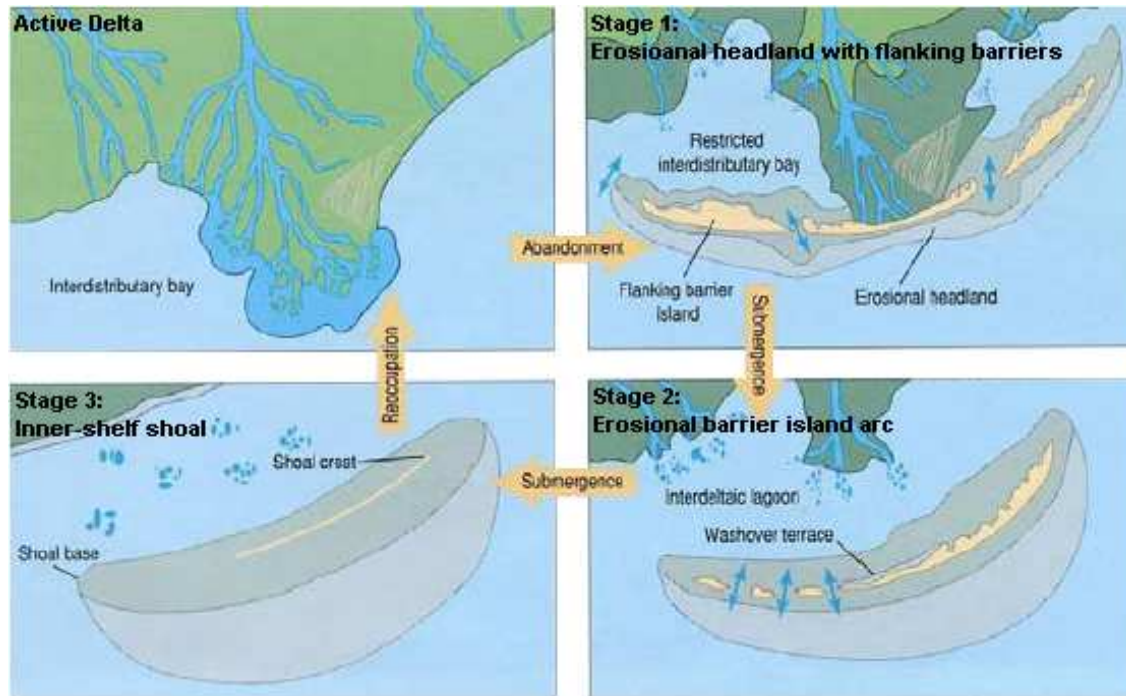


Fig. 3.4: Deltaic cycle - evolution of depositional systems in the Mississippi River Deltaic Plain [20]

The main processes operating on the coast of Louisiana include waves, storms, tides and relative sea level rise. These physical processes are not inherently harmful but a combination with man-made factors could speed the destruction of Louisiana's coast. An immediate result is the conversion of marshes and wetlands into open water and the disintegration of barrier islands. These coastal barrier chains in Louisiana form one of the first lines of defence for protecting wetlands and mainland regions. The barrier systems serve multiple purposes by reducing coastal flooding during storm surges, by preventing direct ocean wave attack and by maintaining gradients between saline and freshwater. The main processes operating on the coast of Louisiana will be briefly discussed:

- Waves

The wave conditions along the Louisiana coast are a product of seasonal wind patterns and the passage of tropical storms. The distribution of deep water wave energy under normal seasonal weather conditions is known from several stations of the National Oceanic and Atmospheric Administration (NOAA) that are located offshore. The period of record ranges widely from 1 to 20 years. Despite this variation, trends are fairly consistent. The data indicate that the mean annual deep water wave height varies from a low of 2.5 ft (0.75 m) to a high of 3.2 ft (0.95 m). Wave periods at all the stations exhibit similar trends. Mean annual wave period ranges from 4.5 to 5.9 seconds. Only one station, located just west of the Mississippi River delta, is used in defining the near shore wave climate for the central Louisiana coast. The waves measured here typically vary from approximately 0.25 to 2.65 ft (0.07 m to 0.8 m).

- Storms

The coast region of the Gulf of Mexico is affected by tropical storms. Tropical storms are generally the forerunners to hurricanes, which form when wind velocity surpasses 75 mph (120 km/h). Hurricane season in the region begins on June 1 and ends on November 30. During the past 100 years, 55 hurricanes and tropical storms have made landfall along the Louisiana coast with the highest incidence occurring in September [Stone et al., 1997]. A graph of the spatial and temporal distribution of large magnitude storms for the 1901–1996 period is presented in figure 3.5. It indicates that hurricanes occur slightly less frequently than tropical storms and hurricanes are least likely to strike eastern Louisiana.

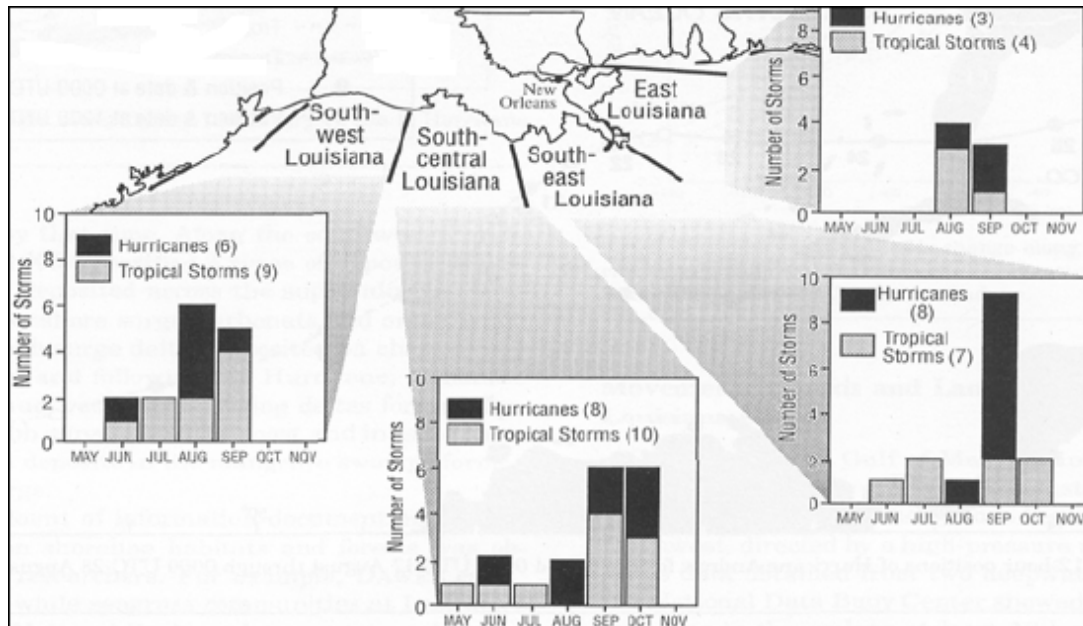


Fig. 3.5: Distribution of hurricanes and tropical storms along the Louisiana coast from 1901–1996 [20]

- Tides

Tides control the elevation and times of high and low tide as well as the flow of water into and out of bays and tidal inlets. Tides interacting with freshwater discharge form rivers and produce salinity gradients in estuaries and wetland areas. Tides along the Louisiana coast change systematically, with an overall decrease in tidal range from the western Chenier Plain eastward toward Mississippi Sound. In western Louisiana, the tides are mixed and have a strong diurnal component. Daily tidal elevations vary in range from a low of 2 ft (0.60 m) to a high of 3.2 ft (0.97 m). At the Chandeleur Islands, located east of the Mississippi River Delta, the tidal wave is dampened, resulting in a smaller tidal range of 0.4 ft (0.12 m) to 2.1 ft (0.64 m).

- Sea level rise

The trend of rising sea level along Louisiana's coast is attributed to several mechanisms. Essentially, the land surface is subsiding and the ocean level is rising. Together these processes are largely responsible for massive shoreline erosion and the transgressive nature of most of the barrier islands in Louisiana. This historical decrease in size and increasing segmentation of Louisiana's barrier systems, as well as the loss of wetlands, has greatly increased the vulnerability of the mainland areas during hurricanes.

As stated before, the immediate result of these physical processes is the conversion of marshes into open water and the disintegration of barrier islands. Over the last century, the rate of erosion has progressively increased. The combination of the natural regression/transgression process and man's attempt to manage natural systems has failed to produce the desired benefits. The Louisiana coastline is changing more rapidly than the coastline of any other part of the U.S. It is experiencing rapid rates of subsidence and relative sea level rise ranging from 1 to 3 ft (0.3 to 1 m) per century [Penland et al., 1989]. The U.S. Geological Survey (USGS) projects that an additional 700 mi² (1,800 km²) of coastal land could be lost by 2050 if no further action is taken to halt or reserve current processes. Figure 3.6 provides insight in these endangered coastal lands.

The deterioration of Louisiana's coastal landscape has made coastal communities vulnerable to hurricane flooding. In particular New Orleans is considered to be increasingly vulnerable, because the city has subsided and most of its surrounding barrier islands and wetlands have disappeared. Over the last 70 years, Louisiana has lost over 1,900 mi² (4900 km²) of coastal land. At the peak of the trend in the 1960s and 70s, Louisiana was losing 40 mi² (102 km²) per year. This loss has slowed in recent years, primarily because the most vulnerable lands had already disappeared. Louisiana is still losing over 10 mi² (25.6 km²) of coastal land per year.

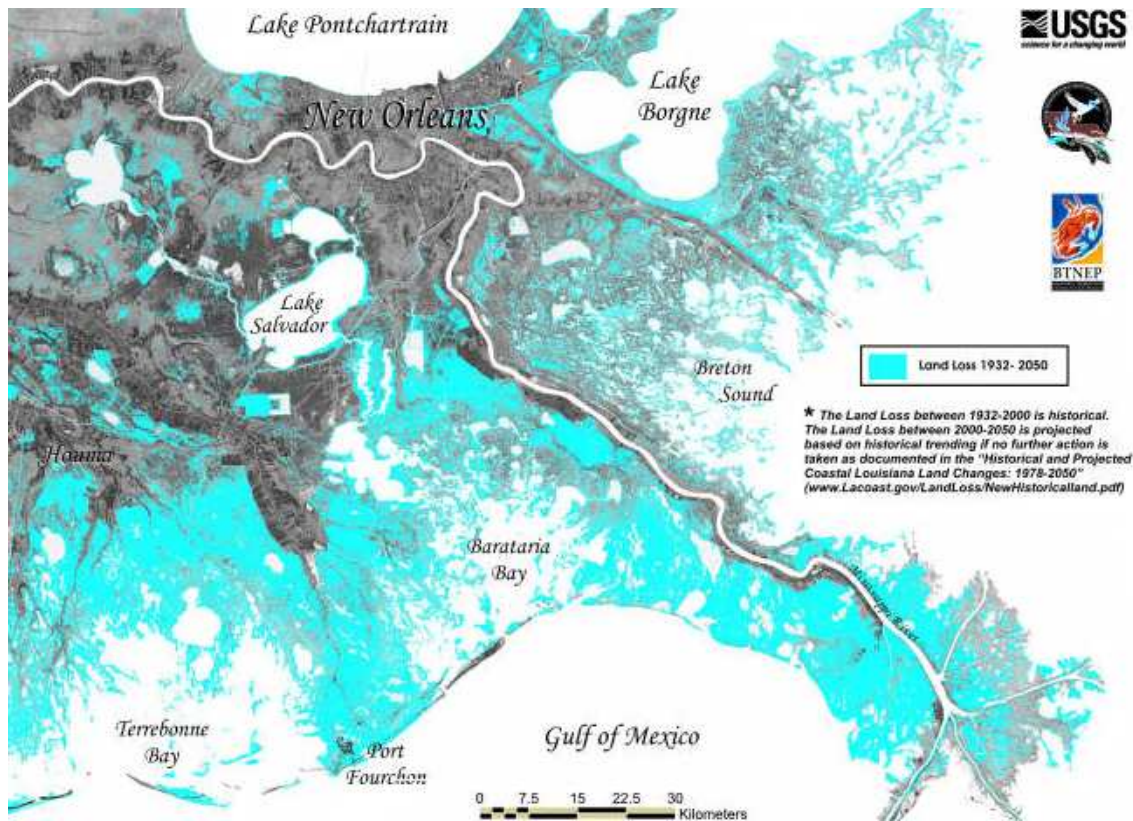


Fig. 3.6: Projected coastal land loss by 2050 [source: USGS]

These changes to Louisiana's coastline have serious implications for the long term sustainability of the region. The combination of land subsidence and predicted global sea level rise during the next 100 years means that areas of New Orleans and vicinity may well 3 ft (0.9 m) more below sea level by 2100 than in the current situation [USGS]. At the same time, the loss of barrier islands and wetlands could eliminate protection from waves and allow for higher and faster moves storm surges. According to the National Agency of Sciences, these trends will make much of Louisiana's southern delta inhabitable without substantial new engineering projects.

Conclusion

The Mississippi River Delta is not alone in being endangered. Deltas worldwide are in trouble because human development is causing the land to sink. Fundamental to the trouble is that for the past century the USACE confined the Mississippi River by building levees to prevent its annual floods. Yet the same levees have starved the region of enormous quantities of sediment, nutrients and freshwater. Natural flooding at the river's mouth had also sent volumes of sediment west and east to a string of barrier islands that cut down surges and waves, rebuilding each year what regular ocean erosion had stolen. Since the mouth is now dredged for shipping lanes, the sediment simply streams out into the deep ocean. This leaves the delta and New Orleans within it vulnerable against the sea.

Sustainability of coastal Louisiana depends on the ability to find solutions that are compatible with nature. There is a growing consensus among engineers involved with Louisiana coastal protection and restoration that future projects for reducing hurricane risks along the Louisiana coast should include plans to sustain or enhance the wetland dominated landscapes. These landscapes are widely recognized for their great value to the nation for the natural resources and ecosystem services, but the also provide a level of protection from hurricane wave action and storm surge. Despite this qualitative knowledge of the potential effects of landscape features on hurricane protection, there has been minimal quantification of these effects in nature. To address this need, a set of idealized numerical modeling tests need to be conducted to evaluate the reduction in surge as a function of landscape feature and vegetation type. This also provides insight in the effect of nourishments and other restoration efforts. Clearly, this modeling is outside the scope of this thesis.

3.3.2 Macro scale – characteristics of the waterways intersecting the study area

Lake Borgne and Lake Pontchartrain

Lake Borgne is located east of the city of New Orleans and is open to the east, connecting with the Gulf of Mexico via Mississippi Sound. It covers an area of 280 square miles (730 km²) with an average depth of 9 to 11 ft (2.7 to 3.3 m, MSL). In Lake Borgne, the tidal range is 1.0 to 1.3 ft (0.3 to 0.4 m) according to the NOAA.

Lake Pontchartrain is a brackish estuary located in southeastern Louisiana. It covers an area of 630 square miles (1630 km²) with an average depth of 12 to 14 ft (about 4 m, MSL). It is roughly oval in shape, about 40 miles (64 km) wide and 24 miles (39 km) deep from south to north. The south shore forms the northern boundary of the city of New Orleans. In Lake Pontchartrain, the tidal range is 0.6 ft (0.2 m) according to the NOAA. In the shallow water bodies, wind driven tides can be substantial and exceed the range of the astronomical tide.

Gulf Intracoastal Waterway

The GIWW forms a protected navigable waterway running approximately 1,050 miles (1,700 km) along the Gulf Coast between Texas and Florida. It links all of the Gulf Coast ports and enables these ports to access the inland waterway system. The GIWW was authorized in 1919. It was excavated in the 1930s to a channel size measuring 12 ft (3.6 m, MSL) deep by a bottom width of 125 ft (38 m) and officially completed in 1949.

The 1930 Rivers and Harbors Act also authorized two improvements in this adjacent western stretch between Mobile Bay, Alabama and New Orleans. By 1929, grounding and collisions of commercial vessel vessels occurred frequently within these restricted confines. Under the new appropriation, this portion of the waterway was straightened and widened to a depth of 18 ft (5.5 m, MSL) and a bottom width of 300 ft (91 m).

Mississippi River Gulf Outlet

The MRGO is a man-made navigational channel connecting the Gulf of Mexico to the city of New Orleans. Approved by the U.S. Congress under the Rivers and Harbor Act of 1956, construction began in 1958 and was completed in 1965. The channel was authorized to a depth of 36 ft (10.9 m, MSL), a surface width of 650 ft (198 m) and a bottom width of 500 ft (152 m), except the portion within the Gulf of Mexico which is authorized to a depth of 38 ft (11.6 m, MSL) and bottom with of 600 ft (182 m). The 76 miles (122 km) long channel bisects the marshes of lower St. Bernard Parish and the shallow waters of Chandeleur Sound. To about 5 miles (8 km) east of the IHNC, the MRGO follows this GIWW before diverting to the southeast.

3.3.3 Meso scale – levee status pre-Katrina and performance during Katrina

The large onshore storm surge caused by Hurricane Katrina overwhelmed Louisiana's coastal landscape features and raised water levels within Lake Borgne. As the storm then passed to the east of New Orleans, the prevailing counterclockwise swirl of the storm winds drove the water of Lake Borgne as a large storm surge to the west against the eastern flank of the protection levees. In this section the two protected areas within the study area are discussed with regard to their performance during Katrina.

St. Bernard Parish

The storm surge level exceeded crest heights of the levees along a nearly 11 miles (17.6 km) long stretch of the northeastern edge of St. Bernard Parish. The levees along this frontage were intended to provide protection to a level of approximately +17.5 (+5.3 m, MSL), but at the time of Hurricane Katrina levees along this frontage had crest elevations 2 to 4 ft (0.6 to 1.2 m) lower than that. Main reason was the fact that the levees not yet been completed. As the levees were being constructed on swampy foundation soils, the levees were planned to be constructed in stages to allow time for consolidation and settlement of the foundations soils. The last major work in this area prior to Katrina had been the construction of the third phase in 1995. Since that time, the USACE had been waiting for Congressional approval of funds necessary to construct the final stage to the full design height.

In addition to the levees along this frontage being well below design grade, the manner of construction was non-typical according to USACE standards. These standards require the use of cohesive (clayey) soils to create an embankment fill that is both strong and relatively resistant to erosion. However, the levees along the MRGO frontage were instead 'sand core levees' [USACE Design Memorandum, 1966]. This means that these levees were constructed using locally available soils, including dredge spoils from the excavation of the adjacent MRGO channel. The most common materials occurring at shallow, relatively accessible depths tend to be predominantly sandy soils that are highly erodible and unsuitable for levee embankment fill.

By the time the storm surge peaked along the MRGO levee frontage, the unfinished sand core levees had been eroded to such an extent that they did little to impede the passage of the storm surge. The storm surge crossed the roughly 10 miles (16 km) stretch of open wetland and reached the Forty Arpent Levee. This levee separates the northern undeveloped wetland from the populated southern section. It was only a secondary levee, with crest heights in the order of +7.5 to +10 ft (2.3 to 3.0 m, MSL). It had not been intended to have to face the full brunt of a largely undiminished rising storm surge. As a result, the storm passed easily over the levee and pushed rapidly into populated areas. It is interesting to note that, although this secondary levee had been massively overtopped, relatively little erosion damage resulted. The levee was properly constructed, using compacted clayey soils. The resulting levee embankment generally performed well with regard to resisting erosion.

Orleans East Parish

The Orleans East Parish encompasses some of the lowest elevation lands in the greater New Orleans populated region. Like the St. Bernard Parish, it includes a secondary levee (Maxtent Lagoon Levee) that separates the developed portions of the region from the wetlands to the east. The primary purpose of this secondary levee is interior drainage control, rather than hurricane protection. Its crest height of +6 ft (1.8 m, MSL) is significantly less than the main frontage levees, which have a crest height of +14 to +18 ft (4.3 to 5.5 m, MSL).

The storm surge from Lake Borgne that topped and eroded the levees along the MRGO frontage also pushed westward over the southeastern corner of the New Orleans East protected area. The protection at this location consisted of an earthen levee with an incline of 1:4, a crest height of 17 ft (5.2 m, MSL) and a 10 ft (3.0 m) wide crown. The damage to this segment was similar to that which occurred along the MRGO levees in St. Bernard Parish as entire sections were completely eroded. Like the MRGO frontage, large portions of this levee frontage section had been constructed using materials excavated from the adjacent navigation channel (GIWW). The flood water subsequently made its way across the undeveloped swamplands and into the populated areas.

As the hurricane passed northwards to the east of New Orleans, the counterclockwise direction of the storm winds also produced a storm surge towards the south shore of Lake Pontchartrain. The water level rose, but it mainly stayed below the crests of most of the lakefront levees. The crest height of these lakefront levees varied from +18 ft (5.5 m, MSL) to the northeast to +14 ft (4.3 m, MSL) at the west end. Moderate overtopping occurred at a number of locations, resulting in minor erosion on the crests and inboard faces of these sections.

Conclusion

The storm surge and waves first attacked the levees of Plaquemines Parish well before Katrina's landfall, causing significant overtopping and erosion. Levees adjacent to the MRGO were soon hit with similar conditions and eventually both Plaquemines and St. Bernard Levees would be overtopped by both high surge and high, long-period waves. The surge and waves had a devastating effect on the sections of the levees along the GIWW (figure 3.7, left) and MRGO (figure 3.7, right) that were constructed with materials dredged from the adjacent channels using hydraulic fill. Even though the levees were capped with clay, they were no match for the energetic environment they experienced. Figure 3.8 shows the correlation between the degree of breaching from overtopping and erosion and the types of materials for New Orleans East protected area.



Fig. 3.7: Examples of levee breach along the GIWW (left) and the MRGO (right) [29]



Fig. 3.8: Levees along the GIWW / MRGO – correlation between erosion and types of material used [32]

3.4 Master plan concepts on *macro scale*

In this section, an assessment of the situation is performed on macro scale. This assessment comprises the southern part of Louisiana and is performed in order to evaluate alternatives with respect to the Grand Plan provided by the LSU, engineering companies and USACE. The assessment results in a no-action alternative, a non-structural alternative and two structural alternatives which would significantly increase the level of protection in the area. Firstly, the sections 3.4.1 and 3.4.2 provide information on the main planning constraints and overall reasoning. The next sections each discuss an alternative on macro scale. Section 3.4.3 presents the no-action alternative, which is not more than an estimation of the direct consequences of doing nothing. Section 3.4.4 presents the alternative of incorporating non-structural measures in contrast to an expensive and comprehensive system of levees and floodgates. Section 3.4.5 presents the first structural alternative, which discusses the improvement of the existing hurricane protection projects. Finally, section 3.4.6 focuses on the Hurricane Barrier Plan, which presents the part of the Grand Plan for southern Louisiana directly adjacent to Lake Borgne. It provides the last step towards the master plan concepts on meso scale.

3.4.1 Planning constraints

The master plan should maintain New Orleans as a viable urban center. It is presumed that there exist certain features within the city of New Orleans that must inarguably be maintained: the Port of New Orleans, the downtown business district, the cultural French Quarter district and sufficient residential areas to support commerce. Thus, no alternative should provide for the relocation of the city of New Orleans en masse.

Many of the issues involved in protecting southeast Louisiana from a major hurricane are ultimately political rather than technical. Forecasting future conditions is challenging in best cases. In a situation in which entire communities with tens of thousands of residents have been virtually destroyed, it is not possible to provide a meaningful description of the future without project based conditions. Many residents of such areas have averred their intentions not to return. Still, these areas prospered for many years with a level of hurricane protection no greater than that provided by existing hurricane protection projects. With time, given the re-establishment of the city's economic base, it is entirely possible that destroyed areas could thrive once again. As there is still a high degree of uncertainty concerning reliable forecasts and future conditions, alternatives involving abandonment of formerly developed areas are not included in this assessment.

As discussed in section 1.3, there are several hurricane protection projects in southeast Louisiana. The revised protection system should benefit from this by incorporating these existing projects. In some areas, the existing features could be utilized as a base upon which a project providing a greater level of protection could be built. In other areas the existing hurricane protection projects could be used as a second line of defence. In this way, the previously authorized projects provide an opportunity to ensure additional security against hurricane flooding. In addition to the second line of levee defences, constructing internal lower level protection levees and structures between basins within the metropolitan area of New Orleans would limit the impacts of a future flood event. Restricting flood damages to one basin would result in an overall reduction in damages. Further investigation on locations where these closures can best be implemented is recommended but outside the scope of this thesis.

3.4.2 No-action alternative

If the existing Lake Pontchartrain and Vicinity Hurricane Protection Project would be completed as designed, its populated areas will not have protection against storms greater than the Standard Project Hurricane (SPH). As discussed in section 1.3, this selected SPH corresponds to a storm surge and rainfall associated with a hurricane that would be roughly the same as what is today classified by the Saffir-Simpson Scale as a fast moving Category 3 hurricane. While such a protection project provides a substantial level of protection, this area would still be vulnerable to relatively infrequent but potentially catastrophic storm events.

Hurricane Katrina caused massive damage to the metropolitan area of New Orleans with direct damages well over \$20 billion [33]. As damaging as Hurricane Katrina was to New Orleans, it was not the worst case scenario. Large areas of the metropolitan area of the city did not retrieve catastrophic damages and the entire West Bank area was not flooded. Hurricane Katrina resulted in the loss of over 1,000 lives but if the entire metropolitan area had been subjected to a catastrophic flooding, this figure could have been higher. Even with excellent evacuation planning, it is likely that many thousands of individuals would remain in the impacted area during the storm. In addition, the impacts to the Port of New Orleans were small. A stronger storm or a storm on a slightly different path could have effectively closed the Port of New Orleans to commerce for a significant length of time. Such an event would have had negative economic impacts throughout much of the nation.

While the return interval for a major hurricane like Hurricane Katrina is not known, it is virtually inevitable that a similar or worse storm will one day strike the New Orleans region again. Even in the absence of a rigorous economic analysis, the direct catastrophic consequences of another event like Hurricane Katrina constitute a compelling argument that the no-action plan is not politically and socially acceptable [27].

3.4.3 Non-structural alternative

In contrast to an expensive and comprehensive system of levees and floodgates, the opportunity exists to also incorporate a wide range of non-structural measures. In general terms, these measures could include:

- Floodplain management
A comprehensive floodplain management plan would be needed to ensure long term success of any adopted plan, including that of structural measures. As mentioned in section 3.3.1 on Louisiana's changing coastal landscape, the sustainability of coastal Louisiana depends on the ability to find solutions that are compatible with nature. There is a growing consensus among engineers involved with Louisiana coastal protection and restoration that future projects for reducing hurricane risks along the Louisiana coast should include plans to sustain or enhance the wetland dominated landscapes.
- Structure raising
Structure raising is usually not a practical alternative in any large scale application. The degree to which the remaining structures would have to be raised in order to remove them from the target flood plain renders most such plan as cost ineffective. The viability of structure raising even as a supplement to a structural plan is conditioned upon the degree of comprehensiveness in its application.
- Land raising
There are some areas where raising of the land surface can be considered. Although it is expected to be a relative expensive option, there are special circumstances in these areas that should be included in its evaluation. Due to social and cultural ties to some of the worst flooded areas, many residents expressed a desire to return and redevelop communities despite of the flooding risk. If these areas are to be redeveloped, one option would be to fill areas that were not as deeply flooded to a safer elevation. The badly damaged St. Bernard Parish might be candidate for such options, as well as selected areas in Orleans East Parish. It should be noted that a land raising solution would generally be implementable only in cases where flooding was so devastating that damaged structures can not be made habitable and complete redevelopment is necessary. Areas flooded by Hurricane Katrina had water depths of 7 to 8 ft (2.1 to 2.4 m) in Orleans East Parish and up to 12 ft (3.6 m) in St. Bernard Parish. Raising the land in these areas to an elevation sufficient to provide safety for this kind of hurricane threat would be a slow, expensive undertaking.
- Construction of ring levees in selected locations
Some areas of southeast Louisiana, while especially subject to the threat of storm surge flooding as a main consequence of their location, are so sparsely developed that conventional structural solutions may not represent the best means of addressing the problems. For instance, Plaquemines Parish extends for many miles along the course of the Mississippi River and forms a narrow stretch of land. This area may afford an opportunity to implement a series of enclosures protecting the more critical areas on either bank of the river.

Since it is impossible to build a comprehensive system without providing protection to some large areas that are currently undeveloped, the key component of any plan will be to insure good floodplain management of the entire southeast of Louisiana. It is apparent that non-structural measures alone are incapable of affording protection from storm surges associated with a hurricane. Nevertheless, the potential is high for non-structural measures to effectively supplement the levee systems. Project features could be designed with flexibility, project performance is enhanced and other needs of the area such as environmental issues and coastal restoration are met.

3.4.4 Improvement of existing hurricane protection projects

The third alternative involves upgrading the existing HPS to improve the level of protection. The existing hurricane protection projects consist of over 120 miles (200 km) of levees and floodwalls. To provide a sufficient level of protection, existing levees are assumed to have to be increased from an average elevation of about 17 ft (5.2 m, MSL) to an elevation of about 30 ft (9.1 m, MSL) in most cases. The levees would have to be rebuilt to accommodate a wider footprint and to reinforce the soil beneath the levees to support the increased elevation. In some cases, this would require extending the protection system into Lake Pontchartrain in order to avoid expensive real estate acquisition. In addition, existing floodwall would have to be replaced and pumping stations would have to be reconstructed to resist the higher water levels.

An option to reduce the impact of raising all of the existing levee system is to raise only levees west of the IHNC, include the western part of Orleans Parish, Jefferson Parish and St. Charles Parish. This decision acknowledges the great amount of destruction in Orleans East Parish and St. Bernard Parish and the possibility that decisions could be made in order not to increase protection levels for these areas. However, there are substantial industrial facilities of value in the eastern part of Orleans East Parish and in St. Bernard Parish that were not destroyed by Hurricane Katrina. These include the NASA Michoud facility, major port facilities and oil refineries. Ring levees would have to be constructed around these facilities.

In conclusion, this alternative is relative expensive due to the modifications of existing systems. At the same time, it does not provide a secondary line levee system that would reduce the risk of flooding. Homes and businesses still would have only one levee stretch or structure protecting them. Any overtopping, breach or other problem with the protective works would compromise the entire system. Finally, improving only the existing project would not provide protection to communities surrounding Lake Pontchartrain outside the existing levee system.

3.4.5 Outlined part of the Grand Plan for southern Louisiana – Hurricane Barrier Plan

In each scheme of the Grand Plan for southern Louisiana, numerous gates would be erected. In the part adjacent to Lake Borgne, gates are projected in the Chef Menteur Pass, Rigolets Pass and in the GIWW/MRGO confluence. These gates should stay open for shipping and for maintaining the natural mixing of freshwater and saltwater but close when needed to prevent storm surges from entering Lake Pontchartrain. This part of the Grand Plan is named the Hurricane Barrier Plan (HBP).

The proposed levee system for the HBP originates on the northeastern shore of Lake Pontchartrain in Slidell and extends across the land bridge between Lake Pontchartrain and Lake Borgne. At this crossing, the levee could follow two optional alignments. Although not further investigated, at first sight the alignment closest to Lake Pontchartrain seems favorable as it requires the shortest stretch of new levee. The system continues around the Lake Borgne shoreline to the vicinity of the existing Bayou Dupree outlet structure. From there it coincides with the existing levee system around St. Bernard Parish and terminates at the Mississippi River levee near Caernarvon. Included in the system are structures at Rigolets Pass, Chef Menteur Pass, GIWW and MRGO. An overview of the HBP is presented in figure 3.9.

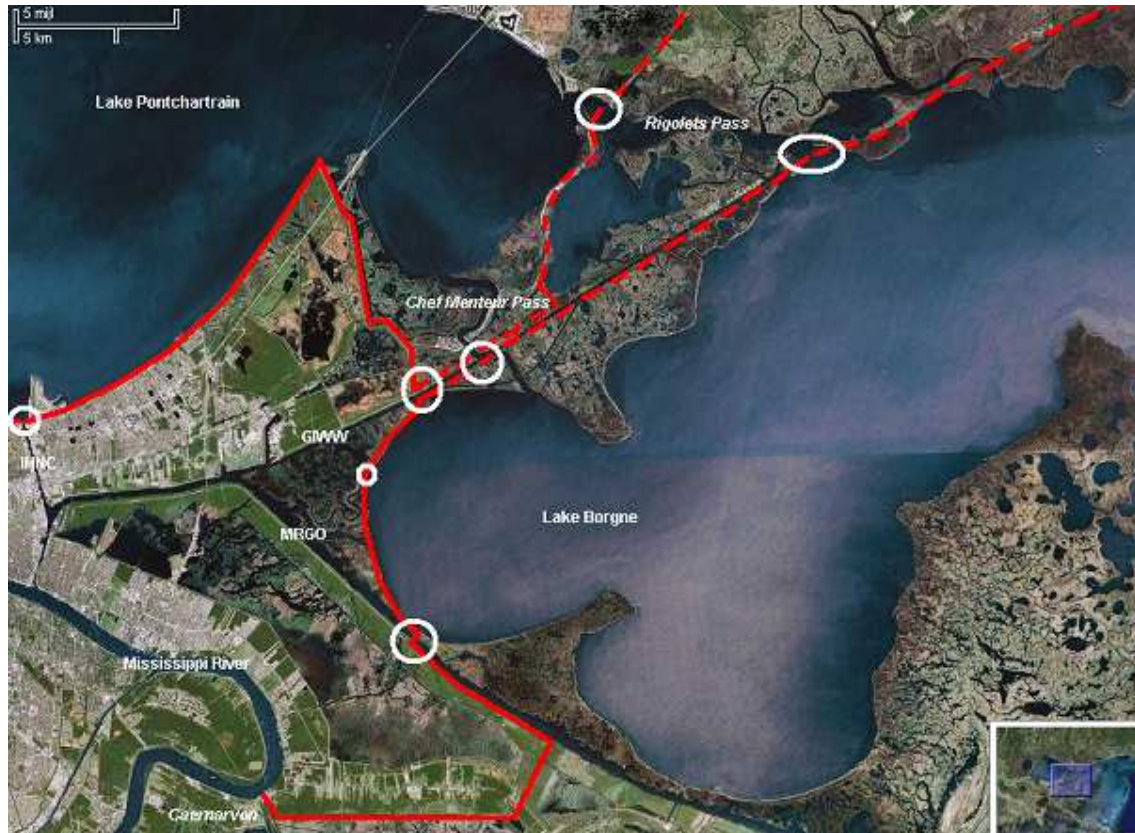


Fig. 3.9: Hurricane Barrier Plan

The intention of the HBP is to keep the storm surges out of Lake Pontchartrain and the IHNC. Closure structures at the IHNC and outfall canals should be included in the plan because the local hydrology of Lake Pontchartrain after closure is still able to generate significant wave conditions during hurricanes by means of wind setup. These structures will keep the local storm surges and wind waves generated solely in Lake Pontchartrain from moving up these canals and entering the heart of the city of New Orleans.

In conclusion, the HPB configuration of this particular part of the Grand Plan for Southern Louisiana is favorable for a number of reasons:

- The Hurricane Barrier Pan provides higher protection levels for all parishes in the Lake Pontchartrain basin, whereas raising the existing protection system would not provide surge protection for the communities in the northern and western part of the Lake Pontchartrain basin. The no-action plan does not provide an increased protection level for any of the communities in the overall Lake Pontchartrain basin.
- The HBP enhances the system reliability because it implements a secondary levee protection system.
- The HBP is expected to be less expensive than raising the levees of the existing hurricane protection systems. It is also expected that it can be constructed in a much shorter time, leaving New Orleans not still vulnerable to flooding for a long period.

3.5 Outlined part of the Hurricane Barrier Plan – Master plan concepts on *meso scale*

This thesis will have its focus on the part of the HBP directly adjacent to Lake Borgne, generally the section between Caernarvon and the connection to the GIWW in the vicinity of the New Orleans East Levee. For this section, this thesis generates several conceptual spatial designs to provide sufficient protection to the populated areas of New Orleans. The general approach taken is to look at the possibilities of using alternative coastal defence strategies. Instead of simply heightening of the primary dikes, a wide coastal defence zone will be proposed using the ComCoast strategy. This strategy is applicable as advantage could be gained from the existing wetlands and open space, both in landward and seaward direction.

After a brief introduction, section 3.5.2 discusses the main design conditions of the coastal defence zone and section 3.5.3 introduces the conceptual spatial designs. Finally, section 3.5.4 evaluates the concepts by using a multiple criteria analysis.

3.5.1 Introduction

As stated in section 2.3.2, the ComCoast project searches for alternative coastal defensive solutions using a multiple line of defence strategy. In comparison with a single line defence, a coastal defence zone has a range of components (lines) each with its own function.

Figure 3.10 present pre-Katrina conditions of the protection levee systems in the study area. It presents the levee systems of St. Bernard Parish and Orleans East Parish, including their secondary levee stretches. As can be seen in the figure, the existing levee system lacks overall unity. The inconsistency in levee heights proves again that the existing HPS can not be seen as a system and that it lacked redundancy. Essentially, the levee system bordering these parishes had only a single line of defence.

Given the extensive flooding of New Orleans, this part of the HPS should be revised according to the redundant strategy of multiple lines of levee defence. As can be seen in figure 3.10, this multiple lines of levee defence strategy is applicable for the part east of the Maxtent Lagoon Levee in Orleans East Parish and for the part northeast of the Forty Arpent Levee in St. Bernard Parish. These parts of the primary levee system do not have to be designed to provide full protection on their own as limited overtopping is allowed. Overtopped water can be stored in the transitional area between the primary and secondary levee. The actual storage quantity depends mainly on the height of the secondary levee and the available storage area surface. In general, the primary levee section backed by such a storage area can be heightened and reinforced in order to resist overtopping values.

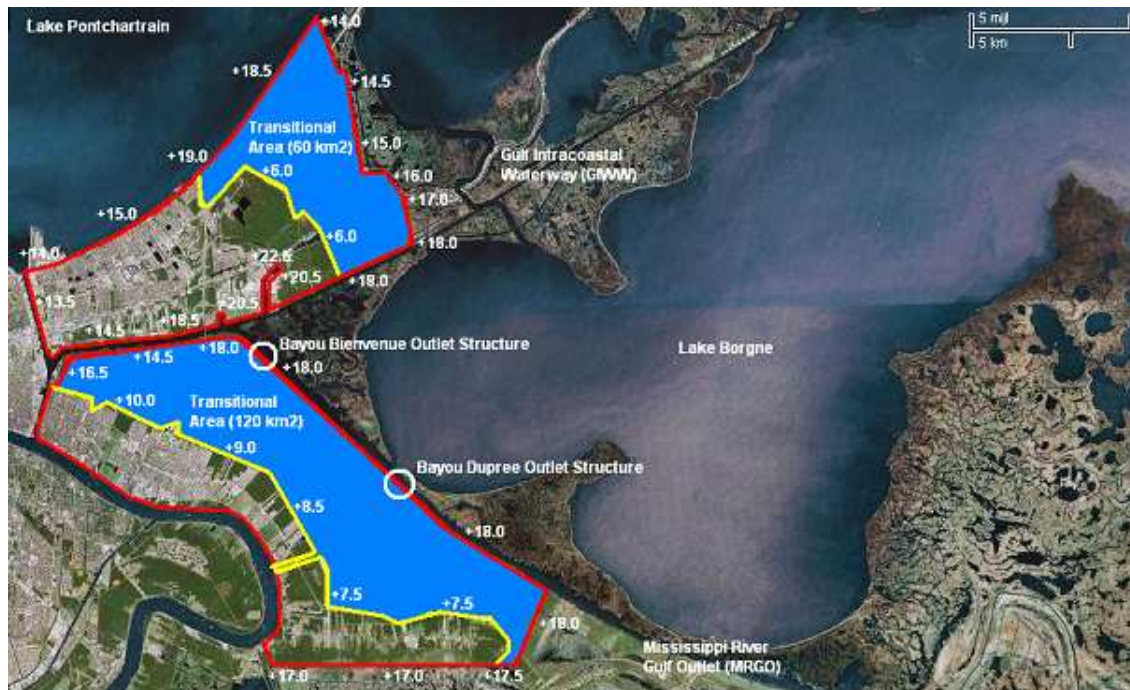


Fig. 3.10: Pre-Katrina levee conditions in the study area (in ft, MSL)

Note that most design documents cite water levels relative to different vertical datums. The data used to in figure 3.10 was converted from the common datum NAVD88 (2004.65) to mean sea level (MSL) in order for it to be used as design input in this thesis. The datum conversion concludes that both levels differ from 0.2 ft to a maximum of 0.5 ft (0.06 to 0.15 m). This difference is neglected in this thesis.

With respect to the ComCoast strategy, the defensive system in both St. Bernard Parish and Orleans East Parish are considered as a coastal defence zone in which four defensive elements can be distinguished [7]:

- A. Secondary levee (water retaining)
- B. Transitional area (water storage)
- C. Primary levee (water retaining)
- D. Shallow foreshore (energy dissipation)

From literature it can be concluded that erosion and overtopping of the primary levee, followed by overflow of the secondary levee caused the flooding of both residential areas [USACE-IPET, 2006]. This means that either the storage capacity of the transitional area was too low or the amount of overtopping and severity of erosion were too high at the primary and/or secondary levees. The main causes can be summarized with their possible solutions, sorted by the coastal defensive measures as described in figure 3.11:

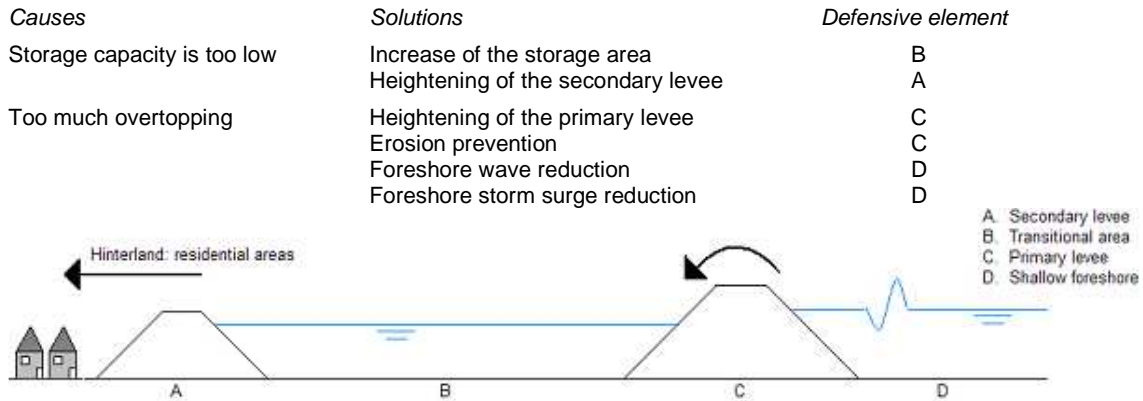


Fig. 3.11: Coastal defensive zone system of both the St. Bernard and Orleans Parish

3.5.2 Design conditions and assumptions

The hydraulic conditions are the most important boundary condition for the design of a coastal defence system. Those hydraulic design conditions usually originate from a certain representative design storm, like the SPH. Although its parameters have been revised a few times afterwards, it is still no proper basis as hurricane varied in intensity and occurrences. The design conditions in the case of hurricanes are still debated a lot, proving it as a complex engineering problem.

Figures 3.12 presents computed time series of water surface elevation at four locations throughout along the MRGO. Wave heights at the shore of Lake Borgne are generally in the order of 5 to 7 ft (1.5 to 2.1 m), as can be extracted from Appendix A.4.

To determine the order of magnitude of the crest elevation needed to provide protection against these wave conditions generated by Hurricane Katrina, a rough estimation of the needed crest elevation can be made by using the (Dutch) general rule of thumb for wave run-up and wave overtopping:

$$H_c = h + 8 * H_s * 8 \tan(\alpha),$$

where: H_c = crest elevation [m];

h = surge level [m];

H_s = wave height [m];

α = the outward face slope [°].

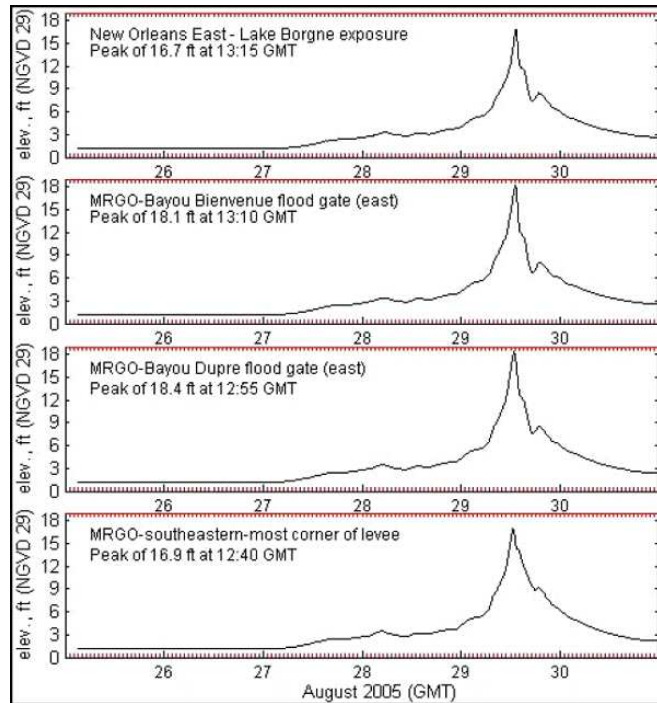


Fig. 3.12: Time series of water surface elevation along the MRGO [28]

The rule of thumb yields the results for the needed crest elevation as presented in table 3.1.

Cross section levee	Surge level [ft]	Wave height [ft]	Crest elevation [ft]
Reference (1:4)	15 – 18	5 – 7	30
Mild slope (1:8)	15 – 18	5 – 7	25
Very mild slope (1:12)	15 – 18	5 – 7	22

Table 3.1: Rough estimation of required crest heights under Hurricane Katrina induced wave conditions

In order to be able to evaluate the concepts, a general safety standard is needed. The safety standard will be set on the fact that no overtopping is allowed at primary levee section directly bordering the urban areas and also no overtopping is allowed at the secondary levees.

To gain insight in the required safety adjustments in each conceptual design, several calculations should be made on the required crest heights and construction materials. As settlement and sea level rise accumulate in time, these parameters should also be included in the calculations. It must be noted that settlement could be important as the levees will have to be constructed on (former) marshlands. The need for higher crests will inevitably lead to more extensive settlement, demanding even higher construction heights.

In this thesis, the alternatives will only be evaluated on a qualitative basis. The quantification of alternative requirements by performing the stated calculations is set to be outside the scope of this thesis. However, some general remarks can be made. Crest height are expected to be high, largely caused by the high storm surge and the long peak wave periods. These long wave period lead to high wave run-up and overtopping values. Ways to reduce the run-up are to adjust the angle of the slope or the roughness of the revetment. A steeper slope results in a higher crest height and on the other hand a less steep slope leads to a wider base. This leads to the effect that there is little different in total required dike construction material between both options. In respect to the settlement prone subsoil in the study area, a less steep slope is expected to be favorable as it will have a lower crest height. In addition, less steep revetments are better resistive against erosion.

3.5.3 'ComCoast' principle – generation of meso-scaled plan concepts

In this section, several conceptual spatial designs will be discussed based on the five ComCoast solutions. Recapitulation of the main ComCoast solutions:

1. Load reduction → foreshore sea defence zone → reduction wave attack
 - *Foreland protection*: To build a sustainable defence in front of the primary defence to provide a brackish area between the defences for habitat or farming practices.
 - *Foreshore recharge*: Eroded sediments are replaced by pumping dredged materials on top of the eroded foreshore. The dredging would otherwise be dumped at sea and lost. The new sediments reinforce the natural flood defence and also help to restore habitats for wildlife.
2. Load admitting → landward sea defence zone → management of water behind the dike
 - *Overtopping defence*: Making the defence resistant to wave overtopping and ensuring that any water that is washed over the top can be temporarily stored and drained away.
 - *Managed realignment*: Allow tidal water to flow onto the coastal floodplain to reduce surge and tide levels. The inter tidal zone may silt up keeping (more or less) pace with sea-level rise and land subsidence.
 - *Regulated tidal exchange*: Allow tidal inundation of the coastal floodplain in a controlled manner. This creates a transitional zone where land can evolve over time into a more saline environment. The transitional zone may silt up keeping more or less pace with sea level rise and land subsidence.

The concept regulated tidal exchange is not further investigated it includes regulated inundation of the transitional area, which is not favorable as this would increase the salinity in these wetlands. The other conceptual spatial designs generally follow the ComCoast strategy and provide protection by either strengthening of the existing protective levee system or by advancing partly into Lake Borgne.

1. *Zero alternative = overtopping defence of primary levee;*
2. *Zero (-) alternative = overtopping defence of secondary levee, which is a form of managed realignment*
3. *Land reclamation alternative = foreshore recharge;*
4. *Breakwater alternative = foreshore protection;*

One of the main causes of flooding of New Orleans was the failure of floodwalls along the IHNC. This failure is predominately subscribed to the funnel shaped levee configuration in the west of Lake Borgne. As a result, several concepts are determined that close of this part of the GIWW/MRGO levee stretch. These concepts are loosely based on two basic principles in Dutch flood protection as noted in section 2.2: shortening of the primary shoreline (first line of defense) to increase it defensibility and the reclamation of land (shortening of wind fetch):

5. *Floodgate(s) alternative, alignment I = shortening of primary shoreline*
6. *Floodgate(s) alternative, alignment II = shortening of primary shoreline and reclamation of 'land'*
7. *Floodgate(s) alternative, alignment III = shortening of primary shoreline and reclamation of 'land'*

Concepts that provide protection by either strengthening of the existing system or advancing into Lake Borgne:

1. Zero alternative

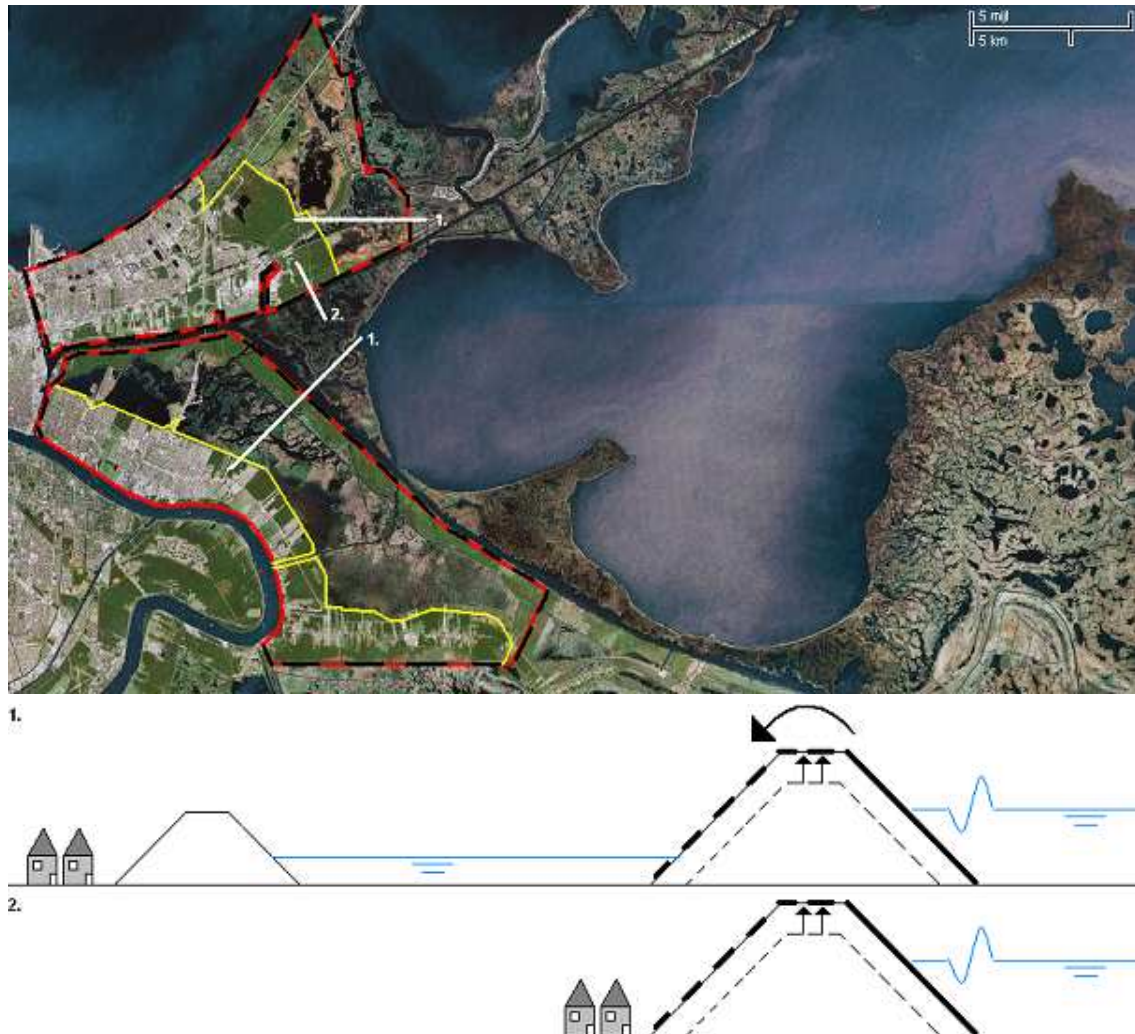


Fig. 3.13: Zero alternative

In this case, hurricane protection is provided by both a primary and a secondary levee. The primary levee is heightened and strengthened to such a level that it can handle large overtopping values. Heightening of the secondary levee will only be needed to increase the storage capacity in order not allow overtopping into the populated areas. The crest and inner slope of the primary levee section backed by a secondary levee need to be overtopping resistant. Then overtopping is allowed as much as the transitional areas are able to store. The crest height for these sections can then be calculated either by limitation of the overtopping discharge or by restriction of the water level inside the transitional area. The primary levees directly adjacent to the populated areas need to have a sufficient crest height in order to prevent overtopping.

Overview of the main characteristics of this alternative:

- As can be seen in figure 3.13, the funnel shaped levee configuration is still present since this alternative only heightening exist levees. Water levels in the IHNC can still rise significantly, which has severe consequences for the floodwall and levees at the east side of the Orleans West Parish. These will have to be strengthened and heightened in order to prevent overtopping.
- In general, the total primary levee system of both Orleans East Parish and St. Bernard Parish need to be adjusted. This adjustment requires a large amount of construction material. Since this material is not readily available in the area, it would make this alternative expensive.
- Adjustment of the primary levee along the MRGO would require expensive modifications to the outlet structures at Bayou Dupree and Bayou Bienvenue.

- When earthen levees are raised with additional earth fill, it can typically only be heightened by increasing the width at the base. In both protected areas, the land has been developed right up to the base of the existing levee. Therefore, raising and widening of the primary levee system would require private property to be purchased and buildings to be removed. Local opposition to such use of land is almost always considerable.
- This alternative could be undesirable for a psychological reason as people in the populated areas of New Orleans want to *feel* safe again. It is likely that the people want to see that the approach in hurricane protection has changed. As levees did not provide the protection people were told to believe, it is possible that an alternative considering only strengthening of the existing levee systems is generally rejected.

2. Zero (-) alternative

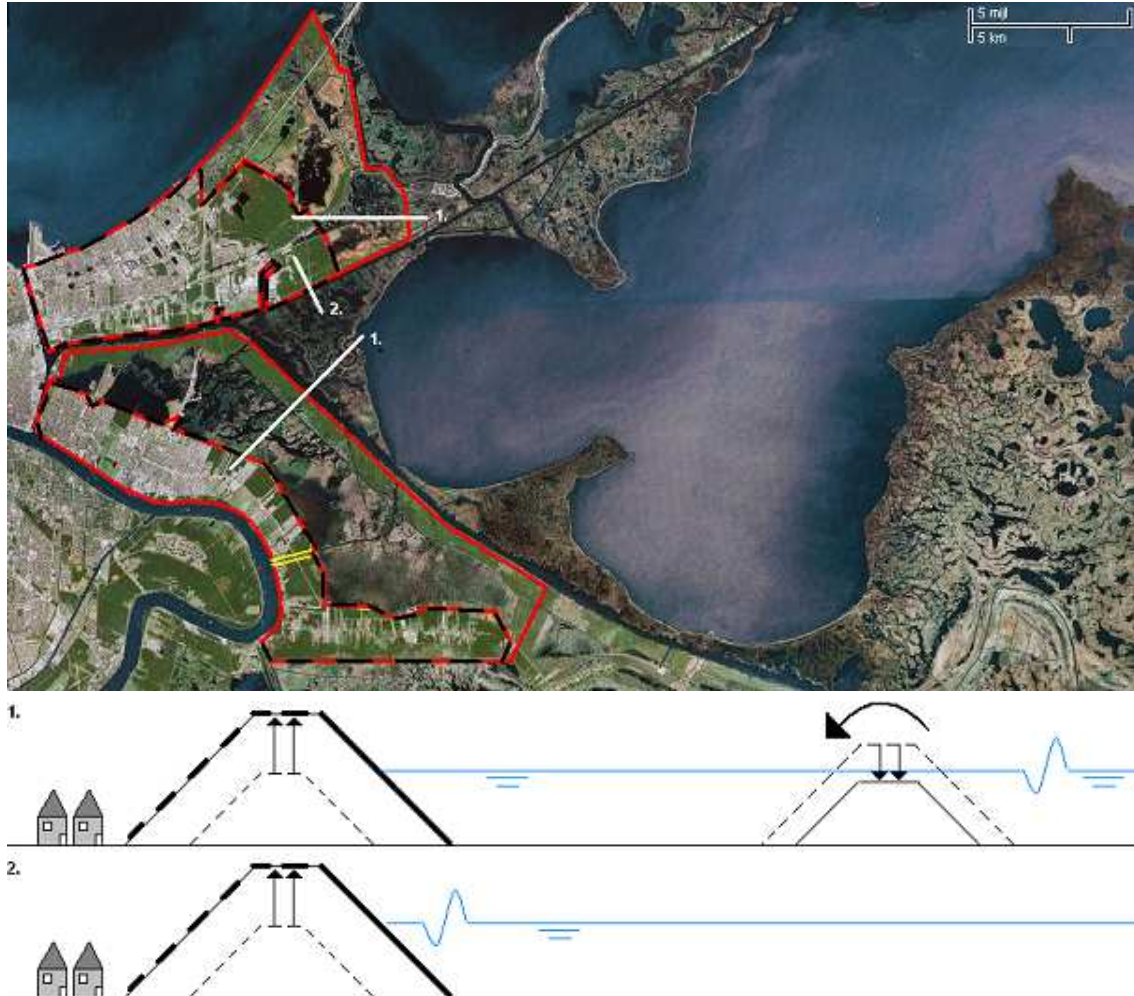


Fig. 3.14: Zero (-) alternative

In this alternative, the primary levee system is not adjusted. It proposes only strengthening of the secondary levees. In this new situation, the secondary levee will have to act as a new primary levee since it now becomes the main line of levee defense. Essentially, this zero (-) alternative is the opposite of the zero alternative, as it has a reversed parallel system. In this zero (-) alternative, the weakest levee section is placed on as a first levee defence and the stronger levee section as the second levee defence.

The change in levee positioning seems to be minimal at first sight but does have several critical consequences:

- This alternative is not consistent with the multiple lines of defence strategy. The main protection levee is now located directly adjacent to the populated areas. Therefore, this alternative lacks redundancy.
- As can be seen in figure 3.14, the funnel shaped levee configuration is still present but has changed considerably. In this case it is even worse as this new levee configuration allows water from Lake Borgne to directly impact the floodwalls and levees at the east side of the Orleans West Parish.

- As the primary protection levees are relatively weak and will only prevent minimal protection to surges from Lake Borgne, the surge waters are expected to completely fill the transitional areas even in moderate hurricane storms. This devaluates the natural retaining opportunity these areas provide.
- The height of the secondary levee need be extensively enhanced in order to accommodate the demand that no overtopping is allowed into the populated areas. At this moment, the existing secondary levees have a height of 6 ft (1.8 m, MSL) for Orleans East Parish and 7.5 to 10 ft (2.3 to 3.0 m, MSL) for St. Bernard Parish, well below the 18 ft (5.5 m, MSL) of the existing primary levees. It is therefore less favorable to heighten the secondary levees, as this requires considerably more construction material and costs.
- In this zero (-) alternative, land has been developed right up to the base of the total levee system that needs to be adjusted. Thus the zero (-) alternative would require even more private property to be purchased or removed than the zero alternative.
- As the existing primary levee along the MRGO is left in its original state, no expensive modifications to the outlet structures at Bayou Dupree and Bayou Bienvenue are required in this zero (-) alternative.
- Like in the zero alternative, the approach in hurricane protection has not changed. It is possible that an alternative considering only strengthening of the existing levee systems is generally rejected by people.

3. *Land reclamation alternative*

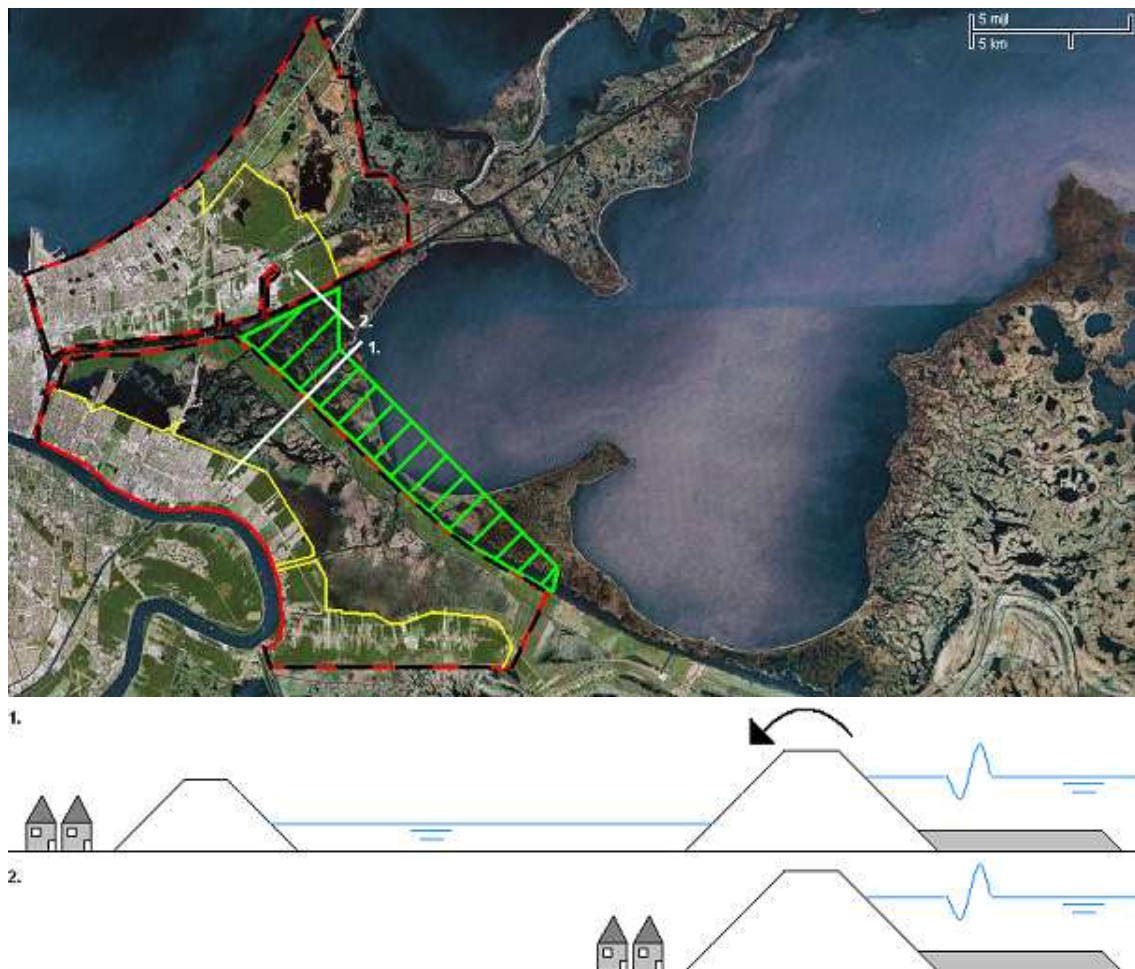


Fig. 3.15: *Land reclamation alternative*

In this alternative, the land directly in front of the primary levees adjacent to Lake Borgne is replenished. The theoretical basis of this alternative is the fact that when waves approach shallow grounds, bottom friction will decrease their speed and wave length. As a result, the waves will get higher and steeper. At a certain point the waves will get too steep and will start to break. Then a lower wave is admitted.

When waves cross a shallow area, the height of the admitted waves strongly depends on the water depth. The dependence can be expressed in a general rule of thumb that the maximum significant wave height in the area is equal to 0.5 times the water depth [Schiereck, 2004]. With this formula, an indicative calculation can be made to determine the actual benefit of the landfill:

*The average depth of Lake Borgne at the toe of the landfill is 7 ft. The maximum storm surge for Hurricane Katrina is equal about 15 ft. Therefore the maximum water depth in the event of a major hurricane is about 22 ft. According to the formula, entering waves will break when their wave height is larger than $22 * 0.5 = 11$ ft. This is larger than the actual wave conditions which state a significant near shore wave height of 5 to 7 ft and a peak wave period of 7 to 16 s. At first sight, this makes the land reclamation alternative still applicable.*

However, as can be seen in figure 3.15, there is still a vegetated stretch of marsh land between Lake Borgne and the MRGO. This small stretch of land will become submerged under the hurricane induced storm surge. Assuming this small stretch of marsh has an elevation of 2 ft above mean sea level

*The maximum water depth in the event of a major hurricane is now reduced to 13 ft. According to the formula, entering waves will break when their wave height is larger than $13 * 0.6 = 7.8$ ft. This is larger than the actual wave conditions which state a significant near shore wave height of 5 to 7 ft and a peak wave period of 7 to 16 s. At first sight, this makes the land reclamation alternative still applicable.*

It follows that the application of this alternatives depends on the actual surge level and the reduction induced by the existing stretch of marshland. If this stretch has an elevation of over 3 to 4 ft above mean sea level at the given surge level, the incoming waves will break before hitting the MRGO levee system.

Overview of the main characteristics / difficulties of this alternative:

- Besides the actual benefit of the landfill, a second direct question is the preservation of the waterways. Extending a landfill from the primary levee section of both protected area will essentially block off both the GIWW and MRGO. Although it is possible, maybe even wanted, to block off the MRGO, the GIWW provides a navigable passage from Texas to Florida and needs to be kept open. Therefore, additional measures are needed in order to protect the GIWW from silting up caused by the sediments that originate from the landfill.
- The actual configuration of the foreshore is difficult to determine. It depends on its construction height, length and vegetation. It is expected that large amounts of sediment will be needed to create a landfill capable of reducing the wave attack on the primary levee. An advantage is that local relatively poor material can be used compared to the construction material needed for the levee adjustments. Therefore the material will be much cheaper.
- Nature can benefit from these regained wetlands. If growth of vegetation is stimulated, new marshes can be created. However, a vegetated foreshore can have both positive and negative effects depending on time [7]:

Positive effect:

Storm surge propagation is dominant when the wetlands/foreshores are still dry and emerged above the water level. The friction force caused by the vegetation works in the opposite direction of the flow. The vegetated areas can therefore delay the storm surge. If it delays the surge longer than the duration of the storm, it can reduce the surge height at the protection levees.

Negative effect:

In the process of wind setup, the wetlands are already submerged. The wind pushes the water of the large flooded area against the levees. Eventually an equilibrium state will be reached between the wind drag force and the gravitational force. The gravitational force depends on the gradient of the water level. When looking at the velocity profile, one can see that the water will flow into the direction of the levee at the surface and in opposite direction at the bottom. This is caused by the fact that the wind pushes water onto the levee at which point it will disperse downwards and flow back as a return current at the bottom of the water column. This process is shown in figure 3.16. If the return flow is obstructed by dense vegetation, it is possible that this results in even higher water surges levels at the levee systems.

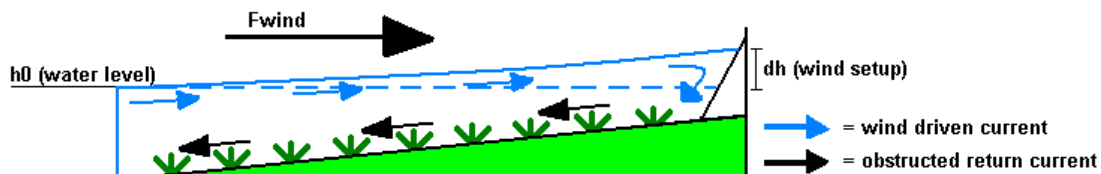


Fig. 3.16: The process of wind setup over vegetated wetlands [7]

- As can be seen in figure 3.17, the funnel shaped levee configuration is still present. The effect of the landfill on the funnel is expected to be minimal as the storm surge could still raise the water level within the IHNC.
- In general, the total primary levee system of both Orleans East Parish and St. Bernard Parish need to be adjusted. This adjustment requires a large amount of construction material. Since this material is not readily available in the area, it would make this alternative expensive.
- Adjustment of the primary levee along the MRGO would require expensive modifications to the outlet structures at Bayou Dupree and Bayou Bienvenue.
- Land has been developed right up to the base of a large part of the primary levee system that needs to be adjusted. This alternative requires an equal amount of private property to be purchased or removed as in the zero alternative.

4. Breakwater alternative



Fig. 3.17: Breakwater alternative

In this alternative a breakwater is constructed in Lake Borgne at a certain distance from the primary levee system of the Orleans East Parish and St. Bernard Parish. The breakwater principle can either comprised of a large breakwater or a series of smaller breakwaters. The basis of this alternative is the fact that waves will break on the breakwater, losing their energy before hitting the primary levee system. The dissipation of energy leads to lower overtopping values.

Overview of the main characteristics / difficulties of this alternative:

- Depending on the extent of energy dissipation, strengthening of the crest and inner slope of the primary levees on the protected side of the breakwater can be eliminated. For Orleans East Parish, only the New Orleans East Back Levee and Lake Pontchartrain fronting levees would need additional strengthening in that case. For the St. Bernard Parish, the southern protection levee near Caernarvon needs to be further investigated. However, for the Hurricane Katrina event this levee section provided sufficient protection even in the absence of additional strengthening.
- One large breakwater would be relative expensive in contrast with several smaller breakwaters. A series of smaller breakwaters is expected to lead to extensive wave diffraction. The superposition of waves diffracting around multiple breakwaters could lead to the build up of additional wave amplitudes, requiring additional shoreline stabilization. Further investigation is needed at this point, but outside the scope of this thesis.
- In order to gain sufficient reduction, the breakwater must be designed at nearly the same height of the water elevation of during the storm surge. This requires a large amount of stones of different sizes. The severe hydrological boundary conditions, expressed in a high significant wave height and long wave period, demand a large stone size on the slopes of the breakwaters in order to provide stability. On the other hand, the generally weak soil layers providing the foundation of the breakwaters require smaller sized stones in order to provide sufficient bearing capacity. Generally stated, the larger heavy stones will sink in the soft soil layers of Lake Borgne. A complex filter bed will be needed for the breakwater alternative in order to reduce settlement and increase the life span of the construction. Both the demand of large quantities of stones not readily available in the area and the complexity of the required filter bed are significant disadvantages in relation to this alternative.
- As can be seen in figure 3.17, the funnel shaped levee configuration is still present. The effect of the breakwaters on the funnel is expected to be minimal as the storm surge could still raise the water level within the IHNC.
- Although the primary line of levee defence is reduced with half of its length and also no expensive modifications to the outlet structures at Bayou Dupree and Bayou Bienvenue are required, these savings are not expected to counterbalance the costs of the breakwaters needed in this alternative.
- This alternative requires the least amount of property to be purchased or removed as only the New Orleans East Back Levee and the levee stretch fronting Lake Pontchartrain would have to be strengthened.

Concepts that provide protection by closing off the funnel shaped levee configuration in the west of Lake Borgne:

5. Floodgate(s) alternative, alignment 1



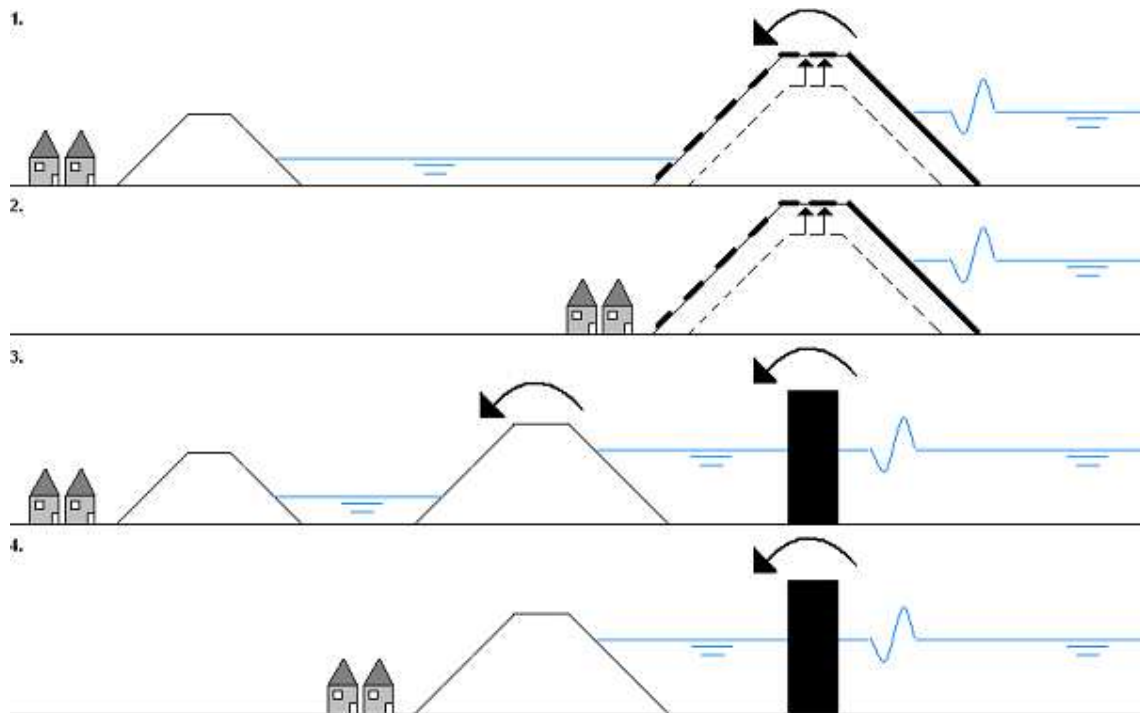


Fig. 3.18: Floodgate(s) alternative, alignment I

The essence of this alternative is shortening of the primary levee system by the implementation of a floodgate. In this alternative, the floodgate is projected within the GIWW/MRGO reach just east of the Paris Road Bridge, as can be seen figure 3.18.

The location of the floodgate has several consequences:

- This alternative would only require one floodgate. The floodgate needs to be navigable as is in located within the GIWW, but should be able to close in the event of storm surges.
- The floodgate provides the possibility to close off the direct connection of between Lake Borgne and Lake Pontchartrain. At this moment, as a result of this connection, the surge experienced within the IHNC and the combined GIWW/MRGO reach is a function of storm surge in both lakes. This is true for both low and high storm surge conditions. The floodgate alternative provides the option to control the flow in this way.
- Another point in relation to the primary levees is that the location of the floodgate does not eliminate the funnel effect. The primary levees along the south side of the Orleans Parish and the northeastern side of the St. Bernard Parish can still locally collect and focus storm surge depending on wind speed and direction. This localized focusing effect can lead to a local increase in storm surge amplitude, demanding for an expensive, non-economical floodgate design.
- The location of the floodgate can also be related to the multiple lines of defence system. By projecting the floodgate relatively far within the heart of the city, the highly populated New Orleans East protected area is still exposed directly to the Lake Borgne induced storm surges. The main protection measure (floodgate), therefore the direct water threat, is pulled towards this populated area, preventing redundancy and thus increasing risks by similar crest heights.
- The location of the floodgate still demands for large portions of the primary levee system of both protected areas to be adjusted. For this reason, the demand for construction materials is still high, even with the proposed floodgate.
- Adjustment of the primary levee along the MRGO would require expensive modifications to the outlet structures at Bayou Dupree and Bayou Bienvenue.
- Land has been developed right up to the base of a large part of the primary levee system that needs to be adjusted. This alternative requires still a lot of private property to be purchased or removed.

6. Floodgate(s) alternative, alignment II

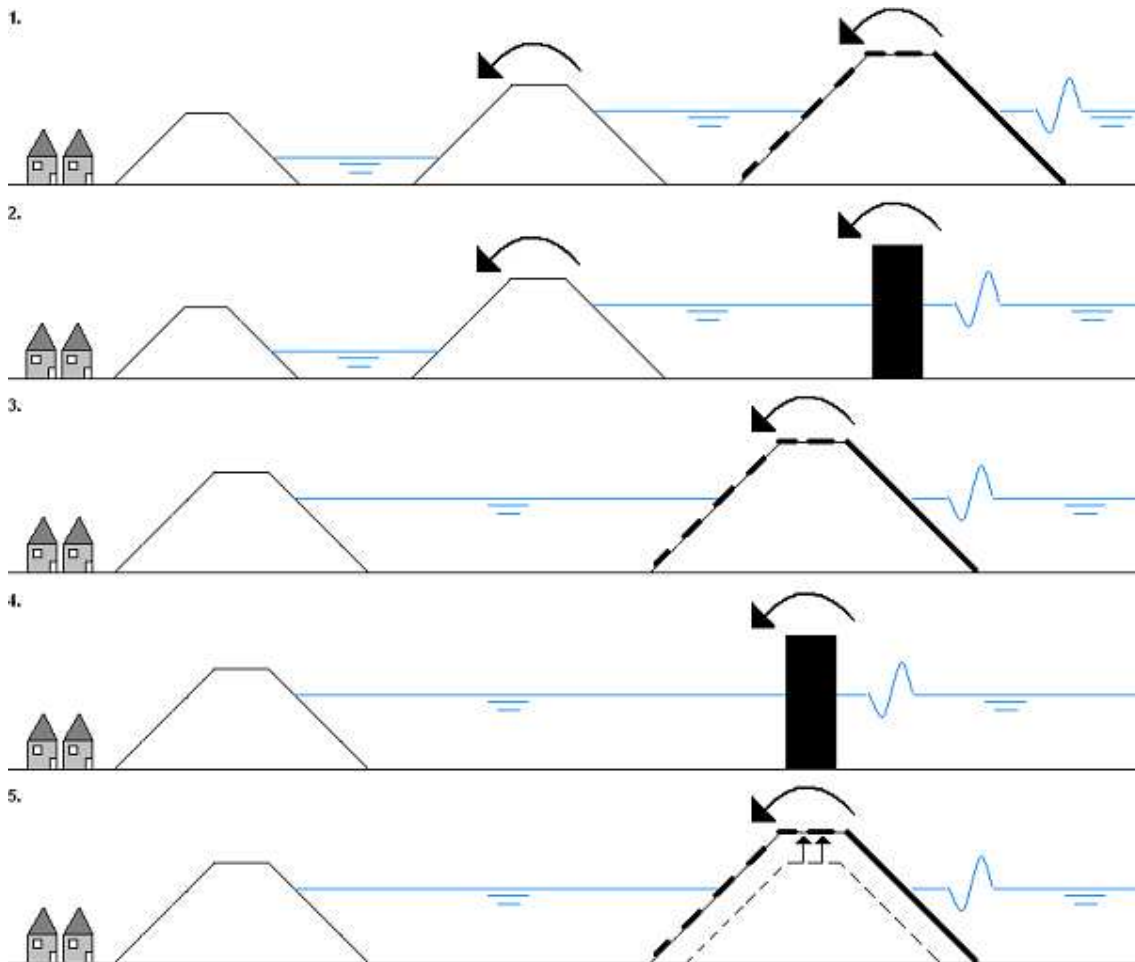


Fig. 3.19: Floodgate(s) alternative, alignment II

This alternative combines the implementation of a defence structure with the multiple lines of defense strategy. As can be seen in figure 3.19, this alternative plans for an extra line of defence. The planned levee alignment spans from the New Orleans East Back Levee in the New Orleans East protected area to the primary levee along the MRGO, just south of the Bayou Dupree outlet structure.

This proposed alignment has significant consequences:

- The alternative requires one floodgate in the GIWW and possibly another one in the MRGO. This latter connection of the new alignment to the primary levee system bordering the St. Bernard Parish is still an open question. It is possible to close off the MRGO, to allow only shallow draft shipping vessels or to sustain the channel's deep draft dimensions, all requiring a different connection at this certain point. Section 4.4 will further elaborate the issues concerning the future of the MRGO.
- The total length of primary levee is reduced significantly in this alternative, further reducing the risks since a smaller total length means a smaller area of possible failure.
- The floodgate(s) provide the possibility to close off the direct connection of between Lake Borgne and Lake Pontchartrain. As can be seen in figure 3.19, the levee alignment between the two connections eliminates the funnel shaped levee configuration. Lake Borgne induced surge level can not reach the IHNC anymore.
- The demand for construction material is relatively large since the new alignment can not be constructed over an existing levee system. This would make the alternative expensive. However, the new alignment does not have to provide absolute protection. Overflow is allowed as much as the combined transitional areas are able to store. Diversion, either in levee height or inlet structure, would have to be constructed to allow water to enter the transitional areas of the parishes before entering their populated areas.
- By including both the Bayou Dupree and Bayou Bienvenue outlet structure within the protected area, adjustments of these structures are not needed as the levee crest heights of this inner section of the primary levee system can be maintained.
- This alternative requires the least amount of property to be purchased or removed as only the New Orleans East Back Levee and the levee stretch fronting Lake Pontchartrain would have to be strengthened.
- An ecological advantage lies in the creation and preservation of an area of marshland between the existing primary levee systems and the new levee alignment. Fresh water diversion from the Mississippi River via the Bayou Dupree outlet structure will fuel the revitalization and growth of the marshland.

7. Floodgate(s) alternative, alignment III



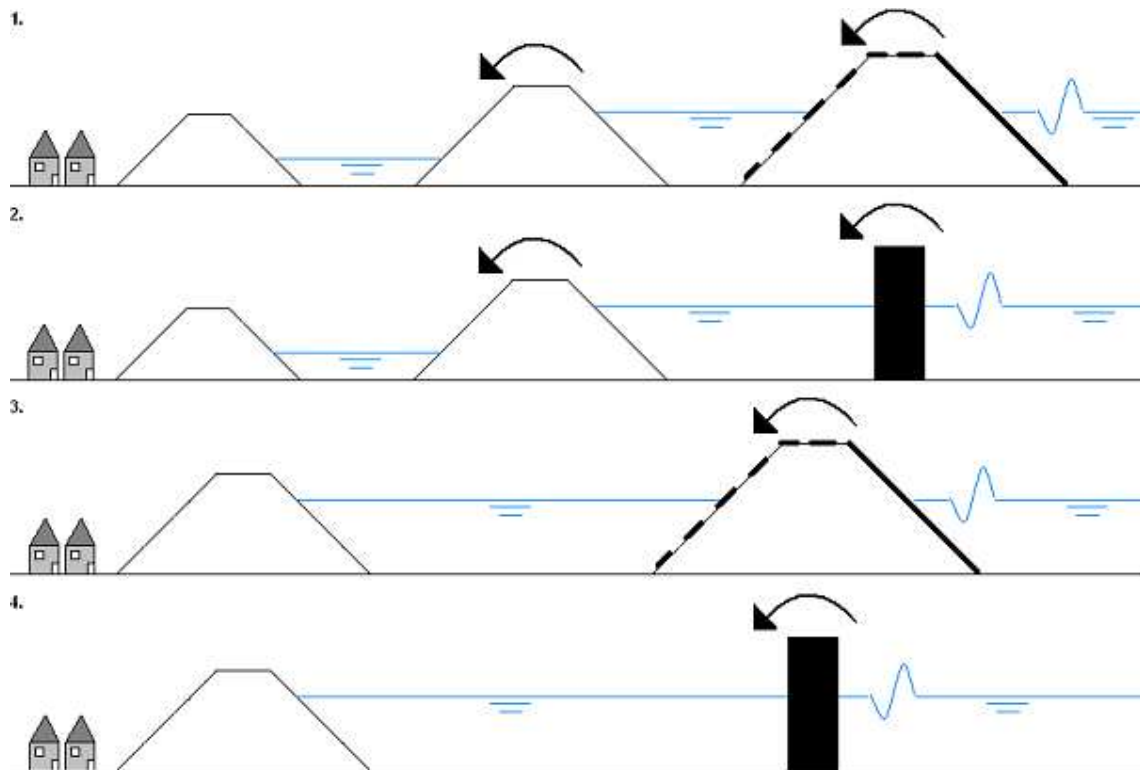


Fig. 3.20: Floodgate(s) alternative, alignment III

Also this alternative combines the implementation of a defence structure with the multiple lines of defense strategy. As can be seen in figure 3.20, this alternative plans for an extra line of defence which extends even further than alignment II. Alignment III plans for an extra line of levee defence that spans all the way from the New Orleans East Back Levee towards the southeastern levee section of the St. Bernard Parish.

This proposed alignment has significant consequences, although most of them are equal those for alignment II:

- The alternative requires one floodgate in the GIWW and possibly another one in the MRGO. This latter connection of the new alignment to the primary levee system bordering the St. Bernard Parish is still an open question. It is possible to close off the MRGO, to allow only shallow draft shipping vessels or to sustain the channel's deep draft dimensions, all requiring a different connection at this certain point. Section 4.4 will further elaborate the issues concerning the future of the MRGO.
- The total length of primary levee is reduced significantly in this alternative, further reducing the risks since a smaller total length means a smaller area of possible failure. Compared with alignment II, the total length of this new alignment is roughly the same.
- The floodgate(s) provide the possibility to close off the direct connection of between Lake Borgne and Lake Pontchartrain. As can be seen in figure 3.20, the levee alignment between the two connections eliminates the funnel shaped levee configuration. Lake Borgne induced surge level can not reach the IHNC anymore.
- The demand for construction material is relatively large since the new alignment can not be constructed over an existing levee system. This would make the alternative expensive. However, the new alignment does not have to provide absolute protection. Overflow is allowed as much as the combined transitional areas are able to store. Diversion, either in levee height or inlet structure, would have to be constructed to allow water to enter the transitional areas of the parishes before entering their populated areas.
- The surface area of the newly retained transitional area is larger than for alignment II, allowing the new alignment to have a slightly smaller strength/height.
- By including both the Bayou Dupree and Bayou Bienvenue outlet structure within the protected area, adjustments of these structures are not needed as the levee crest heights of this inner section of the primary levee system can be maintained.
- This alternative requires the least amount of property to be purchased or removed as only the New Orleans East Back Levee and the levee stretch fronting Lake Pontchartrain would have to be strengthened.

- An ecological advantage lies in the creation and preservation of an area of marshland between the existing primary levee systems and the new levee alignment. Freshwater diversion from the Mississippi River via the Bayou Dupree outlet structure will fuel the revitalization and growth of the marshland. The surface area of the newly retained transitional area that can be used for the development of these marshlands is even larger than for alignment II.

3.5.4 Evaluation of concepts

The proposed concepts are evaluated by means of a multi criteria evaluation, which divides the used criteria in four main categories:

High water safety

- Performance during higher loads than design loads: What are the consequences if the hydraulic loads exceed the design loads? If this would lead to failure, to what extent would it be?
- Adaptability: Is it possible to adjust the proposed defence system if risk or safety levels change in the future?
- No-regret: Is it possible to undo the engineering actions? To what level is it still possible to add other defensive solutions in the future?

Construction costs

- Construction and maintenance: what will be the costs for both construction and maintenance of the project?
- Impact on populated areas: to what extent need property to be purchased or removed.
- Construction materials: What is the availability of the construction materials?

Ecological influence

- What is the impact on the existing ecological system? Will the adjustments preserve the valuable wetlands?
- Salt water intrusion: as wetlands are suffering of increased salt water intrusion, to what extent will the proposed adjustments interfere with the salt and fresh water distribution?

Economical impacts

- Accessibility and disturbance: To what extent will the construction works disturb the infrastructure in the area? Will roads or navigation channels be blocked off during either realization phase or construction phase.
- Will the actual construction lead to any economical opportunities or will it be a drawback for the economical development of the area?

First step is to determine the mutual importance for these four main criteria with the use of a simple matrix. If the criterion in the column of the matrix is more important than the criterion in the corresponding row, a 1 should be noted. If the row criterion is more important, a 0 should be noted. Summation of the horizontal row determines the overall importance of the criteria. The process is presented in table 3.2. It can be concluded that the criterion 'high water safety' is the most important criterion.

	A	B	C	D	Weight Factor (WF)
A: High water safety	1	1	1	1	3
B: Construction costs	0	1	0	1	1
C: Ecological influence	0	1	1	1	2
D: Economical impacts	0	1	0	1	1

Table 3.2: Mutual importance of the stated criteria

Second step is the determine scores for each concept with respect to each of the discussed criteria. The scores are given by values between 1 and 5, where 1 means 'most negative and 5 means 'most positive'. An overview of the scores is given in table 3.3. The total score is determined by incorporating the determined weight factor.

	WF	1	2	3	4	5	6	7
<i>High water safety</i>	3							
– Design level exceedance		3	1	2	3	4	5	5
– Adaptability		3	2	4	5	3	3	3
– No regret		4	4	3	4	2	4	4
<i>Construction costs</i>	1							
– Construction / maintenance		4	4	3	2	3	2	1
– Impact on populated areas		2	1	2	5	4	5	5
– Availability of materials		3	3	2	1	3	2	2
<i>Ecological influence</i>	2							
– Preservation of wetlands		3	1	4	3	3	4	5
– Salt water intrusion		2	1	2	3	2	4	4
<i>Economical influence</i>	1							
– Accessibility & disturbance		3	4	1	2	2	2	2
– Economical opportunities		2	2	4	3	3	3	3
<i>Overall rating</i>		54	39	51	61	52	66	67

Table 3.3: Master plan concepts on meso scale – multi criteria evaluation

- | | |
|---------------------------------|--|
| 1. Zero alternative | 5. Floodgate(s) alternative, alignment I |
| 2. Zero (-) alternative | 6. Floodgate(s) alternative, alignment II |
| 3. Land reclamation alternative | 7. Floodgate(s) alternative, alignment III |
| 4. Breakwater alternative | |

3.6 Principal conclusions

It can be concluded that the floodgate alternative following alignment III holds the most general benefit. It only just scores better than the similar alternative following alignment II. The difference is caused by the gained transitional area, which is larger in the case of alignment III. This transitional area can be used as retention area for overtopped floodwater. A larger surface area thus means a larger storage volume and an increased safety. On the other hand, the costs of this alternative are slightly higher as more material is required to build the straight levee alignment through Lake Borgne. Additional investigation, in both economical and probabilistic safety sense, is needed to make a proper distinction between all alternatives but between these two in particular. This investigation is set to be outside the scope of this thesis. It can be concluded at this point that alternatives 6 and 7 score significantly better than the others. The differences between these two alternatives are only of a limited influence on the design of the flood protection structures as these structures are located at similar positions.

The third floodgate option scores relatively low, mainly to the fact that the funnel effect still exists and no additional line of defence is created for most of the populated areas. This causes it to score lower on the high water safety criteria than the other floodgate alternatives. As more primary levee length is present in this alternative, maintenance is expected to be intensive. The breakwater alternative scores relatively high in this multi criteria evaluation. This is mainly caused by its high water safety and expected positive ecological influence. However, both effects should be investigated more thoroughly in order to justify the given scores and to provide insight in the performance. Waves and surge levels, although decreased, could still damage the primary levee system and enter the non-closed funnel. Finally, the zero (-) alternative scores significantly lower than the others. This alternative scores relatively low on every criterion. In particular the design level exceedance criterion is of importance. No redundancy exists in this alternative as Lake Borgne induced surge level could directly enter the IHNC via a broad stretch of water.

In conclusion, for the part of the Hurricane Barrier Plan directly adjacent to Lake Borgne it is recommended to implement two flood protection structures in combination with a new, straight levee alignment between them. The alternative is presented in figure 3.22. This alternative has the best high water safety and the most positive ecological influence. It is intended to close off the IHNC, forming a first line of man-made defences against storm surges from Lake Borgne to the east. This line of defense would thereby substantially reduce high water and wave action against the interior levees and floodwalls, potentially reducing the costs of future upgrades, maintenance and associated repairs to the system. In addition it accommodates a larger retention area than the curved alignment.

Until now, it was assumed that the flood protection structures would be navigable floodgates at both locations but this is still open for investigation. For this reason, chapter 4 evaluates alternative options.

4. Evaluation Of Barrier Concepts Within Master Plan: *Meso To Micro Scale*

The sections in this chapter outline an evaluation of barrier concepts within both the Gulf Intracoastal Waterway (GIWW) and the Mississippi River Gulf Outlet (MRGO). Section 4.1 presents the location of both barriers and general site parameters. Section 4.2 presents the main boundary conditions on barrier level, including navigation characteristics. It also discusses the assumptions and constraints concerning these boundary conditions. Section 4.3 presents a functional program of requirements on barrier level. Finally, section 4.4 presents the evaluation of the barrier concepts for both locations.

4.1 Location of the flood protection barriers and general site parameters

The proposed flood gates and levee alignment present modifications of the existing Hurricane Protection System (HPS) of New Orleans, in particular the Lake Pontchartrain and Vicinity Project, a system of federal and non-federal levees, floodwalls and pump stations providing protection for the populated areas of New Orleans. The Inner Harbor Navigation Canal (IHNC) appears to have been vulnerable to Hurricane Katrina, contributing to levee and floodwall failures and flooding of adjacent interior areas. As stated earlier, the chosen master plan is intended to close off the IHNC, forming a first line of man-made defences against storm surges from Lake Borgne to the east. Within this chosen master plan, two locations were considered for the construction of a flood protection structure. Figure 4.1 presents the location of these structures, which will perform as connections between the new alignment and the current levee systems in both Orleans East Parish and St. Bernard Parish.

An overview of the main characteristic of both locations:

- Flood protection structure within Gulf Intracoastal Waterway (GIWW):
The new levee alignment will be connected by the flood protection structure to the New Orleans East Back Levee, currently at a height of +18.0 ft (5.5 m, MSL). This section of the GIWW forms the northern boundary of Lake Borgne. The stretch of the GIWW between New Orleans and Mobile Bay is near to straight and has a depth of 18 ft (5.5 m, MSL), a bottom width of 300 ft (91 m) and a surface width of about 600 to 700 ft (185 to 215 m). The channel is directly connected to Lake Borgne and will experience some tidal variation. The influence of it is relatively small and neglected in this thesis, as the tidal range is about 1.0 ft (0.3 m).
- Flood protection structure within Mississippi River Gulf Outlet (MRGO):
The new levee alignment will be connected by the flood protection structure to the southeastern levee section of St. Bernard Parish, currently at a height of +18.0 ft (5.5 m, MSL). This section of the MRGO forms the southeastern boundary of Lake Borgne. It was authorized to a depth of 36 ft (10.9 m, MSL), a surface width of 650 ft (198 m) and a bottom width of 500 ft (152 m).

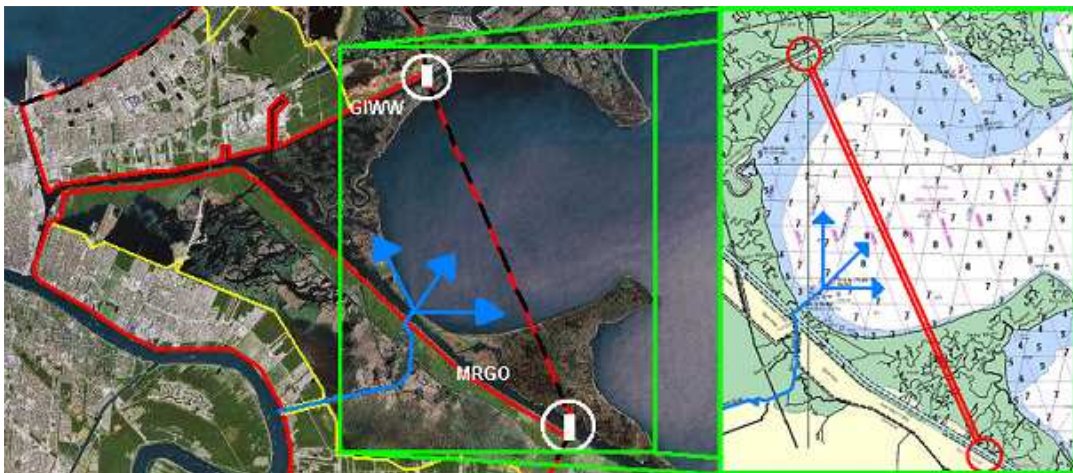


Fig. 4.1: Projected location of both flood protection structures in combination with the local bathymetry of Lake Borgne

This thesis has its focus on the flood protection structures. The levee systems in both parishes are set to be outside the scope of this thesis. For the design of the projected levee alignment in Lake Borgne, the crest height and overflow discharge is calculated in order to determine the surface area elevation of the retention area. This calculation is outlined in section 6.4.3.

4.2 Boundary conditions, assumptions and constraints

The boundary conditions for the evaluation of the barrier concepts are divided into three parts: main hydraulic conditions for Hurricane Katrina, navigation considerations and environmental considerations. These parts are described subsequently in the following sections.

4.2.1 Hydraulic conditions – analytical validation of the hydrodynamic modeling results for Hurricane Katrina

The traditional methods of assessing the frequency of occurrence of hurricanes, dependent primarily on historical data, are too simplistic to capture important characteristics of the hurricane hazard such as time- and space-dependent storm intensity and track patterns. In case of a hurricane in a complex bathymetry, the height of a storm surge depends on many parameters and is therefore difficult to predict. Extensive modeling provides insight into how water surrounding a complex physical system responds to a complex hurricane wind system.

USACE – IPET: Hydrodynamic modeling results for Hurricane Katrina [31]

The ADCIRC storm surge model is used by the USACE-IPET to characterize the storm surge climate produced by Hurricane Katrina. High water marks were used to confirm the accuracy of these model results. In this section, peak wave and water level conditions experienced during Hurricane Katrina are compared to values used in design of the existing Hurricane Protection System (HPS) and to these high water marks. Noted should be that:

- In the series of figures that follow, design values are shown in yellow boxes (label D), values computed by model are shown in blue (label C) boxes and measured values are shown in green boxes (label M).
- Design water levels are cited, not design crest elevations of the protection system levees and floodwalls.
- For wave conditions, design documents cited significant wave height but did not specify whether a peak or mean period was used. At the time, distinction between measures of wave period was probably not made.
- The design documents cite water levels relative to different vertical datums. All design water levels were converted to the common datum NAVD88 (2004.65) for the purposes of comparison. To make this datum conversion from the design MSL, 0.5 ft (0.15 m) is added to the design water level values along the south shore of Lake Pontchartrain and 0.4 ft (0.12 m) is added to values in the vicinity of the GIWW and MRGO.
- For measured water level conditions at sites where hydrographs captured the peak water level, that value is presented. Where high water marks are available, those values are shown. If no high water marks are available in an area of interest, it is listed with a question mark following the listed elevation.

Figure 4.2 (left) presents wave maxima for the eastern section of Orleans Parish. In general, wave conditions generated by Hurricane Katrina were similar to design values for Lake Pontchartrain and the east facing levees. On the back levee along the GIWW, maximum wave heights computed for Katrina were less than design values. Peak wave periods exceed the design values by a factor of 3. These wave model simulations suggest that during Katrina the eastern facing levees were subjected to long period wave propagating in from the Gulf of Mexico. Figure 4.2 (right) presents water level maxima for the area. On the Lake Pontchartrain side, the peak water levels were at the design levels. Along the east facing levees, design water levels increased from 12.0 to 13.4 ft (3.6 to 4.1 m, NAVD88 (2004.65)) at the GIWW. High water marks acquired along this section near the GIWW suggest that design water levels were exceeded by amounts greater than 2 ft (0.6 m) at the southern end of this reach.



Fig. 4.2: Orleans East Parish: comparison of wave maxima (left) and water level maxima (right) with design values

Figure 4.3 (left) presents wave maxima for the eastern portion of St. Bernard Parish. Along the MRGO, the computed significant wave heights were less than design wave heights, but computed peak wave periods were 2.5 times greater. On the south facing portion of the protection levees, the computed significant wave heights computed less than design values by about 2.5 ft (0.8 m), but wave periods exceed design values by a factor of about 3. Design wave conditions at these locations are recommended to be reexamined.

Figure 4.3 (right) presents water level maxima for eastern St. Bernard Parish. Along the MRGO, design water levels ranged from 12.9 to 13.4 ft (3.9 to 4.1 m, NAVD88 (2004.65)). Computed maximum water levels range from 15.4 to 16.8 ft (4.7 to 5.1 m, NAVD88 (2004.65)), reaching about 3 ft (0.9 m) higher. Considered together, model and measured data sources suggest that Katrina peak water levels exceeded design levels by 2 to 5 ft (0.6 to 1.5 m) along the section.

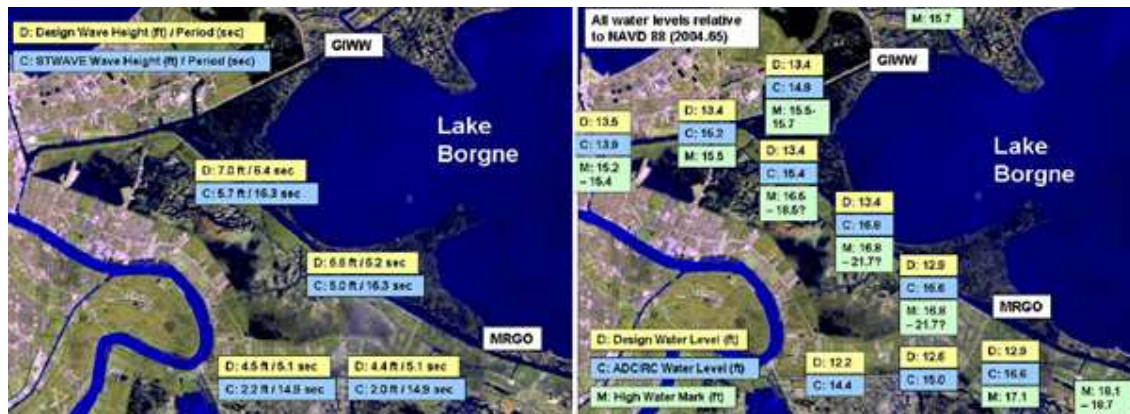


Fig. 4.3: St. Bernard Parish: comparison of wave maxima (left) and water level maxima (right) with design values

Important to note is that both measured and calculated storm surge levels are significantly higher than the design levels in both cases. Calculated wave maxima are generally lower than the design maxima. During the peak of the hurricane, the ARCDIC model predicts storm surge heights a few decimeters lower than the water mark observations. The ARCDIC model is known to underestimate the water levels, partly because it neglects wave setup. In conclusion, one should carefully use the outcome of those hydraulic models as input for calculations where there is a lack of observation data for calibration of these models. To gain a better understanding of the results that originate from these complex hydraulic models, an analytical validation is presented in Appendix B.

Conclusion on the analytical validation of the hydrodynamic modeling results for Hurricane Katrina

The validation can be divided in wave conditions offshore, wave conditions near shore and wind setup:

- In comparison to the regional WAM-model results presented in figure B.2 of Appendix B, the SMB-model for oceanic waters predicts a lower value of both wave height and wave period. As expected, the SPM-model is more suitable for the determination of the offshore conditions associated with a hurricane.
- The SMB-model for coastal waters predicts a higher wave height in comparison to the basin scale WAM-model results presented in figure 4.4. These results could be caused by the fact that the SMB-model does not include the limited depth induced processes of shoaling, refraction and diffraction. The SMB-model predicts and wave height of about 7 s, equal to the lower boundary of the WAM-model results. It is interesting to note that the upper boundary of 16 s corresponds quite well with the generated offshore wave conditions by using the SPM-model. This confirms that during Hurricane Katrina the eastern facing levees adjacent to Lake Borgne were subjected to long period wave propagating in from the Gulf of Mexico.

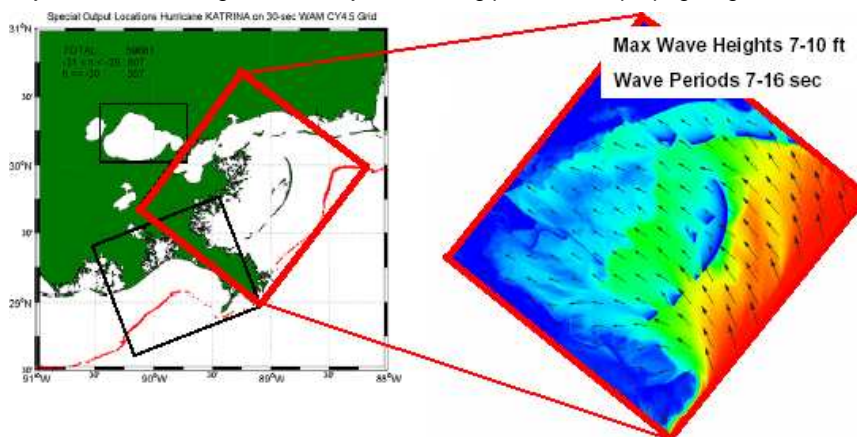


Fig. 4.4: Near shore wave conditions – basin scale WAM model [31]

- In comparison to the basin scale ARCDIC-model storm surge results presented in figure B.5, the used model predict the wind setup well for both offshore and near shore conditions. When waves enter coastal waters, their surge level significantly increases by the limiting water depth, which is represented in the model results.

4.2.2 Navigation considerations

The navigation considerations are divided into two parts: main navigation options around New Orleans and vessel traffic characteristics. These parts are described in this section respectively.

Main navigation options around New Orleans

The busy Port of New Orleans provides a gateway for imports and containerized goods. Thousands of ocean vessels from Europe and other parts of the World move through New Orleans every year. Figure 4.5 provides an overview of the main navigation options around New Orleans. The Port of New Orleans is located within the IHNC and can be reached from the Gulf of Mexico by two main deep draft routes:

- The first and primary route is via the Mississippi River, which may be accessed by ships using Southwest Pass or South Pass. A Federal project provides access to the Head of Passes for a 40 ft (12.2 m, MSL) deep channel through Southwest Pass and for a 17 ft (5.2 m, MSL) deep channel through South Pass. The project also provides for a 40 ft (12.2 m, MSL) deep Mississippi River navigation channel from Head of Passes to New Orleans. Final access from the Mississippi River to the Port of New Orleans is via a 640 ft (195 m) long, 75 ft (22.8 m) wide lock at New Orleans. Sill depth at the lock is 31.5 ft (9.6 m, MSL) at low water. The existing lock is a vital link in the nation's inland waterway navigation system. It connects the Mississippi River with the GIWW, MRGO, IHNC and Lake Pontchartrain.
- A second route to the Port of New Orleans is via the MRGO, a 76 miles (122 km) long channel that extends northwest from deep water in the Gulf of Mexico to the IHNC at New Orleans. This Federal project provides for channel depths ranging from 36 to 38 ft (10.9 to 11.5 m, MSL).



Fig. 4.5: Main navigation options around New Orleans

There are no bridges or cables across the Mississippi River below New Orleans. One bridge and two cables cross the MRGO below the junction with the IHNC at New Orleans. The Paris Road Bridge spans the stretch of the MRGO contiguous with the GIWW and is located 4.3 miles (6.9 km) east of the junction with the IHNC. Figure 4.6 presents its location and characteristics. It is a fixed bridge with a clearance of 135 ft (41.1 m). The overhead power cables across the canal near the Paris Road Bridge have a clearance of 170 ft (51.7 m).

In the current situation, deep draft navigation is possible via the stated main routes. Shallow draft navigation could also use these routes but has several alternative options as presented in figure 4.5:

- The GIWW has an authorized water depth of 18 ft (5.5 m, MSL) and is therefore only suitable for shallow draft navigation. It provides a protected waterway around the main part of the Gulf Coast. At several points along its routes, it is possible for shallow draft vessels to use a direct navigable waterway as a short cut towards the Gulf Of Mexico;
- Regarding the access of the Mississippi River, shallow draft is not restricted to either the Head of Passes or Southwest Pass and could also use several alternative access channels.
- Shallow draft vessels could navigate Lake Pontchartrain, which has a maximum water depth of 14 ft (4.3 m, MSL). At the Rigolets Pass, several bridges span this stretch of water connecting Lake Pontchartrain to Mississippi Sound. Figure 4.6 present the characteristics of these bridges. The minimum vertical clearance of all bridges is determined by the new Rigolets Pass Bridge at 72 ft (21.9 m).

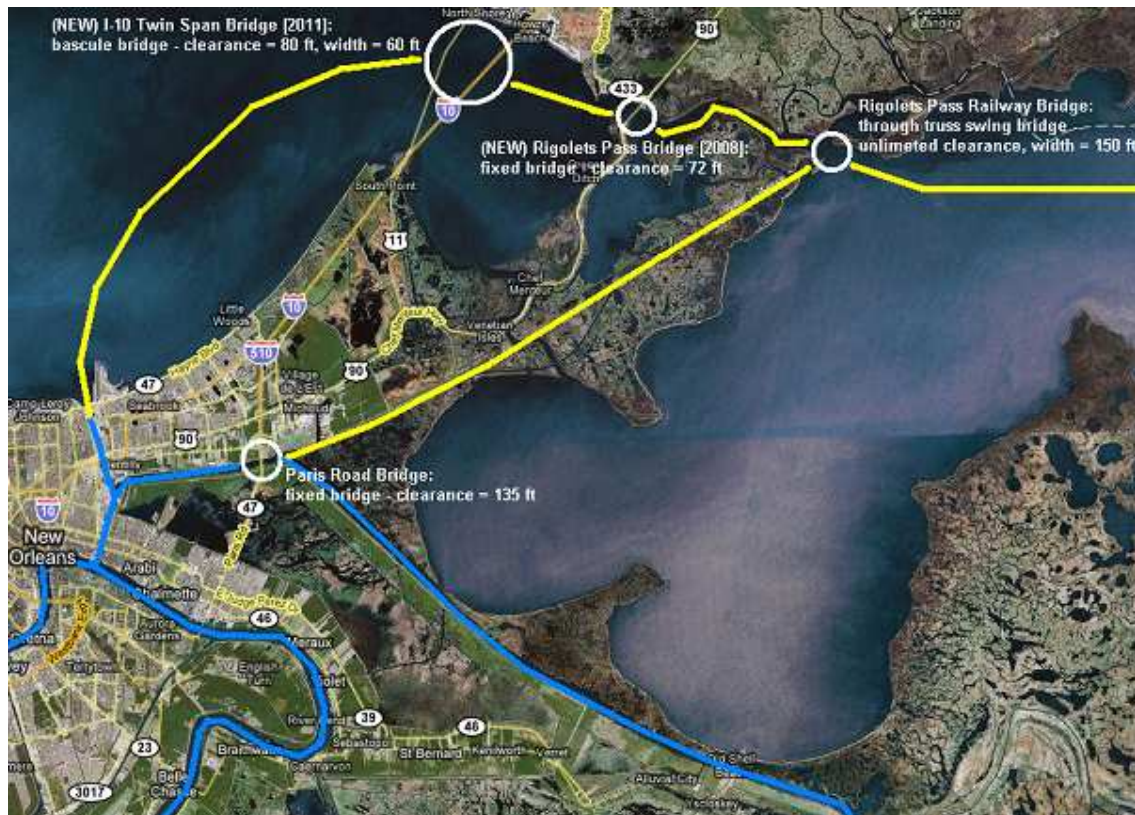


Fig. 4.6: Characteristics of the bridges spanning the Rigolets

Although the MRGO provides a second route to the Port of New Orleans of about 40 miles (64 km) shorter than primary route via the Mississippi River, the use and benefits of it are under heavy debate. As a relatively large federal public works project, the construction of the MRGO provided an initial surge in regional employment. However, since the channel's opening in 1963 its usage by the shipping industry has been less than anticipated and traffic has been well below original projections. The MRGO has provided a conveyance path for regional barge traffic, but the lower Mississippi still leads shipping commerce in southeast Louisiana. It provides more than 40 percent of the region's annual freight tonnage, whereas the MRGO comprised only 3 percent of this commerce in the period 1997 to 2005 [5]. The maintenance expenditures for the MRGO have risen over time and the USACE now estimates dredging costs at \$12.5 million per year. It is therefore instructive to look at the actual vessel traffic that uses this channel in order to determine whether these investments are legitimate.

Vessel traffic characteristics

Before evaluating the actual vessel traffic on both the GIWW and MRGO, the main inland vessel characteristics are discussed. In Europe, each river corresponds to a certain class which refers a maximum vessel size. In other words, navigation requirements are completely defined by specifying the river class. A world wide classification of vessels, including associated waterways is developed by PIANC (Permanent International Association of Navigation Congress). An overview of this PIANC classification is presented in table 4.1.

Type of inland waterway	Classes of navigable Waterways	Motor vessels and barges				Min. required clearance height [m]
		Type of vessel: general characteristics				
		Length [m]	Beam [m]	Draft [m]	Tonnage [T]	
Of regional importance	I	38.5	5.1	1.8 - 2.2	250 - 400	4.0
	II	50 - 55	6.6	2.5	400 - 650	4.0 - 5.0
	III	67 - 80	8.2	2.5	650 - 1,000	4.0 - 5.0
Of international importance	IV	80 - 85	9.5	2.5	1,000 - 1,500	5.25 - 7.0
	Va	95 - 110	11.4	2.5 - 2.8	1,500 - 3,000	5.25
	Vb	-	-	-	-	7.0 - 9.1
	Vla	-	-	-	-	7.0 - 9.1
	Vlb	140	15.0	3.90	-	7.0 - 9.1
Type of inland waterway	Classes of navigable waterways	Pushed convoys				Min. required clearance height [m]
		Type of vessel: general characteristics				
		Length [m]	Beam [m]	Draft [m]	Tonnage [T]	
Of regional importance	I	-	-	-	-	3.0
	II	-	-	-	-	3.0
	III	118 - 132	8.2 - 9.0	1.6 - 2.0	1,000 - 1,200	4.0
Of international importance	IV	85	9.5	2.5 - 2.8	1,250 - 1,450	5.25 - 7.0
	Va	95 - 110	11.4	2.5 - 4.5	1,600 - 3,000	5.25
	Vb	172 - 185	11.4	2.5 - 4.5	3,200 - 6,000	7.0 - 9.1
	Vla	95 - 110	22.8	2.5 - 4.5	3,200 - 6,000	7.0 - 9.1
	Vlb	185 - 195	22.8	2.5 - 4.5	6,400 - 12,000	7.0 - 9.1
	Vlc	270 - 280 193 - 200	22.8 33.0 - 34.2	2.5 - 4.5 2.5 - 4.5	9,600 - 18,000	9.1
	VII	195 - 285	33.0 - 34.2	2.5 - 4.5	14,500 - 27,000	9.1

Table 4.1: Classification of waterways and associated design vessels [source: PIANC]

The vessel traffic records below are provided by the Waterborne Commerce Statistics Center (WCSC):

Gulf Intracoastal Waterway (section New Orleans to Mobile Bay):

Year	Total Tonnage (x 1000)	Self-Propelled Vessel Trips: Loaded Draft Increment (ft)						Tows and Barges		Total Vessels
		13-15	11-12	9-10	7-8	≤ 6	Sub-total	Towboats	Barges	
2001	20,841	12	53	1,279	182	9,516	11,042	9,280	19,774	40,096
2002	20,524	2	70	76	107	11,153	11,408	9,197	18,999	39,604
2003	20,875	49	22	39	222	9,749	10,081	9,849	18,439	38,369
2004	21,808	32	69	5,768	538	3,797	10,204	8,664	19,123	37,991

Table 4.2: Vessel traffic on the Gulf Intracoastal Waterway for the section New Orleans to Mobile Bay [source: WCSC]

The WCSC defines shallow draft as having loaded drafts of less than or equal to 18 ft (5.5 m), while deep draft is defined as having loaded drafts over 18 ft (5.5 m). Note: The USACE commonly uses the definition of deep draft vessels contained in ER-1105-2-100, which defines deep draft as vessels requiring greater than 14 ft (4.3 m). This latter definition is used in this thesis.

The vessel traffic along this stretch of the GIWW, presented in table 4.2, is near to constant in this four year period at about 38,000 to 40,000 trips per year. The transported tonnage, essentially the economical benefit of the GIWW, even increases in this period.

Commercial navigation on the overall GIWW primarily involves tow barge transport of bulk cargo. At certain stretches, the early authorized dimensions (12 ft deep, 125 ft wide at the bottom) limit barge tows to a length of five barges and a width one barge, ranging from 50 to 54 ft (15.2 to 16.5 m) wide by 200 to 300 ft (61 to 92 m) long. Any larger combinations can not negotiate the curves. It should be noted that this limitation is only the part of the stretch of the GIWW to the west of New Orleans. Vessels moving from New Orleans to the east could have larger dimensions. The design barge for this part of the GIWW consists of a pushed convoy combination of 3 barges wide by 5 barges long [USACE, 2006], which has a width of 105 ft (32.0 m) and length of 1,055 to 1,095 ft (320 to 335 m), depending on towboat length. As most vessels move along a significant part of the GIWW, it is expected that the majority of the vessels passing the flood protection structure is composed of traffic equal of smaller than the stated 5x1-barges combination.

Important to note is the fact that the maximum height of all larger commercial vessels is 9.1 m, equal to about 30 ft. Reflecting on figure 4.6, it can be concluded that this clearance height can be used as design criteria. The bridges spanning the Rigolets Pass provide a clearance height of at least 72 ft (21.9 m), assumed to be sufficient for recreational sailing vessels, or other shallow draft vessel requiring significant clearance, to use this as an alternate route for this particular stretch of the GIWW. Since the stretch of the GIWW between New Orleans and Mobile Bay is widened to a bottom width of 300 ft (91 m), barges wider than the stated 54ft (16.5 m) could easily navigate it. This is expressed in a design vessel with a width of 105 ft (31.9).

Mississippi River Gulf Outlet:

Year	Total Tonnage (x 1000)	Self-Propelled Vessel Trips: Loaded Draft Increment (ft)						Tows and Barges		Total Vessels
		34-36	30-33	21-29	19-20	≤ 18	Sub-total	Towboats	Barges	
1970	4,013	16	83	275	80	1,017	1,471	1,225	2,113	4,809
1980	5,541	62	259	744	88	4,951	6,104	1,315	1,540	8,959
1990	6,960	48	214	559	105	391	1,317	1,110	1,883	4,310
1995	5,701	18	230	589	40	186	1,063	620	1,326	3,009
1996	5,042	76	283	503	67	133	1,062	519	982	2,563
1997	5,253	136	400	520	64	2,677	3,797	696	1,098	5,591
1998	4,007	98	277	487	42	796	1,700	462	665	2,827
1999	5,369	117	342	532	48	381	1,420	296	652	2,368
2000	5,850	193	358	590	49	351	1,541	188	657	2,386
2001	4,173	117	282	468	25	658	1,550	377	414	2,341
2002	3,290	83	222	310	10	1,068	1,693	488	409	2,590
2003	2,847	34	99	346	18	1,405	1,902	692	1,303	3,897
2004	1,206	8	13	266	13	1,672	1,972	448	164	2,584

Table 4.3: Vessel traffic on the Mississippi River Gulf Outlet (source: WSCS)

The dominant vessel type in the MRGO is the container ship, in contrast to dry bulk carriers and tankers dominating the Mississippi River. Vessel sizes up to Panamax move through the MRGO. This categorizes a 106 ft (32.5 m) beam and lengths of 750 ft (220 m) for bulk carriers and 950 ft (280 m) for container ships.

Comparison of tonnage volumes for the most recent period of record (2002–2004) with the previous comparable period (1999–2001) shows current volumes down by nearly 50 percent. While total tonnage declined, the percentage of foreign freight maintained a larger share of total tonnage than domestic freight. In spite of these distributional changes, the overall trend line illustrates a downturn for all traffic and tonnage. The 2004 volumes represent an historical low before declining even further in 2005 after Hurricane Katrina. As stated before, the total tonnage transported especially expresses the economical benefit of the waterway.

The pre-Katrina declines were driven by a variety of factors. The MRGO authorized depth of 36 ft (10.9 m) is shallow in comparison to other U.S. Gulf Coast deep draft channels and the current dimensions of the IHNC Lock are the main contributors to the pre-Katrina decline. These limitations of the MRGO likely impeded commercial navigation growth during periods of significant increases in the sizes of large vessels serving U.S. ports. The lack of funds for operational and maintenance dredging during the 1990s is also likely to have contributed to declining trends. In addition, no dredging has occurred on the MRGO since Hurricane Katrina.

Section 4.4.2 discusses the influence of the downturn for all traffic visible in the MRGO traffic records with regard to its future as (deep draft) navigation route towards the Port of New Orleans

4.2.3 Environmental considerations

Information on the hydrological and morphological regime of both waterways is not available at the moment of this thesis. Therefore assumptions are made for both waterways with regard to the discharge of water, discharge of sediments and the preservation of environmental values.

By constructing a new levee alignment across this particular part of Lake Borgne, an additional transitional area is created for the use of water retention. Figure 4.7 present this retention area as part of the chosen master plan. The implementation of this new levee alignment has several significant consequences:

- *Discharge of water*
Water can enter the projected retention area either through diversion from the Mississippi River for the restoration of wetlands via Bayou Dupree (bottom circle in figure 4.7) or as pumped out rainfall runoff from the urban areas via Bayou Bienvenue (upper circle in figure 4.7). This excess water must be periodically discharged by the flood protection structure(s). The retention area also introduces the possibility that the inner water level exceeds the outer water level, causing a reverse differential head.
- *Discharge of sediments*
The discharge of sediment via both waterways is expected to be minimal in normal conditions. At discharging during high internal water level and low outside water level, the high differential head would cause high water velocity. This rush of water could cause scour/erosion and associated sediment transport if the velocity exceeds the critical velocity for scouring. These transported sediments are expected to accumulate just after the flood protection structure due to a steep decrease in particle velocity.
- *Preservation of environmental values*
Environmental values can in this case best be expressed in the preservation of wetlands. Figure 4.6 presents the straight alignment, which will form the outer boundary of a revitalized wetland area. The preservation of it depends mainly on the ability to discharge water from the area.



Fig. 4.7: Retention area for flood protection, retention of rainfall runoff and preservation of wetlands

4.3 Functional program of requirements on barrier concept level

The functional requirements needed in the evaluation of the barrier concepts at both the GIWW and MRGO can be divided into five main groups, including flood protection, navigation, the discharge of water, the discharge of sediments and the preservation of environmental values. Each of these groups is presented in combination with their main content:

Flood protection

- The flood protection structure forms an integral part of the works to protect the New Orleans against hurricane induced storm surges. The operation of the structure should therefore be coordinated within the overall protection plan for New Orleans.
- The risk of failure of the flood protection structure should not exceed a pre-determined probability of failure.
- Although a hurricane can be predicted a few days before its actual arrival, surge levels tend to rise well this moment. The floodgate structure should therefore be fully controllable at all design flow and wave conditions.
- The retention area demands for a flood protection structure with can accommodate reverse differential head.

Navigation

- In the case of implementation in a waterway maintained for navigation, the flood protection structure should provide a safe and smooth passage of vessel traffic during operation.
- During the construction of the flood protection structure, sequencing of its main components must be conducted to ensure sufficient flow opening and undisturbed navigation.

Discharge of water

- The flood protection structure must be able to periodically discharge excess water from the retention area in a controlled manner;

Discharge of sediments

- The flood protection structure must be able to withstand some degree of siltation as scouring of the upstream side of the structure could occur during the discharge of water at high negative differential head. Any transported sediments are expected to accumulate just after the flood protection structure due to a steep decrease in particle velocity. It is expected that sediments could be partly deposited at the structure.

Preservation of environmental values

- The flood protection structure must meet environmental impact criteria.

4.4 Barrier concepts at the Gulf Intracoastal Waterway and Mississippi River Gulf Outlet

This section analyses and evaluates the stated boundary conditions and general functional requirements of both flood protection structure concepts.

4.4.1 Gulf Intracoastal Waterway – navigable storm surge barrier

The GIWW forms a protected navigable waterway running approximately 1,050 miles (1,700 km) along the Gulf Coast between Texas and Florida. It links all of the Gulf Coast ports and enables these ports to access the inland waterway system. Near to 38,000 vessels pass along the stretch of the GIWW between New Orleans and Mobile Bay. This means more than 100 vessel passages per day, making it a highly navigated waterway. The total tonnage transported, thus the economical benefit, even increases over time. The GIWW should therefore remain open for navigation, which requires that a protection barrier in the form of a navigable floodgate structure is built.

4.4.2 Mississippi River Gulf Outlet – permanent closure for all navigation

The MRGO provides a shorter navigation route from the Gulf of Mexico to the Port of New Orleans facilities compared to using the Mississippi River to access the port. The channel extends from the IHNC in New Orleans to the 38 ft (11.6 m, MSL) depth contour in the Gulf of Mexico. The route of the MRGO is presented in figure 4.8. The stretch contiguous with the GIWW is the GIWW Reach (miles 66-60). Where the channel diverts from the GIWW and runs through wetlands is the Inland Reach (miles 60-23). The stretch through Breton and Chandeleur Sounds is the Sound Reach (miles 23-0). All reaches of the MRGO are authorized as a 36 ft (10.9 m, MSL) deep, 500 ft (152 m) bottom width waterway with the exception of the Bar Channel which is authorized at 38 ft (11.5 m, MSL) deep by 600 ft (182 m) wide.

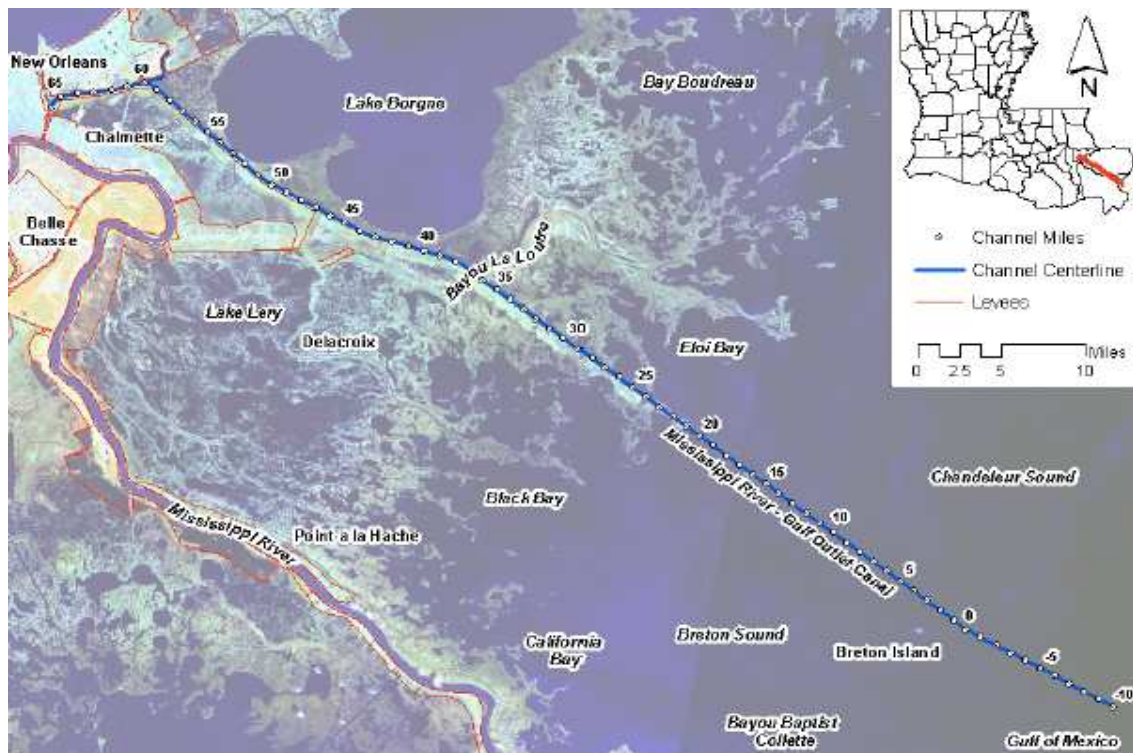


Fig. 4.8: Mississippi River Gulf Outlet – overview and mileage [38]

In 2000 the Environmental Subcommittee of the MRGO Policy Committee prepared a plan to address environmental impacts related to the construction, operation and maintenance of the MRGO [5]. The Committee proposed halting the channel dredging of the MRGO and only limited channel maintenance. These actions would close the MRGO only to oceanic vessels with a draft of more than 12 ft (3.7 m). Along with eliminating deep draft vessels, these initial proposals called for water control structures including floodgates, locks, weirs and sills to be strategically built along the MRGO. The effect of these structures was expected to reduce the potential for water inflow into marshes and bayous from the MRGO channel, thus reducing the potential for storm surges and saltwater intrusion. Clearly, the idea of closing the MRGO has moved beyond the conceptual stage. This particular section discusses permanent closure of the MRGO by focusing on its three main issues: storm propagation, preservation of (deep draft) navigation and its relation to the IHNC Lock Replacement Project.

Storm surge propagation in relation to the Mississippi River Gulf Outlet

Numerous people believe that the Inland Reach of the MRGO exacerbates storm surges in the region and that the MRGO was for a large part responsible for flooding of both St. Bernard and Orleans Parish during Hurricane Katrina. However, several studies indicate that this was not the case:

- A study by Bretschneider and Collins [1966] examined six different storm scenarios using one-dimensional numerical modeling. It concluded that Hurricane Betsy, which occurred in 1965 during the construction of the MRGO, would have produced the same storm surge elevations with or without the MRGO.
- In 2003, a study was completed by the USACE using two-dimensional Advanced Circulation (ADCIRC) modeling for storm surge. Nine different scenarios were modeled, both with and without the MRGO. The model runs demonstrated that the maximum difference in storm surge with and without the MRGO was just over 6 inches (0.15 m).
- Following Hurricane Katrina, the Interagency Performance Evaluation Task Force [IPET, 2006] studied the storm surge, performance of flood protection measures and the consequences of the hurricane. The IPET found that the MRGO had little influence on flooding in St. Bernard Parish during Hurricane Katrina. It concludes that when the marshes surrounding the MRGO are inundated, the water conveyed through the channel is a relatively small part of the total. The IPET report states that during Hurricane Katrina, the MRGO was far from the hurricane highway moniker with which it has been branded. It also concludes that high surge and long period waves overtopped the MRGO levees well before Hurricane Katrina made landfall.
- A study by the Louisiana Department of Natural Resources [2006] also evaluated the impact of the MRGO on storm surge using ADCIRC modeling. This study considered seven different scenarios. The conclusions were that the MRGO does not contribute significantly to peak storm surge during severe storms where the surrounding wetland system is overwhelmed with water. Another important conclusion is that closure would not provide significant, direct mitigation of severe hurricane storm surge.

Studies also demonstrated that the most noticeable effect of the MRGO occurs for small surge events, where the marsh areas are not completely inundated. Further storm surge modeling analyses are underway to consider scenarios with new structural flood protection features, such as levees and floodgates. Solutions to concerns regarding the impact of storm surge include a barrier construction, such as floodgates, at some points along the MRGO and partially or completely filling in the channel.

Conclusions of the MRGO Deep Draft De-Authorization Report [2006]

In 2006, a technical team of the USACE evaluated potential modifications to the current uses of the MRGO navigation channel with the intent of determining if any uses should be maintained. A wide range of initial alternatives was identified for development of this MRGO Deep Draft De-Authorization Report [38], including the total closure of the MRGO. The location of this closure was set to be at Bayou La Loutre (figure 4.11), a place providing relatively stable banks due to the existing natural ridge. Although the location of the proposed flood protection structure located about 10 miles upstream, it is assumed that the influences of both locations on the alternatives is comparable.

Alternative 0 – Future without de-authorization:

The existing MRGO Project was completed in 1968 at the authorized depth and width. Since its construction, the project has been maintained at various depths and widths. For the past years, the Inland Reach, Sound Reach and Bar Channel have not been dredged to full dimensions. Rather, the channel has been maintained for one-way traffic only. Due to shoaling the current controlling depth is approximately 22 ft (6.7 m, MSL). However, to determine whether it is economically feasible to maintain the MRGO Project and evaluate the environmental impacts for various levels of maintenance including closure, the future without de-authorization is assumed to be a project maintained at the authorized dimensions. All alternatives will be compared to this future condition.

Alternative 1 – Maintain a shallow draft MRGO navigation channel:

- *Alternative 1a – Maintain a shallow draft navigation channel without a structure:*
The MRGO would be maintained for commercial and recreational shallow draft navigation only with a depth and width of 12 ft by 125 ft. This alternative was developed to allow continued shallow draft navigation. It is likely to have only a very minimal effect on reducing salinity or storm surge in a tropical storm event. The only environmental benefit could be removal of deep draft vessels from the channel which could significantly reduce bank erosion.
- *Alternative 1b – Construct a salinity control weir at Bayou La Loutre:*
A weir would be constructed just south of Bayou La Loutre to allow passage of shallow draft vessels. The MRGO would be constricted at the weir to 125 ft wide by 14 ft deep. This alternative was developed to allow continued shallow draft navigation and to reduce salinity above the structure which could provide environmental benefits. Removal of deep draft could significantly reduce bank erosion.

- *Alternative 1c – Construct a salinity control gate at Bayou La Loutre (normally closed):*
A gated structure would be constructed just downstream of Bayou La Loutre that would allow passage of shallow draft vessels. The gated structure would have a sill depth of 14 ft and a 125 ft wide opening. The gate would normally be closed to reduce saltwater intrusion, but would be opened for passage of shallow draft vessels. This alternative was developed to allow continued shallow draft navigation and to significantly reduce salinity above the structure. By keeping the gate closed except when vessels are present, it could have the greatest salinity reduction of all the shallow draft alternatives. Removal of deep draft could significantly reduce bank erosion.
- *Alternative 1d – Construct a storm protection gate at Bayou La Loutre (normally open):*
This alternative comprises similar structural components and earthwork as Alternative 1c. This alternative was developed to allow continued shallow draft navigation, to reduce storm surge from tropical storm events and to reduce salinity above the structure. The gate would be operated to close the channel only for a tropical storm event and associated storm surge. Reduction of salinity could be similar to Alternative 1b. Removal of deep draft vessels could significantly reduce bank erosion.

Alternative 2 – Close the MRGO channel to deep draft and shallow draft vessels:

- *Alternative 2a – Construct a total closure structure across the MRGO at Bayou La Loutre:*
This plan was developed to remove both shallow and deep draft vessels from the MRGO, reduce salinity and tropical storm surge and allow the most compatibility with a freshwater diversion. It could reduce salinity more than any of the Alternative 1 options. Removal of deep draft could significantly reduce bank erosion.
- *Alternative 2b – Fill in the entire MRGO channel from the GIWW to the Gulf of Mexico:*
The entire MRGO would be filled from the intersection of the GIWW to Breton Sound. This alternative has been requested by several stakeholders and was frequently noted in public comments. Even recreational shallow draft would not be able to use any portion of the Inland Reach of the MRGO.

Alternative 3 – Cease all MRGO operations and maintenance activities:

If all activities related to maintaining the MRGO would be discontinued, no additional Federal funds would be used to maintain a minimum channel depth on of the MRGO. There would be neither construction nor operation and maintenance costs for this alternative. This was developed as the least cost plan. It would have no impact on storm surge in tropical storm events or salinity reduction. Removal of deep draft vessels could significantly reduce bank erosion.

Alternatives eliminated from further study:

- *Alternatives 1a – 1d:*
All of the alternatives identified that included maintenance of the MRGO channel for shallow draft navigation between the GIWW and the Gulf of Mexico were screened out based on economic analysis. The economic information available indicates that shallow draft traffic on the MRGO between the GIWW and the Gulf of Mexico is not cost-effective. The total average annual costs to maintain a 12 ft shallow draft channel between the GIWW and the Gulf of Mexico is approximately \$6 million, whereas the estimated annual benefits are approximately \$1.2 million.
- *Alternative 2b:*
This alternative was eliminated because of cost. A rough estimate is that it would take approximately 250 to 350 million cubic meters of dredged material to fill the channel from mile 60 to mile 25 at a cost of about \$2.8 billion. A rough estimate is that it could take from 15 to 44 years to fill the channel.

Evaluation and comparison of remaining alternatives:

Alternatives 2a and 3 were analyzed using comparable information. Then the alternatives were evaluated across a series of technical factors including environmental impacts, engineering and economics. Table 4.4 presents the main economics concerning the closure of the MRGO. A comprehensive review on this matter is presented in the MRGO Deep Draft De-Authorization Report. A brief summary comparison of Alternatives 2a and 3:

- *Alternative 2a – Construct a total closure structure across MRGO near Bayou La Loutre:*
 - Alternative 2a yields the most environmental benefits since it is likely that it could prevent a significant percentage of the net acres of marsh estimated to be lost over 50 years under the future without condition. A greater salinity reduction and vegetation change is anticipated to occur over a larger area;
 - Alternative 2a has the highest compatibility with other potential ecosystem restoration efforts, such as a fresh water diversion structure at Violet Canal (figure 4.8);
 - Alternative 2a yields the fewest average annual net economic benefits (estimated to be \$5.7 million) because all navigation benefits are lost as soon as the total closure structure is installed. Alternative 2a immediately closes the MRGO to all navigation, which eliminates the 'free' years of navigation benefits which could be realized prior to the channel filling in naturally. In addition, it requires and an initial investment. The estimated construction cost of the total closure structure is \$13,530,000.

If authorized and funded, Alternative 2a could be built in one construction effort lasting an estimated 170 days. Shallow draft vessel that use the MRGO as an alternate route when the IHNC is congested or unexpectedly closed could no longer do so.

– Alternative 3 – Cease all MRGO operations and maintenance activities:

- Alternative 3 has the fewest environmental benefits: it is estimated that slightly more marsh would be lost than under Alternative 2a, but significantly less than under the future without condition.
- Ecosystem restoration measures, such as a freshwater diversion structure at Violet, could be more difficult to implement than under Alternative 2a. Without a structure in the MRGO, a much larger freshwater diversion would be required at Violet Canal (figure 4.9), which would increase the costs and decrease the ability to control desired environmental results.
- Alternative 3 yields the greatest average annual net economic benefits (estimated to be \$6.8 million) because it requires minimal investment and shallow draft navigation benefits would only be limited by natural shoaling within the channel. Alternative 3 has no construction costs, except aids to navigation and channel markers would be considered for removal.



Fig. 4.9: Freshwater diversion at Violet Canal, St. Bernard Parish [34]

This alternative could be implemented almost immediately after Congressional authorization and appropriation. Shallow draft navigation would be affected over time because the channel would not be maintained. Shallow draft vessel that use the MRGO as an alternative route when the IHNC is congested or unexpectedly closed could no longer do so after about 2014.

	Total average annual costs (millions \$)		Total average annual benefits (millions \$)		Average annual net benefit (millions \$)
Alternative 2a:	construction costs of dam	0.7			
Close the MRGO to deep draft and shallow draft vessels (rock dam closure)	real estate costs	0.08			
	O&M costs of dam	0.1			
	monitoring costs	0.2			
	costs to deep draft traffic	2.5			
	costs to shallow draft traffic	1.2			
	removal of jetties	0.2			
	removal of aids to navigation	0.04			
	O&M foreshore / shoreline	1.8	Avoided 36 ft O&M	12.5	
		6.8		12.5	5.7
Alternative 3:	real estate costs	0.08			
Cease all MRGO operations and maintenance activities (discontinue dredging)	monitoring costs	0.15			
	costs to deep draft traffic	2.5			
	costs to shallow draft traffic	0.9			
	removal of jetties	0.2			
	removal of aids to navigation	0.04			
	O&M foreshore / shoreline	1.8	Avoided 36 ft O&M	12.5	
		5.7		12.5	6.8

Table 4.4: Main economics concerning the closure of the Mississippi River Gulf Outlet [34]

It can be concluded that closing the MRGO is the best option for the future, but an important point is the actual moment of this proposed closure. This will be outlined by reviewing the relation of the IHNC Lock to the aforementioned MRGO closure study.

4.4.3 Advised moment of implementation of the barrier concepts

As stated before, the final access from the Mississippi River to the Port of New Orleans is via the existing IHNC Lock, making it a vital link in the nation's inland waterway navigation system. Growth in waterway traffic over the years had made the IHNC Lock one of the nation's most congested locks with an average wait of 10 hours, but often as much as 24 to 36 hours. The basic problem is that the current lock is simply too small to accommodate the volume of existing and future traffic. Barge tows approaching 12 ft (3.6 m) of draft that move over the GIWW comprise most of the vessel traffic through the lock. Deep draft vessels using the existing lock are limited to 25 ft (7.6 m) draft range, well below drafts demanded of the majority of the present deep draft vessels. In addition, the existing lock requires extraordinary maintenance to continue its level of service.

These developments demanded that actions had to be taken concerning this obstruction in the navigation system around New Orleans, ultimately resulting in the HNC Lock Replacement Project. A general timeline of the main decisions concerning the IHNC Lock:

- The IHNC and IHNC Lock were completed by the Port of New Orleans in 1923 to provide navigation between the Mississippi River and Lake Pontchartrain, a distance of approximately 5 miles (8 km), in order to provide areas away from the Mississippi River for industrial development.
- The River and Harbor Act of 1956 authorized the MRGO. It also provided for the construction of a new lock and connecting channel when economically justified by obsolescence of the existing lock or by increased traffic. Studies were initiated in 1960 for a new lock and connecting channel, because at that time it was estimated that the lock would become dimensionally obsolete by 1970.
- In 1986, this development resulted in the design for a new lock with dimensions of 110 ft (33.5 m) wide by 1,200 ft (365 m) long, with a sill depth sufficient to permit access for vessels with drafts of 36 ft (10.9 m).
- A feasibility study, completed by the USACE in 1997, determined that a larger replacement lock was economically justified and pre-construction activities begun in 2001. The overall construction period for the project was estimated to span 10-12 years, although still heavily depending upon future funding levels.

The IHNC lock was impassable for 16 consecutive days after Hurricane Katrina in 2005. All vessels had to use the only alternate route available, which was via the MRGO. Each year on 2 to 3 occasions, vessels are forced to use the MRGO in order to avoid lengthy delays at the small lock due to high water and resulting traffic backup. At the same time, the mentioned MRGO De-Authorization Report [USACE, 2006] recommends a total, physical closure of the MRGO to all traffic. However, any effort to prevent the use of the MRGO as an alternate route to the IHNC Lock without a concurrent completion of the lock expansion project places a portion of the nation's economy that is dependent upon efficient inland barge transportation in the Gulf Region at risk.

At this point, it is recommended not to allow the total, permanent closure of the MRGO without coupling its timing to coincide with the completion of the IHNC Lock Replacement Project, which is projected to be completed in 2013. This provided an interesting option of combining both remaining alternatives in the mentioned MRGO closure study:

- Alternative 2a provides permanent closure of the MRGO, which is the most beneficial and is therefore advised to be implemented;
- Alternative 3 states that shallow draft navigation would be affected over time since the channel would not be maintained. Shallow draft vessel that use the MRGO as an alternative route when the IHNC is congested or unexpectedly closed could no longer do so after about 2014. This corresponds with the moment of completion of the IHNC Lock Replacement Project, making that it is possible for shallow draft navigation to use the MRGO up to the moment of permanent closure. This results in maximum economical benefit.

Depending on the construction time of the chosen master plan, it could be optimal to first build the flood protection structure within the GIWW and adjacent levee sections including the new alignment. After completion of the IHNC Lock Replacement Project, construction works on the closure of the MRGO will be started. Although this will leave the MRGO open for a longer period of time, storm surge propagation studies have shown that there is no noticeable effect of the MRGO for large storm surge events. The marsh land areas are completely inundated in such event and conveyance of water through the actual channel is not significant. The stated moments of implementation of the concepts is therefore advised.

5. Overview Of Navigable Flood Protection Structures For The Gulf Intracoastal Waterway

The sections in this chapter further analyze the flood protection structure within the Gulf Intracoastal Waterway (GIWW). Before determining if a certain floodgate type is appropriate for a specific location and operational requirements, it is necessary to define a program of requirements and constraints. Section 4.3 presented the main functional requirements for the flood protection structure. The technical requirements are presented in section 5.1. In this particular section also the navigable floodgate opening is determined, in order to apply this important characteristic in the evaluation of floodgate types. Section 5.2 presents an overview and comparative evaluation of different flood protection structures. Section 5.3 outlines the actual comparison of floodgate types, which is performed in the appliance of several killer requirements and on the basis of typical structural concerns. Finally, section 5.4 presents the gate selection rationale and conclusion.

5.1 Qualitative technical program of requirements

The technical program of requirements can be defined by using several key parameters and characteristics that relate to the location, environmental conditions, operation and forces. The quantification of this technical program of requirements is presented in chapter 6.

Location

- Positioning of the structure: The structure should be situated in a position that will minimize the crosscurrent in the areas where ships navigate the gate structure.
- Allowing a straight line for navigation: The structure should be situated to provide a straight line of sight with the gate structure navigational openings to facilitate incoming vessels to enter and exit the opening safely.
- Minimize the structure exposure to environmental loadings: The layout of the structure should minimize its exposure to environmental loading. The structure should be placed not facing the prevailing wind direction.
- Minimize the environmental impact to the surroundings: Modifications to the existing waterway should be selected in a way to minimize the environmental impact of the structure and its size. Ideally, the gate should be built at a site where there is a natural restriction.
- Easy access during construction and maintenance: Easy access to the site during the construction period and during its operation / maintenance is important to minimize the associated costs.

Environmental conditions

- Water discharge: The flow restrictions across the structure and its impact on the retention area should be considered. The structure must periodically discharge excess water from the in a controlled manner;
- Water level and tidal variation: The maximum water level difference between upstream and downstream for all possible scenarios including during an open/closed gate should be defined as it influences hydrodynamic pressure on the structure and the resulting currents and associated erosion of the river bottom.
- Wind magnitude and distribution: The design maximum wind for each of the main prevailing direction should be obtained, as it forms input for ship maneuvering and the effect of loss of control on the drift of the vessel.
- Adaptability: The design should be flexible in order to take into consideration of climatic changes.
- Morphology of the channel: The flood protection structure must be able to withstand some degree of siltation as scouring could occur during the discharge of water at a high negative differential head or during closure of the gate in case of a rapid surge level increase.

Operational requirements

- Protection level: some degree of leakage flow past the sides of the gate is acceptable. Even some overflow is acceptable provided that the gate reduces flood levels sufficiently in the protected area.
- Navigation: The floodgate structure should allow the safe passage of the largest vessel class that is expected to transit the particular stretch of the Gulf Intracoastal Waterway (GIWW). The passage of the structure should be smooth to accommodate the high level of vessel traffic (*). The currents in the channel should be below the critical speed that would create a safety risk to the vessel while passing the structure. During the construction of the flood protection structure, sequencing of its main components must be conducted to ensure sufficient flow opening and undisturbed navigation.

- **Debris protection:** The presence of debris and its accumulation along the face of the structure should be prevented as it can hinder the safe operation of the gates and associated equipments.
- **Erosion and scouring:** The erosion due to local currents generated by waves or from vessel movements close to the structure should be minimized. Opening of the gates also generates local currents that should be considered during the design of bottom scour protection at upstream and downstream ends of the structure.
- **Operation time:** Design gates to be ready for operation within an acceptable preparation time.
- **Maintenance:** The gates and its main elements need to be accessible for inspection and maintenance.

Forces

- **Environmental forces:** The structure should be designed to withstand the hydrostatic pressure during the maximum differential head. In addition, the structure should be fully controllable at all design flow and wave conditions, including reverse differential head conditions;
- **Winds forces:** The structure should withstand the wind effect on loads. The loads include drag forces, wind generated waves including associated waves slamming forces and additional hydrostatic pressure.
- **Ship collision:** The structure should be designed to take into account the impact forces resulting from ship collision. This presents a loading with a low probability but potentially with high consequences.
- **Foundation resistance:** The foundations should be capable of resisting the forces applied by the environment and structural dead weight. The total settlement of the structure should not exceed the allowable settlement.
- **Operating forces:** Friction forces need to be considered where applicable as neglecting or underestimation of these friction forces may lead to floodgate failure.
- **Structural deterioration:** The structure should be designed to resist wear and corrosion and ensure that its structural integrity will not be compromised during the lifetime of the structure. The gate design should also minimize flow or wave induced vibrations and oscillations on the structures.

(*) **Navigations requirements:** Safe passage of vessels

The design vessel for the GIWW is set to be the pushed convoy of 3 barges wide, measuring 105 ft (32.0 m) wide and 1,095 ft (335 m) long, as defined in section 4.2.2. In order to determine leading circumstances for navigation, also the expected average vessel to transit the particular part of the GIWW is included in table 5.1.

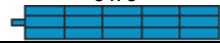
Vessel type	Vessel structure	Beam (USACE)		Draft (PIANC)		Min. clearance (PIANC)	
		[m]	[ft]	[m]	[ft]	[m]	[ft]
Maximum (design) pushed convoy: 3 barges wide	5 x 3 	31.9	105	2.5 - 4.5	8.2 - 14.8	9.1	30.0
Expected average pushed convoy: 1 large barge wide	2 x 1 	16.5	54	2.5 - 4.5	8.2 - 14.8	9.1	30.0

Table 5.1: Design vessels regarding the flood protection structure

For the vessel passage of the floodgate structure three possible situations exist, which include two way traffic through two separate openings, two way traffic through one opening and one way traffic. It should be noted that for the purpose of safe navigation, no combinations of these traffic modes are allowed. This means that the same mode of traffic should be implemented for both the design vessel and expected average vessel.

At first, the minimum navigable profile of the GIWW is determined in order to check whether two way traffic for the design vessel is allowed. The used method for the determination of this navigable profile of the waterway is outlined in Dutch standards provided by the Ministry Of Transport, Public Works And Water Management [11]. In this standard, the waterway is described using normal profile, minimum profile or a profile for one way traffic. The expected vessel traffic along the particular stretch of the GIWW, presented in table 4.2 for the years 2001–2004, is about 38,000 to 40,000 trips per year. This high level of vessel traffic prohibits the use of a minimum profile for the waterway and proposed floodgate structure. The width of the waterway regarding commercial vessel traffic is then determined at three levels:

- At the minimal required water depth (W_d);
- At the keel level of the loaded vessel (W_b);
- At the keel level of the unloaded design vessel, which requires additional width since it is more sensitive to wind loads. Half this width is provided at both sides of the waterway, as outlined in figure 5.1. Table 5.2 presents characteristics for determining the minimum width of a navigable waterway for the design vessels.

The navigable profile of the particular stretch of the GIWW proves to be sufficient to allow two way traffic for the design vessel. The bottom width of the GIWW measures 300 ft (91 m), which is larger than the required width of 210 ft (64 m). The required minimal surface width of 522 ft (160 m) can be accommodated by the GIWW in its length between New Orleans and Mobile Bay, but is not an economical basis as width of the floodgate opening.

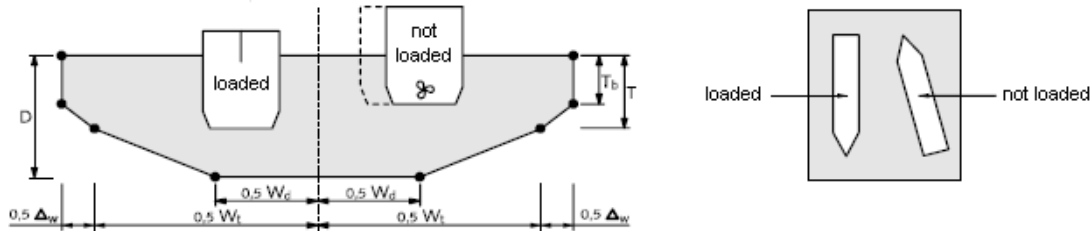


Fig. 5.1: Minimum width of a navigable waterway [11]

Profile	Vessel Type	Minimum width of the navigable waterway						
		Depth	Width		Additional width for wind		Resulting width	
		[ft]	Wt [ft]	Wd [ft]	Inland [m]	Coastal [m]	[ft]	[m]
Normal	Design vessel	21	420 (= 4B)	210 (= 2B)	15	31	522	159
	Average vessel	21	216 (= 4B)	108 (= 2B)	5	11	252	77
One way traffic	Design vessel	19	210 (= 2B)	105 (= 1B)	9	17	266	81
	Average vessel	19	108 (= 2B)	54 (= 1B)	7	15	157	48

Table 5.2: Characteristics for determining the minimum width of a navigable waterway [11]

To determine the actual width of the floodgate opening, the navigability of the structure should be kept in mind. The outer stretch of the GIWW is in open connection to Lake Borgne and the Mississippi Sound and will be influenced by the occurring tidal range. The water level is thus variable in time. The required navigable opening should therefore be relatively wide. Initially it is set at 2 times the beam of the design vessel, in this case resulting in 210 ft (64.0 m). This higher factor accommodates the additional width required for the relatively high wind load in this coastal area, associated crosscurrents and the high level of vessel traffic.

As the length of the surface reduction at floodgate is small, a quick passage of vessels is expected. For that reason, a one way traffic mode is installed regardless of the high level of vessel traffic. Installing a one way traffic mode at the location of the floodgate results in a significant limitation of the vessel speed, which requires the installation of sufficient operating systems and signaling.

It is essential to check the stated navigable opening width of 210 ft (64.0 m) in relation to the limitation speed and the water movement around moving vessels. The vessel speed should at least be equal to 3-4 knots (1.5-2.1 m/s) in order to provide the design vessel with safe maneuverability. The water movement around a moving vessel can be described by combining the theorem of Bernoulli and equation of continuity. This method is known as the method of preservation of energy and is developed by Schijf [1949]. The theorem of Schijf is outlined in Appendix F. Table 5.3 presents calculation results of the limitation speed for both the average and design vessel.

Vessel type	Vessel draft	Max. possible sailing speed		Max. water level depression		Max. return current velocity	
[-]	[ft]	[m/s]	[km/h]	[m]	[ft]	[m/s]	[km/h]
Design vessel (beam = 105 ft)	6	3.80	13.7	1.03	3.38	2.09	7.5
	9	3.06	11.0	1.05	3.44	2.42	8.7
	12	2.45	8.8	1.02	3.35	2.64	9.5
	15	1.94	7.0	0.94	3.08	2.77	10.0
Average vessel (beam = 54 ft)	6	4.77	17.1	0.90	2.95	1.59	5.7
	9	4.21	15.2	0.99	3.25	1.89	6.8
	12	3.76	13.5	1.04	3.41	2.11	7.6
	15	3.35	12.1	1.05	3.44	2.30	8.3

Table 5.3: Results for the limitation speed of vessel passing the floodgate structure – theorem of Schijf

Assumed is that vessels navigate at the maximum attainable speed, which is 90% of the limiting speed. Speeds up to 95% of the limiting speed according to Schijf are attainable for usual power engines, but this requires disproportionately more fuel. The maximum attainable speed for the design vessel at maximum draft can now be calculated as $0.9 \cdot V_{lim} = 0.9 \cdot 7.0 = 6.3$ km/h, which is still more than the required lower boundary of 6 km/h.

The maximum water level depression for the design vessel at maximum draft and maximum possible sailing speed amounts 3.1 ft (0.94 m), slightly more than the available depth under the vessel of 3 ft (0.91m). However, this speed is never reached and the actual water level depression should be determined at the maximum attainable speed of 6.3 km/h. From Appendix F it follows the actual water level depression $Z = 0.53$ m, which proves to be smaller than the maximum allowed depression of 0.91 m.

In conclusion, the required clearance height of 30 ft (9.1 m) is equal for these vessels and can be used as design criteria. Section 4.2.2 concluded that the bridges spanning the Rigolets Pass provide sufficient clearance height in order for it to be used as an alternative route for the particular stretch of the GIWW. The width of the floodgate opening depends on the type of vessel passage, set to be at one way traffic. In combination with the schematization of a guard lock, this leads to a floodgate opening of 210 ft (64.0 m). A check on the navigability of the floodgate opening proves that it is just sufficient to allow the design vessel at maximum draft to pass the structure safely at the minimum required speed of 6 km/h.

The navigable floodgate opening could possibly be reduced based on physical or ship simulation modeling and the placement of aids to navigation. For construction of the gate, consideration should be given to maintaining navigation throughout the construction period. Consequently, it may be necessary for final design to perform detailed hydrodynamic and ship model studies, either numerical or physical, in order to accurately determine the current velocities and flow direction under a wide range of wind and tide conditions with the structure in place. In addition, the final design stage should include an evaluation of guide walls for the approach to the gate in order to assist vessels in entering the passageway during high crosswinds and/or currents. Associated coordination should be induced with the Coast Guard to determine proper aids for navigation to mark this new structure.

5.2 Options for navigable flood protection structures

This section presents an overview and evaluation of navigable flood protection structures considered regarding the GIWW. Most of the gate types presented in the subsequent sections have been constructed and form integral parts of storm surge protection schemes in Europe, in particular in The Netherlands. Additional information on several examples of these completed structures with proven reliability is presented in Appendix D.

The comparative evaluation of different flood protection gate structures focuses on:

- Structural aspects of gates:
 - span of the gate;
 - load concentration / transfer of hydraulic load and wind load to gate supports;
 - responsiveness: sensitivity to hydrodynamic and wind loads (gate stiffness and natural frequencies);
 - driving system.
- Operation of gates:
 - closure in flowing water and waves;
 - effects of silting;
 - readiness of gates for immediate operation when needed;
 - ease of operation.
- Gates not in use:
 - accessibility of gates for inspection, maintenance and replacement;
 - risk of ship collisions.
- Other aspects:
 - abutments, sill and bed protection;
 - construction methods and experiences with similar structures.

The types of flood protection gates considered are presented in figure 5.2:

1. Vertically translating gates

Vertical lifting gates are suspended to hoisting cables in towers. The gate is lifted well above the water level when not in use. Alternatively, the gate is lowered in a deep bottom recess. This option is not further investigated as the weak soils in the region will immediately prevent a safe and economical application of it.

2. Flap gates: pneumatic flap gate and hydraulic flap gate

Flap gate are hinged onto the bottom. The gate is stored in a bottom recess when not in use. The gate rotates in a vertical plane about a horizontal axis and is driven by a hydraulic cylinder. Alternatively, the gate can also be designed as a pneumatic gate with flotation tanks.

3. Horizontally moving or rotating gates: slide gate, sector gate and floating sector gate

Horizontally moving or rotating gates include slide gates, sector gates and floating sector gates. Slide gates move on a slide way or a rail on the sill. The gate is stored in a dock in the abutment. Two gates can be applied, which meet in the center of the flow opening. Sector gates rotate in a horizontal plane about two hinges on a vertical axis. The sector gate is stored in a side chamber and could be made semi-buoyant in order to reduce the hinge forces. Usually, two gates are applied which meet in the center of the flow opening.

4. Vertically rotating gates: segment gate and radial gate

Vertically rotating gates include both segment gates and radial gates. Segment gates rotate in a vertical plane about a horizontal axis. The gate body is connected to circular side plates and is stored in a bottom recess. Radial gates are hinged to side walls or to a high, elevated bridge across the flow opening. The gate is lifted well above the water.

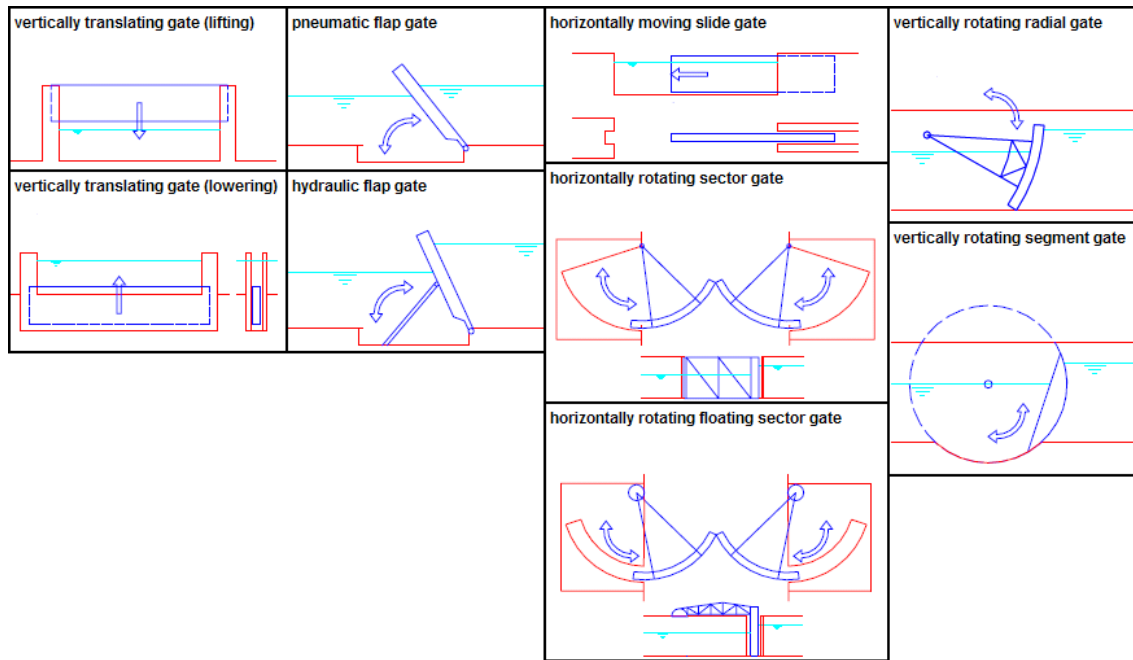


Fig. 5.2: Options for navigable floodgate structures

5.2.1 Vertical lifting gate

Vertical lifting gates have been widely used and have a satisfactory record of operation. As result of their widespread use, much experience on construction techniques and functioning and behaviour under flow and wave conditions has been gained. Table 5.4 presents favorable and unfavorable aspects of vertical lifting gates.

Favorable	Unfavorable
<i>Structural aspects, layout and operation</i>	
<ul style="list-style-type: none"> - A large gate span is feasible; - Little space required for hoisting towers and abutments in the river banks; - Almost no mobilization time as the gate is immediately ready for (easy) operation; - Fully controlled operation under flow and wave conditions; - Gates can be counterweighted in towers; - Raised gate is fully accessible for maintenance; - Wide experience with lifting gates and push and pull hydraulic cylinders. 	<ul style="list-style-type: none"> - Limited clearance height for navigation; - As an alternative, the gate may be stored in a deep bottom recess. This solution, however, requires a deep excavation and is vulnerable to silting; - Gate in raised position is subjected to wind load; - The higher the towers, the greater the rotation moment relative to the base; - The greater the water depth, the higher the gate and the higher the towers. In addition, the length of the hydraulic cylinders increases; - Natural frequencies corresponding to bending modes decrease strongly with span; - Wheel gates: peak pressures in contact points of supporting wheels (concentrations of loads); - Gate guide ways require smooth slide ways to limit friction (attention for growth under the water level).
<i>Hydraulic and hydrodynamic aspects</i>	
<ul style="list-style-type: none"> - Vertical closure of flow opening (no strong flow contraction in horizontal direction); - Gates are suited to reverse differential head and reverse flow during operation; - Gates can be lifted to discharge excess water safely; - Overflow is usually acceptable; - Gate underside may be kept free of silt and therefore little problems with silt on sill; 	<ul style="list-style-type: none"> - As the natural frequencies decrease with span, the sensitivity to flow induced vibration and dynamic loads increases with span; - During operation, the stiffness of hydraulic cylinders is relatively small which reduces the natural frequencies corresponding to vertical bending and translation modes.

Table 5.4: Favorable and unfavorable aspects of vertical lifting gates

Two flood protection schemes in The Netherlands where vertical lifting gates have been used are presented in table 5.5, together with some characteristic properties.

Name of complex	Width of flow opening feet (m)	Height of closed gate above sill feet (m)	Normal water depth above sill feet (m)	Differential design head feet (m)	Remarks
Hartel Canal storm surge barrier	opening 1: 315.0 (96.0) opening 2: 155.2 (47.3)	31.2 (9.5)	21.3 (6.5)	positive head: +15.1 (+4.6) negative head: -3.3 (-1.0)	2 lifting gates shipping lock road bridge
Krimpen storm surge barrier	262.5 (80.0)	37.7 (11.5)	21.3 (6.5)	+ 16.4 (+5.0)	2 lifting gates in tandem shipping lock road bridge
Ravenswaay flood protection barrier	262.5 (80.0)	38.1 (11.6)	24.3 (7.4)	+ 14.8 (+4.5)	1 lifting gate shipping lock

Table 5.5: Vertical lifting gates – proven flood protection schemes

5.2.2 Flap gates – pneumatic flap gate and hydraulic flap gate

Flap gates are not visible when the flood protection barrier is not in use. The gates are stored in a bottom recess and with one end hinged to the sill. The free end emerges above the water surface when the barrier is put in operation. Two gate types are distinguished: gates driven by hydraulic cylinders and pneumatic gates operated by air injection into flotation tanks.

Flap gates are not widely applied in flood protection schemes. This is probably due to the fact that inspection, maintenance and replacement are difficult, while the issue of silting of the gate recess may be an additional drawback. Table 5.6 presents favorable and unfavorable aspects of flap gates.

Favorable	Unfavorable
<i>Structural aspects, layout and operation</i>	
<ul style="list-style-type: none"> - No limitation of the span; - Barrier can be composed of a great number of separate flap gates which reduces the effects of failure of one of the gates; - No clearance height limitation for navigation; - Little space required for abutments in the river banks; - Flap gates can be used in relatively deep water; - Flap gates with hydraulic cylinders: controlled operation under flow and wave conditions; - Flap gates are not subjected to wind load; - Flap gates are invisible when the barrier is not in use. 	<ul style="list-style-type: none"> - Natural frequencies corresponding to rotational modes are relatively low due to relatively small hydrodynamic stiffness/cylinder stiffness and great hydrodynamic mass. Frequencies decrease strongly with increasing water depth; - Pneumatic flap gates: operation of gates under flow and wave conditions may not fully be controlled; - Gates with hydraulic cylinders: hydraulic load concentration in cylinders; - Gates are underwater and subjected to corrosion and biological growth; - Hinges may wear out in sandy environment; - Inspection and maintenance of submerged gates, hinges and driving systems is difficult.
<i>Hydraulic and hydrodynamic aspects</i>	
<ul style="list-style-type: none"> - No strong confinement of flow in horizontal direction when gates are alternately operated; - Flap gates with hydraulic cylinders: excess water may be discharged by lowering the gate crest - One of a series of flap gates can be lowered to discharge excess water. 	<ul style="list-style-type: none"> - Pneumatic gates: the differential head is limited by the thickness of the gate; - Pneumatic gates: a negative head may cause overturning of the gate; - Pneumatic gates: gates cannot safely be operated under reverse flow conditions; - Flap gates with hydraulic cylinders: overflow may cause vibrations; - Silting of gate recesses may cause operational problems; - Flap gates are sensitive to dynamic excitation by waves, this is due to the low natural frequencies; - Passing ships/anchors may cause damage to the gates when stored in bottom recess; - Inclined flap gates may cause breaking of waves and wave slamming on the skin plate.

Table 5.6: Favorable and unfavorable aspects of flap gates

Examples of flood protection schemes where flap gates have been constructed or proposed are presented in table 5.7, together with some characteristic properties.

Name of complex	Width of flow opening feet (m)	Height of closed gate above sill feet (m)	Normal water depth above sill feet (m)	Differential design head feet (m)	Remarks
New Waterway storm surge barrier (alternative design)	1,180 (360)	73.8 (22.5)	55.8 (17.0)	max. pos. head: +11.1 (+3.4)	14 pneumatic gates, width: 84.3 ft (25.7 m)
New Waterway storm surge barrier (alternative design)	1,180 (360)	73.8 (22.5)	55.8 (17.0)	max. pos. head: +11.5 (+3.5)	24 hydraulic gates, width: 49.2 ft (15.0 m)

Table 5.7: Flap gates – proven flood protection schemes

5.2.3 Horizontally moving or rotating gates – slide gate, sector gate and floating sector gate

Flood protection gates that move over a carriage way or slide way on the river bed have some important disadvantages, which may be the reason that they have not yet been applied in major flood protection schemes. Main disadvantages are the necessity of deep side chambers in which the gates are housed when not in use and the risk of malfunctioning when silting occurs on the sill. When the span is limited, gates that rotate about a vertical axis can be kept free of the sill. This may reduce the risk of malfunctioning. To limit the forces in the hinges for longer spans, it may be necessary to install floatation tanks in the gates. Table 5.8 presents favorable and unfavorable aspects of horizontally moving or rotating gates.

Favorable	Unfavorable
<i>Structural aspects, layout and operation</i>	
<ul style="list-style-type: none"> - A large gate span is feasible; - No clearance height limitation for navigation; - Controlled operation under flow and wave conditions; - Gates are not subjected to wind load; - Gates can be applied in relatively deep water; - Floatation tanks reduce vertical loads on sill; - Sector gates with open side chambers: little mobilization time, so the gate is immediately ready for operation; - Sector gates: gate may be kept free of sill when span is not too large (but dynamic flow and wave forces on floatation tanks may not be acceptable); - Straight gates: self stable structure and direct transfer of hydraulic load to foundation (no load concentration); - Straight gates: dry dock for gate housing is possible which enables easy inspection and maintenance and provides protection against ship collisions. 	<ul style="list-style-type: none"> - Side chambers require large, deep excavation in banks; - The slide way or carriage way requires a flat, well founded sill on the river bed and the sill must take up hydraulic load when straight gate is applied; - The slide way must be smooth to limit friction; - Silt on carriage or slide way may hamper gate operation; - Sector gates: gates are underwater and are subjected to corrosion and biological growth; - Sector gates: inspection and maintenance of gate is difficult underwater; - Sector gates: load transfer to hinges on abutments leads to a strong load concentration, making the hinges the critical elements (protection against ship collisions); - Straight gates: sluice gates may be required to limit the hydraulic load and forces on slide way during operation; - Straight gates with dry dock: extra mobilization time is required for filling of dry dock.
<i>Hydraulic and hydrodynamic aspects</i>	
<ul style="list-style-type: none"> - Application of sluice openings in the gate limits the building up of differential head, prevents strong horizontal flow contraction in last stage of closure and can also be used in order to discharge excess water; - Gates are suited to reverse differential head and reverse flow during operation; - Gates on a slide way or carriage way are not particularly sensitive to flow induced vibrations. 	<ul style="list-style-type: none"> - Sector gates: large open side chambers enable ships to collide with the gate; - Sector gates: silting may occur in open side chambers.

Table 5.8: Favorable and unfavorable aspects of horizontally moving or rotating gates

Gates that move over a sill on the river bed are infrequently applied in major flood protection schemes. In the pre-design stage of the storm surge barrier in the New Waterway, two designs with horizontally moving gates were proposed but not selected. Regarding the U.S., the New Bedford hurricane barrier is an example where in a relatively narrow flow opening sector gates have been used. The flood protection barrier in the Harvey Canal near New Orleans, which is presently under construction, will also be provided with sector gates. Characteristic properties of the stated flood protection schemes are presented in table 5.9.

Name of complex	Width of flow opening feet (m)	Height of closed gate above sill feet (m)	Normal water depth above sill feet (m)	Differential design head feet (m)	Remarks
New Waterway storm surge barrier (alternative design)	1,180 (360)	73.8 (22.5)	55.8 (17.0)	max. pos. head: +19.7 (+6.0) max. neg. head: -8.2 (-2.5)	2 straight sliding gates on concrete sill
New Waterway storm surge barrier (alternative design)	1,180 (360)	73.8 (22.5)	55.8 (17.0)	max. pos. head: +15.4 (+4.7) max. neg. head: -6.6 (-2.0)	2 sector gates, rolling on curved concrete sill
New Bedford hurricane barrier	150 (45.7)	60.0 (18.3)	40 (12.2)	positive head: +12.0 (+3.7)	2 sector gates, rolling on curved concrete sill
Harvey Canal flood protection barrier	125 (38.1)	28.0 (8.5)	16.0 (4.9)	positive head: +12.0 (+3.7)	2 sector gates

Table 5.9: Horizontally moving or rotating gates – proven flood protection schemes

Floating sector gates have some noteworthy advantages: the gates can be stored in a relatively inexpensive, shallow dry dock in the abutments, which enables easy maintenance, and the gates can be immersed on the sill also when the sill is covered with silt. A significant disadvantage of the floating gates is the sensitivity to flow induced oscillations and dynamic wave loads. Table 5.10 presents favorable and unfavorable aspects of floating sector gates.

Favorable	Unfavorable
<i>Structural aspects, layout and operation</i>	
<ul style="list-style-type: none"> - A large gate span is feasible; - No clearance height limitation for navigation; - Shallow dry dock enables easy inspection and maintenance and provides protection against ship collisions; - Gates can also be immersed when the sill is covered with silt; - No strict tolerance demands for flatness of the sill. 	<ul style="list-style-type: none"> - Large space is required for dry docks; - The operation of the gates in flowing water may not fully be controlled (vertical gate position depends strongly on flow forces); - A negative differential head may be a threat for the barrier because ball hinges are only capable of taking up small pull forces; - Objects on the sill may damage gates when immersed; - Natural frequencies corresponding with heave and pitch modes of floating gate are relatively low and decrease when floatation tanks of gates get immersed; - Load transfer to ball hinges on abutments leads to strong load concentration, making the hinges critical elements which need to be protected against ship collisions; - Dry docks have to be filled with water which will require extra mobilization time.
<i>Hydraulic and hydrodynamic aspects</i>	
<ul style="list-style-type: none"> - Vertical closure of flow opening (no strong flow contraction in horizontal direction); - Sluice openings can be applied in the gate, which limit the building up of a differential head during closure and may be used to discharge excess water. 	<ul style="list-style-type: none"> - Gates are sensitive to flow induced oscillations when the gate underside is not well designed; - Floating gates are sensitive to dynamic wave forces and the resulting gate oscillations may hamper a controlled landing on the sill; - Gates can only resist a small negative differential head

Table 5.10: Favorable and unfavorable aspects of floating sector gates

Floating sector gates have been used in the New Waterway storm surge barrier and will also be used in the St. Petersburg barrier. Characteristic properties of these protection schemes are presented in table 5.11.

Name of complex	Width of flow opening feet (m)	Height of closed gate above sill feet (m)	Normal water depth above sill feet (m)	Differential design head feet (m)	Remarks
New Waterway storm surge barrier (realized design)	1,180 (360)	73.8 (22.5)	55.8 (17.0)	Max. pos. head: +14.8 (+4.5) Max. neg. head: -2.3 (-0.7)	2 floating sector gates
St. Petersburg storm surge barrier (under construction)	656 (200)	77.1 (23.5)	52.5 (16.0)		2 floating sector gates

Table 5.11: Floating sector gates – proven flood protection schemes

5.2.4 Vertically rotating gates – segment gate and radial gate

Two types of vertically rotating gates are applied in storm surge barrier schemes: segment gates with circular side disks that are stored in a bottom recess and conventional radial gates that are rotated above the water level and leave space for vessels to pass underneath.

When closed gate bodies are used, the torsion stiffness is high, enabling the construction of gates with a long span and supporting gate arms only at the two sides. Segment gates in bottom recesses may be vulnerable to silting. Table 5.12 presents favorable and unfavorable aspects of vertically rotating gates.

Favorable	Unfavorable
<i>Structural aspects, layout and operation</i>	
<ul style="list-style-type: none"> - A large gate span is feasible; - Gates are immediately ready for operation; - Fully controlled operation of gates under flow and wave conditions; - Little space required for abutments; - Gates can be rotated above the water level for inspection and maintenance; - Segment gate: no clearance height limitation for navigation; - Segment gate: gate is not subjected to wind load; - Segment gate: gate can be counterweighted by means of ballast in the side disks. 	<ul style="list-style-type: none"> - Load transfer to pivot bearings results in a strong load concentration; - Segment gate: high tolerance demands for construction of the sill with bottom recess; - Segment gate: vulnerable to silting of the bottom recess and objects between gate and sill may damage the gate when operated; - Segment gate: water filled gate body is vulnerable to silting and corrosion which requires regular maintenance of the interior. - Segment gate: access to the narrow parts of the gate body is difficult; - Radial gate: limitation of clearance height for navigation.
<i>Hydraulic and hydrodynamic aspects</i>	
<ul style="list-style-type: none"> - Vertical closure of flow opening, therefore no strong flow contraction in horizontal direction; - Gates are suited to reverse differential head; - Gates can slightly be lifted to safely discharge the excess water; - Overflow of gates may be acceptable; - Radial gate: gate underside may be kept free of sill, so little problems with silt on sill 	<ul style="list-style-type: none"> - Segment gate: gate may be sensitive to flow induced oscillations in the case of overflow;

Table 5.12: Favorable and unfavorable aspects of vertically rotating gates

Vertically rotating gates have been used in the Thames storm surge barrier and the Ems storm surge barrier. Characteristic properties of these flood protection schemes are presented in table 5.13.

<i>Name of complex</i>	<i>Width of flow opening feet (m)</i>	<i>Height of closed gate above sill feet (m)</i>	<i>Normal water depth above sill feet (m)</i>	<i>Differential design head feet (m)</i>	<i>Remarks</i>
Thames River storm surge barrier	4 main openings: 200 (61.0) 6 smaller openings: 103 (31.5)	53.0 (16.2)	32.8 (10.0)	positive head: +27.6 (+8.4) negative head: -20.0 (-6.1)	navigable openings: segment gates in 4 main openings, smaller segment gates in 2 secondary openings and radial gates in 4 non-navigable openings
Ems storm surge barrier	navigable opening 1: 196.8 (60.0) navigable opening 2: 164.0 (50.0) 5 other openings: 205.1 – 164.0 (62.5 – 50.0)	45.9 (14.0)	22.9 (7.0)	+ 19.7 (+6.0)	navigable openings: segment gate in opening 1, radial gate in opening 2 and 5 lifting gates with upper beams in 5 remaining non-navigable openings

Table 5.13: Vertically rotating gates – proven flood protection schemes

5.3 Comparison of gate types

The comparison of the floodgate types is divided into two parts. First the killer requirements regarding the proposed hurricane protection barrier are stated and evaluated per floodgate types in section 5.3.1. This is performed first in order to eliminate those floodgate types that do not confine with these main requirements at an early stage. Secondly, evaluation of the remaining floodgate types is presented in section 5.3.2 and will be on the basis of typical structural concerns, which will be applied to the location within the GIWW.

5.3.1 Killer requirements

The killer requirements have their focus on the hydrology and morphology of the GIWW. Functional requirements regarding the application for navigation follows in the third requirements.

- The first killer requirement concerns the hydrology of the GIWW / New Orleans region:
"The floodgate structure should be fully controllable at all design flow and wave conditions, including reverse differential head conditions".

Operation under flow and waves conditions is not possible for the sliding gate. The reverse differential head requirement eliminates the pneumatic flap gate and the floating sector gate:

- Pneumatic gates: negative head may cause overturning of the gate, the gates cannot safely be operated under reverse flow conditions and operation under flow and wave conditions may not fully be controlled;
- Floating sector gates: a negative differential head may be a threat because ball hinges are only capable of taking up small pull forces, thus the gates can only resist a very small negative differential head.

- The second killer requirement concerns the morphology of the GIWW:
"The flood protection structure must be able to withstand some degree of siltation as scouring could occur during the discharge of water at high negative differential head".

The morphology and associated sediment transport of the particular section of the GIWW are expected to cause siltation related problems regarding the floodgate structure. The prevention of such problems would minimize the maintenance costs and probability of failure due to dismissal of the moving parts of the gate. This siltation requirement eliminates the hydraulic flap gate and segment gate:

- Hydraulic flap gate: the gate is subjected to corrosion and biological growth, the hinges could wear out and the inspection and maintenance of submerged gates, hinges and driving system is difficult;
- Segment gate: the bottom recess and water filled body are vulnerable to silting which requires regular and expensive maintenance of the interior as access to the narrow parts of the gate body is difficult.

- The third killer requirement concerns the navigation requirements of the GIWW:
"Navigation requirements of span, beam and clearance should impose limited design consequences".

Both the vertical lifting gate and sector gate confine to this requirement as both the required span of 210 ft (61 m) and vertical clearance requirement of 30 ft (9.1 m) can be constructed. For the radial gate, both the span and vertical clearance requirements stretch this type of floodgate structure to its limits. An additional pier should be constructed in the center of the GIWW in order to facilitate a proper gate design, which is not favorable regarding the safety of the high level of vessel traffic.

Application of this requirement on the floodgate types is presented in table 5.14:

	VLG	PFG	HFG	SIG	STG	FSTG	SMG	RG
Killer requirement 1: Fully controllable at all design flow and wave conditions, including reverse differential head conditions;	Yes	No	Yes	No	Yes	No	Yes	Yes
Killer requirement 2: Able to withstand some degree of siltation as scouring is expected to occur during the discharge of excess water	Yes		No		Yes		No	Yes
Killer requirement 3: Navigation requirements should impose limited design consequences and no additional pier is allowed	Yes				Yes			No
<i>Floodgate types that require further investigation regarding their structural concerns</i>	Yes	No	No	No	Yes	No	No	No

Table 5.14: Application of killer requirements
 VLG = vertical lifting gate, PFG = pneumatic flap gate, HFG = hydraulic flap gate, SIG = slide gate, STG = sector gate, FSTG = floating sector gate, SMG = segment gate, RG = radial gate

5.3.2 Structural considerations and concerns

In this section, various structural concerns that could be encountered during the gate operation are discussed. These concerns should be recognized and considered during the design in the evaluation of the gate type in order to prevent major operation problems during its life span. Table 5.16 presents this required evaluation.

Design and construction concerns

The main structural concerns related to the design include structural complexity, internal proportions and impact on required civil works. Table 5.15 presents structural and mechanical characteristics of both selected gate types.

- Complexity of the structure: A more complex structure is difficult to design and later to build. A complex structure has inherently higher risks of error and weaknesses that may in turn have a negative impact on maintenance and durability.
- Proportion with regard to operational requirements (feasibility/costs): Problems can occur when parameters like weight, thickness and superstructures are out of proportion in relation to their operational requirements or handling capabilities. The consequence in that case is that a floodgate type is not feasible and/or too expensive for large dimensions.
- Impact of gate design on other civil works (concentration of load): Often the technical problems does not concern the gate structure itself but the associated civil engineering works it requires. These works, like the foundation and the concrete structures, may become more important, complex and expensive.
In general, the impact of the gate design is depends mainly on the load transfer:
 - If loads permitted to the piers are too concentrated, heavy and expensive concrete reinforcement is required and design limits may be reached;
 - If loads are mobile, special devices and reinforcement must be considered related to wear or blockage.

	<i>Vertical lifting gate</i>	<i>Sector gate</i>
Foundation and operator supports	On the lateral ends of the gates (in slots) with cables or hydraulic cylinders.	Hinged on the bottom of the downstream plate.
Movement and handling	Vertical translation to open/close the gate. Hoisting systems on both sides of the gate.	Rotation around the hinge. The internal water pressure acts as a driving force.
Flow type	Underflow.	Overflow.
Applied loads: - hydraulic loads; - weight and friction; - handling load	Hydraulic load: to the pier on both sides of the gate. Application points change with vertical gate position (mobile loads). Weight and friction: to the piers. Handling load: opposite to the weight.	Hydraulic load: to the floor. Weight and friction: to the floor and piers. Handling load: no real handling load.
Internal forces	- longitudinal bending moment; - dead weight is significant.	Lateral pressure and transverse bending moment on upstream plate.

Table 5.15: Structural characteristics of both vertical lifting gate and sector gate [18]

Operation and maintenance concerns

The operation concerns are the ability to control water height and to handle debris and sediments. The key points for maintenance of movable gate are to define, inspect and maintain the parts that are always under water. In this process, the following should be considered:

- Robustness of all pieces and associated probability of mechanical failure;
- Methods to maintain and replace mechanical pieces, both those submerged and above water;
- Redundancy to maintain acceptable operability in the event that key elements fail;

Degradations of the structure during its period of operation

- Wear due to friction is important in the moving parts, such as hinges and wheels. Excessive wear can create deformation, vibrations and alter the different load distribution.
- Abrasion is the result of contact with the water current, mainly in the presence of sediment transport. It is particularly important for gates that have under water hinges.
- Corrosion can develop for all steel structures near water. Important issue is the problem of accessibility for regular maintenance.
- Vibrations can be the result of either mechanical or water flow causes. The lack of aeration in gate overflow is one of the major causes of vibration. Vibrations can cause higher stresses and large alternate deflection.

	<i>Vertical lifting gate</i>	<i>Sector gate</i>
Design	<p><u>Advantages:</u></p> <ul style="list-style-type: none"> - Large span possible; - Little space required for hoisting towers and abutments; - Avoids long piers; - Simple shape and wide experience concerning hoisting systems; - Ease of fabrication and erection time is short. <p><u>Disadvantages:</u></p> <ul style="list-style-type: none"> - Heavy superstructures and complex mechanic equipment for hoisting system; - Gate in raised position is subjected to wind load; - The higher the towers, the greater the rotation moment relative to the base; - Moving forces in the slot pads; - Mechanisms partly under water (wheel, rails). 	<p><u>Advantages:</u></p> <ul style="list-style-type: none"> - Large span possible; - Simple structure concepts: no torsion and no longitudinal bending; - Not visible under normal conditions and thus not subjected to wind load; - Gates on a slide way or carriage way are not particularly sensitive to flow induced vibrations. <p><u>Disadvantages:</u></p> <ul style="list-style-type: none"> - Side chambers require large, deep excavations; - Heavy steel structure; - Needs a high civil work under the crest; - Load transfer to hinges on abutments leads to a strong load concentration, making the hinges critical elements;
Operation	<p><u>Advantages:</u></p> <ul style="list-style-type: none"> - Fully controlled operation under flow and wave conditions; - Gates are suited to reverse differential head and reverse flow during operation; - Simple and reliable operation (most reliable closure system for emergencies); - Little mobilization time: the gate is immediately ready for easy operation; - Gates can slightly be lifted to discharge the excess water safely and overflow is usually acceptable; - Gate underside may be kept free of sill and therefore little problems with silt on sill. <p><u>Disadvantages:</u></p> <ul style="list-style-type: none"> - During operation, the stiffness of hydraulic cylinders is relatively small which reduces the natural frequencies corresponding to vertical bending and translation modes. - Energy dissipation for underflow (dissipation basin often required, which increases costs). 	<p><u>Advantages:</u></p> <ul style="list-style-type: none"> - Fully controlled operation under flow and wave conditions; - Gates are suited to reverse differential head and reverse flow during operation; - Sector gates with open side chambers: little mobilization time, so the gate is immediately ready for operation; <p><u>Disadvantages:</u></p> <ul style="list-style-type: none"> - The slide way or carriage way requires a flat, well founded sill; - The slide way or carriage way must be smooth to limit friction and because silt on it may hamper gate operation; - Controlled discharge of excess water is difficult.
Maintenance	<p><u>Advantages:</u></p> <ul style="list-style-type: none"> - The gate is easy to inspect and maintain in upper position. <p><u>Disadvantages:</u></p> <ul style="list-style-type: none"> - The complexity of the hoisting systems requires a high level of maintenance; - The guide way of the lifting gate requires a smooth slide way in order to limit friction. 	<p><u>Advantages:</u></p> <ul style="list-style-type: none"> - ... <p><u>Disadvantages:</u></p> <ul style="list-style-type: none"> - Inspection and maintenance of gate is difficult under water.
Degradation	<ul style="list-style-type: none"> - Wheel gates: peak pressures in contact points of supporting wheels and friction may cause wear; - Sensitive to vibrations for small bottom opening or sealing defects; - As the natural frequencies decrease with span, the sensitivity to flow induced vibration and dynamic loads increases with span; 	<ul style="list-style-type: none"> - Hinges are partially or always under water: corrosion risks and sensitive to abrasion. - Friction could be generated by compacted sediments in the under water slots; - Open side chambers enable ships to collide with the gate and silting may occur.

Table 5.16: An overview of the main structural concerns for both vertical lifting gate and sector gate

5.4 Gate selection rationale and conclusion

Table 5.17 presents the final evaluation of the vertical lifting gate and sector gate in the form of a gate selection rationale regarding structural concerns presented in section 5.3.2. Green presents favorable and red unfavorable.

	<i>Vertical lifting gate</i>	<i>Sector gate</i>
Design	<p><u>Complexity of the structure:</u> Characteristic for the lifting gate is the complex mechanic equipment for the hoisting system needed to handle the moving forces in the slot pads. As the loads are mobile, special devices and reinforcement must be considered. The complexity introduces a higher risk of error and a negative impact on maintenance and durability. On the other hand, the gate has a simple shape and there is generally wide experience concerning the hoisting systems.</p> <p><u>Impact of gate design on other civil works:</u> Little space is required for the hoisting towers and abutments and long piers can be avoided. The superstructures are relatively heavy and need a proper foundation. In addition, the gate is subjected to wind load under normal conditions. The higher the towers, the greater the rotation moment relative to the base due to this loading. The required vertical clearance of 30 ft (9.1 m) is relatively small, thus reducing these negative impacts and concerns.</p>	<p><u>Complexity of the structure:</u> The sector gate has a simple structure concept: no torsion and no longitudinal bending.</p> <p><u>Impact of gate design on other civil works:</u> The load transfer to hinges on the abutments leads to a strong load concentration, making the hinges critical elements. These hinges require a high civil work under the crest, resulting in an expensive design and reinforcement. In addition, the sector gate requires a heavy steel structure.</p> <p>The side chambers of the gate require large, deep excavations in the banks. Due to these chambers the gate is not visible under normal conditions and not subjected to wind load.</p>
Operation	<p>A lifting gate has controlled operation under flow and wave conditions and is suited to reverse differential head and reverse flow during operation. The lifting gate also has a minimum mobilization time and a simple, reliable closure system.</p> <p>The gate can slightly be lifted to safely discharge excess water and overflow is usually acceptable. The underside of the gate can be kept free of the sill, thus little problems with silt on the sill. Allowing underflow does require a more complex bottom protection for the dissipation of associated energy.</p>	<p>Also a sector gate has a fully controlled operation under flow and wave conditions and is suited to reverse differential head and reverse flow during operation. A sector gate with side chamber also has minimal mobilization time.</p> <p>However, the operation is less reliable than for the lifting gate. The slide or carriage way must be smooth to limit friction. Silt on it may hamper the gate operation. More importantly, a controlled discharge of excess water is difficult.</p>
Maintenance	<p>The gate is easy to inspect and maintain in upper position, but the complexity of the hoisting systems require a high level of maintenance. Mechanisms are partly under water (wheel, rails).</p>	<p>Inspection and maintenance of the critical gate hinges is difficult under water.</p>
Degradation	<p>The lifting gate is sensitive to vibrations for small bottom opening or sealing defects. As the natural frequencies decrease with span, the sensitivity to flow induced vibration and dynamic loads increases with span. It is important of that the design is checked on this degradation mode.</p> <p>The hydraulic loads are concentrated at the piers on both sides of the gate and mobile. The application points change with the vertical gate position. This introduces several possible modes of degradation, including wear, blockage, friction and corrosion.</p>	<p>A sector gate on a slide or carriage way is not particularly sensitive to flow induced vibrations. The critical hinges are partially or always under water, thus sensitive to corrosion and abrasion. In addition, the under water slots are sensitive to friction due to compacted sediments.</p>

Table 5.17: Gate selection rationale – evaluation of the vertical lifting gate and sector gate

The vertical lifting gate is chosen as the optimal flood protection structure for several main reasons:

- The required vertical clearance height, generally the only limitation of the gate type, is relatively small and applicable. The influences of the expected wind load and the superstructures need to be reviewed;
- The hoisting system is complex but well known, providing a highly reliable closure system;
- The vertical lifting gate has the ability to safely discharge excess water from the retention area, which represents one of the main functions of the gate.
- As the gate can be kept free of the sill, it has little problems with silt on it. On the other hand, allowing this underflow requires a more complex bottom protection. It also introduces vibrations with associated modes of degradation like wear, friction and blockage. It requires a higher level of maintenance, but this is relatively easy as the gate can be lifted out of the water. The relatively large span needed for the gate enforces the need for a review on vibrations and natural frequencies in this preliminary design. This review is presented in chapter 9, after the steel cross-section of the lifting gate is determined.

6. Quantified Program Of Requirements Of The Navigable Storm Surge Barrier Within The Gulf Intracoastal Waterway

This chapter quantifies the main part of the program of requirements stated in the previous chapter. Section 6.1 determines the project site of the vertical lifting gate. Section 6.2 presents the geotechnical schematization to be used in the design. Section 6.3 describes hydraulic design conditions and associated assumptions and constraints. It concludes on a protective levee of safety for the gate design. A detailed hydraulic analysis under predetermined standards, leading water levels and resulting structural requirements is described in section 6.4.

6.1 Site selection

The location of the proposed vertical lifting gate is presented in figure 6.1. It is merely undeveloped as no buildings, power lines or pipelines exist within a couple of miles, except for a railroad and highway located several miles to the north. The only man-made structure close to the gate is the primary levee system it ties into.

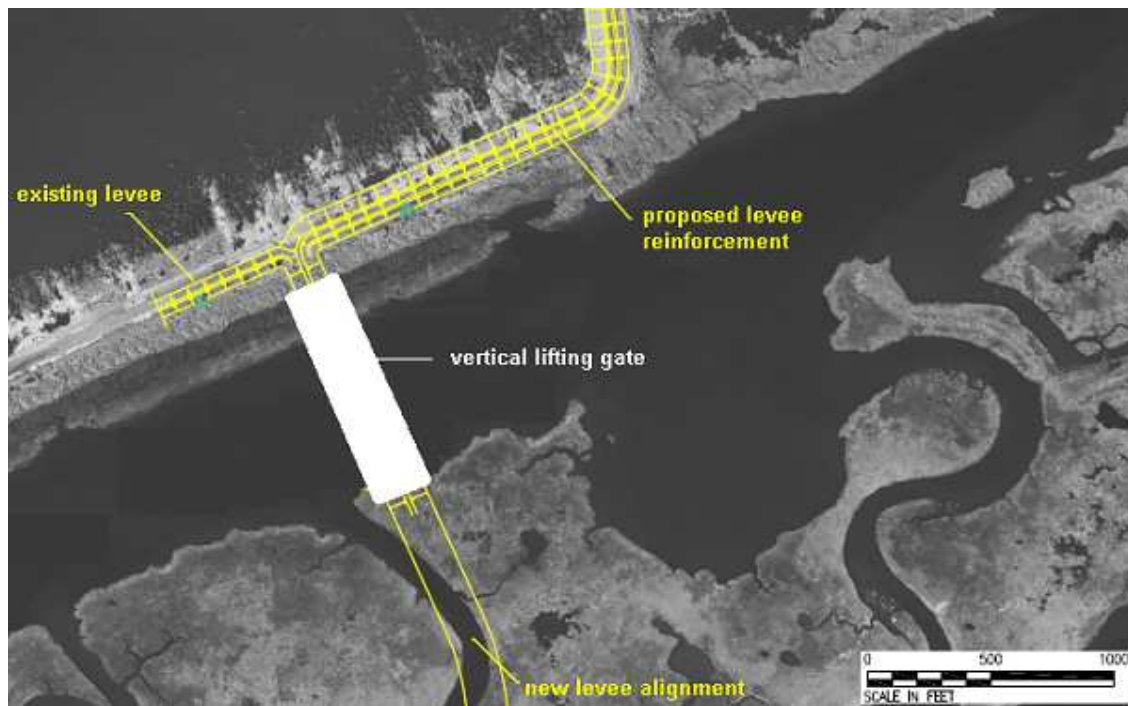


Fig. 6.1: Vertical lifting gate – site selection [2]

The technical program requirement presented in section 5.1 stated several main requirements the location has to perform to. Each of these requirements is discussed concerning the given location as presented in figure 6.1.

- *Modifications to the existing waterway should be selected in a way to minimize the environmental impact of the structure and its size. Ideally, the gate should be built at a site where there is a natural restriction.*

Potential environmental concerns are based on the review of available databases and public records. No sediment data were available for review to determine if the sediments at the location will pose an ecological threat if disturbed. Based on this environmental site assessment, it does not appear that any hazardous, toxic or radioactive waste sites occur within the study area that could have potential impacts to sediments. The cost to dispose impacted sediments significantly increases total cost of the project. Environmental sampling and characterization of sediment quality are recommended. To adequately determine the potential for the presence of endangered species, a biological assessment should also be conducted.

Wetland permits and/or mitigation are required for the construction activities related to realization of the gate structure and levee alignment. Potential impacts of tidal flow fluctuations on wetlands are not expected to be significant because the tidal range is small and normal flow paths and tidal circulation is not altered.

No natural restriction exists as natural wetlands bordering the southern shoreline only provide a soft bank, as depicted in figure 6.1. The requirement is included in the fact that the structure is moved slightly east in relation to the initial plan. The wider surface area at that location could possibly disorientate navigation.

- *The structure should be situated to provide a straight line of sight with the gate structure navigational openings in order to facilitate incoming vessels to enter and exit the gate safely.*

The GIWW is straight for several miles to the east and west of the proposed location. The gate is orientated perpendicular to the GIWW, in order to provide the required straight line of sight for safe navigation.

- *Optimize the use of available space and provide easy access during construction and maintenance.*

Optimization of the use available space is only minorly applicable to this location and floodgate type. The vertical lifting gate already minimizes the need for space compared to other floodgate types and the area surrounding the proposed location is merely undeveloped.

An easy access during construction and maintenance is more troublesome. No roads are located near the projected location yet, but should be constructed. Construction materials could be transported over water.

- *Consideration should be given so the layout of the structure minimizes its exposure to environmental loading.*

The Coastal and Hydraulics Laboratory at Vicksburg, Mississippi reconstructed wind records from 1990 to 1999 for various weather stations along the Gulf coast [26]. The wind rose in figure 6.2 for a station located 70 miles (110 km) east of Lake Borgne. It indicates that winds are about twice as likely to come from the east as from the west but that northerly and southerly winds occur about equally. Lake Borgne is relatively wide, allowing significant fetches for wind setup. The lake is also relatively shallow. The main fetches for the location of the vertical lifting gate are presented in figure 6.2.

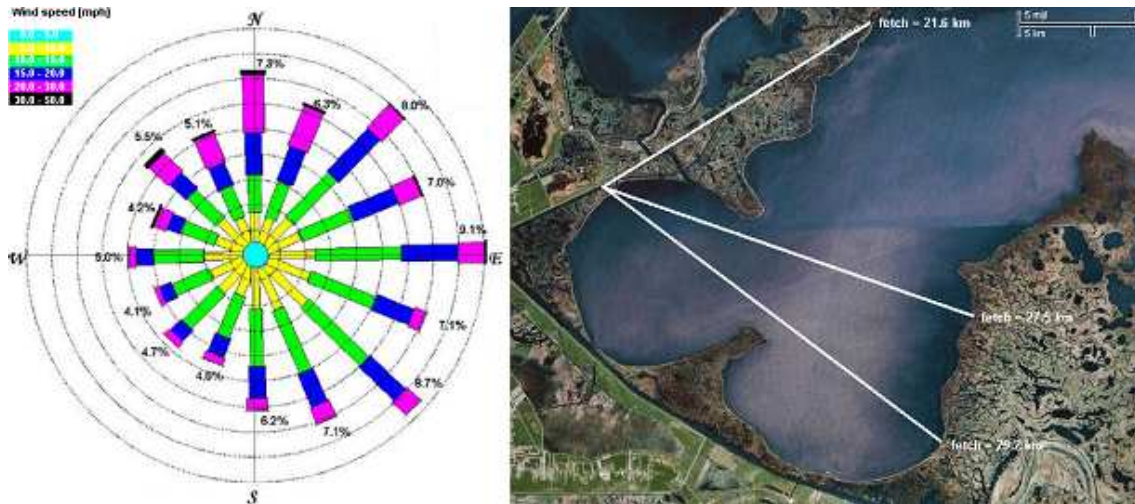


Fig. 6.2: Prevailing winds at Lake Borgne and main wind fetches [26]

The wind field is transferred from a location 70 miles offshore without any reduction for terrestrial friction and is likely higher than what might be expected over Lake Borgne. Table 6.1 provides a statistical presentation of wind speeds for the particular weather station, which is combined for all wind directions. With the calculated fetches and associated average depths, the wave conditions can be determined using the SMB-model for coastal waters as presented in Appendix B. The wind setup is determined by using the approach presented in this appendix. For the calculation, the 90th percentile wind speed is used. Table 6.2 presents the results. The resulting wave conditions are generally mild, with low wave heights and short peak wave periods. Critical wave slamming is not expected.

	All winds	
	[mph]	[m/s]
Max.	62.4	27.9
90%	21.9	9.8
75%	17.4	7.8
50%	13.0	5.8
25%	9.4	4.2
10%	6.7	3.0
Min.	0.4	0.2

Table 6.1: Normal wind speeds [26]

Wind fetch	Average depth		Significant wave height		Peak wave period	Wind setup	
[km]	[ft]	[m]	[ft]	[m]	[s]	[ft]	[m]
21.6	15	4.6	2.3	0.7	3.5	0.6	0.2
27.5	7	2.2	1.6	0.5	2.9	1.2	0.4
29.2	9	2.7	1.8	0.5	3.1	1.1	0.3

Table 6.2: Normal conditions – wave height, wave period and wind setup at location of the structure [26]

6.2 Geotechnical design conditions

6.2.1 General description, assumptions and constraints

Geotechnically, one constraint that should be accounted for in design is the expected soft foundation sediments present. These are compressible materials, which would be expected to allow significant settlement under loads imposed by the levee fill and lifting gate structure. The settlement is likely to continue over an extended period of time. The subsidence occurring over time will lower the level of protection provided by the structures. This condition could be mitigated to some extent by removing some of the soft surface layers and by use of piles beneath the concrete structures.

Settlement analyses were not performed as a part of this conceptual study. As design of the gate structure advances, more detailed and extensive geotechnical investigations and analyses will be required to identify actual conditions and to develop design parameters. Foundation conditions present challenges that must be addressed to ensure safe and satisfactory construction and operation of the project. Investigations will be required at the vertical lifting gate site and along reaches of proposed levee modifications. These investigations could include exploring options for strengthening foundations beneath modified levee sections to reduce settlement and improve shear strength. Specifics of these investigations are beyond the scope of this thesis.

Stability of the levees is also a concern due to the weak shear strength that some of the sedimentary strata are likely to display. Stability analyses were not performed as a part of the thesis. As the design of the structure progresses, stability analyses should be completed for the various components of the gate structure. Chapter 7 presents only an indicative calculation of the stability of the substructure for several loading scenario. More detailed analyses should be included for this structural design, any excavations and modified levee sections.

6.2.2 Geotechnical analysis

The modern Mississippi Delta has been laid down by an intricate system of distributary channels that periodically overflowed into shallow swamps and marshes lying between the channels. The combination of channel extension and sea level rise has served to flatten the grade of the river and its adjoining flood plains. This process created the land on which New Orleans is now built. When floods occur on a major river, water mixed with sediments spills over the banks. The coarsest sediments settle out first close to the river, thus forming natural levees near the river banks. The finer sediments settle out much further away from the river. Over the many floods and river alterations in the course of the Mississippi River channel, this natural process has created a complex and variable geology in the New Orleans area. Layers of gravel, sand, silt and clay are intersected with layers of organic marsh deposits at various locations. An impression of the geological complexity of the New Orleans region is given in figure 6.3.

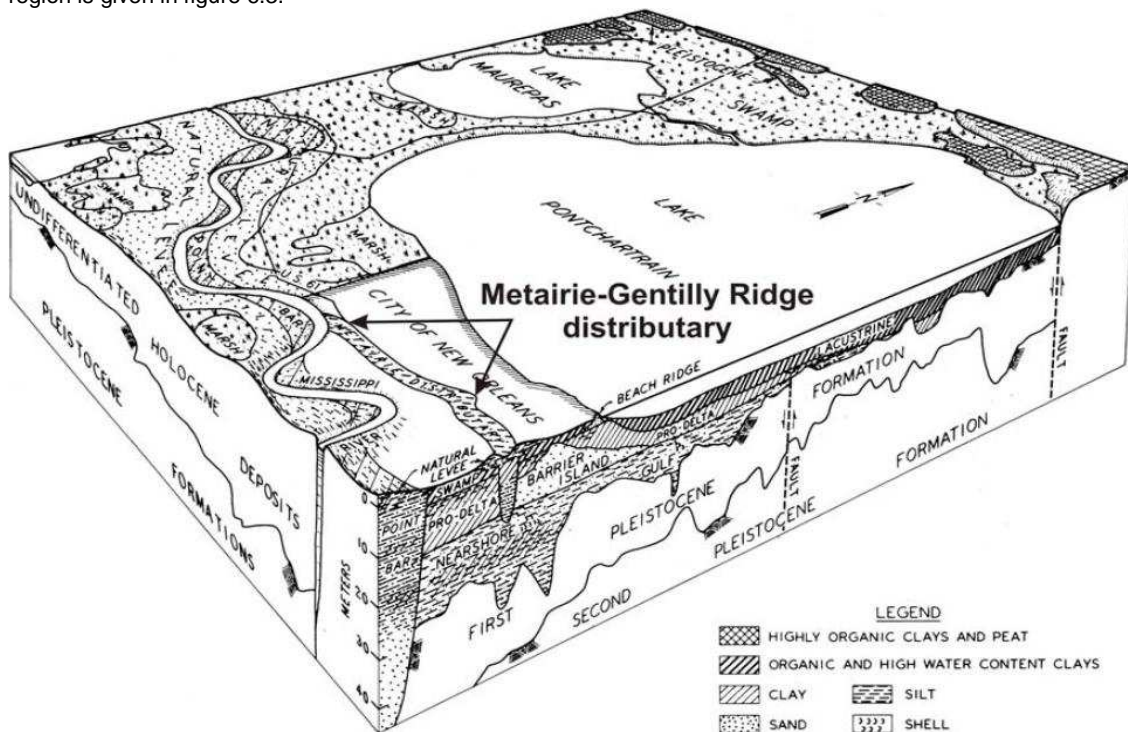


Fig. 6.3: Geological complexity of the New Orleans region [21]

This geological complexity influences the engineering properties of the soils. The Holocene deposits generally have low to very low cohesive strengths, high to very high water contents and high to very high settlement potential. In contrast, Pleistocene sediments have higher shear strengths and lower water contents and settlement potential. Based on data collected by the United States Geological Survey (USGS) from benchmarks located in Orleans Parish for the time period 1951–1995, subsidence has been estimated to occur at an average rate of 0.2 inches/year (5 mm/year). Rates in excess of 1 inch/year (25 mm/year) occurred in some locations.

The site for the projected lifting gate is located in lowlands bounded on the south by the natural levee ridges of the Mississippi River and on the north by a natural levee of an ancient distributary. The lowlands are composed of recent marine deltaic and marsh soil deposits. These recent soil deposits are underlain by moderately stiff clays of the Pleistocene age. The top of the Pleistocene clays is indicated by the borings to be at approximate elevation minus 50 ft (15.3 m) with respect to NAVD88 (2004.65). In section 3.5 it was stated that the difference between this datum and mean sea level (MSL) can be neglected for the location of New Orleans.

Recent deposits include clays, organic layers and sandy and silty soils. Limited information is available to characterize subsurface conditions at the site. Subsurface conditions along the then-proposed MRGO channel alignment are documented in Design Memorandum (DM) No. 1-A Mississippi River Gulf Outlet Channel [1957]. A subsurface profile along the combined MRGO/GIWW channel alignment is described in DM 1-A as follows:

The soil borings disclose that the soils along the proposed waterway consists of a surface layer of peat 3 to 10 ft (0.9 to 3.0 m) thick with water contents of 200 to 700% overlying fat clay with water contents of 50 to 100% which extends to elevation -38 to -44 ft NAVD88 (2004.65) (equal to -11.6 to -13.4 m MSL). Beneath the clay is a layer of silty sand and fine sand with lenses of clay and with few thin lenses of shell about 5 to 20 ft (1.5 to 6.1 m) thick which is underlain by firm clays of the Pleistocene formation.

The geotechnical conditions of the region should be extracted from the little information available. On basis of several global surveys and report, the geological cross-section depicted in figure 6.6 was composed [4]. It generally follows the proposed new barrier alignment and serves as input for any geotechnical calculations in this thesis. Information regarding the soil characteristics of the presented geological cross-section is not available at the time of this thesis. The approach is taken to assign these characteristics according to engineering justice. For this approach Appendix E.1 is used, which is extracted from the Dutch engineering standard NEN 6740. Table 6.4 present the results of this conversion.

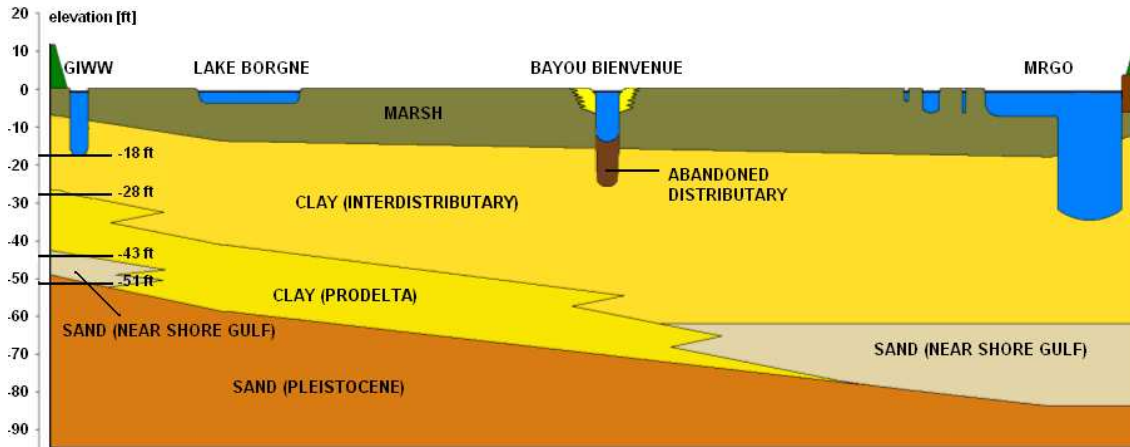


Fig. 6.4: Geological cross-section [4]

Soil type	Soil character (density or strength)	Volume weight (dry)	Volume weight (wet)	Av. cone resistance	Internal friction angle	Cohesion	Undrained shear stress
		$\gamma_{dry} [kN/m^3]$	$\gamma_{wet} [kN/m^3]$	$q_c [MPa]$	$\Phi' [^\circ]$	$C' [kPa]$	$f_{undr} [kPa]$
Marsh	peat, weak not pre-loaded	10/12	10/12	0.1	15	2/5	10/20
Clay (inter-distributary)	clay: weakly sanded moderate strength	18	18	1.5	22.5	10	80
Clay (Pro-Delta)	clay: strongly sanded	18/20	18/20	1.0	25/30	0/2	0/10
Sand (Near shore Gulf)	sand: weakly silted	18/19	20/21	12	27.5/32.5	-	-
Sand (Pleistocene)	sand: clean, dense	19/20	21/22	25	35/40	-	-

Table 6.3: Soil characteristics according to Dutch standards [source: NEN 6740]

6.3 Hydraulic design conditions

Section 6.3.1 presents general assumptions and constraints concerning available hydraulic data. The proposed level of protection extracted from this data is presented in section 6.3.2. Leading circumstances regarding differential head, reverse head, retention area and structural heights are presented in section 6.4.

6.3.1 General description, assumptions and constraints

The design conditions used for the analysis are expected to produce maximum hydraulic loads on the vertical lifting gate. Maximum hydraulic loads on the gates could be produced for intermediate conditions that were not addressed as a part of this thesis. Further investigation is needed at this point. Also in the actual definition of hydraulic design conditions, several assumptions should be noted:

- Design storm information regarding storm surge levels and wave conditions is used to determine the height of the flood protection gate. Changes to the definition of the design storm will therefore affect this height.
- Design storm information is used to calculate hydraulic forces on the gates, thus contributing to the structural design of the gate. Changes to the definition of the design storm will affect the structural design of the gates.
- Design storm characteristics could play a role in determining the type of flood protection gate to be built. In principle, significant changes to the design storm could even affect this decision making.
- Planned height of the surrounding levee system. The New Orleans East Back Levee is expected to be significantly lower than the proposed gate structure. This thesis assumes that the existing levee system has already been raised to a sufficient flood protection level.

Modification to the storm surge and wave transformations resulting from local effects such as the presence of surrounding structures, the configuration of the gates themselves and near shore bathymetric changes were not addressed in this preliminary design thesis. It is understood that the likelihood and significance of these effects will have to be evaluated in the development of the final design of these gates.

Storm surge is a function of many factors including, wind speed, translation speed, landfall location, orientation of the storm track at landfall to the shoreline, levee alignment orientation and storm size. Therefore, there is the need to abandon an event-driven approach that considers only particular storms and move towards a risk based approach that addresses how often assets and populations become inundated and how severe that inundation is for storm events of particular characteristics. This risk-based approach is outside the scope of this thesis.

6.3.2 Hydraulic analysis of the Probable Maximum Hurricane – required level of protection

Comprehensive modeling should be performed in order to determine the level of protection required in the study area. Hydrodynamic modeling of storm surge and waves has been conducted by the USACE to predict wave action for input to engineering and design processes in the future. This is presented in the comprehensive report ‘Louisiana Coastal Protection And Restoration’ (LACPR) [37]. Appendix A.1 summarizes this modeling, in which a single screening storm was selected and simulated on ten separate tracks. The storm selected for the rough order of magnitude estimations is based on the Probable Maximum Hurricane (PMH) as documented in NOAA’s Technical Report NWS 23 [1979]. The PMH criteria for the Louisiana coast describe a storm of Category 5 intensity on the Saffir-Simpson Scale. It should be noted that ten tracks will not provide comprehensive coverage in order to define water levels at every location and it would be incorrect to assume that protective levels described in this thesis provide protection against surges associated with Category 5 hurricanes in all cases.

In the LACPR report [37], the return period of the central pressure associated with this PMH is calculated for a certain coastal stretch of the Gulf of Mexico. The length of the particular coastal stretch is 400 miles (640 km). The return period of the PMH, which has a central pressure of 890 mbar, is then calculated using probabilistic equations. The results are presented in figure 6.5. The return period of the PMH can be extracted from this figure and is set on 200 years.

In general, one can say that a hurricane needs to be with a range of 30 to 40 miles (48 to 64 km) in order to cause real danger. This leads to a return period of PMH in vicinity of New Orleans area equal to:

$$(400/40) * 200 = 2,000 \text{ years.}$$

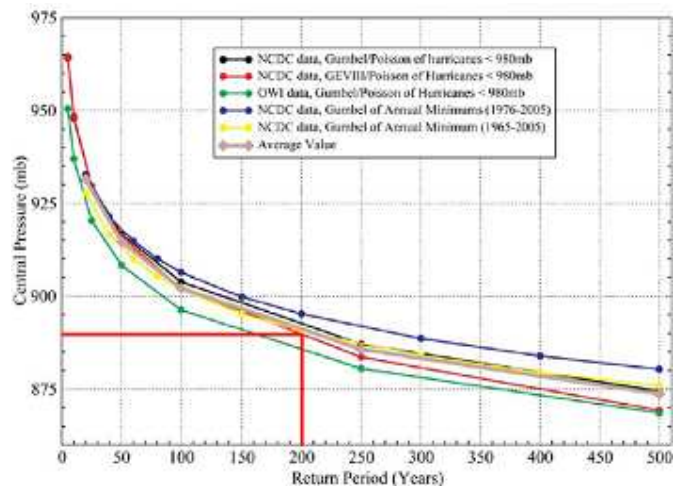


Fig. 6.5: Zone B Gulf of Mexico Hurricanes – central pressure return periods [37]

The probability that this PMH strength hurricane which makes landfall in the stated coastal stretch causes the worst case possible further depends on the exact location of landfall, its path and forward speed. This indicates that the return period for this worst case scenario results in an even larger return period than 2,000 years. However, the level of protection of 1/2,000 [1/year] is used in this thesis.

The hydrodynamic modeling of storm surge and waves has been conducted in order to predict wave action at several proposed levee alignments in combination with the water level response. The alignment corresponding to the central Grand Plan [Louisiana State University, 2006], presented in section 3.1 as the overall basis of this thesis, places a barrier levee across Lake Pontchartrain and along the southwest edge of Lake Borgne. The Rigolets and Chef Menteur Passes, the two major channels that connect Lake Pontchartrain to Lake Borgne and the Gulf of Mexico, are left open under normal conditions. It then generally follows the alignments of existing and proposed hurricane protection projects to Morgan City and runs along the GIWW in the western part of the state. Figure 6.6 present both the modeled levee alignment (upper left corner) and the Grand Plan (bottom). In addition to the levee alignment, figure 6.6 also present the maximum hydraulic conditions for this particular alignment.

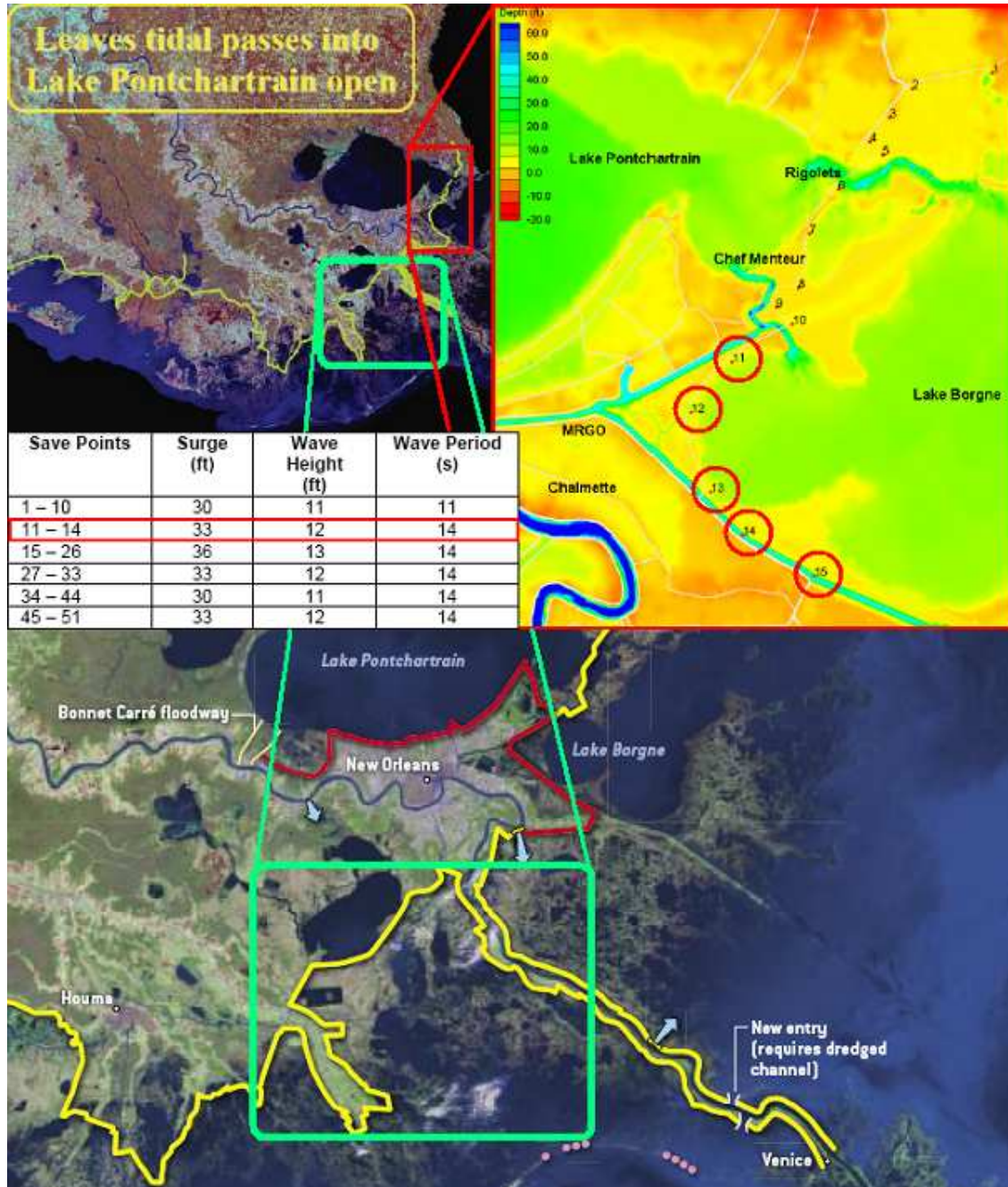


Fig. 6.6: Modeled levee alignment presenting maximum hydraulic conditions [14, 37]

6.4 Appliance and quantification of Dutch standards

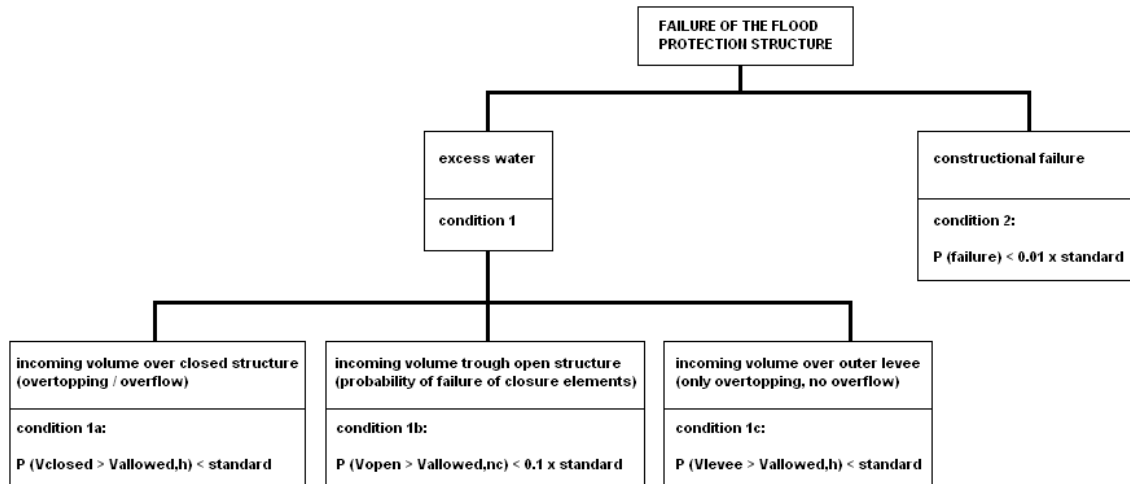
For the preliminary design of the flood protection structure, Dutch standards are followed as documented in the report 'Leidraad Kunstwerken' [9]. Flood protection structures in primary flood schemes need to be constructed with a sufficient level of safety. For this reason, several main requirements concerning the design of these structures are distinguished in the stated document, which are elaborated in the subsequent sections.

Section 6.4.1 outlines the main standards, which can be divided into several main conditions. Section 6.4.2 quantifies the boundary conditions required in these standards. Section 6.4.3 determines the retaining height of the lifting gate and associated maximum incoming volume of water over the closed flood protection structure. Section 6.4.4 outlines the probability of failure of closure elements and associated maximum incoming volume of water through the open protection structure if failure occurs. The stability of the concrete substructure and strength of the steel lifting gate are determined in chapter 7 and 8 respectively.

6.4.1 Overview of main design standards

Figure 6.7 present an overview of the main design standards regarding a flood protection structure as used in The Netherlands. The structure needs to perform to these standards during its entire life span. Besides these general requirements, the structure still needs to perform to the requirements and functions stated earlier in section 4.3 (functional) and section 5.1 (technical).

The essence of this approach is twofold. On one hand, the primary requirements are stated for the probability of exceedance of the allowable volume of water. This volume could enter the retention area either over the closed structure (overflow and overtopping), through the open structure (failure of closure elements) or over the outer levee alignment (overtopping). These conditions can be put under a general condition of excess water. The other main condition concerns constructional failure. The probability of such failure under design conditions should be small compared to the probability of exceedance of the allowable incoming volume.



The mentioned parameters in the formulas can be described as follows:

- $P (V_{closed} > V_{allowed,h}) < \text{standard}$
Probability of exceedance per year of the allowed incoming volume via overtopping and overflow over the closed structure [1/year].
- $P (V_{open} > V_{allowed,nc}) < 0.1 \times \text{standard}$
Probability of exceedance per year of the allowed incoming volume through the open structure as a result of failure of the closure elements [1/year].
- $P (V_{levee} > V_{allowed,h}) < \text{standard}$
Probability of exceedance per year of the allowed incoming volume via overtopping over the outer levee alignment bordering the retention area [1/year].
- $P (\text{failure}) < 0.01 \times \text{standard}$
Probability of constructional failure per year, when given that no exceedance of the design conditions will occur [1/year].
- Standard = the design frequency, which is set on the predetermined 1/2,000 [1/year].

Fig. 6.7: Main standards regarding a flood protection structure [9]

With the exception of condition 2 on constructional failure, each of the standards and conditions are discussed in the subsequent sections. Condition 1a and 1c combined determine the retaining height of the lifting gate. Condition 1b provides insight in the actual safety of the structure, which can be seen independent of the retaining height. It focuses in the probability of failure of various components and also on failure as result of human actions. It is important to outline this in order to provide insight in the measure to be taken to increase safety once the structure is in place. Condition 2 focuses on constructional failure, presenting standards to be used regarding strength and stability of the overall structure. The safety factor used in this thesis is mentioned in chapter 8.

6.4.2 Quantification of required boundary conditions

The requirements regarding the water retaining ability of the vertical lifting gate as presented in figure 6.7 have their focus on the probability of occurrence of excess water in the form of flooding of the hinterland. This leads to conclude that, in order to determine and check the actual design, both the leading outer water levels and wave conditions should be known in correlation with the level to which excess water can be stored in the hinterland. Table 6.4 presents an overview of the minimum required hydraulic boundary conditions for the determination of the influence of excess water and for the design of structural elements. In the quantification of the stated boundary conditions, it should be kept in mind the conditions are time dependent processes and could therefore change over time. The projected sea level rise and subsidence rate should be integrated in the design.

Design requirement	Failure mode	Boundary Conditions	Boundary Conditions
Retaining height (vertical lifting gate and outer levee)	Incoming volume and/or discharge over the closed structure	<ul style="list-style-type: none"> - Maximum surge level; - Variation surge level in time; - Wave conditions at maximum surge level; - Rainfall and local wind setup; 	Maximum allowable surface elevation in the retention area at the time of maximum surge level
Reliability of closure (vertical lifting gate)	Incoming volume and/or discharge through the open structure	<ul style="list-style-type: none"> - Frequency of exceedence of leading high water levels - Rainfall and local wind setup; - Variation water level in time; - Wave conditions at leading high water level; 	Maximum allowable surface elevation in the retention area at the time of maximum surge level
Strength and stability (vertical lifting gate and outer levee)	Constructional failure	<ul style="list-style-type: none"> - Maximum surge level; - Wave conditions at maximum surge level; - Rainfall and local wind setup; 	Surface elevation in the retention area at the time of maximum surge level

Table 6.4: Boundary conditions divided per design requirement [9]

Maximum surge level and the variation of the surge level in time

The maximum surge level is determined in section 6.3 at +33 ft (+10.1 m, MSL), a surge level with a return period of 2,000 years. The variation of the surge level is modeled lightly in accordance to the event of Hurricane Katrina. Figure 3.12 presented time series of water surface elevation along the MRGO for this event. It appears that the offset of the surge takes a longer time than the rise of it. This is used in the model by stating the offset 2 times longer than the rise of the water level. Figure 7.2 presents the modeled variation of the surge level in time. In the design of the lifting gate a slow moving hurricane is modeled, thus opposite to the fast moving Hurricane Katrina. The slower moving hurricane prolongs the surge level elevation and thus represents a more severe situation.

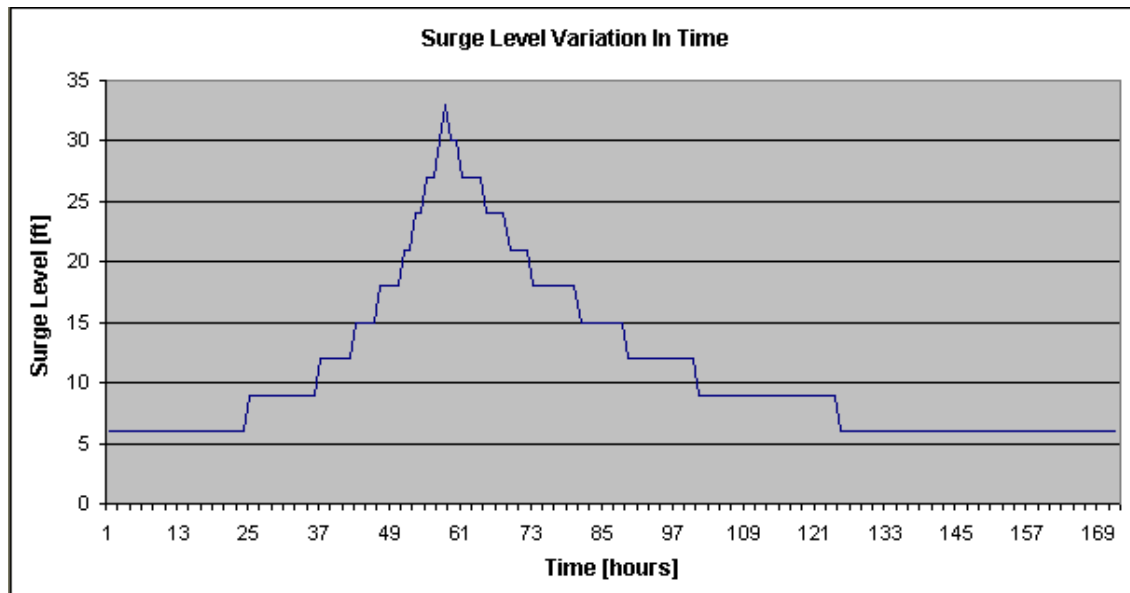


Fig. 6.8: Modeled variation of the surge level in time

Also at this point, it should be noted again that a hurricane could follow an infinite number of paths at a wide range of forward speed. The modeled variation should therefore be handled with care as it only presents a rough indicative relation. Further investigation and numerical modeling is highly recommended.

Wave conditions at maximum surge level: storm conditions

The wave conditions associated with the maximum surge level were determined in section 6.3. The significant wave height is equal to 12 ft (3.7 m) and the peak wave period is equal to 14 seconds. In the preliminary design calculations for the determination of the retaining height and the stability of the structure, it is assumed that these severe wave conditions are present all the time. This is an overestimation of the actual situation and will lead to a higher overtopping discharge. For a more accurate calculation of this overtopping discharge, thus more optimal design, also the wave conditions should have a variation in time. For a final design stage, it could be beneficial to implement this variation. Regarding the check on stability of the structure, the use of maximum wave conditions is justified as this represents the maximum loading state. Information on the variation in time thus not needed.

Rainfall, sea level rise and subsidence

The average total rainfall during Hurricane Katrina is introduced in section 1.2 and derived to be 1 ft (0.3 m). In the modeling of the maximum storm surge level this rainfall is expected to be incorporated. It is not possible to verify this assumption, as the input variables of the PMH-modeling are not available for review.

The time dependent processes of sea level rise and subsidence can be determined for a 100-year period. Section 3.1 stated the expected sea level rise to be 3 ft (0.9 m) per 100 year, a conservative value that could be debated as other sources claim it to be significantly less. The average subsidence is stated in section 6.2 to be 5 mm/year, equal to 0.5 m per 100 year or 1.5 ft per 100 year. Regular checks should be performed regarding these processes to determine if any structural adjustments are needed for strength, stability and retaining height.

Initial surface elevation in the retention area at the time of maximum surge level and maximum level at closure

The maximum surface elevation in the retention area at the time of a required closure of the lifting gate is set to be +5 ft (1.5 m, MSL). This value is used in all following calculations. It should be noted that this is a rough order assumption with significant consequences. A lower allowed value drastically increases the retention ability due to the large surface area of the retention area. Further investigation at this point is therefore highly recommended. The maximum outside water level at the time of closure is set to be +9 ft (2.74 m, MSL). This value denotes the maximum surge level allowed for a safe and reliable closure of the lifting gate.

Maximum allowable surface elevation in the retention area at the time of maximum surge event

This maximum allowable surface elevation in the retention area at the time of the hurricane can be calculated by computing the overtopping and overflow of both the levee alignment and the floodgate structure for the modeled variation of the surge level in time. These calculations are described in section 6.4.3.

In order to determine this vital parameter, the overall defence system regarding the implementation of the gained retention area should be drawn up first. Figure 6.9 presents this system, provided with its main characteristics. Figure 6.10 presents the leading cross-section over the retention area. Levee heights are presented for some parts of the current system, more information on current levee heights is presented in figure 3.20.

Several points of notice regarding figure 6.9 and associated cross-section 1-1':

- Important to mention is the available surface area of the retention basin, which amounts 90 km². This area is fairly large and can be closed at all sides. As can be seen in figure 6.9, in the northwestern tip of the area is closed by the proposed floodgate at the Seabrook location, thus the entrance of the Inner Harbor Navigation Canal (IHNC). The southwestern tip is closed by the proposed new lock (IHNC Lock Replacement Project, see section 4.4.2). The MRGO is also proposed to be permanently closed off (section 4.4.2), leaving only the lifting gate at the GIWW in the northeastern part to close in the event of a hurricane.
- It is assumed that that only incoming volume over this lifting gate and outer levee alignment influence the retention water level. In practice, water levels inside the retention area will rise as excess rainfall and potential floodwaters are pumped in it from out of the populated area via either the Bayou Dupree or Bayou Bienvenue outlet structure. However, for this preliminary design it is assumed that this pumping discharge and associated surface elevation will start after the hurricane event has passed. At this time a higher water level is allowed temporarily as the hurricane induced wind setup is not present anymore.
- The transitional areas in St. Bernard Parish and New Orleans East Parish amount 120 km² and 60 km² respectively. The surface elevation of these areas is about +2 ft (+0.6 m, MSL) and 0 ft (MSL) respectively.
- In this preliminary design stage, the transitional areas are only minimally used as a cost-benefit analysis should be performed for these areas to determine the allowance of flooding. As this information is yet not available, an overtopping discharge of 1 l/s per meter width is set to be as maximum allowed in these areas. This value also accommodates the relatively weak levees, whose non-adjusted grass cover could not handle larger overtopping discharges. The incline of these current primary levees is generally equal to 1:4.
- The total length of the proposed outer alignment between the southeastern tip of St. Bernard Parish and the floodgate structure amounts 18 km. This outer levee is strengthened with a single layer of armour rock to allow a higher overtopping discharge, thus reducing the required crest height. The maximum allowed overtopping discharge over the outer levee is set to be 100 l/s per meter width. The armour layer should be designed for discharge. This calculation is set to be outside the scope of this thesis. Only the crest height of the outer levee will be determined as this directly influences the retaining height needed for the lifting gate.

- The bottom level near the toe of the current primary levee is set to be 0 ft (MSL), whereas the bottom of Lake Borgne is set at -8 ft (-2.5 m, MSL) at both side of the proposed levee alignment.

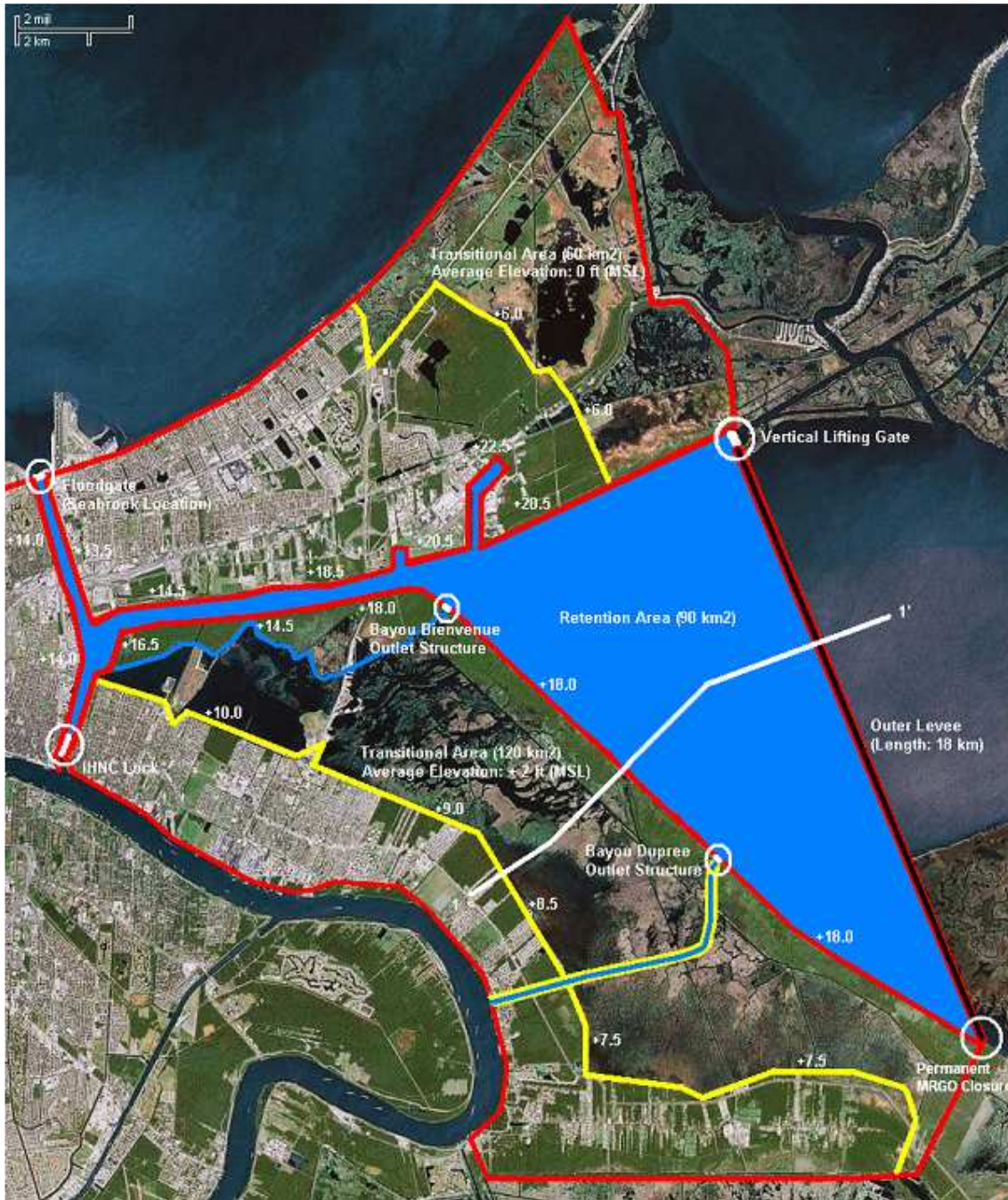


Fig. 6.9: Overview of the projected defence system – characteristics of the retention area

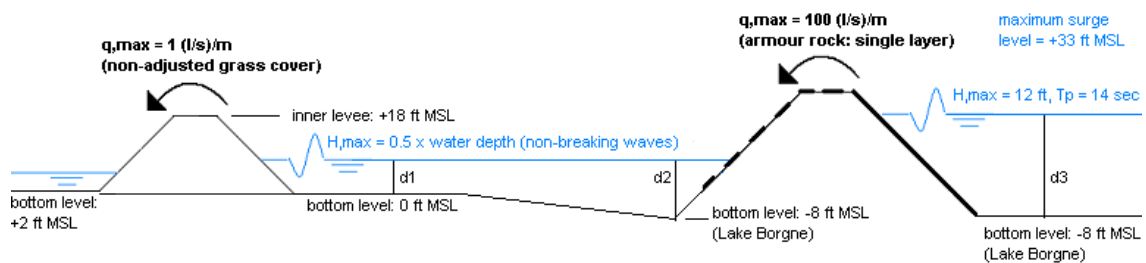


Fig. 6.10: Cross-section 1-1' – retention area and associated design conditions

6.4.3 Retaining height – maximum incoming volume of water over the closed structure

Condition 1a stated that the probability of exceedence per year of the allowed incoming volume via overtopping and overflow over the closed structure should be smaller than the projected standard of once in 2,000 years. Also the probability of exceedence per year of the allowed incoming volume via overtopping over the outer levee bordering the retention area should be smaller than this projected standard. With these conditions, the minimum retaining height of the gate can be determined by using hydraulic conditions corresponding to that standard: Maximum surge level = +33 ft (10.6 m, MSL), maximum wave height = 12 ft (3.7 m) and peak wave period = 14 s.

Figure 6.11 presents a cross-section at the lifting gate, presenting the maximum hydraulic conditions. In order to prevent large forces on the backside of the gate structure, the maximum combined discharge of overtopping and overflow is set at 10 m³/s per meter width of the structure. This value is large but still a factor 1.5 smaller than to which the Hartel Canal Barrier was designed. However, the differential head is significantly larger in this hurricane environment than for that particular barrier. As the influence of the differential head on the resultant loading of overflow on the structure is uncertain, the presumed safe value of 10 m³/s per meter width is used.

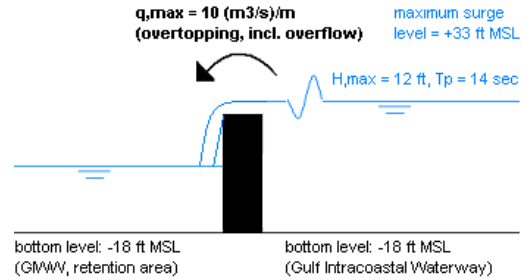


Fig. 6.11: Cross-section 2-2' – lifting gate and conditions

In order to determine the most optimal retaining height of the lifting gate, which would comply with stated limitations and requirements, the approach is taken to subsequently determine the following parameters:

- Maximum allowable surface elevation in the retention area at the time of the maximum surge event;
- Minimum required crest height of the outer levee and associated overtopping discharge over the total event;
- The overtopping and/or overflow allowed over the lifting gate, as direct consequence of the difference between the maximum allowed surface elevation and the share of the elevation caused by overtopping of the levee alignment. This latter parameter iteratively determines the minimum required height of the lifting gate.
- Optimize the height of the lifting gate with introduction of allowed leakage.

Maximum allowable surface elevation in the retention area at the time of the maximum surge event

For wave overtopping, the crest height of a levee is lower than the wave run-up levels at the highest waves. The parameter used to describe the height difference is the free crest height R_c , which is the difference in height between the still water line and the crest height. The crest height of these existing levees is presented in figure 6.9 in relation to mean sea level (MSL) at +18.0 ft (+5.5 m). Wave overtopping is usually given as an average discharge per meter linear width, as is done in this thesis.

Wave overtopping can be described in two formulae, which are linked to each other: one for breaking waves and one for non-breaking waves. The breaker index to distinguish them is given as a function of the wave steepness and the incline of the levee. Breaking waves generally have a breaker index < 2 and non-breaking waves an index > 2 [10]. The wave overtopping formulae for both cases are exponential functions and given by:

$$\frac{q_b}{\sqrt{g \cdot H_s^3}} = \frac{0.067}{\sqrt{\tan(\alpha)}} \cdot \gamma_b \cdot \xi_0 \cdot \exp\left(-4.3 \cdot \frac{R_c}{H_s} \cdot \frac{1}{\xi_0 \cdot \gamma_b \cdot \gamma_f \cdot \gamma_\beta}\right)$$

And a maximum of:
$$\frac{q_{nb}}{\sqrt{g \cdot H_s^3}} = 0.2 \cdot \exp\left(-2.3 \cdot \frac{R_c}{H_s} \cdot \frac{1}{\gamma_f \cdot \gamma_\beta}\right)$$

- In which:
- q = average overtopping discharge [m³/s per meter width];
 - g = acceleration of gravity [m/s²];
 - H_s = significant wave height [m];
 - ξ_0 = breaker index [-];
 - s_0 = wave steepness [-];
 - R_c = free crest height above the still water line [m];
 - γ_b = influence factor for a berm [-];
 - γ_f = influence factor for roughness elements on slope [-];
 - γ_β = influence factor for angled wave attack [-];

The dimensionless wave overtopping discharge at the left part of the inequality and the relative crest height R_c/H_s are both related to the breaker index and/or slope of the levee. In order to take into account the influence of different conditions, the dimensionless crest height is increased by dividing by several influence factors. Wave overtopping for non-breaking waves is no longer dependent on the breaker index. The formula for breaking waves is valid up to the maximum, which is in the region of $\gamma_b \cdot \xi_0 = 2$ [10]. A check must still be performed as the whether the formula for breaking waves exceeds the stated maximum.

The maximum allowable surface elevation in the retention area at the time of the maximum surge event can now be calculated by combining three aforementioned criteria:

- An overtopping discharge of 1.0 l/s per meter width is maximum allowed in transitional areas;
- Significant wave heights within the retention area, in this case induced by the high hurricane wind velocity, can reach a maximum value of 0.5 times the water depth before breaking.
- The incline of the current primary levee is set at 1:4 and the crest height at +18.0 ft (+5.5 m, MSL).

Appendix H1.1 presents the iterative calculation of the maximum required water level under given conditions. The calculation is iterative as the depth influences both H_s and R_c . Since the significant wave height is assumed under non-breaking conditions, the presence of a berm is of no influence and a maximum value for the overtopping discharge is found. This is a safe but conservative approach. As the particular levee has a grass cover and could have a perpendicular wave attack, both influence factors are equal to 1.0.

It follows that the maximum water level allowed in the retention area during a major hurricane event is +2.25 m MSL, equal to +7.4 ft MSL. The maximum surface elevation in the retention area at the time of closure of the floodgate structure was set to be +5 ft (1.5 m, MSL), so the maximum allowed surface level elevation due to overtopping and/or overflow of the outer levee and vertical lifting gate at the time of the maximum surge event is equal to $7.4 - 5 = 2.4 \text{ ft} = 0.73 \text{ m}$.

Minimum required crest height of the outer levee and associated overtopping discharge over the total event

In order to determine the share of the allowed elevation in the retention area that consists of overtopping of the outer levee, the crest height of this levee must be determined first. The approach taken is similar as to the previous calculation. In this case, the prescribed maximum allowed overtopping discharge over this outer levee is set to be 100 l/s per meter width as this levee is projected to be strengthened with a single layer of armour rock.

Appendix H.1.2 presents the calculation of the minimum required crest height of this proposed outer levee. It appears that under the leading wave conditions, which were assumed to be constant over the total event, the formula for non-breaking waves should be used. Given a perpendicular wave attack and armour rock slope strengthening, the corresponding influence factors are equal to 1.0 and 0.7 respectively. It follows that the minimum required crest height of the outer levee under given conditions is equal to 6.77 m above the maximum surge level. This results in a minimum crest height of +47 ft (14.3 m, MSL).

Now the crest height of the outer levee is known, the overtopping discharge can be calculated as a function of the occurring surge level. Table 6.5 present the results of this calculation. The surge level is modeled as a variable in time. The data presented corresponds to the graph of figure 6.8. The overtopping volume per meter linear width for each surge level is calculated as the product of the overtopping discharge and associated duration. The overtopping volume per meter linear width spanning the total event is the sum of these results. The resulting water level elevation of the retention area is equal to this sum of results times the length of the levee alignment (18 km), divided by the surface area of the retention area.

<i>Outer levee alignment - requirement: maximum overtopping discharge $\approx 100 \text{ (l/s)/m}$</i>					
tan α = incline of the outer slope of the levee		1/4 [-]			
h _c = crest level		47 ft			
combined reduction factor		0,7 [-]			
<i>crest height outer</i>	<i>surge level</i>	<i>overtopping discharge</i>	<i>duration</i>		<i>overtopping volume</i>
<i>levee: + 47 ft MSL</i>	<i>[ft]</i>	<i>[(l/s)/m]</i>	<i>[hour, <- l]</i>	<i>[hour, l ->]</i>	<i>[m³/m]</i>
<i>slow moving</i> <i>(PMH, max)</i>	6	0,06	24	x (no diff. head)	5,2
	9	0,13	12	24	16,8
	12	0,30	6	12	19,4
	15	0,69	4	8	29,8
	18	1,56	4	8	67,4
	21	3,55	2	4	76,7
	24	8,06	2	4	174,1
	27	18,33	2	4	395,9
	30	41,68	1	2	450,1
	33	94,78	1	1	341,2
total overtopping volume			1576,7 [m ³ /m]		
length levee alignment			18 [km]		
surface area retention basin			90 [km ²]		
surface elevation retention basin			0,32 [m]		

Table 6.5: Surface elevation of the retention area as a result of overtopping of the outer levee

The minimum required gate height as direct result of overtopping and/or overflow allowed over the lifting gate

The maximum allowed water level increase due to overtopping of the outer levee and overtopping and/or overflow of the lifting gate was calculated to be 7.4 – 5.0 = 2.4 ft = 0.73 m. The surface elevation of the retention area as a result of overtopping of the outer levee over the total event is equal 0.32. This results in an allowed surface elevation due to overtopping and/or overflow of the lifting gate of 0.41 m. This value serves as input for the iterative calculation of the minimum required gate height.

The total overtopping volume is expected to be a combination of overtopping and overflow. In order to determine total overtopped volume of water, both formulae are applied. The basic formula for the overtopping discharge of vertical structures is given by:

$$q = 0.13 * \sqrt{g * H_s^3} * \exp\left(-3.0 * \frac{h_{kr}}{H_s} * \frac{1}{\gamma_\beta * \gamma_n}\right), \text{ given that } h_{kr} > 0.$$

- In which: q = average overtopping discharge [m³/s per meter width];
 g = acceleration of gravity [m/s²];
 H_s = significant wave height in front of the structure [m];
 h_{kr} = crest height of the structure above the still water line [m];
 γ_β = influence factor for angled wave attack [-];
 γ_n = influence factor for the shape of tip of the gate [-];

This formula is valid in the case that there is no severe wave breaking action right in front of the structure [9]. In the case of variable surge level under maximum wave conditions, it possible that such action takes place at some point during lower surge levels. However, as this is highly uncertain, the influence of it is neglected. Further investigation at this point is recommended in order to determine whether the use of the formula is justified. For this preliminary design calculation, both the influence factor for the angled wave attack and for the shape of the tip of the gate is set at 1.0.

As a result of the large retention area, it is expected that some overflow is allowed. This will result in a gate height under maximum surge level. As stated earlier, in order to prevent large forces on the backside of the gate structure, the maximum combined discharge of overtopping and overflow is set at 10 m³/s per meter width. The total discharge over the structure in the case overflow is given as a sum of two contributing parts:

$$q = 0.6 * \sqrt{-g * h_{kr}^3} + 0.13 * \sqrt{g * H_s^3}$$

The first term describes the overflow of a short weir in absence of waves [9]. The second term states the maximum overtopping discharge. This is equal to the overtopping discharge at h_{kr} = 0. For negative values of the parameter it is assumed that this term is constant.

Appendix H.2.1 presents the calculation model for determining the overtopping discharge at a variable surge level. If h_{kr} is positive than the formula for overtopping is used and if h_{kr} is negative the formula for overflow is used. Table 6.6 present the calculation results for a variable surge level. The approach taken is similar to the calculation performed for the outer levee.

<i>Vertical lifting gate - requirement: maximum allowed surface elevation retention basin = 0,73 - 0,32 = 0,41 m</i>					
<i>vertical lifting gate: + 22 ft MSL</i>	<i>surge level [ft]</i>	<i>overtopping discharge [(m³/s)/m]</i>	<i>duration</i>		<i>overtopping volume [m³/m]</i>
			<i>[hour, <-- l]</i>	<i>[hour, l -->]</i>	
	6	0,05	24	x (no diff. head)	4493
<i>slow moving (PMH, max)</i>	9	0,11	12	24	14256
	12	0,23	6	12	15163
	15	0,50	4	8	21384
	18	1,05	4	8	45274
	21	2,22	3	4	55894
	24	3,75	3	4	94475
	27	6,41	2	4	138499
	<u>30</u>	<u>10,06</u>	<u>1</u>	<u>2</u>	<u>108670</u>
	<u>33</u>	<u>14,48</u>	<u>1</u>		<u>52124</u>
	total overtopping volume			550231	[m ³ /m]
width structure			64	[m]	
surface area retention basin			90	[km ²]	
surface elevation retention basin			0,39	[m]	

Table 6.6: Minimum required gate height as direct result of overtopping and/or overflow allowed over the lifting gate

It can be concluded that the minimum crest height of the lifting gate regarding the allowed water surface elevation in the retention area is equal to +22 ft (6.7 m, MSL). However, this crest height is not desired since for a surge level higher than +30 ft, the maximum allowed combined discharge of overtopping and overflow is exceeded. This means that the crest height needs to be increased in order to decrease maximum discharge over the structure. In the determination of this minimum gate height, time dependent sea level rise and subsidence are not included. These processes would even further increase the combined overtopping discharge.

Increasing the gate height has the additional benefit that some leakage around the structure can be allowed as less water enters the retention area over the structure. This given provides some margins in the design and construction of the gate. It could possibly reduce the need for maintenance as the rubber seals needed to provide water tight closures tend to degrade relatively fast in a salt water environment. Immediate replacement is not needed in the case leakage is allowed. For this reason, it is important to determine an optimal combination of the actual gate height and the allowed leakage volume.

The optimal combination of gate height and allowed leakage volume

The amount of leakage allowed is equal to the water surface elevation allowed in the retention area in addition to the overtopping discharge over the outer levee and lifting gate. Appendix H.2.2 present the calculation model used to determine the leakage discharge per meter width of the structure. The conversion to this parameter is performed in order to implement the results into the model for a variable surge level. For flow under the gates, the discharge efficiency is affected by the gate seat location relative to the top of the sill. It is difficult to quantify a specific discharge coefficient for a vertical lifting gate, as it is strongly dependent on the lip configuration at the bottom of the gate. In this preliminary design stage, an overestimated discharge coefficient of 1.0 is assumed for both the bottom and sides of the gate.

Appendix G.3 presents an iterative calculation for several combinations of leakage width at the sides and bottom and the corresponding required height of the gate. Table 6.7 present the calculation results for three elaborated combinations. The approach taken is again similar to the previous calculations in the use of a variable surge level. This can be seen in table 6.8, which presents the calculation overview of combination 3.

Requirement: maximum surface elevation retention basin due to leakage + overtopping / overflow \leq 0.41 m			
<i>Combination 1</i>	<i>Leakage width:</i> 0.05 m at sides and bottom	total leakage volume	163397 [m ³ /m]
		surface elevation retention basin	0,12 [m]
	<i>Required height lifting gate:</i> + 24 ft MSL	maximum discharge over the gate	11,46 [(m ³ /s)/m]
		total overtopping volume	371711 [m ³ /m]
		surface elevation retention basin	0,26 [m]
<i>Combination 2</i>	<i>Leakage width:</i> 0.10 m at sides and bottom	total leakage volume	333385 [m ³ /m]
		surface elevation retention basin	0,24 [m]
	<i>Required height lifting gate:</i> + 27 ft MSL	maximum discharge over the gate	7,53 [(m ³ /s)/m]
		total overtopping volume	208926 [m ³ /m]
		surface elevation retention basin	0,15 [m]
<i>Combination 3</i>	<i>Leakage width:</i> 0.05 m at sides, 0.15 m at bottom	total leakage volume	454720 [m ³ /m]
		surface elevation retention basin	0,32 [m]
	<i>Required height lifting gate:</i> + 30 ft MSL	maximum discharge over the gate	4,50 [(m ³ /s)/m]
		total overtopping volume	113289 [m]
		surface elevation retention basin	0,08 [m ³ /m]

Table 6.7: Calculated combinations of leakage width and required gate height

From table 6.7 can be concluded that the minimum leakage width of 0.05 m at all sides is not desirable. The associated minimum required gate height of +24 ft (7.3 m, MSL) still results in a maximum combined overtopping discharge larger than the prescribed maximum of 10 m³/s per meter width. Time dependent processes are not even included at this point. Quantifying the time dependent processes of seal level rise and subsidence leads to conclude that the optimal combination of allowed leakage and minimum required gate height is combination 3. The sum of both processes predicts a relative maximum surge elevation rise of 3 + 1.5 = 4.5 ft per 100 year, equal to 1.4 m. Computing the maximum overflow discharge results in:

$$h_{kr} = 30 \text{ ft (gate height)} - (\text{max. surge level} + 4.5 \text{ ft}) = -7.5 \text{ ft, which gives: } q = 9.4 \text{ (m}^3\text{/s)} / \text{m} < \text{allowed maximum}$$

This gate height at +30 ft MSL has the additional benefit that no perfect closure is needed at the bottom of the gate during a storm event. A space of 0.15 m can be allowed between the gate and the top of the sill, which reduces the need for maintenance of the sill regarding siltation.

0.05/0.15 m – requirement: max. surface elevation retention basin due to leakage + overtopping/overflow ≤ 0.41 m						
leakage width:	surge level	leakage discharge	duration		overtopping volume	
			[hour, <--]	[hour, -->]		
0.05 at sides	[ft]	[(m ³ /s)/m]			[m ³ /m]	
0.15 m at bottom	6	0,39	24	x (no diff. head)	33782	
	9	0,78	12	24	101218	
	12	1,03	6	12	66938	
	15	1,24	4	8	53352	
	18	1,41	4	8	60826	
	slow moving	21	1,56	2	4	33739
	(PMH, max)	24	1,70	2	4	36763
		27	1,83	2	4	39571
		30	1,95	1	2	21092
		33	2,07	1		7438
	total leakage volume		454720	[m ³ /m]		
	width structure		64	[m]		
	surface area retention basin		90	[km ²]		
	surface elevation retention basin		0,32	[m]		
vertical lifting	surge level	overtopping discharge	duration		overtopping volume	
			[hour, <--]	[hour, -->]		
gate: + 30 ft MSL	[ft]	[(m ³ /s)/m]			[m ³ /m]	
slow moving	6	0,01	24	x (no diff. head)	656	
	9	0,02	12	24	1944	
	(PMH, max)	12	0,03	6	12	2074
		15	0,07	4	8	2894
		18	0,14	4	8	6134
		21	0,30	3	4	7560
		24	0,64	3	4	16002
		27	1,35	2	4	29052
		30	2,85	1	2	30758
		33	4,50	1		16214
	total overtopping volume		113289	[m ³ /m]		
	width structure		64	[m]		
	surface area retention basin		90	[km ²]		
	surface elevation retention basin		0,08	[m]		

Table 6.8: Calculation overview of the leading combination of allowed leakage volume and minimum required gate height

Conclusion and recommendations concerning the maximum incoming volume of water over the closed structure

From this point on, this thesis assumes the height of the vertical lifting gate height at +30 ft (9.1 m, MSL). The maximum overtopping discharge at the time of realization is about 5 m³/s per meter width, which is about half the prescribed maximum. Due to the time dependent change of sea level rise and subsidence, the maximum allowed discharge is reached in about 100 years.

Some final remarks and recommendations:

- The significant wave height in the retention area during the leading storm event is assumed maximum under non-breaking conditions, leading to a wave height of 0.5 times the water depth and a maximum value for the overtopping discharge. This is a safe but conservative approach. Since this directly influences the allowed surface elevation in the retention area, it could be beneficial to further investigate this local wave climate.
- In order to reduce the probability of failure regarding overtopping discharge, it is advised to monitor the time dependent changes and to regularly check whether the retaining height of the gate is still sufficient. If checks suggest that the maximum overtopping discharge could be exceeded, additional height must be created.
- It is also advised to monitor the outer levee, in particular regarding failure of the protective armour layer and regarding subsidence. This structure acts independent in relation to the lifting gate. The outer levee should be maintained in such a manner that its overtopping volume during the leading storm event does not result in a surface level elevation in the retention area larger than 0.32 m.

6.4.4 Safety of closure elements – maximum incoming volume of water through the open structure [9]

Condition 1b stated that the probability of exceedence per year of the allowed incoming volume through the open structure due to failure of closure elements should be smaller than 0.1 times the projected standard of once in 2,000 years. On the basis of the requirement, an open retaining level (ORL) can be determined in coherence with a maximum allowed probability of failure of the closure process. This is described in the following formula:

$$P(V_{\text{open}} > V_{\text{allowed};nc}) = P(h_{\text{surge}} > \text{ORL}) * P_{nc} = n_{\text{year}} * P_{nc} < 0.1 \times \text{standard} = 5 * 10^{-5}$$

in which: $P(h_{\text{surge}} > \text{ORL})$ = frequency of exceedence of the surge level in relation to the open retaining level;

ORL = open retaining level. This is the maximum outside surge water level at which it is allowed for water to enter the retention area through the open structure;

P_{nc} = probability of failure of the closure elements at the time the open retaining level is exceeded;

n_{year} = required closing frequency of the lifting gate, which is equal to $P(h_{\text{surge}} > \text{ORL})$.

The main difference in the check on the water retaining safety of a closed structure and open structure is the subsequent steps of reasoning. The minimum retaining height of the structure is determined on the basis of the maximum occurring surge level and wave conditions. In the case of an open structure as consequence of failure of closure elements, the geometry of it and the associated open retaining level is the basis of the check on safety. In the definition of the open retaining level, it is assumed that after exceedence of this level the probability of safety and reliable closure can be neglected. This results in a conservative approach. Once the open retaining level and frequency of exceedence of this level are determined, the required closing frequency of the lifting gate can be calculated. Finally, the probability of failure of the closure elements at the time this open retaining level is exceeded needs to be estimated. This requires an analysis of the safety of the closing process of the lifting gate.

In this preliminary design, first a rough order assessment is carried out regarding the safety of the closing process of the lifting gate. According to the used standard [9], the probability of non-closure of a single gate has an order of magnitude of 10^{-3} . This is a general value and does not accommodate the gate driving system or any external conditions. A more thorough analysis is therefore presented in this thesis in order to distinguish the influence human induced failures, failure of mechanical components and external causes. The discrete criteria used in this detailed analysis are stated in four main categories [9]:

A High water warning system

The main requirements regarding the high water warning system:

- There should be two independently functioning warning systems. The main failure modes of one system should not cause failure of other. In the case multiple measuring devices are projected, each of these devices should have its own power supply and wiring. A complementary requirement is that the system should be automatic and self-registering.
- If during potential high water people have to be warned via human actions, the particular procedures need to be put down in manuals and be practiced at least once a year.

B Procedure for mobilization

If the lifting gate is not permanently manned, it should fulfil the following requirements:

- There is a procedure present that states how the required mobilization of personnel is arranged, not only those need for operating the gate but also supportive technical and maintenance personnel.
- There is a pre-warning system and feed-back system should be present.
- Regarding personnel, there should always be a sufficient number of people attainable and employable. To accommodate this, replacement schedules including tasks and responsibilities should be drawn up.
- All operating and supportive personnel should be adequately trained. A comprehensive practice run should be performed at least once a year.
- The lifting gate should be accessible during extreme conditions.

C Procedure for closure of the lifting gate

The high water warning system could generate an automatic closure of the lifting gate. In the absence of such a system, operation of the lifting gate should be performed by trained personnel. In either case, the following main requirements should be fulfilled:

- There is a procedure present that describes a non-automatic closure of the gate.
- There is a procedure or manual present that stated the required actions needed to allow a safe and reliable closure of the gate. It should state tasks and responsibilities, the order in which the actions should take place and the procedure in case of disturbances.
- Potential abusive actions could be noticed in time and be corrected.
- All operating and supportive personnel should be familiar with the stated procedures. A practice run should be performed at least once a year.
- The main parts of the lifting gate should be alight if visibility is low.
- Adequate communication of personnel on site should be possible.

D Guaranteed proper operation of the closure elements

The main requirements regarding the operation of the closure elements:

- Disturbance during normal gate operation should be adequately intercepted by either a manual or alternative operation system including an emergency generator.
- The flood protection structure should be checked at least twice a year and fully tested once a year.
- The probability of a ship collision, expected to lead to immediate failure and non-availability of the gate, should be kept sufficiently small.

In this safety analysis of technical and/or human induced failure of the closing process of the lifting gate, two quantities are used to describe failure of a particular component. The quantities include the probability of failure per time interval and the probability of non-availability of the component. The probability of failure per time interval is denoted by λ [1/time unity] and is always applicable on a component with a continuous function. If the particular component has a constant failure frequency, the probability of failure of the component of given by:

$$F(t) = 1 - e^{-\lambda t}, \text{ which equals } F(t) = \lambda t \text{ for } \lambda t < 0.1$$

The probability of non-availability of a component during a required action can be caused by spontaneous failure, non-noticeable failure in the precedent time period, testing or repairs. These causes can be denoted as:

$$U = Q + U_{\text{non-noticeable}} + U_{\text{test}} + U_{\text{repair}}$$

Spontaneous failure is related to a component that has to perform only one monetary movement. A probability of failure Q is introduced every time the monetary condition is adjusted. The non-availability caused by testing of components can be neglected as these tests should always be performed outside the storm season.

The probability of non-availability due to repair of the component can be determined analogously to the probability of non-availability due to non-noticeable failure in a precedent time interval. The latter is therefore treated first. If components not permanently have to fulfill a particular function, these components could transit from non-failure conditions into failed conditions without notice. If the failed component is not operated during a certain time period, this failure is not noticed. In order to avoid these non-noticeable failures, regular maintenance and testing is required. The probability of non-availability of a component proceeds from 0 at the start to λt at the end of a test interval. The average probability of non-availability due to non-noticeable failure therefore equals:

$$U_{\text{non-noticeable}} = \frac{1}{2} \lambda T$$

Analogously, if the average repair time for a component is denoted by Θ , then the probability of non-availability during a required action due to repair of the particular component is equal to:

$$U_{\text{repair}} = \lambda \Theta$$

The overall probability of non-availability of a component during a required action can now be denoted as follows:

$$U = Q + U_{\text{non-noticeable}} + U_{\text{test}} + U_{\text{repair}} = Q + \frac{1}{2} \lambda T + \lambda \Theta$$

Description of the projected situation – high water warning system, power and control system and personnel

The projected lifting gate protects the populated areas of St. Bernard Parish and Orleans Parish from Lake Borgne induced flooding during major hurricane events. The design frequency for this structure equals the expected return period of a major hurricane in this area and is set at 1/2,000 [1/year]. The main function of the gate is the stated protection against flooding. Other functions of the gate include the safe passage of vessel and the discharge of excess water during normal conditions.

The lifting gate is composed of one steel gate. The maximum surface elevation inside the retention area at the time of a required closure of the gate is set to be +5 ft (1.5 m, MSL). The maximum outside water level to allow a safe and reliable closure is set to be +9 ft (2.74 m, MSL). The exceedence of this outside water level is assumed to be once per year. It should be noted that this is a rough order assumption with significant consequences. No information regarding the development of water levels in the area is available at the time of this thesis. This value should therefore be handled with care as it is not verified.

Initial assumptions should be made with regard to the high water warning system. At this point it is projected that there are two independent, continuous water level measuring devices which are tested every month in order to guarantee a proper operation. Two staff members are responsible for an adequate reading of these devices. This personnel and measuring devices can be seen as two independent warning systems. Once the allowed water level inside the retention area is exceeded, the lifting gate needs to be closed. In addition, there is a premonishment system for extreme weather conditions.

The operation procedure is put down in a manual. It is expected that there are sufficient possibilities to check performed actions and sufficient time for recovery in the event of minor operation faults.

An important design criterion in the safety of the closing process is whether the lifting gate is permanently staffed. Initially, the scenario is projected that the gate is not permanently staffed. If the water level inside the retention area is expected to be exceeded within the hour, a staff member is send to the gate in order to operate it on site. The lifting gate is projected at remote location as no road connection to the lifting gate is available yet. However, it is not that far located from the populated areas of Orleans Parish and the Chef Menteur Highway. Figure 6.12 present the actual location of the gate in relation these existing features. Constructing a road connection to the lifting gate is would allow a fast and easy access for personnel for operating and regular maintenance. The main procedures concerning the mobilization of personnel are put down in manuals, including stand-by arrangements for additional or replacement members.

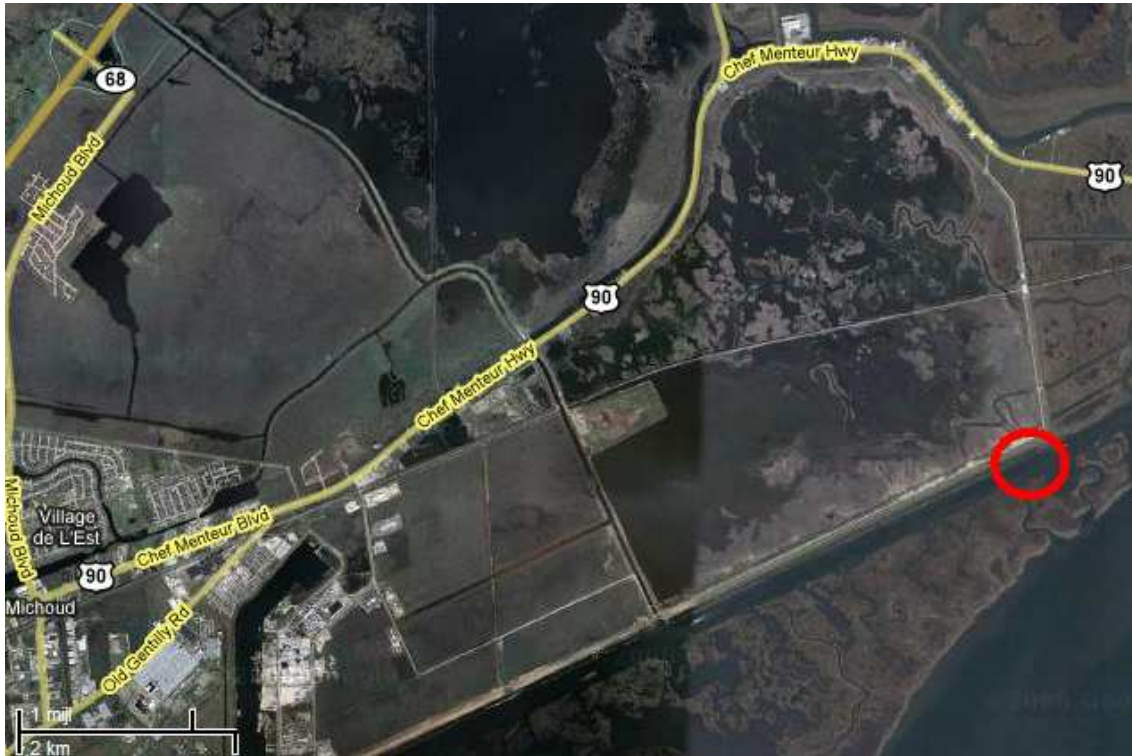


Fig. 6.12: Mobilization of personnel – the accessibility of the projected site

In general, two optional gate driving types can be considered in contemporary vertical lifting gate projects. These types include an electromechanical system and an electro-hydraulic system. Most existing lifting gates are driven by a system of the first type. Nevertheless, the latter is considered to be a better solution for the projected lifting gate. It is chosen at this point despite the very long lifting height, which is never before realized by a single cylinder, as there is a general development of an increasing quality and reliability of hydraulic technology. The most important advantages of an electro-hydraulic system are the better automatic control possibilities it provides, the relatively easy maintenance and the good environmental performances.

An electro-hydraulic hoisting system consists in principle of several main components per hoisting tower, which include an oil tank and oil pipe system, a pump driven by an electrical engine and a hydraulic cylinder. In the projected lifting gate, the most impressive of these components will be the hydraulic cylinders. Important in the design of the cylinder is their function. This means that it should be determined whether the cylinders should only be used to move the gates, or also to hold them in a lifted position. The second view appears to be more convincing. Its main advantage is of a failure-analytical nature. A gate locking device in the tower, having an own probability of failure, would increase the malfunctioning chance of the entire system at the moment of closure. This is expected to be more hazardous than setting the hydraulic system under continuous oil pressure [18].

The lifting gate operation is projected to be powered by the city power net. As is usual for such important structures, emergency generators should be installed as a back-up to the possible net power failure. During failure of the closing mechanism, no manual or alternative back-up operation system is present except these generators. The closing proceeds fully automatically but there should be staff present at the lifting gate to monitor this procedure. When the gate is in lifted position, no staff members are usually present in the operation center at the site of the gate. The actual closing time of the gate is estimated to be about 2 hours.

Check on safety of the closure element

The following steps are subsequently taken in the check on safety of the closure element:

- 1) Determination of the open retaining level;
- 2) Determination of the frequency of exceedence of the open retaining level;
- 3) Determination of the probability of failure of the closing process of the lifting gate;
- 4) Check the probability of failure of the closing process with regard to the predetermined standard.

Each of these parameters is quantified subsequently:

- 1) Determination of the open retaining level

Starting point in the determination of the open retaining level is the maximum allowed incoming volume of water through the open structure, denoted in the maximum allowed surface level elevation with the retention area. At this point it is possible to distinguish two possible scenarios:

- The modeled maximum hurricane with associated surge level development and leading wave conditions. This scenario allows the maximum initial water level in the retention area to be at + 5 ft MSL. An additional 2.4 ft (0.73 m) surface level elevation is expected to be caused by overtopping discharges over the outer levee and lifting gate. The occurrence of this leading event is equal to the projected level of protection and therefore not suitable to determine the open retaining level. A different approach should be taken.
- A severe surge level rise in both wind induced surge level development and wave conditions, but not with hurricane proportions. This scenario allows the maximum initial water level in the retention area to be higher, probably at level of up to +9 ft (2.74 m, MSL). Figure 6.9 presented an overview of the current crest heights of levees and/or floodwalls. The estimated maximum water level leaves a sufficient free-board at the levees and floodwall adjacent to the Inner Harbor Navigation Channel (IHNC). Assuming a mild wave development due to the moderate wind climate, a value of +9 ft (2.74 m, MSL) seems reasonable. A check could be made to validate this assumption. The occurring wave conditions in this scenario are set to be equal to a significant wave height of 3 ft (0.91 m) and peak wave period of 4 s. The maximum allowable surface level in the retention area at the time of these wave conditions can now be calculated by combining the criteria that a maximum overtopping discharge of 1.0 l/s per meter width is allowed over the current primary levees and that the general crest height at +18.0 ft (+5.5 m, MSL). The waves are non-breaking, thus the following formula can be used:

$$\frac{q_{nb}}{\sqrt{g} * H_s^3} = 0.2 * \exp\left(-2.3 * \frac{R_c}{H_s} * \frac{1}{\gamma_f * \gamma_\beta}\right), \text{ thus: } \frac{1 * 10^{-3}}{\sqrt{9.807} * 0.91^3} = 0.2 * \exp\left(-2.3 * \frac{R_c}{0.91} * \frac{1}{1.0 * 1.0}\right)$$

This results in a value for $R_c = 2.51 \text{ m} = 8.3 \text{ ft}$. The estimated open retaining level of +9 ft MSL is valid.

- 2) Determination of the frequency of exceedence of the open retaining level

The frequency of exceedence of the open retaining level determines the average number of times per year the lifting gate has to be closed. This frequency of exceedence equals the frequency of required closure of the gate and can be denoted as:

$$n_{\text{year}} = P(h_{\text{surge}} > \text{ORL}) = 10^{-(x-A)/B}, \text{ in which:}$$

A = outer surge level with a probability of exceedence of once per year. This value is assumed to be equal to +5 ft (1.52 m, MSL);

B = constant decimation value = 0.42 [-]

$$x = \text{ORL} = +9 \text{ ft (2.74 m MSL)}, \text{ thus: } n_{\text{year}} = P(h_{\text{surge}} > \text{ORL}) = 10^{-(2.74-1.52)/0.42} = 1.25 * 10^{-3}$$

It should be noted that this value is highly dependent on the previously stated assumptions regarding the outer surge level with a probability of exceedence of once per year and the open retaining level. Table 6.9 presents this dependency by calculating the frequency of exceedence for a variable value of $x - A$.

$x - A$ [ft]	5	4	3	2	1	0
n_{year} [-]	$2.35 * 10^{-4}$	$1.25 * 10^{-3}$	$6.65 * 10^{-3}$	$3.54 * 10^{-2}$	$1.88 * 10^{-1}$	1.0

Table 6.9: Dependency of the frequency of exceedence of open retaining level

Although not available for this thesis, basic hydraulic information of the region provides the first parameter. The occurring wave conditions determine the second parameter and need to be defined adequately. For the difference of 4 ft (1.22 m), the predetermined probability of non-closure of a single gate proves sufficient:

$$P(V_{\text{open}} > V_{\text{allowed;nc}}) = P(h_{\text{surge}} > \text{ORL}) * P_{\text{nc}} = 1.25 * 10^{-3} * 10^{-3} = 1.25 * 10^{-6} < 0.1 \times \text{standard} = 5 * 10^{-5}$$

It appears that even for a difference of 2 ft (0.6 m), the closing process proves to be sufficiently safe. Now the predetermined value of 10^{-3} is further investigated. The influences of human induced failures, failure of mechanical components and due to external causes are distinguished.

3) Determination of the probability of failure of the closing process of the lifting gate

The probability of failure of the closing process of the lifting gate can best be presented with the use of an event tree as depicted in figure 6.13. In the event the start scenario of a surge level exceeds +9 ft MSL, inundation will occur in case the lifting gate fails to close. This can be caused by:

- Failure of the alarm – measuring devices and reading;
- Failure of mobilization of staff members;
- Failure during operation – human induced failures;
- Failure during operation – failure of the electro-hydraulic system;
- Failure due to external causes – non-availability caused by ship collision;
- Failure due to external causes – the occurrence of blockage by debris and/or siltation of the sill.

These failure modes are quantified subsequently. The overall probability of failure of the lifting gate is found by summation of each separate failure mode.

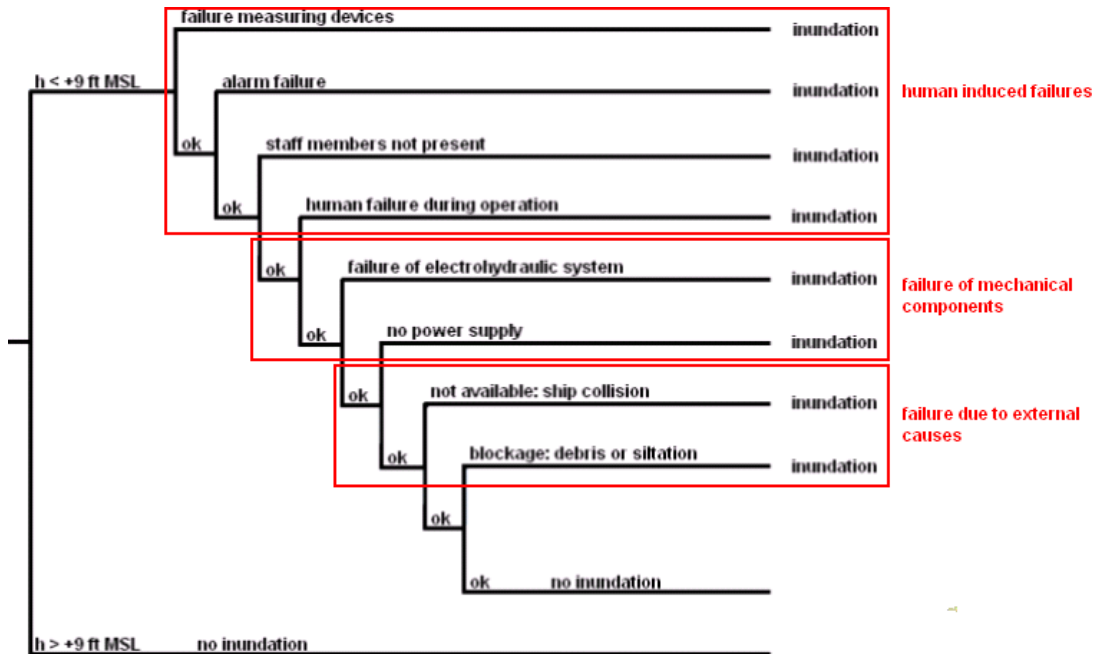


Fig. 6.13: Event tree describing the probability of failure of the closing process of the lifting gate [9]

Failure of the alarm – measuring devices and reading

At the occurrence of a high water, the first potential point of failure of the closing process is within the measuring devices as part of the high water warning system. The failure frequency of the measuring devices is presented in table E.2 of Appendix E. It is of the order 10^{-5} per hour. The probability of non-availability of the devices can now be determined given the fact that the devices should be checked every month and by neglecting any repair times:

$$U_{md} = \lambda T / 2 = 10^{-5} * (30 * 24) / 2 = 3.6 * 10^{-3}$$

In the case the measuring devices perform sufficiently, personnel responsible for reading the devices still have to perform adequately. Initially, it is set that two staff members are responsible for an adequate reading of these measuring devices. The probability that the alarms and/or measuring devices are wrongfully acted upon by both persons is equal to the probability of misinterpretation of the first person times the probability of misinterpretation of the second person. The failure frequency of these human errors is presented in table E.5 of Appendix E. The total probability of wrongfully assessing the alarms is given by:

$$P_{alarm} = P_1 * P_2 = (1.0 * 10^{-3}) * (5 * 10^{-2}) = 5 * 10^{-5}$$

Introducing an additional staff member would further reduce this probability by a factor of $5 * 10^{-2}$.

Failure of mobilization of staff members

Initially, the scenario is projected that the gate is not permanently staffed. If the water level inside the retention area is expected to be exceeded within the hour, a staff member is sent to the gate in order to operate it on site. Constructing a road connection to the lifting gate allows a fast and easy access for personnel for operating and regular maintenance.

Assume an operating team of 4 staff members. A work shift requires at least 1 person and one additional person should always be available as stand-in. Failure of the closing process of the gate occurs if all four staff members are not available. The probability of that a person is sick can be extracted from table E.4 in Appendix E and equals $5 \cdot 10^{-2}$. The probability of non-availability of the stand-in person equals $1.0 \cdot 10^{-2}$ if proper arrangements are made and $2 \cdot 10^{-1}$ if no arrangements are made. The main procedures concerning the mobilization of personnel are put down in manuals, including stand-by arrangements for additional or replacement members. The following failure modes can occur:

No person sick but none available	$P = 1[\text{combination}] \cdot (10^{-2})^2 \cdot (0.2)^2 = 4.0 \cdot 10^{-6}$
One person sick, others not available	$P = 4[\text{combinations}] \cdot (5 \cdot 10^{-2}) \cdot (10^{-2})^2 \cdot 0.2 = 4.0 \cdot 10^{-6}$
Two people sick, others not available	$P = 6[\text{combinations}] \cdot (5 \cdot 10^{-2})^2 \cdot (10^{-2})^2 = 1.5 \cdot 10^{-6}$
Three people sick, fourth not available	$P = 4[\text{combinations}] \cdot (5 \cdot 10^{-2})^3 \cdot 10^{-2} = 5.0 \cdot 10^{-6}$
Four people sick	$P = 1[\text{combination}] \cdot (5 \cdot 10^{-2})^4 = 6.3 \cdot 10^{-6}$

The total probability of failure during the mobilization of operating personnel equals $21 \cdot 10^{-6}$. This approach is conservative because it is assumed that no additional measures are undertaken in the case that the four members of the operation team are all not available. This situation should always be avoided.

Failure during operation – human induced failures

The operation procedure is put down in a manual. It is expected that there are sufficient possibilities to check performed actions and sufficient time for recovery in the event of minor operation faults. Suppose a situation without proper training of personnel, then the probability of failure of the closure process due to human errors can be determined by the summation of possible errors. The failure frequencies of these human errors are presented in table E.5 of Appendix E. The following errors can be distinguished:

- Fault in handling sequence of about 5 items: $4.0 \cdot 10^{-1}$ [q]
- Fault by neglecting a particular action, although the presence of checklist: $1.0 \cdot 10^{-2}$ [q]
- Fault in the operation of particular parts: $1.0 \cdot 10^{-2}$ [q]
- Fault in selection of proper switch or display: $1.0 \cdot 10^{-2}$ [q]

The total probability of failure equals $4.3 \cdot 10^{-1}$ [q], which is relatively high. A proper training is required and a comprehensive practice run should be performed at least once a year. It is assumed that this would decrease the probability of failure to $1.0 \cdot 10^{-3}$ [q].

Failure during operation – failure of the electro-hydraulic system

An electro-hydraulic hoisting system is chosen over the electro-mechanical system and consists of the following components per hoisting tower: an oil tank and oil pipe system, a pump driven by an electrical engine and a hydraulic cylinder. The electro-hydraulic system fails if a failure occurs in one of the two separate systems. It is assumed that all mentioned components of per system act independently, thus all with a distinctive probability of failure, and that failure occurs if one of the components fails. The failure frequencies per main component of the hydraulic system are presented in table 6.10, which is extracted from table E.3 in Appendix E. The probability of failure during the closure process of 2 hours equals $1.8 \cdot 10^{-3}$.

Component	Failure mechanism	λ [/h] or Q [/q]	Probability of failure during closure process of 2 hours
Cylinder	Fails	1.0×10^{-7} [/h]	2.0×10^{-7}
Filter	Blockage	1.0×10^{-5} [/h]	2.0×10^{-5}
Non-return valve	Fails to open	1.5×10^{-4} [/q]	1.5×10^{-4}
	Fails to close	1.6×10^{-3} [/q]	1.6×10^{-3}
	Opens not in time	9.5×10^{-7} [/h]	9.0×10^{-6}
Piston	Leakage along the cylinder	5.0×10^{-7} [/h]	1.0×10^{-6}
Pressure vessel	Leakage	5.0×10^{-6} [/h]	1.0×10^{-5}
Regulating valve	Internal leakage	5.2×10^{-6} [/h]	1.1×10^{-5}
	Fails to regulate	2.6×10^{-5} [/h]	5.2×10^{-5}
	Blockage	1.7×10^{-6} [/h]	3.4×10^{-6}
Tank	Leakage	5.0×10^{-7} [/h]	1.0×10^{-6}
		total	1.8×10^{-3}

Table 6.10: Safety of closure elements – hydraulic components of moving locking devices [9]

It should be noted that this probability of failure only describes the main parts of the electro-hydraulic system. The failure frequencies of the switches, displays, hoses and other smaller components of the system are not included. The calculated value represents therefore an underestimation. For this reason, a value of two times the calculated probability of failure is advised to be incorporated at this point, leading to a value of $4 \cdot 10^{-3}$.

The lifting gate operation is projected to be powered by the city power net. Emergency generators are installed as a back-up to a possible net power failure. The probability that there is no electric power to start the electro-hydraulic system is assumed to be equal to the probability of net power failure times the probability of failure of the emergency generators. It is estimated that failure frequency of a power cut-off equal 10^{-3} per hour, with an estimated duration $T = 6$ hours. The emergency generators are schematized as diesel generator, a probability of failure according to table E.3 in Appendix E. This results in:

$$P = P_{\text{supply}} * P_{\text{generator}} = (10^{-3} * 6) * 10^{-2} = 6 * 10^{-5}$$

Failure due to external causes – non-availability caused by ship collision

The non-availability of the gate due to a ship collision can be estimated according to the following formula:

$$U = \lambda \Theta = (N * P * L) * \Theta, \text{ in which:}$$

N = number of ships per time interval. About 40,000 ships per year pass the particular stretch of the Gulf Intracoastal Waterway. Assume a maximum value of 200 passing ships a day.

P = probability of a ship collision per unity of length = 10^{-6} per ship per km.

L = length the projected concrete substructure of the gate, which is estimated to be 100 m

Θ = average repair time, estimated to be 2 months = 60 days.

$$\text{This results in: } U = \lambda \Theta = (N * P * L) * \Theta = (200 * 10^{-6} * 100) * 60 = 1.2 * 10^{-3}$$

Failure due to external causes – the occurrence of blockage by debris and/or siltation of the sill

The probability of failure caused by debris and/or siltation of the sill is expected to be relatively small. The projected lifting gate design allows for a sufficient opening under the gate in order to diminish any inference due to these external causes. The combined probability of failure is set at an order of 10^{-5} .

4) Check the probability of failure of the closing process of the lifting gate with the predetermined standard

According to the standard, the required safety of the closing process can be described with:

$$P(V_{\text{open}} > V_{\text{allowed;nc}}) = P(h_{\text{surge}} > \text{ORL}) * P_{\text{nc}} = n_{\text{year}} * P_{\text{nc}} < 0.1 \times (1/2,000) = 5 * 10^{-5}, \text{ in which:}$$

$$n_{\text{year}} = P(h_{\text{surge}} > \text{ORL}) = 10^{-(2.74-1.52)/0.42} = 1.25 * 10^{-3}$$

$$P_{\text{nc}} = 3.6 * 10^{-3} + 5 * 10^{-5} + 21 * 10^{-6} + 1.0 * 10^{-3} + 4 * 10^{-3} + 6.5 * 10^{-5} + 1.2 * 10^{-3} = 1 * 10^{-2}$$

It can be concluded that the safety standard is met. However, as the detailed hydrological information required for an adequate determination of the retaining level is not available for this thesis, it is advised to lower the probability of failure of the closing process of the gate (P_{nc}). A sufficient target value for this probability is the order of $10^{-3} - 10^{-4}$. This requires a reevaluation of any larger contributors:

- The probability of failure of the measuring devices is one of the highest contributors. It is advised to design an additional, parallel measuring device system. This reduces the probability of non-availability to:

$$U_{\text{md}} = (\lambda T)^2 / 3 = (10^{-5} * (30 * 24))^2 / 3 = 1.8 * 10^{-5}, \text{ which appears to be reasonably small.}$$

- Human induced failures are still relatively high. Additional expertise and/or training are required in order to decrease the probability of such failure. Manuals and procedures should be put down and familiar to all operating staff.
- The probability of failure of the electro-hydraulic system during the closure process is high since the failure of one hydraulic system leads to failure of the overall closure process. This probability could be decreased by designing an alternative back-up operation system or manual system. It is also advised to investigate the design of a system which allows the gate to be lowered under its own weight. Failure of the hydraulic system would then only result in a closed gate for a longer period of time. This is unfavorable for navigation purposes but independency of hydraulic cylinders increases the safety of the hinterland in the potential event of a major hurricane.
- The non-availability due to ship collision can be decreased by designing a fender wall within the prone substructure of the lifting gate. The probability of a ship collision remains the same, but would not immediately lead to failure of the substructure and/or steel gate. The failure frequency decreases.

7. Preliminary Design Of The Navigable Storm Surge Barrier Within The Gulf Intracoastal Waterway – Concrete Civil Works

In the preliminary design presented in this thesis, two main parts of the barrier will be reviewed. The barrier can roughly be divided in the concrete civil works, forming the substructure of the barrier, and the steel lifting gate. This chapter presents an indicative order of magnitude calculation to determine a first estimation of the needed concrete civil works. For this calculation, the stability of the structure and the potential of shearing are reviewed. Section 7.1 introduces the calculation approach and presents general assumptions and constraints. Section 7.2 determines the loading of the subsurface during maximum storm surge. It determines whether this is critical by reviewing several loading scenarios. Section 7.3 comments on the potential of failure due to piping. Section 7.4 concludes on the results and calculation method.

7.1 Calculation method, assumptions and constraints

The substructure is formed by the abutments, which include the hoisting towers, the concrete sill and the pile plan beneath it. As the substructure forms the outer border of the steel barrier gate, it will be reviewed as a single structure. This assumption will be discussed at the end of this section, after the calculation method is introduced.

7.1.1 Calculation method

The calculation method is rooted in the actual functions of the substructure, which include the transmission of forces from the upper structure (steel lifting gate) to the subsurface. These forces main concern the water induced forces on the gate and substructure and their own weight. Figure 7.1 presents a schematization.

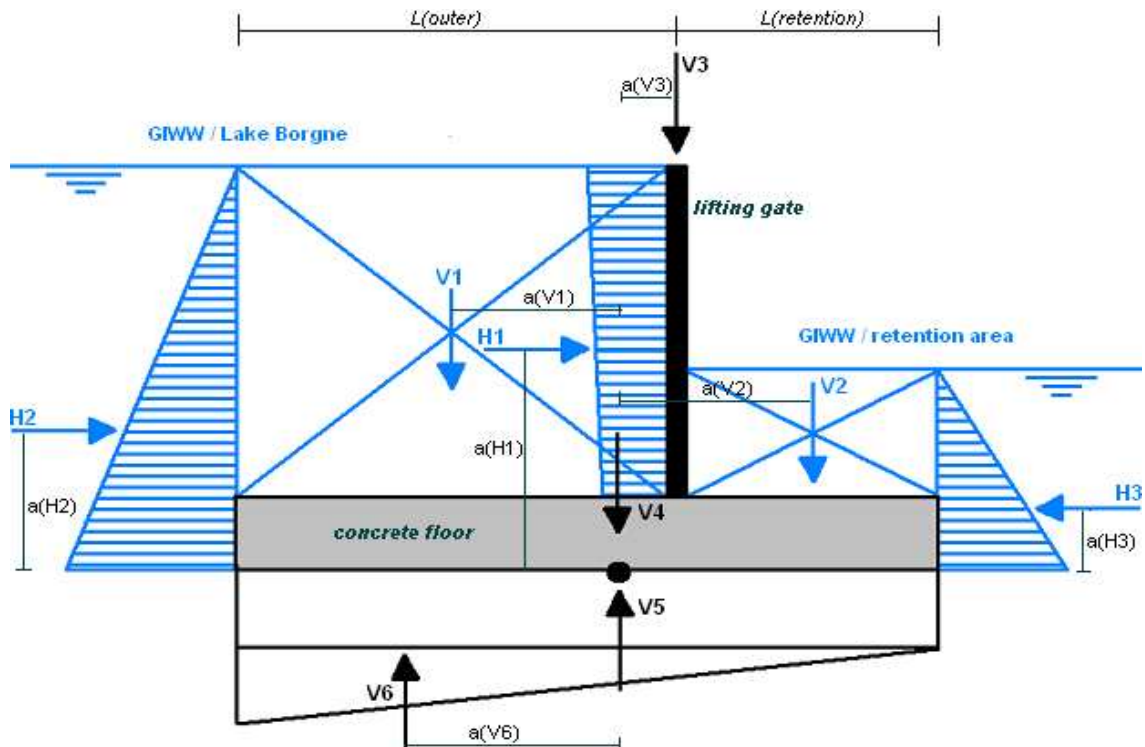


Fig. 7.1: Schematization loading of the concrete substructure

- H1: Resultant horizontal wave force on the vertical lifting gate, which is elaborated in section 7.1.2;
- H2: Resultant hydrostatic water pressure at Gulf Intracoastal Waterway (GIWW) / Lake Borgne;
- H3: Resultant hydrostatic water pressure at GIWW / retention area;
- V1: Resultant vertical water pressure at GIWW / Lake Borgne;
- V2: Resultant vertical water pressure at GIWW / retention area;
- V3: Weight of the hoisting towers and steel lifting gate (assumption, to be checked!);
- V4: Weight of the substructure: concrete walls plus floor
- V5+V6: Resultant upward water pressure under the substructure

The following failure criteria should be determined:

Shearing of the structure

In order to prevent shearing, the friction force between the substructure and the subsurface should be larger than the sum of the horizontal forces. The friction force is determined by the product of the shearing coefficient f and the sum of the vertical forces.

$$\frac{\Sigma V * f}{\Sigma H} > 1.0$$

$$f = \tan(\delta), \text{ with } : \delta = 0.8\phi$$

This means that the angle of the resultant loading force R in relation to the vertical axis should be smaller than the friction angle between the substructure and subsurface (δ), thus also smaller than the internal friction angle of the subsurface (ϕ).

Stability of the structure

As a result of the eccentric loading of the foundation plate, the subsurface may shear causing the structure to tilt over. With the theorem of Prandtl, the safety regarding tilting can be determined. For this preliminary design is it sufficient to check the occurring granular stress and to keep the eccentricity of the resultant loading force small. In general, it is stated that the whole foundation plate should participate in the transmission of forces and that the granular stress should not exceed a predetermined maximum value. This leads to conclude that the eccentricity of resultant loading force R should not only be within the foundation plate but within the central part of it. This is generally stated to be equal to the central 1/3 part of the plate. The

$$e_R = \frac{\Sigma M_H + \Sigma M_V}{\Sigma V} < \frac{1}{6} * L_{\text{plate}}$$

If the eccentricity of the resultant loading force is within the central part of the foundation plate, the occurring granular stress can be determined by using the following formula:

$$\sigma_{\text{granular}} = \frac{\Sigma V}{B_{\text{plate}} * L_{\text{plate}}} \pm \frac{\Sigma M_H + \Sigma M_V}{\frac{1}{6} * B_{\text{plate}} * L_{\text{plate}}^2} < \sigma_{\text{granular,max}}$$

The predetermined maximum granular stress of the subsurface is set to be 300 kN/m². If the occurring granular stress exceeds the predetermined maximum, the dimensions of the substructure should be adjusted.

It should be noted that this approach assumes a foundation *without* piles. However, the use of piles is likely in the design as the high surge level and associated high differential head results in both high vertical forces and high horizontal forces. In addition, the layers with sufficient bearing capacity are located relatively deep (Pleistocene sand layer at -16 m MSL, see table 6.3). The use of inclined piles is preferred as this would accommodate the relatively large horizontal forces to be expected.

In essence, two types of foundation configurations can be distinguished: a single substructure of concrete walls and floor or separate pier connected by a sill. Figure 7.2 presents both types. In order to apply the check on shearing and stability, the structure should be seen as a single structure. A reason to state that this is a more suitable substructure can be related to the local geology. The relative weak layers present form a serious threat of subsidence. Constructing heavy hoisting towers at two separate piers could result in a disproportionate subsidence of the piers, potentially causing the gate to jam if lowered. For this reason, at this preliminary design stage, the potential for shearing and stability is checked for a configuration of combined concrete walls and floor.

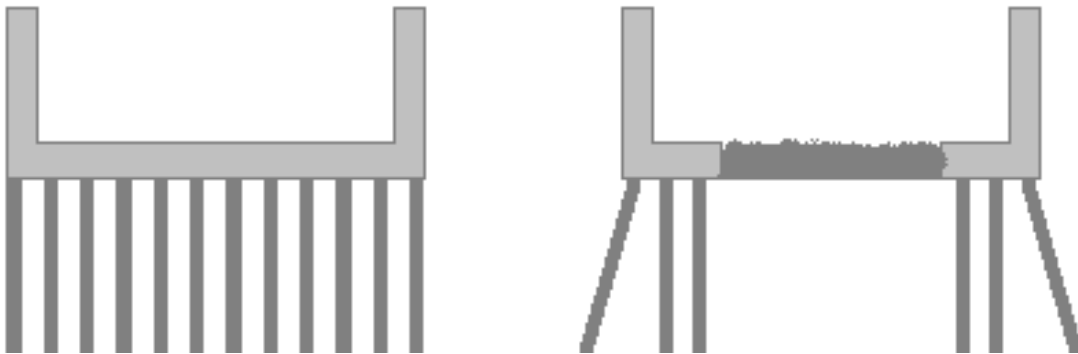


Fig. 7.2: Front view of main types of foundation configurations: combined concrete walls / floor (left) and separate piers (right)

7.1.2 Resultant horizontal wave force on the vertical lifting gate – modified model of Goda

Generally, three types of waves are distinguished for the determination of wave loading. These types include breaking waves, non-breaking waves and broken waves. In the case of non-breaking waves, the forces on a vertical wall or gate can be determined using the linear wave theorem and associated pressure distribution.

An indication of this pressure distribution according the linear wave theorem is sketched in figure 7.2 for a depth of 20 m and a wave height of 6 m. The figure present the wave pressures for several wave lengths. The pressures should be added to the hydrostatic pressure corresponding with the still water level. It can be concluded that the wave pressure approaches the hydrostatic pressure for very large wave lengths. This summation is included in the calculation method for shearing and stability by introducing both H_1 (resultant wave force) and H_2 (resultant hydrostatic pressure).

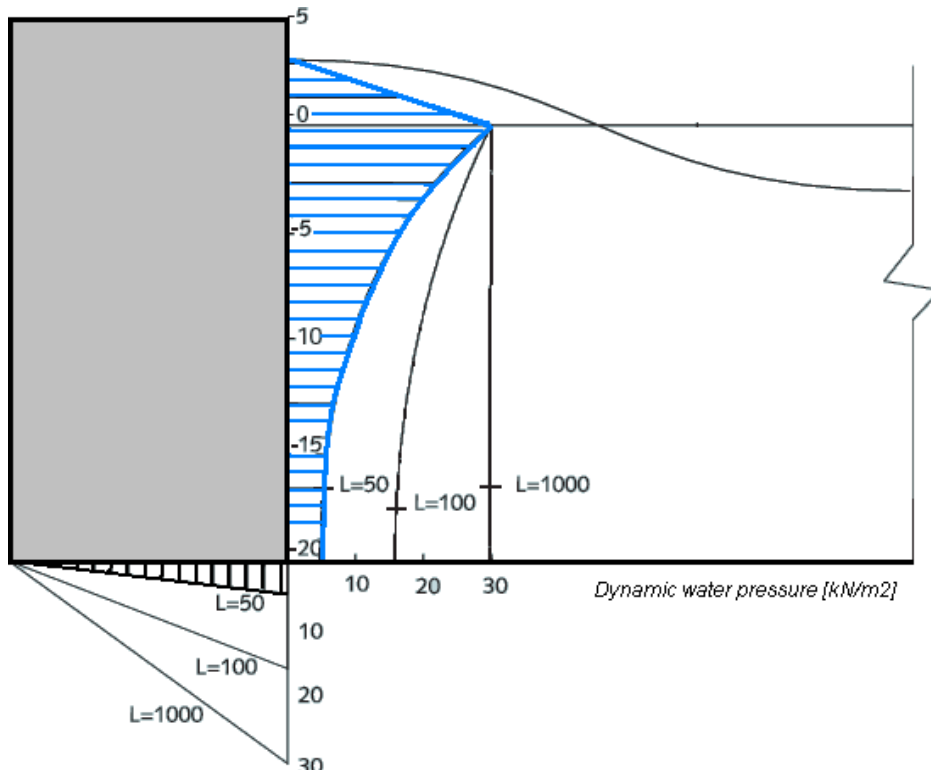


Fig. 7.3: Indication of the wave pressure distribution according the linear wave theorem [9]

In the case of breaking waves, the actual form of the breaking wave and the inclusion of air between the breaking wave and the construction both have a significant influence on the maximum wave impact and the development of pressure distribution in time. Depending on the way the waves break at the structure, the loading should be characterized as a strong impact force or more uniform distributed loading. As limited information on waves and wave development is available for this thesis, this distinction is not made here. As the high impact occurs over a small period in time, it does not influence the shearing and stability of the structure. However, it does influence the strength and could lead to partial failure of the structure or some of its elements. In the final design stage, this impact loading should therefore be kept in mind.

For the calculation of the wave loading, several models exist. Most common are the relatively simple model of Sainflou and the more comprehensive model of Goda. For non-breaking waves, both models can be used. For breaking waves and broken waves, only the model of Goda is applicable. As the structure should be checked for a variety of loading scenarios, all three types of wave could occur in theory. Therefore the model of Goda is chosen for the calculation of the wave loading. It should be noted that optimization can be achieved by calculation with spectral wave theory and frequencies. This is set to be outside the scope of this thesis.

Modified model of Goda

Goda presented a general formulation of the wave pressure distribution on a caisson on a rock-fill sill. It should be noted that the model is based on curve-fitting and results from various experiments. The formulation of the model is adjusted by Takahashi et al. in order to be able to use the model for waves breaking at the structure.

The modified model of Goda is outlined in Appendix H.3. Before reviewing the results, some general remarks should be made:

- Although originally derived for breakwater on a rock-fill sill, the model is also commonly used for vertical wall without a sill [9]. This is an important given, since the configuration of the structure within the GIWW depicted in figure 7.3 does not include a sill. This sill would interfere with the predetermined navigation requirements.

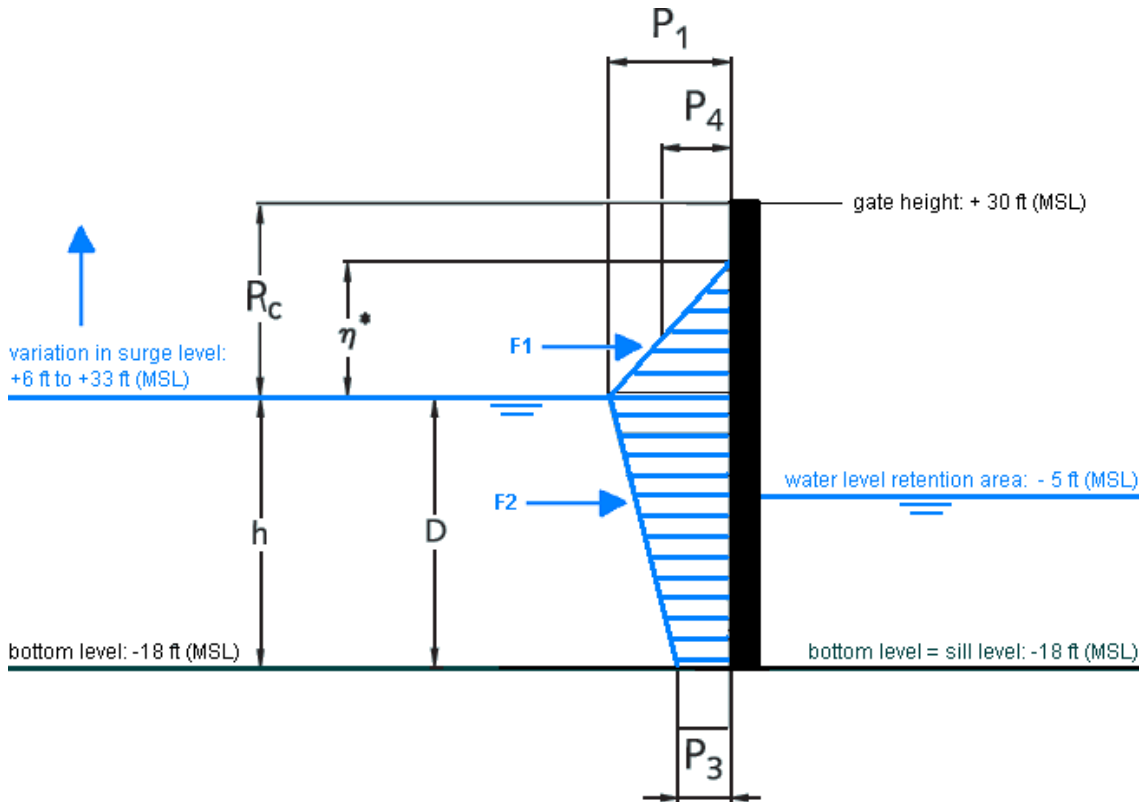


Fig. 7.4: Modified model of Goda

- The model equations do not change in the case of overtopping. As stated, the structure should be checked for a variety of loading scenarios. These scenarios include surge levels with significant overtopping, in which this model has the benefit of still being applicable.
- Only for the maximum surge level of +33 ft (+10.1 m, MSL) overflow occurs, at which point the use of the model is highly questionable and not recommended. This will be avoided by computing the maximum surge level in the model at +30 ft (+9.1 m, MSL), equal to the gate height. For the check on shearing and stability, this value is used in combination with and hydrostatic pressure of +33 ft (+10.1 m, MSL).

Table 7.1 presents an overview of the wave load for a variable external surge level elevation. It should be noted that the water level within the retention area does not influence the wave loading.

	storm surge level (MSL)										[ft] [m]
	6 1,8	9 2,7	12 3,7	15 4,6	18 5,5	21 6,4	24 7,3	27 8,2	30 9,1	33 10,1	
Pressures:											
P ₁	87,8	87,5	87,1	86,7	86,3	85,9	85,4	84,9	84,4	83,9	[kN/m ²]
P ₃ = P ₄ (no berm)	86,8	86,2	85,6	84,9	84,2	83,4	82,6	81,7	80,7	79,8	[kN/m ²]
Forces:											
F ₁	447	411	369	321	268	209	144	74,7	0,0	0,0	[kN/m]
F ₂	638	715	790	863	935	1006	1075	1143	1208	1195	[kN/m]
Lever Arms:											
a ₁	10,44	11,05	11,62	12,17	12,69	13,20	13,69	14,17	-	-	[m]
a ₂	3,66	4,12	4,59	5,05	5,51	5,97	6,44	6,90	7,37	7,37	[m]
Res. Force: F_H											
Res. Moment: M _H	1086	1126	1159	1185	1203	1215	1220	1217	1208	1195	[kN]
	7012	7491	7911	8267	8554	8766	8898	8946	8904	8814	[kNm/m]

Table 7.1: Modified model of Goda – overview of results

Figure 7.5 presents the development of the horizontal wave pressures for a variable surge level. Pressure P_1 represents the maximum wave pressure. Pressure P_3 is equal to $\alpha_3 \cdot P_1$ and represents the steady decrease of the wave pressure over the water depth. Pressure P_4 is equal to $\alpha_4 \cdot P_1$ and represents the reduction of the wave force due to overtopping of waves. Appendix H.3 outlines the equations regarding these factors.

Figure 7.6 presents the development of the resulting horizontal wave forces for a variable surge level, directly dependent on the wave pressures. Force F_1 represents the resultant horizontal force of the wave pressure above the water surface, whereas force F_2 represents the resultant horizontal force of the wave pressure under the water surface. Force F_u present the upward pressure under the gate. However, as the hydraulic thickness of the gate is small (set to be 2ft, equal to 0.6 m), this resultant forces is of minor influence and can be neglected.

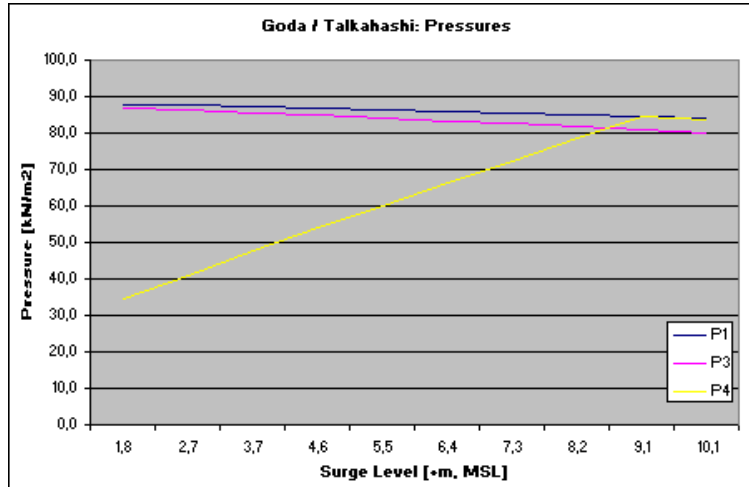


Fig. 7.5: Modified model of Goda – wave pressures

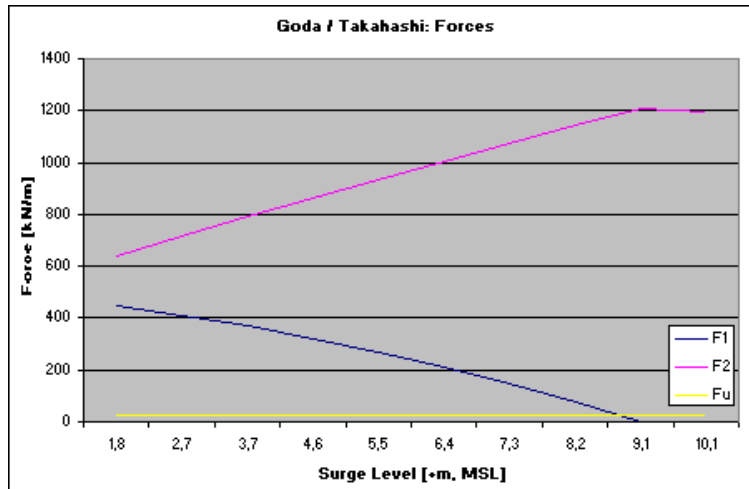


Fig. 7.6: Modified model of Goda – resulting wave forces

Several point of notice regarding both figures:

- The large peak wave period of 14 s results in a large wave length, equal to about 1000 ft (306 m). As a result of this, the wave pressure approaches the hydrostatic pressure in accordance with the linear wave theory. This can be seen in the fact that the difference between P_1 and P_3 is small.
- As the surge level rises, more waves will overtop the structure. The reduction represented by pressure P_4 will decrease and approach pressure P_1 . From figure 7.4 can be seen that for a surge level of +30 ft and larger, no reduction is achieved. This is to be expected as the top of the gate is at this position. Any higher water level elevation will directly lead to overtopping and overflow.
- Force F_1 decreases for an increasing surge level. This is a result of the reduction by wave overtopping. For a surge level equal to the gate height or larger, this load is becomes equal to zero. This is to be expected as the total wave pressure above the water surface ‘falls’ over the structure. Force F_2 increases linearly for an increasing surge level. This is to be expected as, for the known large wave length, this pressure approaches the hydrostatic pressure. For a surge level equal to the gate height, this forces has reached is maximum. Force F_u decreases equal to the decrease of pressure P_3 , as its resultant is proportional to this pressure.

7.2 Determination of the critical loading scenario and associated substructure

Several loading scenarios will be reviewed in this section. The approach is taken to first outline the expected leading scenario of maximum surge level in combination with maximum wave conditions and minimum water level in the retention area. The required concrete cross-sections for this scenario are determined. The other scenarios are checked to these stated dimensions. An overview of the additional reviewed loading scenarios:

- Introducing a reduction as result of a pile plan: halve the resultant horizontal forces and double the central part of the foundation plate;
- Maximum negative differential head: malfunction of the lifting gate after closure;
- Maximum surge level and maximum wave conditions in combination with the occurrence of a wave low;
- Wind load on the gate in lifted position: maximum surge level for closure in combination with the maximum wind speed under normal conditions;
- Severe conditions during a temporary closure of the substructure for maintenance;
- Ship collision: indicative calculation to estimate order of magnitude and expected influence.

7.2.1 Maximum surge level and wave conditions under maximum differential head

To schematize this expected critical loading scenario, one main assumption should be made. The bottom of the GIWW with the structure in place should be a smooth surface, as higher sill is allowed that could interfere with navigation. The sill should rather be integrated in the bottom, thus having a top level of -18 ft (MSL). The bottom adjacent to the structure should be schematized as a permeable layer, as presented in figure 7.7. Hydrostatic water pressure now also produces a horizontal pressure against the concrete floor, which forms the sill of the structure. Figure 7.8 presents the actual loading scheme used in the calculation and associated check of shearing and stability, not only for this expected critical scenario but also for all other scenarios.

The water level in the retention area is set at -5 ft (-1.5 m, MSL), rather than the maximum water level allowed in the area at the moment of closure of +5 ft (+1.5 m, MSL). The significantly lower water level accommodates the large wind offset expected in the event of a hurricane. It represents a more critical situation for the check on stability and shearing of the substructure as the resultant overturning moment (eccentricity and granular stress) and resultant horizontal force (shearing) increases.

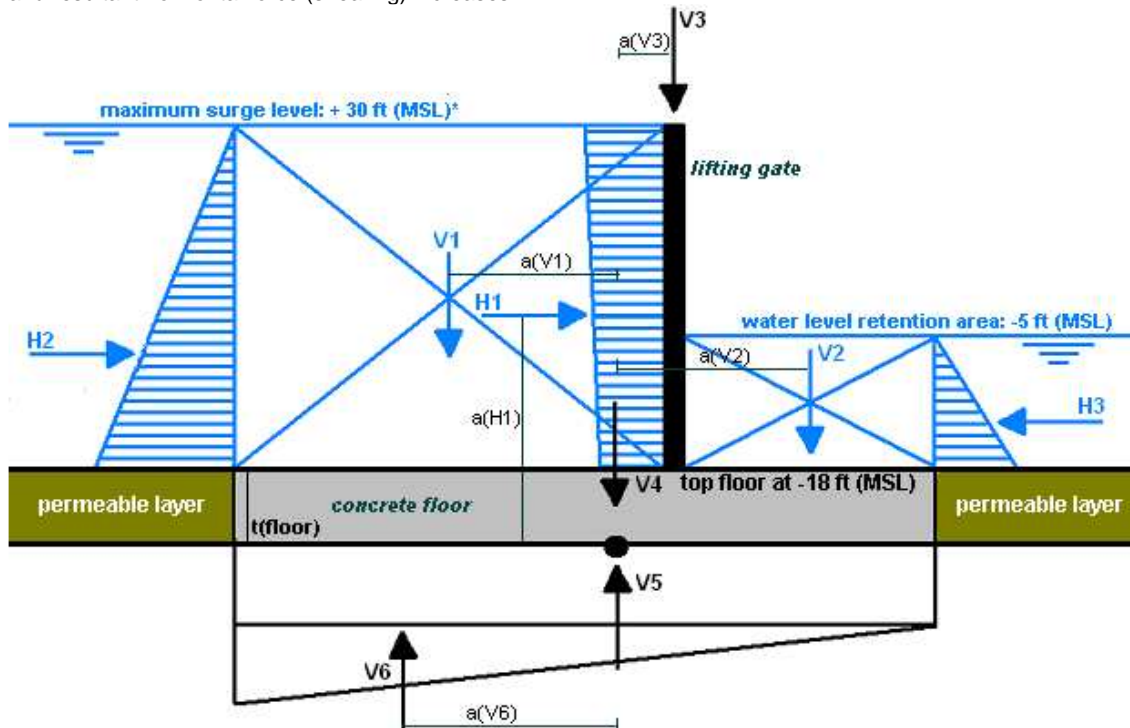


Fig. 7.7: Maximum surge level and wave conditions under maximum differential head - influence (im)permeable layer

An overview of the calculation for this particular scenario is presented in Appendix H.4.1, which provides insight in different parameters and their use in the formulae. The calculations for all other scenarios are presented appendices H.4.2 to H.4.5. The results are outlined and reviewed in this thesis. A mass of 4500 tonnes is estimated for each hoisting tower. The steel lifting gate is estimated at 750 tonnes at this point. Chapter 8 provides a preliminary design of the steel gate. The estimated mass of the steel gate is evaluated afterwards.

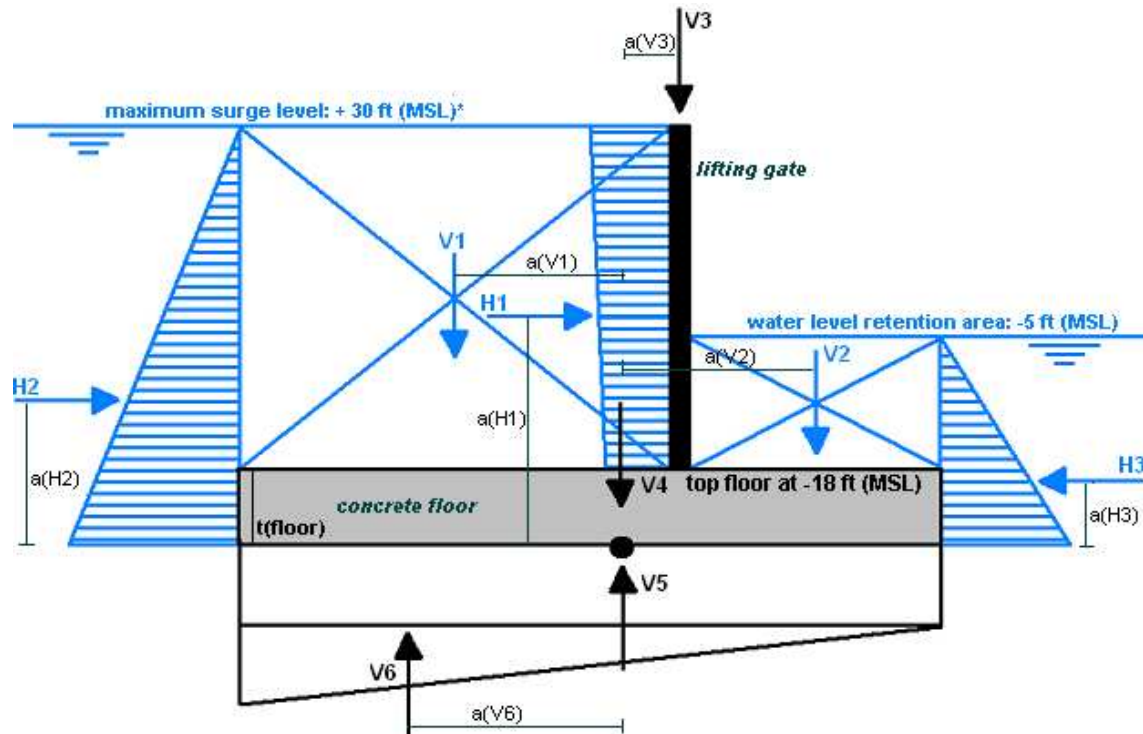


Fig. 7.8: Maximum surge level and wave conditions under maximum differential head - loading scheme used for calculations

	Maximum surge level and wave conditions under maximum differential head
Dimensions barrier:	$L_{\text{outer}} + L_{\text{retention}} = 130 + 35 = 165 \text{ ft (50.3 m)}$
External forces:	Differential head = 35 ft = 10.7 m.
- hydrostatic pressure:	$P_{\text{outer}} = 217.5 \text{ kN/m}^2$ $P_{\text{retention}} = 98.6 \text{ kN/m}^2$
- resultant wave force (Goda):	$F_H = 1208 \text{ kN/m}$ $P_{\text{bottom}} = 80.7 \text{ kN/m}^2$
Unity check shearing:	$\Sigma V = 5.85 \times 10^8$, $\Sigma H = 2.08 \times 10^8$ $\Sigma V \cdot \tan(25) / \Sigma H = 1.03 > 1.0$
Check on eccentricity:	$e_R = 6.3 < 50.3 / 6 = 8.4$
Check on granular stress:	$\sigma_{\text{granular}} = 289.9 \text{ kN/m}^2 < 300 \text{ kN/m}^2$

Table 7.2: Calculation results for maximum surge level and wave conditions under maximum differential head

The calculation results lead to conclude that shearing is critical for this expected critical scenario. The concrete substructure needs to be enlarged substantially in order to create enough down force and to prevent shearing. This is a result of the high differential head and associated high resultant horizontal force. This enlargement can be generated directly by enlarging the thickness of the floor and walls or the length of the substructure. With regard to the realization, maximum values in this preliminary design are set at a wall thickness of 10 ft (3.0 m) a floor thickness of 20 ft (6.1 m). If these values are reached, enlarging the length generates additional vertical force. Additionally, this directly increases the maximum allowed eccentricity of the resultant force R. It is more beneficial to increase the outer part of the concrete stretch than the inner part, as this increases the resultant vertical force more effectively. The total length of the concrete civil works is equal to $130 + 35 = 165 \text{ ft (50.3 m)}$.

In coherence with shearing, also the overturning moment depends on the horizontal force and length of the substructure. As stated, a relative large outer part is favorable as this would counterbalance the moment generated by the large horizontal forces H1 and H2. The eccentricity at the presented configuration is well under the stated maximum: $6.3 \text{ m} < 50.3 / 6 = 8.4 \text{ m}$.

The granular stress is also at the critical point, as the occurring stress is close to the predetermined maximum. To lower the occurring granular stress, it is more beneficial to increase this part of the structure than the outer part.

In conclusion, the checks present a minimal boundary in which the structure has to be designed. The check on shearing and eccentricity determines the minimal length and thickness of the outer part of the substructure, and the check on maximum granular stress determines these parameters for the inner part of the substructure.

The influence of the two main assumptions regarding the calculation method is quantified. Besides the mentioned assumption of a permeable layer all the way to the bottom of the floor or foundation plate, another important point is the introduction or absence of piles. As stated in the introduction of the calculation method, this approach assumes a foundation *without* piles. The use of piles, preferably inclined piles, was stated to be likely in order to accommodate the high resultant vertical and horizontal forces. As the configuration of the pile plan is outside the scope of this thesis, two rough assumptions are made:

- Halve the resultant horizontal forces: part of the horizontal force will be transmitted to the inclined piles (*);
- Double the central part of the foundation plate: the resultant force (R) could have a larger eccentricity as tensile stresses are transmitted to the piles instead of the direct subsurface (**).

Table 7.3 presents the calculation results for both assumed loading scenarios, essentially variations of the used calculation method. Reduction of the horizontal loading significantly reduces the length of the substructure. For the impermeable layer scenario, shearing is critical. An equal inner and outer part is due to the check on granular stress. By combining both, a minimal length under optimal proportion is achieved. For the assumed pile plan, the check on eccentricity and shearing are both critical. However, the real meaning of both is questionable and should be handled with care. The check on granular stress for this latter scenario is not performed as the influence of the piles on this check is hard to quantify.

	<i>Impermeable layer</i>	<i>Assumed Influence pile plan</i>
Dimensions barrier:	$L_{outer} + L_{retention} = 50 + 50 = 100 \text{ ft (30.5 m)}$	$L_{outer} + L_{retention} = 50 + 30 = 80 \text{ ft (30.5 m)}$
External forces:	Differential head = 35 ft = 10.7 m.	Differential head = 35 ft = 10.7 m.
- hydrostatic pressure:	$p_{outer} = 156.3 \text{ kN/m}^2$ $p_{retention} = 38.9 \text{ kN/m}^2$	$p_{outer} = 217.5 \text{ kN/m}^2$ $p_{retention} = 98.6 \text{ kN/m}^2$
- resultant wave force (Goda):	$F_H = 1208 \text{ kN/m}$ $P_{bottom} = 80.7 \text{ kN/m}^2$	$F_H = 1208 \text{ kN/m}$ $P_{bottom} = 80.7 \text{ kN/m}^2$
Unity check shearing:	$\Sigma V = 4.55 \times 10^8$, $\Sigma H = 1.57 \times 10^8$ $\Sigma V * \tan(25) / \Sigma H = 1.06 > 1.0$	$\Sigma V = 3.03 \times 10^8$, $\Sigma H = 1.04 \times 10^8$ (**) $\Sigma V * \tan(25) / \Sigma H = 1.06 > 1.0$
Check on eccentricity:	$e_R = 1.7 < 30.5 / 6 = 5.1$	$e_R = 7.6 < 30.5 / 3 = 8.1$ (*)
Check on granular stress:	$\sigma_{granular} = 283.9 \text{ kN/m}^2 < 300 \text{ kN/m}^2$	-

Table 7.3: Calculation results for variations on the calculation method: impermeable layer and assumed influence pile plan

7.2.2 Maximum negative differential head: malfunction of the lifting gate after closure

The maximum negative differential head is reached during malfunction of the gate during a rapid increase of the water level inside the retention area. This scenario is imaginable to take place after the presence of a hurricane. Figure 7.10 schematizes this loading scenario. If the gate is in lowered position after a hurricane has struck the area, it is vital to lift it if normal conditions have restored at the outer side of the gate and levee alignment. This allows discharge of the excess water from the retention area. If the hurricane has damaged the gate, it is possible that it can not be lifted. Water levels inside the retention area will rise as excess rainfall and potential floodwaters are pumped in it from out of the populated area via either the Bayou Dupree or Bayou Bienvenue outlet structure. The maximum water level elevation inside the retention area in such an event is set to be +12 ft (+3.7 m, MSL).

Table 7.4 presents the calculation results for this scenario. As the minimal dimensions of the substructure are laid down by the expected critical loading scenario, only a check of those dimensions regarding a maximum negative head scenario is required. The calculation results lead to conclude that the maximum negative head is not critical.

	<i>Maximum negative differential head</i>
Dimensions barrier:	$L_{outer} + L_{retention} = 130 + 35 = 165 \text{ ft (50.3 m)}$
External forces:	Differential head = (-) 12 ft = 3.7 m.
- hydrostatic pressure:	$p_{outer} = 116.4 \text{ kN/m}^2$ $p_{retention} = 149.5 \text{ kN/m}^2$
- resultant wave force (Goda):	$F_H = 0 \text{ kN/m}$ (normal conditions at outer side of the gate) $P_{bottom} = 0 \text{ kN/m}^2$
Unity check shearing:	$\Sigma V = 4.51 \times 10^8$, $\Sigma H = 3.26 \times 10^7$ (resultant horizontal force is now: ←) $\Sigma V * \tan(25) / \Sigma H = 5.05 > 1.0$
Check on eccentricity:	$e_R = 4.7 < 50.3 / 6 = 8.4$
Check on granular stress:	$\sigma_{granular} = 199.7 \text{ kN/m}^2 < 300 \text{ kN/m}^2$

Table 7.4: Calculation results for the maximum negative differential head

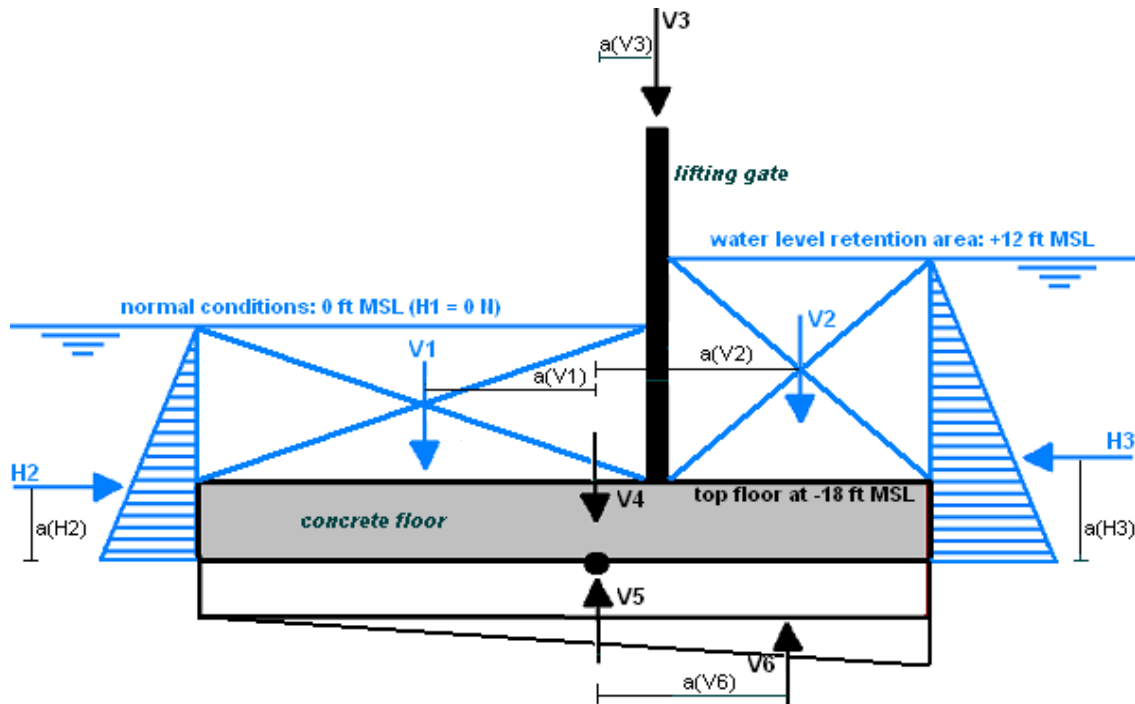


Fig. 7.10: Maximum negative differential head

7.2.3 Maximum surge level and maximum wave conditions in combination with the occurrence of a wave low

In order to estimate the influence of a wave low, the significant wave height should be known. Depending on the local geometry, hydraulic phenomenon like shoaling, refraction and diffraction could all influence this wave height. In this preliminary design, these influences are neglected. The design wave height in the Goda-model assumed in such a manner that the probability of exceedence during the peak of the storm is equal to about 10%. Assuming a Rayleigh-distribution for the wave height, a safe value for the design wave height is determined by: $H_d = 2.2 \cdot H_s$. This value is used in this thesis, but corresponds to Dutch storm conditions (North Sea) and results should therefore be handled with care. Further investigation is required to adequately determine the multiplication factor needed to determine the design wave height. With the assumed factor, the maximum water level in front of gate during a wave low can be determined as $+33 - 2.2 \cdot 12 = +6.6$ ft (+2.0 m, MSL). The hydrostatic pressure should be determined at the base of the structure and depends on the wave length. This wave length is a function of the peak wave period of 14 s: $L = g \cdot T^2 / 2\pi = 306$ m. The precise development of a wave low over the outer part of the substructure is unknown. A water level of +12 ft (3.7 m, MSL) is estimated at this point. Figure 7.11 schematizes this loading scenario.

Table 7.5 presents the calculation results of this scenario. It can be concluded that this is not a critical scenario as all checks are well within safety. The critical check is the one on shearing as the influence of hydrostatic pressure at the outer side of the substructure could be underestimated. If this pressure would actually increase, the safety on shearing would decrease as the vertical down force would not be sufficient in this case.

<i>Maximum conditions in combination with the occurrence of a wave low</i>	
Dimensions barrier:	$L_{outer} + L_{retention} = 130 + 35 = 165$ ft (50.3 m)
External forces:	Differential head = 12 ft = 3.7 m (determines hydrostatic pressure at the time of wave the low)
- hydrostatic pressure:	$p_{outer} = 153.2$ kN/m ² $p_{retention} = 98.6$ kN/m ²
- resultant wave force (Goda):	$F_H = 1159$ kN/m, see table 7.1 under surge = 12 ft $P_{bottom} = 85.6$ kN/m ²
Unity check shearing:	$\Sigma V = 5.35 \times 10^8$, $\Sigma H = 1.21 \times 10^8$ $\Sigma V \cdot \tan(25) / \Sigma H = 1.61 > 1.0$
Check on eccentricity:	$e_R = 5.1 < 50.3 / 6 = 8.4$
Check on granular stress:	$\sigma_{granular} = 244.1$ kN/m ² < 300 kN/m ²

Table 7.5: Calculation results for maximum surge level and wave conditions in combination with the occurrence of a wave low

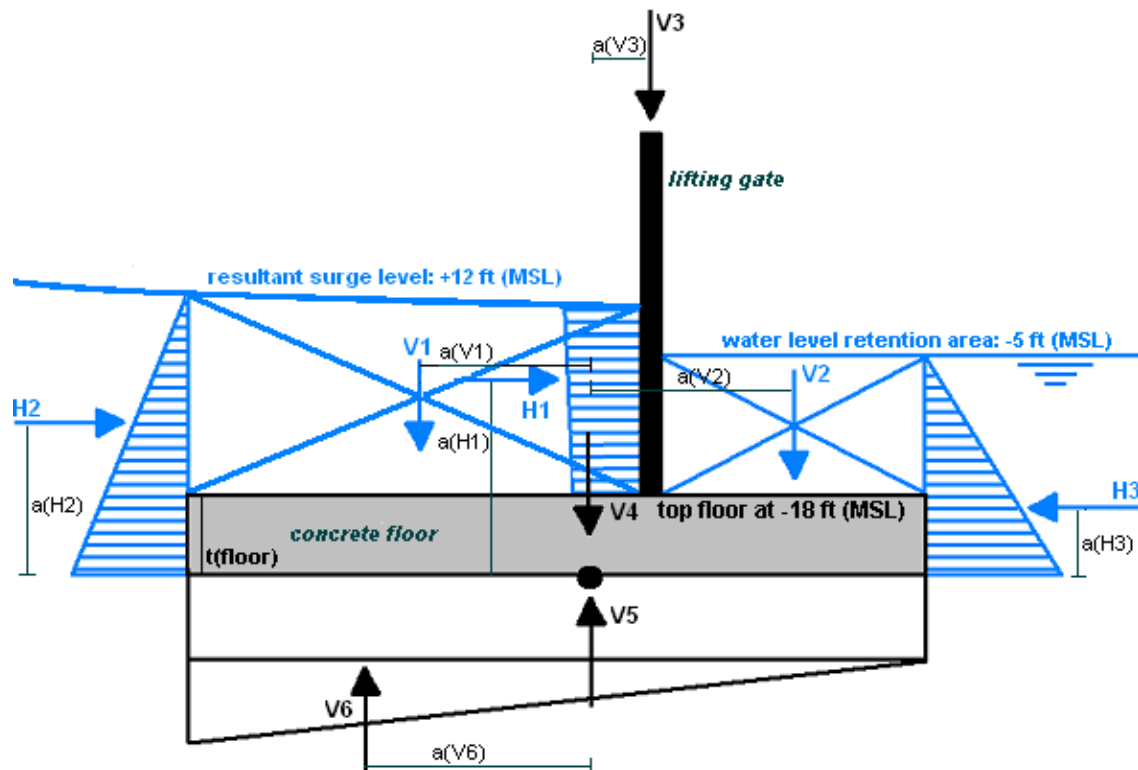


Fig. 7.11: Maximum surge level and maximum wave conditions in combination with the occurrence of a wave low

7.2.4 Representative wind load on the gate in lifted position

When the gate is in lifted position, it can become subject to wind load. As the surface of the gate is significant, an evaluation of this non-hydraulic scenario is required for a leading wind speed from either sides of the gate. Wind pressure occurs when the wind velocity is decelerated. The relation between the pressure and the velocity can be derived from Bernoulli's law, which states that the sum of the kinetic energy of airflow and the potential energy along a streamline is constant.

Appendix H.4.4 calculates the maximum wind pressure on the gate surface at normal conditions, which means that the gate is in upper position. Figure 7.12 schematizes this loading scenario. The maximum wind speed under normal conditions can be extracted from table 6.1 as 27.9 m/s. No hurricane wind speeds are included in the calculation of the wind load as these correspond to a gate in closed position. If this would gate would have been in lifted position at that time, flooding would occur in the hinterland anyway.

As wind is a complex and dynamic parameter, the best approach is to assume that the vertical lifting gate in lifted position is dynamically loaded. The main causes of these dynamic influences are wind gusts, which consist of fluctuations of the wind velocity around the mean. This can occur in the wind direction but also perpendicular to it. Just as wind velocity, the basic stagnation pressure ($q = \frac{1}{2} \rho v^2$) can be divided into a constant and variable part:

$$q = \frac{1}{2} \rho v^2 = \frac{1}{2} \rho (\bar{v} + \tilde{v})^2 \approx \frac{1}{2} \rho \bar{v}^2 + \rho \bar{v} \tilde{v} = \frac{1}{2} \rho \bar{v}^2 \left[1 + 2 \frac{\tilde{v}}{\bar{v}} \right] \text{ in which the term } \frac{1}{2} \rho \tilde{v}^2 \text{ is neglected}$$

As the stated term is neglected, a linear relation is obtained between q and \tilde{v} . For a structure that reacts statically, choosing an appropriate value for this variable wind speed is sufficient. For this, a value is taken that on average is exceeded once an hour. This delivers the following equations:

$$q_{\text{static}} = \frac{1}{2} \rho \bar{v}^2 (1 + 2dl), \text{ in which } l \text{ presents the turbulence intensity and } d \text{ introduces the influence of the duration.}$$

If the structure reacts dynamically, in theory a spectral analysis should be performed. However, it is possible to approximate the result of that by accounting for the dynamical effect of the load:

$$q_{\text{dynamic}} = \frac{1}{2} \rho \bar{v}^2 \left[1 + 2dl \sqrt{1 + \frac{\pi f_n S(f_n)}{4 \zeta_{\text{steel}} \sigma^2(\tilde{v})}} \right]$$

It can be seen that the wind load now depends on the natural frequency (f_n) and material damping (c_{steel}) of the structure and the spectrum of the wind velocity ($S(f_n)$). Appendix H.4.4 outlines the parameters of both the static and dynamic response. The following results can be found:

$$A_{gate} = (\text{width} * \text{height})_{gate} = 210 \text{ ft} * (30 + 18) \text{ ft} = 936.5 \text{ m}^2$$

$$q_{static} = \frac{1}{2} \rho v^2 (1 + 2dl), \text{ which results in: } F_{static} = q_{static} * A_{gate} = 1254.4 \text{ kN}$$

$$q_{dynamic} = \frac{1}{2} \rho v^2 \left[1 + 2dl \sqrt{1 + \frac{\pi}{4c_{steel}} \frac{f_n S(f_n)}{\sigma^2(\tilde{v})}} \right], \text{ which results in: } F_{dynamic} = q_{dynamic} * A_{gate} = 2949.2 \text{ kN}$$

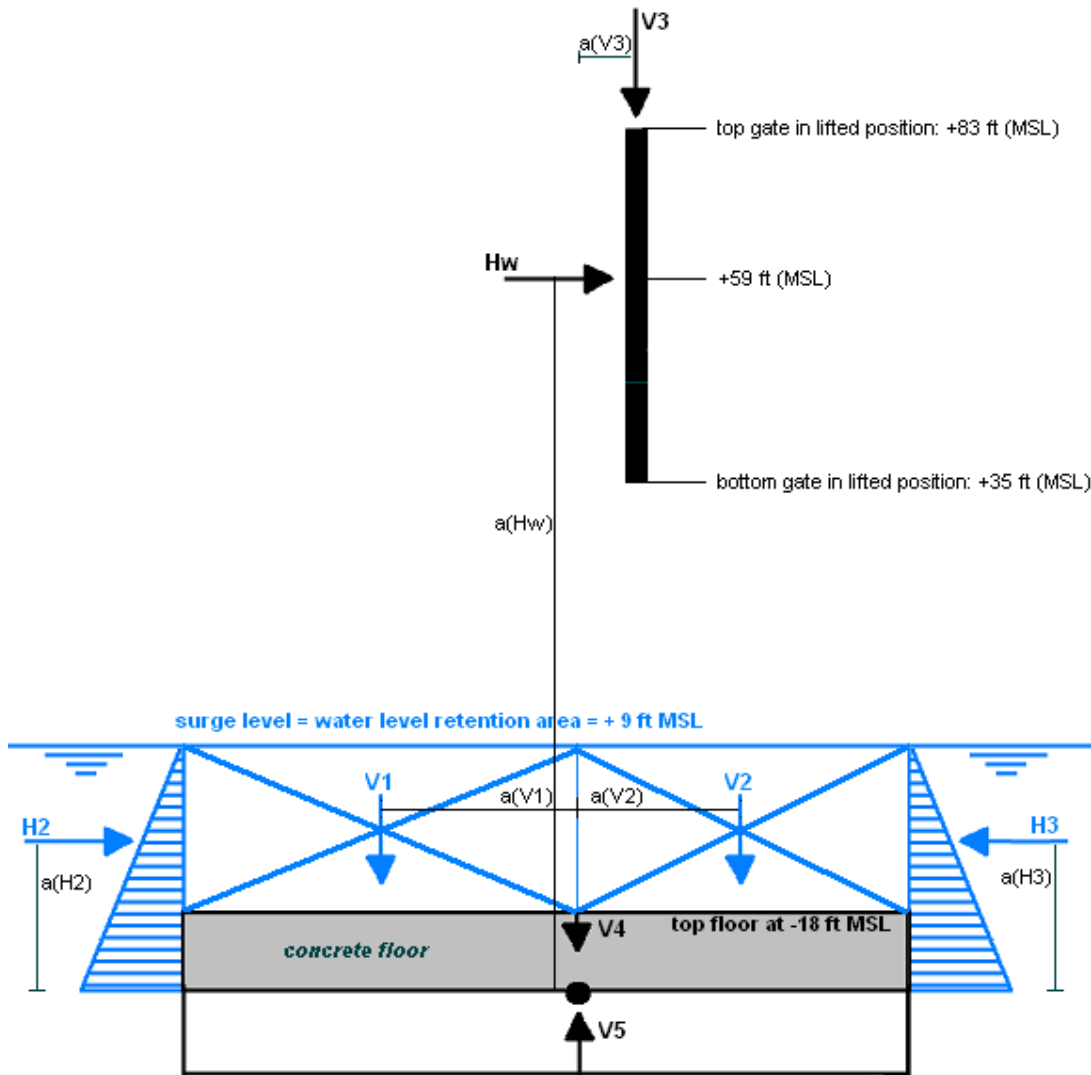


Fig. 7.12: Representative wind load on the gate in lifted position

A dynamic load of the structure is about 2.4 times higher than the static load. The dynamic load will therefore be used in the check on shearing and stability. Table 7.6 presents the calculation results for this scenario.

It can be concluded that the representative wind load has no significant influence on the structure despite the significant force and lever arm. The resultant moment of $2950 \text{ kN} \times 29.5 = 8.7 \times 10^4 \text{ kNm}$ is still over a factor 10 smaller than the moments caused by the vertical forces V1, V2 and V3. These vertical forces represent the water pressures and weight of the gate plus hoisting towers respectively. As the structure is design on the differential head of over 10 m, the vertical constant vertical forces (V3 and V4) are significantly higher than the wind load. As the gate is in lifted position, there is no differential head over the structure. The resulting horizontal hydraulic force can be neglected. The only horizontal force, besides the additional wind load, is caused by a difference in water density. Shearing is thus not critical.

<i>Wind load on the gate in lifted position</i>		
Dimensions barrier:	$L_{outer} + L_{retention} = 130 + 35 = 165 \text{ ft (50.3 m)}$	
External forces:	Differential head = 0 ft	
- hydrostatic pressure:	$P_{outer} = 144.0 \text{ kN/m}^2$ $P_{retention} = 140.5 \text{ kN/m}^2$ (difference caused by density of salt/fresh water)	
- resultant wave force (Goda):	$F_H = 0 \text{ kN/m}$ (gate is in lifted position) $P_{bottom} = 0 \text{ kN/m}^2$	
- additional wind load	2950 kN (dynamic response, see Appendix H.4) Lever arm: $59 + 18 + 20 = 97 \text{ ft} = 29.5 \text{ m}$	
	Wind towards retention area	Wind from retention area
Unity check shearing:	$\Sigma V = 4.82 \times 10^8$, $\Sigma H = 4.71 \times 10^8$ (\rightarrow) $\Sigma V * \tan(25) / \Sigma H = 37.3 \gg 1.0$	$\Sigma V = 4.82 \times 10^8$, $\Sigma H = 1.19 \times 10^8$ (\leftarrow) $\Sigma V * \tan(25) / \Sigma H = 148.0 \gg 1.0$
Check on eccentricity:	$e_R = 3.1 < 50.3 / 6 = 8.4$	$e_R = 2.8 < 50.3 / 6 = 8.4$
Check on granular stress:	$\sigma_{granular} = 187.8 \text{ kN/m}^2 < 300 \text{ kN/m}^2$	$\sigma_{granular} = 181.9 \text{ kN/m}^2 < 300 \text{ kN/m}^2$

Table 7.6: Calculation results for the representative wind load on the gate in lifted position

For a wind load from the retention area, checks on shearing and granular stress become even safer compared to a wind load towards it. The first is caused by the fact that the resulting horizontal forces as a result of difference in density is from the salt outer part towards the fresh retention area, thus opposite to the wind load. The resulting horizontal force decreases. The latter is caused by the fact the result moment in the case of $v = 0 \text{ m/s}$ is clockwise in figure 7.12. Wind from the retention area cause a counterclockwise moment, thus reducing the resulting moment. The small difference in eccentricity and granular stress between wind load from and towards the retention area outlines again the minimum influence it presents on the structure.

7.2.5 Severe conditions during a temporary closure of the substructure for maintenance

As the gate is located in a salt water environment, regular maintenance to prevent corrosion is required. Other forms of degradation could also lead to a temporary closure of the substructure for maintenance. It is possible that during maintenance severe, unforeseen hydraulic conditions occur. Figure 7.13 schematizes this loading scenario. In this scenario it is assumed that maintenance takes place with the gate in closed position, thus requiring the closure of the substructure.

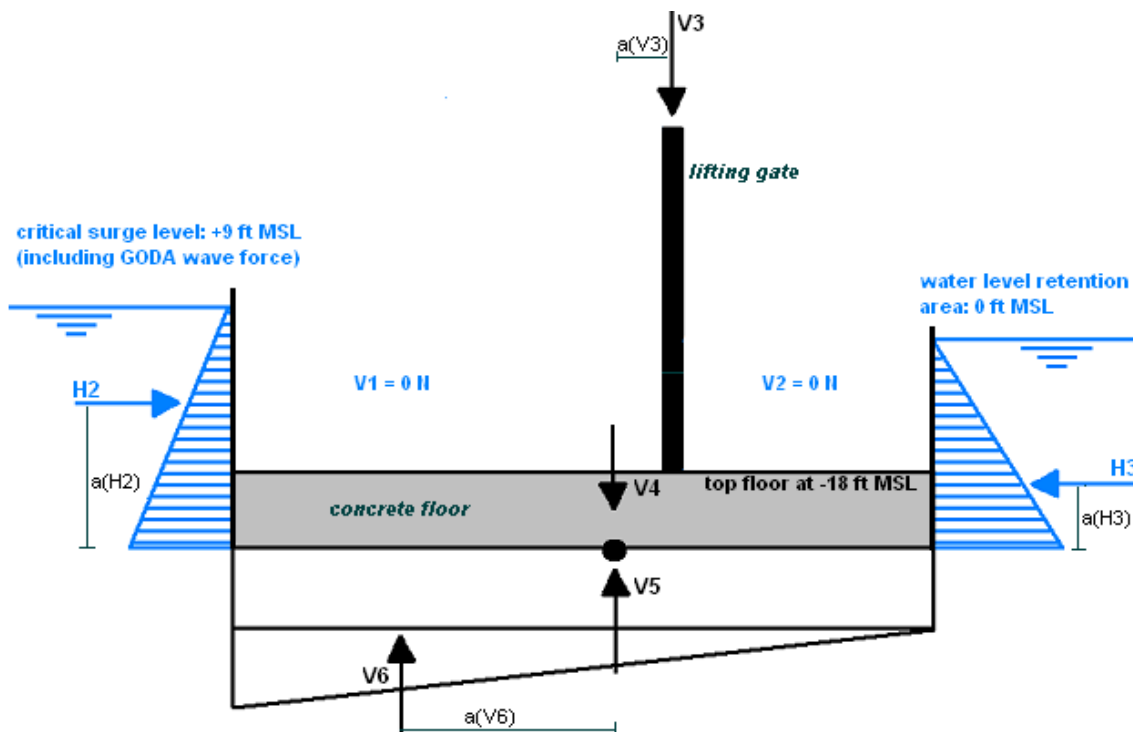


Fig. 7.13: Severe conditions during temporary closure of the substructure for maintenance

The critical surge level is set to be at +9 ft (2.8 m, MSL), equal to the maximum water level at which the gate is projected to be closed. The influence of waves is incorporated by assuming wave conditions with a wave height of 4 ft (1.2 m) and period of 7 s. The water level in the retention area is set on 0 ft MSL, as no significant wind offset is expected to occur in these conditions. Table 7.7 presents the calculation results for this scenario. It can be concluded that the structural dimension are just sufficient to allow a closure of the substructure. The eccentricity of the resulting moment is critical. This can be explained by the fact that only the relatively small force H3 produces a counterclockwise moment. All other forces contribute to a moment in clockwise direction. Another way present this conclusion is that the eccentricity is near to critical. Maintenance and associated closure of the substructure is not allowed for an outer water level higher that +9 ft (2.8 m, MSL).

<i>Severe conditions during a temporary closure of the substructure for maintenance</i>	
Dimensions barrier:	$L_{outer} + L_{retention} = 130 + 35 = 165 \text{ ft (50.3 m)}$
External forces: - hydrostatic pressure: - resultant wave force (Goda):	Differential head = 9 ft = 2.8 m (maximum water level before closure) $p_{outer} = 144.0 \text{ kN/m}^2$ $p_{retention} = 113.6 \text{ kN/m}^2$ $F_H = 225.0 \text{ kN/m}$ (assumed wave conditions: $H_s = 12 \text{ ft} / 3 = 1.2 \text{ m}$, $T_p = 14 / 2 = 7 \text{ s}$) $P_{bottom} = 19.2 \text{ kN/m}^2$
Unity check shearing:	$\Sigma V = 2.65 \times 10^8$, $\Sigma H = 4.06 \times 10^7$ $\Sigma V * \tan(25) / \Sigma H = 2.38 > 1.0$
Check on eccentricity:	$e_R = 8.2 < 50.3 / 6 = 8.4$
Check on granular stress:	$\sigma_{granular} = 148.5 \text{ kN/m}^2 < 300 \text{ kN/m}^2$

Table 7.7: Calculation results for severe conditions during temporary closure of the substructure for maintenance

7.2.6 Ship collision: indicative calculation to estimate order of magnitude and expected influence

Another significant loading scenario is the event of a ship collision, earlier mentioned in the safety analysis of the closure elements presented in section 6.4.4. Although this loading scenario should be avoided at all time, it is instructive to determine the order of magnitude. Appendix H.4.6 presents the calculation of the design kinetic energy during a ship collision. It can be concluded that for the design vessel sailing at its limiting speed of about 2 m/s, the kinetic energy to be transmitted by the upper structure to the subsurface is equal to $2.35 \times 10^4 \text{ kNm}$. It is not meaningful to incorporate this value in the check on shearing and stability. This collision causes such an impact force that the substructure and/or steel lifting gate is expected to fail locally. This could be avoided by designing a fender wall inside that navigable gate opening, which was already advised in section 6.4.4 in order to decrease the probability of such an event. It is also advised to extent this wall at both side of the opening in order to guide incoming vessel safely in and through the opening.

7.3 Potential of failure due to piping

Specific foundation requirements are largely based on the objectives of the structure and must be adapted to the site conditions. In general, the foundation should provide a stable support for the entire structure. Secondly, it should provide resistance to under seepage, preventing excessive water losses and degradation of soil components and prevent sand from washing away from under the barrier piers. A seepage analysis is central in assessing the lifting gate structure for this boil forming and piping. Guiding principle for the assessment is that there should be sufficient resistance to boil forming and piping along every possible seepage line under and around the structure. Ideally, a good 3D-analysis of possible normative seepage lines is needed. This is outside the scope of this thesis. Only basic remarks are made concerning the potential of failure due to piping.

At hydraulic structures piping and/or boil forming only occurs if there is sand directly under or alongside it. The sensitivity to piping depends on the seepage line, the configuration and material composition of the potential erosion sensitive sand layer and on the differential head per meter structural length. In the projected scenario with hydraulic preconditions of maximum surge level and wave conditions under maximum differential head, a large differential head gradient over the structure is found. In principle, the seepage length is the distance between the entry point for groundwater flow through the sand layer on the outside of the structure and the exit point on the inside. In some cases, those points can be indicated in a natural way but mostly this is not possible. If a crack sensitive top layer is present on the inside of the structure, the crack nearest to it should be selected as exit point. If vertical cut-off walls are introduced, the location and length of those screens are important. Screens on the outside of the structure are intended to extent the seepage line and are usually relatively long. Screens on the inside of the structure have the same purpose but should also ensure the seepage flows out vertically.

Figure 6.3 presented a geotechnical cross-section of the site location. Based on this figure it is concluded that the undisturbed subsurface profile consists of an impermeable body of interdistributary clay on another impermeable Holocene package formed by pro-deltaic clay. It is assumed that this Holocene package is sufficiently thick to accommodate the cut-off wall and to ensure that cracking in the package will not occur. The substructure of the lifting gate is also projected to be founded on piles. In this case, minimum dimensions of anti-seepage vertical and horizontal screens suffice to guarantee the connection of the substructure to the undisturbed impermeable subsurface. The background to this is that a perfect connection of the structure to the ground next to it is often difficult to guarantee. In the course of time, spaces can be created due to differences in settlement, temperature effects and other causes. This could result in micro-instability beside the structure. The clay package around the structure will settle faster over time than the pile founded structure. This leads to hollow space could eventually provide a relatively short seepage line over the structure, as the impermeable layer is now cracked. Hollow spaces could also be assumed under the pile foundation, which must also be closed with a short screen.

7.4 Principal conclusions – review on the calculation method and results

The calculation results lead to conclude that the loading under maximum surge level and significant wind offset in the retention area is the critical loading scenario and that shearing is critical for it. The concrete substructure needs to be sufficiently large to create enough down force and to prevent shearing. This is a direct result of the high differential head and associated high resultant horizontal force. The enlargement is generated in two ways:

- By enlarging the thickness of the floor and walls. However, with regard to the production process, maximum values assumed in this preliminary design are a thickness of 10 ft (3.0 m) for the walls and a thickness of 20 ft (6.1 m) for the floor. The large width for the side walls is chosen with regard to the very high overhead load. This load consists of the heavy hoisting tower including half the weight of the steel lifting gate and of a significant increased granular pressure at the wall caused by the adjacent levee body. Kept in mind that the height of the wall should be $+30 - -18 = 48$ ft (14.6 m), a value of the thickness of 0.2 times the height seems reasonable at this point. Although not set to be part of this thesis, it is advised to review the deformation of the concrete wall under the high overhead loading. By determining the maximum allowed deformation, an optimal wall thickness can be determined. It should be noted however, that this would not decrease the overall need in concrete. As the shearing capacity is critical under the presented resultant horizontal loading, the resultant vertical forces must generate a certain minimum value. The weight 'saved' by optimizing the concrete wall size should be included elsewhere in the design.
- By enlarging the length of the substructure. If the maximum thickness values are reached or lower values for it are preferred, enlarging the length is the easiest way of generated additional vertical force. Additional benefit is gained as this directly increases the maximum allowed eccentricity of the resultant force R. This parameter is not critical in the maximum loading scenario, but increases the safety level in the critical case of a closed substructure during maintenance. Regarding the enlargement in length, it is more beneficial to increase the outer part of the concrete substructure than the inner part, as this increases the resultant vertical force more effectively. The total length of the concrete civil works is equal to $130 + 35 = 165$ ft (50.3 m). However, the inner part can not be too small as this would increase the granular stress above its predetermined maximum. A balance between them should be found. The checks together present a minimal boundary in which the structure has to be designed. The check on shearing and eccentricity determines the minimal length and thickness of the outer part of the substructure, whereas the check on maximum granular stress determines the minimal length and thickness of the inner part of the substructure.

The overall conclusion is that the result of this calculation approach should be handled with the up most care as it assumes a foundation *without* piles. However, the use of piles is likely in the design as the high surge level and associated high differential head results in both high vertical forces and high horizontal forces. The method is therefore not sophisticated enough for in order for it to be used as an optimal design tools. It acts as an indicative order of magnitude calculation to determine a first estimation of the needed concrete civil works. The most significant contribution of this method is that it provides insight in the relative criticalness of each scenario:

- Loading under maximum surge level and significant wind offset in the retention area is the critical loading scenario. The check on shearing and maximum granular stresses are both critical in this event;
- The occurrence of a wave low during extreme conditions is not critical;
- The influence on shearing and stability of maximum winds on the gate in lifted position is minimal as the resulting moment is over a factor 10 smaller than the moments caused by the vertical forces V1, V2 and V3.

As stated in section 7.3, a seepage analysis is central in assessing the lifting gate structure for boil forming and piping. Ideally, a good 3D-analysis of possible normative seepage lines is needed. Additional geotechnical information is required to determine the soil characteristic at the site location. Based on the information available, it is concluded that the undisturbed subsurface profile consists of an impermeable body of interdistributary clay on another impermeable Holocene package formed by pro-deltaic clay. The substructure of the lifting gate is projected to be founded on piles. In this case, minimum dimensions of anti-seepage vertical and horizontal screens suffice to guarantee the connection of the substructure to the undisturbed impermeable subsurface. Actual design of those screens is outside the scope of this thesis.

8. Preliminary Design Of The Navigable Storm Surge Barrier Within The Gulf Intracoastal Waterway – Steel Lifting Gate

This chapter presents a preliminary design of the steel lifting gate. Section 8.1 introduces the reference project and calculation method. Section 8.2 calculates the lens-shaped barrier cross-section and transverse girders. It determines the optimal gate curvature and arch pitches. Section 8.3 introduces two distinctive analytical calculation methods for the design of the retaining wall of the gate. Section 8.4 concludes on the required structural components and presents optimizations within the design. The total mass and center of gravity of the steel gate are determined. Finally, section 8.5 concludes on the calculation method, results and consequences.

8.1 Introduction of the reference project, calculation method and assumptions

In the structural design of the steel gate, the Hartel Canal Barrier is used as reference project. Its main features are described in section 8.1.1. Section 8.1.2 introduces the calculation method with associated assumptions and determines the leading loading scenario.

8.1.1 Reference project for the gate design – Hartel Canal Barrier

Reference point of the design of the steel lifting gate is the Hartel Canal Storm Surge Barrier. Appendix D.1 introduces this barrier as one of the leading storm surge barrier consisting of a vertical lifting gate. The barrier consists of two vertical lift gates with the span lengths of 98.0 m (321.5 ft, southern gate) and 49.3 m (161.5 ft, northern gate). The southern gate is one of the longest of this kind in the world. The sliding gates are driven by hydraulic cylinders with a long piston, which are hinged to the side towers

Typical for the Hartel Canal Barrier is that both gates are lens-shaped. This shape has been chosen in order to place their centers of gravity close to the plane of suspension. The overturning moment atop the towers as result of the eccentric suspension can in this way been kept small. The hydraulic load is transferred to the supports in the gate recesses of the towers. The lens-shaped retaining wall is less easy to manufacture than a flat wall, but it enables to use the material strength in a more economical manner. This will be explained in section 8.1.2.

Another special feature of the barrier is its overflowing service. A gap of 0.25 m (about 0.8 ft) remains above the gate sill. Under extreme circumstances, statistically set at once every 10000 years, there is an overflow of 3.7 m above the top edge of the gate. This will result in overflow of the gates, but also in a limitation of the horizontal hydraulic load. In the case of overflow, the gates still act as a reductor. These arrangements do not jeopardize the safety of the inner land. However, it introduces a problem of gate vibrations in flowing water.

Some remarks regarding main structural components of the Hartel Canal Barrier to be designed for the proposed lifting gate. Figure 8.1 presents an overview of these components and describes the terms used to name them.

– *Retaining wall*

The retaining wall consists of a front plate, crossbeams and longitudinal stiffeners. The beams and stiffeners are on the downstream side. The top edge is round shaped in order to conduct the stream of overflowing water in such a way that no disturbances or vibrations occur. The bottom edge has been constructed as a flat, sharp ended plate stroke, which results in a well defined departure point of the water flow. Such a solution guarantees a stable behavior with no significant vibrations.

– *Rear chords and traverses*

The hydraulic loads are collected by the retaining wall and passed on two main girders. The front chord of each girder is the effective width of the retaining wall itself, while the rear chord is a welded I-shaped section. This section has a web of 1200 mm on the larger gate and 800 mm on the smaller gate. The flange thickness varies from 30 to 50 mm. The distance between the top and the bottom rear chords is held by x-type bracings which also provide sufficient stability of both chords under vertical loads like falling water (overflow) and own weight. The load transfer between the front and the rear chord takes place through traverse girders. Alike the main girders, the transverse girder also have an x-type bracing system.

In the case of the Hartel Canal Barrier, the wall arch pitch is half a size of the back chord pitch. The number of system fields is uneven and the field lengths are comparable in both gates. All these arrangements satisfied structural as well as aesthetical requirements. No major contradictions or compromises between these criteria can be traced in the gate design. An exception is the primarily aesthetical choice of the retaining wall position on the upstream side. A wall on the downstream side is also acceptable in structural view and would have possibly been less vulnerable to the damage by floating objects.

– *Guide posts and suspension*

The guide posts are components where the main system forces come together: the reaction from hydraulic load, the tensile force in the rear chord and the compressive force in retaining wall and front chord. The guide post should therefore be relatively massive.

An important function of the guide posts is to provide a stable, rigid support for the post guide lining. Atop the guide posts, gate lifting lugs are constructed. The lugs carry the gate own weight and friction on guide beams during lifting. The system is designed in such a way that the gate own weight is sufficient to lower the gates under all circumstances. The lifting lugs and the drive cylinders never come under compression.

– *Piers and towers*

The barrier piers have been constructed as an extension to the piers carrying the existing road bridge. Between the piers, a sill and an extensive erosion protection of the bottom were laid, with stone deposition of up to 3 tones a piece. The piers serve not only as barrier supports; but also contain machine rooms, shafts and equipment of the gate lifting system.

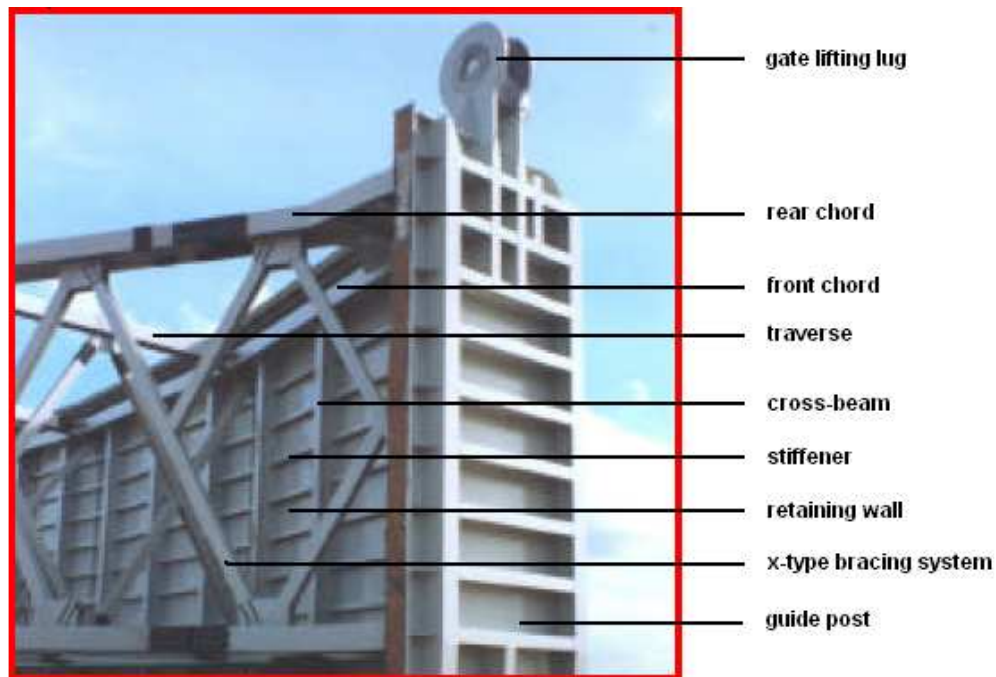
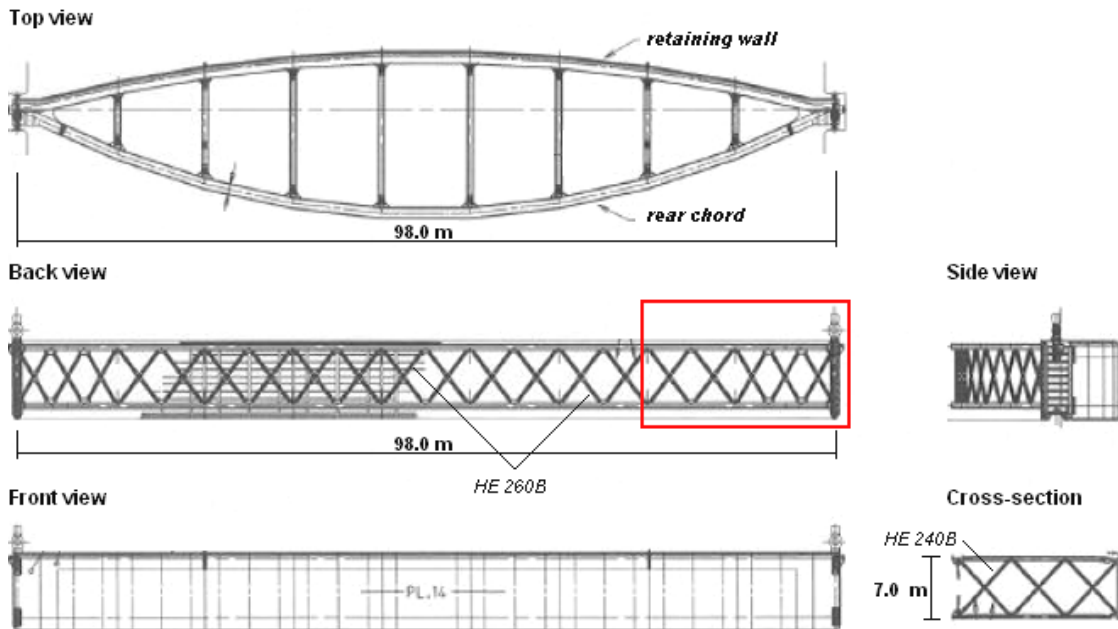


Fig. 8.1: Hartel Canal Barrier – overview of the barrier and introducing its main component [19]

To provide insight in the projected difference between the reference project and the proposed lifting gate, table 8.1 presents an overview of the main characteristics of each barrier. These characteristics are roughly divided in four groups: concrete civil works, steel gate dimensions, hydraulic lifting system and hydraulic conditions. The projected civil works and gate dimensions of both barriers are generally equal, with the exception of the gate height. The proposed lifting gate has a gate height of 1.5 times that of the Hartel Canal Barrier, which reflects the difference in hydraulic design conditions. In addition, the Hartel Canal Barrier allows for a larger overtopping discharge, thus for an even lower gate height.

Characteristics	Hartel Canal Barrier (reference project)	Proposed lifting gate
Pier bottom level	NAP -10.25 / -7.50 m	-38 ft MSL = -11.6 m MSL
Barrier sill level	NAP -6.50 m	-18 ft MSL = -5.5 m MSL
Lift tower height	35.0 m	150 ft = 45.8 m
Tower section dimensions	11.80 x 4.80 m	Estimated to be 50 x 25 ft = ca. 15 x 7.5 m
Gate span length	South: 98.0 m, North: 49.2 m	210 ft = 64.0 m
Gate system widths	South: 18.78 m, North: 11.56 m	To be determined
Gate own weights	South: 650 tonnes, North: 280 tonnes:	To be determined
Gate top in closed position	NAP +3.00 m	+ 30 ft MSL = +9.1 m MSL
Gate bottom in closed position	NAP -6.30 m	ca. -18 ft MSL = -5.5 m MSL
Gate bottom in open position	NAP +14.0 m	+ 35 ft MSL = 10.7 m MSL
Gate retaining wall height	At supports: 9.50 m, in between 9.30 m	48 ft = 14.65 m
Gate cylinder lifting heights	Nominal 20.30 m, maximum 21.10 m	Estimated to be 30 m *
Oil volumes in cylinder tanks	South: 2 x 9000 liters, North: 2 x 6300 liters	Estimated volumes: 2 x 1200 liters *
Oil pressure in hydraulic system	Operating: 5 bar, maximum: 10 bar	Estimated maximum is 10 bar
Average high / low tide levels	NAP +1.05 / -0.40 m	Tidal range is 1.5 ft (0.5 m)
Hydraulic design conditions	Conditions occurring once in 10,000 years: <ul style="list-style-type: none"> - water level outside: + 6.70 m - water level inside: +1.20 m - $H_s = 0.6$ m - $q_{\text{overflow}} = 13.6$ m³/s per meter width Conditions occurring once in 100 years: <ul style="list-style-type: none"> - water level outside: + 5.50 m - water level inside: +1.20 m - $H_s = 0.5$ m - $q_{\text{overflow}} = 7.6$ m³/s per meter width 	Conditions occurring once in 2,000 years: <ul style="list-style-type: none"> - water level outside: + 33 ft = 10.1 m - water level inside: -5 ft = -1.5 m - $H_s = 12$ ft = 3.7 m - $q_{\text{overflow}} = 4.5$ m³/s per meter width

Table 8.1: Dimensions projected lifting gate compared to the Hartel Canal Barrier [19] (NAP is the standard Dutch chart datum)

(*) It is assumed that this height and oil volume is applicable. As the gate cylinder used in the Hartel Canal Barrier were unique at the time of construction, further investigation is needed whether this assumed hydraulic system is

8.1.2 Calculation method and assumptions

The main goal of the design calculations presented in this chapter is to determine a proper estimation of the steel cross-sections of the various parts of the lifting gate. To achieve this, the software package MatrixFrame S3.0 is used. This package allows mechanical analysis of 2D frames and 2D trusses with both graphical and numerical input options. The 2D calculation program is based on linear elastic analysis according to the displacement method. It allows for the calculation of nodal forces, member forces and displacements. In addition, it allows for the calculation of section forces using numerical integration. The use of a 2D calculation program is preferred in this thesis over a comprehensive 3D program, as it provides a better insight in direct mechanical consequences of adjustment to certain parts of the gate. For the final design stage, usage of the 3D software package is advised. This package allows for more detailed design checks and for a distribution of forces in all three directions. This results in a more realistic, thus safer and more economical design output.

Several assumptions used in the design calculations of this chapter:

– Type of steel

It is assumed that the lifting gate is constructed in one single steel quality. Steel is available in various types and classes. Important in the choice of a particular type of steel is sufficient strength and the ability for it to deform to some extent. In addition, it should be homogeneous in order to exclude high stress concentration. For hydraulic engineering, two types of steel are generally used: construction steel and stainless steel. Construction steel is the type most used in the design of supporting structures. Disadvantage of this type is its vulnerability to corrosion in this salt environment, demanding for a more severe maintenance routine. Although maintenance costs are higher for construction steel, it is still chosen over stainless steel as it is much cheaper in purchase. Table 8.2 presents an overview of several main qualities of construction steel.

According to the Dutch steel standard NEN 6770, the maximum calculation value for the yield point is equal to 355 N/mm². To reduce the overall weight of the lifting gate, it could be beneficial to use a high steel quality. If the use of S420 or S460 is preferred, additional checks must be performed besides the most common checks on moment, shear force and normal force. For this reason, in this preliminary design the steel quality used is set to be S355. Figure 8.2 presents the stress-strain curve of steel, in which the main material properties are indicated.

Material property	Quantity	Unity	Construction steel qualities				
			S235	S275	S355	S420*	S460*
Unit weight	ρ_{rep}	[kg/m ³]	7850	7850	7850	7850	7850
Elastic modulus	E_{rep}	[N/mm ²]	210×10^3	210×10^3	210×10^3	210×10^3	210×10^3
Calculation value yield point **	$f_{y,d}$	[N/mm ²]	235	275	355	420	460
Calculation value tensile strength **	$f_{t,d}$	[N/mm ²]	360	430	510	–	–
Yield point	$\epsilon_{y,d}$	[%]	1.12	1.31	1.69	–	–
Shear modulus	G_{rep}	[N/mm ²]	8.1×10^4	8.1×10^4	8.1×10^4	8.1×10^4	8.1×10^4

Table 8.2: Overview of construction steel qualities – strength and stiffness

(*) According to the Dutch steel standard NEN 6770, the maximum calculation value for the yield point is equal to 355 N/mm². If the use of S420 or S460 is preferred, additional checks must be performed.

(**) According to the Dutch steel standard NEN-EN 10025, the presented for the yield point and tensile strength are valid for plates and flanges with a thickness $t \leq 40$ mm.

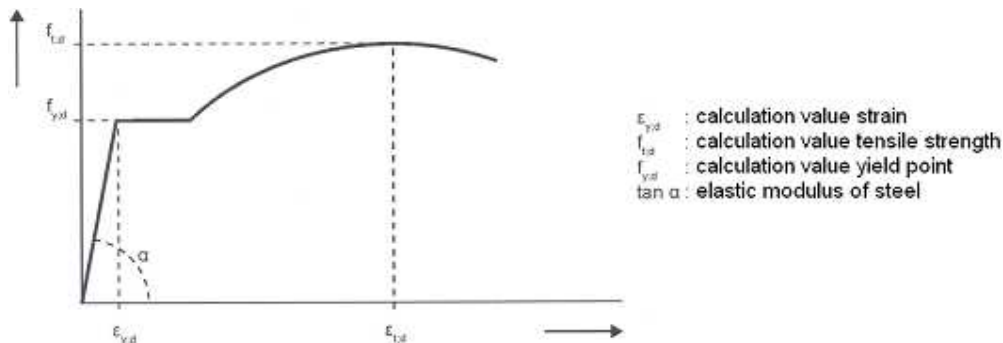


Fig. 8.2: Stress-strain curve of steel

- All steel checks performed are based on the elastic theory

As stated, the used software program is based on linear elastic analysis. The steel checks performed will therefore all be based on the elastic theory. This means that there is always equilibrium in the undistorted state. As a result, there will be proportionality between the applied loading and corresponding distortions in the structure. Practically, the steel is characterized as failing if it begins to yield under the applied loading. Only the first, linear part of figure 8.2 is used in the calculation.

As simplification in the calculations used is the fact that the own weight of the components is 'neglected'. As the gate is calculated using only the linear part of the steel-strain curve, it allows for additional loading to some extent. It is assumed that this allowed additional loading is sufficient to cope with the relatively high own weights of the steel components. In the detailed design stage, this assumption should be evaluated.

- Initial structural assumptions

The distance between the traverses is assumed to be the only constant and is set at 8.0 m. This divided the gate into 8 equal system fields, as is depicted in figure 8.3. The wall arch pitch and rear chord pitch are still variable. The wall arch pitch is not initially set to be equal to half a size of the back chord pitch, a proper ratio is determined in section 8.2.

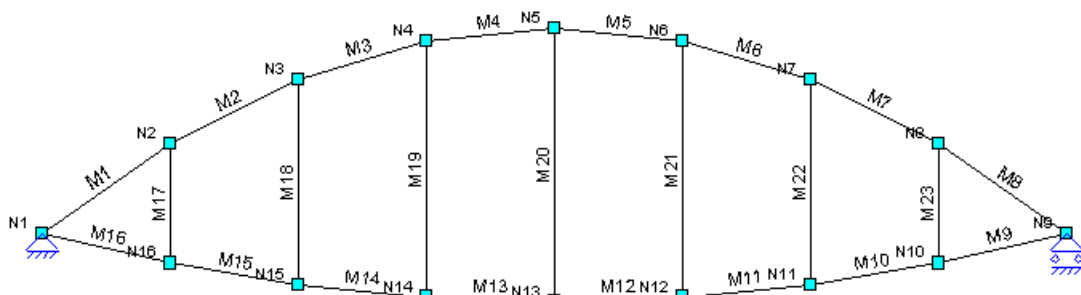


Fig. 8.3: First impression of the calculation model, in which the transverse girders are set at a constant 8.0 m interval

The joints of the x-type bracing system and adjacent transverses and rear chord are initially assumed to be hinged joints. This simplifies the checks and associated calculations significantly as it provides a structure that is only loaded by normal forces.

It should be noted that in practice, the realization of hinged joints is difficult and labor-intensive. As a result, no pure hinged joints exist in the structure and the joints are always clamped to some extent. In addition to the normal force, also moments and shear forces can be introduced in those joints. It is therefore important to evaluate the initial assumption of hinged joints. The evaluation is presented in section 8.2.3.

– *Load factor to determine calculation value of the representative load*

In order to check the steel structure on strength and stiffness, the calculation values of the loads should be determined: $F_d = \gamma * F_{rep}$, in which F_d = calculation value of the load, γ = load factor and F_{rep} = representative value of the load. The most important load factor to be used in the structural check on strength and stiffness:

- o Own weight of the structure is only type of loading: $\gamma = 1.35$;
- o Permanent load in a load combination: $\gamma = 1.2$;
- o Permanent load in a load combination but relieving: $\gamma = 0.9$;
- o Water pressures and waves: $\gamma = 1.25$. If this value is used, no correction is needed related to material factor as all other factors are included in this value [9]. This factor of 1.25 is used in this thesis.

– *Representative loading scenario: maximum surge and waves in combination with $h_{retention} = -5$ ft MSL*

The maximum possible differential head results in the maximum loading on the lifting gate. The maximum representative loading scenario is presented in figure 8.4. The lower the water level in the retention area, the lower the bend in the resulting horizontal pressure curve (orange), which is the sum of the three water pressure curves. This results in a higher resultant water pressure.

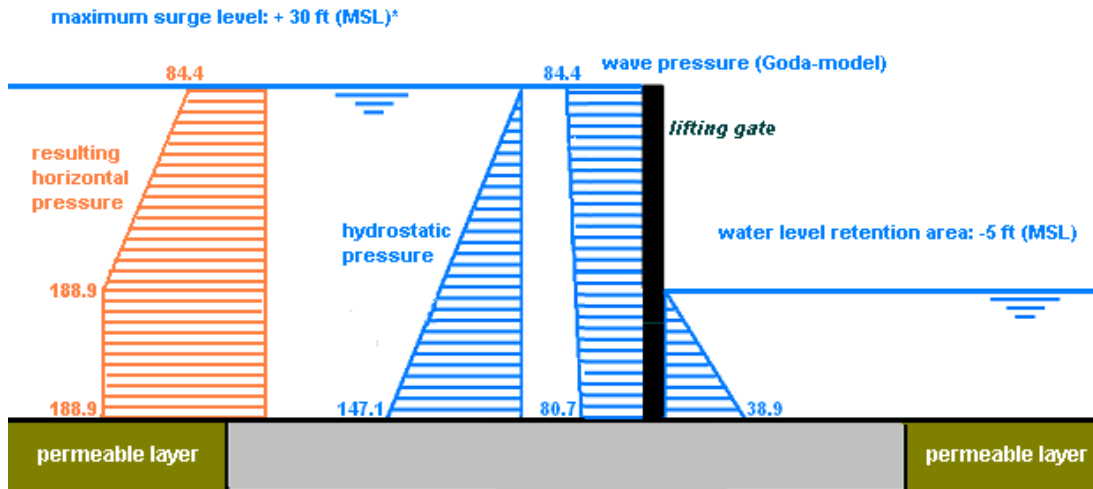


Fig. 8.4: Leading loading scenario for the design of the lifting gate

The values in figure 8.3 are derived as follows:

- o The hydrostatic pressure in the retention area:
depth retention area = -5 (water level) – -18 (bottom sill) = 13 ft = 4.0 m.
 $p_{retention} = 9.807 \times 1,000$ (density of fresh water) $\times 4.0 = 388864$ N/m² = 38.9 kN/m²
- o The wave pressure is determined according to the modified model of Goda for a surge level of +30 ft (+9.1 m, MSL) equal to the retaining height of the lifting gate. In section 7.1.2 it was concluded that only for the maximum surge level of +33 ft (+10.1 m, MSL) overflow occurs, at which point the use of Goda-model is highly questionable and not recommended. This is avoided by computing the maximum surge level in the model at +30 ft (+9.1 m, MSL).
- o The hydrostatic pressure in the retention area:
depth at the outer side of the gate = +30ft – -18 (bottom sill) = 48 ft = 14.6 m.
 $p_{outer;30ft} = 9.807 \times 1,025$ (density of salt water) $\times 14.6 = 147084$ N/m² = 147.1 kN/m²
- o The resulting horizontal force at the bottom of the structure can now be calculated:
 $p_{res} = 147.1 + 80.7 - 38.9 = 188.9$ kN/m²

To incorporate the maximum surge level in the resulting horizontal pressure, a water column of 3 ft (0.9 m) is added to the hydrostatic pressure: $p_{outer;add} = 9.807 \times 1,025 \times 0.91 = 9.2$ kN/m². Including the predetermined load factor, this determines the following calculation factor for the load:

$$q_{top;d} = (84.4 + 9.2) \times 1.25 = 117 \text{ kN/m}^2 \text{ and } q_{bottom;d} = (188.9 + 9.2) \times 1.25 = 248 \text{ kN/m}^2$$

8.2 Design of the barrier cross-sectional components

The structural design of the main lens-shaped barrier cross-sections can be divided in several subsequent steps, to be outlined in the following sections:

- Determination of the reaction forces of the cross beam on the front chord. The actual steel cross-section of this beam is determined in section 8.3. This is possible since for 1D bending beams, the member forces are independent of the cross-sectional area, moment of inertia and material dependent elastic modulus and yield point. The reaction forces can be presented as a uniform distributed load on the lens-shaped barrier section. This enables for the overall barrier cross-section to be designed before the retaining wall is determined.
- A first guess can be determined for the cross-sectional area of the front chord, rear chord and transverses. At this point, two variations regarding the lens-shaped barrier section are reviewed:
 - Optimum type of gate curvature: circular or parabolic;
 - Optimum ratio between the wall arch pitch and back chord pitch.
- The predetermined loading of the 2D frame with the preferred configuration presented at this point does depend on the earlier stated cross-section parameters. Calculations to find the optimal steel cross-sections should therefore have an iterative character. The transverse girder dimensions should be varied first, in order to check whether this has an influence on the moment distribution in the front chord. Subsequently, this girder, front chord, rear chord and general x-type bracing system can be designed.

8.2.1 Determination leading reaction forces of the cross beam on the front chord

A uniform distributed load can be projected on the cross beam equal to the resulting horizontal pressure per meter width. The reaction forces retrieved from the mechanical calculation of this continuous beam on multiple supports can be regarded as a uniform distributed load on the associated barrier cross-section. The actual steel cross-section of this beam is determined in section 8.3. This is possible since for 1D bending beams, the member forces are independent of the cross-sectional area, moment of inertia, elastic modulus and yield point.

Essential in the determination of the leading uniform load on the barrier cross-section is the number of supports, equal to the number of lens-shaped section. The Hartel Canal Barrier consists of two of these lenses with a mutual distance of 7.0 m, as can be seen in figure 8.1. The gate height of this barrier is equal to 9.5 m. For the proposed lifting gate with a total height of 14.6 m, the mutual distance of the upper and lower lens-shaped section is initially set at 12.0 m. The larger mutual distance under the high resulting pressure is expected to result in a large field moment between the two sections. The addition of an extra lens-shaped section can possibly reduce this moment significantly. For this reason, both situations are modeled and reviewed. Appendix I.1 presents an overview of the model calculations for the determination of the support reactions and member forces for the stated situations. Table 8.3 presents an overview of the main results.

	<i>Support reactions (per meter width)</i>	<i>Maximum moment (per meter width)</i>	<i>Maximum shear force (per meter width)</i>
Cross beam at two supports with field lengths: 2.0 / 12.0 / 0.65 [m]	F1 = 1853 kN F2 = 1083 kN	Field moment supports 1-2: 3313 kNm	Shear force at first support: 1354 kN
Cross beam at two supports with field lengths: 3.0 / 9.0 / 2.65 [m]	F1 = 1826 kN F2 = 1041 kN	Field moment ≈ support moment: 1288 kNm ≈ 1116 Km	Shear force at second support: 1082 kN
Cross beam at three supports with field lengths: 2.0 / 6.0 / 6.0 / 0.65 [m]	F1 = 1175 kN F2 = 1357 kN F3 = 405 kN	Moment at second support: 761 kNm	Shear force at second support: 712 kN
Cross beam at three supports with field lengths: 1.5 / 6.0 / 6.0 / 1.15 [m]	F1 = 1011 kN F2 = 1440 kN F3 = 486 kN	Moment at second support: 825 kNm	Shear force at second support: 775 kN

Table 8.3: Cross beam – overview of support reactions and leading member forces, all per meter structural width

From the results in table 8.3 can be concluded that it is favorable to design an additional lens-shaped section. The addition of an extra support without changing the outer supports halves the leading field length. This reduces the maximum moment with a factor of 4 and nearly halves the maximum shear force. As a result, the cross beam itself could be constructed much finer. In addition, it is expected favorable for the x-type brace system between the sections, whose buckling length is reduced. As the normal force is quadratic proportional to this length, reducing it has significant influence. Section 8.2.3 provides more detailed information regarding buckling.

In order to determine its positive or negative influence, the initial mutual distance is varied for both two and three supports. The most optimal configuration for two supports requires a field moment about equal to the leading support moment. This results in a moment of 1288 kNm and leading shear force of 1082 kN. The leading support reaction changes only minimally and is still relatively high, thus not favorable. Furthermore, the influence of the larger ‘cantilever’ end fields is hard to determine. At the same time, the dynamic loads are higher at these points.

From the results for three supports, it follows that is favorable to have a small top field length and larger bottom field length than a more uniformly distribution. The 'cantilever' field of 2.0 at the bottom of the gate reduces the leading maximum moment at the second support. Also the maximum support reaction and shear force are reduced. In conclusion, the cross beam is designed with three 'supports' forming field lengths of 2.0 m, 6.0 m, 6.0 m and 0.65 m respectively. An additional lens-shaped steel section is advised compared to the reference project.

8.2.2 Configuration of the lens-shaped barrier sections

The uniform distributed load on the leading lens-shaped section is equal the maximum support reaction of the cross beams, thus 1357 kN/m. In this thesis, the three lens-shaped sections are divided into two designs. As the support reaction at the bottom 'support' is near to equal to that of the middle 'support' (ratio of forces: 1175 / 1357 = 0.9), these sections are designed to have similar cross-sectional properties. The upper lens can be designed significantly lighter as its uniform distributed load is a factor 405 / 1357 = 0.3 smaller. The leading lens-shaped sections are elaborated first. The reductions regarding the upper lens-shaped design are reviewed in section 8.4.

A first guess can be determined for the cross-sectional areas of the front chord, rear chord and transverses by reviewing the total barrier as a beam on two supports with a uniform distributed force $q = 1357$ kN/m. This leads the following characteristic support reaction: $V_{max} = 0.5 \times q \times L = 0.5 \times 1357 \times 64 = 43424$ kN, see figure 8.5.

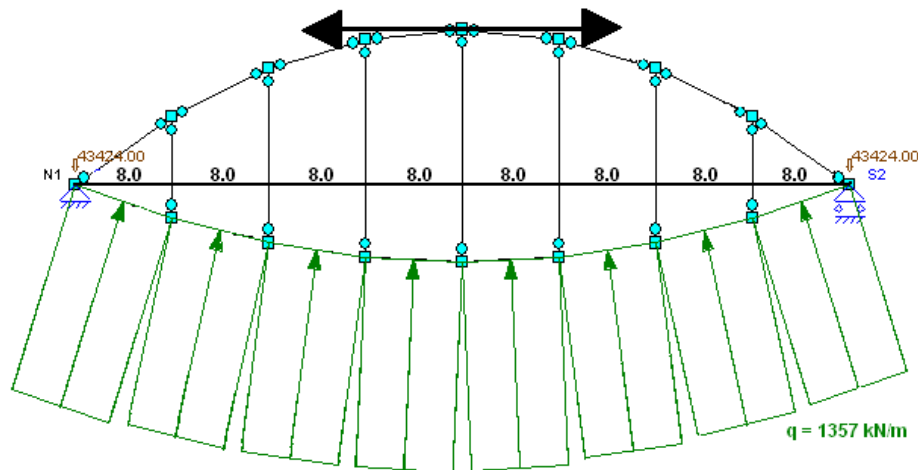


Fig. 8.5: Initial analysis of the lens-shaped barrier section

It is expected that the normal forces in the chords have a similar order of magnitude as the predetermined support reaction. The tensile force in the rear chord can be determined as a direct result of the bending moment. The maximum moment of the modeled beam on two supports can be found by applying the common formula: $M_{max} = 1/8 \times q \times L^2 = 1/8 \times 1357 \times 64^2 = 694784$ kNm. This bending moment should be divided by the distance between the arches to find a proper estimate of the tensile force in the rear chord. Initially assuming a wall arch pitch of 4.0 m and a rear chord pitch of 12.0 m, the tensile force results in $694784 / (4.0 + 12.0) = 43424$ kN. This value is equal to the support reaction but only valid for a combined pitch of 16.0 m. Altering this distance changes the tensile force. A minimum steel cross-section can be now determined:

$$A_{min} = \frac{N}{f_{y;d}}, \text{ in which } N = 4.4 \times 10^4 \text{ kN and } f_{y;d} = 355 \text{ N/mm}^2: A_{min} = 124 \times 10^3 \text{ mm}^2$$

In order to account for the expected local bending moments and shear forces in the front chord, this minimum cross-sectional area is multiplied by a factor of 1.5. A similar cross-sectional area is used for the rear chord. The cross-sectional configuration of the front and rear chords needs to be determined in order to calculate their moment of inertia. The chords are initially designed as square box profiles. This symmetric shaped profile has a uniform moment of inertia in both directions, thus a constant stiffness regarding buckling. With a maximum allowed flange thickness of 40 mm for it to be calculated with the provided values of tensile strength and yield point, the required dimensions result in:

$$\text{Front chord, rear chord: } A_{min} = 190 \times 10^3 \text{ mm}^2 \quad a_{outer} = 1250 \text{ mm, } a_{inner} = 1170 \text{ mm: } A = 193.6 \times 10^3 \text{ mm}^2$$

These dimensions present only a first guess in order to determine the corresponding moment of inertia. In the iterative design calculation regarding both chords, changes are expected. The resulting moment of inertia for both chords can be determined by assuming a squared inner section:

$$\text{Front chord, rear chord: } I_{zz} = I_{yy} = 1/12 \times (a_{outer}^4 - a_{inner}^4) = 4.73 \times 10^{10} \text{ mm}^4$$

For the transverse girders, a box profile with $a = 500$ mm and $t = 20$ mm is estimated at this point. This results in a cross-sectional area of $3.84 \times 10^4 \text{ mm}^2$ moment of inertia of $1.48 \times 10^9 \text{ mm}^4$

At this point, two variations regarding the lens-shaped barrier section are reviewed subsequently:

1) *Optimum type of gate curvature: circular or parabolic*

First step in modeling both gate curvatures is to determine the actual coordinates of the nodes. This can be done by assuming a ratio between the wall arch pitch and rear chord pitch at this point of 3. The wall arch pitch is set at 4 m. The second part of this section determines whether this is a favorable configuration.

– Circular gate curvature

Figure 8.6 presents the used schematization to determine the required coordinates for describing the circular gate curvature. The approach is given for the rear chord pitch of $4 \times 3 = 12$ m. This method makes use of the given constant radius:

$$\sqrt{(4 \cdot 8)^2 + y_R^2} = (12 + y_R)^2$$

$$32^2 = 144 + 24 \cdot y_R,$$

thus $y_R = 36.67$ m

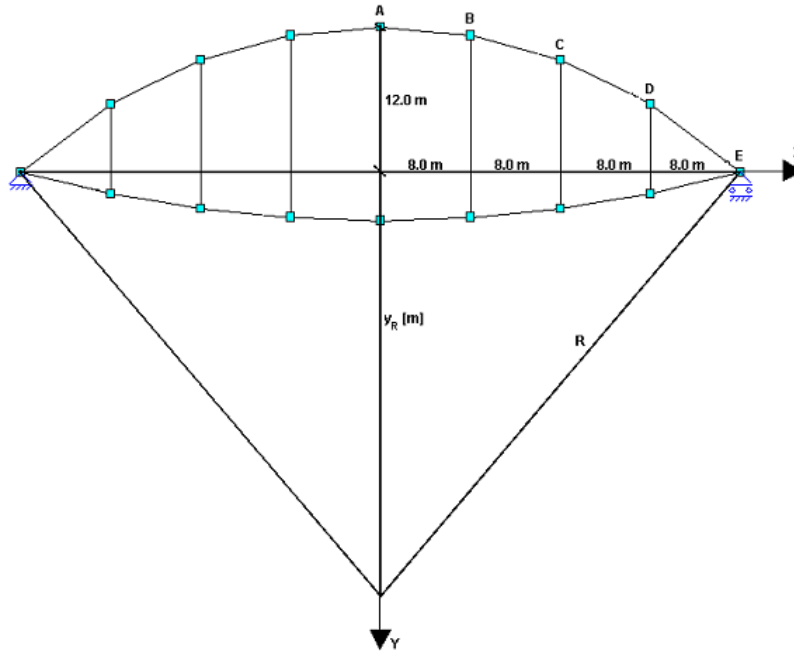


Fig. 8.6: Schematization of a circular gate curvature

The coordinates of nodes A–E can now be calculated with $R^2 = x^2 + y^2$, in which $R = 12 + 36.67 = 48.67$ m. As the gate is symmetric in relation to the y-axis, only these nodes suffice. This calculation results in:

Node	A	B	C	D	E
Coordinate	(0.0; 12.0)	(8.0; 11.34)	(16.0; 9.30)	(24.0; 5.67)	(32.0; 0.0)

The same approach can be used in order to determine the coordinates of the nodes at front chord. Given the wall arch of 4 m: $y_R = 126$ m, thus $R = 130$ m. This results in:

Node	A	B	C	D	E
Coordinate	(0.0; 4.0)	(8.0; 3.75)	(16.0; 3.01)	(24.0; 1.77)	(32.0; 0.0)

– Parabolic gate curvature

The coordinates for a parabolic curvature can be calculated by introducing the boundary conditions to a standard quadratic function $y = ax^2 + b$:

Rear chord pitch = 12.0 m and $y = 0$ at $x = 32$ m: $0 = 12 - a \cdot 32^2 = 0$, thus $a = 3/256$

Node	A	B	C	D	E
Coordinate	(0.0; 12.0)	(8.0; 11.25)	(16.0; 9.00)	(24.0; 5.25)	(32.0; 0.0)

Wall arch pitch = 4.0 m and $y = 0$ at $x = 32$ m: $0 = 4 - a \cdot 32^2 = 0$, thus $a = 1/256$

Node	A	B	C	D	E
Coordinate	(0.0; 4.0)	(8.0; 3.75)	(16.0; 3.00)	(24.0; 1.75)	(32.0; 0.0)

Appendix I.2.1 and I.2.2 present the support reactions and member forces of the circular and parabolic shaped gate configuration respectively. In order to compare the results, both configurations have similar cross-sectional parameters, corresponding to those derived at the beginning of this section. Both gate curvatures are modeled with hinged joints and with a wall arch pitch of 4.0 m and a rear chord arch of 12.0 m. Finally, also the loading is similar and equal the leading support reaction per meter linear structural width, thus equal to 1357 kN/m.

In order to determine the favorable configuration, the member forces of moment, shear force and normal force are reviewed. Several conclusions can be stated:

- The development of shear force is not similar for both configurations. The circular shaped design has a shear force range at its front chord of about 3,500 kN to about 7,000 kN. The parabolic configuration has a fairly constant shear force with a significantly smaller range of about 5,100 kN to 5,800 kN.

- The development of the bending moment in the front chords is not similar for both configurations. Like for the shear force, the circular shaped design has a wider range of moments, including both high field moments and support moments. The parabolic configuration has a more uniform distributed moment along the front chord. Only at the end field a significantly higher field moment is found. This could be due to the rough order steel cross-sections assumptions, in which all transverses were stated to be similar. The influence of these transverses on the overall development is determined in the next part of this section.
- The development of normal forces for is near to similar for both configurations. In both configurations the front and rear chords are loaded by a normal force in the range of 43,000 to 52,000 kN. Important to note is that these model results clearly present the manner in which forces are transmitted to the substructure. The wall arch or front chord is purely loaded by a compressive force, whereas the rear arch is purely loaded by a tensile force. The transverse girder allows for the transmission of forces between those two arches.

From these stated developments of member forces it is concluded that a parabolic gate curvature is favorable over the circular curvature. The maximum moment and shear force is smaller and also the range of these forces is smaller. The first allows for a finer design, which means that the gate will be lighter. The latter allows for a more optimal use of the steel cross-sectional as the loading is more uniform distributed of the length of the chord. The significant changes in member forces are remarkable in respect to the small changes in coordinates of the nodes. It can be concluded that it is really important to adequately determine this lens-shaped design, as minimal differences in the curvature can have significant influence on the development of the member forces.

2) *Optimum ratio between the wall arch pitch and rear chord pitch*

The parabolic curvature is stated to be the most optimal configuration. Now the ratio between the wall arch and rear chord pitch is varied in order to find an optimum. The coordinates for a parabolic curvature with a certain wall arch pitch a rear chord pitch can be calculated as previously described. Table 8.4 presents an overview for several ratios between the pitches.

A) Wall arch pitch = 4.0 m and rear chord pitch = 8.0 m, thus ratio = 2: <i>Appendix I.2.3</i>							
wall arch	a = 1 / 256	Node	A	B	C	D	E
		Coordinate	(0.0; 4.0)	(8.0; 3.75)	(16.0; 3.00)	(24.0; 1.75)	(32.0; 0.0)
rear chord	a = 2 / 256	Node	A	B	C	D	E
		Coordinate	(0.0; 8.0)	(8.0; 7.5)	(16.0; 6.00)	(24.0; 3.50)	(32.0; 0.0)
B) Wall arch pitch = 6.0 m and rear chord pitch = 12.0 m, thus ratio = 2 with and increase in pitches: <i>Appendix I.2.4</i>							
wall arch	a = 3 / 512	Node	A	B	C	D	E
		Coordinate	(0.0; 6.0)	(8.0; 5.625)	(16.0; 4.50)	(24.0; 2.625)	(32.0; 0.0)
rear chord	a = 3 / 256	Node	A	B	C	D	E
		Coordinate	(0.0; 12.0)	(8.0; 11.25)	(16.0; 9.00)	(24.0; 5.25)	(32.0; 0.0)
C) Wall arch pitch = 4.0 m and rear chord pitch = 12.0 m, thus ratio is 3: <i>Appendix I.2.2</i>							
wall arch	a = 1 / 256	Node	A	B	C	D	E
		Coordinate	(0.0; 4.0)	(8.0; 3.75)	(16.0; 3.00)	(24.0; 1.75)	(32.0; 0.0)
rear chord	a = 3 / 256	Node	A	B	C	D	E
		Coordinate	(0.0; 12.0)	(8.0; 11.25)	(16.0; 9.00)	(24.0; 5.25)	(32.0; 0.0)

Table 8.4: Overview of coordinates to describe variable arch pitches

Appendices I.2.2 to I.2.4 present the three configurations stated in table 8.4. All consist of parabolic curvatures, similar cross-sectional parameters, hinged joints and are loaded by the leading uniform distributed load of 1357 kN/m. Only the wall arch pitch and rear chord pitch are varied. In order to determine the favorable configuration, the member forces of moment, shear force and normal force are reviewed. Several conclusions can be stated:

- The development of shear force is fairly similar in the stated configurations. The range of fairly small, with a general value of about 5,000 kN. It can therefore be concluded that the influence of the gate curvature on this shear force is minimum and can be neglected.
- The development of the bending moment depends on the curvature of the gate, thus on the ratio of the pitches. At the center of the wall arch, configuration A has a relative uniform distributed moment line as support moments are generally equal to associated field moments. For configuration C, the support moments are about two times the associated field moments. In configuration B, this factor increase to about 10 times the field moments at the center of the arch. This factor rapidly decreases per field length, thus resulting in a non-uniform distributed moment of the front chord. The stated differences can be explained by focusing on the arch of the rear curvature. It can be concluded that the steeper the rear arch curvature with regard to the front curvature, the higher the support moments in the front chord. This results in lower field moment in the adjacent fields. The support moments in configurations with the larger rear chord (B and C, rear chord = 12.0 m) should thus be larger than the support moments in configuration A. Figure 8.7 present the moment lines of the three configurations with their deformations, in which the lower support moments of configuration A are visible.

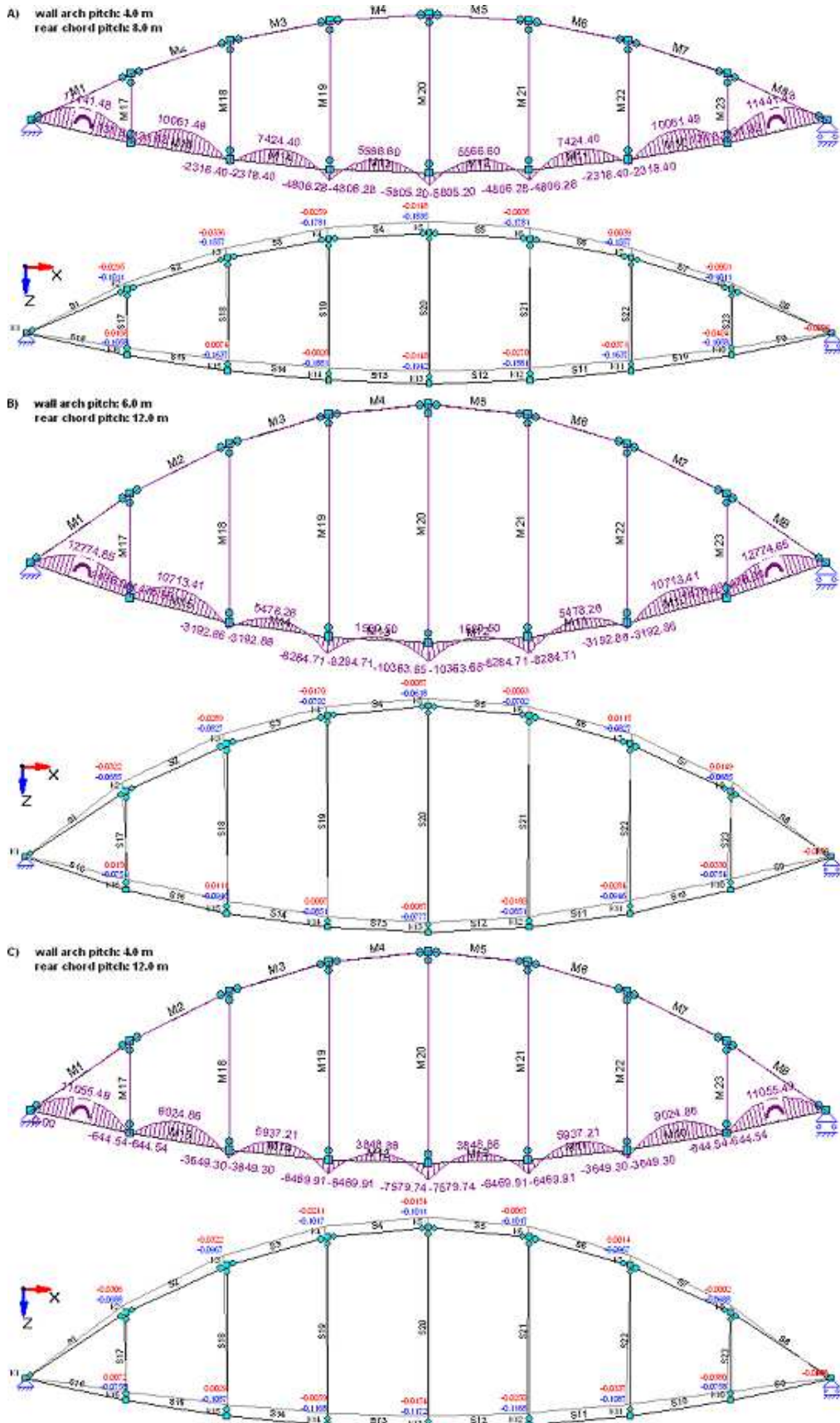


Fig. 8.7: Bending moment development for variable arch pitches

Comparing the moment lines of configurations B and C leads to conclude that it is not simply the curvature of the rear chord, thus the rear chord pitch, which causes the moment line to change. It is instructive to further focus on the relative curvature of this rear chord, thus on the ratio of the pitches. The larger ratio of 3 at configuration C corresponds to a larger relative curvature, which generally leads to higher support moments. The shallower the curvature of the rear chord arch, the larger the local deformation at their connection and thus the lower the support moment is provided at the front chord end.

By concluding this, it should be noted the moment line in all configurations can still be adjusted by variation of the transverse girder. This girder essentially provides the supports of the front chord. Variation of this parameter led to conclude that this influence is only minimal. It is the relative curvature that determines the forces which the girders can transmit towards the rear chord.

- The development of the normal force over the front and rear chord for the stated configurations is presented in figure 8.8. It provides an image of the influence of a particular arch pitch itself and the ratio between the wall arch and rear chord pitch.

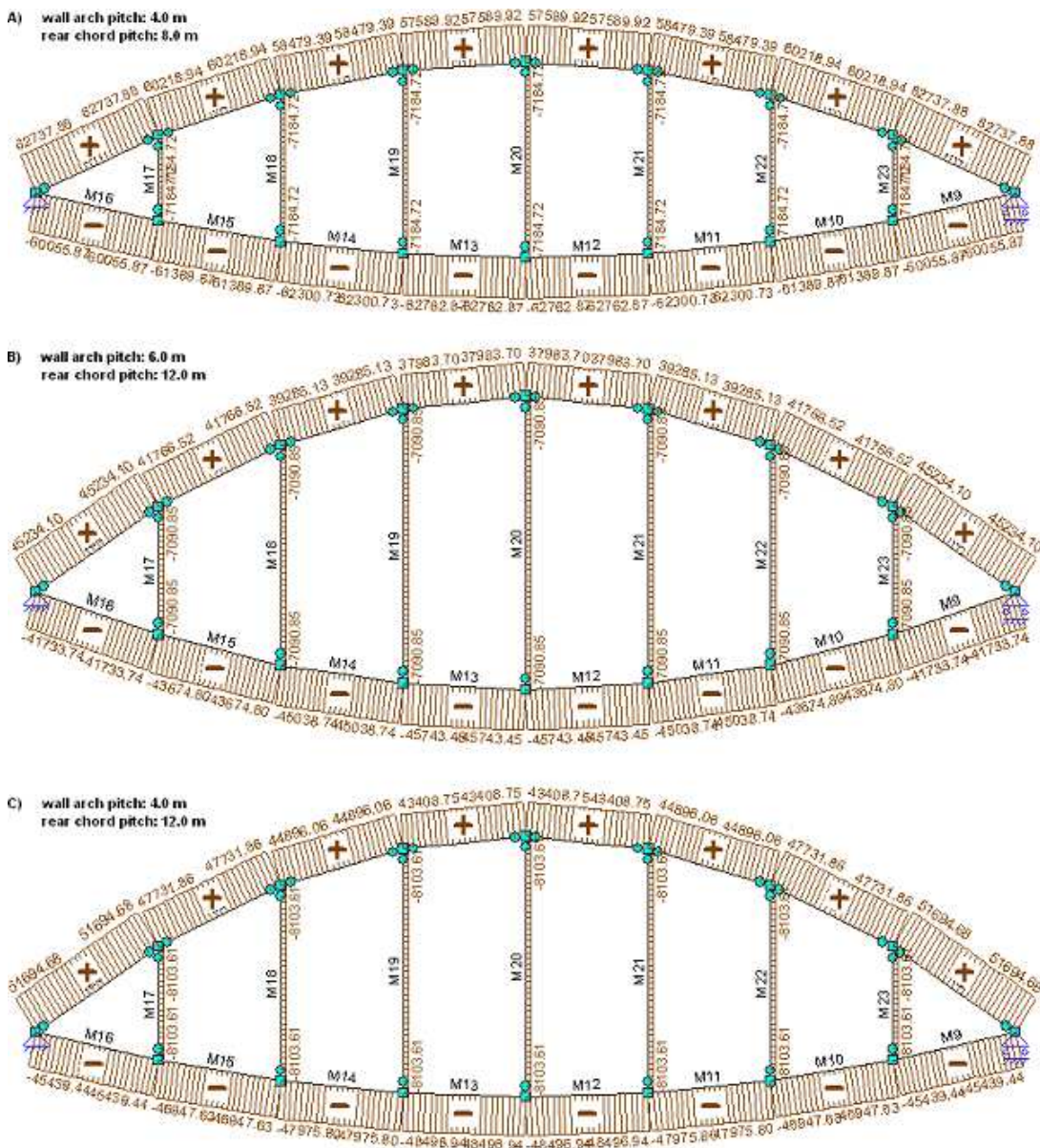


Fig. 8.8: Normal force development for variable arch pitches

- Configuration A consists of the smaller wall arch pitch of 4.0 m and a pitch ratio of 2. This combination results in significantly larger compressive and tensile forces with regard to the other configurations. In configuration A, both forces have a small range around a general value of about 60,000 kN. The force compressive force in the transverse girder is constant at about 7,200 kN
- Configuration B consists of the larger wall arch pitch of 6.0 m and a pitch ratio of 2. The front chord has general compressive force of 41,000 to 45,000 kN. The rear chord has a general tensile force of about 38,000 to 45,000 kN. Also in this configuration, the compressive and tensile forces are near to equal. However, both forces are significantly lower than those in configuration A. The compressive force in the transverse girders is about equal to that of A.
- Configuration C consists of the smaller wall arch pitch, but now with a pitch ratio of 3. This configuration results in small ranged compressive and tensile force, both with a general value of about 45,000 to 50,000 kN. The compressive force in the transverse girders is constant at 8,100 kN, about 10% higher than that of configuration A and B.

From the stated developments of member forces it is concluded that a the parabolic gate curvature with an wall arch pitch of 6.0 m and pitch ratio of 2 is the most favorable lens-shaped configuration. It has the benefit that the compressive and tensile forces are near to equal and significantly smaller than those of configuration A. The only disadvantage is the fact that the buckling length of the transverse girder increases. As the length is quadratic proportional to the required moment of inertia of the girder, its cross-section and weight increases.

With respect to configuration C, the normal force is generally equal. The leading support moment at the center node is significantly higher. The leading field moments at the end fields are only slightly higher. This difference is not expected to be critical. At the maximum field moment of 12,775 kNm, the shear force is equal to zero and at the support moment of 10,360 kNm, the shear force is about 5700 kN. It is estimated that the contribution of the shear force is minimal due to the large cross-sectional area required for the normal forces. The resulting stresses at the leading field and leading support section are thus expected to about equal. This is favorable because it leads to a more optimal use of the provided steel cross-section as it is about uniformly loaded over it total length.

Another reason to prefer configuration B is that a pitch ratio of 2 is expected to place the center of gravity of the lens-shaped section closer to the plane of suspension. In this way, the overturning moment atop the towers is kept smaller. This reduces the moment at the foundation of the towers and decreases the probability of friction during vertical movement of the gate. A pitch ratio of 3 in C would place the center of gravity further towards the rear arch. Reason for this to expect is the fact that the front and rear chord will have to be relatively large in order to transmit the high normal forces. This means that the weight of the gate wall at the smaller arch will contributes less to the center of gravity of the lens-shaped section. A smaller ratio of distances of the chords is thus advised. With respect to structural stability, this eccentricity with a pitch ratio of 3 results in an additional overturning moment 'towards' the retention area. From the stability analysis presented in chapter 7, it can be concluded that the resultant moment in that direction is already critically high due to the high horizontal forces and asymmetric gate positioning. Any significant increase is thus not desirable.

8.2.3 Iterative calculations to find optimal steel cross-sections: front chord, rear chord and transverse girders

The preliminary design of the front chord, rear chord and transverse on the occurring member forces is essentially applying a combination of the checks on the equivalent stress and buckling. At first, both checks will be briefly explained. After this introduction, the steel components are designed iteratively.

Equivalent stress should be smaller than the yield point

The equivalent stress of the bending moment, shear force and normal force can be determined according to the simplified formula of Hubert-Hensky. This results in a minimum cross-sectional area and moment of inertia. In used linear elastic theory, a maximum is reached if at some point in the steel cross-section the yield point is reached. For a 3D configuration of steel stress, the yield criterion of Hubert-Hensky states [39]:

$$\sigma_{\text{eq}} = \sqrt{\sigma_x^2 + \sigma_y^2 + \sigma_z^2 - \sigma_x\sigma_y - \sigma_y\sigma_z - \sigma_x\sigma_z + 3\tau_{xy}^2 + 3\tau_{yz}^2 + 3\tau_{xz}^2} \leq \text{yield point } f_{y,d}$$

In a beam, with the assumption that it follows the direction of the y-axis, the equivalent stress formula results in:

$$\sigma_{\text{eq}} = \sqrt{\sigma_y^2 + 3\tau_{yz}^2} \leq \text{yield point } f_{y,d}$$

The quantities within this equation present the combination of the three main member forces:

- The quantity σ represents the calculation value of the combination of the normal force and bending moment. As stated earlier, according to the elastic theory, the stresses at some point in the steel cross-section should not exceed the yield point. This can be denoted by.

$$\sigma_x = \frac{N}{A} \leq f_y \quad \sigma_x = \frac{N}{A} + \frac{M_y}{W_y} \leq f_y \quad \sigma_x = \frac{N}{A} + \frac{M_z}{W_z} \leq f_y$$

The interaction of the normal force and the bending moment gives:

$$\sigma_x = \frac{N}{A} + \frac{M_y}{W_y} + \frac{M_z}{W_z} \leq f_y$$

- The quantity τ represents the absolute value of shear stress, which can be denoted in its general form as:

$$\tau = \frac{V_z S_y^a}{b l_y}, \text{ in which:}$$

V_z = the leading shear force;

S_y^a = the static moment of the shearing part in relation to the center line of gravity;

b = width of the shearing part at a certain location;

I_y = moment of inertia of the total cross-section.

In the elastic theory, the separate check of the cross-section on the leading shear stress states that this stress should be smaller than the yield point for shearing. This can be denoted as:

$$\tau = \frac{V_z S_y^a}{b l_y} \leq \frac{f_{y;d}}{\sqrt{3}}$$

Sufficient moment of inertia should prevent buckling

The transverse girders can be modeled as a beam with hinged joints at both ends. The critical buckling force for this situation is derived by Euler and is given by [39]:

$$F_{\text{Euler}} = \frac{\pi^2 EI}{L^2} (2n-1), n > 0, \text{ in which the critical force is found in case } n = 1$$

The compressive force in the front could potentially lead to buckling. Although expected to be the leading cause of failure due to the large dimensions of the chord, it should be checked. For a beam with clamped joints at both ends, Euler derived a critical buckling force 4 times that of the beam on hinged joints. If one of the clamped joint could move in one direction, a similar critical buckling force should be used as for a beam on hinged joints. In this preliminary design, the latter is used as this is more critical. If this beam configuration suffices, the beam with non-moving clamped joints will too.

Rewriting the equation of Euler for a beam with hinged joints presents an indication for the minimum moment of inertia required in the particular steel cross-section in order to prevent buckling:

$$I_{\text{min}} = \frac{F_{\text{Euler}} \cdot L^2}{\pi^2 \cdot E_{\text{steel}}}, \text{ in which } F_{\text{Euler}} \text{ corresponds to the occurring normal force in the steel component}$$

Design calculations the steel components – front chord, rear chord and transverse girders

The approach is taken to design the component iteratively. The first input of cross-sectional parameters was determined in section 8.2.1. The front chord, rear chord and transverses were assumed square box profiles as this provides a constant stiffness regarding buckling. The rear chord can not fail due to buckling since it is purely loaded by tensile forces.

With a maximum allowed flange thickness of 40 mm for it to be calculated with provides tensile strength and yield point, the required chords resulted in an outer dimension of $a = 1250$ mm. Both chords were set to have similar dimensions. For the transverse girders, a box profile with $a = 500$ mm and $t = 20$ mm was chosen.

Front chord

In the front chord, two leading sections exist: one at the end field and one at the center of the front chord. These sections will be checked subsequently. The third check concerns the minimum moment of inertia required to avoid local buckling of the chord.

- At the end fields, the field moment represents the maximum occurring moment in the chord: 12775 kNm. At this location, the shear force equal zero. The normal force amounts 41734 kN. As the shear force is zero, the check regarding the yield point reduces to the interaction of normal force moment. Again the own weight of the barrier parts is neglected, so the check results in:

$$\sigma = \frac{N}{A} + \frac{M_y}{W_y} \leq 355 \text{ N/mm}^2, \text{ in which } W \text{ is the moment of inertia divided the distance to the outer steel fiber.}$$

Moment of inertia of the front chord, rear chord: $I_{zz} = I_{yy} = 1/12 \times (a_{\text{outer}}^4 - a_{\text{inner}}^4) = 4.73 \times 10^{10} \text{ mm}^4$

$$\sigma = \frac{41734 \cdot 10^3}{193.6 \cdot 10^3} + \frac{12775 \cdot 10^6 \cdot (1250/2)}{4.73 \cdot 10^{10}} = 215.6 + 168.8 = 384.4 \text{ N/mm}^2$$

It can be concluded that the initially assumed dimensions are not sufficient as the yield point is exceeded. For the purpose of comparison, also the other leading section is determined at these failing dimensions.

- At the center transverse girder, the support moment represents the maximum moment in combination with a shear force. The moment amounts 10364 kNm and the shear force amounts 5694 kN. At this location, the normal force amounts 45744 kN. As the shear force is non-zero, the check regarding the yield point requires the determination of the equivalent stress. This check results in:

$$\sigma_{eq} = \sqrt{\sigma_y^2 + 3\tau_{yz}^2} = \sqrt{\left(\frac{N}{A} + \frac{M_y * e}{I_y}\right)^2 + 3\tau_{yz}^2} \leq 355 \text{ N/mm}^2$$

The center line of gravity of the square profile is located at $a/2 = 625 \text{ mm}$. The shearing part of the cross-section of the square box profile in relation to this line equals:

$$S_z^a = (a - 2t) * \left(\frac{1}{2}a - t\right) + 2 * \left(\frac{1}{2}at\right)\left(\frac{1}{4}a\right)$$

$$S_z^a = (1250 - 2 * 40) * \left(\frac{1}{2} * 1250 - 40\right) + 2 * \left(\frac{1}{2} * 1250 * 40\right) * \left(\frac{1}{4} * 1250\right) = 16.31 * 10^6 \text{ mm}^3$$

The stress due to the bending moment and shear force can now be determined:

$$\tau = \frac{V_z S_y^a}{b I_y} = \frac{(5694 * 10^3) * (16.31 * 10^6)}{(40 + 40) * (4.73 * 10^{10})} = 24.6 \text{ N/mm}^2$$

$$\sigma = \frac{N}{A} + \frac{M_y * e}{I_y} = \frac{45744 * 10^3}{193.6 * 10^3} + \frac{10364 * 10^6 * (1250/2)}{4.73 * 10^{10}} = 236.3 + 137.0 = 373.3 \text{ N/mm}^2$$

The equivalent stress results in:

$$\sigma_{eq} = \sqrt{\left(\frac{N}{A} + \frac{M_y * e}{I_y}\right)^2 + 3\tau_{yz}^2} = \sqrt{372.1^2 + 3 * 24.6^2} = 374.5 \text{ N/mm}^2$$

Not only at the end field, but also at the center transverse girder the yield point is exceeded. Note that the shear force has no significant influence. This corresponds to the earlier stated estimation. The stresses at the leading end field and this leading support section are about equal, resulting in optimal use of the steel.

- The initially assumed moment of inertia of the front chord equals $1/12 * (a_{outer}^4 - a_{inner}^4) = 4.73 * 10^{10} \text{ mm}^4$. The minimum required value to avoid buckling can be determined for the maximum compressive force equal to 45744 kN by assuming the field length equal to 8.0 m. This results in:

$$I_{min} = \frac{F_{Euler} * L^2}{\pi^2 * E_{steel}} = \frac{45744 * 10^3 * 8000^2}{\pi^2 * 210 * 10^3} = 1.42 * 10^9 \text{ mm}^4$$

This value is significantly smaller (factor > 30) than the moment of inertia for the initial assumed cross-section. It can therefore be concluded that buckling is not critical for the front chord.

Rear chord

In the rear chord, only one leading section exists: the maximum tensile force at the end field. Due to the assumed hinged joints, the bending moments and shear forces are zero. Only the minimal cross-sectional area should be determined with the check on the yield point. The maximum tensile stress in the rear chord equals 51695 kN. The check results in:

$$\sigma = \frac{N}{A} \leq 355 \text{ N/mm}^2, \text{ thus: } A_{min} = \frac{51695 * 10^3}{355} = 146 * 10^3 \text{ mm}^2$$

The initially assumed cross-sectional area equals $1.5 * 127 * 10^3 = 190 * 10^3 \text{ mm}^2$ and would suffice.

Transverse girders

The joints of the x-type bracing system and adjacent transverses and rear chord are initially assumed to be hinged joints. As a result of this modeling, the transverse girder, rear chord and x-type bracing system are only loaded by a normal force. The minimum cross-sectional area and minimum moment of inertia of the girder can be determined combining the following checks:

- The yield point determines the minimum required cross-sectional area: $\sigma_x = \frac{N}{A} \leq f_y$

The yield point is equal to 355 N/mm^2 . The normal force for the chosen lens-shaped configuration can be extracted from figure 8.7 and is equal to 7091 kN. This results in a minimum steel cross-sectional area of $7091 * 10^3 / 355 = 20.0 * 10^3 \text{ mm}^2$.

- The critical buckling force derived by Euler determines the minimum required moment of inertia:

$$I_{\min} = \frac{F_{\text{Euler}} * L^2}{\pi^2 * E_{\text{steel}}}$$

As the normal forces are equal for each transverse girder, the minimum moment of inertia solely depends on the buckling length L. This length is not constant, but can be determined by the summation of the local gate eccentricities. Table 8.5 presents the calculation results regarding the design of the transverse girders. A constant flange thickness of 20 mm is chosen and the outer dimension (a) is varied.

Location (fig 8.8)	Normal force	A_{\min}	L_{buckling}	I_{\min}	Design transverse girder			
					a [mm]	t [mm]	A [mm ²]	I [mm ⁴]
	[N]	[mm ²]	[m]	[mm ⁴]				
A	7091x10 ³	20.0x10 ³	12.0 + 6.0 = 18.0	1.11x10 ⁹	500	20	38.4x10 ³	1.47x10 ⁹
B	7091x10 ³	20.0x10 ³	11.25 + 5.625 = 16.875	9.75x10 ⁸	450	20	34.4x10 ³	1.06x10 ⁹
C	7091x10 ³	20.0x10 ³	9.00 + 4.5 = 13.5	6.24x10 ⁸	400	20	30.4x10 ³	7.34x10 ⁸
D	7091x10 ³	20.0x10 ³	5.25 + 2.625 = 7.875	2.13x10 ⁸	300	20	22.4x10 ³	2.94x10 ⁸

Table 8.5: Bottom / center lens-shaped section – design transverse girder, hinged joint model – constant flange thickness

The quadratic dependence on the buckling length results in a significant variation of required properties. The initially constant transverse girders result in a severe overestimation of the actual required steel components. It is also possible to variation the flange thickness in relation to a constant outer dimension a. This outer dimension is set at 400 mm. Table 8.6 presents the calculation results.

Location (fig 8.8)	Normal force	A_{\min}	L_{buckling}	I_{\min}	Design transverse girder			
					a [mm]	t [mm]	A [mm ²]	I _z [mm ⁴]
	[N]	[mm ²]	[m]	[mm ⁴]				
A	7091x10 ³	20.0x10 ³	12.0 + 6.0 = 18.0	1.11x10 ⁹	400	40	57.6x10 ³	1.26x10 ⁹
B	7091x10 ³	20.0x10 ³	11.25 + 5.625 = 16.875	9.75x10 ⁸	400	30	44.4x10 ³	1.02x10 ⁹
C	7091x10 ³	20.0x10 ³	9.00 + 4.5 = 13.5	6.24x10 ⁸	400	20	30.4x10 ³	7.34x10 ⁸
D	7091x10 ³	20.0x10 ³	5.25 + 2.625 = 7.875	2.13x10 ⁸	400	15 *	23.1x10 ³	5.71x10 ⁸

Table 8.6: Bottom / center lens-shaped section – design transverse girder, hinged joint model – constant outer dimension

*) the minimum steel cross-section becomes critical, therefore and flange thickness of 10 mm not allowed

It can be concluded that the results in table 8.5 present a more optimal configuration. The required amount of steel is significantly less for a constant flange thickness than for a constant outer dimension. The distance of the steel area in relation to the center of gravity of the cross-section is the critical optimization parameter. The larger this distance, the more the steel contributes to the moment of inertia.

A check on the initially neglected own weight of the central transverse girder is made in order to validate this assumption. The density of steel amounts 7850 kg/m³. The bending of the girder can be modeled as a uniform distributed load on a beam at two supports. The load is denoted as weight per meter length: q = 7850 x 38400 x 10⁻⁶ = 301.5 kg/m = 3 kN/m. The maximum bending moment equals: M_{max} = 0.125 x 3 x 18² = 121.5 kNm. The bending moment produces an increase of stress: Δσ = (M*e)/I_z = (121.5x10⁶ x 250) / 1.26x10⁹ = 24.2 N/mm². The minimum required cross-sectional area for this combined loading of a normal force and a bending moment: 355 N/mm² = (N/A) + 24.2, thus A_{min} = 7091x10³ / (355 - 24.2) = 21.4x10³ mm², an increase of 7%. For this preliminary design, this appears to be sufficiently small. All presented transverse girder configurations still suffice.

X-type bracing system – design of center frame

The distance between the top and the bottom rear chords is held by x-type bracings which should provide sufficient stability of both chords under vertical loads like falling water (overflow) and own weight. These loads are not included in this preliminary design. The dynamic load of falling water should be investigated for the final design stage. The own weights of the front plate / front chord on one hand and rear chord / bracings on the other hand cause an internal bending of the overall lens-shaped section. This could cause significant internal stresses. This influence can not be included in the taken 2D calculation approach, but is important to include in a detailed 3D design analysis.

As stated at the beginning of this section, the three lens-shaped sections are divided into two designs. The bottom and center lens-shaped sections are designed to have similar cross-sectional properties. The upper lens can be designed significantly lighter as its uniform distributed load is a factor 405 / 1357 = 0.3 smaller than for the center lens-shaped section. The design of the transverse girders of the upper section is presented in table 8.7.

The dimensions of the beams that form the x-type bracing system can be determined by separating it from the adjacent front and rear chord. The normal forces in the transverse girder are defined as external nodal forces at the front chords side of the frame. Figure 8.9 presents the schematization of the center frame of 18.0 m and figure 8.10 presents the calculation results regarding the normal forces in the particular frame.

Location (fig 8.8)	Normal force [N]	A_{min} [mm ²]	$L_{buckling}$ [m]	I_{min} [mm ⁴]	Design transverse girder			
					a [mm]	t [mm]	A [mm ²]	I_z [mm ⁴]
A	2128×10^3	6.0×10^3	$12.0 + 6.0 = 18.0$	3.33×10^8	350	15	20.1×10^3	3.77×10^8
B	2128×10^3	6.0×10^3	$11.25 + 5.625 = 16.875$	2.93×10^8	350	15	20.1×10^3	3.77×10^8
C	2128×10^3	6.0×10^3	$9.00 + 4.5 = 13.5$	1.88×10^8	300	15	17.1×10^3	2.32×10^8
D	2128×10^3	6.0×10^3	$5.25 + 2.625 = 7.875$	0.64×10^8	250	15	14.1×10^3	1.30×10^8

Table 8.7: Upper lens-shaped section – design transverse girder, hinged joint model

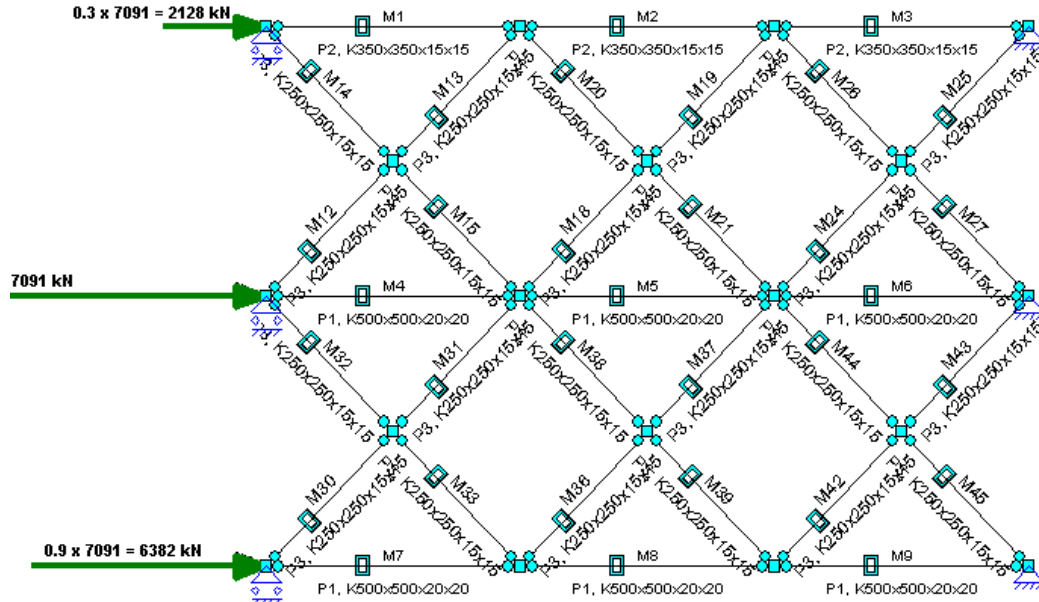


Fig. 8.9: Schematization of the center frame

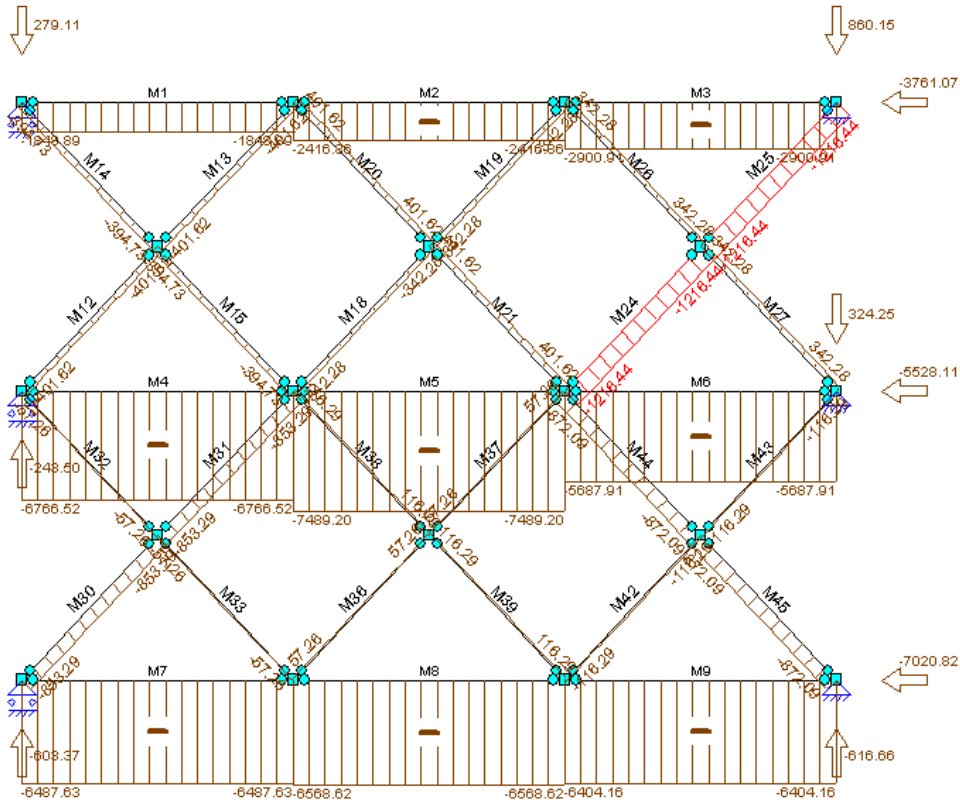


Fig. 8.10: Center frame – development of normal forces, hinged joint model

Center transvers	Normal force	A_{min}	$L_{buckling}$	I_{min}	Design transverse girder / x-type beam			
	[N]				[mm ²]	[m]	[mm ⁴]	a [mm]
Upper	2900x10 ³	8.2x10 ³	12.0 + 6.0 = 18.0	4.47x10 ⁸	350	15 *	20.1x10 ³	3.77x10 ⁹
Center	7490x10 ³	21.1x10 ³	12.0 + 6.0 = 18.0	1.18x10 ⁹	500	20	38.4x10 ³	1.47x10 ⁹
Bottom	6569x10 ³	21.1x10 ³	12.0 + 6.0 = 18.0	1.03x10 ⁹	500	20	38.4x10 ³	1.47x10 ⁹
x-type beam	1217x10 ³	3.5x10 ³	6.0√2 = 8.5	4.25x10 ⁷	250	15 **	14.1x10 ³	1.30x10 ⁸

Table 8.8: X-type bracing system – design center frame, hinged joint model – first guess

The results of table 8.8 indicate that the current design is not sufficient. The flange thickness of the transverse of the upper lens-shaped section (*) is increased to 20 mm. The flange thickness of the x-type bracing beams appears to be overestimated and it therefore decreased to 10 mm (**). Appendix I.2.5 presents the member forces of the adjusted frame. Table 8.9 presents the design calculations for this configuration, which all suffice.

Center transvers	Normal force	A_{min}	$L_{buckling}$	I_{min}	Design transverse girder			
	[N]				[mm ²]	[m]	[mm ⁴]	a [mm]
Upper	3059x10 ³	8.2x10 ³	12.0 + 6.0 = 18.0	4.78x10 ⁸	350	20	20.1x10 ³	4.81x10 ⁸
Center	7054x10 ³	21.1x10 ³	12.0 + 6.0 = 18.0	1.11x10 ⁹	500	20	38.4x10 ³	1.47x10 ⁹
Bottom	6790x10 ³	21.1x10 ³	12.0 + 6.0 = 18.0	1.07x10 ⁹	500	20	38.4x10 ³	1.47x10 ⁹
x-type beam	758x10 ³	3.5x10 ³	6.0√2 = 8.5	2.65x10 ⁷	250	10	9.6x10 ³	9.23x10 ⁷

Table 8.9: X-type bracing system – design center frame, hinged joint model – preliminary design

Review on assumed hinged joints at the rear chord, transverse girders and x-type bracing system

At this point, it is interesting to review the influence of the assumption that the x-type bracing system, including the rear chord and transverse girders, consists of hinged joints. Appendix I.3.1 presents the member forces of the predetermined lens-shaped configuration with clamped joints instead of hinged joints. In this adjusted model, both the front and rear are loaded by a combination of bending moments, shear forces and normal forces. The critical cross-section of both chords can be determined and checked in the same manner as is presented above. These checks results in:

- Front chord, clamped joints, maximum support moment (M = 7605 kNm, V = 5553 kN, N = 45636 kN):

$$\sigma_{eq} = \sqrt{\left(\frac{N}{A} + \frac{M_y * e}{I_y}\right)^2} + 3\tau_{yz}^2 = \sqrt{\left(\frac{45636 * 10^3}{193.6 * 10^3} + \frac{7605 * 10^6 * 625}{4.73 * 10^{10}}\right)^2} + 3\left(\frac{5553 * 10^3 * 16.31 * 10^6}{(40 + 40) * 4.73 * 10^{10}}\right)^2 = 338.8 \text{ N/mm}^2$$

- Front chord, clamped joints, maximum field moment (M = 8332 kNm, V = 0 kN, N = 43646 kN):

$$\sigma = \frac{N}{A} + \frac{M_y * e}{I_y} = \frac{43646 * 10^3}{193.6 * 10^3} + \frac{8332 * 10^6 * 625}{4.73 * 10^{10}} = 225.4 + 110.1 = 335.5 \text{ N/mm}^2$$

- Rear chord, clamped joints, max. moment at end support (M = 6268 kNm, V = 253 kN, N = 44958):

$$\sigma_{eq} = \sqrt{\left(\frac{N}{A} + \frac{M_y * e}{I_y}\right)^2} + 3\tau_{yz}^2 = \sqrt{\left(\frac{44958 * 10^3}{193.6 * 10^3} + \frac{6268 * 10^6 * 625}{4.73 * 10^{10}}\right)^2} + 3\left(\frac{253 * 10^3 * 16.31 * 10^6}{(40 + 40) * 4.73 * 10^{10}}\right)^2 = 315.1 \text{ N/mm}^2$$

All these checks suffice for the initially assumed cross-sectional dimensions. This leads to conclude that a lens-shaped barrier section as calculated here is more critical with purely hinged joints than with clamped joints. The hinged joints model results in stresses of about 10% higher than the model with clamped joints. The clamped joints present a more uniform distribution of the bending moment in the lens-shaped section, which are partly transmitted to the rear chord. The changes in normal force and shear force can be neglected. As stated before, the realization of hinged joints is more difficult and labor-intensive. This extra effort is not even beneficial and therefore not advised.

The clamped joints also affect the member forces in the transverse girders. In addition to a large normal force, a bending moment and shear force are introduced. The approach taken is to dimension the girder first with respect to only the normal force, in order to determine the minimum moment of inertia to avoid buckling. The resulting cross-sectional dimensions determine the equivalent stress, which will be checked on the yield point. Table 8.7 presents the design of the transverse girder for the lens-shaped model with clamped joints. As the normal forces are about equal those of the model with hinged joints, the same transverse girder configurations are found.

Location (fig 8.8)	Normal force	A_{min}	$L_{buckling}$	I_{min}	Design transverse girder			
	[N]	[mm ²]	[m]	[mm ⁴]	a [mm]	t [mm]	A [mm ²]	I_z [mm ⁴]
A	6819x10 ³	19.2x10 ³	12.0 + 6.0 = 18.0	1.07x10 ⁹	500	20	38.4x10 ³	1.47x10 ⁹
B	6895x10 ³	19.4x10 ³	11.25 + 5.625 = 16.875	9.48x10 ⁸	450	20	34.4x10 ³	1.06x10 ⁹
C	7212x10 ³	20.3x10 ³	9.00 + 4.5 = 13.5	6.34x10 ⁸	400	20	30.4x10 ³	7.34x10 ⁸
D	6940x10 ³	19.6x10 ³	5.25 + 2.625 = 7.875	2.08x10 ⁸	300	20	22.4x10 ³	2.94x10 ⁸

Table 8.10: Bottom / center lens-shaped section – design transverse girder, clamped joint model - constant flange thickness

Table 8.8 presents the check of the equivalent stress on the yield point. For transverse D the surface area is relatively small. In addition, the moment of inertia decreases disproportional to the outer dimension (a) and flange thickness (t). This combined results in a stress higher than the yield point. Increasing the value of the outer dimension to 350 mm proves to be sufficient.

	Normal force	Bending Moment	Shear force	Design transverse girder				Stress due to N + M	Shear stress	Equivalent stress
	[kN]	[kNm ²]	[kN]	a [mm]	t [mm]	A [mm ²]	I_z [mm ⁴]	[N/mm ²]	[N/mm ²]	[N/mm ²]
A	6819	0.0	0.0	500	20	38.4x10 ³	1.47x10 ⁹	177.6	0.0	177.6
B	6895	116.4	13.3	450	20	34.4x10 ³	1.06x10 ⁹	225.2	0.35	225.6
C	7212	160.5	22.0	400	20	30.4x10 ³	7.34x10 ⁸	281.0	0.65	281.7
D	6940	110.0	13.6	300	20	22.4x10 ³	2.94x10 ⁸	366.0	0.56	366.6 *

Table 8.11: Bottom / center lens-shaped section – check designed transverse girder on equivalent stress < yield point

*) This stress exceeds the yield point. The outer dimension (a) should be increased to 350 mm.

The design of the transverse girders of the upper section is presented in table 8.12. At least the same dimensions are needed as presented in table 8.7 in order to avoid buckling. These dimensions are checked regarding the introduced bending moments and shear forces.

	Normal force	Bending Moment	Shear force	Design transverse girder				Stress due to N + M	Shear stress	Equivalent stress
	[kN]	[kNm ²]	[kN]	a [mm]	t [mm]	A [mm ²]	I_z [mm ⁴]	[N/mm ²]	[N/mm ²]	[N/mm ²]
A	2036	0.0	0.0	350	15	20.1x10 ³	3.77x10 ⁸	101.4	0.0	101.4
B	2058	34.8	4.0	350	15	20.1x10 ³	3.77x10 ⁸	118.5	0.18	118.5
C	2153	47.9	6.6	300	15	17.1x10 ³	2.32x10 ⁸	156.9	0.41	156.9
D	2071	32.8	4.1	250	15	14.1x10 ³	1.30x10 ⁸	178.4	0.28	178.4

Table 8.12: Upper lens-shaped section – check designed transverse girder on equivalent stress < yield point

The member forces of the design center transverse girder are presented in Appendix I.3.2. The flange thickness of the transverse of the upper lens-shaped section is increased to 20 mm since this force is expected to increase in relation to the other girders. Tables 8.13 and 8.14 present the design calculations.

Center transvers	Normal force	A_{min}	$L_{buckling}$	I_{min}	Design transverse girder / x-type beam			
	[N]	[mm ²]	[m]	[mm ⁴]	a [mm]	t [mm]	A [mm ²]	I_z [mm ⁴]
Upper	2899x10 ³	8.2x10 ³	12.0 + 6.0 = 18.0	4.53x10 ⁸	350	20	26.4x10 ³	4.81x10 ⁸
Center	6621x10 ³	18.6x10 ³	12.0 + 6.0 = 18.0	1.04x10 ⁹	500	20	38.4x10 ³	1.47x10 ⁹
Bottom	5990x10 ³	16.9x10 ³	12.0 + 6.0 = 18.0	9.36x10 ⁸	500	20	38.4x10 ³	1.47x10 ⁹
x-type beam	684x10 ³	2.0x10 ³	6.0√2 = 8.5	2.39x10 ⁷	250	10	9.6x10 ³	9.23x10 ⁷

Table 8.13: X-type bracing system – design center frame, clamped joint model – preliminary design

Center Transvers	Normal force	Bending Moment	Shear force	Design transverse girder				Stress due to N + M	Shear stress	Equivalent stress
	[kN]	[kNm ²]	[kN]	a [mm]	t [mm]	A [mm ²]	I_z [mm ⁴]	[N/mm ²]	[N/mm ²]	[N/mm ²]
Upper	2899	20.8	3.9	350	20	26.4x10 ³	4.81x10 ⁸	154.0	0.14	154.0
Center	6620	19.6	2.8	500	20	38.4x10 ³	1.47x10 ⁹	175.8	0.16	175.8
Bottom	5990	55.5	10.5	500	20	38.4x10 ³	1.47x10 ⁹	165.5	0.58	165.5
x-type beam	684	10.9	5.2	250	10	9.6x10 ³	9.23x10 ⁷	86.1	0.51	86.1

Table 8.14: Upper lens-shaped section – check designed x-type bracing system on equivalent stress < yield point

The other x-type bracing systems of the transverse girders can be determined by using a similar approach. This detailed design is set to be outside the scope of this thesis. The calculation of the center frame is presented in order to conclude on the development of member forces. A final check is made for the x-type bracing system of the rear chords. The contribution of the own weight of the rear chords is modeled, as depicted in figure 8.11.

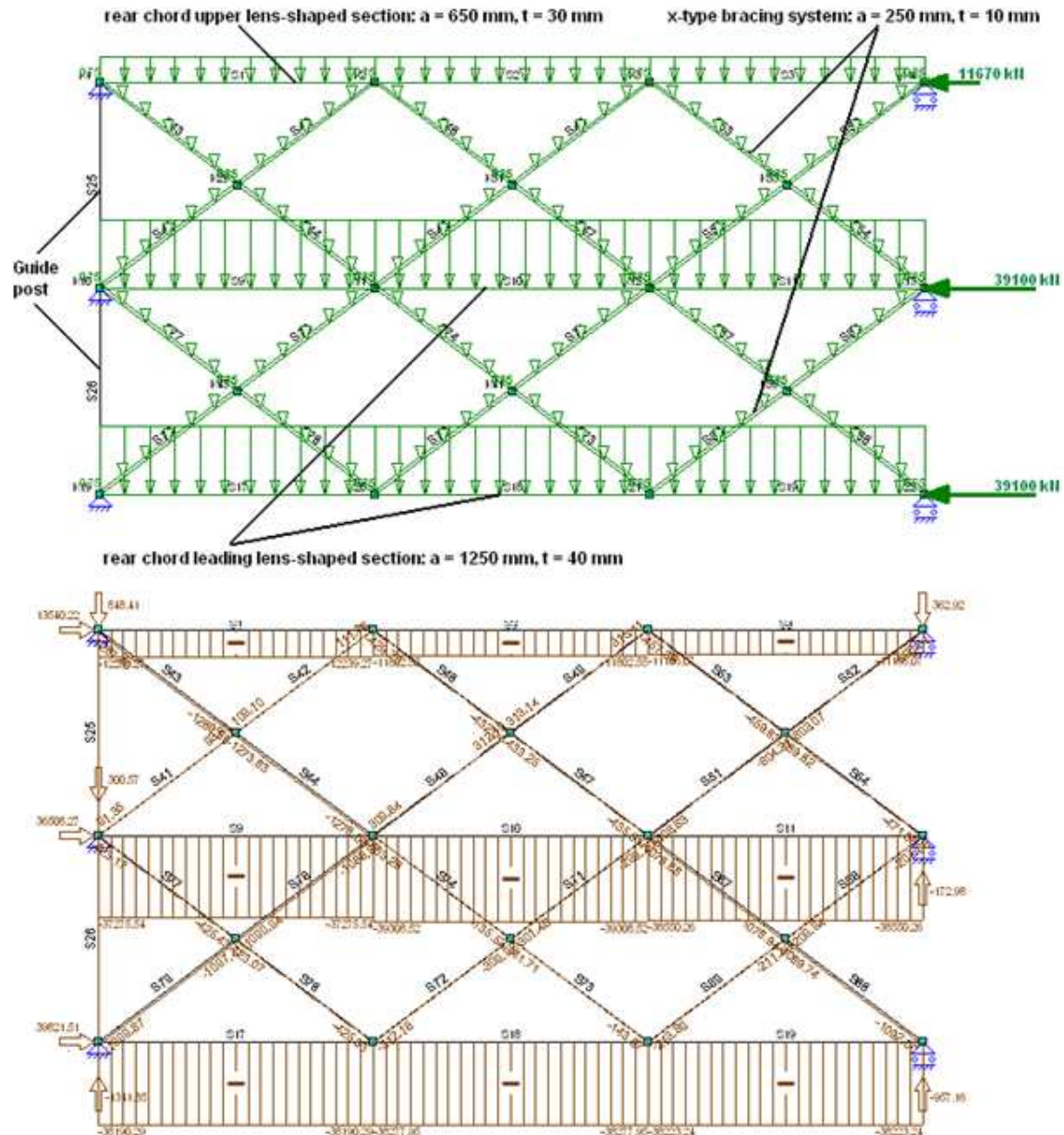


Fig. 8.11: Introducing the own weight of the x-type bracing system of the rear chord

Appendix I.3.3 present an overview of the member forces for this leading x-type bracing system configuration. It can be concluded that the influence of the own weight of the rear chords is limited and that the designed cross-sectional dimensions suffice. In conclusion, some remarks are stated in the design of the x-type bracing system:

- The shear force can be neglected in the design of the transverse girder and bracing system and the influence of the bending moment is also marginal.
- The normal force in the upper transverse increases with about 50% due to the bracing system. This girder should be designed to this additional loading. The normal forces in the center and bottom girder decrease as a result of this process.
- The actual cross-sectional area used for the x-type bracing system influences the development of forces. The larger this cross-section, the larger its member forces and the more it influences the member forces in the transverse girders. In theory, optimizing this x-type bracing beam would decrease its cross-sectional area towards zero. This is not realistic as the bracing system should still be able to perform to its original functions of providing rigidity to the overall barrier and of absorbing vertical forces on the girders and/or rear chord.

8.3 Design of the retaining wall – front plate thickness, stiffeners and cross beams

The retaining wall consists of a front plate, longitudinal stiffeners and cross beams. Figure 8.12 presents a schematization of the wall. The beams and stiffeners are on the downstream side of the front plate. The mutual distance of the stiffeners is fixed and set a 1.0 m in order to reduce the front plate thickness. The mutual distance of the cross beam is variable and needs to be optimized. This variable is denoted as Δx in figure 8.12.

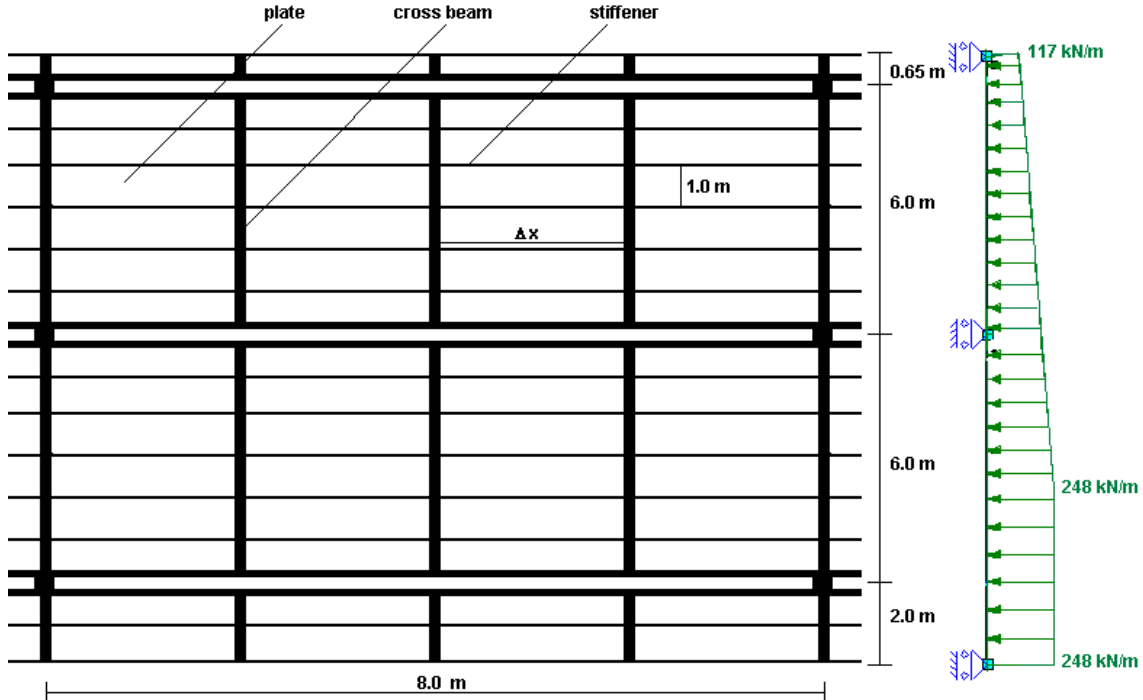


Fig. 8.12: Schematization of the retaining wall – front plate, longitudinal stiffeners and cross beams

Section 8.3.1 determines the minimum required front plate thickness. The longitudinal stiffeners and the cross beams can be designed by using either the method of the separation of components or the method of the equivalent cross-section. The first method is discussed in section 8.3.2, the latter in section 8.3.3.

8.3.1 Front plate thickness

From the front plate as slice is taken over a field in between the cross beams. It is modeled as a continuous bending beam on multiple supports. The model is presented in figure 8.13. The supports are actually the longitudinal stiffeners. The mutual distance of these stiffeners equals the fixed value of 1.0 m.



Fig. 8.13: Model front plate and schematized loading

Figure 8.14 presents the development of the moment and shear force of the modeled slice of the front plate. The largest moment and shear force occur at the second last stiffer. The numerical values equal 26.21 kNm and 150.21 kN respectively. It is important to note that the modeling causes these values to be an overestimation. In reality, the stiffeners can also move in the direction of the load. This movement causes the support moment to decrease, but also the field moment to increase. However, the field moment can not increase to a higher value than the adjacent support moment. Movement of the supporting longitudinal stiffeners therefore results in a more uniform distribution of the moment and shear force. This scenario is more favorable than the reviewed non-moving support and thus not critical.

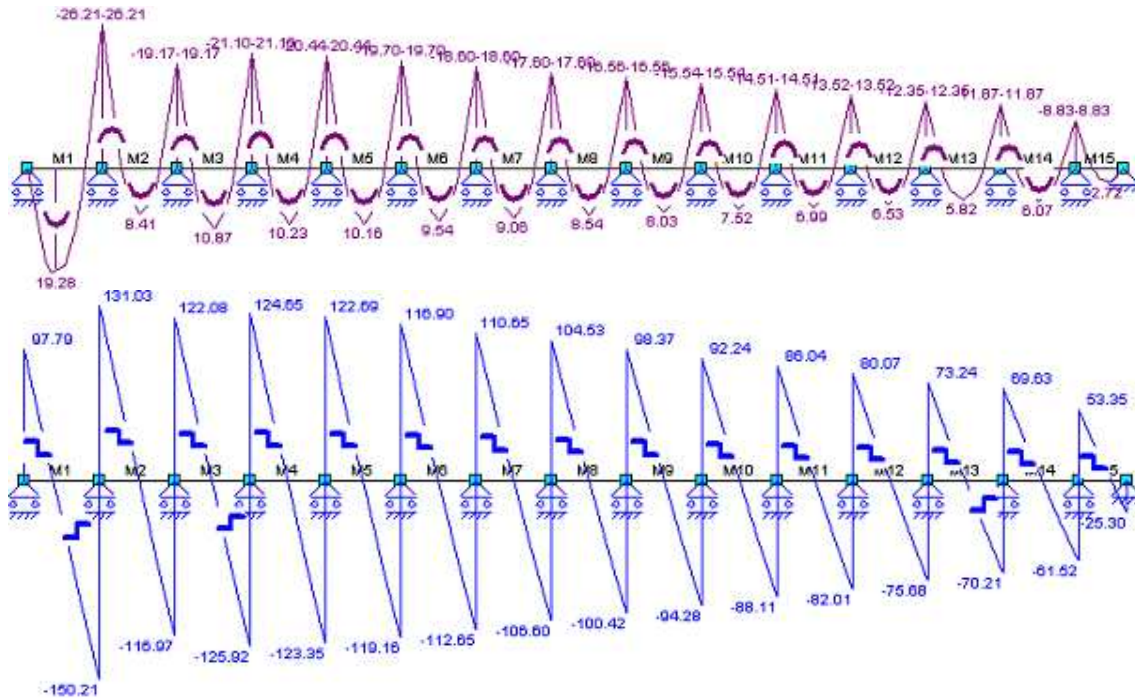


Fig. 8.14: Front plate – development of member forces: moment (upper) and shear force (lower)

In this modeled bending beam on multiple supports, no normal force occurs. In reality, the projected retaining wall curvature causes a normal force not only in the front chord but also in the front plate. The value of this normal force should be determined in a final design stage. At this point, a value of 10% of the occurring normal force in the front chord is assumed to act on the front plate.

As a result, the plate section is loaded by a combination of a bending moment, shear force and normal force. The equivalent stress should be smaller than the yield point. Both the cross-sectional area and moment of inertia depend on the required thickness of the front plate. To find the optimum front plate thickness, an iterative calculation should be performed. Appendix H.5.1 presents this calculation. For the leading moment and shear force in combination with a normal force of 5,000 kN, a front plate thickness of 30 mm is found. Appendix H.5.1 also presents the dependency of the front plate thickness on the occurring normal force. For large values of this force, the influence of the bending moment and shear force can be neglected and a linear relation exists. In the absence of a normal force, a front plate thickness of 22 mm is found.

8.3.2 Method of the separation of components

In this section, the method of the separation of elements is used to determine the cross-sectional dimensions of the longitudinal stiffeners and cross beams.

Longitudinal stiffener

The longitudinal stiffener can be modeled as a continuous bending beam on multiple supports. The supports of the stiffener are actually the cross beams. The critical uniform distributed load can be found by multiplying the critical water pressure with the mutual distance of the stiffener. As this distance is 1.0 m, the uniform distributed load on the modeled beam equals 248 kN/m. Appendix I.5.1 presents the model and member forces under the predetermined loading for a field length of 1.0 m. The leading member forces correspond to those determined at the front plate. In this front plate, the gradually decreasing load apparently has no influence over several field lengths. Numerical values for the leading moment and shear force equal 26.21 kNm and 150.21 kN respectively.

The mutual distance of the supportive cross beams is variable. The maximum moment in the longitudinal stiffener is quadratic proportional to this distance and the maximum shear force linear proportional. The leading cross-section of the stiffener is subjected to a combination of a bending moment and shear force. The normal force induced loading is assumed to act purely on the front plate. Appendix H.5.2 presents a calculation overview from which the results are summarized in table 8.15.

It should be noted that the deformation of the stiffener is not included. The used model denies any vertical movement of the stiffeners and presents an underestimation of the actual deformation. In order to model this deformation more accurately, supports in the form of springs should be used. However, the deformation of is not critical. Structural components should suffice with respect strength and stiffness under leading circumstances.

Field length [m]	Maximum moment [kNm]	Maximum shear force [kN]	Minimum required IPE-profile			Stress due to bending moment [N/mm ²]	Shear stress [N/mm ²]	Equivalent stress [N/mm ²]
			[-]	A [mm ²]	I _z [mm ⁴]			
1.0	26.21	150.21	IPE 180	23.9x10 ²	1317x10 ⁴	179.5	173.1	349.4
2.0	104.9	300.4	IPE 300	53.8x10 ²	8356x10 ⁴	188.2	152.4	324.3
3.0	235.9	450.6	IPE 400	84.5x10 ²	23130x10 ⁴	204.1	140.3	317.3
4.0	419.4	600.8	IPE 500	116x10 ²	48200x10 ⁴	217.5	128.8	311.5

Table 8.15: Method of the separation of components – required longitudinal stiffener for variable field width

According to the elastic theory, the combined stresses due to a bending moment and normal force at some point in the steel cross-section should not exceed the yield point. The separate check of the cross-section on the leading shear stress states that this stress should be smaller than the yield point for shearing, which is equal to $355 / \sqrt{3} = 205 \text{ N/mm}^2$. The results in table 8.15 indicate that both these checks suffice. Relatively, the influence of the bending moment increases with an increasing field width as it is quadratic proportional to this parameter. The shear stress decreases as the surface area and associated moment of inertia increases faster than the linear proportional increasing shear force.

Cross beam

For the design of the cross beam, their mutual distance should be determined. An increasing mutual distance increases the moment and shear force in the cross beam proportionally. It also requires a larger stiffener, which can be extracted from table 8.15. A reasonable first estimate is a mutual distance equal to 2.0 m, which requires a stiffener of IPE 300.

The dimensions of the cross beam can be determined by modeling it as a continuous bending beam on three supports. The predetermined field lengths are equal to 2.0 m, 6.0 m, 6.0 m and 0.65 m respectively. The resultant load on the beam has a similar development as presented for the front plate, but is two times larger as the mutual distance of the beams equals 2.0 m. Figure 8.15 presents this load and resulting member forces.

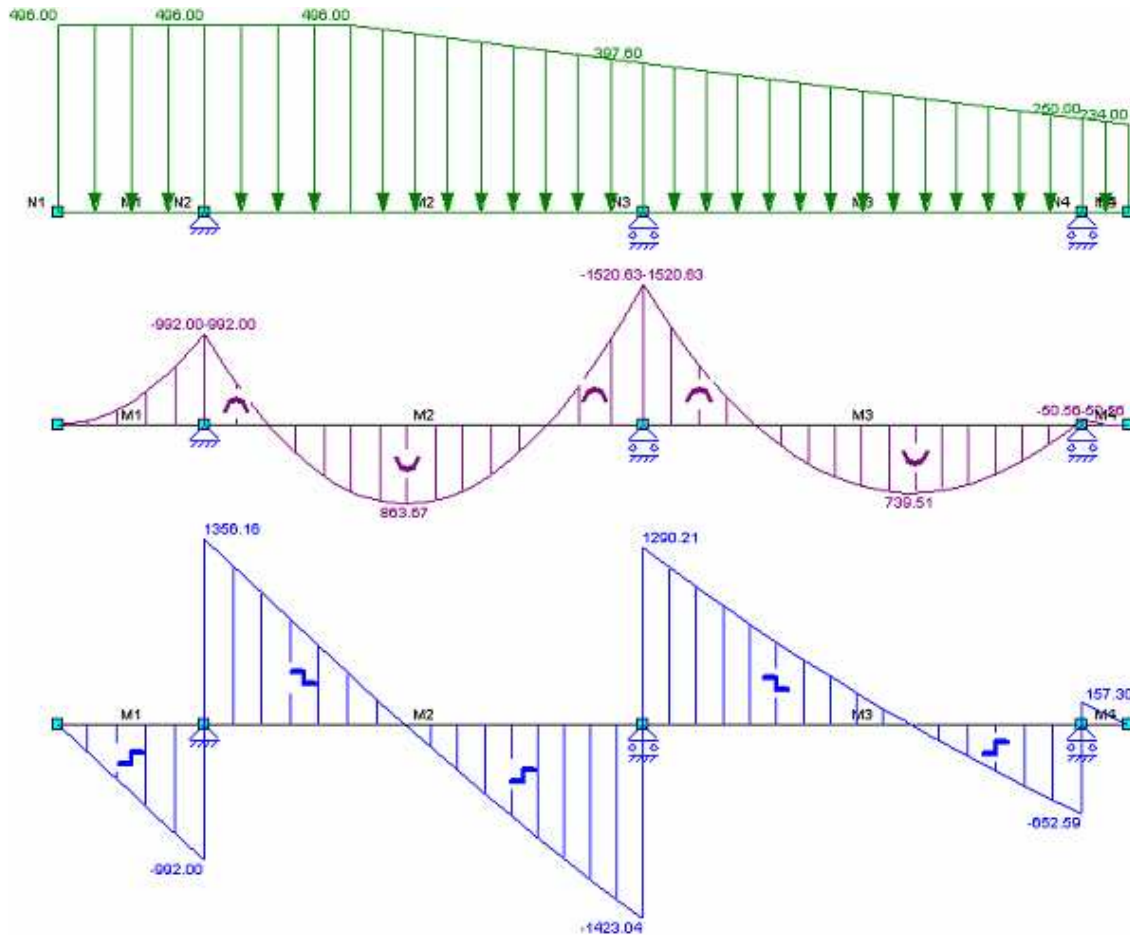


Fig. 8.15: Cross beam – model and member forces for a mutual distance of 2.0 m: moment (center) and shear force (lower)

The maximum moment in the cross beam occurs at the center support. The resulting minimum required section factor regarding this bending moment can be determined by dividing this moment by the yield point:

$$\text{min. section factor : } W_{el,min} \geq \frac{M_{max}}{f_{y;d}} = \frac{1521 \cdot 10^6}{355} = 4.29 \cdot 10^6 \text{ mm}^3$$

This value appears to be too large for any standard IPE-profile to be used. The minimum standard HEA-profile to provide a sufficient section factor is HE 600A. As the shear force at the center support is significant, this profile is not expected to suffice in the check that the equivalent stress should be less than the yield point. For this reason, a HE 700A profile is checked first. If this profile is still not sufficient, a HE 800A profile should be checked. Table 8.16 presents the characteristics of both profiles.

	Height	Width	Center thickness	Flange thickness	Cross-sectional area	Moment of inertia	Section factor
	h [mm]	b [mm]	t_w [mm]	t_f [mm]	A_{tot} [mm ²]	I_{zz} [mm ⁴]	$W_{el,z}$ [mm ³]
HE 450A	440	300	11.5	21.0	178×10^2	63720×10^4	2896×10^3
HE 500A	490	300	12.0	23.0	198×10^2	86970×10^4	3550×10^3
HE 550A	540	300	12.5	24.0	212×10^2	111990×10^4	4146×10^3
HE 600A	590	300	13.0	25.0	226×10^2	141200×10^4	4787×10^3
HE 650A	640	300	13.5	26.0	242×10^2	175300×10^4	5474×10^3
HE 700A	690	300	14.5	27.0	260×10^2	215300×10^4	6241×10^3
HE 800A	790	300	15.0	28.0	286×10^2	303400×10^4	7682×10^3
HE 900A	890	300	16.0	30.0	321×10^2	422100×10^4	9485×10^3
HE 1000A	990	300	16.5	31.0	347×10^2	553800×10^4	11190×10^3

Table 8.16: Overview of available HEA-profiles

At the center support, the moment equals 1521 kNm and the shear force equals 1423 kN. As the cross beams are projected vertically, no normal force is assumed to be transmitted by the front plate on the beams. It is expected that the moment and deformation of the beam are influenced. This is not incorporated in this preliminary design stage. The assumed absence of normal force also neglects the own weight of the beams, stiffeners and front plate. The cross beams should therefore be designed with some surplus to accommodate these additional forces. The check regarding the yield point requires the determination of the equivalent stress and results in:

$$\sigma_{eq} = \sqrt{\sigma_y^2 + 3\tau_{yz}^2} = \sqrt{\left(\frac{N}{A} + \frac{M_y \cdot e}{I_y}\right)^2 + 3\tau_{yz}^2} \leq 355 \text{ N/mm}^2$$

The shearing part of the cross-section of the HE 700 A in relation to its center line equals:

$$S_z^a = b \cdot t_f \cdot \left(\frac{h}{2} - \frac{t_f}{2}\right) + \frac{1}{2} \cdot t_w \cdot \left(\frac{1}{2}h - t_f\right)^2 = 300 \cdot 27.0 \cdot \left(\frac{690}{2} - \frac{27.0}{2}\right) + \frac{1}{2} \cdot 14.5 \cdot \left(\frac{690}{2} - 27.0\right)^2 = 3.42 \cdot 10^6 \text{ mm}^3$$

The stress due to the bending moment and shear stress can now be determined:

$$\tau = \frac{V_z S_y^a}{b I_y} = \frac{(1423 \cdot 10^3) \cdot (3.42 \cdot 10^6)}{(14.5) \cdot (215300 \cdot 10^4)} = 155.8 \text{ N/mm}^2 \leq \frac{355}{\sqrt{3}} = 205 \text{ N/mm}^2$$

$$\sigma = \frac{N}{A} + \frac{M_{max}}{W_{z,el}} = 0 + \frac{1521 \cdot 10^6}{6241 \cdot 10^3} = 0 + 243.7 = 243.7 \text{ N/mm}^2$$

The equivalent stress results in:

$$\sigma_{eq} = \sqrt{243.7^2 + 3 \cdot 155.8^2} = 363.6 \text{ N/mm}^2 > 355 \text{ N/mm}^2$$

It appears that the HE 700A is not sufficient. Increasing the cross beam to a HE 800A profile is sufficient as this leads to an equivalent stress of 302.1 N/mm². In a similar manner, the required HEA-profiles for the other mutual distances are calculated. Table 8.17 presents an overview of the calculation results.

Mutual distance	Maximum moment	Maximum shear force	Minimum required HEA - profile			Stress due to bending moment	Shear stress	Equivalent stress
			[-]	A [mm ²]	I _z [mm ⁴]			
1.0	760.5	711.5	HE 500A	198×10^2	86970×10^4	214.3	130.0	311.0
2.0	1521	1423.0	HE 800A	286×10^2	303400×10^4	198.0	131.7	302.1
3.0	2281.5	2134.5	HE 1000A	321×10^2	422100×10^4	203.9	145.7	324.5

Table 8.17: Method of the separation of components – required cross beam for variable mutual distance

A mutual distance of 3.0 requires the largest standard HEA-profile available. Increasing the distance even further would require the manufacturing of unique profiles, which is not cost-effective.

The required volume of steel for the three combinations of cross beam and stiffeners can now be calculated. This essentially determines which combination is favorable. The front plate length is assumed to be 66 m. The 14 stiffeners are equally distributed of the height of the gate and span this total length. The length of the cross beams equals the height of the gate, thus equal to about 14.5 m. Table 8.18 presents the calculation results.

Mutual distance cross beams [m]	Profile combination stiffener / cross beam [-]	Cross-sectional area [mm ²]	Number of profiles used [-]	Profile length [m]	Required volume of steel [m ³]
1.0	IPE 180	23.9x10 ²	14	66.0	2.2
	HE 500A	198x10 ²	65	14.5	18.7
2.0	IPE 300	53.8x10 ²	14	66.0	5.0
	HE 800A	286x10 ²	32	14.5	13.3
3.0	IPE 400	84.5x10 ²	14	66.0	7.8
	HE 1000A	347x10 ²	21	14.5	10.6

Table 8.18: Method of the separation of components – required volume of steel for longitudinal stiffeners and cross beams

A mutual distance of 1.0 is not favorable as expected. It requires the most steel of all three configurations. The configuration with a mutual distance of 2.0 is most favorable, although it requires the same volume of steel as for a distance of 3.0 m. Reason for this is that the first has the most capacity left to handle additional stresses due to the own weight of the components. Secondly, a mutual distance of 3.0 m requires relocation of transverses.

8.3.3 Method of the equivalent cross-section

In this section, the method of equivalent cross-section is used to determine the cross-sectional dimensions the longitudinal stiffeners and cross beams.

Longitudinal stiffener

The model, loading and resulting member forces for the stiffener in this method are equal to those presented in section 8.2.3. Appendix I.5.1 presents the model and member forces under the predetermined loading for a field length of 1.0 m. Numerical values for the leading moment and shear force equal 26.21 kNm and 150.21 kN respectively. The mutual distance of the supportive cross beams is variable. The maximum moment in the longitudinal stiffener is quadratic proportional to this distance and the maximum shear force linear proportional. In addition to these member forces, for this equivalent cross-section a normal force is introduced. Per equivalent cross-section of front plate and 2 stiffeners, a normal force of maximum half the predetermined 10%-value of 5,000 kN is assumed. In other words, it is expected that the maximum normal force in the front plate is divided over at least over 2 stiffeners.

The method of equivalent cross-section determines an alternate cross-sectional area and center of gravity, which determine the shearing part and equivalent moment of inertia. Appendix H.5.3 presents a general calculation overview of this calculation method for a variable field width. The predetermined field width of 2.0 m is calculated in this thesis. The results for a varied field width are summarized in table 8.19.

A field width of 2.0 m results in a maximum moment equal to 2² * 26.21 = 104.9 kNm and a maximum shear force equal to 2 * 150.21 = 300.4 kN. The normal force per stiffener equals 5,000 / 2 = 2,500 kN. The check regarding the yield point requires the determination of the equivalent stress and results in:

$$\sigma_{eq} = \sqrt{\sigma_y^2 + 3\tau_{yz}^2} = \sqrt{\left(\frac{N}{A} + \frac{M_y * e}{I_y}\right)^2 + 3\tau_{yz}^2} \leq 355 \text{ N/mm}^2$$

Figure 8.16 presents the equivalent cross-section. The thickness of the front plate (1) equals 30 mm. The proposed profile to be used as longitudinal stiffener (2) is IPE 240, which can be estimated by determining the minimum required section factor regarding only the bending moment.

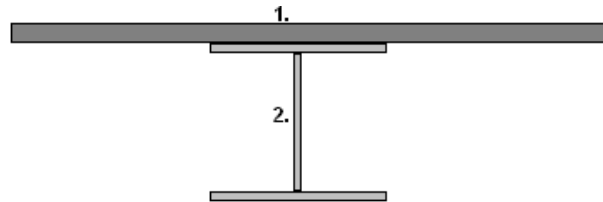


Fig. 8.16: Equivalent cross-section

The combination of the projected front plate and this IPE-profile results in a center of gravity of:

$$\Sigma A = A_{plate} + A_{IPE240} = 30 * 1000 + 39.1 * 10^2 = 33910 \text{ mm}^2, \text{ as the mutual distance of stiffeners is equal to 1.0 m}$$

$$\Sigma Sz_c = A_{plate} * z_{c;plate} + A_{IPE240} * z_{c;IPE240} = 3 * 10^4 * (30 / 2) + 39.1 * 10^2 * (30 + 240 / 2) = 1.04 * 10^6 \text{ mm}^3$$

$$z_c = \frac{\Sigma Sz_c}{\Sigma A} = 30.57 \text{ mm}, \text{ which is in relation to the top of the front plate}$$

The equivalent moment of inertia of the cross-section can be determined as follows:

$$I_{z,eq} = I_{z,eigen} + I_{z,steiner}, \text{ in which: } I_{z,steiner} = A_i * (\Delta z_c)_i^2$$

$$I_{z,eigen,plate} = \frac{1}{12} * \Delta x_{stiffener} * t_{plate}^3 = \frac{1}{12} * 1000 * 30^3 = 2.25 * 10^6 \text{ mm}^4$$

$$I_{z,steiner,plate} = 3 * 10^4 * (30.57 - 15.0)^2 = 7.27 * 10^6 \text{ mm}^4$$

$$I_{z,eigen,IPE240} = 3892 * 10^4 \text{ mm}^4$$

$$I_{z,steiner,IPE240} = 39.1 * 10^2 * (150 - 30.57)^2 = 5.58 * 10^7 \text{ mm}^4$$

$$I_{z,eq} = I_{z,eigen,plate} + I_{z,steiner,plate} + I_{z,eigen,IPE240} + I_{z,steiner,IPE240} = 1.042 * 10^8 \text{ mm}^4$$

The stress due to the bending moment and normal force can now be determined:

$$\sigma = \frac{N}{A} + \frac{M_y * e}{I_y}, \text{ in which } e \text{ equals the maximum distance to the outer steel fibers or cross-section, thus:}$$

$$\sigma = \frac{N}{\Sigma A} + \frac{M_{max} * (t_{plate} + h_{IPE240} - z_c)}{I_{z,eq}} = \frac{2500 * 10^3}{33910} + \frac{104.9 * 10^6 * (30 + 240 - 30.57)}{1.042 * 10^8} = 73.7 + 240.9 = 314.6 \text{ N/mm}^2$$

The center of gravity is positioned in the flange of the IPE 240 profile. The width of the shearing parts is therefore equal to 120 mm. The location of the center of gravity thus influences the shear stress significantly and should always be checked. The static moment of the shearing part can be calculated for either the upper or lower half of the cross-section. In theory, the moments should be similar. Neglecting the curved corners within the IPE-profile causes both results to differ slightly. The highest value produces the highest shear stress and is therefore used. The stress due shear force can now be determined.

$$S_z^a = A_{plate} * (z_c - z_{c,plate}) + \frac{1}{2} * b_{IPE} * (z_c - t_{plate})^2 = 4.67 * 10^5 \text{ mm}^3$$

$$S_z^a = \frac{1}{2} * b_{IPE} * (t_{plate} + t_f - z_c)^2 + t_w * (h_{IPE} - 2 * t_f) * (z_{c,IPE} - z_c) + b_{IPE} * t_f * (t_{plate} + h_{IPE} - \frac{t_f}{2} - z_c) = 4.45 * 10^5 \text{ mm}^3$$

$$\tau = \frac{V_z S_z^a}{b I_{z,eq}} = \frac{(300.4 * 10^3) * (4.67 * 10^5)}{(120) * (1.042 * 10^8)} = 11.2 \text{ N/mm}^2 \leq \frac{355}{\sqrt{3}} = 205 \text{ N/mm}^2$$

The equivalent stress results in:

$$\sigma_{eq} = \sqrt{314.6^2 + 3 * 11.2^2} = 315.2 \text{ N/mm}^2 < 355 \text{ N/mm}^2$$

It can be concluded that the IPE 240 profile is sufficient to use as a stiffener for a field width of 2.0 m. Table 8.19 presents the calculation results for a variable field width. As Δx increases to 3.0 m or more, the influence of the front plate diminishes and no benefit is gained anymore by using the equivalent cross-section method over the separation method. In combining table 8.19 and table 8.20, it can be seen that the location of the center of gravity is critical for the determination of the shear stress. As the stiffener increases, the center will be located in the web of the IPE-profile. The associated width at this section for the shearing part is relatively small which causes the shear stress to increase rapidly.

Field length	Max. moment	Max. shear force	Normal force	Min. required IPE-profile combined with 30 mm plate		Stress due to N + M	Shear stress	Equivalent stress
[m]	[kNm]	[kN]	[kN]	[-]	ΣA [mm ²]	$I_{z,eq}$ [mm ⁴]	[N/mm ²]	[N/mm ²]
1.0	26.21	150.21	2500	IPE 140	31640	1.89x10 ⁷	287.9	1.5
2.0	104.9	300.4	2500	IPE 240	33910	1.04x10 ⁸	314.6	11.2
3.0	235.9	450.6	2500	IPE 400	38450	5.38x10 ⁸	226.2	137.9
4.0	419.4	600.8	2500	IPE 500	41600	1.07x10 ⁹	232.7	126.8

Table 8.19: Method of the equivalent cross-section – required longitudinal stiffener for variable field width

Field length	Minimum required IPE-profile in combination with a 30 mm front plate					
[m]	[-]	ΣA [mm ²]	z_c [mm] (with respect to top of the front plate)	b [mm] (width at section shearing part)	S_z [mm ³]	$I_{z,eq}$ [mm ⁴]
1.0	IPE 140	31640	19.41	$\Delta x_{stiffener} = 1000$	1.88x10 ⁵	1.89x10 ⁷
2.0	IPE 240	33910	30.75	$b_{profile} = 120$	4.67x10 ⁵	1.04x10 ⁸
3.0	IPE 400	38450	62.25	$t_w = 8.6$	1.42x10 ⁵	5.38x10 ⁸
4.0	IPE 500	41600	88.89	$t_w = 10.2$	2.31x10 ⁵	1.07x10 ⁹

Table 8.20: Method of the equivalent cross-section – longitudinal stiffener – additional cross-sectional parameters

Cross beam

The method of equivalent cross-section determines an alternate cross-sectional area and center of gravity, which determine the shearing part and equivalent moment of inertia. Appendix H.5.4 presents a general calculation overview of this calculation method for a variable mutual distance of the cross beams. The cross beam for the predetermined expected optimal mutual distance of 2.0 m is calculated in this thesis, which requires a stiffener of IPE 240. The model, loading and resulting member forces for the cross beam in this method are equal to those presented in section 8.2.3. Appendix I.5.2 presents the model and member forces under the predetermined loading and field lengths equal to 2.0 m, 6.0 m, 6.0 m and 0.65 m respectively. Numerical values for the leading moment and shear force, both acting at the center support, are equal to 1521 kNm and 1423 kN respectively.

Again it can be stated that, as the cross beams are projected vertically, no normal force is assumed be transmitted by the front plate on the beams. The expected influence on the bending moment and deformation of the beam is not incorporated in this preliminary design stage. This assumed absence of normal force neglects the own weight of the beams, stiffeners and front plate. The cross beams should therefore be designed with some surplus to accommodate these additional forces.

The minimum standard HEA-profile to provide a sufficient section factor with respect to the loading is HE 600A, as determined in section 8.3.2. In the same section, a HE 700A profile was checked by using the method of the separation of the component. It appeared to be not sufficient. For the method of the equivalent cross-section, this HE 700A profile is checked first. If this profile is still not sufficient, a HE 800A profile should be checked. The combination of the projected front plate and this HEA-profile results in a center of gravity of:

$$\begin{aligned}\Sigma A &= A_{\text{plate}} + A_{\text{HE700A}} = 30 * 2000 + 260 * 10^2 = 8.6 * 10^4 \text{ mm}^2, \text{ as the mutual distance of the beams is 2.0 m} \\ \Sigma Sz_c &= A_{\text{plate}} * z_{c;\text{plate}} + A_{\text{HE700A}} * z_{c;\text{HE700A}} = 6 * 10^4 * (30/2) + 260 * 10^2 * (30 + 690/2) = 10.65 * 10^6 \text{ mm}^3 \\ z_c &= \frac{\Sigma Sz_c}{\Sigma A} = 123.84 \text{ mm}, \text{ which is in relation to the top of the front plate}\end{aligned}$$

The equivalent moment of inertia of the cross-section can be determined as follows:

$$\begin{aligned}I_{z;\text{eq}} &= I_{z;\text{eigen}} + I_{z;\text{steiner}}, \text{ in which: } I_{z;\text{steiner}} = A_i * (\Delta z_c)_i^2 \\ I_{z;\text{eigen};\text{plate}} &= \frac{1}{12} * \Delta x * t_{\text{plate}}^3 = \frac{1}{12} * 2000 * 30^3 = 4.5 * 10^6 \text{ mm}^4 \\ I_{z;\text{steiner};\text{plate}} &= 6 * 10^4 * (123.84 - 15.0)^2 = 7.11 * 10^8 \text{ mm}^4 \\ I_{z;\text{eigen};\text{IPE240}} &= 175200 * 10^4 \text{ mm}^4 \\ I_{z;\text{steiner};\text{IPE240}} &= 260 * 10^2 * (375 - 123.84)^2 = 1.64 * 10^9 \text{ mm}^4 \\ I_{z;\text{eq}} &= I_{z;\text{eigen};\text{plate}} + I_{z;\text{steiner};\text{plate}} + I_{z;\text{eigen};\text{IPE240}} + I_{z;\text{steiner};\text{IPE240}} = 4.508 * 10^9 \text{ mm}^4\end{aligned}$$

The stress due to the bending moment and normal force can now be determined:

$$\begin{aligned}\sigma &= \frac{N}{A} + \frac{M_y * e}{I_y}, \text{ in which } e \text{ equals the maximum distance to the outer steel fibers or cross-section, thus:} \\ \sigma &= \frac{N}{\Sigma A} + \frac{M_{\text{max}} * (t_{\text{plate}} + h_{\text{HE700A}} - z_c)}{I_{z;\text{eq}}} = 0 + \frac{1521 * 10^6 * (30 + 690 - 123.84)}{4.508 * 10^9} = 201.1 \text{ N/mm}^2\end{aligned}$$

The center of gravity is positioned in the web of the HE 700A profile. The width of the shearing parts is therefore equal to 14.5 mm. The static moment of the shearing part can again be calculated for either the upper or lower half of the cross-section. In theory, the moments should be similar but neglecting the curved corners within the IPE-profile causes both results to differ slightly. The highest value produces the highest shear stress and is therefore used. The stress due shear force can now be determined, with the use of table 8.16.

$$\begin{aligned}S_z^a &= A_{\text{plate}} * (z_c - z_{c;\text{plate}}) + b_{\text{HEA}} * t_f * (z_c - (t_{\text{plate}} + \frac{t_f}{2})) + \frac{1}{2} * t_w * (z_c - (t_{\text{plate}} + t_f))^2 = 7.21 * 10^6 \text{ mm}^3 \\ S_z^a &= \frac{1}{2} * t_w * (t_{\text{plate}} + h_{\text{HEA}} - 2 * t_f - z_c)^2 + b_{\text{HEA}} * t_f * (t_{\text{plate}} + h_{\text{HEA}} - \frac{t_f}{2} - z_c) = 7.07 * 10^6 \text{ mm}^3 \\ \tau &= \frac{V_z S_z^a}{b I_{z;\text{eq}}} = \frac{(1423 * 10^3) * (7.30 * 10^6)}{(14.5) * (4.508 * 10^9)} = 157.0 \text{ N/mm}^2 \leq \frac{355}{\sqrt{3}} = 205 \text{ N/mm}^2\end{aligned}$$

The equivalent stress results in:

$$\sigma_{\text{eq}} = \sqrt{201.1^2 + 3 * 157.0^2} = 338.2 \text{ N/mm}^2 < 355 \text{ N/mm}^2$$

Table 8.21 presents the calculation results for a variable mutual distance of the cross beams. By using the method of the equivalent cross-section, a smaller minimum required HEA-profile is found compared to the previously described method of separation of the components. In this first method, the influence of the normal force is even included. The use of the method of the equivalent cross-section is preferred, as it better describes the inner coherence of components within the retaining wall.

Mutual distance	Maximum moment	Maximum shear force	Min. required HEA-profile combined with 30 mm plate			Stress due to bending moment	Shear stress	Equivalent stress
[m]	[kNm]	[kN]	[-]	ΣA [mm ²]	$I_{z,eq}$ [mm ⁴]	[N/mm ²]	[N/mm ²]	[N/mm ²]
1.0	760.5	711.5	HE450A	4.78x10 ⁴	1.26x10 ⁹	222.4	149.3	341.0
2.0	1521	1423.0	HE700A	8.60x10 ⁴	4.51x10 ⁹	201.1	157.0	338.2
3.0	2281.5	2134.5	HE900A	1.22x10 ⁵	9.23x10 ⁹	193.7	169.7	352.0
4.0	3042	2846	HE1000A	1.55x10 ⁵	1.25x10 ¹⁰	215.9	200.0	408.1 *

Table 8.21: Method of the equivalent cross-section – required cross beam for mutual distance

Field length	Minimum required IHEA-profile in combination with a 30 mm front plate					
[m]	[-]	ΣA [mm ²]	z_c [mm] (with respect to top of the front plate)	b [mm] (width at section shearing part)	S_z [mm ³]	$I_{z,eq}$ [mm ⁴]
1.0	HE450A	4.78x10 ⁴	102.51	$t_w = 11.5$	3.03x10 ⁶	1.26x10 ⁹
2.0	HE700A	8.60x10 ⁴	123.84	$t_w = 14.5$	7.21x10 ⁶	4.51x10 ⁹
3.0	HE900A	1.22x10 ⁵	135.93	$t_w = 16.0$	1.17x10 ⁷	9.23 x10 ⁹

Table 8.22: Method of the equivalent cross-section – cross beam – additional cross-sectional parameters

The required volume of steel for the three combinations of cross beam and stiffeners can now also be calculated for this method. It essentially determines which combination is favorable and also quantifies the differences in the presented calculation approaches.

The front plate length is again assumed to be 66 m. The 14 stiffeners are equally distributed of the height of the gate and span this total length. The length of the cross beams equals the height of the gate, thus equal to about 14.5 m. Table 8.18 presents the calculation results.

Mutual distance cross beams	Profile combination stiffener / cross beam	Cross-sectional area	Number of profiles used	Profile length	Required volume of steel
[m]	[-]	[mm ²]	[-]	[m]	[m ³]
1.0	IPE 140	16.4x10 ²	14	66.0	1.5
	HE 450A	178x10 ²	65	14.5	16.8
2.0	IPE 240	39.8x10 ²	14	66.0	3.7
	HE 700A	260x10 ²	32	14.5	12.1
3.0	IPE 400	84.5x10 ²	14	66.0	7.8
	HE 900A	321x10 ²	21	14.5	9.8

Table 8.23: Method of the equivalent cross-section – required volume of steel for longitudinal stiffeners and cross beams

As expected, a mutual distance of 1.0 is still not favorable. It requires the most steel of all three configurations, although the differences are smaller than for the method of the separation of components. An equivalent cross-section of front plate and relatively small stiffener diminishes the influence of the shear force. It therefore leads to an even smaller stiffener, thus reducing the required volume of steel. The configuration with a mutual distance of 2.0 is most favorable. It requires the least volume of steel of all three configurations and has the most capacity left to handle additional stresses due to own weight of the components. In addition, the mutual distance of 3.0 m requires a relocation of the transverses.

Table 8.24 summarizes the required volumes of steel for both calculation methods and for a variable mutual distance for the cross beams, which is equal to the field length of the longitudinal stiffeners.

Mutual distance cross beams	Method of the separation of components		Method of the equivalent cross-section	
	Profile combination stiffener / cross beam	Required volume of steel	Profile combination stiffener / cross beam	Required volume of steel
[m]	[-]	[m ³]	[-]	[m ³]
1.0	IPE 180 HE 500A	2.2 + 18.7 = 20.9	IPE 140 HE 450A	1.5 + 16.8 = 18.3
2.0	IPE 300 HE 800A	5.0 + 13.3 = 18.3	IPE 240 HE 700A	3.7 + 12.1 = 15.8
3.0	IPE 400 HE 1000A	7.8 + 10.6 = 18.4	IPE 400 HE 900A	7.8 + 9.8 = 17.6

Table 8.24: Required volumes of steel for both calculation methods and for a variable mutual distance for the cross beams

8.4 Overview of structure components and optimizations in the steel gate design

This section provides an overview and quantification of the main optimization in the steel lifting gate design. It concludes in a distribution of mass over the lifting gate. The optimizations are presented in section 8.4.1 and the determination of the total mass and its distribution of the steel lifting gate is presented in section 8.4.2.

8.4.1 Quantifying optimizations in the steel gate design

In this chapter, four main optimizations are quantified. These optimizations were already encountered during the design of the components in the previous sections of this chapter. The mentioned optimizations include the introduction of clamped joints over hinged joints, the opportunity to design the upper lens-shaped barrier section finer than the leading sections and the influence of the calculation method to design the retaining wall. The latter essentially includes or excludes the fact that steel components can enforce each other when working together. Each optimization is discussed subsequently.

– Extra lens-shaped section – reducing cross-sectional dimensions of cross beam, front chord and rear chord

Table 8.3 presented the support reaction, maximum moment and maximum shear force of the cross beam for both two and three supports. Reviewing the initial case of two ‘supports’, essentially the number of lens-shaped barrier sections, the leading member forces of bending moment and shear force are equal to 3313 kNm and 1354 kN respectively. It should be noted that these values are valid for a mutual distance of the beam of 1.0 m. As this is concluded to be non-favorable, the values should be multiplied by a factor 2. A quick review on the resulting stress due to only a bending moment for the maximum standard cross beam of HE 1000A determines its applicability. Appendix H.5.4 presents the general calculation method. The stress due to the bending moment and normal force can now be determined:

$$\sigma = \frac{M_y * e}{I_y}, \text{ in which } e \text{ equals the maximum distance to the outer steel fibers or cross-section}$$

It can be found that the center of gravity $z_c = 201.87$ mm and that the equivalent moment of inertia $I_{z;eq} = 1.126 * 10^{10}$ mm⁴. This results in:

$$\sigma = \frac{M_{max} * (t_{plate} + h_{HE1000A} - z_c)}{I_{z;eq}} = \frac{6626 * 10^6 * (30 + 990 - 201.87)}{1.126 * 10^{10}} = 481.9 \text{ N/mm}^2 > 355 \text{ N/mm}^2$$

As the maximum stress exceeds the yield point, it can be concluded that no standard profile suffices. For a mutual distance of 1.0 m, this profile would suffice but lead to an immense weight. It is important to note that this large weight at the front plate and reduced weight at the rear due to the absence of one chord, results in a large eccentric moment atop the tower. This is not favorable for various reasons as earlier described in the review of the gate curvature configurations.

The leading support reaction, essentially equal to the uniform distributed load on the lens-shaped barrier section, increases in the absence of the center section with a factor 1.4 to 1853 kN. This would further increase the dimension of the front and rear chord, whose profiles are already designed at their limits. An extra lens-shaped section is therefore not an actual saving of steel volume but a practical necessity.

– Clamped joints – more uniform distribution of the member forces over the lens-shaped barrier section

Appendix I.4 presents the member forces of the predetermined lens-shaped configuration with clamped joints instead of hinged joints. In this adjusted model, both the front and rear are loaded by a combination of bending moments, shear forces and normal forces. In the hinged model, the rear chord is only loaded by normal forces. For both configurations, the initially assumed chords dimensions of an outer dimension $a = 1250$ mm and a flange thickness $t = 40$ mm were checked.

For the clamped joints configuration, these cross-sectional dimensions appeared to be sufficient. For the hinged joints configuration, it can be determined that a minimum increased outer dimension of 1350 mm is required. The use of clamped joint thus leads to a reduction in volume of steel per meter length of the chords, which is equal to:

$$\Delta A_{steel;joints} = (1350^2 - 1270^2) - (1250^2 - 1170^2) = 209600 - 193600 = 16 * 10^3 \text{ mm}^2/\text{m}$$

The length of the parabolic front chord and front plate and parabolic rear chord can be adequately estimated by assuming them to be circular. In the evaluation of both gate curvatures, it appeared that the difference in coordinates of the nodal point is sufficiently small.

Figure 8.5 graphically presents the schematization to determine the required coordinates for describing the circular gate curvature. The taken approach uses the constant radius.

Rear chord – pitch = 12 m: $\sqrt{(4 * 8)^2 + y_R^2} = (12 + y_R)^2$
 $32^2 = 144 + 24y_R$, thus $y_R = 36.67$ m. The radius $R = 12 + 36.67 = 48.67$ m
 $\alpha = \arctan\left(\frac{32.0}{36.67}\right) = 41.1^\circ$

$$L_{\text{rear}} = \left(\frac{2 * \alpha}{360}\right) * 2\pi R = \left(\frac{2 * 41.1}{360}\right) * 2\pi * 48.67 = 69.8 \text{ m}$$

Front chord – pitch = 6 m: $\sqrt{(4 * 8)^2 + y_R^2} = (6 + y_R)^2$
 $32^2 = 36 + 12y_R$, thus $y_R = 82.33$ m. The radius $R = 6 + 82.33 = 88.33$ m
 $\alpha = \arctan\left(\frac{32.0}{82.33}\right) = 21.3^\circ$

$$L_{\text{rear}} = \left(\frac{2 * \alpha}{360}\right) * 2\pi R = \left(\frac{2 * 21.3}{360}\right) * 2\pi * 88.33 = 65.5 \text{ m}$$

In this thesis, the front and rear chord are taken at similar cross-sectional dimensions. The reduction in steel volume for the leading lens-shaped cross-section caused by the use of clamped joints over hinged joints can now be calculated as follows:

$$\Delta V_{\text{steel;joints}} = 16 * 10^3 \text{ mm}^2/\text{m} * (69.8 + 65.5) = 2.17 \text{ m}^3 \text{ per leading lens-shaped section}$$

With the given unit weight of steel ($\rho_{\text{rep}} = 7850 \text{ kg/m}^3$), this volume is equal to $2.17 * 7850 = 17.0 * 10^3 \text{ kg} = 17.0 \text{ tonnes}$ per leading lens-shaped barrier section.

– *Upper lens-shaped barrier section with clamped joints – reducing weight by more optimum use of steel*

The uniform distributed load on the leading lens-shaped section is equal the maximum support reaction of the cross beams, thus 1357 kN/m. In this thesis, the three lens-shaped sections are divided into two designs. As the support reaction at the bottom lens is near to equal to that of the middle lens (ratio of forces: $1175 / 1357 = 0.9$), the lenses are designed to have similar cross-sectional properties. The upper lens can be designed significantly lighter as its uniform distributed load is a factor $405 / 1357 = 0.3$ smaller.

The predetermined ratio of forces can be applied to all member forces. Appendix I.4 presents these member forces for the upper lens-shaped barrier section. A first guess for the minimum cross-sectional dimensions can be made by multiplying the moment of inertia of the front and rear chord of the leading barrier sections by the predetermined factor. An extra factor of 0.25 is added to account for the non-linear relation within the equivalent stress equation and the equation of the moment of inertia. These factors combined results in:

$$I_{\text{upper;firstguess}} = \frac{1}{4} * \left(\frac{405}{1357}\right) * I_{\text{bottom/center}} = \frac{1}{4} * \left(\frac{405}{1357}\right) * 4.73 * 10^{10} = 3.53 * 10^9 \text{ mm}^4 .$$

Assuming a square box profile with a flange thickness of 40 mm, this minimum required moment of inertia results in an outer dimension of 600 mm:

$$A = 600^2 - 520^2 = 89600 \text{ mm}^2 \text{ and } I_z = \frac{1}{12} (600^4 - 520^4) = 4.71 * 10^9 \text{ mm}^4$$

As stated earlier, steel is more beneficial at a larger distance of the center of gravity of the cross-section. Based on this theory, assuming a square box profile with flange thickness of 30 mm results in an outer dimension of 650 mm and the following values for the cross-sectional area and moment of inertia:

$$A = 650^2 - 590^2 = 74400 \text{ mm}^2 \quad I_z = \frac{1}{12} (650^4 - 540^4) = 4.78 * 10^9 \text{ mm}^4$$

It can be seen that the moment of inertia increases while the cross-sectional area decreases. For internal stability of the cross-section, lower values for the flange thickness are not reviewed at this point. In theory, reducing the flange thickness would further reduce the cross-sectional area at the minimum required moment of inertia. The outer dimension would significantly increase at the same time, leading to non-favorable internal proportions. The flange thickness of 30 mm results in a significant reduction:

$$\Delta A_{\text{steel;upper;flange}} = 89600 - 74400 = 15.2 * 10^3 \text{ mm}^2/\text{m}$$

$$\Delta V_{\text{steel;upper;flange}} = 15.2 * 10^3 \text{ mm}^2/\text{m} * (69.8 + 65.5) = 2.06 \text{ m}^3 \text{ for the total upper lens-shaped section}$$

With the given unit weight of steel ($\rho_{\text{rep}} = 7850 \text{ kg/m}^3$), this volume is equal to $2.06 * 7850 = 16.2 * 10^3 \text{ kg} = 16.2 \text{ tonnes}$. This reduction is only due to the projected reduction in flange thickness for this barrier section.

In the clamped joints model, both the front and rear are loaded by a combination of bending moments, shear forces and normal forces. The critical cross-sections of both chords can be determined and checked for the square box profile with a flange thickness of 30 mm in a similar manner as is presented in section 8.2. These checks results in:

Front chord – upper lens-shaped barrier section – clamped joints – maximum support moment:

$$M_{\max} = \left(\frac{405}{1357}\right) * 7605 = 2270 \text{ kNm}, \quad V_{\max} = \left(\frac{405}{1357}\right) * 5553 = 1658 \text{ kN}, \quad N_{\max} = \left(\frac{405}{1357}\right) * 45636 = 13621 \text{ kN}$$

$$S_z^a = (a - 2t) * \left(\frac{1}{2}a - t\right) + 2 * \left(\frac{1}{2}at\right)\left(\frac{1}{4}a\right)$$

Static moment:

$$S_z^a = (650 - 2 * 30) * \left(\frac{1}{2} * 650 - 30\right) + 2 * \left(\frac{1}{2} * 650 * 30\right) * \left(\frac{1}{4} * 650\right) = 3.35 * 10^6 \text{ mm}^3$$

$$\sigma_{\text{eq}} = \sqrt{\left(\frac{N}{A} + \frac{M_y * e}{I_y}\right)^2 + 3\tau_{yz}^2} = \sqrt{\left(\frac{13621 * 10^3}{74.4 * 10^3} + \frac{2270 * 10^6 * 325}{4.78 * 10^9}\right)^2 + 3\left(\frac{1658 * 10^3 * 3.35 * 10^6}{(30 + 30) * 4.78 * 10^9}\right)^2} = 339.1 \text{ N/mm}^2$$

Front chord – upper lens-shaped barrier section – clamped joints – maximum field moment:

$$M_{\max} = \left(\frac{405}{1357}\right) * 8332 = 2487 \text{ kNm}, \quad V_{\max} = 0 \text{ kN}, \quad N_{\max} = \left(\frac{405}{1357}\right) * 43646 = 13027 \text{ kN}$$

$$\sigma = \frac{N}{A} + \frac{M_y * e}{I_y} = \frac{13027 * 10^3}{74.4 * 10^3} + \frac{2487 * 10^6 * 325}{4.78 * 10^9} = 175.1 + 169.1 = 344.2 \text{ N/mm}^2$$

Rear chord – upper lens-shaped barrier section – clamped joints – maximum moment at end support:

$$M_{\max} = \left(\frac{405}{1357}\right) * 6268 = 1871 \text{ kNm}, \quad V_{\max} = \left(\frac{405}{1357}\right) * 253 = 76 \text{ kN}, \quad N_{\max} = \left(\frac{405}{1357}\right) * 44958 = 13418 \text{ kN}$$

$$\sigma_{\text{eq}} = \sqrt{\left(\frac{N}{A} + \frac{M_y * e}{I_y}\right)^2 + 3\tau_{yz}^2} = \sqrt{\left(\frac{13418 * 10^3}{74.4 * 10^3} + \frac{1871 * 10^6 * 325}{4.78 * 10^9}\right)^2 + 3\left(\frac{76 * 10^3 * 3.35 * 10^6}{(30 + 30) * 4.78 * 10^9}\right)^2} = 307.6 \text{ N/mm}^2$$

All checks suffice with regard to the yield point. Now the chords of both the leading and upper lens-shaped barrier sections are known, the difference in required steel volume can be calculated:

Leading lens-shaped section	front chord = rear chord: a = 1250 mm, t = 40 mm	A = 193600 mm ²
Upper lens-shaped section	front chord = rear chord: a = 650 mm, t = 30 mm	A = 74400 mm ²

$$\Delta A_{\text{steel;upper}} = 193600 - 74400 = 119.2 * 10^3 \text{ mm}^2/\text{m}$$

$$\Delta V_{\text{steel;upper}} = 119.2 * 10^3 \text{ mm}^2/\text{m} * (69.8 + 65.5) = 16.2 \text{ m}^3 \text{ for the total upper lens-shaped section}$$

With a given unit weight of steel ($\rho_{\text{rep}} = 7850 \text{ kg/m}^3$), this volume is equal to $16.2 * 7850 = 126.6 * 10^3 \text{ kg} = 126.6 \text{ tonnes}$. This reduces the weight by an estimated 10%, as the expected total weight was initially set at 1000 tonnes. In this difference, the cross-sectional reduction of the transverse girders is not even included. The reduction in weight is significant and favorable as it reduces the costs of the steel. More importantly, it reduces the forces on the hydraulic cylinders and moving parts of the barrier. The actual total weight of the gate, including all optimized components, is determined in section 8.4.2. It serves as data input for the calculations on vibrations presented in chapter 9.

– *Designing the retaining wall with the method of equivalent cross-section – reduction by calculation method*

Section 8.3 already determined the differences in required steel volumes for both design calculation methods. Table 8.24 summarized these volumes of steel for both methods and for a variable mutual distance for the cross beams, which is equal to the field length of the longitudinal stiffeners. For the designed optimum mutual distance of 2.0 m, the reduction in weight can be calculated as follows:

$$\text{Method of separation of components} \quad \text{stiffener} = \text{IPE 300, cross beam} = \text{HE 800A}: \quad V_{\text{steel;soc}} = 18.3 \text{ m}^3$$

$$\text{Method of equivalent cross-section} \quad \text{stiffener} = \text{IPE 240, cross beam} = \text{HE 700A}: \quad V_{\text{steel;eqcs}} = 15.8 \text{ m}^3$$

With a given unit weight of steel ($\rho_{\text{rep}} = 7850 \text{ kg/m}^3$), this difference in required volume of steel in both calculation methods is equal to $(18.3 - 15.8) * 7850 = 19.7 * 10^3 \text{ kg} = 19.7 \text{ tonnes}$. It should be noted that the used values are based on a length of the front plate of 66.0 m instead of the actual length of 65.5 m. However, the influence of this minimum difference can be neglected.

8.4.2 Overview of structural components – determination of the mass distribution over the steel lifting gate

This section presents an overview of the structural components of the steel lifting gate. The height and flange thickness of the used square box profiles result in a cross-sectional area. In combination with the main length of the components and the number of components used, this cross-sectional area results in a required steel volume per component. Table 8.25 presents this overview of required steel volume per structural component and provides insight in the way the mass is distributed over the steel lifting gate.

	Cross-sectional dimensions (height, flange thickness)	Cross-sectional area component	Component main length	Number of components	Required steel volume component
	[mm]	[mm ²]	[m]	[-]	[m ³]
<u>Leading lens-shaped barrier section</u>					
- Front chord	a = 1250 mm, t = 40 mm	193600	65.5	2	25.4
- Rear chord	a = 1250 mm, t = 40 mm	193600	69.8	2	27.2
- Transverse girders (table 8.10 and 8.11)					
A	a = 500 mm, t = 20 mm	38400	18.0	2	1.4
B	a = 450 mm, t = 20 mm	34400	16.9	2	1.2
C	a = 400 mm, t = 20 mm	30400	13.5	2	0.82
D	a = 350 mm, t = 20 mm	26400	7.9	2	0.42
				subtotal	55.2
<u>Upper lens-shaped barrier section</u>					
- Front chord	a = 650 mm, t = 30 mm	74400	65.5	1	4.9
- Rear chord	a = 650 mm, t = 30 mm	74400	69.8	1	5.2
- Transverse girders (table 8.12: t = 20 mm)					
A	a = 350 mm, t = 20 mm	26400	18.0	1	0.48
B	a = 350 mm, t = 20 mm	26400	16.9	1	0.45
C	a = 300 mm, t = 20 mm	22400	13.5	1	0.30
D	a = 250 mm, t = 20 mm	18400	7.9	1	0.15
				subtotal	11.5
<u>Retaining wall</u>					
- Front plate	h = 14650 mm, t = 30 mm	439500	65.5	1	28.6
- Longitudinal stiffener	IPE 240	3910	2.0	14 x 33	3.6
- Cross beam	HE 700 A	26000	14.5	32	12.1
				subtotal	44.3
<u>x-type bracing system</u>					
- Transverse girders					
A	a = 250 mm, t = 10 mm	9600	8.5	12	0.98
B	a = 250 mm, t = 10 mm	9600	10.3	8	0.79
C	a = 250 mm, t = 10 mm	9600	9.0	8	0.69
D	a = 250 mm, t = 10 mm	9600	9.9	4	0.38
- Rear chord	a = 250 mm, t = 10 mm	9600	10.0	32	3.2
				subtotal	6.0
<u>Guide posts</u>					
	h = 14650 mm, t = 200 mm (t is eq. plate thickness)	2930000	3.0	2	17.6

Table 8.25: Overview of structural components – determination of the mass distribution over the steel lifting gate

The components that form the lens-shaped barrier sections and the retaining with its front plate, longitudinal stiffeners and cross beam are all determined in sections 8.2 and 8.3. The x-type bracing system is determined for the leading transverse girder at the center of the lens-shaped barrier section. For the calculation of the total mass of the lifting gate, it is assumed that all beams in the x-type bracing system are composed of equal cross-sectional dimensions. The length of each beam can be determined by assuming a number of x-type bracings and by including the fixed mutual distance of the lens-shaped barrier sections of 6.0 m. At the rear chord, the length of the x-type bracing system beams can thus be determined as $\sqrt{(8^2 + 6^2)} = 10.0$ m.

The guide posts are not designed in this thesis. It is known that the guide posts are components where the main system forces come together should therefore be relatively massive. For this reason, an equivalent plate thickness of 200 mm is assumed. The width of the guide post is set at 3.0 m.

The total mass of the gate can be determined by the summation of the five main structural parts, which results in:

$$m_{\text{gate}} = 7850 * (55.2 + 11.5 + 44.3 + 6.0 + 17.6) = 7850 * 134.6 = 1060 * 10^3 \text{ kg} = 1060 \text{ tonnes}$$

The main contributors to this total mass are the bottom and center lens-shaped barrier sections, with a volume of 27.6 m³ each, and the retaining wall. The front plate has a volume of 28.6 m³ and forms the largest single contributor at 20% of the total mass of the gate. In the detailed design stage, efforts should be made to investigate any possible reduction of the front plate thickness. This would significantly decrease the mass of the gate.

The upper lens-shaped barrier section requires only 11.5 / 27.6 = 40% of the steel volume needed for the leading lens-shaped sections. This results in the predetermined weight reduction of (27.6 – 11.5) * 7850 = 126 tonnes, which is equal to about 12% of the current total weight of the gate.

Finally, it is instructive to review the expected overturning moment atop the hoisting towers. An estimation of the balance of components determines whether the center of gravity of the lens-shaped section is close to the plane of suspension. The pitch ratio between the parabolic front and rear gate curvature is 2, which implies that the weight of the front chords and retaining wall may only be two times larger than the weight of the rear chords and x-type bracing systems. The check on the expected overturning moment results in the following:

Front arch: mass = ρ [retaining wall + front chord upper barrier section + 2 * front chord leading barrier section]
mass = 7850 * [44.3 + 4.9 + 25.4] = 7850 * 74.6 = 588 tonnes

Rear arch: mass = ρ [rear chord upper barrier section + 2 * rear chord leading barrier section + x-type bracing]
mass = 7850 * [5.2 + 27.2 + 3.2] = 7850 * 35.6 = 280 tonnes

It can be concluded that the overturning moment is sufficiently small. The mass of the rear arch multiplied by two nearly equals the mass of the front arch. In addition, the center of gravity of the transverse girders and associated x-type bracing systems is located in the rear arch. This means that the overturning moment is even smaller.

8.5 Principal conclusions – review on the calculation method and results

As stated in the introduction of the calculation method, a 2D software package is used in this thesis over a comprehensive 3D program, as it provides a better insight in direct mechanical consequences of adjustment to certain parts of the gate. For the final design stage, usage of the 3D software package is advised. This package allows for more detailed design checks and for a distribution of forces in all three directions. This results in a more realistic, thus safer and more economical design output. The calculated results in this chapter should therefore be handled with care and should not directly be used as design input.

The calculated total weight of 1060 tonnes is about 25% higher than the initial assumed value. The actual higher mass of the steel gate influences both the stability of the substructure described in chapter 7 and the potential sensibility to vibrations described in chapter 9. With regard to the reference project, it appears that the weight of the structure increases non-linear with the span and/or depth. The span of the largest gate of the Hartel Canal Barrier is about 1.5 times larger than the projected lifting gate, but it also about 1.5 times lower than it. The total mass of the projected lifting gate is 1060 tonnes, which is about 1.5 times larger than the largest gate of the Hartel Canal Barrier. It appears the height of the gate is the predominant factor for the mass. In particular for the projected lifting gate, in which the required crest height required an additional lens-shaped barrier section. The stated non-linear relation can be expected as the leading loading scenario is predominantly dependent on the hydrostatic pressure. This pressure, thus the load on the lifting gate, is quadratic proportional to the water depth.

9. Review On Degradations – General Maintenance And Analysis On Vibrations

This chapter describes a preliminary review on the expected modes of degradation of the structure during its period of operation. Section 9.1 describes the main modes of degradations and presents a general maintenance approach. Section 9.2 focuses on a particular degradation in the form of vertical vibrations of the lifting gate.

9.1 Main modes of degradations and general maintenance approach

The main modes of degradation are described in this section correspond to those stated in section 5.3.1. For each mode, the expected problems are briefly mentioned.

- *Wear* due to friction is important in the moving parts, such as hinges and wheels. Excessive wear can create deformation, vibrations and alter a normal load distribution. This is of less importance for the projected gate.
- *Abrasion* is the result of contact with the water current, mainly in the presence of sediment transport. It is particularly important for gates that have under water hinges, thus of less importance for the projected gate.
- *Corrosion* can develop for all steel structures near water, especially in this salt water environment. Regular maintenance is required. Important issue is the problem of accessibility for this maintenance. The advised construction of a road connection in section 6.4.4 accommodates this need.
- *Vibrations* can be the result of either mechanical or water flow causes. The lack of aeration in gate overflow is one of the major causes of vibration. Vibrations can cause higher stresses and large alternate deflection. Section 9.2 further analyses this mode of degradations.

There should be a detailed maintenance program to accommodate the stated modes of degradations. In general, the required maintenance activities can be considered as belonging to one of the three following groups. The following remarks refer to the maintenance of the lifting gate. A more detailed description, including all other components, goes beyond the scope of this thesis.

- *Periodical inspections:*
The periodical inspections can be scheduled or unscheduled. The latter could take place after a test closure, if the gate condition and/or behavior give a reason for that. Such a reason can be the occurrence of friction on guide linings, small dents caused by obstacles on the barrier sill or by floating objects. The scheduled inspections should take place unconditionally once every 3 to 4 years. The program of both types of inspection is in principle the same. The main concerns are the condition of the paint coating, wear of guide lining and the condition of the bolted connections which are particularly susceptible to corrosion.
- *Small maintenance services as result of the inspections:*
Based on inspection reports, small maintenance services should be scheduled. Such services are usually limited to cleaning and very local paint corrections. The gates can be lowered to any level in order to make them accessible by boat for this purpose. Section 7.2 proved that even temporary closure of the substructure is possible for moderate weather conditions. Closure of the substructure should always be planned outside the storm season, since for severe weather conditions stability of the structure is not guaranteed. During small maintenance services, additional regulation concerning navigation is required.
- *Periodical full maintenance services:*
The full maintenance services shall take place once every 15 to 25 years and should comprise, among other measures, an entire blast cleaning and painting of the gates. For proper results, this can not be performed in situ. The gate should be coupled off and shipped there in basically the same way as during the first installation. Naturally, this full maintenance service should be scheduled outside the storm season.

9.2 Analysis on vibrations

The main causes of vibration concern the gate lip and the bottom and/or side seals designs. Fluttering of rubber seals can also generate vibrations of the gate. These flow-induced vibrations can be caused either by the shifting of the flow control point between the skin plate lip and other gate bottom members or by the flexibility of the rubber seals which causes them to flutter [Pickering, 1971].

Schmidgall [1972] found that vibration tendencies could be reduced if a rubber seal is not used. This leads to leakage when the gate is closed and this leakage must be tolerated at the project for this strategy to be useful. Section 6.4.3 concluded that for the given dimensions of the gate a leakage width of 50 mm is allowed at both sides of the gate. At the same time, a bottom leakage opening of 150 mm is tolerated. Rubber seals are therefore not advised in the design.

9.2.1 Schematization and principal data

The concrete structure of the barrier consists of two lifting towers on deep foundations, which are connected by a prefab sill. In chapter 7, this configuration is schematized as a single substructure which is checked on stability for several loading scenarios. As mentioned in section 7.3 of this chapter, around the foundations and below the sill a seepage screen has been projected. These can be realized by using sheet pile, but this is not further analyzed in this thesis. The closing element of the barrier is a steel lifting gate. Chapter 8 determined the configuration and mass of it. The lifting gate is lowered and raised by hydraulic cylinders on top of the towers.

The lifting gate can be characterized as an elastically suspended gate in a flow [43]. Figure 9.1 presents the schematization of the dynamically loaded structure. In the following, harmonic loading caused by an unsteady flow will be examined. The vertical lifting gate has a natural frequency and can be loaded dynamically by:

- extraneous excitation, which could be induced by an unsteady flow or wave action;
- instability induced excitation, which could be induced by vortex shedding from the lip of the gate or water flow separation and/or reattachment to the gate;
- movement induced excitation, when the water flow or the hydraulics enhance the movement to which the gate is already subjected (by the lifting/lowering equipment)

Theoretically, the gate as a whole has 6 degrees of freedom. In this thesis, vertical vibration will be analyzed. Generally this results in the leading problems from a gate structure collision point of view. The vibration behavior of the gate changes with the water depth. In this case the leading situation of an almost closed gate is examined.

Differential equation of motion [42]:

$$(m + m_w) \frac{d^2 y}{dt^2} + (c + c_w) \frac{dy}{dt} + (k + k_w) y = F_w(t, y), \text{ in which:}$$

- m = mass [kg]
- m_w = added water mass [kg]
- c = damping [Ns/m]
- c_w = added water damping [Ns/m]
- k = spring stiffness [N/m]
- k_w = added water stiffness [N/m]
- L = representative length [m]
- v = flow velocity
- F_w = all static or dynamic forces by water [N]
- y = direction of analysis, which here is vertical [-]

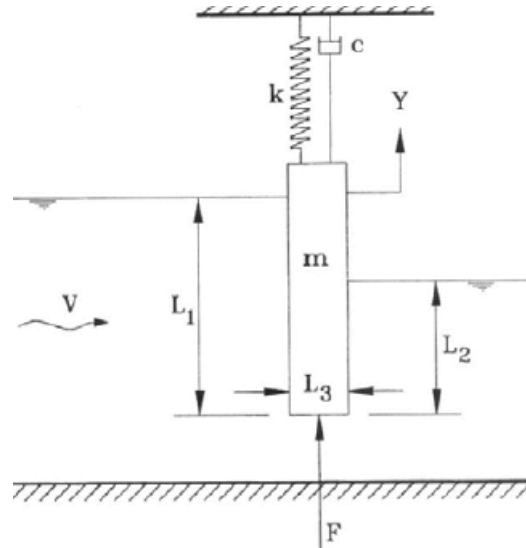


Fig. 9.1: Schematization of an almost closed gate [43]

Data

Gulf Intracoastal Waterway bottom and top of sill level: $h_{\text{bottom}} = -18 \text{ ft} = -5.49 \text{ m}$

The gate has to retain water to a level up to: $h_{\text{max}} = +33 \text{ ft} = +10.06 \text{ m}$

Height of the gate: $h_{\text{gate}} = 48 \text{ ft} = 14.65 \text{ m}$

The gate will be closed at a water level of: $h_{\text{closing,max}} = +9 \text{ ft} = 2.74 \text{ m}$

The length of the span between the towers: $w_{\text{span}} = 210 \text{ ft} = 64.0 \text{ m}$

Mass of the vertical lifting gate: $m_{\text{gate}} = 1060 \cdot 10^3 \text{ kg}$

Specific density of steel and water: $\rho_{\text{steel}} = 7850 \text{ kg/m}^3$ and $\rho_{\text{water}} = 1025 \text{ kg/m}^3$

Computed 'equally distributed thickness' of the gate: $t_{\text{eq,dis}} = \frac{m_{\text{gate}}}{\rho_{\text{steel}} \cdot w_{\text{span}} \cdot h_{\text{gate}}} = 0.144 \text{ m}$

Assumed hydraulic thickness of the gate: $t_{\text{hyd}} = 1.0 \text{ m}$

9.2.2 Calculation of all main parameters pertaining to the vertical lifting gate vibration

The values for all parameters pertaining to the vertical lifting gate vibration are determined in the following order:

- 1) Establish the total suspended mass;
- 2) Establish the spring rigidity of the suspension system;
- 3) Determine the added mass;
- 4) Calculate the damping forces: slide/roller friction, roller bearing friction and seal friction;
- 5) Determine the critical damping coefficient and damping ratio;
- 6) Calculate the resonance frequency;
- 7) Calculate the excitation frequency;
- 8) Establish the transmissibility ratio and magnification factor.

Each of these parameters is quantified subsequently:

- 1) Establish the total suspended mass

By using the underwater mass for steel, the buoyancy force has been taken into account in the differential equation. In case there would be closed hollow spaces, the resulting buoyancy force translated into mass should have to be subtracted from the total suspended mass. The total lifting gate is under water during the maximum storm surge of +33 ft (10.6 m, MSL). The underwater mass of the gate than results in:

$$m_{uw} = 1.0 * \left(\frac{\rho_{steel} - \rho_{water}}{\rho_{steel}} \right) * m_{gate} = 1.0 * \left(\frac{7850 - 1025}{7850} \right) * 1060 * 10^3 = 9.22 * 10^5 \text{ kg}$$

Enclosed water, paint, possible pieces of debris and other items could add to the mass. The retaining wall, front chord, rear chord and framework enclose a certain water body. Consequently, these components interfere with the passing flow together. The enclosed water body is estimated as 25% of the water volume between the stiffeners. This contributes significantly and results in:

$$m_{enclosed} = 0.25 * t_{hyd} * h_{gate} * w_{span} * \rho_{water} = 2.40 * 10^5 \text{ kg}$$

The contribution of paint, debris and other items is estimated as 5% of the mass of the gate. This results in:

$$m_{additional} = 0.05 * m_{gate} = 0.05 * 1060 * 10^3 = 5.30 * 10^4 \text{ kg}$$

The total suspended mass of the gate can now be calculated as follows:

$$m_{total} = m_{uw} + m_{enclosed} + m_{additional} = (922 * 240 * 53) * 10^3 = 1215 * 10^3 \text{ kg}$$

- 2) Establish the spring rigidity of the suspension system

The gate is lifted up and down by a hydraulic jack system. Assume that the jack has been fixed to infinitely stiff concrete and that the housing of the jack is infinitely stiff as well. What remains to be schematized as a spring is the oil in the cylinder and the piston, which is moving the gate up and down.

Stiffness of the steel piston

Combining the general formulae for the strain in a prismatic bar under a constant normal force and the definition of a spring results in:

$$\Delta L = \frac{N * L}{E * A} \text{ and } k = \frac{N}{\Delta L}, \text{ which provides a formula for the steel spring stiffness: } k = \frac{E * A}{L}$$

The required diameter and length of the piston rod are rough order estimates. The gate cylinder lifting height, thus the length of the cylinder, of the Hartel Canal Barrier are about 21 m, which is very long and had never before been realized at the time the barrier was designed. For the projected lifting gate a gate cylinder lifting height is expected of about 30 m. At this point in the thesis, it is assumed that these cylinders can be designed. No limitations regarding their operability are included. Further analysis is needed at this point.

Ideally, the system should be designed in such a way that the gate own weight is sufficient to lower the gates under all circumstances. The lifting lugs and the drive cylinders should never come under compression. The minimum required diameter of the piston rod can initially be calculated by using the yield point of steel and the assumption that one cylinder is subjected to the mass of the lifting gate in the case of partial failure of one of the cylinders. This results in:

$$F = m_{total} * g = 1215 * 10^3 * 9.807 = 11.92 * 10^6 \text{ N}$$

$$A_{min} = \frac{F}{f_{y;d}} = \frac{11.92 * 10^6}{355} = 33578 \text{ mm}^2, \text{ which results in a diameter of 210 mm}$$

Friction and blockage are forms of degradations that could cause difficulties during lowering of the gate. The own weight of the gate is expected to be sufficient to overcome these problems in most cases. Any inequality in the lowering process due to these local degradations could possibly have to be corrected by a compressive force of the cylinders. A compressive force of 10% of the mass of the lifting gate is stated as the absolute maximum. The minimum required diameter of the piston can then be calculated by using the critical buckling force derived by Euler. This determines the minimum required moment of inertia and diameter as follows:

$$I_{\min} = \frac{F_{\text{Euler}} * L^2}{\pi^2 * E_{\text{steel}}}, \text{ thus: } I_{\min} = \frac{(0.10 * 11.92 * 10^6) * 30000^2}{\pi^2 * 210 * 10^3} = 5.18 * 10^8 \text{ mm}^4$$

Moment of inertia for a massive circle: $I_{\text{circle}} = \frac{1}{4} * \pi * R^4$, which results in a diameter of 320 mm

The diameter of the steel piston is designed to be 320 mm, as this accommodates both the own weight of the gate on a single piston and a compressive force of 10% to overcome potential friction and blockage. With a piston length of 30 m, the steel piston stiffness can be calculated:

$$k_{\text{piston}} = \frac{E_{\text{steel}} * A_{\text{piston}}}{L_{\text{piston}}} = \frac{210 * 10^3 * (0.25 * \pi * 320^2)}{30.0} = 5.63 * 10^8 \text{ N/m}$$

Stiffness of the oil in the cylinder

The formula to describe the stiffness of the oil in the cylinder can be derived as follows [42]:

$$\kappa = \frac{\vartheta}{\Delta p} = \frac{\vartheta}{N/A} = \frac{\vartheta * A}{N} = \frac{\Delta L * A}{L * N}, \text{ where } \vartheta = \frac{\Delta V}{V} \approx \frac{A * \Delta L}{A * L} = \frac{\Delta L}{L} \text{ has been used. The parameter used:}$$

κ = compressibility of a fluid at $T = 293 \text{ K}$ or 20° C . For oil this equals: $\kappa_{\text{oil}} = 675 * 10^{-12} \text{ m}^2/\text{N}$

ϑ = relative change in volume of the oil body

Δp = pressure difference. Here it has been assumed that the diameter of the oil cylinder remains constant and that only the vertical movement of the piston results in a pressure difference

Given $k = \frac{N}{\Delta L}$, this provides a formula for the stiffness of the oil in the cylinder: $k = \frac{A}{\kappa * L}$

The stiffness of the oil in the cylinder can now be determined:

$$k_{\text{oil}} = \frac{A_{\text{piston}}}{\kappa_{\text{oil}} * L_{\text{piston}}} = \frac{(0.25 * \pi * 320^2) * 10^{-6}}{675 * 10^{-12} * 30} = 3.97 * 10^6 \text{ N/m}$$

The piston and the oil reservoir act in a serial system, regarding the total spring stiffness of the system:

$$k_{\text{total}} = \frac{1}{\frac{1}{k_{\text{piston}}} + \frac{1}{k_{\text{oil}}}} = \frac{1}{\frac{1}{5.63 * 10^8} + \frac{1}{3.97 * 10^6}} = 3.94 * 10^6 \text{ N/m}$$

Added water stiffness

Immersion, stationary flow and sudden movement of the gate result in an added water stiffness. The added water stiffness due to immersion can be calculated with the following formulae [43]:

$$k_w = \rho_{\text{water}} * g * A_{\text{intersection}}, \text{ in which } A_{\text{intersection}} \text{ is the steel area cutting through the water surface.}$$

Introducing the equally distributed thickness of the gate of 0.144 m and the gate width of 64.0 results in:

$$A_{\text{intersection}} = w_{\text{span}} * t_{\text{eq;dis}} = 64.0 * 0.144 = 9.22 \text{ m}^2, \text{ thus: } k_w = 1025 * 9.807 * 9.22 = 9.27 * 10^4 \text{ N/m}$$

This is can almost be neglected in comparison to the rigidity of the suspension system.

3) Determine the added mass

A lifting gate with the projected longitudinal stiffeners has a considerably larger added mass than a smoother type of gate, because a larger volume of water that moves along with the gate. This added mass should be quantified by using the following formulae:

$$m_w = C_L * \rho * D^2 \text{ or } C_m = \frac{m_w}{\rho * D^2 * L}, \text{ which can be rewritten to: } C_L = \frac{m_w}{\rho * D^2} = L * C_m, \text{ in which:}$$

m_w = added water mass [kg], C_m = added mass coefficient [-], $C_L = L * C_m$ [m]

ρ = density of water [kg/m^3], D = characteristic immersed gate dimension [m], L = width of the gate [m]

Both formulae can be used. Since graphs are available for C_m , presented in figure 9.2, this coefficient is used to determine the added mass. In order to find this coefficient, multiple iterative steps of trial and error need to be taken. An important initial parameter is the last possible moment the gate can be safely closed. The corresponding maximum water level at closure is set to be at +9 ft MSL, thus at a water depth of $h = 18 + 9 = 27$ ft (8.23 m). This value is described earlier in section 6.4.3.

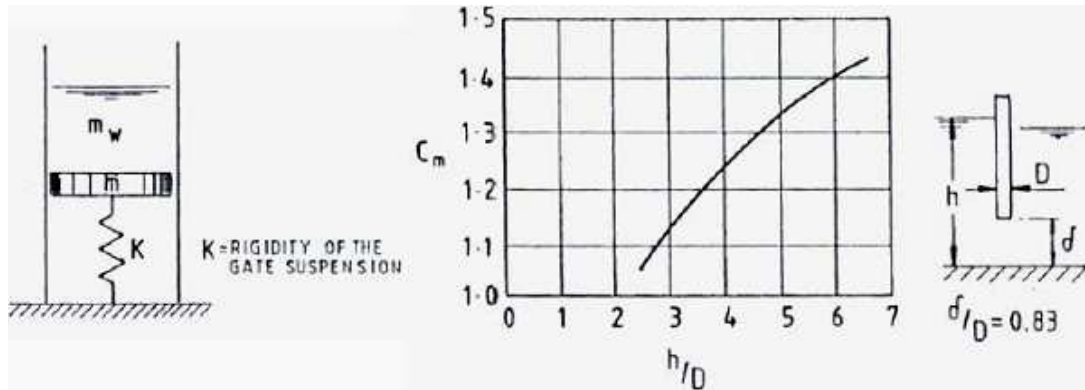


Fig. 9.2: Graphical presentation of the added mass coefficient [44]
 Note: the graph assumes $\delta/D = 0.83$, which implies that the gate is almost completely closed.

Trial & Error Step 1:

D is equal to the overall distributed thickness of the gate, provided that this thickness is larger than the height of the submerged part of the gate. When the thickness is smaller than the height of the submerged part of the gate, the latter dimension should be used for D . When the lowering procedure starts and the gate hits the water, D is equal to the height of the submerged part. A little later, it is equal to the gate thickness. The predetermined equally distributed thickness of the gate = 0.144 m.

Ratio $h/D = 8.23 / 0.144 = 57.2$ and $\delta = 0.83 \cdot 0.144 = 0.12$ m.

The calculated value for h / D is beyond the applicable range in the graph used to determine C_m . This could have been expected when the very small value of 0.144 m was used for D . Using the computed average thickness is not in line with the physical reality.

Trial & Error Step 2:

A more realistic approach is to use a thickness related to the actual dimensions of the gate or parts of the gate, such as the longitudinal stiffeners behind the front plate of the steel gate. The estimated hydraulic thickness of the gate of 1.0 m is used, which is slightly related to the stiffener and girder size.

Ratio $h/D = 8.23 / 1.0 = 8.23$ and $\delta = 0.83 \cdot 1.0 = 0.83$ m – extrapolate the graph of figure 9.3: $C_m = 1.5$

The calculated value for h/D is still beyond the applicable range in the graph used to determine C_m . The value found by extrapolation of the graph is not really reliable, but used in this preliminary design. The added mass can now be determined:

$$m_w = C_m \cdot \rho \cdot D^2 \cdot L = 1.5 \cdot 1025 \cdot 1.0^2 \cdot 64.0 = 9.84 \cdot 10^4 \text{ kg}$$

The added mass has the same order of magnitude as the enclosed water. It is realistic to take both enclosed and entrapped water into account with regard to the mass of the gate.

4) Calculate the damping forces

Damping in a structure may consist of different types of damping and different parts of the structure may contribute. Everything should be added together to find the total damping of the structure. In reality, the damper and spring of the considered suspension system may be frequency dependent. For sake of simplicity, a frequency independent damper is assumed for every separate motion of vertical translation, horizontal translation and rotation.

Material damping

Material damping due to stress changes can be expressed by means of a dimensionless damping coefficient ζ [-]. The damping coefficient presents the force [N] that can be damped from the excitation [Hz = 1/s] every second, per m length of the structure. A reasonable estimate for steel $\zeta = 7 \cdot 10^{-8} \cdot \sigma^2$ [N/mm²] [42]. This leads to a value of the total damping coefficient for the steel gate equal to: $\zeta = 7 \cdot 10^{-8} \cdot 355^2 = 0.0088$ [-].

The material damping can now be determined:

$$c_{\text{material}} = 2 * \zeta_{\text{steel}} * \sqrt{k_{\text{total}} * m_{\text{uw}}} = 2 * 0.0088 * \sqrt{(3.94 * 10^6) * (9.22 * 10^5)} = 3.36 * 10^4 \text{ Ns/m}$$

Friction in the suspension structure: slide and roller friction, roller bearing friction and seal friction

A value for the damping of the entire suspension structure of 1000 Ns/m is used. This value is part of the total damping of the structure and is rather small compared to the predetermined material damping. It is based on experience and mainly used to compare results.

Added damping caused by resistance in air and water

This could be the largest contributor to the total damping. However, in this case the lifting gate moves vertically, hence perpendicular to the flow of water. The resulting damping will be zero or next to nothing even if the gate moves with a small angle to the flow.

- 5) Determine the critical damping coefficient and damping ratio

$$c_{\text{critical}} = 2 * \sqrt{k_{\text{total}} * m_{\text{uw}}} = 2 * \sqrt{(3.94 * 10^6) * (9.22 * 10^5)} = 3.81 * 10^6 \text{ Ns/m}$$

Taking the calculated critical damping, the damping ratio $\zeta = 0.0088$. Since $\zeta \ll 1$ oscillations occur with diminishing amplitude and the system is stable or positively damped.

- 6) Calculate the resonance frequency

The resonance frequency is not equal to the natural or eigenfrequency. In the resonance frequency the added mass and added stiffness should be taken into account. In general, the eigenfrequency is given as:

$$f_{\text{natural}} = \frac{1}{2\pi} * \sqrt{\frac{k_{\text{total}}}{m_{\text{uw}}}} = \frac{1}{2\pi} * \sqrt{\frac{3.94 * 10^6}{9.22 * 10^5}} = 0.329 \text{ Hz} \quad T_{\text{natural}} = \frac{1}{f_{\text{natural}}} = 3.04 \text{ s}$$

Due to the presence of enclosed and added water, paint, debris, etc., the previous formula changes to:

$$f_{\text{resonance}} = \frac{1}{2\pi} * \sqrt{\frac{k_{\text{total}} + k_w}{m_{\text{total}} + m_w}} = \frac{1}{2\pi} * \sqrt{\frac{3.94 * 10^6 + 9.27 * 10^4}{(1215 * 10^3 + 98.4 * 10^3)}} = 0.279 \text{ Hz} \quad T_{\text{resonance}} = \frac{1}{f_{\text{resonance}}} = 3.59 \text{ s}$$

- 7) Calculate the excitation frequency

The excitation source is the underflow of water. By the separation of vortices from the lifting gate, practically periodical loads in the direction of the water flow, but especially perpendicular to the water flow direction will occur. The general formulae used to describe this vortex shedding during underflow [44]:

$$\text{Strouhal's number } S = f * \frac{L}{V}, \text{ in which } V = \sqrt{2 * g * H_e}$$

The calculation of the energy head is presented graphically in figure 9.3.

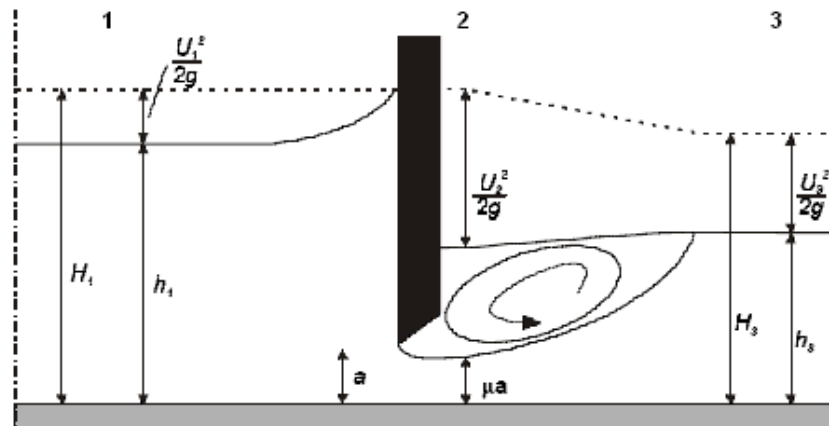


Fig. 9.3: Graphical presentation of the development of energy head [42]

- Data**
- $a = 0.83 \text{ m}$, but could be actually variable. This value is used in the calculation of the added mass.
 - $\mu = \text{contraction coefficient} = 0.70$. This value is commonly used.
 - $h_1 = \text{maximum water level outside at the time of closure} = 18 + 9 = 27 \text{ ft} = 8.23 \text{ m}$.
 - $h_2 = \text{minimum water level inside near the lifting gate at the time of closure} = 18 - 5 = 13 \text{ ft} = 3.96 \text{ m}$

The formulae describing the conservation of energy and volume should be used for the intersection 1-2:

– Conservation of energy (Bernoulli) $H_{1-2} = h_1 + \frac{u_1^2}{2 \cdot g} = h_2 + \frac{u_2^2}{2 \cdot g}$

– Conservation of volume $h_1 \cdot u_1 = \mu a \cdot u_2$

In order to solve these equations, initially it is assumed that $\frac{u_1^2}{2 \cdot g} \ll h_1 - h_2 = 8.23 - 3.96 = 4.27 \text{ m}$.

Then the velocity u_2 is given by: $u_2 = \sqrt{2 \cdot g \cdot (h_1 - h_2)} = \sqrt{2 \cdot g \cdot (8.23 - 3.96)} = 9.15 \text{ m/s}$

Velocity u_1 can now be determined: $u_1 = \frac{\mu a \cdot u_2}{h_1} = \frac{0.70 \cdot 0.83 \cdot 9.15}{8.23} = 0.65 \text{ m/s}$.

Check: $\frac{u_1^2}{2 \cdot g} = \frac{0.65^2}{2 \cdot 9.807} = 0.022 \text{ m}$, which is sufficiently small to allow the initial assumption.

The water level in the retention area further away from the lifting gate can be determined with the equation describing the conservation of impulse:

$$\frac{1}{2} \rho g h_2^2 + \rho u_2^2 \mu a - \frac{1}{2} \rho g h_3^2 + \rho \frac{q^2}{h_3} = 0$$

$$\frac{1}{2} \cdot 1025 \cdot 9.807 \cdot 3.96^2 + 1025 \cdot 9.15^2 \cdot 0.70 \cdot 0.83 - \frac{1}{2} \cdot 1000 \cdot 9.807 \cdot h_3^2 - 1000 \cdot \frac{(9.15 \cdot 0.70 \cdot 0.83)^2}{h_3} = 0$$

$$[\text{kN/m}] \cdot \left(78.82 + 49.86 - 4.91 \cdot h_3 - \frac{5.316^2}{h_3} \right) = 0, \text{ which results in: } h_3 = 5.0 \text{ m}$$

The energy head at this location: $H_3 = h_3 + \frac{q}{2 \cdot g \cdot h_3^2} = 5.0 + \frac{(9.15 \cdot 0.70 \cdot 0.83)^2}{2 \cdot 9.807 \cdot 5.0^2} = 5.06 \text{ m}$

It should be noted that the influence of the wind offset, essentially the cause of the low initial water level at section 2, is not be incorporated in this calculation. These calculated values should therefore be handled with care and only used in this preliminary design stage to assess the influence of vibrations.

The energy head in section 1, 2 and 3 is respectively 8.25, 8.25 and 5.06 m. To determine the frequency of a vortex trail shed from the bottom edge of a partly open gate, the following formula can be used:

$$f_{\text{excitation}} = \frac{\sqrt{2 \cdot g \cdot H_e}}{7 \cdot L}$$

The submerged depth of the lifting gate under the projected circumstances is equal to 5.0 m. The eddy behind the gate has a length of 7 times the submerged depth. In this case the length L is assumed to be equal to this distance, thus $L = 7 \cdot 5 = 35 \text{ m}$. The frequency of the vortex trail can now be calculated:

$$f_{\text{excitation}} = \frac{\sqrt{2 \cdot g \cdot H_e}}{7 \cdot L} = \frac{\sqrt{2 \cdot 9.807 \cdot 8.252}}{7 \cdot 35} = 0.052 \text{ Hz} \quad T_{\text{excitation}} = \frac{1}{f_{\text{excitation}}} = 19.26 \text{ s}$$

8) Establish the transmissibility ratio and magnification factor

The magnification factor is calculated by dividing the excitation frequency over the resonance frequency:

$$MF = \frac{f_{\text{excitation}}}{f_{\text{resonance}}} = \frac{0.052}{0.279} = 0.19$$

The transmissibility ratio is given by:

$$TR = \frac{1}{1 - (f_{\text{excitation}} / f_{\text{resonance}})^2} = \frac{1}{1 - (0.052 / 0.279)^2} = 1.034$$

Figure 9.4 presents the graph for the magnification factor versus the transmissibility ratio. The calculated TR of about 1.0 leads to conclude that there might be a problem regarding vibrations for higher eigenfrequency modes. It is advised that the resonance frequency should be substantially different from the excitation frequency. At least a factor 3 higher or lower is advised [43].

The excitation frequency is smaller than the eigenfrequency and well below the resonance peak. The system can be described as quasi-static, which means that the structure may show some minor response to the excitation source.

9.2.3 Conclusion on the gate vibration in vertical direction

Based on the calculation results of the main parameters pertaining to the lifting gate vibration in vertical direction, major problem should not be expected for two main reasons:

- 1) The system is positively damped.
- 2) The excitation frequency is sufficiently small compared to the first eigenfrequency.

During the detailed design stage, the situation regarding vertical vibration should be kept in close watch. From literature, some remarks can be made at this point. As stated, the reviewed flow induced vibrations of the lifting gate can be a forced motion resulting from shedding vortices. Researchers have focused on vertical lifting gates and findings of these efforts have shown that flat-bottomed gates have to be avoided. The inclination of the lip should be 45 degrees and the skin plate should be at the upstream side of the gate [18].

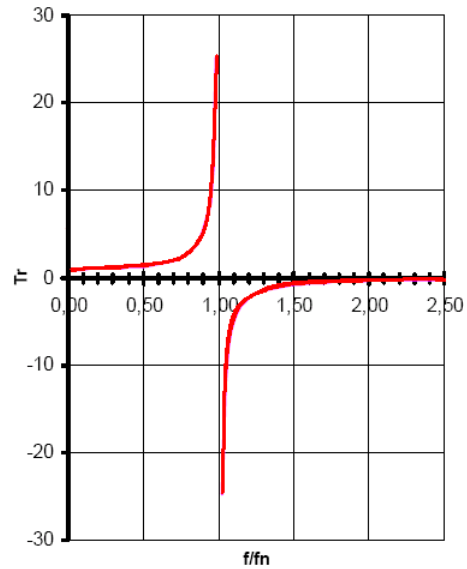


Fig. 9.4: Transmission coefficients [42]

Another structural feature to reduce vibrations is the design of the proper hinges between the cylinder arms and the gate lugs. These are projected to be Cardan joints. Generally, this is a joint in a rigid rod that allows the rod to bend in any direction. It consists of a pair of ordinary hinges located close to each other, but orientated at 90° relative to each other. In choosing this type of joints, all possible movements of the gates can be tolerated including a disturbed, unequal lifting movement. The Cardan joints are also used in the Hartel Canal Barrier. A global view on the cylinders used in this proven scheme and a detail of cylinder joint to one of the gates are depicted in figure 9.5. The cylinder support joints on the towers also allow for rotations in both vertical planes.



Fig. 9.5: Hartel Canal Barrier – global view of projected cylinders and detail of the cylinder joint to one of the gates [19]

10. Principal Conclusions And Recommendations

Chapter 1 to 5 – From Hurricane Katrina to projected barrier concepts

Hurricane Katrina generated a storm surge and wave environment unparalleled in the history of New Orleans, generating water levels that exceeded the design criteria at several locations. It leads to conclude that storm surge and waves are the hazard, not the storm. Meteorological designations such as the Saffir-Simpson Scale by themselves are not adequate to characterize the distributed surge and wave conditions that a protective system will face. These traditional methods of assessing the frequency of occurrence of hurricanes, which depend primarily on historical data, are too simplistic to capture important characteristics of the hurricane hazard such as time- and space-dependent storm intensity and track patterns. Wave and storm surge modeling provides insight into how water surrounding a complex physical system responds to an also complex hurricane wind system.

In the validation of the used model results, it appeared that both measured and calculated storm surge levels are significantly higher than the design levels in both cases. Calculated wave maxima are generally lower than the design maxima. For the peak Hurricane Katrina, the ARCDIC model predicted storm surge heights a few decimeters lower than the actual water mark observations. The ARCDIC model is known to underestimate the water levels, partly because it neglects wave setup. In conclusion, one should carefully use the outcome of those hydraulic models as input for any design at location with is a lack of observation data for calibration of them.

The Hurricane Protection System (HPS) did not perform as a system. All components that contribute to the performance of the overall system should be treated as an integral part of the system. Also interior drainage is advised to be an integral part of the system because it can limit the amount and duration of flooding. Most important of all, the design methods need frequent review to determine whether they represent best practice and knowledge. An example of this lack of review is the use of the Standard Project Hurricane (SPH), which has been the heart of most hurricane protection projects since the 1960s. Over time the SPH went from being a general indicator of threat levels to a guarantee of safety. The methods used to define the SPH were forgotten, along with their potential flaws and questionable assumptions. As a result, the design approaches taken were not conservative enough to deal with the unknowns. They should consider a broader spectrum of possible behaviors, including redundancy within designed systems and resilience to catastrophic breaching.

Fundamental to the trouble in the Mississippi River Delta is that for the past century the U.S. Army Corps of Engineers (USACE) confined the river by building levees to prevent its annual floods. Yet the same levees have starved the region of enormous quantities of sediment, nutrients and freshwater. Natural flooding at the its mouth had sent volumes of sediment west and east to a string of barrier islands that cut down surges and waves, rebuilding each year what regular ocean erosion had stolen. Since the mouth is now dredged for shipping lanes, the sediment simply streams out into the deep ocean. This leaves the delta and New Orleans within it vulnerable against the sea. Sustainability of coastal Louisiana depends on the ability to find solutions that are compatible with nature. To address this need, numerical modeling tests need to be conducted to evaluate the reduction in surge as a function of landscape features and vegetation types. This provides insight in the effect of nourishments and other restoration efforts.

In Katrina's wake, the blueprints for structures are rapidly being dusted off and integrated into a Grand Plan for southern Louisiana. The idea that improving only the existing project would not provide protection to communities outside the existing levee system was the basis for this Grand Plan. Another fundamental point is the fact that this plan maintains New Orleans as a viable urban center. No alternative provided in any reviewed literature that evaluates relocation of the city of New Orleans en masse. Many of the issues involved in protecting New Orleans from a major hurricane are ultimately political rather than technical. Forecasting future conditions is challenging in best cases. As there is still a high degree of uncertainty concerning reliable forecasts and future conditions, alternatives involving abandonment of formerly developed areas are not included in this thesis. It could be interesting perform this evaluation, resulting in a possible abandonment of St. Bernard Parish and Orleans Parish. Detailed information and a wide range of variable should be known in order to adequately evaluate this subject. As this information is not available at the time of this thesis, no further analysis is made.

For the part of the Grand Plan adjacent to Lake Borgne it is recommended to implement two flood protection structures in combination with a new, straight levee alignment between them. This alternative has the best high water safety and the most positive ecological influence. It is intended to close off the IHNC, thereby substantially reducing high water and wave action against the interior levees and floodwalls, potentially reducing the costs of future upgrades, maintenance and associated repairs to the system. From literature, it appears to be favorable to permanently close the Mississippi River Gulf Outlet (MRGO), on of the projected flood protection barriers. The highly navigated Gulf Intracoastal Waterway can not be permanent closed. As navigable floodgate structure is recommended in the form of a vertical lifting gate.

The projected protection level of the lifting gate presents one of the main uncertainties of the thesis. The lack of proper hydraulic information requires the level of protection to be derived in an unusual manner, making that the value is not absolute and should be handled with care. The other hydraulic boundary conditions required to determine the crest level of the outer levee, crest height of the lifting gate and the safety of the closure elements are near to all assumed according to engineering justice. Also for these values, a more thorough investigation of detailed hydraulic conditions is recommended in order to adequately describe those characteristic design parameters. Any changes in the design storm information affect the crest heights, the structural design of the steel lifting gate and could even affect the decision of the type of flood protection structure to be built.

Geotechnically, the compressible materials present are expected to allow significant settlement under loads imposed by the levee fill and lifting gate structure. The settlement is likely to continue over an extended period of time. The subsidence occurring over time will lower the level of protection provided by the structures. It is recommended to investigate whether this condition could be mitigated to some extent by removing some of the soft surface layers and/or by use of piles beneath the concrete structures. Settlement analyses were not performed as a part of this conceptual study. As design of the gate structure advances, more detailed and extensive geotechnical investigations and analyses will be required to identify actual conditions and to develop proper design parameters. Investigations should include options to reduce settlement and improve shear strength. Stability of the levees is also a concern due to this weak shear strength that some of the sedimentary strata are likely to display. Stability analyses were not performed as a part of the thesis. As the design of the structure progresses, stability analyses should be completed for the various components of the gate structure. More detailed analyses should also be performed for any excavations and modified levee sections.

In this thesis, an indicative order of magnitude calculation is presented in order to determine a first estimation of the needed concrete civil works. For this calculation, the stability of the structure and the potential of shearing are reviewed. It should be noted that the results of this calculation approach are not absolute and should be handled with the up most care as it assumes a foundation *without* piles. However, the use of piles is likely in the design as the high surge level and associated high differential head results in both high vertical forces and high horizontal forces. The method is therefore not sophisticated enough for in order for it to be used as an optimal design tool. The most significant contribution of this method is that it provides insight in the relative criticalness of each scenario. The calculation results lead to conclude that the loading under maximum surge level and significant wind offset in the retention area is the critical loading scenario. The checks on shearing and maximum granular stresses are both critical in this event. It appears that the occurrence of a wave low during extreme conditions is not critical and the influence of the representative wind load on the gate in lifted position can be neglected.

A 2D software package is used for the steel design calculations presented in this thesis over a comprehensive 3D program, as it provides a better insight in direct mechanical consequences of adjustment to certain parts of the gate. For the final design stage, usage of the 3D software package is advised. This package allows for more detailed design checks and for a distribution of forces in all three directions. This results in a more realistic, thus safer and more economical design output. The calculated results in this thesis should not directly be used as design input. In the design of the steel lifting gate reference is made to the Hartel Canal Barrier, a proven protection scheme in the Netherlands consisting of a lifting gate. Typical for this barrier are the lens-shaped barrier section. This shape has been chosen in order to place their centers of gravity close to the plane of suspension. In the design of this particular section of the lifting gate, several conclusions can be made:

- During the design it appeared favorable to introduce an additional lens-shaped section. The addition of an extra support halves the leading field length. As a result, the cross-beam can be constructed much finer.
- From the investigated development of member forces it can be concluded that a parabolic gate curvature is favorable over a circular curvature. The maximum moment and shear force is smaller and also the range of these forces is smaller. This allows for a finer design, which means that the gate can be lighter. It also allows for a more optimal use of the steel as the loading is more uniformly distributed over the length of the chord.
- A lens-shaped barrier section as calculated in this thesis is more critical with purely hinged joints than with clamped joints. The hinged joints model results in stresses of about 10% higher than the model with clamped joints. The clamped joints model presents a more uniform distribution of the bending moment, which is partly transmitted to the rear chord. Changes in normal and shear force can be neglected. The realization of hinged joints is more difficult and labor-intensive. This extra effort is not even beneficial and therefore not advised.
- The upper lens-shaped barrier section can be designed much finer, thus reducing the overall weight and resulting in more optimum use of steel. The reduction in weight is significant and reduces the costs of the steel. More importantly, it reduces the forces on the hydraulic cylinders and moving parts of the barrier.

Based on the calculation results of the main parameters pertaining to the lifting gate vibration in vertical direction, major problems are not expected as the system is positively damped and the excitation frequency is sufficiently small compared to the first eigenfrequency. There could be problems with higher eigenfrequency modes. During the detailed design stage, the situation regarding vertical vibration should be kept in close watch. A proper configuration of the gate lip, the use of Cardan joints to connect the gate to the hoisting towers and the fact that rubber seals can be avoided due to a proper amount of allowed leakage, all contribute to an even safer design with regard to these flow-induced vibrations.

References

General reports and presentations

- [1] American Society Of Civil Engineers [2006] – Hurricane Katrina External Review Panel – ‘The New Orleans Hurricane Protection System: What Went Wrong And Why?’, *Final Report*
- [2] ARCADIS G&M, Inc. [2006] – ‘Inner Harbor Navigation Canal Floodgates Conceptual Study’, *Draft Report*
- [3] ARCADIS G&M, Inc. I USACE [2006] – Inner Harbor Navigation Canal Flood Gate Alternative Study, *Final Report*
- [4] ARCADIS G&M, Inc. [2006] – ‘Inner Harbor Navigation Canal Flood Protection: Geotechnical Challenges’, *Presentation*
- [5] Caffey, R.H. [2002] – ‘Closing The Mississippi River Gulf Outlet: Environmental And Economic Considerations’, *Paper*
- [6] ComCoast [2002] – ‘Innovative Flood Management Solutions And Spatial Development: A Wider Approach In Coastal Management’, *Brochure*
- [7] Dijkman, M. [2007] – ‘Protecting St. Bernard Parish, New Orleans: Revision Of The Coastal Defence Zone’, *Master Thesis, Delft University Of Technology*
- [8] Dutch Ministry Of Transport, Public Works And Water Management [1998] – ‘The Delta Project For Safety, Wildlife, Space And Water’, *Report*
- [9] Dutch Technical Advisory Committee On Flood Defences [2003] – ‘Leidraad Kunstwerken’, *Report*
- [10] Dutch Technical Advisory Committee On Flood Defences [2003] – ‘Technical Report Wave Run-up And Wave Overtopping At Dikes’, *Report*
- [11] Dutch Ministry Of Transport, Public Works And Water Management [2005] – ‘Richtlijnen Vaarwegen’, *Report*
- [12] Dutch Ministry Of Transport, Public Works And Water Management [2006] – ‘The Dutch Approach To Flood Protection’, *Presentation*
- [13] Federal Emergency Management Agency [2007] – ‘Guidelines And Specifications For Flood Hazard Mapping’, *Report*
- [14] Fischetti, M. [2006] – Scientific American – ‘Protecting New Orleans’, *Article*
- [15] Kent, J.D. [2005] – Louisiana Geographic Information Center – ‘Louisiana Hurricane Impact Atlas’, *Report*
- [16] Knabb, R.D. et al. [2005] – National Hurricane Center – ‘Tropical Cyclone Report On Hurricane Katrina’, *Report*
- [17] Lopez, J.A. [2006] – ‘Multiple Lines Of Defense To Sustain Coastal Louisiana’, *Final Report*
- [18] PIANC InCom Working Group 26 [2005] – ‘Design Of Movable Weirs And Storm Surge Barriers’, *Final Report*
- [19] PIANC InCom Working Group 26 [2005] – ‘Design Of Movable Weirs And Storm Surge Barriers – Project review: Hartel Canal Barrier’, *Report*
- [20] Stone et al. [2003] – ‘Louisiana Ecosystem Restoration Study’, *App. D – Louisiana Gulf Shoreline Restoration Report*
- [21] Seed, R.B. et al. [2006] – Independent Levee Investigation Team – ‘Investigation Of The Performance Of The New Orleans Flood Protection Systems In Hurricane Katrina on August 29, 2005’, *Final Report*
- [22] Van der Ven, G.P. [1993] – ‘Leefbaar Laagland’, *Book*
- [23] Voortman, H.G. [2003] – ‘Risk Based Design Of Large Scale Flood Defense Systems’, *Doctoral Thesis, Delft University Of Technology*

Reports provided by the U.S. Army Corps of Engineers

- [24] U.S. Army Corps Of Engineers [1957] – Design Memorandum 1A – ‘Mississippi River Gulf Outlet’, *Report*
- [25] U.S. Army Corps Of Engineers [1959] – Design Memorandum 1B – ‘Mississippi River Gulf Outlet’, *Report*
- [26] U.S. Army Corps Of Engineers [2004] – ‘Coastal Wetlands Planning, Protection And Restoration Act: Lake Borgne – Mississippi River Gulf Outlet Shoreline Protection (PO-32)’, *Final Design Report*
- [27] U.S. Army Corps Of Engineers [2005] – ‘Assessment Of Hurricane Protection In Southeast Louisiana’, *Final Report*
- [28] U.S. Army Corps Of Engineers [2006] – Interagency Performance Evaluation Taskforce – ‘Performance Evaluation Of The New Orleans And Southeast Louisiana Hurricane Protection System’, *Draft Report*
- [29] U.S. Army Corps Of Engineers [2006] – Interagency Performance Evaluation Taskforce – ‘Performance Evaluation Of The New Orleans And Southeast Louisiana Hurricane Protection System’, *Final Report – Volume 1: Executive Summary And Overview*
- [30] U.S. Army Corps Of Engineers [2006] – Interagency Performance Evaluation Taskforce – ‘Performance Evaluation Of The New Orleans And Southeast Louisiana Hurricane Protection System’, *Final Report – Volume 3: The Hurricane Protection System*
- [31] U.S. Army Corps Of Engineers [2006] – Interagency Performance Evaluation Taskforce – ‘Performance Evaluation Of The New Orleans And Southeast Louisiana Hurricane Protection System’, *Final Report – Volume 4: The Storm*
- [32] U.S. Army Corps Of Engineers [2006] – Interagency Performance Evaluation Taskforce – ‘Performance Evaluation Of The New Orleans And Southeast Louisiana Hurricane Protection System’, *Final Report – Volume 5: The Performance – Levees And Floodwalls*
- [33] U.S. Army Corps Of Engineers [2006] – Interagency Performance Evaluation Taskforce – ‘Performance Evaluation Of The New Orleans And Southeast Louisiana Hurricane Protection System’, *Final Report – Volume 7: The Consequences*
- [34] U.S. Army Corps Of Engineers [2006] – ‘Mississippi River Gulf Outlet Deep Draft De-Authorization Interim Report To Congress’, *Report*
- [35] U.S. Army Corps Of Engineers [2006] – ‘Mississippi River Gulf Outlet Environmental Restoration Features’, *A Near Term Critical Feature For The Louisiana Coastal Area Plan*
- [36] U.S. Army Corps Of Engineers [2006] – Louisiana Coastal Protection And Restoration (LACPR) – ‘Preliminary Technical Report to United States Congress’, *Final Report*
- [37] U.S. Army Corps Of Engineers [2006] – Louisiana Coastal Protection And Restoration (LACPR) – ‘Preliminary Technical Report to United States Congress’, *Enclosure F: Engineering Investigations*
- [38] U.S. Army Corps Of Engineers [2007] – ‘Mississippi River Gulf Outlet Deep Draft De-Authorization Report: Draft Integrated Final Report And Legislative Environmental Impact Statement’, *Final Report*

Course books

- [39] Bijlaard, F.S.K. and Abspoel, R. [2004] – ‘Steel Structures’, *Course Book, Delft University Of Technology*
- [40] Groeneveld, R. [2002] – ‘Inland Waterways’, *Course Book, Delft University Of Technology*
- [41] Holthuijsen, L.H. [2006] – ‘Waves In Oceanic And Coastal Waters’, *Course Book, Delft University Of Technology*
- [42] Jongeling, T.H.G. [2006] – Analysis Of A Gate On Vibrations’, *Paper, Delft University Of Technology*, which uses:
 - [43] Kolkman, P.A. and Jongeling, T.H.G. [1996] – Dutch Technical Advisory Committee On Flood Defences – ‘Dynamic Behavior Of Hydraulic Structures’, *Report*
 - [44] Lewin, J. [1995] – American Society Of Civil Engineers – ‘Hydraulic Gates And Valves In Free Surface Flow And Submerged Outlets’, *Book*
- [45] Vrouwenvelder, A.W.C.M. [2006] – ‘Structural Dynamics’, *Course Book, Delft University Of Technology*

PROTECTING NEW ORLEANS:

***REVISION OF THE HURRICANE PROTECTION SYSTEM IN ORDER TO
PREVENT LAKE BORGNE INDUCED FLOODING DURING HURRICANES***

APPENDICES

E.A. van Vugt

23/05/2008



APPENDIX A – Hydrodynamic Modeling: General Overview (Including PMH) And Results For Hurricane Katrina [37]

A.1 General overview and introduction of the Probable Maximum Hurricane (PMH)

Hydrodynamic modeling of storm surge and waves has been conducted by the U.S. Army Corps of Engineers' Interagency Performance Evaluation Task Force (USACE-IPET) in order to predict wave action at several proposed levee alignments in combination with the water level response. The modeling results will be input to engineering and design processes in the future. For this modeling, a single screening storm was selected and simulated on ten separate tracks. It should be noted that ten tracks will not provide comprehensive coverage in order to define water levels at every location.

This appendix also briefly describes wind and atmospheric pressure modeling, storm surge modeling and offshore / near shore wave modeling. Results from these various models are used to estimate maximum waves and water levels along the proposed levee alignments presented in figure A.1.

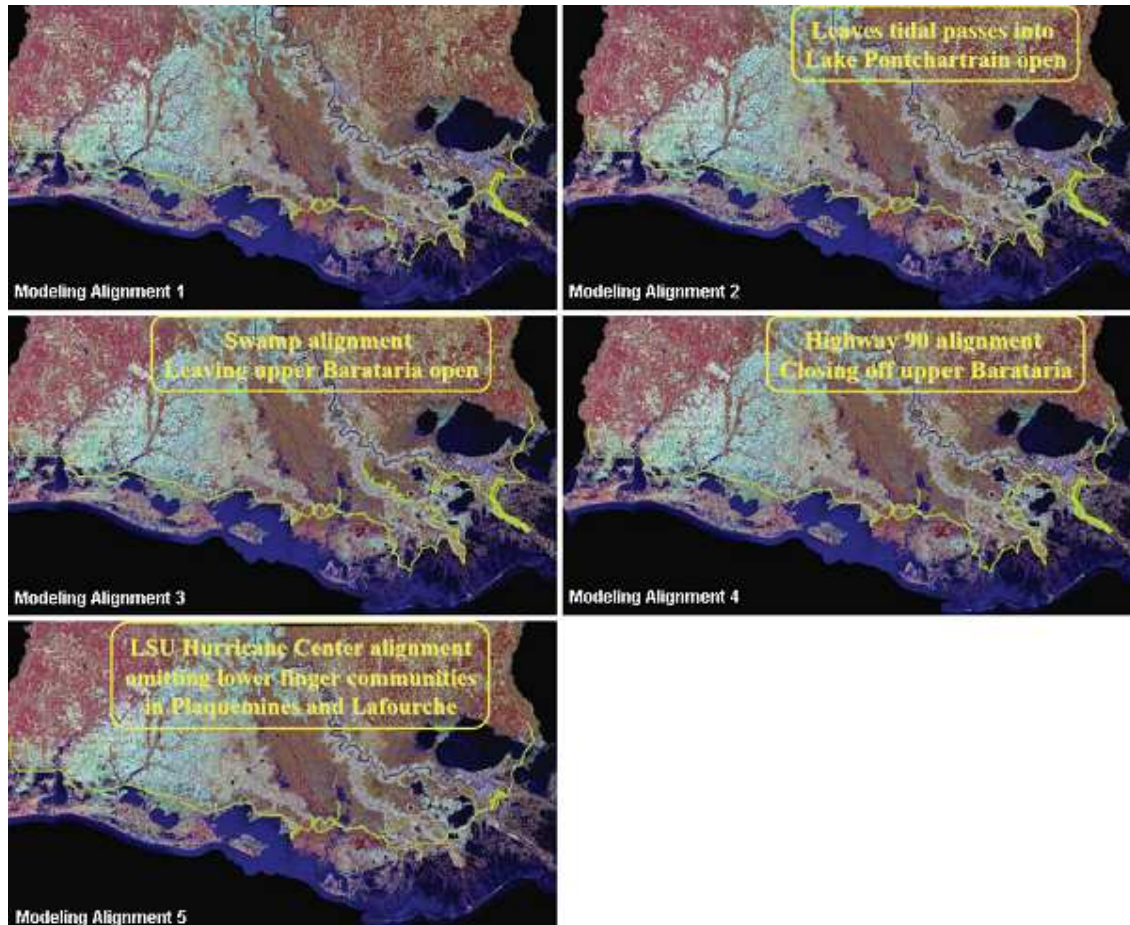


Fig. A.1: Proposed levee alignments along which the maximum waves and water levels are modeled [37]

- Modeling Alignment 1 places a barrier levee across Lake Pontchartrain and along the southwest edge of Lake Borgne. It then generally follows the alignments of existing and proposed hurricane protection projects to Morgan City and runs along the GIWW in the western part of the state. The protection ties into high ground near the Texas border. This alignment includes barrier structures across Lake Pontchartrain in the Rigolets and Chef Passes.
- Modeling Alignment 2 is the same as Alignment 1 except that the Rigolets and Chef Mentour Passes, the two major channels that connect Lake Pontchartrain to Lake Borgne and the Gulf of Mexico, are left open.
- Modeling Alignment 3 is the same as Alignment 1 except that the interior of the Barataria Basin is left open and highly developed areas are protected by levees extending up the wetland interface on both sides of the basin.
- Modeling Alignment 4 is the same as Alignment 1 except that the levee across the Barataria Basin follows Highway 90.
- Modeling Alignment 5 follows Alignment 1 except that it cuts through St. Bernard Parish and leaves out most of Plaquemines Parish and other communities in the southwestern part of the state.

The storm selected for the rough order of magnitude estimations is based on the probable maximum hurricane (PMH) as documented in NOAA's Technical Report NWS 23 [1979]. The PMH-criteria for the Louisiana coast describe a storm of Category 5 intensity on the Saffir-Simpson Scale. Several characteristic parameters:

- The radius to maximum winds is set at 11 NM (20.4 km), corresponding to the only Category 5 hurricane that ever struck the area at landfall [Hurricane Camille, 1966];
- For storm surge modeling, the storms were translated both at the historical hurricane track speed and at a constant 10 knots (19.4 m/s);
- The PMH was run on ten historical tracks with landfalls across coastal Louisiana with different approach angles. The tracks were selected to result in Category 5 hurricane surge levels at locations across proposed structural alignments. The selected tracks are summarized in table A.1 and plotted in figure A2.

Track	Description	Naming convention
1	Hurricane Katrina	T1 — blue line with circles
2	Hurricane Andrew shifted 1.0 deg east	T2 — red line with circles
3	1947 storm shifted 0.25 deg south	T3 — green line with circles
4	Hurricane Rita	T4 — cyan line with circles
5	Hurricane Carmen	T5 — red line with circles
6	1915 storm	T6 — green line with circles
7	1893 storm shifted 0.5 deg west	T7 — magenta line with circles
8	Hurricane Rita shifted 1.0 deg east	T8 — cyan line with circles
9	Hurricane Camille shifted 0.5 deg west	T9 — blue line with circles
10	1893 storm shifted 2.5 deg west	T10 — magenta line with circles

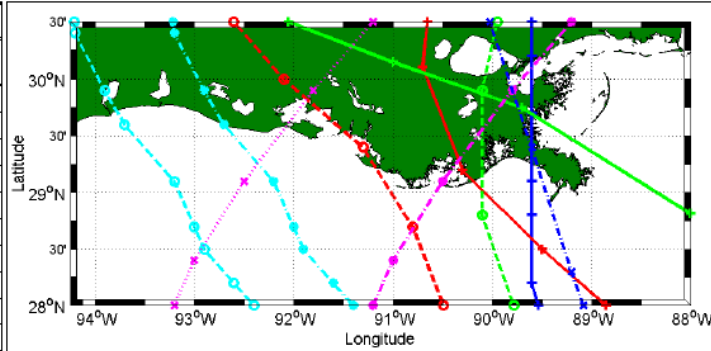


Table A.1: Modeled hurricane tracks [37]

Fig. A.2: Modeled hurricane tracks [37]

Storm surge is a function of many factors including, wind speed, translation speed, landfall location, orientation of the storm track at landfall to the shoreline, levee alignment orientation and storm size. Therefore, there is the need to abandon an event-driven approach that considers only particular storms and move towards a risk based approach that addresses how often assets and populations become inundated and how severe that inundation is for storm events of particular characteristics. This is outside the scope of this report.

Wind and atmospheric pressure

The wind and pressure fields were developed with a highly refined numerical model for the specification of surface wind and pressure fields in tropical cyclones. This model specifies the surface wind and pressure field in tropical cyclones and is referred to as the Planetary Boundary Layer Model [Thompson and Cardone, 1996]. Model inputs include the central pressure index (CPI), radius to maximum wind (RMW), forward velocity and storm track locations. The simulation assumes that a hurricane is steady state offshore and does not begin to weaken until the center arrives at the coast. Model calibration was required to explore and define additional storm criteria that are not included in the PMH criteria. The calibration effort required a period of experimentation with recent Gulf of Mexico storms of intensity comparable to the PMH. Hurricanes Ivan [2004] and Katrina [2005] were selected. The main objective of the calibration is to ensure that the surface marine wind field specified is consistent with modern thinking as to the relationship between the storm criteria and inner core maximum surface winds for modern averaging intervals.

The maximum wind speed generated over space and time is approximately 135 mph (60 m/s). This speed is based on a 10-m equivalent neutrally stable, 30-minute average wind speed. If the maximum wind speed is converted to a 1- minute average, which is the general average interval to quantify the Saffir-Simpson Hurricane Scale, the magnitude would be about 166 mph (74 m/s) or an intense Category 5 hurricane. The final 30-minute wind and pressure fields provided input to the surge and wave models.

Storm surge modeling

The ADvanced CIRCulation (ADCIRC) hydrodynamic model [Leutlich et al., 1992] is being applied to estimate the storm surge generated by the PMH. ADCIRC is a finite-element hydrodynamic circulation numerical model for the simulation of water level and current over an unstructured gridded domain. ADCIRC is a two-dimensional depth-integrated model that can simulate tide-, wind- and wave-driven circulation in coastal waters as well as hurricane storm surge and flooding. Extensive storm surge model development, application and validation efforts have been conducted in southern Louisiana. [Westerink et al., 2005 and Feyen et al., 2005]. ADCIRC was chosen by IPET for simulating long wave hydrodynamic processes. Imposing the wind and atmospheric pressure fields, the ADCIRC model can replicate tide-induced and storm-surge water levels and currents. The ADCIRC model uses the finite-element approach in solving governing equations over a complicated bathymetry, commonly encompassed by irregular sea and shore boundaries.

Hurricane surge water surface elevations were generated for all ten storm tracks. The storm surge can be sensitive to the hurricane translation speed as a slower moving storm allows more time for the winds to push the water toward the coast. Therefore, the storms were run at both historical translation speeds and at a constant 10 knots (19.4 m/s). Model results also indicate that surges tend to be larger in levee 'pockets', which are areas along the levee alignment with acute angles. The levees in these areas confine the surge, not allowing it to spread along the coast. This effect is seen on a larger scale east of the Mississippi River, as the geography of the Lake Borgne area catches the surge of hurricanes making landfall to the east. The sensitivity of surge potential is intensified on this part of southern Louisiana coast due to the complex geometry of the levees and the coast.

Sensitivity runs were performed to compare the surges estimated by the model for the PMH to historical storms to put the estimated surges for the screening storm into a historical context. The surges estimated by the model for the PMH track T1 were compared to that calculated for Hurricane Katrina. Some of the stretches of the Louisiana levees most impacted by T1 and T9 are the south shore of Lake Pontchartrain and from Slidell (on the eastern shore of Lake Pontchartrain) to English Turn (near Caernarvon, along the Mississippi River). Relative to Hurricane Katrina, the PMH surges were 1 to 2 ft (0.3 to 0.6 m) lower from Slidell to English Turn and surges were 3 to 5 ft (0.9 to 1.5 m) higher along the south shore of Lake Pontchartrain.

Offshore wave modeling

The generation of the wave field and directional wave spectra for the various hurricane storm tracks is based on the implementation of a third generation discrete spectral wave model called WAM [Komen et al., 1994]. Each packet of energy in frequency and direction is propagated based on the group speed for the frequency band and water depth. This assumes linear theory and superposition of wave packets. In a fixed longitude and latitude grid system curvature effects are resolved where the energy is propagated in a spherical coordinate system. As the water depth decreases, the full dispersion relationship is applied and wave shoaling and refraction effects the propagation of the energy packets. The wave model simulations reflect the time and spatial variation of one hurricane wind field projected onto various storm tracks. This will depict the growth and propagation of the wave energy in the target domains. The analysis continues into the Region-scale modeling domain. The overall maximum H_{mo} estimates are provided for each of the 10 hurricane track simulations are displayed in table A2.

Maximum Wave Height Locations		Basin				Region			
Trk #	Description	H_{mo} (ft)	Storm Duration (Days)	Location		H_{mo} (ft)	Storm Duration (Days)	Location	
				Long	Lat			Long	Lat
1	Hurricane Katrina	56	4.50	-87.40	24.50	54	4.50	-89.40	28.65
2	Hurricane Andrew shifted 1.0-deg east	59	3.50	-88.20	27.80	57	3.50	-89.25	28.55
3	1947 Storm shifted 0.25-deg south	60	3.25	-88.05	29.10	60	3.25	-88.15	29.15
4	Hurricane Rita	57	5.00	-85.80	24.50	48	5.00	-92.60	28.50
5	Hurricane Carmen	56	4.25	-90.10	26.80	48	4.25	-90.40	28.50
6	1915 Storm	56	4.75	-88.40	26.10	55	4.75	-89.80	28.50
7	1893 Storm shifted 1.0-deg east	56	6.50	-86.70	25.60	45	6.50	-90.50	28.50
8	Hurricane Rita shifted 1.0-deg east	55	4.75	-90.50	27.30	48	4.75	-91.60	28.50
9	Hurricane Camille shifted 0.5-deg west	57	4.25	-89.10	28.60	58	4.25	-89.15	28.75
10	1893 Storm shifted 2.5-deg west	53	6.50	-92.60	24.60	49	6.50	-92.70	28.50

Table A.2: Maximum wave height estimates for each of the 10 hurricane track simulations [37]

Near shore wave modeling

Near shore waves need to be determined in order to calculate wave run-up, overtopping on structures and wave forces on structures. The numerical model STWAVE [Smith, Sherlock and Resio, 2001 / Thompson, Smith and Miller, 2004] was applied to generate and transform waves to the shore. The STWAVE-model can be implemented as either a half-plane model, meaning that only the waves propagating toward the coast are represented, or a full-plane model allowing generation and propagation in all directions. The source terms include wind input, nonlinear wave-wave interactions, dissipation within the wave field and surf zone breaking. The assumptions made in the STWAVE-model are as follows:

- Mild bottom slope and negligible wave reflection.
- Steady waves, currents and winds.
- Linear refraction and shoaling.
- Depth-uniform current.

The STWAVE-model outputs a zero-moment wave height, peak wave period and mean wave direction at all grid points. An option is added to input variable wind and surge fields. The surge significantly alters the wave transformation and generation for the hurricane simulations in shallow areas like Lake Pontchartrain and Lake Borgne. Spatially varying wind input is important to simulate the complex wind fields in hurricanes.

Conclusion – Estimated maximum waves and water level

The storms simulated for the initial screening provide limited coverage across the Louisiana coast. The simulated storm tracks impact short reaches of the levee with the highest waves and surge. However, these impacts could occur over extensive reaches of the levee with changes in storm landfall location. Therefore, for rough order of magnitude cost estimation purposes, the estimated maximum surge elevations and waves were spread along the levee applying engineering judgment. Track T3 produced the worst conditions for the south shore of Lake Pontchartrain and on the easterly reaches north of English Turn, while track T7 generated the greatest surge at the levee south of English Turn. Tracks T2 and T7 produced the most severe conditions in the Barataria reach. Track T10 produced the most severe conditions along the central and westerly reaches and track T4 produced the most extreme conditions on the far western reaches.

A summary of the maximum wave and surge levels applied for the levee cost estimation for each alignment is provided in the following table A.3. Figure A.3 presents an overview of the used save points.

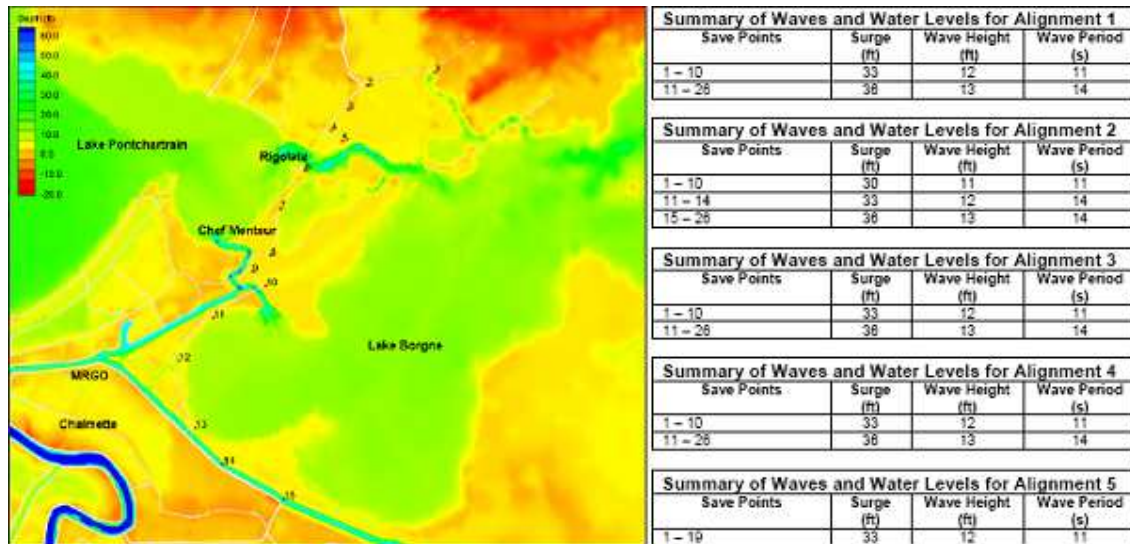


Fig. A.3: Save points adjacent to Lake Borgne [37]

Table A.3: Summary of waves and water levels [37]

Maximum surge elevations range from 15 to 20 ft (4.6 to 6.1 m) in Lake Pontchartrain and 30 to 40 ft (9.1 to 12.2 m) elsewhere along the coast. Maximum waves range from about 10 to 15 ft (3.0 to 4.6 m) with peak wave periods of 8 to 14 s. For the PMH storm, opening of the tidal passes decreases surges on the levee at the Pontchartrain land bridge by about 3 ft (0.9 m) and increases water levels in the lake by about 1.5 ft (0.5 m).

It should be noted, that the impact of allowing the tidal passes to remain open could increase water levels further in Lake Pontchartrain for larger, slower moving storms and additional analysis is required. Opening Barataria Basin (Alignments 3 and 4) reduces surges along the levees by several feet but requires substantially longer levees. Smoothing the levee alignment (Alignment 5) reduces the surges east of the river 3 to 5 ft (0.9 to 1.5 m).

A.2 Southern Louisiana – storm peak water levels for *Hurricane Katrina* using the ADCIRC model

Figure A.4 shows color shaded contours of the maximum water level computed for the storm at each grid node of the ADCIRC model, in feet NAVD88 (2004.65), for the southern Louisiana region. Figure A.5 shows maximum water level contours for the metropolitan New Orleans vicinity in feet NAVD88 (2004.65).

The maximum water level occurred mid-way along the levee system and decreases to the north. Adjacent to the levees along the MRGO, maximum computed water levels are 16 to 17 ft (4.9 to 5.2 m). The model predicts a low gradient in water level within the GIWW/MRGO, decreasing water levels from east to west, with a peak water level of about 14 ft (4.3 m) at the confluence of the GIWW/MRGO and the IHNC. From this point south to the IHNC Lock, water levels are fairly constant at approximately 14 ft (4.3 m). From the confluence to the northern extent of the IHNC, a high water level gradient is computed. Along the south shore of Lake Pontchartrain, maximum levels were computed to range of 9 to 10 ft (2.7 to 3.0 m). Note that these computed peak water levels do not include the effects of wave setup or run-up at the levee systems.

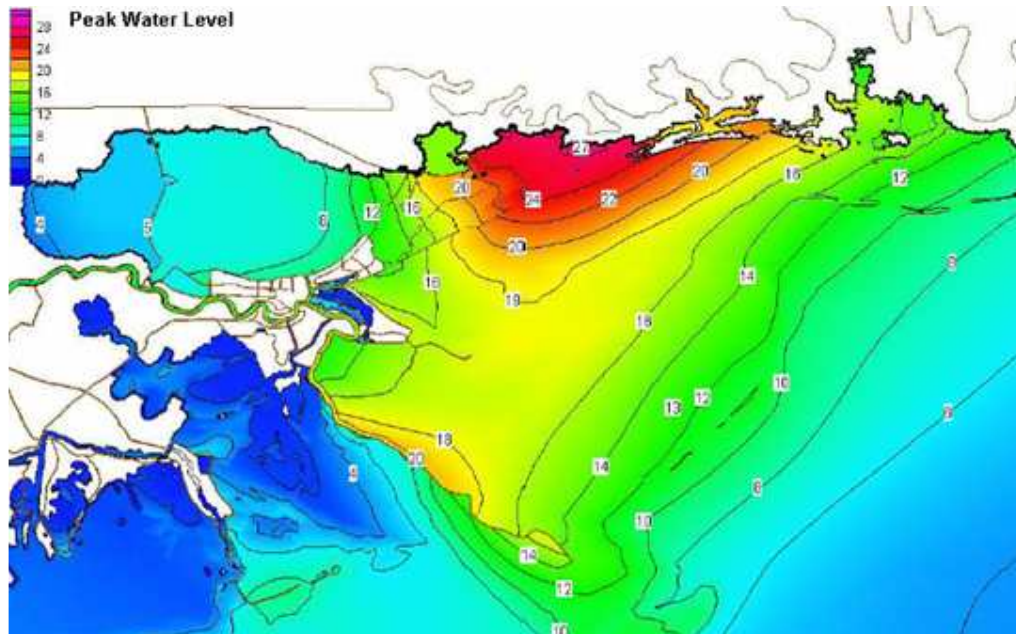


Fig. A.4: Southern Louisiana – maximum computed storm water level using the ADCIRC model (in ft NAVD88 (2004.65)) [31]

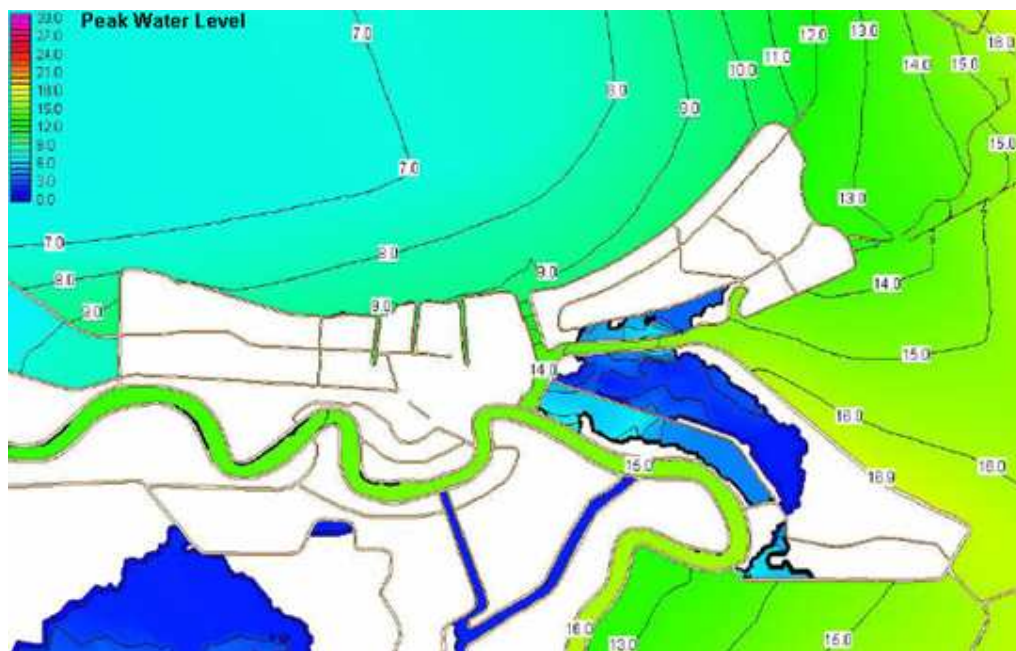
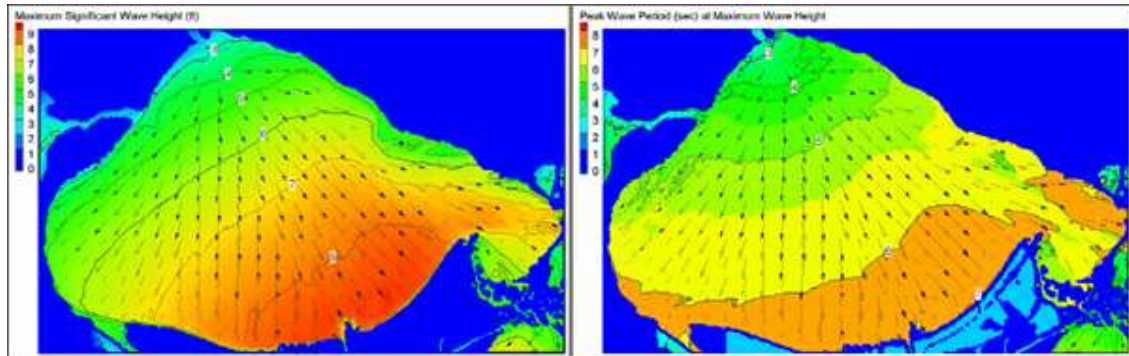


Fig. A.5: New Orleans area – maximum computed storm water level using the ADCIRC model (in ft NAVD88 (2004.65)) [31]

A.3 Southern Louisiana – maximum wave conditions for *Hurricane Katrina* using the STWAVE model

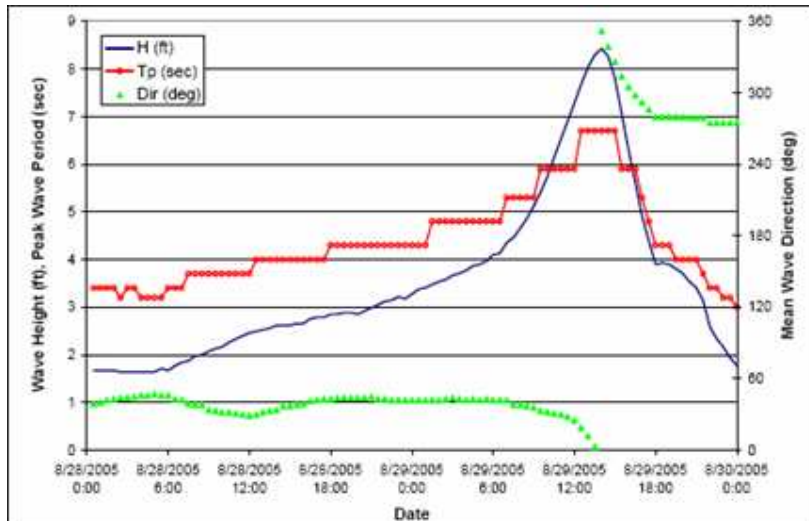
Lake Pontchartrain

The peak wave conditions on the south shore of Lake Pontchartrain occur at approximately 1330–1430 UTC on 29 August 2005. Figure A.6 (left) shows the maximum significant wave height for the entire simulation period for each grid cell within the domain, along with the corresponding mean wave direction. Figure A.6 (right) shows the peak wave period corresponding to the maximum wave height for each cell. The maximum wave heights range from 8.0 to 8.7 ft (2.4 to 2.6 m) on the New Orleans lakefront and the associated peak periods are 6.5 to 7.5 s.



A.6: Left – Lake Pontchartrain: maximum significant wave height and mean direction (wave heights in feet) [31]
 Right – Lake Pontchartrain: peak wave period corresponding to the maximum wave height (periods in seconds) [31]

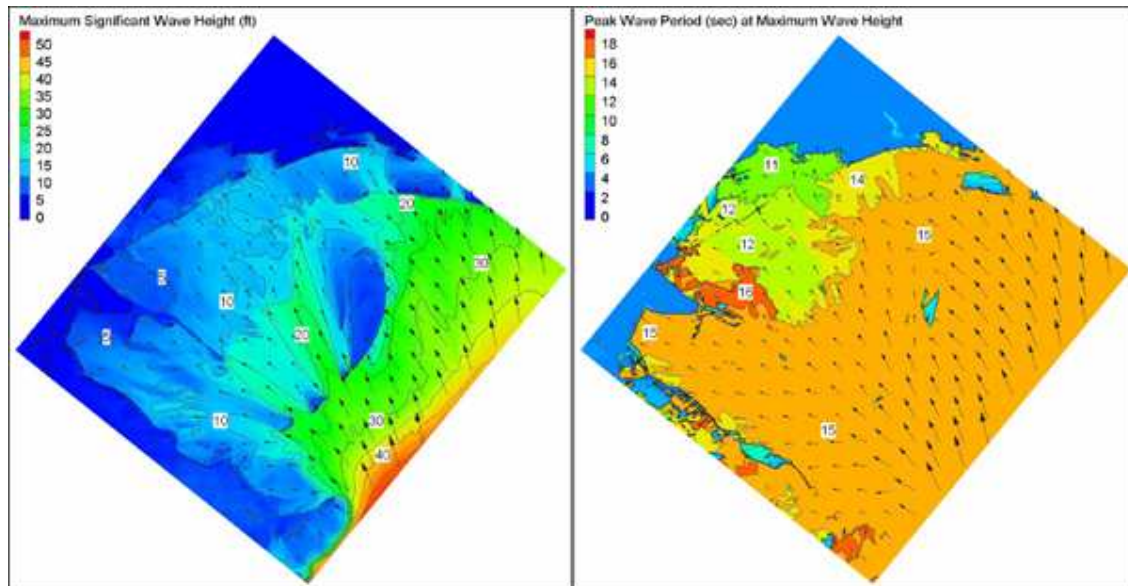
Figure A.7 shows the variation of significant wave height, peak period and mean wave direction at a site along the southern shoreline of Lake Pontchartrain in the vicinity of the entrance to Orleans Avenue Canal. In the early stages of the storm just before landfall, winds are from the northeast and waves approach from the same direction. As the storm approaches, winds increase in speed and both wave height and wave period steadily increase. As the storm makes landfall and its center moves northward, winds begin to shift blowing from the northeast then from the north. Winds are blowing out of the north at the time peak wave conditions are generated along the south shoreline of the lake. Local wave generation within the lake tracks closely with the local wind speed and wind direction. Peak wave heights are about 8.4 ft (2.5 m) and peak periods are 6.7 s. As the storm passes and moves into the state of Mississippi, winds continue to shift, finally blowing from the northwest. Wave heights and periods decrease rapidly following passage of the storm.



A.7: Temporal variation of significant wave height, peak period and mean wave direction along the southern shoreline of Lake Pontchartrain (time is referenced to UTC) [28]

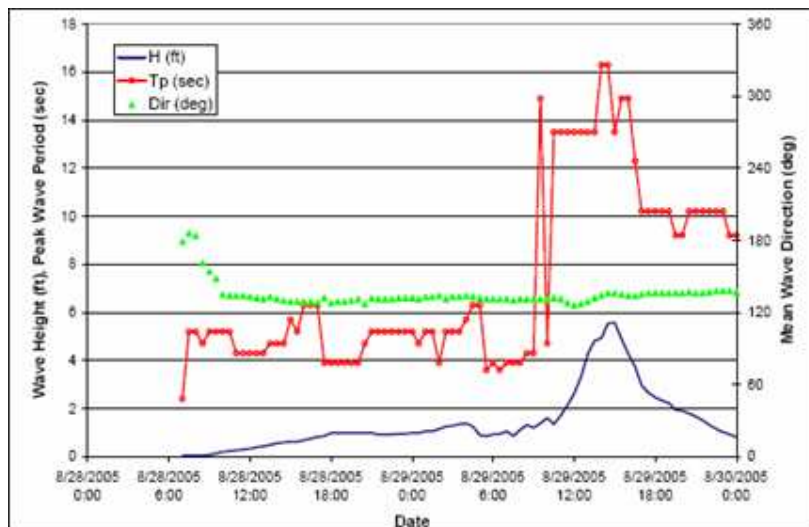
Southeastern Louisiana / Lake Borgne

The peak wave conditions on the southeast grid occur between approximately 1000 and 1500 UTC on 29 August 2005. The highest waves along the Mississippi River Levees occur around 1000-1200 UTC and along the Lake Borgne Levees around 1400-1500 UTC. Figure A.8 shows the maximum wave height with its corresponding wave direction and wave period for the entire simulation period for each grid cell within the domain. The maximum wave heights range from 4 to 10 ft (1.2 to 3.0 m) along the hurricane protection system levees and the associated periods are 7 to 16 s. The longer wave periods originate from wave energy traveling between and over the islands from the Gulf of Mexico. Large wave heights occur in lower Plaquemines Parish. The peak periods are relatively large, reaching up to 16 s, caused by wave penetration through and over the barrier islands.



A.8: Left – Southeast Louisiana: maximum wave height and corresponding mean direction (wave heights in feet) [31]
 Right – Southeast Louisiana: peak wave period corresponding to the maximum wave height (periods in seconds) [31]

Figure A.9 shows the variation of significant wave height, peak period and mean wave direction near Bayou Bienvenue along the MRGO. In the early stages of the storm wave heights are quite low, on the order of 1 to 1.5 ft (0.3 to 0.5 m). Wave periods range between 4 and 6 s. These periods are typical of locally generated wind sea conditions. Waves approach from the southeast (direction of 135 degrees). As the hurricane makes landfall, wave energy begins to increase, as does the wave period as larger swells from the gulf arrive at the levee. The peak significant wave height reaches 5.7 ft (1.7 m) and the peak period reaches 16 s. Wave direction remains constant out of the southeast the entire time. As the storm passes wave heights decrease rapidly, peak wave periods decrease to 10 s.



A.9: Temporal variation of significant wave height, peak period and mean wave direction at Bayou Bienvenue outlet structure (time is referenced to UTC) [28]

A.4 Hurricane Katrina – comparison of wave maxima and water level maxima with design values

Peak wave and water level conditions experienced during Hurricane Katrina are compared to values used in design of the hurricane protection system. In the series of figures that follow, design values are shown in yellow boxes (label D), values computed by model are shown in blue (label C) boxes and measured values are shown in green boxes (label M).

Design values were taken from design documents. Design water levels are cited in this section, not design crest elevations of the protection system. For wave conditions, design documents cited significant wave height and period. These documents do not specify whether a peak or mean period was used. At the time the projects were designed, the distinction between measures of wave period was probably not made. Computed wave maxima are based on regional STWAVE model results (significant wave height, peak wave period).

The design documents cite water levels relative to a number of different vertical datums, such as mean sea level (MSL), National Geodetic Vertical Datum (NGVD) and still-water level (SWL). The earliest design documents cited SWL and MSL, later design documents tended to cite NGVD. All design water levels were converted to the common datum NAVD88 (2004.65) for the purposes of comparison. In all areas of the protection system considered here, local mean sea level (LMSL) datum is above the NAVD88 (2004.65) datum. The local mean sea level term is used, rather than simply mean sea level, to indicate that the correction does vary depending on location. To make the datum conversion from the design MSL to NAVD88 (2004.65), 0.5 ft (0.15 m) is added to the design water level values along the south shore of Lake Pontchartrain and in the Inner Harbor Navigation Canal (IHNC) and 0.4 ft (0.12 m) is added to values in the vicinity of the Gulf Intracoastal Waterway (GIWW) and Mississippi River Gulf Outlet (MRGO) channels.

For measured water level conditions at sites where hydrographs captured the peak water level, that value is presented. Where high water marks are available, those values are shown. If no high water marks are available in an area of interest, it is listed with a question mark following the listed elevation. Computed water level maxima were based on regional ADCIRC model results and relative to NAVD88 (2004.65).

Orleans Parish (Lake Pontchartrain)

Figure A.10 (left) presents wave maxima for the south shore of Lake Pontchartrain in Jefferson and Orleans Parishes. Significant wave heights measured for Katrina exceeded design wave heights by 0.6 to 1.6 ft (0.18 to 0.5 m). Computed wave heights are about 0.5 ft (0.15 m) higher than design heights. Peak wave periods during Katrina were about equal to the design values. In general, Katrina wave conditions are similar to design values along the south shoreline of Lake Pontchartrain.

Figure A.10 (right) presents water level maxima for the same area. The design water level is 12.0 ft (3.6 m) NAVD88 (2004.65) throughout this region. Observed peak water levels during Katrina occurred at the entrances to the outfall canals, ranging from 0.6 to 1.2 ft (0.18 to 0.4 m) below design values. The peak values were based on the trend in high water mark data along the south shore of the lake.



Fig. A.10: Left – Jefferson and Orleans Parishes: comparison of wave maxima with design values [31]
 Right – Jefferson and Orleans Parishes: comparison of water level maxima with design values [31]

Orleans East Parish

Figure A.11 (left) presents wave maxima for the eastern section of Orleans Parish. On Lake Pontchartrain, significant wave heights computed for Katrina exceeded design wave heights up to 1.6 ft (0.5 m). Peak wave periods were slightly less than the design values. On the east-facing side of the parish, significant wave heights computed for Katrina exceeded the design value by 1 ft (0.3 m). Wave period are about equal to the design value. In general, for these two reaches of the project, Katrina wave conditions were similar to design values.

On the back levee of Orleans Parish, along the GIWW with exposure to Lake Borgne, maximum significant wave heights computed for Katrina were less than design values, but the peak wave periods exceed the design values by about a factor of 3. The design wave periods are more typical for conditions with a restricted fetch. Wave model simulations suggest that during Katrina the eastern facing levees were subjected to longer-period wave propagating in from the Gulf of Mexico.

Figure A.11 (right) shows water level maxima for the area. On the Lake Pontchartrain side, the design water level is 12.0 ft (3.6 m) NAVD88 (2004.65) and the measured peak water level at the entrance to the IHNC was 11.8 ft (3.6 m). At this location, the peak water levels were at the design levels. Along the east-facing levees adjacent to Chef Menteur Pass, design water levels increased from 12.0 ft (3.6 m) at South Point to 13.4 ft (4.1 m) at the GIWW. High water marks acquired along this section of levee and near the GIWW at Chef Menteur suggest that design water levels were exceeded by amounts greater than 2 ft (0.6 m) at the southern end of this reach.



Fig. A.11: Left – Eastern section of Orleans Parish: comparison of wave maxima with design values [31]
 Right – Eastern section of Orleans Parish: comparison of water level maxima with design values [31]

St. Bernard Parish

Figure A.12 (left) shows wave maxima for the eastern portion of St. Bernard Parish. Along the MRGO, the significant wave heights computed for Katrina were less than the design wave heights. However, peak wave periods computed for Katrina were 2.5 times greater than the design values. On the south-facing portion of the protection levees, the computed significant wave heights computed less than design values by about 2.5 ft (0.8 m), but wave periods exceed design values by a factor of about 3. Design wave conditions at these locations should be reexamined. Lower wave heights will reduce run-up but the higher wave periods increase wave run-up. Figure A.12 (right) shows water level maxima for eastern St. Bernard Parish and the back levee of Orleans Parish. On the back levee adjacent to the GIWW, the design water level is 13.4 ft (4.1 m) NAVD88 (2004.65). Reliable high water mark data suggest that design water levels were exceeded along this reach by at least 2 ft (0.6 m). Along the MRGO adjacent to the protection levees, design water levels ranged from 12.9 to 13.4 ft (3.9 to 4.1 m). Computed maximum water levels range from 15.4 to 16.8 ft (4.7 to 5.1 m). Reliable high water marks near Shell Beach, which is located further to the southeast and not fronting the hurricane protection levee, ranged from 17.1 to 18.7 ft (5.2 to 5.7 m). Reliable marks from Paris Road Bridge, further to the northwest but in the GIWW channel, were 15.5 ft (4.7 m). Considered together, model and measured data sources suggest that Katrina peak water levels exceeded design levels by 2 to 5 ft (0.6 to 1.5 m) along the section.

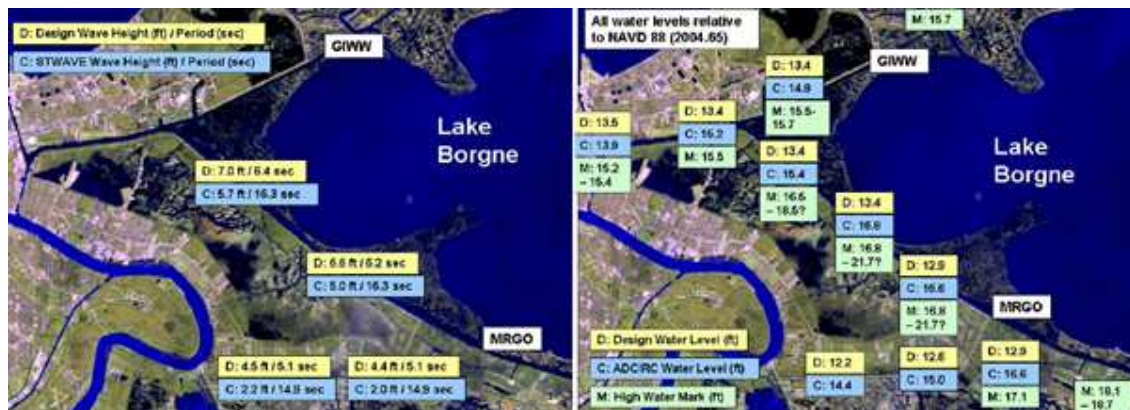


Fig. A.12: Left – St. Bernard Parish: comparison of wave maxima with design values [31]
 Right – St. Bernard Parish: comparison of water level maxima with design values [31]

APPENDIX B – Analytical Validation Of The Hydrodynamic Modeling Results For Hurricane Katrina

B.1 Wave conditions offshore and near shore

Strong winds can cause extreme wave conditions, characterized by high wave heights and long wave periods. In shallow water near shore, wind causes a considerable increase in the water level with respect to the astronomic tide. This wind setup and wave conditions depend on the same driving force. A strong dependence between the two is expected under extreme conditions. The hydraulic conditions in front of a protection system can be considered to be the result of two influences:

- The weather system determines the hydraulic conditions;
- The local bathymetry influences transfer of offshore conditions to the flood protection system or structure and influences local generation of wind setup and waves.

The weather system can be considered the dominating factor for hydraulic conditions if the water depth is sufficiently large [23]. Influence of bathymetry occurs in a relatively small region near the coast. Based on this image of hydraulic conditions, Vrijling and Bruinsma [1980] devised a conceptual model indicating a relation between weather system and hydraulic conditions offshore and near shore.

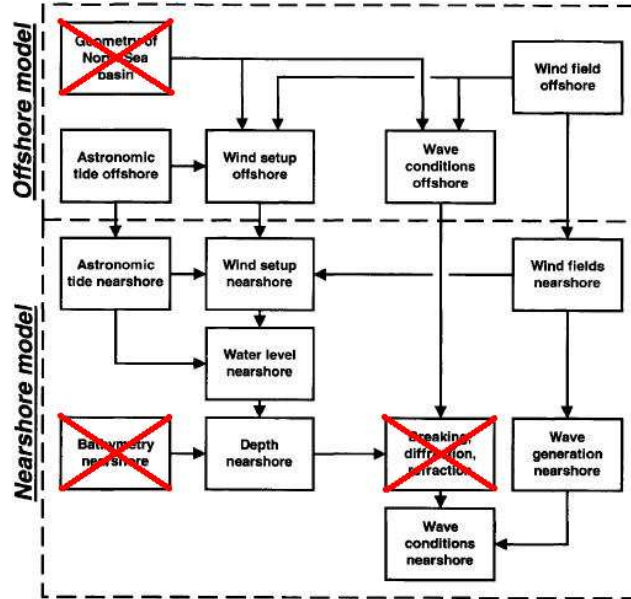


Fig. B.1: Conceptual model of hydraulic boundary conditions for a flood defence structure Vrijling and Bruinsma, 1980) [23]

Wave observations that are required to estimate past, present and future wave conditions are not always available. This is either because no instrument was operating at the required time and specific location or because the required conditions have not yet occurred. The only alternative in the absence of observations is to simulate the wave conditions, using wind information. For this analytical validation effort, models are used that are essentially just a generalization of observations made under ideal conditions. The models are simple in the sense that a few variables are involved and that the geometry offshore, bathymetry near shore and depth induced processes like breaking, diffraction and refraction are neglected.

B.1.1 SMB-model – wave conditions offshore: oceanic waters [41]

The wave model considered for the validation of the numerical model results in *deep water* is essentially a generalization of wave observations under conditions that approximate the following idealization: A constant wind field (constant in time and space) is blowing over deep water (waves not affected by the bottom, typically more than half wavelength), perpendicularly off a straight and infinitely long coastline. The waves are described with only a characteristic wave height and period. In this approach of idealized conditions, the waves depend only on the wind speed and the distance to the upwind coastlines (fetch) or the time elapsed since the wind started to blow (duration). In the idealized situation of wave generation, the wind is assumed to be constant. This introduces errors in estimating the significant wave height of up to 20%, even in such idealized situations [41].

The first systematic observations of the wave height and period under fetch limited conditions were made by Sverdrupp and Munk [1947], later modified by Bretschneider [1952]. Their results have been used widely. The corresponding parameterizations are generally known as the SMB-model, a model based on dimensionless parameters. The SMB-model is predominately suited for a basin with a constant depth and a constant wind speed over the length of the basin (uniform wind field). It should be noted again that there is no typical hurricane nor associated storm surge. The actual wind, wave and storm surge loadings imposed at any location during a hurricane are a function of location relative to the storm, wind speed, wind direction, offshore conditions, levee orientation, etc. These loadings vary over time as the hurricane moves progressively through the region.

For short fetches, simple power laws are generally used in the SMB-model:

$$\tilde{H} = a_1 \left(\tilde{F}^{b_1} \right) \quad \text{and} \quad \tilde{T} = a_2 \left(\tilde{F}^{b_1} \right)$$

Later, such observations were carried out by many other investigators. To represent these young sea states, the fully developed sea state and the transition between them, a tanh-function is often used. The reason is that this function has the property that, for small arguments, it approaches its argument: $\tanh(x) \rightarrow x$ for $x \ll 1$ and for large values of its argument it approaches unity: $\tanh(x) \rightarrow 1$ for $x \gg 1$.

Young and Verhagen [1996] added two parameters, p and q, to the tanh-expressions to control the transition from young sea states to the fully developed sea state:

$$\tilde{H} = \tilde{H}_\infty \left[\tanh \left(k_1 \tilde{F}^{\tilde{m}_1} \right) \right]^p \quad \text{and} \quad \tilde{T} = \tilde{T}_\infty \left[\tanh \left(k_2 \tilde{F}^{\tilde{m}_2} \right) \right]^q$$

Breugem and Holthuijsen [2006] corrected the results by evaluating more observations. The resulting coefficients are summarized below:

	Pierson and Moskowitz [1964]: <i>fully developed sea states</i>	Kahma and Calkoen [1992]: <i>young sea states</i>	Breugem and Holthuijsen [2006]: <i>all sea states</i>
$\tilde{H} = \tilde{H}_\infty$	$\tilde{H}_\infty = 0.24$	$\tilde{H} = a_1 \left(\frac{\tilde{F}^{\tilde{b}_1}}{\tilde{F}} \right)$ $a_1 = 2.88 \times 10^{-3}, \tilde{b}_1 = 0.45$	$\tilde{H}_\infty = 0.24$ $k_1 = 4.14 \times 10^{-4}, m_1 = 0.79$ $p = 0.572$
$\tilde{T} = \tilde{T}_\infty$	$\tilde{T}_\infty = 7.69$	$\tilde{T} = a_2 \left(\frac{\tilde{F}^{\tilde{b}_1}}{\tilde{F}} \right)$ $a_2 = 0.459, \tilde{b}_2 = 0.27$	$\tilde{T}_\infty = 7.69$ $k_2 = 2.77 \times 10^{-7}, m_2 = 1.45,$ $q = 0.187$

B.1.2 SMB-model – wave conditions near shore: coastal waters [41]

When waves enter coastal waters, their amplitude and direction will be affected by the limiting water depth:

- The phenomenon of waves changing in the direction of propagation due to variations in the wave group velocity in that direction is called *shoaling*. Near the coast this results in an increase in wave height.
- The phenomenon of the wave direction changing due to depth induced variations in the phase speed in lateral direction, thus along the wave crest, is called *refraction*. It turns the wave direction towards shallower water and results in either an increase or a decrease in wave height, depending on the actual changes in wave direction. These depth induced changes in amplitude and direction are usually sufficiently small over the distance of one wave length that locally the linear wave theory for waters with a horizontal bottom can be used.
- In some cases, variations in amplitude are not slow and the linear wave theory needs to be expanded. This is particularly true for wave propagating around obstacles such as breakwaters, small islands or headlands. The wave amplitude may vary rapidly across the geometric shadow line of such obstacles. The variation in amplitude causes waves to turn into areas with lower amplitude. This phenomenon is called *diffraction*.

The idealized case for wave growth in shallow waters is essentially the same as for deep water, except that water depth d is added as an extra parameter: A constant wind field (constant in time and space) is blowing perpendicularly off a straight and infinitely long coastline over water with a limited, constant depth. The waves are described with only the significant wave height and peak wave period. In this approach, the waves depend only on the wind speed, the distance to the upwind coastline (fetch), the time elapsed since the wind started to blow (duration) and the water depth.

In water with a constant, limited depth observations indicate that initially the water depth has no effect on the waves. The wave lengths at short fetches are so short that the depth/wavelength ratio is large and the water relatively deep. As the waves grow along the fetch, the wave length becomes longer and the depth becomes increasingly important. At very large fetch the waves are fully developed, but with lower values of the significant wave height and period than in deep water. Observations show that these limit values depend on the dimensionless water depth [19]. This dependence can be approximated with the following tanh-expressions:

$$\tilde{H}_{\infty,d} = \tilde{H}_\infty \tanh \left(k_3 \tilde{d}^{\tilde{m}_3} \right) \quad \text{and} \quad \tilde{T}_{\infty,d} = \tilde{T}_\infty \tanh \left(k_4 \tilde{d}^{\tilde{m}_4} \right)$$

Probably the best shallow water data set that is at present available to determine the coefficients of these tanh-expressions is obtained by Young and Verhagen [1996]. To control the transition for a young sea state to a fully developed sea state, Young and Verhagen [1996] added two extra parameters, p and q, to these expressions:

$$\tilde{H}_{\infty,d} = \tilde{H}_\infty \left[\tanh \left(k_3 \tilde{d}^{\tilde{m}_3} \right) \tanh \left(\frac{k_1 \tilde{F}^{\tilde{m}_1}}{\tanh \left(k_3 \tilde{d}^{\tilde{m}_3} \right)} \right) \right]^p \quad \text{and} \quad \tilde{T}_{\infty,d} = \tilde{T}_\infty \left[\tanh \left(k_4 \tilde{d}^{\tilde{m}_4} \right) \tanh \left(\frac{k_2 \tilde{F}^{\tilde{m}_2}}{\tanh \left(k_4 \tilde{d}^{\tilde{m}_4} \right)} \right) \right]^q$$

Breugem and Holthuijsen [2006] corrected the results by evaluating more observations. The resulting coefficients are summarized below:

	Pierson and Moskowitz [1964]: <i>fully developed sea states</i>	Kahma and Calkoen [1992]: <i>young sea states</i>	Breugem and Holthuijsen [2006]: <i>all sea states, all water depths</i>
$\tilde{H} = \tilde{H}_\infty$	$\tilde{H}_\infty = 0.24$	$\tilde{H} = a_1 \left(\frac{\tilde{b}_1}{F} \right)$	$\tilde{H}_\infty = 0.24$
		$a_1 = 2.88 \times 10^{-3}, b_1 = 0.45$	$k_1 = 4.14 \times 10^{-4}, m_1 = 0.79$
			$k_3 = 0.343, m_3 = 1.14, p = 0.572$
$\tilde{T} = \tilde{T}_\infty$	$\tilde{T}_\infty = 7.69$	$\tilde{T} = a_2 \left(\frac{\tilde{b}_1}{F} \right)$	$\tilde{T}_\infty = 7.69$
		$a_2 = 0.459, b_2 = 0.27$	$k_2 = 2.77 \times 10^{-7}, m_2 = 1.45$
			$k_4 = 0.10, m_4 = 2.01, q = 0.187$

B.1.3 SPM-model – calculating deep water wave characteristics associated with a hurricane [13]

The Shore Protection Manual (SPM) provides recommendations for the calculation of deep water wave characteristics associated with a hurricane. This method includes two equations, one for the maximum significant wave height and one for the associated wave period. The corresponding parameters are shown in table B.1:

Parameter	Dimension
Δp = central pressure deficit	[inches mercury]
V_F = forward translational speed	[knots]
R = radius to maximum winds	[nautical miles]
U_R = maximum sustained wind speed	[knots]
α = coefficient depending on hurricane speed	[-]

Table B.1: Parameters used in the SPM-model

The Coriolis parameter is given by: $f = 0.524 * \sin(\phi)$, where ϕ is the latitude at the location of interest. New Orleans is located at 30° N. The equation for maximum significant wave height and associated period are:

$$H'_{0,max} = 16.5 * e^{\frac{R * \Delta p}{100}} * \left[1 + \frac{0.208 * \alpha * V_F}{\sqrt{U_R}} \right] \quad T_p = 8.6 * e^{\frac{R * \Delta p}{200}} * \left[1 + \frac{0.104 * \alpha * V_F}{\sqrt{U_R}} \right]$$

The parameter U_R used in these equations is expressed in terms of the maximum sustained wind speed:

$$U_{max} = 0.868 * (73 * \sqrt{\Delta p} - 0.575 * R * f) \quad U_R = 0.865 * U_{max} + 0.5 * V_F$$

The value of the parameter α is recommended as unity (value of 1) for slowly translating hurricanes and this value is recommended for use here. This approach only provides reliable wave conditions offshore as the water depth is not taken into account. Therefore, only the offshore results will be presented.

B.1.4 Overview of input parameters and evaluation of analytical model results regarding wave conditions

The basin geometry is described only by basin the length (fetch) and depth, both deterministic values. The wave conditions depend mainly on the wind direction because of the highly irregular shape of the basin, both in depth and contour. For hurricanes the wind direction is of less importance and the radius of maximum winds becomes the characteristic parameter. The wind field characteristics of Hurricane Katrina are presented in table B.2:

Hurricane Katrina		wind field offshore	wind field near shore
Strength (Saffir-Simpson scale)	[-]	Category 5	Category 3
Maximum wind speed	[mph] [m/s]	> 155 > 70	111 – 130 50 – 58
Radius to maximum winds	[NM] [km]	25 – 30 45 – 55	25 – 30 45 – 55
Pressure hurricane	[mbar]	902	930
Forward translational speed	[m/s]	15	15

Table B.2: Wind field characteristics of Hurricane Katrina

Calculation results offshore wave conditions

– Results SMB-model (wave conditions offshore: oceanic waters):

Input: offshore wind field characteristics

U = maximum wind speed	75	[m/s]
D = storm duration	10	[hours]
R = radius to maximum winds	55	[km]

Offshore component:

H_s = significant wave height	12.6	[m]	=	41.4	[ft]
T_p = peak wave period	12.0	[s]			

- Results SPM-model (calculating deep water wave characteristics associated with a hurricane):

$$H'_{0,max} = \text{maximum significant wave height} \quad 51.6 \text{ [ft]} = 15.7 \text{ [m]}$$

$$T_s = \text{peak wave period associated to } H'_{0,max} \quad 15.2 \text{ [s]}$$

In comparison to the regional WAM-model results presented in figure B.2, the SMB-model for oceanic waters predicts a lower value of both wave height and wave period. As expected, the SPM-model is more suitable for the determination of the offshore conditions associated with a hurricane.

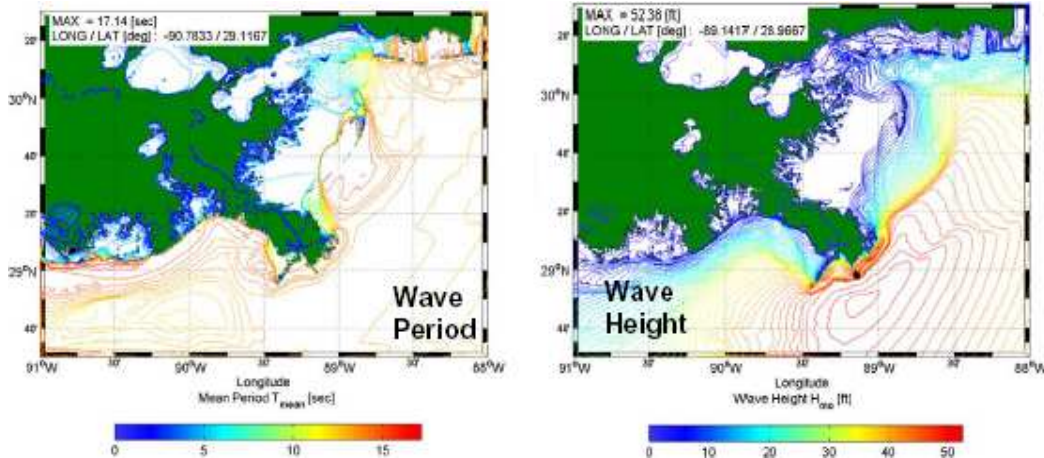


Fig. B.2: Offshore wave conditions – regional scale WAM model [31]

Calculation results offshore wave conditions – SMB-model (wave conditions near shore: coastal waters)

Input: near shore wind field characteristics

d = water depth (incl. surge)	8 [m]
U = maximum wind speed	55 [m/s]
D = storm duration	10 [hours]
R = min (radius to maximum winds, F_{eff})	40 [km]

Lake Borgne has an representative near shore wind fetch of 40 km.

Offshore component:

H_s = significant wave height	3.7 [m] = 12.2 [ft]
T_p = peak wave period	7.1 [s]

In comparison to the basin scale WAM-model results presented in figure B.3, the SMB-model for coastal waters predicts a higher wave height. The higher wave height results for the SMB-model could be caused by the fact that the model does not include the limited depth induced processes of shoaling, refraction and diffraction. When waves enter coastal waters, their amplitude and direction will be affected significantly by the limiting water depth and associated processes. The SMB-model predicts a wave height of about 7 s, equal to the lower boundary of the WAM-model results.

It is interesting to note that the upper boundary of 16 s corresponds with generated offshore wave conditions by using the SPM-model. This confirms the statement made that during Hurricane Katrina the eastern facing levees adjacent to Lake Borgne were subjected to long period wave propagating in from the Gulf of Mexico.

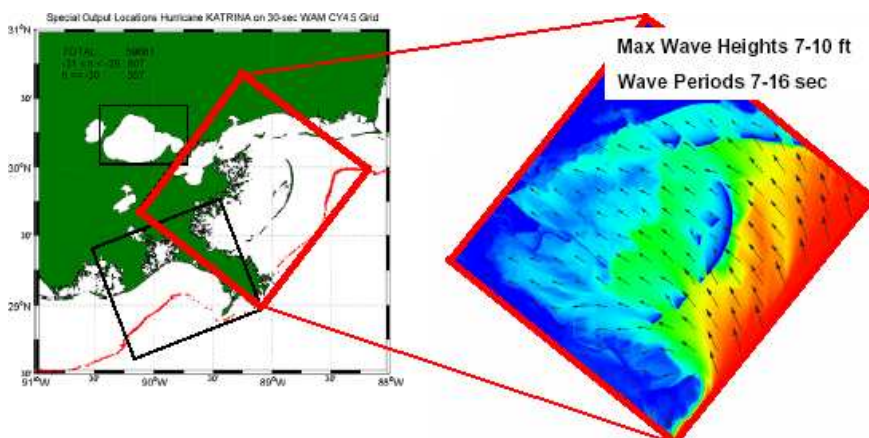


Fig. B.3: Near shore wave conditions (basin scale WAM model) [31]

B.2 Wind setup offshore and near shore [23]

Wind setup is defined as the increase of the water level with respect to the astronomical tide, as a direct consequence of a wind field. It can therefore be calculated by subtraction of the astronomical tide from the observed water level. A model to describe wind setup can be derived from an analysis of the equilibrium wind setup in a two-dimensional basin in a uniform wind speed. A simple model for the water level gradient over an infinitesimal part of a two-dimensional water body is given by:

$$\frac{dh}{dx} = \frac{cu(x)^2}{g(d(x) + h(x))}$$

where: h = wind setup; u = wind speed; g = acceleration of gravity; d = depth with respect to mean sea level.

This equation shows that for the same depth d , the water level gradient decreases if the wind setup increases. It therefore suggests a negative feedback, where an existing high wind setup limits the possibility of an even higher wind setup [23]. In the case of a rectangular basin and uniform wind speed over the basin, the equation can be integrated analytically, leading to an expression for the downwind wind setup. The approximating formula is only valid as long as $d \gg h$:

$$h(u, F, d) = h_{upwind} - d + \sqrt{d^2 + 2 \frac{cu^2 F}{g}} \approx h_{upwind} + F \frac{cu^2}{gd}$$

where: F = basin length (fetch); h_{upwind} = wind effect on the upwind side of the basin

This simplified model implies a uniform wind speed and a uniform depth over the full length of the basin. As stated before, the actual loadings imposed at any location during a hurricane, vary over time as the hurricane moves progressively through the region. Furthermore, the depth of the 'basin' varies significantly. The value of the wind effect on the upwind side of the basin h_{upwind} depends on the boundary condition on that side. Since conservation of mass must hold for the wind setup process, the possibility of inflow of water at the upwind boundary determines the boundary condition.

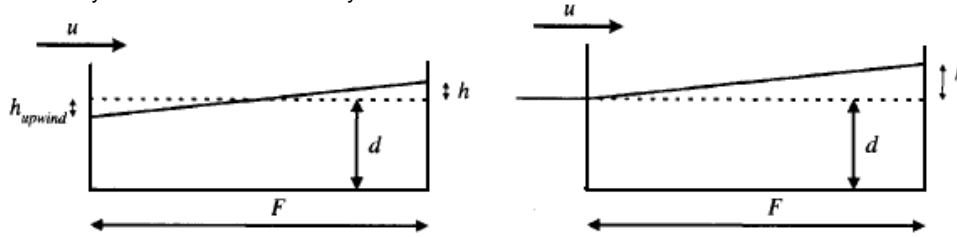


Fig. B.4: Longitudinal sections of rectangular basin with wind setup (left: enclosed basin / right: basin open on upwind end) [23]

In an enclosed basin, any increase of the water level on the down side needs to be compensated by a decrease of the water level on the upwind side. In case of a marginal sea connected to a large ocean, the large supply of water from the ocean ensures that mass is conserved without a decrease of the upwind water level. The latter is the case for both Lake Borgne and Lake Pontchartrain since both are connected to the Gulf of Mexico. Therefore, in the remainder of this study, h_{upwind} will be set to zero.

In a situation with tides, the astronomical tide influences the available depth which in turn influences the wind setup. This effect can be crudely modeled by including the astronomic tide in the definition of the depth in the wind setup calculation. Adopting the modifications outlined above, the wind setup equation results in:

$$h(d, h_a, u, F) = -(d + h_a) + \sqrt{(d + h_a)^2 + 2 \frac{cu^2 F}{g}}, \text{ where } h_a \text{ denotes the astronomical tide.}$$

The effect of a high astronomic tide is the same as that of an increase in water depth d . The wind setup for the same wind speed gets lower. This is in contrast to the study by Vrijling and Bruinsma [1980] who assumed independence of wind setup and astronomic tide. The water level as a function of the wind speed is found by superposition of the wind setup on the astronomic tide.

The wind setup near shore is considered to be the result of a superposition of the wind setup offshore and locally generated wind setup. When the depth with respect to a fixed datum, the astronomic tide and wind setup offshore are considered constant over the full length of the near shore wind fetch, substitution in the wind setup equation for offshore conditions then leads to:

$$h(h_{os}, h_{a,ns}, d_{ns}, u, F_{ns}) = h_{os} - (d_{ns} + h_{a,ns} + h_{os}) + \sqrt{(d_{ns} + h_{a,ns} + h_{os})^2 + 2 \frac{cu^2 F_{ns}}{g}}$$

where: h_{os} = wind setup offshore; $h_{a,ns}$ = astronomic tide near shore with respect to mean sea level;
 d_{ns} = representative near shore water depth with respect to mean sea level;
 F_{ns} = representative near shore wind fetch.

The locally generated wind setup is negatively influenced by the wind setup offshore. The water level near shore is found by superposition of the astronomical tide and the wind setup near shore. Tides are mostly diurnal in the study area, as described in section 3.1. The normal range of tides along the coast portion of the study area is in the range of 1.0 to 1.3 ft (0.3 to 0.4 m).

Results

Offshore component (Gulf of Mexico):

depth offshore with respect to MSL	1000	[m]			
U = maximum wind speed	75	[m/s]			
F _{eff} = effective fetch	55000	[m]			
wind set-up	0.1	[m]	=	0.4	[ft]

Offshore component (edge of the continental shelf):

depth offshore with respect to MSL	100	[m]			
U = maximum wind speed	75	[m/s]			
F _{eff} = effective fetch	100000	[m]			
wind set-up	1.1	[m]	=	3.6	[ft]

Offshore component (perpendicular to coast):

U = maximum wind speed		[m/s]			
depth near shore with respect to MSL	10	[m]			
F _{eff} = effective fetch	100000	[m]			
wind set-up	8.5	[m]	=	27.9	[ft]

Near shore component (Lake Borgne, locally generated):

depth near shore with respect to MSL	7	[m]			
U = maximum wind speed		[m/s]			
F _{eff} = effective fetch (about 40 km, less than RMW)	40000	[m]			
wind set-up	5.3	[m]	=	17.6	[ft]

In comparison to the basin scale ARCDIC-model storm surge results presented in figure B.5, the used model predict the wind setup quite well for both offshore and near shore conditions. When waves enter coastal waters, their surge level significantly increases by the limiting water depth, as can be seen in the model results.

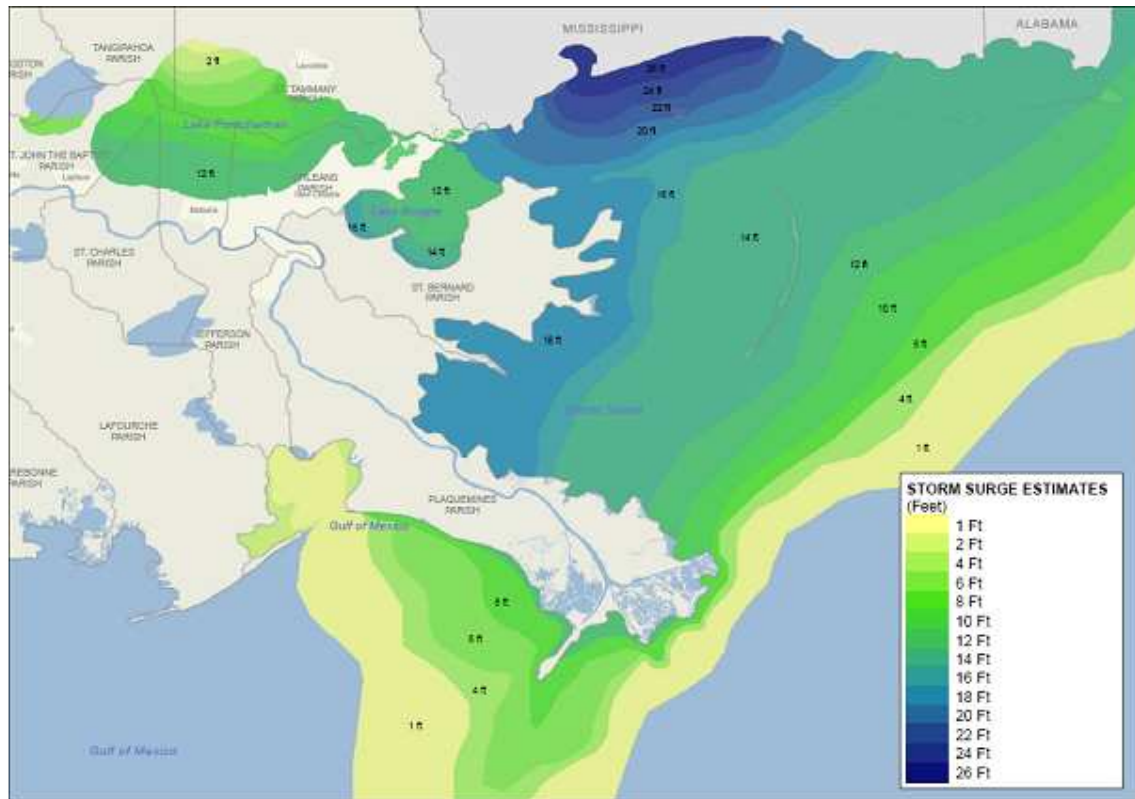


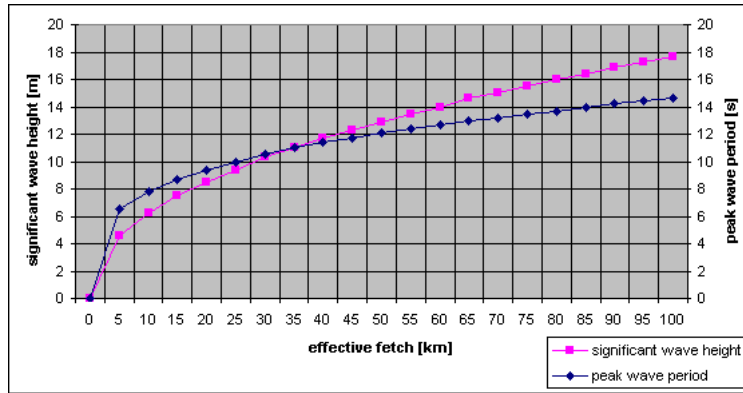
Fig. B.5: Storm surge estimates for Hurricane Katrina [15]

B.3 Sensitivity analysis of the analytical models

B.3.1 SMB-model – wave conditions offshore: oceanic waters

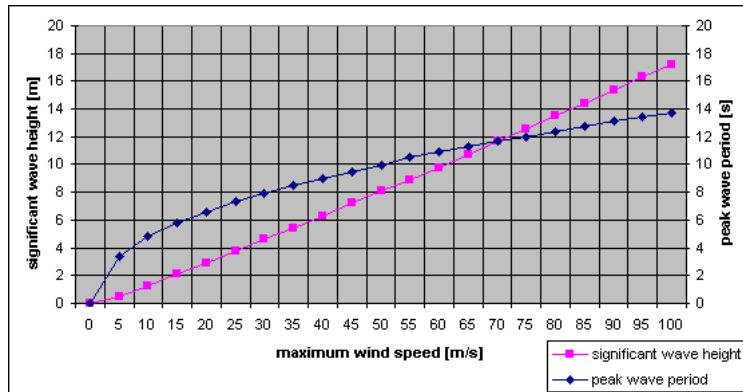
Effective fetch (radius to maximum winds) ($u = 80 \text{ m/s}$, $depth = \infty$)

	0	5	10	15	20	25	30	35	40	45	50
significant wave height [m]	0	4,6	6,2	7,5	8,5	9,4	10,3	11,0	11,7	12,3	12,9
peak wave period [s]	0	6,5	7,8	8,7	9,4	10,0	10,5	11,0	11,4	11,7	12,1
	55	60	65	70	75	80	85	90	95	100	
	13,5	14,0	14,6	15,0	15,5	16,0	16,4	16,9	17,3	17,7	
	12,4	12,7	13,0	13,2	13,5	13,7	14,0	14,2	14,4	14,6	



Maximum wind speed (fixed wind fetch of 55 km (radius to maximum winds), $d = \infty$)

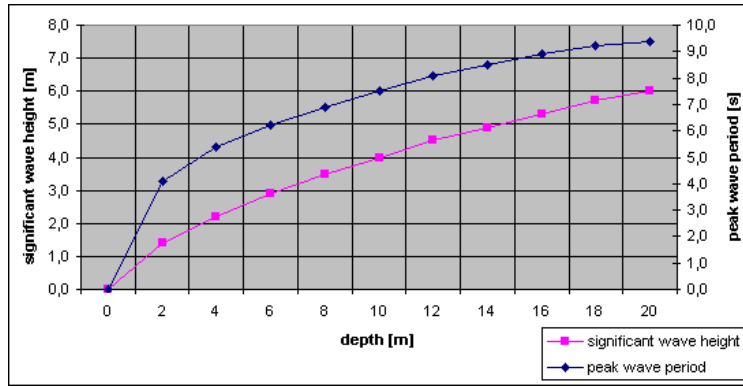
	0	5	10	15	20	25	30	35	40	45	50
significant wave height [m]	0	0,5	1,3	2,1	2,9	3,8	4,6	5,4	6,3	7,2	8,1
peak wave period [s]	0	3,4	4,8	5,8	6,6	7,3	7,9	8,5	9,0	9,5	10,0
	55	60	65	70	75	80	85	90	95	100	
	8,9	9,8	10,7	11,7	12,6	13,5	14,4	15,4	16,3	17,2	
	10,5	10,9	11,3	11,7	12,0	12,4	12,8	13,1	13,4	13,7	



B.3.2 SMB-model – wave conditions near shore: coastal waters

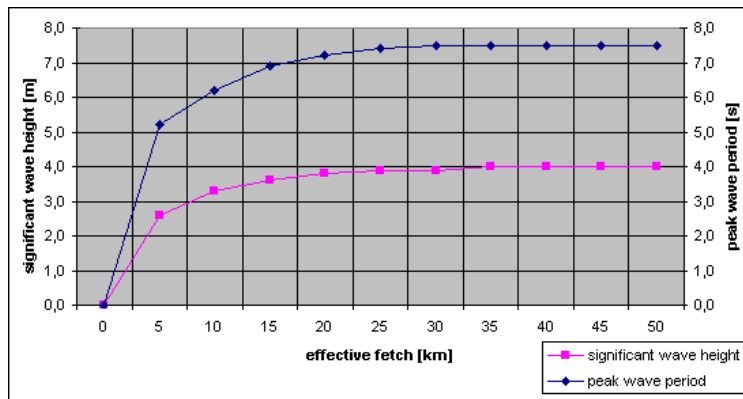
Depth (fixed wind fetch of 55 km (radius to maximum winds), $u = 50$ m/s)

	0	2	4	6	8	10	12	14	16	18	20
significant wave height [m]	0,0	1,4	2,2	2,9	3,5	4,0	4,5	4,9	5,3	5,7	6,0
peak wave period [s]	0,0	4,1	5,4	6,2	6,9	7,5	8,1	8,5	8,9	9,2	9,4



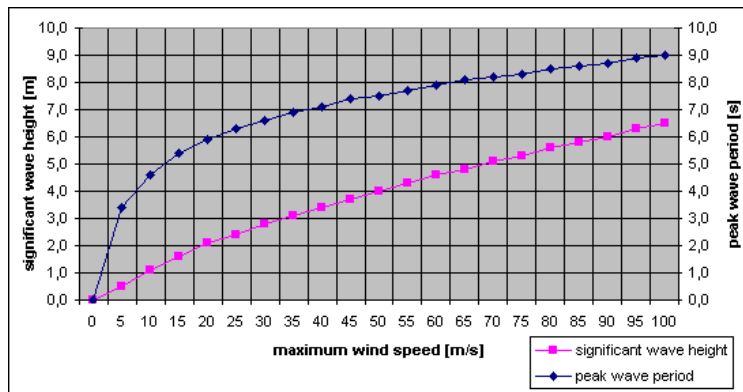
Effective fetch / radius to maximum winds ($u = 50$ m/s, $d = 10$ m)

	0	5	10	15	20	25	30	35	40	45	50
significant wave height [m]	0,0	2,6	3,3	3,6	3,8	3,9	3,9	4,0	4,0	4,0	4,0
peak wave period [s]	0,0	5,2	6,2	6,9	7,2	7,4	7,5	7,5	7,5	7,5	7,5



Maximum wind speed (fixed wind fetch of 55 km (radius to maximum winds), $d = 10$ m)

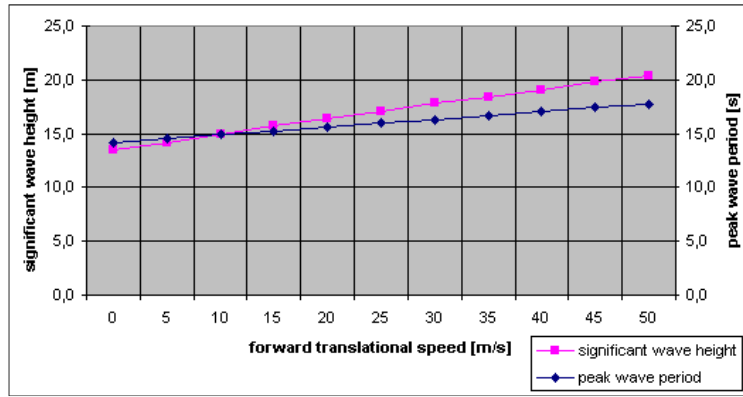
	0	5	10	15	20	25	30	35	40	45	50
significant wave height [m]	0,0	0,5	1,1	1,6	2,1	2,4	2,8	3,1	3,4	3,7	4,0
peak wave period [s]	0,0	3,4	4,6	5,4	5,9	6,3	6,6	6,9	7,1	7,4	7,5
	55	60	65	70	75	80	85	90	95	100	
	4,3	4,6	4,8	5,1	5,3	5,6	5,8	6,0	6,3	6,5	
	7,7	7,9	8,1	8,2	8,3	8,5	8,6	8,7	8,9	9,0	



B.3.3 SPM-model – calculating deep water wave characteristics associated with a hurricane

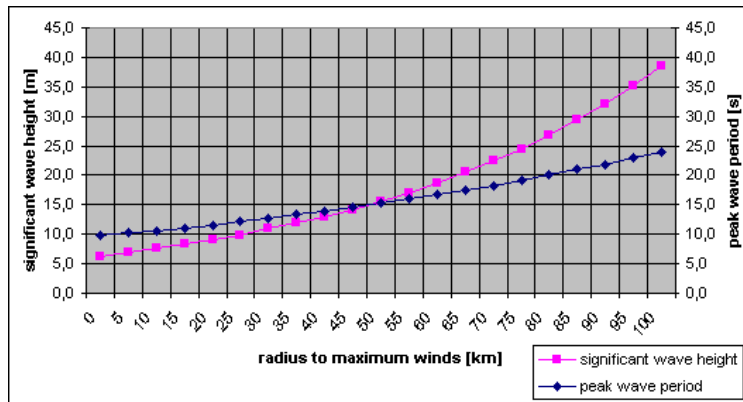
Forward translational speed ($p_A = 1015 \text{ mbar}$, $p_H = 902 \text{ mbar}$, $R = 55 \text{ km}$, $d = \infty$)

	0	5	10	15	20	25	30	35	40	45	50
significant wave height [m]	13,5	14,2	15,0	15,7	16,4	17,1	17,8	18,4	19,1	19,8	20,4
peak wave period [s]	14,1	14,5	14,9	15,2	15,6	16,0	16,3	16,7	17,0	17,4	17,7



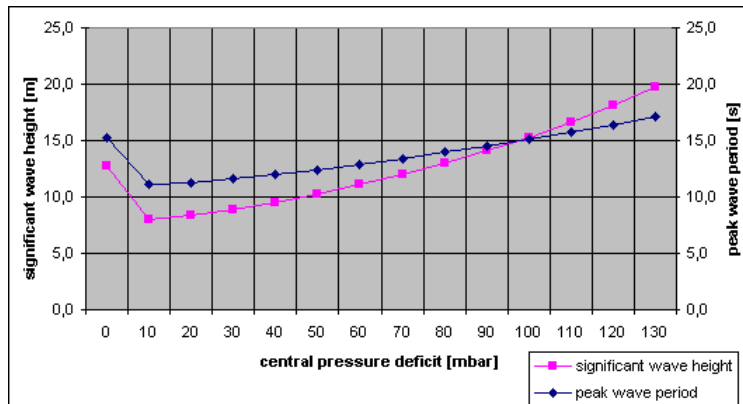
Radius to maximum winds ($p_A = 1015 \text{ mbar}$, $p_H = 902 \text{ mbar}$, $V_F = 25 \text{ m/s}$, $d = \infty$)

	0	5	10	15	20	25	30	35	40	45	50
significant wave height [m]	6,3	6,9	7,6	8,3	9,1	9,9	10,9	11,9	13,0	14,2	15,6
peak wave period [s]	9,7	10,2	10,6	11,1	11,6	12,2	12,7	13,3	13,9	14,6	15,3
	55	60	65	70	75	80	85	90	95	100	
	17,1	18,7	20,5	22,4	24,5	26,8	29,4	32,1	35,2	38,5	
	16,0	16,7	17,5	18,3	19,1	20,0	21,0	21,9	22,9	24,0	



Central pressure deficit ($R = 55 \text{ km}$, $V_F = 25 \text{ m/s}$, $d = \infty$)

	0	10	20	30	40	50	60	70	80	90	100
significant wave height [m]	12,7	8,0	8,4	8,9	9,5	10,3	11,1	12,0	13,0	14,1	15,3
peak wave period [s]	15,2	11,1	11,3	11,6	12,0	12,4	12,9	13,4	14,0	14,5	15,1



APPENDIX C – Hurricane Protection System and its flooding characteristics

C.1 Lake Pontchartrain and Vicinity Protection Project - finalized reaches divided in parishes

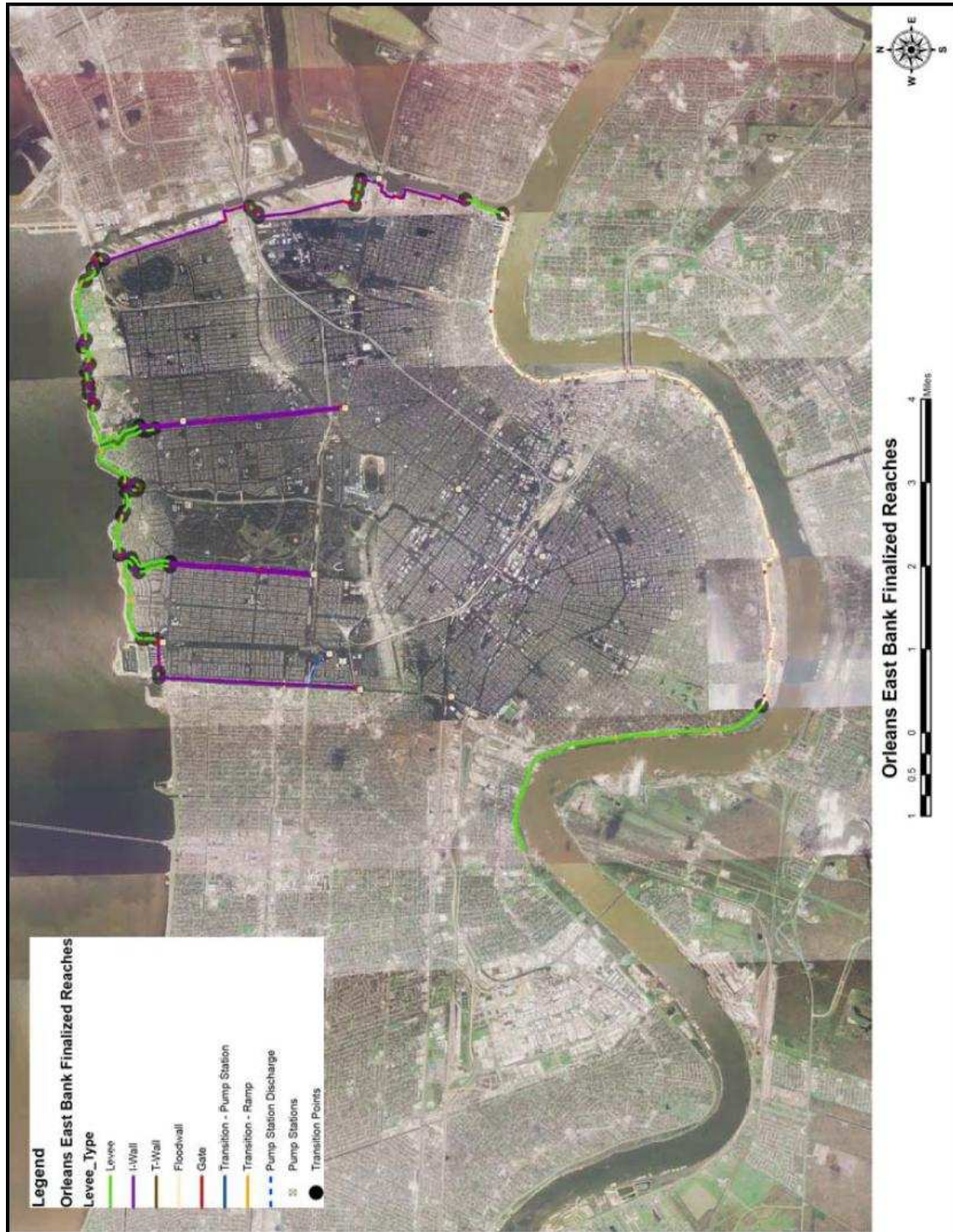


Fig. C.1: Finalized Reaches – Orleans East Bank [29]

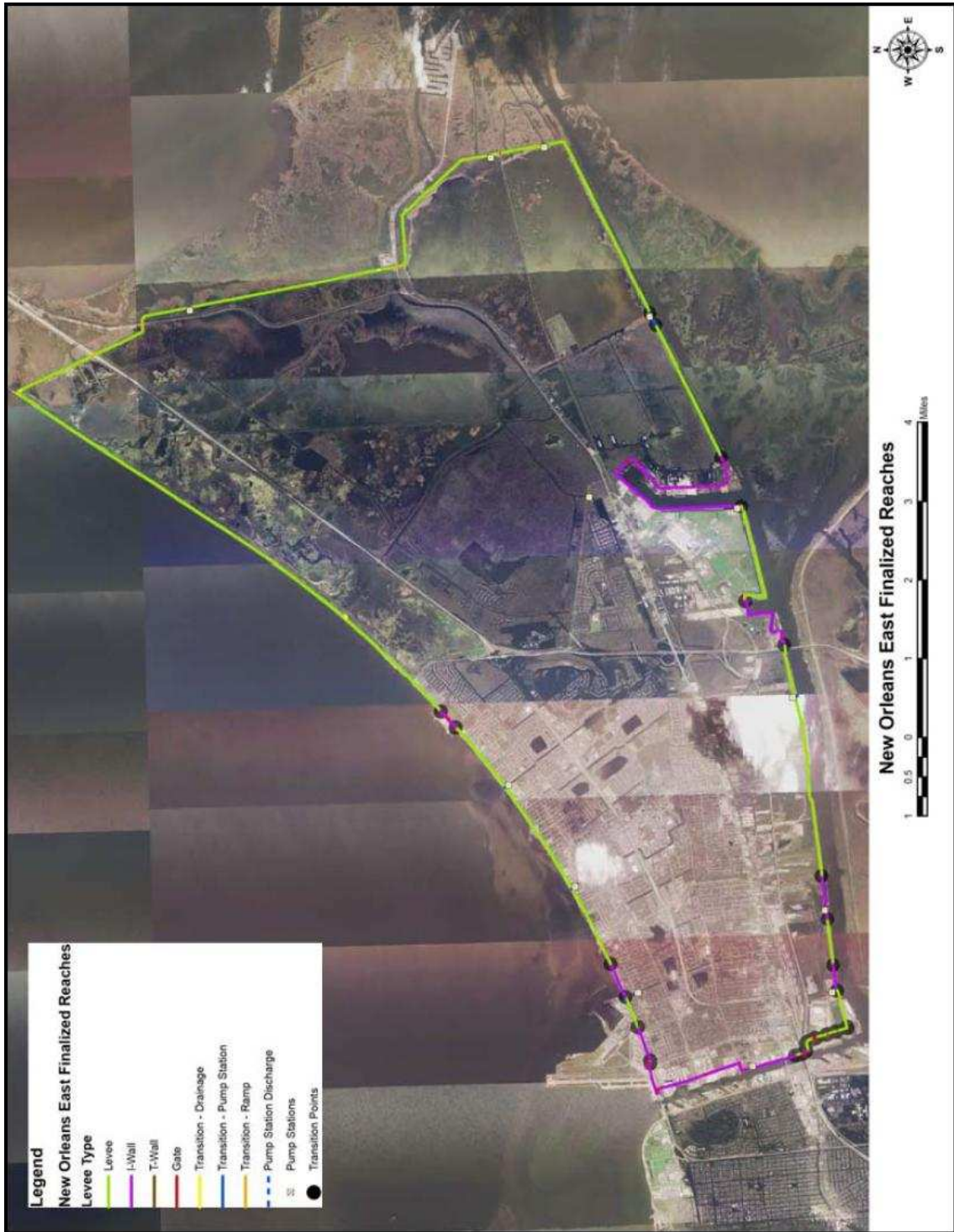


Fig. C2: Finalized Reaches – New Orleans East [29]

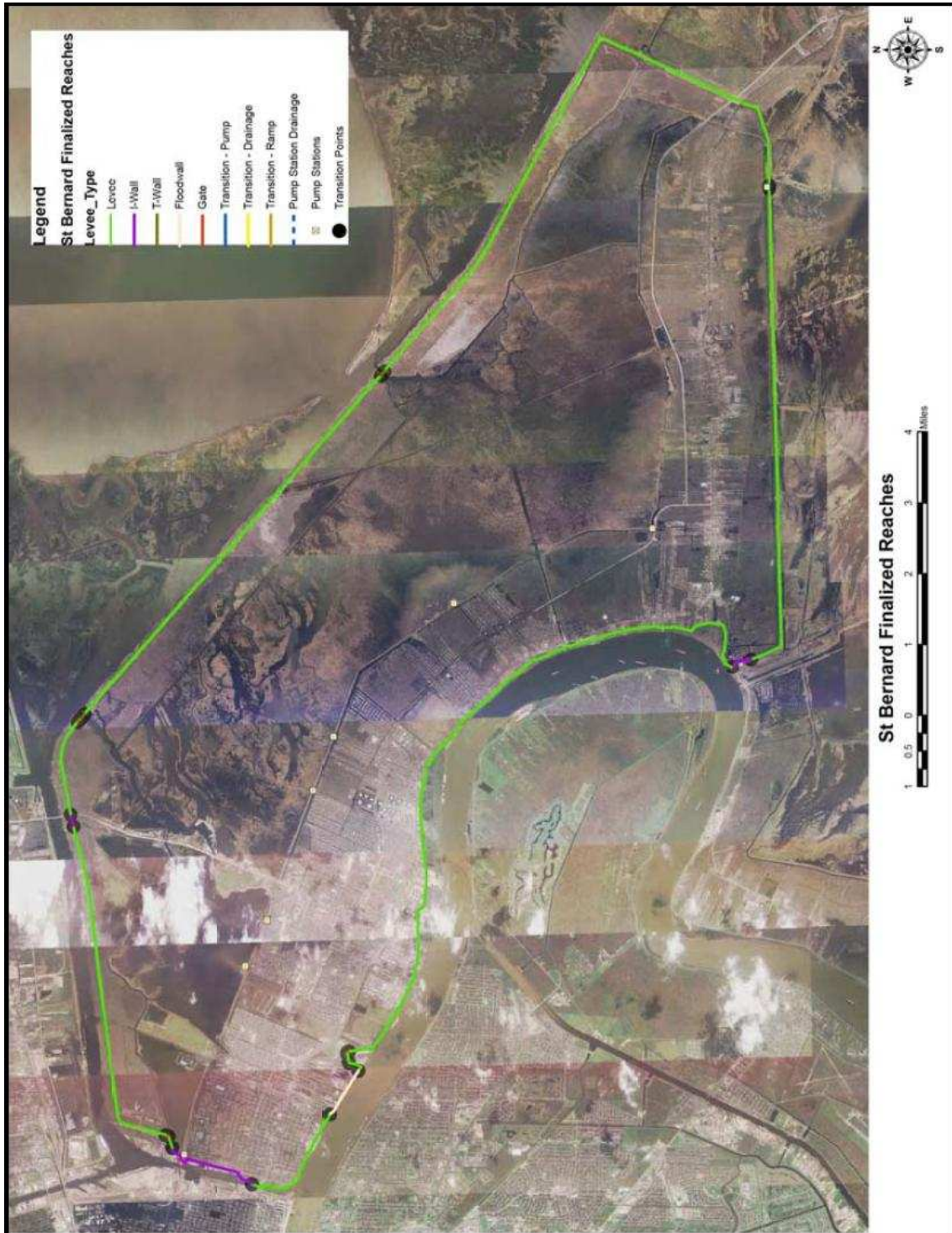


Fig. C3: Finalized Reaches – St. Bernard [29]

C.2 Technical background on the causes of failure for the main levee and floodwall breaches [1]



Fig. C.4: Overview of the failures of several I-walls and levees along the canals into New Orleans [1]

17th Street Canal breach

At about 6:30 a.m. on August 29, a 450 ft (140 m) long section of I-wall along the east side of the 17th Street Canal failed, sending water into New Orleans's Lakeview neighborhood. The water level in the 17th Street Canal at the time of failure was about 5 ft (1.5 m) lower than the top of the wall, well below the design water level. A cross-section of the levee and flood wall is shown in figure C.5.

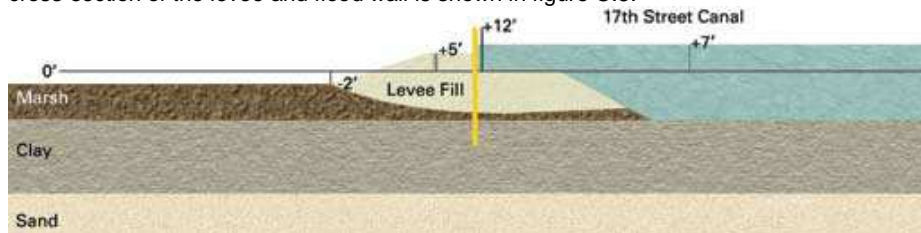


Fig. C.5: Cross section of 17th Street Canal levee and floodwall [1]

The levee and floodwall were built over a layer of organic soil, which overlays a layer of soft clay. A principal concern with levees founded on soft soil is the possibility that the entire levee might slide either into the canal or away from the canal because of the low strength of the soft soil. To prevent the failure of a levee or I-wall such as that along the 17th Street Canal, the resisting forces (strength of the underlying soil) must be greater than the driving forces imposed upon it (weight of the levee and pressure of the canal water acting against the levee and floodwall). The factor of safety against failure occurring is the ratio of the shear resistance of the soil divided by the shear force that develops along a potential sliding surface. If the factor of safety is less than one, failure will occur. As the factor of safety is directly proportional to the soil strength, determining the soil strength is certainly one of the most important decisions that an engineer makes for the levee design. However, the engineers responsible for the design of the levee and I-wall overestimated the soil strength, meaning that the soil strength used in the design calculations was greater than what actually existed under and near the levee during Katrina. The cause of this overestimation is twofold:

- The data used to determine the soil parameters was extracted from borings drilled along the centerline of the levee over a distance of 8,000 feet (2.4 km). Lumping together data over distances is not uncommon. However, care must be taken in areas where there is geologic variability such as the New Orleans area.
- The data was obtained from borings drilled along the *centerline* of the levee. Clay soil is consolidated and strengthened by the weight of overlying soil. The soft clay below the centerline of the levee was therefore stronger than the soil below and beyond the edge of the levee.

Overestimating the soil strength below the levee set the stage, but was not the sole cause of the 17th Street Canal failure. The target factor of safety chosen by the design engineers for the 17th Street Canal levee and floodwall design was 1.3. A target factor of safety of 1.3 is inconsistent with current USACE standards which call for a target factor of safety of at least 1.4 to 1.5 under long term conditions. The cumulative effect of using a target factor of safety of 1.3 and overestimating the soil strength resulted in disaster. The design was simply too close to the margin of safety, allowing little or no room to account for variables or uncertainties.

Another critical engineering oversight that led to the failure of the 17th Street Canal involves not taking into account the possibility of a water-filled gap, which is illustrated in the diagram in figure C.6. The water-filled gap turned out to be a very important aspect of the failures of the I-walls around New Orleans.

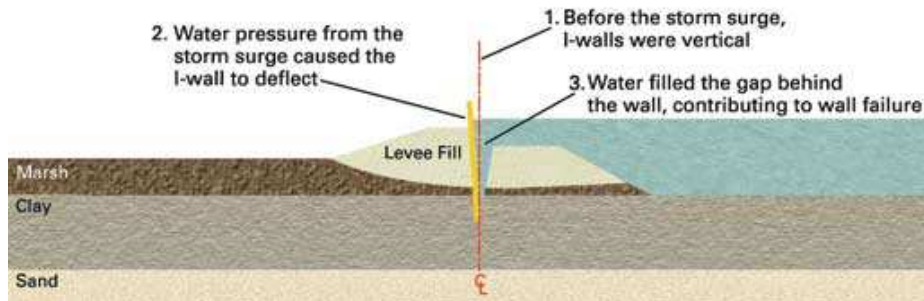
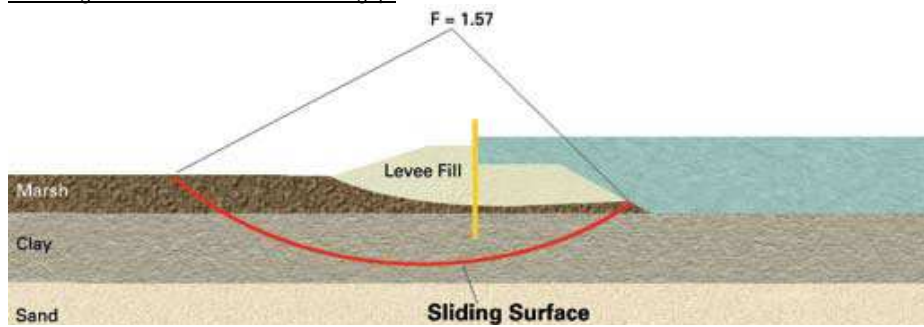


Fig. C.6: The water-filled gap [1]

Figure C.7 illustrates the reason the water-filled gap led to failure of several I-walls. The first diagram shows the critical sliding surface passing beneath the 17th Street Canal I-wall and through soil between the wall and the canal without a water-filled gap. The shearing resistance provided by this segment along the failure surface adds to the stability. In the second diagram, representing the actual situation with a gap, the critical sliding surface starts at the base of the water-filled gap. The sliding surface cuts through less soil, so that less resisting soil strength can be mobilized. In addition, the pressure on the wall generated by the water in the gap adds to the forces tending to slide the wall away from the canal.

1: Sliding surface without a water-filled gap:



2: Sliding surface with a water-filled gap:

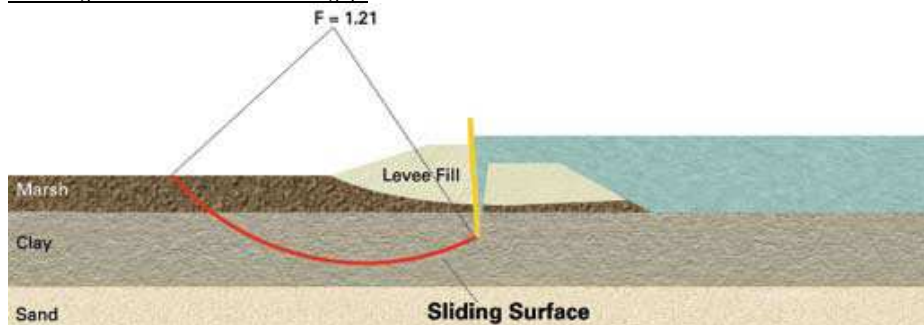


Fig. C.7: 17th Street Canal failure mechanism [1]

Analyses indicate that, with the presence of a water-filled gap, the factor of safety is about 30 percent lower. Since a factor of safety of 1.3 was used for design, a reduction by 30 percent would reduce the factor of safety to approximately 1.0: the condition of incipient failure.

London Avenue Canal: south breach

The London Avenue Canal south breach occurred around 6:00 to 7:00 a.m. on August 29th. As with the 17th Street Canal, the water level in the London Avenue Canal at the time of failure was well below the design water level. The soil beneath the London Avenue Canal south breach area is sand beneath a marsh layer, rather than soft clay as was the case at the 17th Street Canal breach location. A cross section describing the failure mechanism is shown in figure C.8.

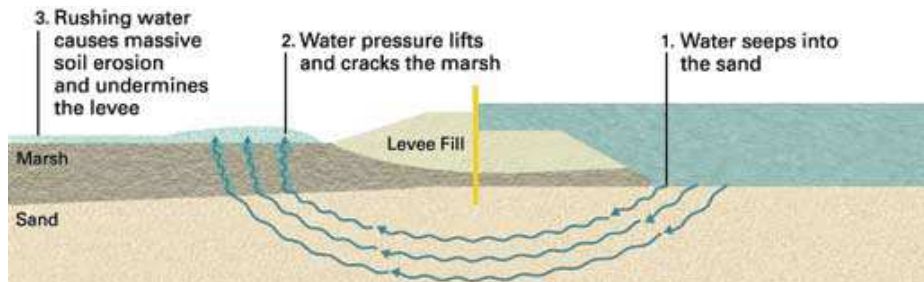
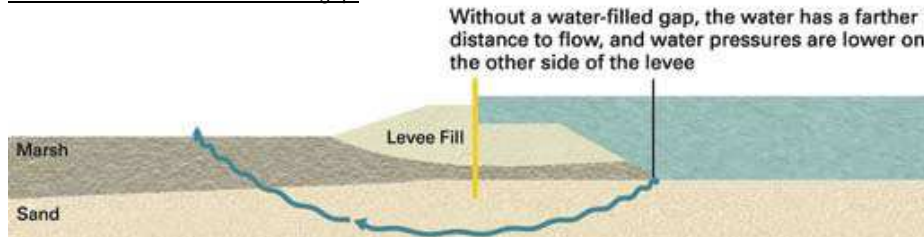


Fig. C.8 : Cross section of London Avenue Canal levee and floodwall [1]

As the water level rose in the canal, water seeped into the highly permeable sand and flowed under the levee toward the land-side of the wall. The water pressure acted upward on the bottom of the marsh layer. The stability of the levee in this type of situation depends on whether the weight of the overlying material is large enough to resist the uplift water pressure acting upward. In well designed structures, the uplift water pressure is never allowed to come close to the weight of the overlying soil. At the London Avenue Canal south breach, the water pressure exceeded the weight of the marsh layer and the topsoil above it. The marsh layer was lifted off the sand and cracked open, which allowed water to rush through the cracks. After the cracks developed, the upward-rushing water carried sand with it. This scouring rapidly expanded and worked its way back under the levee.

The failure of the London Avenue Canal I-wall was influenced by the water-filled gap that developed behind the wall. As with the 17th Street Canal, the water in the London Avenue Canal pushed the I-wall away from the canal side, leaving a gap between the I-wall and the levee. The elevated water pressures were brought much closer to the land-side of the levee, significantly increasing the uplift forces on the clay and worsening the situation. This process is shown in figure C.9.

1: Conditions without a water-filled gap:



2: Conditions with a water-filled gap:

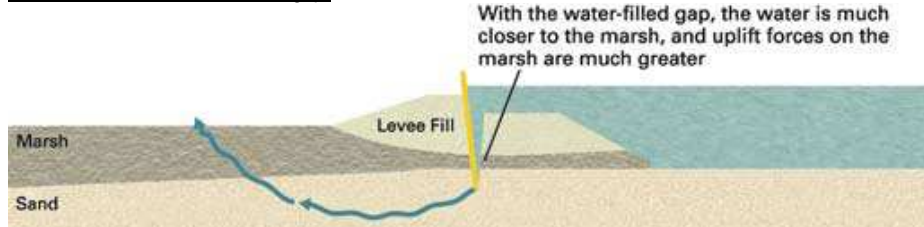


Fig. C.9: London Avenue Canal south breach failure [1]

London Avenue Canal: north breach

The London Avenue Canal North Breach occurred on the west side of London Avenue Canal around 7:00 to 8:00 a.m. on August 29th. The upper 15 ft (4.6 m) of soil beneath the London Avenue Canal north breach consists of marsh underlain by a thick layer of sand, similar to the conditions at the London Avenue Canal south failure. However, the sand at the north breach was much looser and weaker than the sand at the south breach. The levee and I-wall probably failed in much the same way as the 17th Street Canal failure, in which the driving forces exceeded the resisting forces. The sliding failure was amplified by seepage.

Orleans Avenue Canal breach

The Orleans Avenue Canal did not suffer breaching, but near the south end of the canal a section of floodwall topping the earthen levee of approximately 300 ft (91 m) in length had been left incomplete. This effectively reduced the level of protection for this canal from about 12 ft (3.6 m) above mean sea level, which is the height of the tops of the floodwalls lining the canal, to an elevation of about 7 ft (2.1 m) mean above sea level. This is the height of the earthen levee crest along the 300 ft (91 m) length where the floodwall that should have topped this levee was omitted. As a result of the missing floodwall section, flow passed through this gap and began filling the heart of the main New Orleans protected basin.

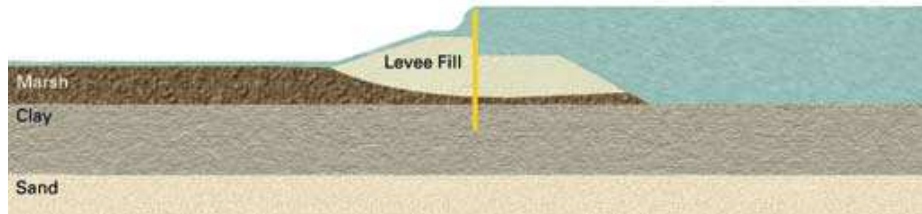
Inner Harbor Navigation Canal: east bank, north breach

The failure of the north I-wall of the Inner Harbor Navigation Canal's east bank was likely the source of the earliest flooding in the Lower Ninth Ward. The water level in the IHNC was below the top of the floodwall. The soil conditions in this area consisted of marsh deposits overlying soft clay, which overlies sand. The particular I-wall failed in much the same way as the 17th Street Canal I-wall failed: by slope failure along a sliding surface in the marsh. As with the 17th Street Canal, the presence of a water-filled gap was not considered during the design but greatly reduced the factor of safety.

Inner Harbor Navigation Canal: east bank, south breach and west bank breach

At both locations the I-walls were overtopped by floodwaters from Hurricane Katrina. The peak water level was estimated to be 1.7 ft (0.5 m) above the tops of the floodwalls and levees. The apparent failure mechanism is shown in figure C.10. Water flowing over the floodwalls scoured and eroded the land-side of the levee at the base of the walls. The sheet piles that support the I-walls were undermined. In some locations, the sheet pile walls may have lost all of their foundation support, resulting in failure of the wall.

1: Flood water overtops the I-wall, scours soil from the land-side of the I-wall and washes it away:



2: I-wall fails due to lack of foundation support:

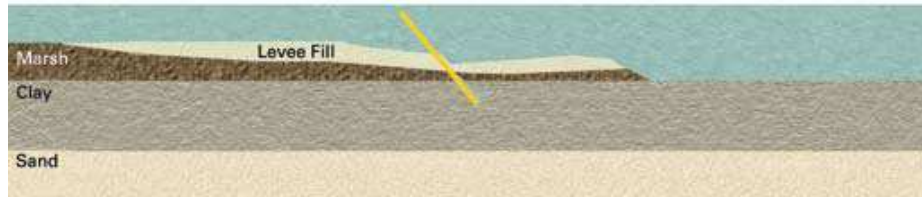
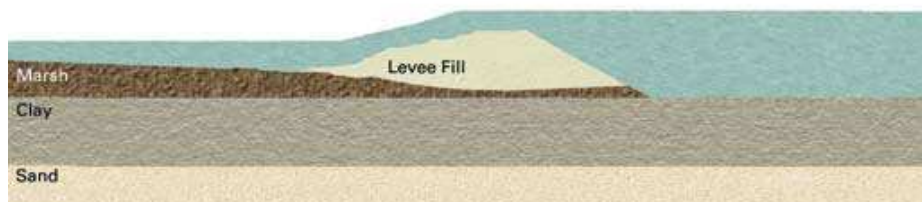


Fig. C.10: Overtopped I-wall failure mechanism [1]

Inner Harbor Navigation Canal: west bank, south breach. All other levee breaches

Earthen levees without I-walls all around New Orleans, including the west bank levee at the IHNC, were overtopped by Hurricane Katrina's storm surge. Out of the 50 total estimated levee breaches system wide, the majority can be attributed to overtopping and erosion. The failure mechanism from overtopping is shown in figure C.11. Levees constructed with properly compacted clay with a good grass cover appeared to have withstood the storm the best. Levees with higher silt and sand content in the embankment material and levees built with hydraulic fill sustained the most severe damage. In some cases they were completely washed away.

1: Flood water overtops the levee, scours soil from the crest and land-side of the levee and washes it away:



2: Some levees constructed of sand and silt washed away completely:



Fig. C.11: Overtopped levee erosion failure mechanism [1]

APPENDIX D – Navigable Flood Protection Structures: Examples Of Proven Protection Schemes [2]

D.1 Vertical lifting gate

Hartel Canal Storm Surge Barrier, The Netherlands

The Hartel Canal Barrier (known also as the Europoort Barrier) is one of the two large storm surge barriers protecting the Dutch province of South Holland with its Rotterdam harbor against the intrusion of sea water. The second, larger barrier is the Maeslant Barrier near Hoek van Holland, known also as the New Waterway Barrier. The construction of the Hartel Canal Barrier made it possible to open a new excess to the Rotterdam harbor. The barrier solution has been selected as an alternative to a large scale dike raising program, which would have required private property to be purchased and buildings to be removed at an immense scale.

The barrier consists of two vertical lift gates with the span lengths of 98.0 m (321.5 ft, southern gate) and 49.3 m (161.5 ft, northern gate). The sliding gates are driven by hydraulic cylinders with a long piston, which are hinged to the side towers. The gates are lens-shaped and the retaining plate at the high water side is through vertical beams connected to the arched truss girders. The hydraulic load is transferred to the supports in the gate recesses of the towers. When not in use, the clearance height between the mean water level and the gate underside amounts to 14 m (46 ft).

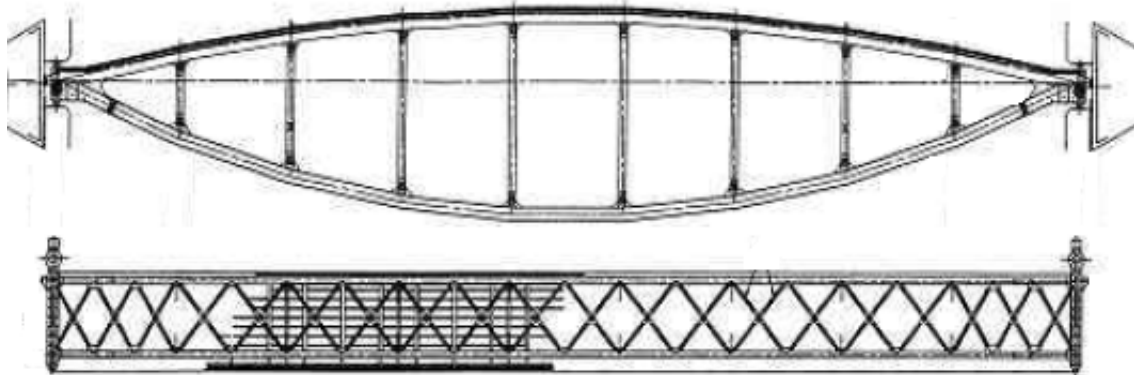


Fig. D.1: Hartel Canal Storm Surge Barrier, The Netherlands [19]

Another special feature of the barrier is its overflowing service. In order to make economic use the water storage capacity inside the protected area, the gates do not entirely seal the canal. A gap of 0.25 m (about 0.8 ft) remains always above the gate sill. Under extreme circumstances, statistically once every 10,000 years, there is also an overflow of 3.7 m above the top edge of the gate. This will result in overflow of the gates, but also in a limitation of the horizontal hydraulic load. In the case of overflow, the gates still act as a reductor for the storm. These arrangements do not jeopardize the safety of the inner land, in fact even increasing it. However, it introduces a problem of gate protection against vibrations in flowing water.

As water can flow over, it can also carry containers or other floating objects under extreme circumstances. In order to protect the gates against collision a floating arm (200 m long) has been constructed. The arm is moored along the southern bank and hinged to it at one end. It gets towed to the closing position by a tugboat. Opening of the barrier, floating arm and lock takes place when the water level on both sides becomes equal with the tolerance fall of about 0.5 m.

The operational closing of the barrier has been synchronized in with the closing of the Maeslant Barrier. Test closings can be separately conducted from the barrier own operation center. When the barrier is closed, navigation can still continue for a few hours through the 24 m wide Hartel Lock next to it. Then also the lock closes and becomes a part of the barrier.

Krimpen Storm Surge Barrier, The Netherlands

The Krimpen storm surge has been constructed at a junction about 30 km (20 miles) away from the point where the Rhine River flows into the North Sea. The Krimpen complex forms a part of the sea defense system of the Netherlands. For security reasons, a double barrier system with two gates in tandem has been constructed.

The main support system of the gate consists of arched truss girders, essentially like an arched bridge at its side. The retaining plate is supported by vertical beams that are connected to the truss girders. The gate is lifted by means of hoisting cables in the side towers and is counterweighted with the help of ballast blocks. The hydraulic load is transferred to the side supports in the towers. Wheels provide guidance and support during lifting. When not in use, the underside of the flood protection gate is lifted 55.8 ft (17.0 m) above the sill, leaving a clearance height of about 33 ft (10 m) above the normal water level. The gate is lowered when high floods occur on the river. Shipping locks beside the floodgate enable the passage of ships when the barrier is closed.



Fig. D.2: Krimpen Storm Surge Barrier, The Netherlands [2]

D.2 Flap gate: pneumatic flap gate and hydraulic flap gate

New Waterway Storm Surge Barrier, The Netherlands: design with flap gates

The storm surge barrier in the New Waterway, the lower reach of the Rhine River and the shipping channel to the Ports of Rotterdam, forms the final link in the sea defence system of The Netherlands. In the pre-design stage, contractors were asked to submit a proposal for the design and construction of the barrier on the basis of a limited feasibility study. Some starting points were: minimum width of flow and navigation opening 1180 ft (360 m), sill level 55.8 ft (17.0 m) below mean water level, no clearance height limitation for navigation.

Several designs were proposed, among which were two flap gate designs. Neither of these two designs was selected as the preferred design, but the two gate designs (referred to as A and B) are presented here to give an impression of construction possibilities.

The first design concerns a barrier with pneumatic flap gates. The barrier consists of seven embedded concrete caissons, each caisson housing two flap gates with a breadth of 84.3 ft (25.7 m). The river bed adjacent to the caissons is riprap protected. The hydraulic load is transferred through the hinges to the foundation. Because flow openings underneath the gates are provided, the barrier acts only as a reductor for the storm surge on the river. As a result, the differential head across the barrier is limited. The flow openings may reduce the height of the translation wave that is generated when the barrier is closed, in particular when all gates are operated simultaneously. When not in use, the gates rest in their recesses and the hollow compartments of the gates are filled with water. In the case of an expected storm surge at sea, air is blown into the gates, forcing the gates to emerge. Each gate can be removed for maintenance purposes by means of a special lifting pontoon.

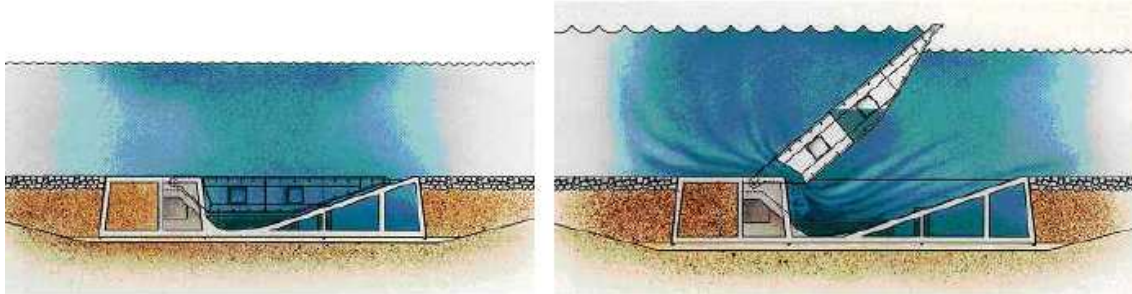


Fig. D.4: New Waterway Storm Surge Barrier – Flap Gate Design A: Pneumatic [18]

The flap gates in the second alternative barrier design are operated by means of hydraulic cylinders. The barrier consists of three embedded concrete caissons, each caisson housing eight gates with a breadth of 49.2 ft (15 m).

Each gate is served independently by a set of two hydraulic cylinders, which are placed in the gate recesses underwater. The hydraulic cylinders control the position of the gate and enable the application of a desired overflow discharge. The hydraulic load is transferred through the hinges and the hydraulic cylinders to the foundation. In lowered position, the gates close off the recesses fully. Each recess can be pumped dry, which allows for inspection and maintenance of hydraulic cylinders and flap gate.

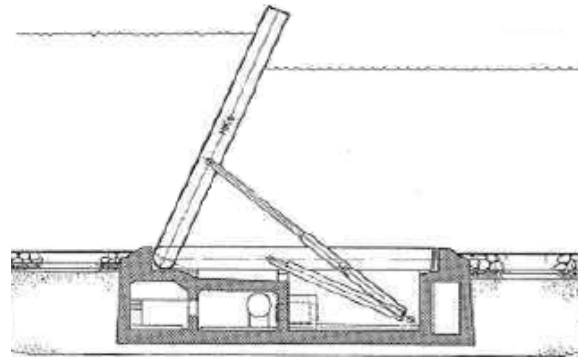


Fig. D.5: New Waterway Storm Surge Barrier – Flap Gate Design B: Hydraulic [18]

D.3 Horizontally moving or rotating gate: slide gate, sector gate and floating sector gate

New Waterway Storm Surge Barrier, The Netherlands: Design with straight sliding gates

This alternative barrier design comprises two straight sliding gates with a length of 722 ft (220 m) each, which are housed in long chambers in the abutments when not in use. The chambers can be closed off and pumped dry. The gates are thus fully accessible for inspection and maintenance.

The gates have large flow openings in the retaining plate, which are closed with vertically movable bulkheads when the gates are in position. The openings limit the building up of a differential head and the corresponding hydraulic load during the sliding operation, thus reducing contact pressures on the slide way. The sill consists of two pre-fabricated concrete caissons. The frame of the self-stable gates has a triangular shape and is built up of pipes. The lower pipes are partly filled with ballast to ensure stability while, simultaneously, contact pressures on the slide way are kept low to minimize friction forces. The gates are pushed from both sides into the river by a rack and pinion gear. The estimated closure time is about 1 hour.

New Waterway Storm Surge Barrier, The Netherlands: Design with non-floating sector gates

This alternative barrier design consists of two sector gates with a radius of 968 ft (295 m). The gate arm of a gate is connected to a set of two vertically aligned hinges on the abutment. The gates are provided with retractable wheels and roll on a carriage way on the sill. The wheels are retracted when the gates are in position and the gates then rest on special support blocks.

The horizontal load is for the greater part transferred to the hinges on the abutments. Each abutment consists of a huge concrete structure that is filled with sand. The gates have large openings in the retaining plate, which are closed when the gates are in position. These openings limit the building up of the differential head during operation. When not in use, the gates are housed in large chambers in the banks. These chambers cannot be closed off, so that inspection and maintenance underwater is difficult.

The gates are driven by a locomotive, which runs on a rack and pinion rail on the abutments. The sill, which consists of pre-fabricated concrete caissons, is founded on piles to ensure a firm base for the carriage way. The gates are provided with flotation tanks and ballast tanks, so that the vertical load on the wheels can be controlled during operation. Estimated closure time is about 0.5 hour.

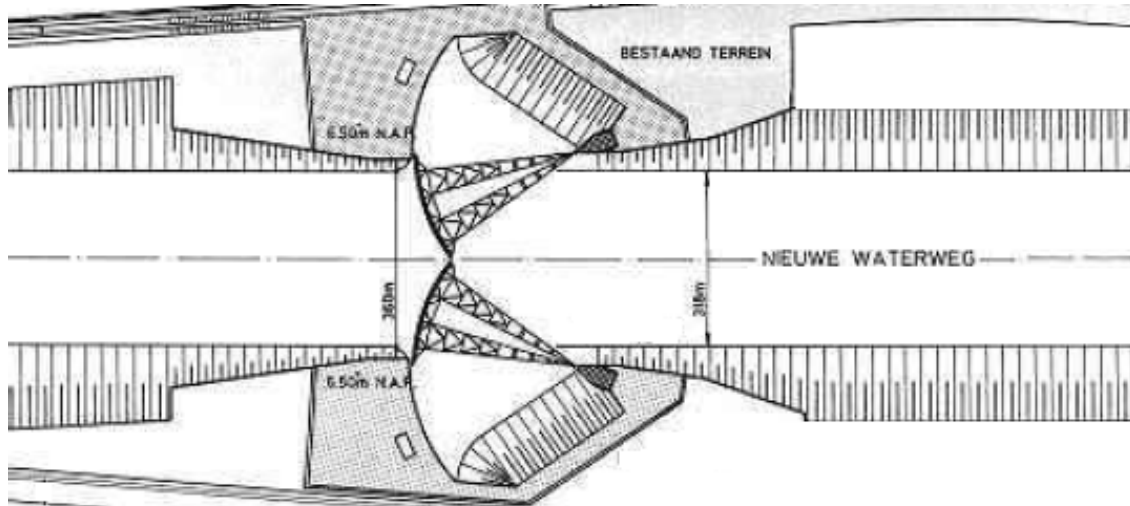


Fig. D.6: New Waterway Storm Surge Barrier – Design with non-floating sector gates [18]

New Waterway Storm Surge Barrier, The Netherlands: Design with floating sector gates

The flood barrier consists of two floating sector gates, each with a radius of 807 ft (246 m) and arch length of 682 ft (208 m). The gate arm is connected to a single ball hinge on the abutments. When not in use, the gates are housed in side docks. These relatively shallow docks, with high elevated floor, can be closed off fully and pumped dry. This enables an inspection and maintenance in the dry. The gates can be floated into the river and immersed within 1.5 hours. Additionally, mobilization and filling of the docks with water requires about 1.0 hour.

Each gate is driven by a locomotive engine that is connected to the abutment by means of a rod that can move along a vertical pile. The locomotive itself runs on a rack and pinion rail on top of the gate. After the gates have been floated into the river, the floatation boxes are filled with water, and the gates sink down onto the sill. The gates stand on fender blocks that are affixed to the underside of the gate at a center-to-center distance of 19.7 ft (6.0 m). The sill consists of large rectangular concrete blocks, 10.5 ft (3.2 m) thick, on a gravel base. The gravel base has been constructed in a trench that was cleared of silt and filled with sand; the gravel top layer was flattened within a tolerance range of +/- 0.16 ft (+/- 0.05 m), using floating equipment. Subsequently, the sill blocks were placed with the help of a lifting crane on a barge. The horizontal hydraulic load is transferred to the ball hinges. The ball hinges are constructed on top of huge concrete gravity caissons, which are filled with sand. The hinges are elevated well above the mean water level.

Much attention was paid in the design stage to the behavior of the floating gates under flow and wave conditions. From experimental studies, it appeared that the floating gates are sensitive to flow-induced oscillations, in particular in the last stage of immersion. These oscillations could be prevented by a reshaping of the gate underside, while also increasing the hydrodynamic rigidity of the gates.



Fig. D.7: New Waterway Storm Surge Barrier – Design with floating sector gates [14]

There are leaks in the barrier, but are not for concern. The barrier does not need to hold all the water. Generally, it is only a redactor. It proved simpler to leave a gap of about 1.5 m between the gates in order to prevent them from banging against one another in closed position. The opening means that water can pass through the barrier. Water can also pass beneath the wall, while under heavy storm conditions water will also spill over the top. Another leakage takes place through the parking dock. In total, the leaks have a surface area of some 125 m², equal to about 2.5 percent of the total retaining surface.

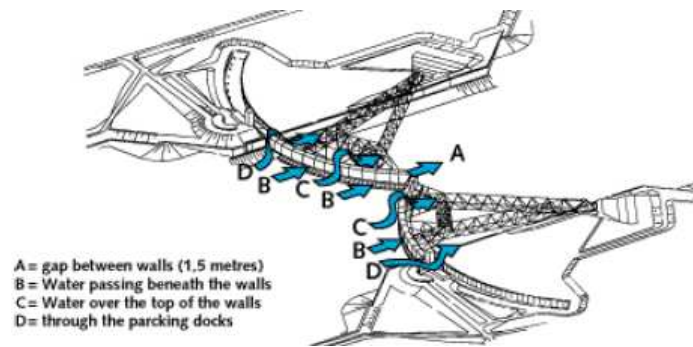


Fig. D.8: Definitive design – allowed types of leakage [18]

D.4 Vertically rotating gate: segment gate and radial gate

Thames Storm Surge Barrier, UK

The storm surge barrier in the Thames River comprises four main navigable openings with a breadth of 200 ft (61 m) and two smaller navigable openings with a breadth of 103 ft (31.5 m), which are closed off by means of segment gates. Four non-navigable openings with a breadth of 103 ft (31.5 m) are closed by radial gates. The gates span the space between concrete piers.

The segment gates have a radius of 40.0 ft (12.2 m) and are stored in a bottom recess in the concrete sill when not in use. The hollow, box-type gate body of the segment gates has high torsion stiffness. The gate body is connected to circular side disks, also with a radius of 40.0 ft (12.2 m), which rotate in a vertical plane about central pivot bearings. The side disks are partly filled with cast iron to counterbalance the weight of the gate body and are driven by hydraulic jacks. The hollow gate body is filled with water when the gate is immersed. When the gate body is lifted, the internal water flows out through check valves near the toe of the body. Simultaneously air flows in through openings in the side disks. This process is presented in figure D.7. Conversely, when the gate body is lowered, water flows into the hollow gate through openings in the side disks, and simultaneously air is blown off through the air vents in the side disks. This water filling system is chosen to minimize the entering of silt into the gate interior.

The hydraulic forces on the curved skin plate have their working line through the rotation axis of the gate. Hydraulic forces on the straight inner skin plate balance with the water inside the gate body and do not cause a rotation moment (but during lifting or lowering operations these forces do not balance; the resulting rotation moment has to be taken up by the hydraulic cylinders). The segment gates can be rotated 180° so that the gate body is fully lifted above the water and is accessible for inspection and maintenance. The accessibility of the narrow interior of the gate body is difficult, however, as appears in practice.

The radial gates in the non-navigable openings have more or less a similar closed gate body as the segment gates, but the two gate arms, one at either side, are designed as non-circular conventional gate arms. When not in use, these gates are lifted above the water level. The full barrier can be closed within 1 hour.

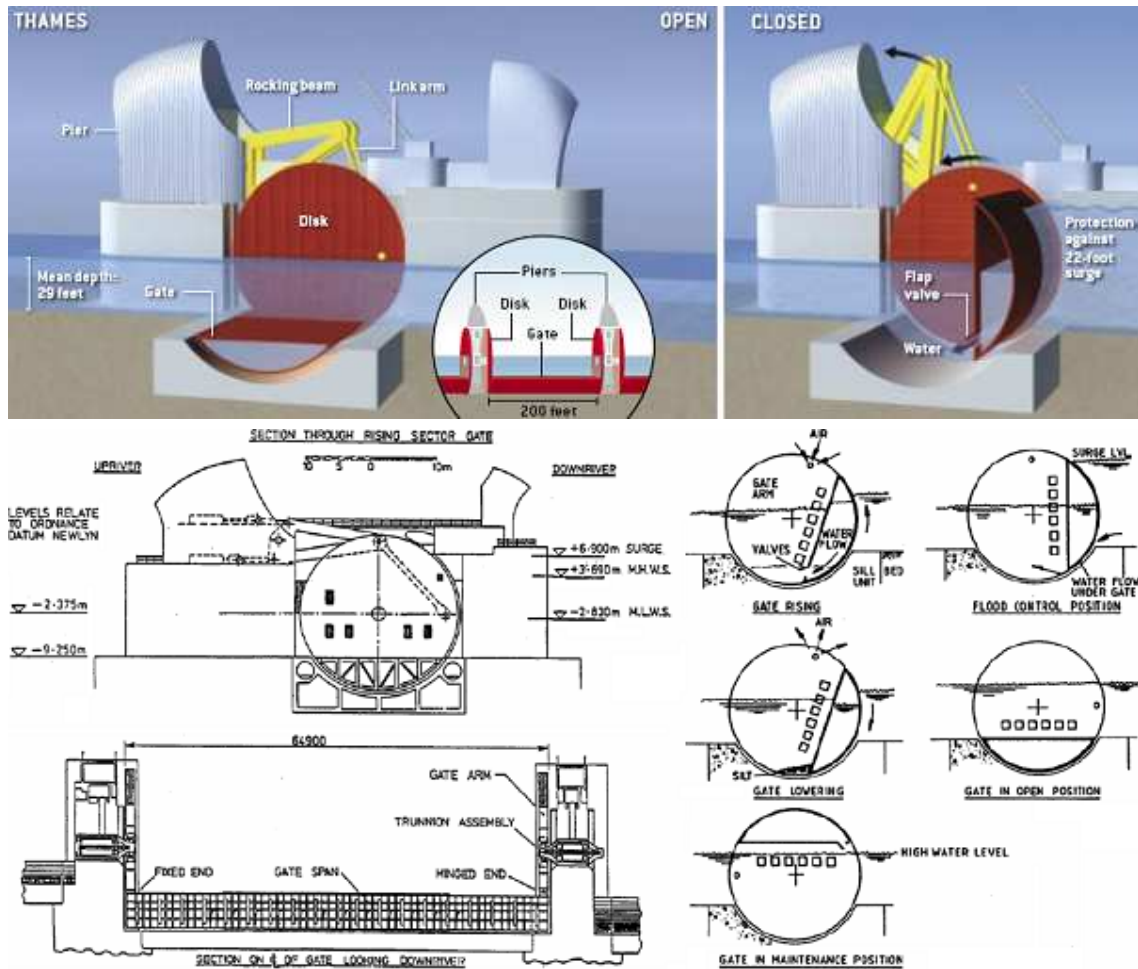


Fig.D.9: Thames Storm Surge Barrier – design and operation [upper: 24, bottom: 18]

Ems Storm Surge Barrier, Germany

The Ems storm surge barrier has recently been constructed in the Ems River. The barrier protects against storm surges from the North Sea, but it is also used to dam up the water in the river temporarily. The latter enables big ships to sail from the ship yard upstream of the river to the sea.

The barrier has two navigable flow openings and five non-navigable openings. The main navigable opening with a width of 196.8 ft (60.0 m) has been provided with a segment gate that is stored in a recess in the sill when not in use. The segment gate, having a closed gate body, has circular side disks with a radius of 39.4 ft (12.0 m). For inspection and maintenance purposes, the segment gate can be rotated above the water level. The secondary navigable opening with a breadth of 164.0 ft (50.0 m) has been provided with a radial gate, with two gate arms, that is rotated above the water when not in use, leaving a clearance height for shipping of 24.1 ft (7.35 m). Both gates are driven by hydraulic cylinders. The five remaining non-navigable flow openings with a breadth of 205.1 ft to 164.0 ft (62.5 m to 50.0 m) have been provided with vertical lifting gates. These gates are combined with a fixed upper structure. The full barrier can be closed in about 30 minutes.

APPENDIX E – General Design Requirements

E.1 Geotechnical design requirements

Information regarding the soil characteristics of the presented geological cross section is limited. Therefore the approach is taken to assign these characteristics according to engineering justice. For this approach table E.1 will be used, which is extracted from the Dutch Standards for engineering (NEN 6740).

Type	Character	Density / Strength	γ_{dry} kN/m ³	γ_{wet} kN/m ³	q_c MPa	C'_p	C'_s	C_c	C_a	C_{sw}	E MPa	Φ'	C' kPa	f_{undr} kPa
Gravel	weakly silted	loose	17	19	15	500	-	0.008	0	0.003	75	32.5	-	-
		moderate	18	20	25	1000	-	0.004	0	0.002	125	35	-	-
		dense	19/20	21/22	30	1200/ 1400	-	0.003/ 0.002	0	0.001/ 0	150/ 200	37.5/ 40	-	-
	strongly silted	loose	18	20	10	400	-	0.009	0	0.003	50	30	-	-
		moderate	19	21	15	600	-	0.006	0	0.002	75	32.5	-	-
		dense	20/21	22/ 22.5	25	1000/ 1500	-	0.003/ 0.002	0	0.001/ 0	125/ 150	35/ 40	-	-
Sand	clean	loose	17	19	5	200	-	0.021	0	0.007	25	30	-	-
		moderate	18	20	15	600	-	0.006	0	0.003	75	32.5	-	-
		dense	19/20	21/22	25	1000/ 1500	-	0.003/ 0.002	0	0.001/ 0	125/ 250	35/ 40	-	-
	weakly silted		18/19	20/21	12	450/ 650	-	0.008/ 0.006	0	0.003/ 0.001	25/ 35	27.5/ 32.5	-	-
		strongly silted		18/19	20/21	8	200/ 400	-	0.019/ 0.009	0	0.006/ 0.001	20/ 30	25/ 30	-
	Loam	weakly sanded	weak	19	19	1	25	650	0.168	0.004	0.056	2	27.5/ 30	0
moderate			20	20	2	45	1,300	0.084	0.002	0.028	5	27.5/ 32.5	2	100
dense			21/22	21/22	3	70/ 100	1,900/ 2,500	0.049/ 0.030	0.001	0.017/ 0.005	10/2 0	27.5/ 35	5/ 7.5	200/ 300
strongly sanded			19/20	19/20	2	45/70	1,300/ 2,000	0.092/ 0.055	0.002	0.031/ 0.005	5/10	27.5/ 35	0/2	50/ 100
Clay	clean	weak	14	14	0.5	7	80	1.357	0.013	0.452	1	17.5	0	25
		moderate	17	17	1.0	15	160	0.362	0.006	0.121	2	17.5	10	50
		dense	19/20	19/20	2.0	25/30	320/ 500	0.168/ 0.126	0.004	0.056/ 0.042	4/10	17.5/ 25	25/ 30	100/ 200
	weakly sanded	weak	15	15	0.7	10	110	0.759	0.009	0.253	1.5	22.5	0	40
		moderate	18	18	1.5	20	240	0.237	0.005	0.079	3	22.5	10	80
		dense	20/21	20/21	2.5	30/50	400/ 600	0.126/ 0.069	0.003	0.042/ 0.014	5/10	22.5/ 27.5	25/ 30	120/ 170
	strongly sanded		18/20	18/20	1.0	25/ 140	320/ 1680	0.190/ 0.027	0.004	0.063/ 0.025	2/5	25/ 30	0/2	0/10
	organic	weak	13	13	0.2	7.5	30	1.690	0.015	0.550	0.5	15	0/2	10
		moderate	15/16	15/16	0.5	10/15	40/60	0.760/ 0.420	0.012	0.250/ 0.140	1.0/2 .0	15	0/2	25/ 30
Peat	not pre-loaded	weak	10/12	10/12	0.1	5/7.5	20/30	7.590/ 1.810	0.023	2.530/ 0.600	0.2/0 .5	15	2/5	10/ 20
	Moderately pre-loaded	moderate	12/13	12/13	0.2	7.5/10	30/40	1.810/ 0.900	0.016	0.600/ 0.300	0.5/1 .0	15	5/1 0	20/ 30

Table E.1: Soil characteristics according to Dutch Standards [source: NEN 6740]

E.2 Safety of closure elements – general failure frequencies per structural component

The safety of closure element is determined in accordance to the Dutch report 'Leidraad Kunstwerken' [9]. In this report, an overview is presented of general failure frequencies per structural component. It has references to several books and reports, which are not analyzed as part of this thesis. The presented values should therefore be handled with care.

Component	Failure mechanism	λ [/h] or Q [/q]	5% - lower boundary	95% - upper boundary
Accumulator battery	No power supply	6.6×10^{-3} [/q]	7.1×10^{-4}	2.1×10^{-2}
	Premature stop	1.9×10^{-6} [/h]	1.8×10^{-7}	6.4×10^{-6}
Cable (above ground)	Cable breaks	3.0×10^{-6} [/km/hr]	2.4×10^{-7}	9.0×10^{-6}
Cable (under ground)	Cable breaks	1.0×10^{-6} [/km/h]	7.0×10^{-7}	1.4×10^{-6}
Cable (signal/control)	Cable breaks	1.0×10^{-5} [/km/h]	1.0×10^{-7}	2.0×10^{-5}
Coax connection	No contact	1.7×10^{-7} [/h]	1.2×10^{-7}	2.5×10^{-7}
Connection power supply	Connection fails	4.0×10^{-5} [/h]	1.0×10^{-5}	1.0×10^{-4}
Converter	Provides no alternating current voltage	1.2×10^{-5} [/h]	4.0×10^{-6}	2.1×10^{-5}
Fusible cut-out	Fails to open	1.0×10^{-5} [/q]	3.8×10^{-7}	3.8×10^{-5}
	Opens spontaneously	1.0×10^{-7} [/h]	3.8×10^{-9}	3.8×10^{-7}
High voltage line	50 kV supply fails	0.9×10^{-5} [/h]	0.6×10^{-5}	1.3×10^{-5}
	110-220 kV supply fails	0.8×10^{-6} [/h]	0.5×10^{-6}	1.0×10^{-6}
	30 kV supply fails	0.3×10^{-6} [/h]	0.2×10^{-6}	0.5×10^{-6}
Limit switch	Fails to open	3.0×10^{-5} [/q]	3.7×10^{-6}	9.3×10^{-5}
	Fails to close	3.0×10^{-5} [/q]	3.7×10^{-6}	9.3×10^{-5}
	Opens spontaneously	1.0×10^{-6} [/h]	3.8×10^{-8}	3.8×10^{-6}
Measuring device	Fails	1.0×10^{-5} [/q]	1.2×10^{-6}	3.6×10^{-5}
Push button	No contact	1.0×10^{-5} [/q]	1.2×10^{-6}	3.6×10^{-5}
Rectifier: stabilized power supply (24 kV)	Provides no rectified voltage	7.8×10^{-6} [/h]	3.5×10^{-7}	2.9×10^{-5}
Switch (manual)	Fails to switch	3.0×10^{-5} [/q]	1.1×10^{-6}	1.1×10^{-4}
Switch (power)	Fails to open/close	3.0×10^{-3} [/q]	1.1×10^{-4}	1.1×10^{-2}
	Opens spontaneously	5.0×10^{-7} [/h]	1.8×10^{-8}	1.8×10^{-6}
Thermal protection	Fails to protect	3.0×10^{-7} [/q]	1.1×10^{-8}	1.1×10^{-6}
	Premature stop	3.0×10^{-7} [/h]	1.1×10^{-8}	1.1×10^{-6}
Transformer	Transformer fails	1.0×10^{-6} [/h]	3.8×10^{-8}	3.8×10^{-6}

Table E.2: Safety of closure elements – electric and electronic components of moving locking devices [9]

Component	Failure mechanism	λ [/h] or Q [/q]	5% - lower boundary	95% - upper boundary
Ball valve	Fails to open/close	3.5×10^{-4} [/q]	2.6×10^{-5}	1.2×10^{-3}
	Blockage	1.9×10^{-7} [/h]	2.8×10^{-8}	5.8×10^{-7}
Cylinder	Fails	1.0×10^{-7} [/h]	3.7×10^{-9}	3.7×10^{-7}
Filter	Blockage	1.0×10^{-5} [/h]	3.7×10^{-7}	3.7×10^{-5}
Gasket	Leakage	5.0×10^{-7} [/h]	1.8×10^{-8}	1.8×10^{-6}
Gearbox	Blockage	1.5×10^{-7} [/h]	4.0×10^{-8}	3.6×10^{-7}
	Premature failure	1.3×10^{-6} [/h]	3.5×10^{-7}	3.1×10^{-6}
Non-return valve	Fails to open	1.5×10^{-4} [/q]	3.5×10^{-5}	3.6×10^{-4}
	Fails to close	1.6×10^{-3} [/q]	1.1×10^{-4}	5.7×10^{-3}
	Opens not in time	9.5×10^{-7} [/h]	5.0×10^{-8}	3.4×10^{-6}
Piston	Leakage along the cylinder	5.0×10^{-7} [/h]	1.8×10^{-8}	1.8×10^{-6}
Pressure vessel	Leakage	5.0×10^{-6} [/h]	1.8×10^{-7}	1.8×10^{-5}
Regulating valve	Internal leakage	5.2×10^{-6} [/h]	1.4×10^{-6}	1.3×10^{-5}
	Fails to regulate	2.6×10^{-5} [/h]	1.0×10^{-6}	6.7×10^{-5}
	Blockage	1.7×10^{-6} [/h]	9.0×10^{-8}	8.2×10^{-6}
Tank	Leakage	5.0×10^{-7} [/h]	1.8×10^{-8}	1.8×10^{-6}
Winch	Fails during operation	7.9×10^{-5} [/h]	5.3×10^{-6}	1.1×10^{-4}

Table E.3: Safety of closure elements – hydraulic, mechanical and pneumatic components of moving locking devices [9]

Component	Failure mechanism	λ [/h] or Q [/q]	5% - lower boundary	95% - upper boundary
Air cooler	Fails to start	2.1×10^{-4} [/q]	9.4×10^{-6}	7.7×10^{-4}
	Premature stop	1.1×10^{-5} [/h]	1.6×10^{-6}	3.1×10^{-5}
Diesel generator	Fails to start	1.0×10^{-2} [/q]	1.2×10^{-3}	3.1×10^{-2}
	Premature stop	3.0×10^{-3} [/h]	1.1×10^{-4}	1.1×10^{-2}
Electric motor	Fails to start	3.0×10^{-5} [/q]	1.1×10^{-6}	1.1×10^{-4}
	Premature stop	3.0×10^{-5} [/h]	1.1×10^{-6}	1.1×10^{-4}
Electric motor – operating valve	Fails to close	6.0×10^{-3} [/q]	6.7×10^{-4}	1.9×10^{-2}
	Fails to open	5.1×10^{-3} [/q]	1.4×10^{-3}	1.2×10^{-2}
	Premature stop	1.4×10^{-6} [/h]	2.4×10^{-7}	3.8×10^{-6}
Electric motor – driving pump	Fails to start	4.8×10^{-3} [/q]	5.5×10^{-4}	1.5×10^{-2}
	Premature stop	8.5×10^{-5} [/h]	3.7×10^{-6}	3.1×10^{-4}

Table E.4: Safety of closure elements – electromechanical components of moving locking devices [9]

Component	Failure mechanism	λ [/h] or Q [/q]
Alarm fault	Ordered staff member	1.0×10^{-3} [/q]
	Other staff member	5.0×10^{-2} [/q]
Fault in handling sequence	2 items	6.0×10^{-3} [/q]
	5 items	4.0×10^{-1} [/q]
Fault by neglecting	With checklist	$1.0 \times 10^{-3} - 3.0 \times 10^{-2}$ [/q]
	Without checklist	$3.0 \times 10^{-3} - 1.0 \times 10^{-2}$ [/q]
Fault in operation	Switch at wrong position	$5.0 \times 10^{-4} - 5.0 \times 10^{-1}$ [/q]
	Wrong reading	$1.0 \times 10^{-3} - 5.0 \times 10^{-2}$ [/q]
Fault in selection	Wrong switch	$5.0 \times 10^{-4} - 3.0 \times 10^{-3}$ [/q]
	Wrong display	$1.0 \times 10^{-3} - 5.0 \times 10^{-2}$ [/q]
Non-availability staff	Sickness	5.0×10^{-2} [/q]
	Accident during transport	1.0×10^{-5} [/km]
	Not attainable (arranged)	1.0×10^{-2} [/q]
	Not attainable (not arranged)	2.0×10^{-1} [/q]

Table E.5: Safety of closure elements – human errors [9]

Component	Failure mechanism	λ [/h] or Q [/q]
Banks navigation channel	Ship collision	1.0×10^{-6} [/km/vessel]
Sliding gate / lifting gate	Failure moveable parts	$3.0 \times 10^{-5} - 3.0 \times 10^{-3}$ [/q]
	Obstacle at the sill	$1.0 \times 10^{-4} - 1.0 \times 10^{-2}$ [/q]
	Sand/debris at the sill	1.0×10^{-2} [/q]
	Ship collision at closed gate	2.0×10^{-5} [/closure]
Stop log	Not be able to install in the dry	1.0×10^{-2} [/h]
	Not be able to install in the wet	1.0×10^{-1} [/h]
	Not be able to install in the wet, given failure of the gate	3.0×10^{-1} [/h]

Table E.6: Safety of closure elements – gates and stop logs [9]

APPENDIX F – Water Movement Around Moving Vessels: Theorem Of Schijf [1949] [40]

In this appendix the water movement around moving vessels is presented. This is done by the approach of Schijf [1949], by which the vessel maximum possible vessel speed (V_{lim}), water level depression (Z_{lim}) and return current (U_{lim}) can be computed.

Introduction: Theorem of Bernoulli

The water movement around moving vessels is complicated, particularly because of the three-dimensional current pattern under and next to the vessel. The shape of inland vessel is generally not ideal because of a large cross-sectional area and blockage coefficient. Furthermore, the presence of a free water level and waterway restrictions of width and depth play an important role in the water movement.

In this thesis, the three-dimensional current is simplified to a one-dimensional current in order to find an exact analytical solution. Although additional modeling could be useful in a detailed design, this one-dimensional model provides sufficient possibilities for a quantitative implementation. The following assumptions are made:

- The channel section has no significant current during normal conditions;
- The cross-sectional restriction at the vertical lifting gate is straight and prismatic, as is the channel;
- A prismatic cross-section over the total length of the vessel;
- A constant speed of the vessel;
- Uniform return current over the total navigable profile next and under the vessel;
- Uniform water level depression of the total width of the navigable profile;
- Depression of the ship is equal to the water level depression;
- No energy losses: omitting of shear stress and inertia losses;
- No influence of waves initiated by the moving vessel;

The axes of the coordinate system are considered to move together with the vessel. With regard to this system the vessel is not moving and the water in the channel is flowing with a permanent velocity equal to the vessel speed V_s . Alongside and under the vessel the velocity is equal to the vessel speed plus the return current, denoted as $V_s + U$. Figure F.1 present and overview of stated parameters.

Using the theory of Bernoulli between cross-sections I and II gives:

$$Z = \frac{(V_s + U)^2}{2g} - \frac{V_s^2}{2g} = \frac{V_s * U}{g} + \frac{U^2}{2g}$$

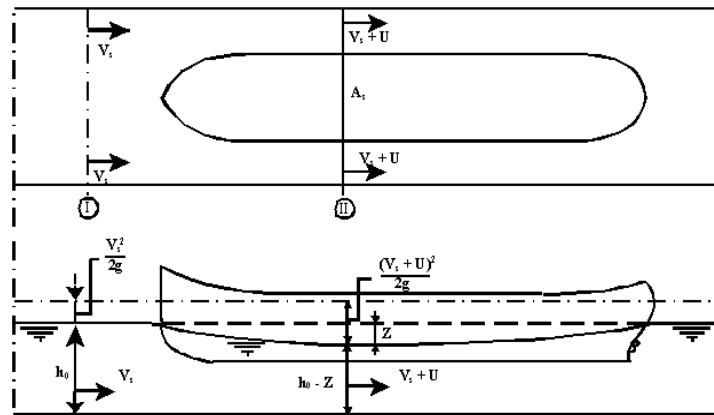


Fig.F.1: Ship-fixed coordinate system [40]

The condition of continuity applied for cross-sections I and II gives:

$$Q = V_s * A_c = (V_s + U) * (A_c - A_s - B * Z)$$

$A_c = b * h =$ wet cross-section area of undisturbed channel [m^2]

$A_s = b * d =$ underwater cross-section of the design vessel [m^2]

$h =$ water depth of the undisturbed channel [m]

$B =$ width at water level of the undisturbed channel [m^2]

$b =$ beam of the design vessel [m]

$d =$ draft of the design vessel [m]

$V_s =$ vessel speed [m/s]

$Z =$ maximum water level depression at amidships section [m]

$U =$ return current velocity along vessel at amidships section [m/s]

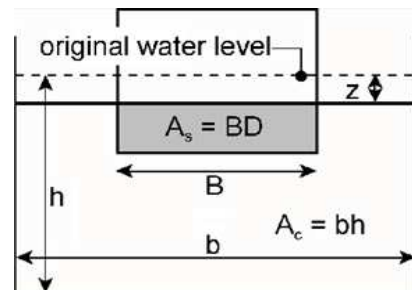


Fig. F.2: Cross-section navigable opening [40]

Method of preservation of energy: Theorem of Schijf

The restrictions of the waterway in depth and width have an impact on the speed of the vessel. Schijf developed a method based on preservation of energy in order to compute the natural limiting speed. This speed is the maximum possible sailing speed (V_{lim}) for a certain vessel in a restricted waterway of given dimensions. The approach of Schijf is limited to shallow water conditions, thus applicable for the Gulf Intracoastal Waterway.

According to Schijf, the limiting speed of the vessel is reached when the return flow is at maximum as a function of the water level depression. The water depth alongside the vessel is thereby equal to the critical water depth for flowing water. When the vessel's speed would still further increase, the water movement next to the vessel would pass from a sub-critical into a critical discharge. Because of the strong decrease of the water depth, which will occur in such a situation, the condition of continuity can not be fulfilled anymore despite the increase of the water velocity. The increase of the water velocity and the decrease of the water depth would cause an accumulation of water in front of the bow. A self-propelled vessel is not able to overcome such an accumulation, making the theorem of Schijf is limited self-propelled vessels.

First step in the theorem of Schijf is combining the equations introduced by Bernoulli. These two equations only contain two unknowns (Z and U). Eliminating one of them results in a pair of equations with only one unknown. Making these equations dimensionless results in:

$$1 - \frac{A_s}{A_c} - \frac{Z}{h} - \left(1 + \frac{4 * Z/h}{V_s^2 / gh}\right)^{-1/2} = 0$$

$$1 - \frac{A_s}{A_c} - \frac{1}{2} * \frac{V_s^2}{gh} - \left[\left(1 - \frac{U/\sqrt{gh}}{V_s/\sqrt{gh}}\right) - 1\right]^2 - \left(1 + \frac{U/\sqrt{gh}}{V_s/\sqrt{gh}}\right)^{-1} = 0$$

These equations can be used after the maximum discharge has been determined. The maximum discharge can be found with the help of the equation of motion and equation of continuity defined by Bernoulli. The equation of continuity results in: $Q_{max} = V_s * A_c = (V_{lim} + U) * (A_c - A_s - B * Z)$

The equation of motion can be rewritten into: $(V_{lim} + U) = (V_{lim}^2 + 2 * g * Z)^{1/2}$

Combining these equations gives: $Q_{max} = V_s * A_c = (V_{lim}^2 + 2 * g * Z)^{1/2} * (A_c - A_s - B * Z)$

Differentiating to Z then gives: $\frac{dQ}{dz} = g * (V_{lim}^2 + 2 * g * Z)^{-1/2} * (A_c - A_s - B * Z) - B * (V_{lim}^2 + 2 * g * Z)^{1/2} = 0$

Using the first dimensionless equation and the well known Froude number, Z can be eliminated which results in:

$$1 - \frac{A_s}{A_c} + \frac{1}{2} Fr^2 - \frac{3}{2} Fr^3 = 0, \text{ with: } Fr = \frac{V_{lim}}{\sqrt{gh}}$$

For the extremes, the following holds: $A_s/A_c = 0, Fr = 1$ and $A_s/A_c = 1, Fr = 0$. This means that at unrestricted width a vessel is able to sail at a maximum speed equal to the velocity of a wave in shallow water. For sailing at the limiting speed, the following relations for the water level depression and return current are found:

$$\frac{Z_{lim}}{h} = \frac{1}{3} * \left(1 - \frac{A_s}{A_c} + \frac{V_{lim}^2}{gh}\right) \text{ and } \frac{U_{lim}}{\sqrt{gh}} = \left[\frac{2}{3} * \left(1 - \frac{A_s}{A_c} + \frac{1}{2} * \frac{V_{lim}^2}{gh}\right)\right]^{1/2} - \frac{V_{lim}}{\sqrt{gh}}$$

Figure F.3 presents $\frac{V_{lim}}{\sqrt{gh}}, \frac{Z_{lim}}{h}$ and $\frac{U_{lim}}{\sqrt{gh}}$ as a function of $\frac{A_s}{A_c}$.

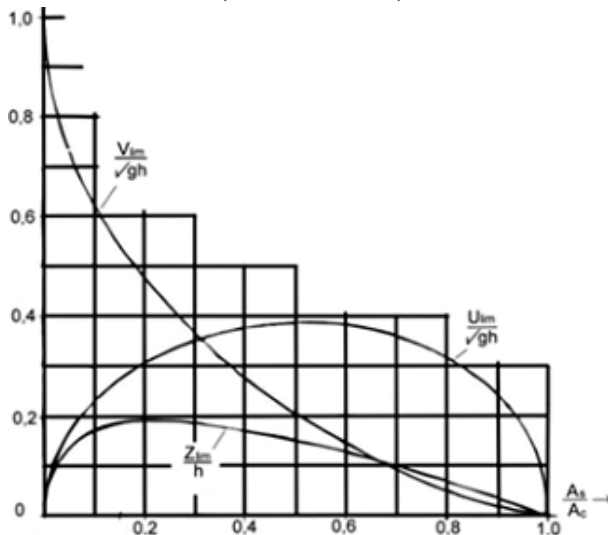


Fig. F.3: Limiting values according to the theorem of Schijf [40]

Calculation

Navigable opening: $h_0 := 18\text{ft}$ $B_0 := 210\text{ft}$
 Design Vessel: $L_{\text{vessel}} := 1095\text{ft}$ $B_{\text{vessel}} := 105\text{ft}$ $D_{\text{vessel}} := 15\text{ft}$

$$A_s := B_{\text{vessel}} \cdot D_{\text{vessel}} = 146.3 \text{ m}^2 \quad A_c := B_0 \cdot h_0 = 351.2 \text{ m}^2 \quad \frac{A_s}{A_c} = 0.417$$

$$\text{eq}(F_r) := 0$$

Guess value: $F_r := 0.5$

Given

$$\text{eq}(F_r) = 1 - \frac{A_s}{A_c} + \frac{1}{2} \cdot F_r^2 - \frac{3}{2} \cdot F_r^3$$

$$\text{Find}(F_r) = 0.265$$

$$V_{\text{lim}} := 0.265 \cdot \sqrt{g \cdot h_0} = 1.94 \frac{\text{m}}{\text{s}}$$

$$Z_{\text{lim}} := h_0 \cdot \left[\frac{1}{3} \cdot \left(1 - \frac{A_s}{A_c} - \frac{V_{\text{lim}}^2}{g \cdot h_0} \right) \right] = 0.94 \text{ m}$$

$$U_{\text{lim}} := \sqrt{g \cdot h_0} \cdot \left[\frac{2}{3} \cdot \left(1 - \frac{A_s}{A_c} + \frac{1}{2} \cdot \frac{V_{\text{lim}}^2}{g \cdot h_0} \right) \right]^{\frac{1}{2}} - \frac{V_{\text{lim}}}{\sqrt{g \cdot h_0}} = 2.77 \frac{\text{m}}{\text{s}}$$

Table F.1 present an overview of the calculation results for the design vessel (beam = 105 ft)

Vessel draft	Max. possible sailing speed		Max. water level depression		Max. return current velocity	
[ft]	[m/s]	[km/h]	[m]	[ft]	[m/s]	[km/h]
6	3.80	13.7	1.03	3.38	2.09	7.5
9	3.06	11.0	1.05	3.44	2.42	8.7
12	2.45	8.8	1.02	3.35	2.64	9.5
15	1.94	7.0	0.94	3.08	2.77	10.0

Table F.1: Calculation results for the design vessel using the theorem of Schijf

Assumed is that vessels navigate at the maximum attainable speed, which is 90% of the limiting speed. Speeds up to 95% of the limiting speed according to Schijf are attainable for usual power engines, but this demands disproportionately more fuel. The maximum attainable speed for the design vessel at maximum draft can now be calculated as $0.9 \cdot V_{\text{lim}} = 0.9 \cdot 7.0 = 6.3 \text{ km/h}$, which is still more than the required lower boundary of 6 km/h.

The maximum water level depression for the design vessel at maximum draft and maximum possible sailing speed amounts 3.1 ft (0.94 m), slightly more than the available depth under the vessel of 3 ft (0.91m). However, this speed is never reached and the actual water level depression at a vessel speed of 6.3 km/h should be determined by using the following formulas, in which A_c and A_s are defined for the situation at hand:

$$0 = \frac{\alpha \cdot (V_s + U)^2 - V_s^2}{2gh} - \frac{U}{V_s + U} + \frac{A_s}{A_c}, \text{ in which: } \alpha = 1.4 - 0.4 \cdot \frac{V_s}{V_{\text{lim}}} = 1.4 - 0.36 = 1.04$$

Iteration of this formula, with $A_s = 105 \times 15 \text{ ft}^2 = 146.3 \text{ m}^2$ and $A_c = 210 \times 18 \text{ ft}^2 = 351.2 \text{ m}^2$, provides the actual return current $U = 1.84 \text{ m/s}$.

The water level depression can be determined by using:

$$Z = \frac{\alpha \cdot (V_s + U)^2 - V_s^2}{2g}$$

Substitution of α , U and $V_s = 0.9 \times 1.94 = 1.75 \text{ m/s}$ provides the actual water level depression $Z = 0.53 \text{ m}$. This water level depression at the actual attained navigation speed proves to be smaller than the maximum allowed depression of 0.91 m, equal to the clearance of 3 ft.

APPENDIX G – Excel Results

G.1 Overtopping discharge at the outer levee under variable surge level

Hurricane input (PMH)

h_w = maximum surge level	24 ft	=	7,3 m
H_s = significant wave height	12 ft	=	3,7 m
T_p = peak wave period	14 sec		
g = acceleration of gravity	9,8 m/s ²		

Proposed levee design

average depth Lake Borgne at levee alignment	10 ft		3,0 m
$\tan\alpha$ = angle outer slope of the outer levee	1/4 [-]		
h_c = crest level	47 ft	=	14,3 m
γ_β = influence factor for angled wave attack	1,0 [-]		
γ_f = influence factor for roughness elements on slope	0,7 [-]		
γ_b = influence factor for a berm	1,0 [-]		
combined reduction factor	0,7 [-]	≥	0,4 OK

*) Wave approach - wave breaking index $\gamma = 0.5 = H_s / d$

d = water depth	34 ft	=	10,4 m
γ = breaker index	0,35 [-]	<	0,5 non-breaking

*) Wave overtopping (only valid of $h_c > h_w$)

breaker index

S_{op} = wave steepness	0,014 [-]		
ξ = breaker index	2,1 [-]	>	2 non-breaking

overtopping discharge

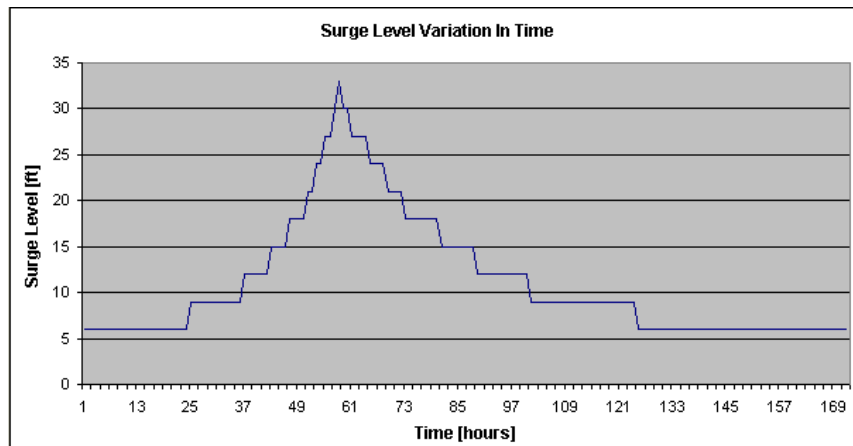
$$\frac{q_b}{\sqrt{g * H_s^3}} = \frac{0.067}{\sqrt{\tan(\alpha)}} * \gamma_b * \xi_0 * \exp\left(-4.3 * \frac{Rc}{H_s} * \frac{1}{\xi_0 * \gamma_b * \gamma_f * \gamma_\beta}\right)$$

Hydraulic Formulas: TAW - Wave Run-up And Wave Overtopping At Dikes, 2002

and a maximum of: $\frac{q_{nb}}{\sqrt{g * H_s^3}} = 0.2 * \exp\left(-2.3 * \frac{Rc}{H_s} * \frac{1}{\gamma_f * \gamma_\beta}\right)$

q_b = overtopping discharge for breaking waves	21,09 (l/s)/m		
q_n = overtopping discharge for non-breaking waves	8,06 (l/s)/m		maximum

*) Modeled time-dependent surge level



G.2 Vertical lifting gate – minimum required retaining height at moment of installation

Maximum water level retention area regarding inner levee (+) 7,4 ft MSL
 Maximum water level retention area regarding time of closure (+) 5,0 ft MSL

Allowed water level increase due to overtopping of outer levee
 and overtopping/overflow of navigable floodgate structure: 2,4 ft = 0,73 m

Outer Levee Alignment - requirement: maximum overtopping discharge ≈ 100 (l/s)/m

$\tan\alpha$ = incline of the outer slope of the levee 1/4 [-]
 h_c = crest level 47 ft
 combined reduction factor 0,7 [-]

crest height outer	surge level	overtopping discharge	duration		overtopping volume
levee: + 47 ft MSL	[ft]	[(l/s)/m]	[hour, <-- l]	[hour, l -->]	[m ³ /m]
	6	0,06	24	x (no diff. head)	5,2
	9	0,13	12	24	16,8
	12	0,30	6	12	19,4
	15	0,69	4	8	29,8
	18	1,56	4	8	67,4
	21	3,55	2	4	76,7
	24	8,06	2	4	174,1
	27	18,33	2	4	395,9
	30	41,68	1	2	450,1
	33	94,78	1		341,2
	total overtopping volume		1576,7	[m ³ /m]	
	length levee alignment		18	[km]	
	surface area retention basin		90	[km ²]	
	surface elevation retention basin		0,32	[m]	

Vertical Lifting Gate - requirement: maximum allowed surface elevation retention basin = 0,73 - 0,32 = 0,41 m

vertical lifting	surge level	overtopping discharge	duration		overtopping volume
gate: + 22 ft MSL	[ft]	[(m ³ /s)/m]	[hour, <-- l]	[hour, l -->]	[m ³ /m]
	6	0,05	24	x (no diff. head)	4493
	9	0,11	12	24	14256
	12	0,23	6	12	15163
	15	0,50	4	8	21384
	18	1,05	4	8	45274
	21	2,22	3	4	55894
	24	3,75	3	4	94475
	27	6,41	2	4	138499
	30	10,06	1	2	108670
	33	14,48	1		52124
	total overtopping volume		550231	[m ³ /m]	
	width structure		64	[m]	
	surface area retention basin		90	[km ²]	
	surface elevation retention basin		0,39	[m]	

Minimum retaining height of the vertical lifting gate without leakage and time dependent changes = + 22 ft MSL.

G.3 Vertical lifting gate – iterative calculation to determine optimum combination for leakage width and gate height

width = 0.05 m - requirement: maximum surface elevation retention basin due to leakage + overtopping/overflow \leq 0.41 m

leakage width:	surge level	leakage discharge	duration		overtopping volume
0.05 m around	[ft]	[(m ³ /s)/m]	[hour, <-- l]	[hour, l -->]	[m ³ /m]
	6	0,14	24	x (no diff. head)	12096
	9	0,28	12	24	36418
	12	0,37	6	12	24041
	15	0,44	4	8	19181
	18	0,51	4	8	21859
	21	0,56	2	4	12118
	24	0,61	2	4	13219
	27	0,66	2	4	14213
	30	0,70	1	2	7582
	33	0,74	1		2671
	total leakage volume		163397	[m ³ /m]	
	width structure		64	[m]	
	surface area retention basin		90	[km ²]	
	surface elevation retention basin		0,12	[m]	

vertical lifting	surge level	overtopping discharge	duration		overtopping volume
gate: + 24 ft MSL	[ft]	[(m ³ /s)/m]	[hour, <-- l]	[hour, l -->]	[m ³ /m]
	6	0,03	24	x (no diff. head)	2592
	9	0,07	12	24	9072
	12	0,14	6	12	9202
	15	0,30	4	8	12960
	18	0,64	4	8	27432
	21	1,35	2	4	29052
	24	2,85	2	4	61517
	27	4,50	2	4	97286
	30	7,53	1	2	81356
	33	11,46	1		41242
	total overtopping volume		371711	[m ³ /m]	
	width structure		64	[m]	
	surface area retention basin		90	[km ²]	
	surface elevation retention basin		0,26	[m]	

width = 0.10 m - requirement: maximum surface elevation retention basin due to leakage + overtopping/overflow \leq 0.41 m

leakage width:	<i>surge level</i>	<i>leakage discharge</i>	<i>duration</i>		<i>overtopping volume</i>
0.10 m around	[ft]	[(m ³ /s)/m]	[hour, <-- l]	[hour, l -->]	[m ³ /m]
	6	0,29	24	x (no diff. head)	24710
	9	0,57	12	24	74261
	12	0,76	6	12	49118
	15	0,91	4	8	39096
	18	1,03	4	8	44582
	21	1,15	2	4	24732
	24	1,25	2	4	26957
	27	1,34	2	4	29009
	30	1,43	1	2	15466
	33	1,52	1		5454
	total leakage volume		333385	[m ³ /m]	
	width structure		64	[m]	
	surface area retention basin		90	[km ²]	
	surface elevation retention basin		0,24	[m]	

vertical lifting	<i>surge level</i>	<i>overtopping discharge</i>	<i>duration</i>		<i>overtopping volume</i>
gate: + 27 ft MSL	[ft]	[(m ³ /s)/m]	[hour, <-- l]	[hour, l -->]	[m ³ /m]
	6	0,02	24	x (no diff. head)	1296
	9	0,03	12	24	4147
	12	0,07	6	12	4342
	15	0,14	4	8	6134
	18	0,30	4	8	12960
	21	0,64	2	4	13716
	24	1,35	2	4	29052
	27	2,85	2	4	61517
	30	4,50	1	2	48643
	33	7,53	1		27119
	total overtopping volume		208926	[m ³ /m]	
	width structure		64	[m]	
	surface area retention basin		90	[km ²]	
	surface elevation retention basin		0,15	[m]	

width = 0.05/0.15 m - requirement: max. surface elevation retention basin due to leakage + overtopping/overflow ≤ 0.41 m

leakage width:	<i>surge level</i>	<i>leakage discharge</i>	<i>duration</i>		<i>overtopping volume</i>
0.05 m at sides	[ft]	[(m ³ /s)/m]	[hour, <-- l]	[hour, l -->]	[m ³ /m]
0.15 m at bottom	6	0,39	24	x (no diff. head)	33782
	9	0,78	12	24	101218
	12	1,03	6	12	66938
	15	1,24	4	8	53352
	18	1,41	4	8	60826
	21	1,56	2	4	33739
	24	1,70	2	4	36763
	27	1,83	2	4	39571
	30	1,95	1	2	21092
	33	2,07	1		7438
			total leakage volume	454720	[m ³ /m]
			width structure	64	[m]
			surface area retention basin	90	[km ²]
			surface elevation retention basin	0,32	[m]

vertical lifting	<i>surge level</i>	<i>overtopping discharge</i>	<i>duration</i>		<i>overtopping volume</i>
gate: + 30 ft MSL	[ft]	[(m ³ /s)/m]	[hour, <-- l]	[hour, l -->]	[m ³ /m]
	6	0,01	24	x (no diff. head)	656
	9	0,02	12	24	1944
	12	0,03	6	12	2074
	15	0,07	4	8	2894
	18	0,14	4	8	6134
	21	0,30	3	4	7560
	24	0,64	3	4	16002
	27	1,35	2	4	29052
	30	2,85	1	2	30758
	33	4,50	1		16214
			total overtopping volume	113289	[m ³ /m]
			width structure	64	[m]
			surface area retention basin	90	[km ²]
			surface elevation retention basin	0,08	[m]

APPENDIX H – MathCAD Results

H.1 Maximum water level allowed in the retention area and minimum required crest height of the outer levee with associated overtopping discharge (results serve as input Excel-calculations)

H.1.1 Inner levee – maximum water level allowed in the retention area

Influence factor for roughness elements on the outer slope: $\gamma_{f,inner} := 1.0$ (grass cover)

Influence factor for angled wave attack: $\gamma_{\beta,inner} := 1.0$ (incoming waves perpendicular to levee)

==> Maximum significant wave height for non-breaking waves = 0.5 x water depth (d)

$$q_{nb,inner}(d) := \frac{1}{1000} \cdot \frac{\left(\frac{m^3}{s}\right)}{m}$$

Guess value: $d := 3m$ (+m MSL)

$$\text{Given } q_{nb,inner}(d) = \sqrt{g \cdot (0.5d)^3} \cdot 0.2 \cdot e^{\left(-2.3 \cdot \frac{18ft-d}{0.5d} \cdot \frac{1}{\gamma_{f,inner} \gamma_{\beta,inner}}\right)}$$

Find(d) = 2.25 m = maximum water level allowed in retention area (+m MSL)

H.1.2 Outer levee – minimum required crest height of the outer levee with associated overtopping discharge

Breaker index - determination breaking/non-breaking waves

$$g = 9.807 \frac{m}{s^2} \quad H_s := 12ft = 3.66m \quad T_p := 14 \cdot s$$

steepness of the outer slope: $\tan(\text{angle}) := \frac{1}{4}$

$$\text{wave steepness: } s_0 := \frac{2\pi H_s}{g \cdot \left(\frac{T_p}{1.1}\right)^2} = 0.014, \text{ which leads to the breaker index: } \xi_0 := \frac{\tan(\text{angle})}{\sqrt{(s_0)}} = 2.08$$

Overtopping discharge for non-breaking waves - critical height levee alignment

Influence factor for roughness elements on the outer slope: $\gamma_{f,outer} := 0.70$ (armour rock - single layer)

Influence factor for angled wave attack: $\gamma_{\beta,outer} := 1.0$ (incoming waves perpendicular to levee)

$$q_{nb,outer}(h_{kr}) := \frac{10}{1000} \cdot \frac{\left(\frac{m^3}{s}\right)}{m}$$

Guess value: $h_{kr} := 3m$

$$\text{Given } q_{nb,outer}(h_{kr}) = \sqrt{g \cdot H_s^3} \cdot 0.2 \cdot e^{\left(-2.3 \cdot \frac{h_{kr}}{H_s} \cdot \frac{1}{\gamma_{f,outer} \gamma_{\beta,outer}}\right)}$$

Find(h_{kr}) = 6.77 m = required crest height above maximum surge level

Overtopping discharge for non-breaking waves

$$H_s = 3.66m \quad \gamma_{f,outer} = 0.7 \quad \gamma_{\beta,outer} = 1 \quad +$$

Variable: surge level (+ft MSL): $h_{surge} := 30ft$

$$q_{nb} := \sqrt{g \cdot H_s^3} \cdot 0.2 \cdot e^{\left[-2.3 \cdot \frac{(47ft - h_{surge})}{H_s} \cdot \frac{1}{\gamma_{f,outer} \gamma_{\beta,outer}}\right]} = 0.0417 \frac{m^2}{s}$$

H.2 Retaining height of the vertical lifting gate and allowed leakage

H.2.1 Retaining height of the vertical lifting gate – additional water allowed in the retention area

Crest height structure above maximum surge level ($h_{kr} > 0$) - overtopping discharge

$$g = 9.807 \frac{\text{m}}{\text{s}^2} \quad H_s := 12\text{ft} = 3.66 \text{ m}$$

$\gamma_\beta := 1.0$ and $\gamma_n := 1.0$ (reduction coefficients for the angle of incidence and gate configuration respectively)

Variable: $h_{kr,above} := 6\text{ft}$

$$q_{\text{overtopping}} := 0.13 \cdot \sqrt{g \cdot H_s^3} \cdot e^{\left(-3.0 \frac{h_{kr,above}}{H_s} \frac{1}{\gamma_\beta \gamma_n}\right)} = 0.635 \cdot \left(\frac{\text{m}^3}{\text{s}}\right) \quad +$$

Crest height structure under maximum surge level ($h_{kr} < 0$) - overflow discharge

$m_{\text{constant}} := 1.1$ Variable: $h_{kr,under} := -3\text{ft}$

$$q_{\text{overflow}} := 0.55 \cdot m_{\text{constant}} \cdot \sqrt{-g \cdot h_{kr,under}^3} = 1.657 \cdot \left(\frac{\text{m}^3}{\text{s}}\right)$$

Total discharge total discharge as an combination of overtopping and overflow

$$q_{\text{overflow.overtopping}} := q_{\text{overflow}} + 0.13 \cdot \sqrt{g \cdot H_s^3} = 4.504 \cdot \left(\frac{\text{m}^3}{\text{s}}\right)$$

H.2.2 Leakage – allowed volume of water in the retention area in addition to the overtopping discharges

Leakage width: $w_{L,under} := 0.15\text{m}$ and $w_{L,side} := 0.05\text{m}$

Dimensionless discharge coefficient: $\mu_{\text{side}} := 1.0$ and $\mu_{\text{under}} := 1.0$ (preliminary design)

Width gate opening: $w_{\text{gate}} := 210\text{ft}$

Proposed gate height (+ ft MSL): $h_{\text{gate}} := 30\text{ft}$

Water level inside retention area (+ ft MSL): $h_{\text{retention}} := 5\text{ft}$ (fixed at this minimum water level at closure)

Variable: surge level (+ ft MSL): $h_{\text{surge}} := 33\text{ft}$

$$Q_{\text{under}} := \mu_{\text{under}} \cdot w_{L,under} \cdot w_{\text{gate}} \cdot \sqrt{2 \cdot g \cdot (h_{\text{surge}} - h_{\text{retention}})} = 124.22 \frac{\text{m}^3}{\text{s}}$$

$$Q_{\text{side}} := \mu_{\text{side}} \cdot w_{L,side} \cdot (h_{\text{gate}} - h_{\text{retention}}) \cdot \sqrt{2 \cdot g \cdot \left(\frac{2}{3}\right) \cdot (h_{\text{surge}} - h_{\text{retention}})} = 4.02 \frac{\text{m}^3}{\text{s}}$$

$$\text{Total discharge per meter: } q_{\text{leakage}} := \frac{(Q_{\text{under}} + 2 \cdot Q_{\text{side}})}{w_{\text{gate}}} = 2.07 \cdot \left(\frac{\text{m}^3}{\text{s}}\right)$$

H.3 Modified model of Goda – wave forces on a vertical wall

Hydraulic boundary conditions:

$$h_{\text{surge}} := 24\text{ft} = 7.32\text{ m (MSL)} \quad H_s := 12\text{ft} = 3.66\text{ m} \quad T_p := 14\text{ s} \quad \beta := 0\text{-deg}$$

$$g = 9.807 \frac{\text{m}}{\text{s}^2} \quad \rho_w := 1025 \frac{\text{kg}}{\text{m}^3} \quad \gamma_w := \rho_w g = 10.05 \frac{\text{kN}}{\text{m}^3}$$

$$H_d := 2.2 \cdot H_s = 8.05\text{ m} \quad L := \frac{g \cdot T_p^2}{2 \cdot \pi} = 305.9\text{ m}$$

Geometrics:

$$h_{\text{bottom.outer}} := -18\text{ft} = -5.49\text{ m (MSL)}$$

$$h_{\text{bottom.inner}} := -18\text{ft} = -5.49\text{ m (MSL)}$$

$$h_{\text{bottom.sill}} := -18\text{ft} = -5.49\text{ m (MSL)}$$

$$h_{\text{bottom.foundation}} := -18\text{ft} = -5.49\text{ m (MSL)}$$

$$d_{\text{toplayer}} := 0\text{ft} \quad \text{and} \quad w_{\text{berm}} := 0\text{ft}$$

Dimensions lifting gate

$$h_{\text{height.gate}} := 30\text{ft} = 9.14\text{ m (MSL)}$$

$$t_{\text{gate}} := 2\text{ft} = 0.61\text{ m}$$

$$\lambda_1 := 1 \quad \lambda_2 := 1 \quad \lambda_3 := 1 \quad (\text{modification factors: depend on the structural form, but set to be 1 in this preliminary design stage})$$

$$\text{Results: } h_s := h_{\text{surge}} - h_{\text{bottom.outer}} = 12.8\text{ m}$$

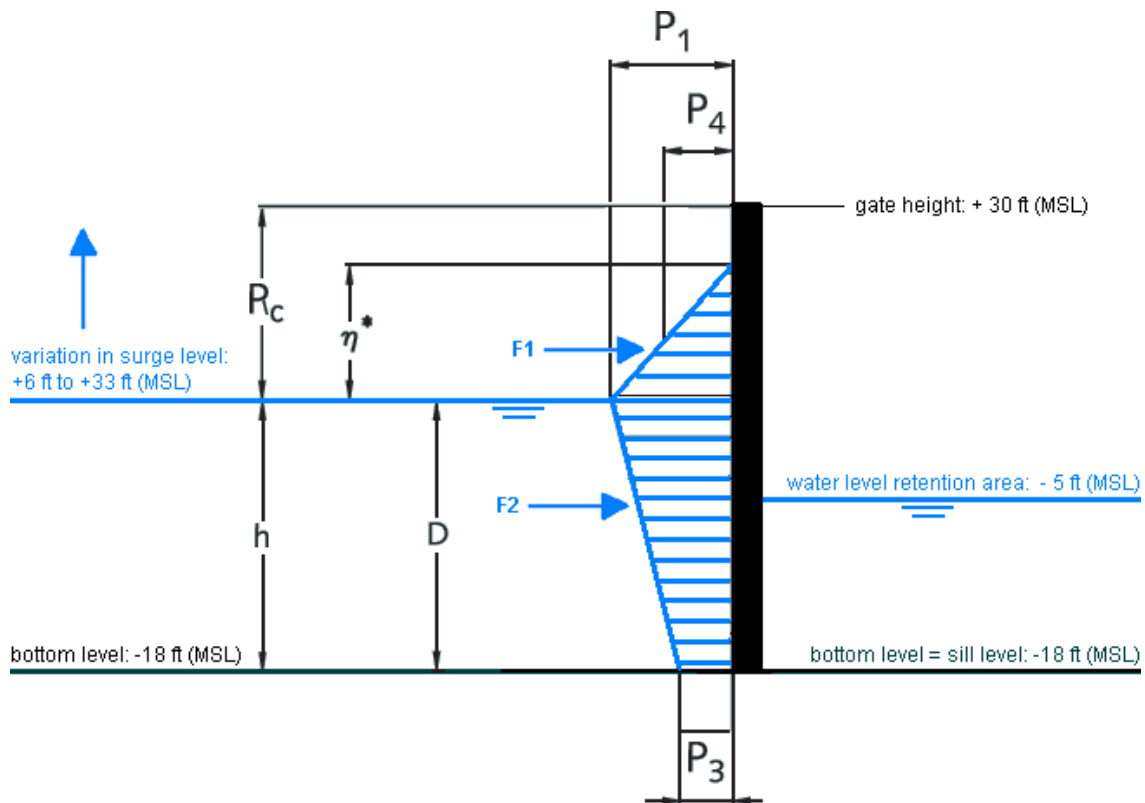
$$d_c := d_{\text{toplayer}} = 0$$

$$d := h_{\text{surge}} - h_{\text{bottom.sill}} = 12.8\text{ m}$$

$$B_b := w_{\text{berm}} = 0$$

$$h_c := h_{\text{height.gate}} - h_{\text{bottom.sill}} = 14.63\text{ m}$$

$$B_c := t_{\text{gate}} = 0.61\text{ m}$$



Vertical lifting gate - crest height: $R_d(h_c, d, d_c) = h_c - d - d_c$
 Crest elevation: $\eta(H_d, \beta, \lambda_1) = 0.75 \lambda_1 (1 + \cos(\beta)) H_d$

$R_d(h_c, d, d_c) = 1.83 \text{ m}$
 $\eta(H_d, \beta, \lambda_1) = 12.07 \text{ m}$

Coefficients for the wave pressure:

$$\alpha_1(h_s, L) = 0.6 + \frac{1}{2} \left(\frac{\frac{4\pi h_s}{L}}{\sinh\left(\frac{4\pi h_s}{L}\right)} \right)^2$$

$\alpha_1(h_s, L) = 1.058$

$$\alpha_{21}(H_d, h_s, d) = \frac{1}{3} \left(\frac{h_s - d}{h_s} \right) \left(\frac{H_d}{d} \right)^2$$

$\alpha_{22}(H_d, d) = \frac{2-d}{H_d}$

$$\alpha_2(H_d, h_s, d) = \min \left(\alpha_{21}(H_d, h_s, d), \alpha_{22}(H_d, d) \right)$$

$\alpha_2(H_d, h_s, d) = 0$

$$\alpha_3(H_d, h_s, d, d_c, L) = 1 - \frac{d + d_c}{h_s} \left(1 - \frac{1}{\cosh\left(\frac{2\pi h_s}{L}\right)} \right)$$

$\alpha_3(H_d, h_s, d, d_c, L) = 0.866$

$$\delta_{11}(H_d, L, h_s, d, B_b) = 0.93 \left(\frac{B_b}{L} - 0.12 \right) + 0.36 \left(\frac{h_s - d}{h_s} - 0.6 \right)$$

$\delta_{11}(H_d, L, h_s, d, B_b) = -0.328$

$$\delta_{22}(H_d, L, h_s, d, B_b) = -0.36 \left(\frac{B_b}{L} - 0.12 \right) + 0.93 \left(\frac{h_s - d}{h_s} - 0.6 \right)$$

$\delta_{22}(H_d, L, h_s, d, B_b) = -0.515$

$$\delta_1(H_d, L, h_s, d, B_b) = \text{if}(\delta_{11}(H_d, L, h_s, d, B_b) > 0.15 \delta_{11}(H_d, L, h_s, d, B_b), 20 \delta_{11}(H_d, L, h_s, d, B_b)) \quad \delta_1(H_d, L, h_s, d, B_b) = -6.552$$

$$\delta_2(H_d, L, h_s, d, B_b) = \text{if}(\delta_{22}(H_d, L, h_s, d, B_b) > 0.3 \delta_{22}(H_d, L, h_s, d, B_b), 4.9 \delta_{22}(H_d, L, h_s, d, B_b))$$

$$\alpha_n(H_d, L, h_s, d, B_b) = \text{if} \left(\delta_2(H_d, L, h_s, d, B_b) > 0, \frac{1}{\cosh(\delta_1(H_d, L, h_s, d, B_b)) \sqrt{\cosh(\delta_2(H_d, L, h_s, d, B_b))} \cosh(\delta_1(H_d, L, h_s, d, B_b))} \cos(\delta_2(H_d, L, h_s, d, B_b)) \right)$$

$\alpha_n(H_d, L, h_s, d, B_b) = -2.325 \times 10^{-3}$

$$\alpha_0(H_d, d) = \text{if} \left(\frac{H_d}{d} > 2, 2, \frac{H_d}{d} \right)$$

$\alpha_0(H_d, d) = 0.629$

$\alpha_l(H_d, L, h_s, d, B_b) = \alpha_0(H_d, d) \alpha_n(H_d, L, h_s, d, B_b)$

$\alpha_l(H_d, L, h_s, d, B_b) = -1.461 \times 10^{-3}$

$$\alpha_{2l}(H_d, L, h_s, d, B_b) = \max \left(\alpha_l(H_d, L, h_s, d, B_b), \alpha_2(H_d, h_s, d) \right)$$

$\alpha_{2l}(H_d, L, h_s, d, B_b) = \alpha_2(H_d, h_s, d)$

Pressures:

$$p_1(H_d, L, h_s, d, B_b, \beta, \lambda_1, \lambda_2, \gamma_w) = \frac{1}{2} (1 + \cos(\beta)) \left(\lambda_1 \alpha_1(h_s, L) + \lambda_2 \alpha_{2l}(H_d, L, h_s, d, B_b) \cos(\beta)^2 \right) \gamma_w H_d \quad p_1(H_d, L, h_s, d, B_b, \beta, \lambda_1, \lambda_2, \gamma_w) = 85.44 \frac{\text{kN}}{\text{m}^2}$$

$$p_3(H_d, L, h_s, d, d_c, B_b, \beta, \lambda_1, \lambda_2, \gamma_w) = \alpha_3(H_d, h_s, d, d_c, L) p_1(H_d, L, h_s, d, B_b, \beta, \lambda_1, \lambda_2, \gamma_w)$$

$$p_d(H_d, L, h_s, d, d_c, B_b, \beta, \lambda_1, \lambda_2, \gamma_w) = \begin{cases} p_1(H_d, L, h_s, d, B_b, \beta, \lambda_1, \lambda_2, \gamma_w) \left[\alpha_3(H_d, h_s, d, d_c, L) \left(1 - \frac{h_c}{d + d_c} \right) + \frac{h_c}{d + d_c} \right] & \text{if } R_d(h_c, d, d_c) < 0 \\ 0 & \text{if } R_d(h_c, d, d_c) > \eta(H_d, \beta, \lambda_1) \\ \left(1 - \frac{R_d(h_c, d, d_c)}{\eta(H_d, \beta, \lambda_1)} \right) p_1(H_d, L, h_s, d, B_b, \beta, \lambda_1, \lambda_2, \gamma_w) & \text{otherwise} \end{cases}$$

$$p_u(H_d, L, h_s, d, d_c, \beta, \gamma_w, \lambda_2) = \frac{1}{2} (1 + \cos(\beta)) \alpha_1(h_s, L) \alpha_3(H_d, h_s, d, d_c, L) \lambda_2 \gamma_w H_d$$

Wave forces:

$$F_1(H_d, L, h_c, h_s, d, d_c, B_b, \beta, \lambda_1, \lambda_2, \gamma_w) = \begin{cases} \frac{p_1(H_d, L, h_s, d, B_b, \beta, \lambda_1, \lambda_2, \gamma_w) + p_d(H_d, L, h_c, h_s, d, d_c, B_b, \beta, \lambda_1, \lambda_2, \gamma_w)}{2} \min \left(\frac{\eta(H_d, \beta, \lambda_1)}{R_d(h_c, d, d_c)} \right) & \text{if } R_d(h_c, d, d_c) > 0 \\ \beta p_1(H_d, L, h_s, d, B_b, \beta, \lambda_1, \lambda_2, \gamma_w) \eta(H_d, \beta, \lambda_1) & \text{otherwise} \end{cases}$$

$$F_2(H_d, L, h_c, h_s, d, d_c, B_b, \beta, \lambda_1, \lambda_2, \gamma_w) = \begin{cases} \frac{p_1(H_d, L, h_s, d, B_b, \beta, \lambda_1, \lambda_2, \gamma_w) + p_3(H_d, L, h_s, d, d_c, B_b, \beta, \lambda_1, \lambda_2, \gamma_w)}{2} (d + d_c) & \text{if } R_d(h_c, d, d_c) > 0 \\ \frac{p_3(H_d, L, h_s, d, d_c, B_b, \beta, \lambda_1, \lambda_2, \gamma_w) + p_d(H_d, L, h_c, h_s, d, d_c, B_b, \beta, \lambda_1, \lambda_2, \gamma_w)}{2} h_c & \text{otherwise} \end{cases}$$

$$F_u(H_d, L, h_c, h_s, d, d_c, \beta, \gamma_w, \lambda_2) = \frac{1}{2} p_u(H_d, L, h_s, d, d_c, \beta, \gamma_w, \lambda_2) B_c$$

Lever arms:

$$a_1(H_d, L, h_c, h_s, d, d_c, B_b, \beta, \lambda_1, \lambda_2, \gamma_w) = d + d_c + \frac{p_1(H_d, L, h_s, d, B_b, \beta, \lambda_1, \lambda_2, \gamma_w) + 2 p_d(H_d, L, h_c, h_s, d, d_c, B_b, \beta, \lambda_1, \lambda_2, \gamma_w)}{3 (p_1(H_d, L, h_s, d, B_b, \beta, \lambda_1, \lambda_2, \gamma_w) + p_d(H_d, L, h_c, h_s, d, d_c, B_b, \beta, \lambda_1, \lambda_2, \gamma_w))} \min \left(\frac{R_d(h_c, d, d_c)}{\eta(H_d, \beta, \lambda_1)} \right)$$

$$a_2(H_d, L, h_c, h_s, d, d_c, B_b, \beta, \lambda_1, \lambda_2, \gamma_w) = \frac{2 p_1(H_d, L, h_s, d, B_b, \beta, \lambda_1, \lambda_2, \gamma_w) + p_3(H_d, L, h_s, d, d_c, B_b, \beta, \lambda_1, \lambda_2, \gamma_w)}{3 (p_1(H_d, L, h_s, d, B_b, \beta, \lambda_1, \lambda_2, \gamma_w) + p_3(H_d, L, h_s, d, d_c, B_b, \beta, \lambda_1, \lambda_2, \gamma_w))} (d + d_c) \text{ if } R_d(h_c, d, d_c) > 0$$

$$a_u(B_c) = \frac{B_c}{6} \frac{2 p_d(H_d, L, h_c, h_s, d, d_c, B_b, \beta, \lambda_1, \lambda_2, \gamma_w) + p_3(H_d, L, h_s, d, d_c, B_b, \beta, \lambda_1, \lambda_2, \gamma_w)}{3 (p_d(H_d, L, h_c, h_s, d, d_c, B_b, \beta, \lambda_1, \lambda_2, \gamma_w) + p_3(H_d, L, h_s, d, d_c, B_b, \beta, \lambda_1, \lambda_2, \gamma_w))} h_c \text{ otherwise}$$

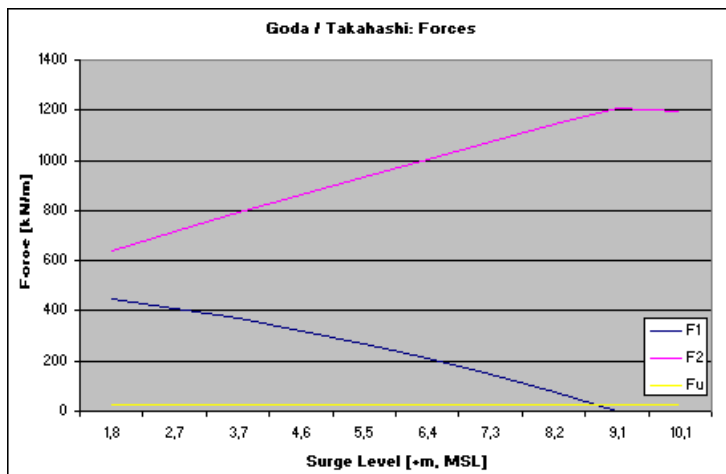
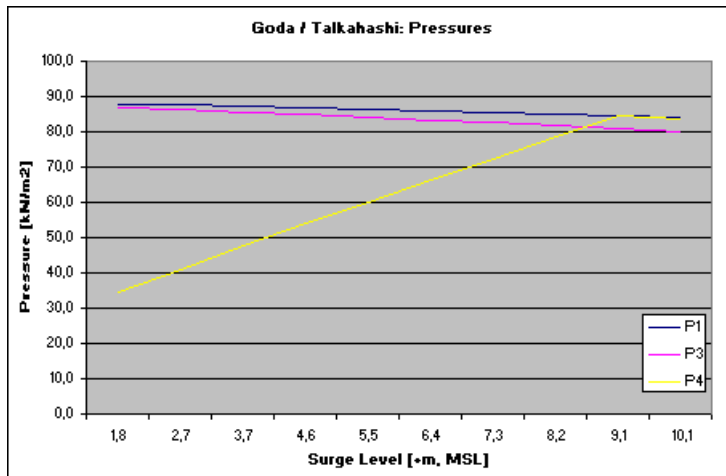
Resulting horizontal force and moment

$$F_H(H_d, L, h_c, h_s, d, d_c, B_b, \beta, \lambda_1, \lambda_2, \gamma_w) = F_1(H_d, L, h_c, h_s, d, d_c, B_b, \beta, \lambda_1, \lambda_2, \gamma_w) + F_2(H_d, L, h_c, h_s, d, d_c, B_b, \beta, \lambda_1, \lambda_2, \gamma_w)$$

$$M_H(H_d, L, h_c, h_s, d, d_c, B_b, \beta, \lambda_1, \lambda_2, \lambda_3, \gamma_w) = a_1(H_d, L, h_c, h_s, d, d_c, B_b, \beta, \lambda_1, \lambda_2, \gamma_w) F_1(H_d, L, h_c, h_s, d, d_c, B_b, \beta, \lambda_1, \lambda_2, \gamma_w) - a_2(H_d, L, h_c, h_s, d, d_c, B_b, \beta, \lambda_1, \lambda_2, \gamma_w) F_2(H_d, L, h_c, h_s, d, d_c, B_b, \beta, \lambda_1, \lambda_2, \gamma_w)$$

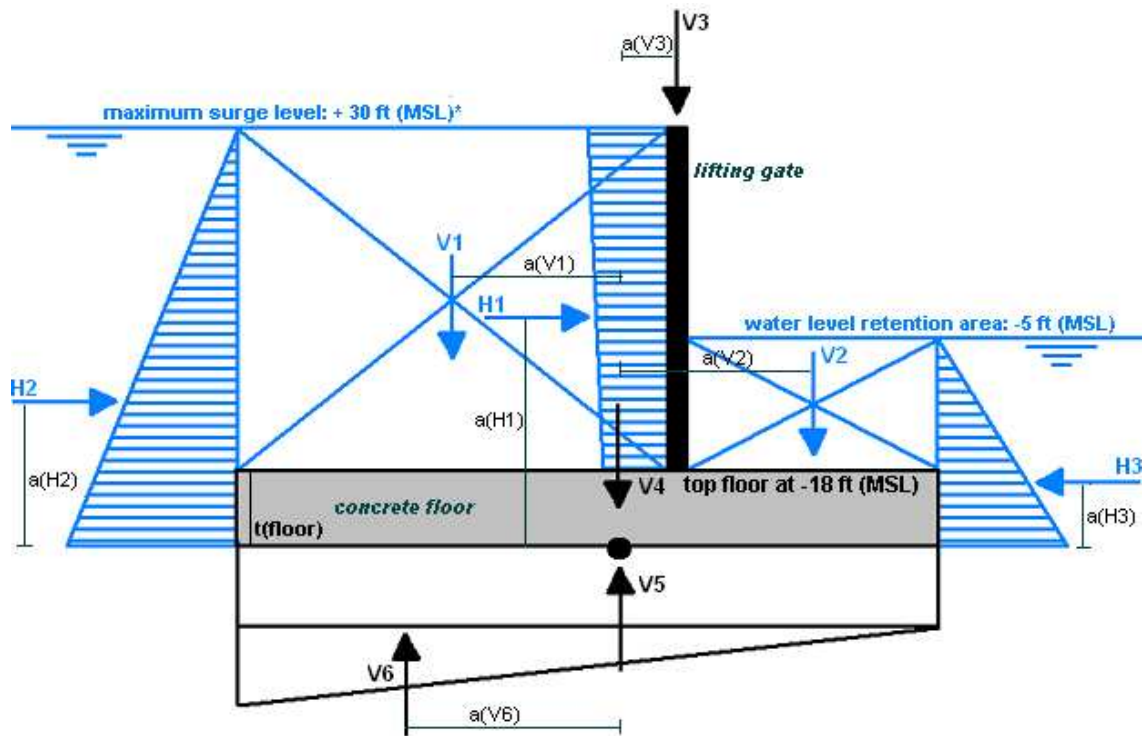
Goda / Takahashi Model: Results

	storm surge level (MSL)										
	6	9	12	15	18	21	24	27	30	33	[ft]
	1,8	2,7	3,7	4,6	5,5	6,4	7,3	8,2	9,1	10,1	[m]
Pressures:											
P ₁	87,8	87,5	87,1	86,7	86,3	85,9	85,4	84,9	84,4	83,9	[kN/m ²]
P ₃	86,8	86,2	85,6	84,9	84,2	83,4	82,6	81,7	80,7	79,8	[kN/m ²]
P ₄	34,6	41,1	47,5	53,9	60,2	66,4	72,5	78,5	84,4	83,6	[kN/m ²]
P _u = P ₃ (no berm)	86,8	86,2	85,6	84,9	84,2	83,4	82,6	81,7	80,7	79,8	[kN/m ²]
Forces:											
F ₁	447	411	369	321	268	209	144	74,7	0,0	0,0	[kN/m]
F ₂	638	715	790	863	935	1006	1075	1143	1208	1195	[kN/m]
F _u	26,5	26,3	26,1	25,9	25,7	25,4	25,2	24,9	24,6	24,3	[kN/m]
Lever Arms:											
a ₁	10,44	11,05	11,62	12,17	12,69	13,20	13,69	14,17	-	-	[m]
a ₂	3,66	4,12	4,59	5,05	5,51	5,97	6,44	6,90	7,37	7,37	[m]
a _u	0,102	0,102	0,102	0,102	0,102	0,102	0,102	0,102	0,102	0,102	[m]
Res. Force: F _H	1086	1126	1159	1185	1203	1215	1220	1217	1208	1195	[kN]
Res. Moment: M _H	7012	7491	7911	8267	8554	8766	8898	8946	8904	8814	[kNm/m]



H.4 Check on shearing and stability of the required concrete civil works – multiple loading scenarios

H.4.1 Maximum surge level and wave conditions under maximum differential head – wind offset retention area



Data:

$$h_{\text{bottom}} := -18\text{ft (MSL)} \quad h_{\text{sill}} := h_{\text{bottom}}$$

$$\text{soil characteristics: MSL -8 to -25 = clay (interdistributary): } p_{\text{wet,ci}} := 15 \cdot \frac{\text{kN}}{\text{m}^3} \quad \text{and } \phi_{\text{ci}} := 22.5^\circ$$

$$\text{MSL -25 to -45 = clay (pro-delta): } p_{\text{wet,pd}} := 18 \cdot \frac{\text{kN}}{\text{m}^3} \quad \text{and } \phi_{\text{cpd}} := 25.0^\circ$$

Dimensions barrier:

$$h_{\text{pier}} := 30\text{ft (MSL)} \quad h_{\text{tower}} := 180\text{ft (MSL)} \quad M_{\text{tower}} := 4500 \cdot 10^3 \text{kg} \quad P_{\text{concrete}} := 24 \frac{\text{kN}}{\text{m}^3}$$

$$w_{\text{span}} := 210\text{ft} \quad M_{\text{gate}} := 750 \cdot 10^3 \text{kg}$$

$$t_{\text{wall}} := 10\text{ft} \quad t_{\text{floor}} := 20\text{ft} \quad b_{\text{floor}} := w_{\text{span}} + 2 \cdot t_{\text{wall}}$$

$$L_{\text{outer}} := 130\text{ft} \quad L_{\text{retention}} := 35\text{ft} \quad L_{\text{floor}} := L_{\text{outer}} + L_{\text{retention}}$$

External Forces (water/wave pressures):

$$h_{\text{surge}} := 33\text{ft (MSL)} \quad h_{\text{retention}} := -5\text{ft (MSL)} \quad P_{\text{outer}} := 1025 \frac{\text{kg}}{\text{m}^3} \quad P_{\text{retention}} := 1000 \frac{\text{kg}}{\text{m}^3}$$

$$F_{\text{Goda.H}} := 1208 \frac{\text{kN}}{\text{m}} \quad P_{\text{Goda.bottom}} := 80.7 \frac{\text{kN}}{\text{m}^2}$$

$$P_{\text{hydro.outer}} := P_{\text{outer}} \cdot g \cdot [h_{\text{surge}} - (h_{\text{bottom}} - t_{\text{floor}})] = 217.5 \frac{\text{kN}}{\text{m}^2}$$

$$P_{\text{hydro.retention}} := P_{\text{retention}} \cdot g \cdot [h_{\text{retention}} - (h_{\text{bottom}} - t_{\text{floor}})] = 98.6 \frac{\text{kN}}{\text{m}^2}$$

$$H_1 := F_{\text{Goda.H}} \cdot w_{\text{span}} = 7.73 \times 10^7 \text{ N}$$

$$H_2 := \left[\frac{1}{2} p_{\text{outer}} \cdot g \cdot [h_{\text{surge}} - (h_{\text{bottom}} - t_{\text{floor}})]^2 \right] \cdot (w_{\text{span}} + 2 \cdot t_{\text{wall}}) = 1.65 \times 10^8 \text{ N}$$

$$H_3 := \left[\frac{1}{2} p_{\text{retention}} \cdot g \cdot [h_{\text{retention}} - (h_{\text{bottom}} - t_{\text{floor}})]^2 \right] \cdot (w_{\text{span}} + 2 \cdot t_{\text{wall}}) = 3.48 \times 10^7 \text{ N}$$

$$V_1 := p_{\text{outer}} \cdot g \cdot (h_{\text{surge}} - h_{\text{bottom}}) \cdot L_{\text{outer}} \cdot w_{\text{span}} = 3.96 \times 10^8 \text{ N}$$

$$V_2 := p_{\text{retention}} \cdot g \cdot (h_{\text{retention}} - h_{\text{bottom}}) \cdot L_{\text{retention}} \cdot w_{\text{span}} = 2.65 \times 10^7 \text{ N}$$

$$V_3 := M_{\text{gate}} \cdot g + 2 \cdot M_{\text{tower}} \cdot g = 9.56 \times 10^7 \text{ N}$$

$$V_4 := p_{\text{concrete}} \cdot [2 \cdot t_{\text{wall}} \cdot (h_{\text{pier}} - h_{\text{bottom}}) + b_{\text{floor}} \cdot t_{\text{floor}}] \cdot L_{\text{floor}} = 6.23 \times 10^8 \text{ N}$$

$$V_5 := p_{\text{hydro.retention}} \cdot L_{\text{floor}} \cdot b_{\text{floor}} = 3.48 \times 10^8 \text{ N}$$

$$V_6 := \frac{1}{2} \cdot (p_{\text{hydro.outer}} - p_{\text{hydro.retention}}) \cdot L_{\text{floor}} \cdot b_{\text{floor}} = 2.1 \times 10^8 \text{ N}$$

$$\Sigma V := V_1 + V_2 + V_3 + V_4 - V_5 - V_6 = 5.85 \times 10^8 \text{ N}$$

$$\Sigma H := H_1 + H_2 - H_3 = 2.08 \times 10^8 \text{ N}$$

unity check: $\phi := 25^\circ$ $\text{delta}(\delta) := 0.8\phi$ $\tan(\text{delta}(\delta)) = 0.36$

$$\frac{\Sigma V \cdot \tan(\text{delta}(\delta))}{\Sigma H} = 1.03 > 1.0$$

Lever arm

$$a_{H1} := 7.37 \text{ m} + t_{\text{floor}} = 13.47 \text{ m}$$

$$a_{H2} := \left(\frac{1}{3} \right) \cdot [h_{\text{surge}} - (h_{\text{bottom}} - t_{\text{floor}})] = 7.21 \text{ m}$$

$$a_{H3} := \left(\frac{1}{3} \right) \cdot [h_{\text{retention}} - (h_{\text{bottom}} - t_{\text{floor}})] = 3.35 \text{ m}$$

$$a_{V1} := \left(\frac{L_{\text{floor}}}{2} \right) - \frac{1}{2} \cdot L_{\text{outer}} = 5.33 \text{ m}$$

$$a_{V2} := \left(\frac{L_{\text{floor}}}{2} \right) - \frac{1}{2} \cdot L_{\text{retention}} = 19.81 \text{ m}$$

$$a_{V3} := \left(\frac{L_{\text{floor}}}{2} \right) - L_{\text{retention}} = 14.48 \text{ m}$$

$$a_{V4} := 0 \text{ m}$$

$$a_{V5} := 0 \text{ m}$$

$$a_{V6} := \frac{L_{\text{floor}}}{6} = 8.38 \text{ m}$$

$$\Sigma M_H := M_{H1} + M_{H2} - M_{H3}$$

$$\Sigma M_V := -M_{V1} + M_{V2} + M_{V3} + M_{V4} + M_{V5} + M_{V6}$$

$$\text{check: eccentricity} := \frac{\Sigma M_H + \Sigma M_V}{\Sigma V} = 6.27 \text{ m} < \frac{L_{\text{floor}}}{6} = 8.38 \text{ m}$$

check on maximum soil stresses:

$$\sigma_{\text{com}} := \frac{\Sigma V}{b_{\text{floor}} \cdot L_{\text{floor}}} + \frac{\Sigma M_H + \Sigma M_V}{\frac{1}{6} \cdot b_{\text{floor}} \cdot L_{\text{floor}}^2} = 289.9 \frac{\text{kN}}{\text{m}^2} < 300 \frac{\text{kN}}{\text{m}^2}$$

Moment

$$M_{H1} := a_{H1} \cdot H_1 = 1.04 \times 10^6 \text{ kN}\cdot\text{m}$$

$$M_{H2} := a_{H2} \cdot H_2 = 1.19 \times 10^6 \text{ kN}\cdot\text{m}$$

$$M_{H3} := a_{H3} \cdot H_3 = 1.17 \times 10^5 \text{ kN}\cdot\text{m}$$

$$M_{V1} := a_{V1} \cdot V_1 = 2.11 \times 10^6 \text{ kN}\cdot\text{m}$$

$$M_{V2} := a_{V2} \cdot V_2 = 5.26 \times 10^5 \text{ kN}\cdot\text{m}$$

$$M_{V3} := a_{V3} \cdot V_3 = 1.38 \times 10^6 \text{ kN}\cdot\text{m}$$

$$M_{V4} := a_{V4} \cdot V_4 = 0 \text{ kN}\cdot\text{m}$$

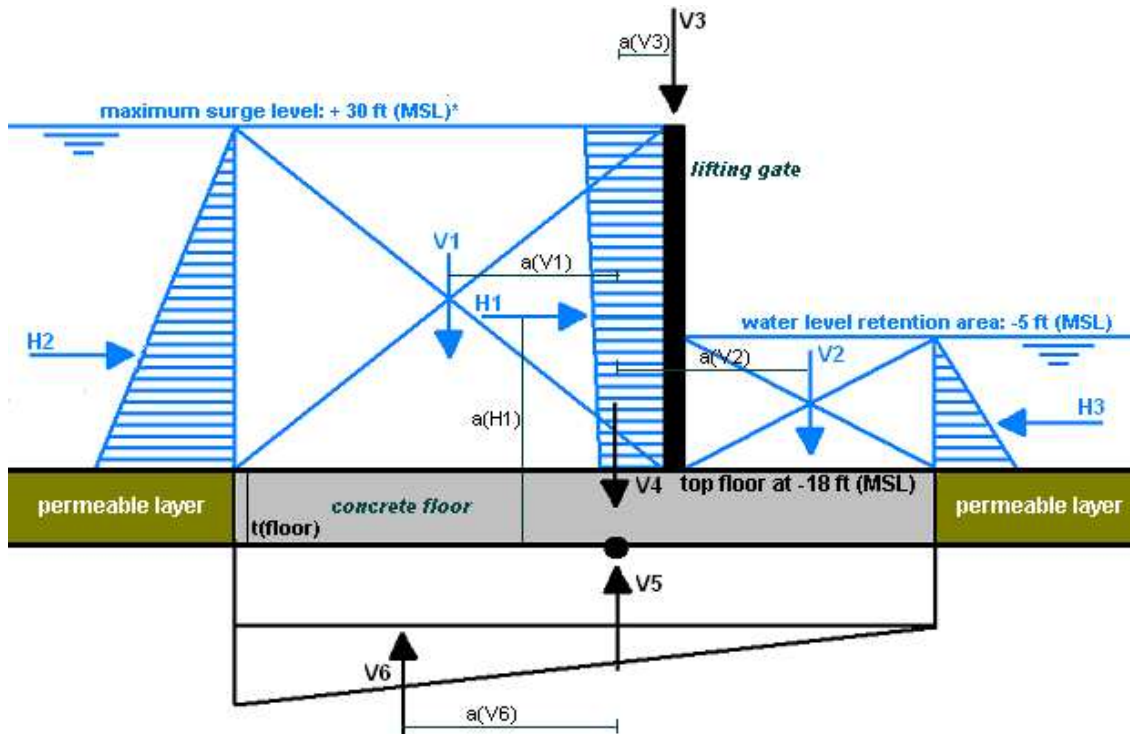
$$M_{V5} := a_{V5} \cdot V_5 = 0 \text{ kN}\cdot\text{m}$$

$$M_{V6} := a_{V6} \cdot V_6 = 1.76 \times 10^6 \text{ kN}\cdot\text{m}$$

$$e_H := \frac{\Sigma M_H}{\Sigma H} = 10.19 \text{ m}$$

$$e_V := \frac{\Sigma M_V}{\Sigma V} = 2.66 \text{ m}$$

(Im) permeable layer



Data:

$h_{\text{bottom}} := -18\text{ft (MSL)}$ $h_{\text{sill}} := h_{\text{bottom}}$

soil characteristics: MSL -8 to -25 = clay (interdistributary): $\rho_{\text{wet,ci}} := 15 \cdot \frac{\text{kN}}{\text{m}^3}$ and $\phi_{\text{ci}} := 22.5^\circ$
 MSL -25 to -45 = clay (pro-delta): $\rho_{\text{wet,pd}} := 18 \cdot \frac{\text{kN}}{\text{m}^3}$ and $\phi_{\text{cpd}} := 25.0^\circ$

Dimensions barrier:

$h_{\text{pier}} := 30\text{ft (MSL)}$ $h_{\text{tower}} := 180\text{ft (MSL)}$ $M_{\text{tower}} := 4500 \cdot 10^3 \text{kg}$ $\rho_{\text{concrete}} := 24 \cdot \frac{\text{kN}}{\text{m}^3}$
 $w_{\text{span}} := 210\text{ft}$ $M_{\text{gate}} := 750 \cdot 10^3 \text{kg}$
 $t_{\text{wall}} := 10\text{ft}$ $t_{\text{floor}} := 20\text{ft}$ $b_{\text{floor}} := w_{\text{span}} + 2 \cdot t_{\text{wall}}$
 $L_{\text{outer}} := 50\text{ft}$ $L_{\text{retention}} := 50\text{ft}$ $L_{\text{floor}} := L_{\text{outer}} + L_{\text{retention}}$ **$L_{\text{outer}} = L_{\text{retention}} = 50\text{ft}$**

External Forces (water/wave pressures):

$h_{\text{surge}} := 33\text{ft (MSL)}$ $h_{\text{retention}} := -5\text{ft (MSL)}$ $\rho_{\text{outer}} := 1025 \cdot \frac{\text{kg}}{\text{m}^3}$ $\rho_{\text{retention}} := 1000 \cdot \frac{\text{kg}}{\text{m}^3}$
 $F_{\text{Goda,H}} := 1208 \cdot \frac{\text{kN}}{\text{m}}$ $\rho_{\text{Goda,bottom}} := 80.7 \cdot \frac{\text{kN}}{\text{m}^2}$
 $\rho_{\text{hydro,outer}} := \rho_{\text{outer}} \cdot g \cdot (h_{\text{surge}} - h_{\text{bottom}}) = 156.3 \cdot \frac{\text{kN}}{\text{m}^2}$
 $\rho_{\text{hydro,retention}} := \rho_{\text{retention}} \cdot g \cdot (h_{\text{retention}} - h_{\text{bottom}}) = 38.9 \cdot \frac{\text{kN}}{\text{m}^2}$

$$H_1 := F_{\text{Goda.H}} \cdot w_{\text{span}} = 7.73 \times 10^7 \text{ N}$$

$$H_2 := \left[\frac{1}{2} p_{\text{outer}} \cdot g \cdot (h_{\text{surge}} - h_{\text{bottom}})^2 \right] \cdot (w_{\text{span}} + 2 \cdot t_{\text{wall}}) = 8.51 \times 10^7 \text{ N}$$

$$H_3 := \left[\frac{1}{2} p_{\text{retention}} \cdot g \cdot (h_{\text{retention}} - h_{\text{bottom}})^2 \right] \cdot (w_{\text{span}} + 2 \cdot t_{\text{wall}}) = 5.4 \times 10^6 \text{ N}$$

$$V_1 := p_{\text{outer}} \cdot g \cdot (h_{\text{surge}} - h_{\text{bottom}}) \cdot L_{\text{outer}} \cdot w_{\text{span}} = 1.52 \times 10^8 \text{ N}$$

$$V_2 := p_{\text{retention}} \cdot g \cdot (h_{\text{retention}} - h_{\text{bottom}}) \cdot L_{\text{retention}} \cdot w_{\text{span}} = 3.79 \times 10^7 \text{ N}$$

$$V_3 := M_{\text{gate}} \cdot g + 2 \cdot M_{\text{tower}} \cdot g = 9.56 \times 10^7 \text{ N}$$

$$V_4 := p_{\text{concrete}} \left[2 \cdot t_{\text{wall}} \cdot (h_{\text{pier}} - h_{\text{bottom}}) + b_{\text{floor}} \cdot t_{\text{floor}} \right] \cdot L_{\text{floor}} = 3.78 \times 10^8 \text{ N}$$

$$V_5 := p_{\text{hydro.retention}} \cdot L_{\text{floor}} \cdot b_{\text{floor}} = 8.3 \times 10^7 \text{ N}$$

$$V_6 := \frac{1}{2} \cdot (p_{\text{hydro.outer}} - p_{\text{hydro.retention}}) \cdot L_{\text{floor}} \cdot b_{\text{floor}} = 1.25 \times 10^8 \text{ N}$$

$$\Sigma V := V_1 + V_2 + V_3 + V_4 - V_5 - V_6 = 4.55 \times 10^8 \text{ N}$$

$$\Sigma H := H_1 + H_2 - H_3 = 1.57 \times 10^8 \text{ N}$$

$$\text{unity check: } \phi := 25^\circ \quad \text{delta}(\delta) := 0.8\phi \quad \tan(\text{delta}(\delta)) = 0.36$$

$$\frac{\Sigma V \cdot \tan(\text{delta}(\delta))}{\Sigma H} = 1.06 > 1.0$$

Lever arm

$$a_{H1} := 7.37 \text{ m}$$

$$a_{H2} := \left(\frac{1}{3} \right) \cdot (h_{\text{surge}} - h_{\text{bottom}}) = 5.18 \text{ m}$$

$$a_{H3} := \left(\frac{1}{3} \right) \cdot (h_{\text{retention}} - h_{\text{bottom}}) = 1.32 \text{ m}$$

$$a_{V1} := \left(\frac{L_{\text{floor}}}{2} \right) - \frac{1}{2} \cdot L_{\text{outer}} = 7.62 \text{ m}$$

$$a_{V2} := \left(\frac{L_{\text{floor}}}{2} \right) - \frac{1}{2} \cdot L_{\text{retention}} = 7.62 \text{ m}$$

$$a_{V3} := \left(\frac{L_{\text{floor}}}{2} \right) - L_{\text{retention}} = 0 \text{ m}$$

$$a_{V4} := 0 \text{ m}$$

$$a_{V5} := 0 \text{ m}$$

$$a_{V6} := \frac{L_{\text{floor}}}{6} = 5.08 \text{ m}$$

$$\Sigma M_H := M_{H1} + M_{H2} - M_{H3}$$

$$\Sigma M_V := -M_{V1} + M_{V2} + M_{V3} + M_{V4} + M_{V5} + M_{V6}$$

$$\text{check: eccentricity} := \frac{\Sigma M_H + \Sigma M_V}{\Sigma V} = 1.69 \text{ m} < \frac{L_{\text{floor}}}{6} = 5.08 \text{ m}$$

check on maximum soil stresses:

$$\sigma_{\text{com}} := \frac{\Sigma V}{b_{\text{floor}} \cdot L_{\text{floor}}} + \frac{\Sigma M_H + \Sigma M_V}{\frac{1}{6} \cdot b_{\text{floor}} \cdot L_{\text{floor}}^2} = 283.9 \frac{\text{kN}}{\text{m}^2} < 300 \frac{\text{kN}}{\text{m}^2}$$

Moment

$$M_{H1} := a_{H1} \cdot H_1 = 5.7 \times 10^5 \text{ kN}\cdot\text{m}$$

$$M_{H2} := a_{H2} \cdot H_2 = 4.41 \times 10^5 \text{ kN}\cdot\text{m}$$

$$M_{H3} := a_{H3} \cdot H_3 = 7.13 \times 10^3 \text{ kN}\cdot\text{m}$$

$$M_{V1} := a_{V1} \cdot V_1 = 1.16 \times 10^6 \text{ kN}\cdot\text{m}$$

$$M_{V2} := a_{V2} \cdot V_2 = 2.89 \times 10^5 \text{ kN}\cdot\text{m}$$

$$M_{V3} := a_{V3} \cdot V_3 = 0 \text{ kN}\cdot\text{m}$$

$$M_{V4} := a_{V4} \cdot V_4 = 0 \text{ kN}\cdot\text{m}$$

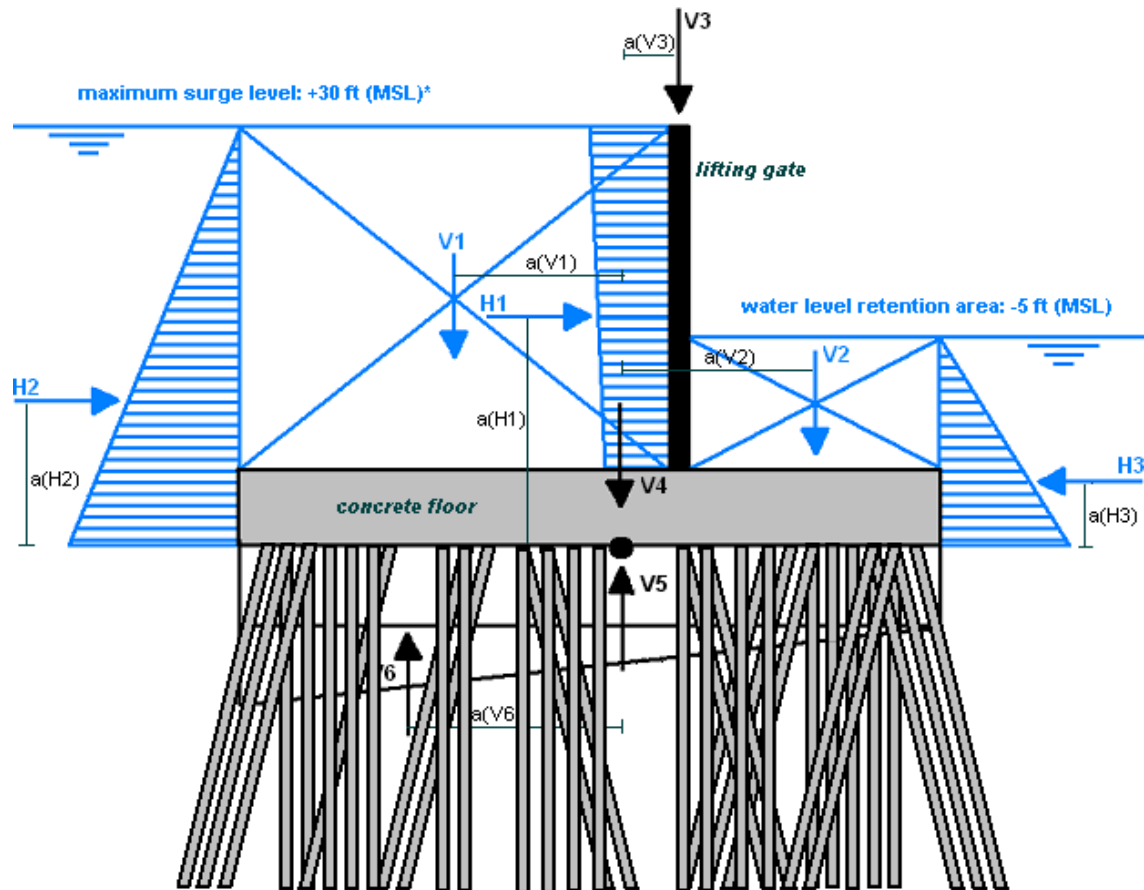
$$M_{V5} := a_{V5} \cdot V_5 = 0 \text{ kN}\cdot\text{m}$$

$$M_{V6} := a_{V6} \cdot V_6 = 6.37 \times 10^5 \text{ kN}\cdot\text{m}$$

$$e_H := \frac{\Sigma M_H}{\Sigma H} = 6.39 \text{ m}$$

$$e_V := \frac{\Sigma M_V}{\Sigma V} = -0.52 \text{ m}$$

Assumed Influence pile plan (indicative calculation: sketches piles do not represent design output)



Data:

$$h_{\text{bottom}} := -18\text{ft (MSL)} \quad h_{\text{sill}} := h_{\text{bottom}}$$

soil characteristics: MSL -8 to -25 = clay (interdistributary): $p_{\text{wet,ci}} := 15 \cdot \frac{\text{kN}}{\text{m}^3}$ and $\phi_{\text{ci}} := 22.5^\circ$
 MSL -25 to -45 = clay (pro-delta): $p_{\text{wet,pd}} := 18 \cdot \frac{\text{kN}}{\text{m}^3}$ and $\phi_{\text{cpd}} := 25.0^\circ$

Dimensions barrier:

$$h_{\text{pier}} := 30\text{ft (MSL)} \quad h_{\text{tower}} := 180\text{ft (MSL)} \quad M_{\text{tower}} := 4500 \cdot 10^3 \text{kg} \quad p_{\text{concrete}} := 24 \frac{\text{kN}}{\text{m}^3}$$

$$w_{\text{span}} := 210\text{ft} \quad M_{\text{gate}} := 750 \cdot 10^3 \text{kg}$$

$$t_{\text{wall}} := 10\text{ft} \quad t_{\text{floor}} := 20\text{ft} \quad b_{\text{floor}} := w_{\text{span}} + 2 \cdot t_{\text{wall}}$$

$$L_{\text{outer}} := 50\text{ft} \quad L_{\text{retention}} := 30\text{ft} \quad L_{\text{floor}} := L_{\text{outer}} + L_{\text{retention}}$$

External Forces (water/wave pressures):

$$h_{\text{surge}} := 33\text{ft (MSL)} \quad h_{\text{retention}} := -5\text{ft (MSL)} \quad p_{\text{outer}} := 1025 \frac{\text{kg}}{\text{m}^3} \quad p_{\text{retention}} := 1000 \frac{\text{kg}}{\text{m}^3}$$

$$F_{\text{Goda.H}} := 1208 \frac{\text{kN}}{\text{m}} \quad p_{\text{Goda.bottom}} := 80.7 \frac{\text{kN}}{\text{m}^2}$$

$$p_{\text{hydro.outer}} := p_{\text{outer}} \cdot g \cdot [h_{\text{surge}} - (h_{\text{bottom}} - t_{\text{floor}})] = 217.5 \frac{\text{kN}}{\text{m}^2}$$

$$p_{\text{hydro.retention}} := p_{\text{retention}} \cdot g \cdot [h_{\text{retention}} - (h_{\text{bottom}} - t_{\text{floor}})] = 98.6 \frac{\text{kN}}{\text{m}^2}$$

$$H_1 := F_{\text{Goda.H}} \cdot w_{\text{span}} = 7.73 \times 10^7 \text{ N}$$

$$H_2 := \left[\frac{1}{2} p_{\text{outer}} \cdot g \cdot [h_{\text{surge}} - (h_{\text{bottom}} - t_{\text{floor}})]^2 \right] \cdot (w_{\text{span}} + 2 \cdot t_{\text{wall}}) = 1.65 \times 10^8 \text{ N}$$

$$H_3 := \left[\frac{1}{2} p_{\text{retention}} \cdot g \cdot [h_{\text{retention}} - (h_{\text{bottom}} - t_{\text{floor}})]^2 \right] \cdot (w_{\text{span}} + 2 \cdot t_{\text{wall}}) = 3.48 \times 10^7 \text{ N}$$

$$V_1 := p_{\text{outer}} \cdot g \cdot (h_{\text{surge}} - h_{\text{bottom}}) \cdot L_{\text{outer}} \cdot w_{\text{span}} = 1.52 \times 10^8 \text{ N}$$

$$V_2 := p_{\text{retention}} \cdot g \cdot (h_{\text{retention}} - h_{\text{bottom}}) \cdot L_{\text{retention}} \cdot w_{\text{span}} = 2.27 \times 10^7 \text{ N}$$

$$V_3 := M_{\text{gate}} \cdot g + 2 \cdot M_{\text{tower}} \cdot g = 9.56 \times 10^7 \text{ N}$$

$$V_4 := p_{\text{concrete}} \cdot [2 \cdot t_{\text{wall}} \cdot (h_{\text{pier}} - h_{\text{bottom}}) + b_{\text{floor}} \cdot t_{\text{floor}}] \cdot L_{\text{floor}} = 3.02 \times 10^8 \text{ N}$$

$$V_5 := p_{\text{hydro.retention}} \cdot L_{\text{floor}} \cdot b_{\text{floor}} = 1.69 \times 10^8 \text{ N}$$

$$V_6 := \frac{1}{2} \cdot (p_{\text{hydro.outer}} - p_{\text{hydro.retention}}) \cdot L_{\text{floor}} \cdot b_{\text{floor}} = 1.02 \times 10^8 \text{ N}$$

$$\Sigma V := V_1 + V_2 + V_3 + V_4 - V_5 - V_6 = 3.03 \times 10^8 \text{ N}$$

$$\Sigma H := 0.5(H_1 + H_2 - H_3) = 1.04 \times 10^8 \text{ N}$$

$$\text{unity check: } \phi := 25^\circ \quad \text{delta}(\delta) := 0.8\phi \quad \tan(\text{delta}(\delta)) = 0.36$$

$\Sigma H \times 0.5$

$$\frac{\Sigma V \cdot \tan(\text{delta}(\delta))}{\Sigma H} = 1.06 > 1.0$$

Lever arm

$$a_{H1} := 7.37 \text{ m} + t_{\text{floor}} = 13.47 \text{ m}$$

$$a_{H2} := \left(\frac{1}{3} \right) \cdot [h_{\text{surge}} - (h_{\text{bottom}} - t_{\text{floor}})] = 7.21 \text{ m}$$

$$a_{H3} := \left(\frac{1}{3} \right) \cdot [h_{\text{retention}} - (h_{\text{bottom}} - t_{\text{floor}})] = 3.35 \text{ m}$$

$$a_{V1} := \left(\frac{L_{\text{floor}}}{2} \right) - \frac{1}{2} \cdot L_{\text{outer}} = 4.57 \text{ m}$$

$$a_{V2} := \left(\frac{L_{\text{floor}}}{2} \right) - \frac{1}{2} \cdot L_{\text{retention}} = 7.62 \text{ m}$$

$$a_{V3} := \left(\frac{L_{\text{floor}}}{2} \right) - L_{\text{retention}} = 3.05 \text{ m}$$

$$a_{V4} := 0 \text{ m}$$

$$a_{V5} := 0 \text{ m}$$

$$a_{V6} := \frac{L_{\text{floor}}}{6} = 4.06 \text{ m}$$

$$\Sigma M_H := M_{H1} + M_{H2} - M_{H3}$$

$$\Sigma M_V := -M_{V1} + M_{V2} + M_{V3} + M_{V4} + M_{V5} + M_{V6}$$

$$\text{check: eccentricity} := \frac{\Sigma M_H + \Sigma M_V}{\Sigma V} = 7.58 \text{ m} < \frac{L_{\text{floor}}}{3} = 8.13 \text{ m}$$

$$2 \times L_{\text{floor}}/6 = L_{\text{floor}}/3$$

Moment

$$M_{H1} := a_{H1} \cdot H_1 = 1.04 \times 10^8 \cdot \text{kN} \cdot \text{m}$$

$$M_{H2} := a_{H2} \cdot H_2 = 1.19 \times 10^6 \cdot \text{kN} \cdot \text{m}$$

$$M_{H3} := a_{H3} \cdot H_3 = 1.17 \times 10^5 \cdot \text{kN} \cdot \text{m}$$

$$M_{V1} := a_{V1} \cdot V_1 = 6.97 \times 10^5 \cdot \text{kN} \cdot \text{m}$$

$$M_{V2} := a_{V2} \cdot V_2 = 1.73 \times 10^5 \cdot \text{kN} \cdot \text{m}$$

$$M_{V3} := a_{V3} \cdot V_3 = 2.91 \times 10^5 \cdot \text{kN} \cdot \text{m}$$

$$M_{V4} := a_{V4} \cdot V_4 = 0 \cdot \text{kN} \cdot \text{m}$$

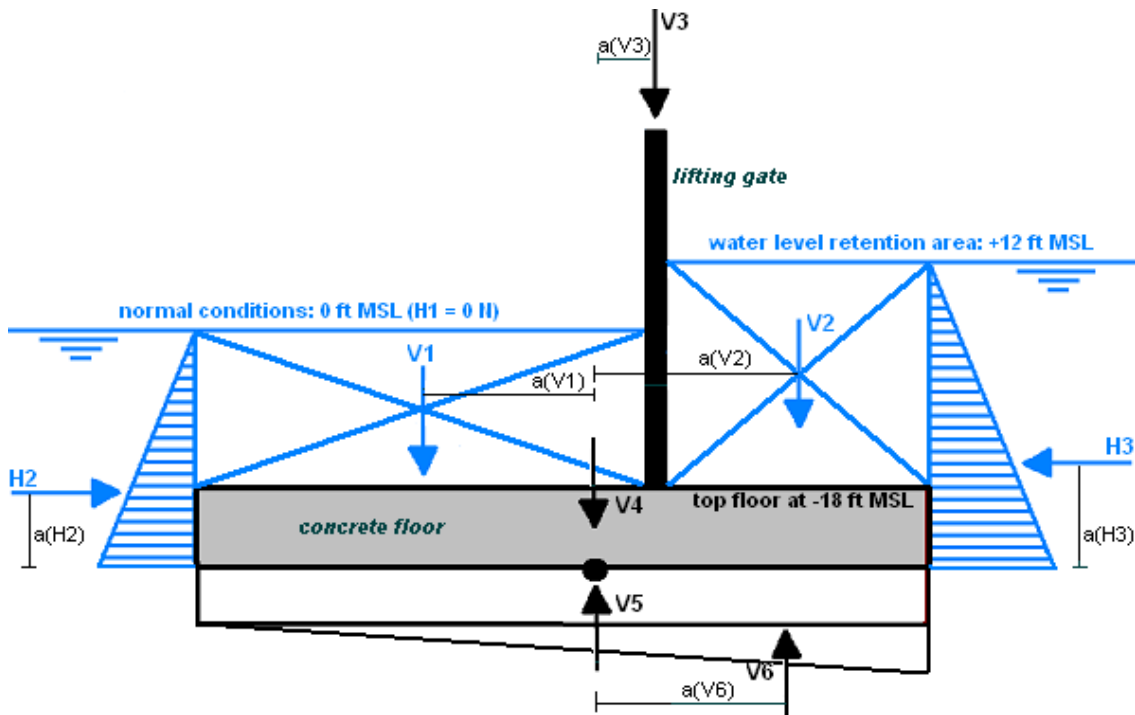
$$M_{V5} := a_{V5} \cdot V_5 = 0 \cdot \text{kN} \cdot \text{m}$$

$$M_{V6} := a_{V6} \cdot V_6 = 4.13 \times 10^5 \cdot \text{kN} \cdot \text{m}$$

$$e_H := \frac{\Sigma M_H}{\Sigma H} = 20.38 \text{ m}$$

$$e_V := \frac{\Sigma M_V}{\Sigma V} = 0.6 \text{ m}$$

H.4.2 Maximum negative differential head – malfunction of the gate after closure



Data:

$$h_{\text{bottom}} := -18\text{ft (MSL)} \quad h_{\text{sill}} := h_{\text{bottom}}$$

$$\text{soil characteristics: MSL -8 to -25 = clay (interdistributary): } p_{\text{wet,ci}} := 15 \cdot \frac{\text{kN}}{\text{m}^3} \text{ and } \phi_{\text{ci}} := 22.5^\circ$$

$$\text{MSL -25 to -45 = clay (pro-delta): } p_{\text{wet,pd}} := 18 \cdot \frac{\text{kN}}{\text{m}^3} \text{ and } \phi_{\text{cpd}} := 25.0^\circ$$

Dimensions barrier:

$$h_{\text{pier}} := 30\text{ft (MSL)} \quad h_{\text{tower}} := 180\text{ft (MSL)} \quad M_{\text{tower}} := 4500 \cdot 10^3 \text{kg} \quad p_{\text{concrete}} := 24 \frac{\text{kN}}{\text{m}^3}$$

$$w_{\text{span}} := 210\text{ft} \quad M_{\text{gate}} := 750 \cdot 10^3 \text{kg}$$

$$t_{\text{wall}} := 10\text{ft} \quad t_{\text{floor}} := 20\text{ft} \quad b_{\text{floor}} := w_{\text{span}} + 2 \cdot t_{\text{wall}}$$

$$L_{\text{outer}} := 130\text{ft} \quad L_{\text{retention}} := 35\text{ft} \quad L_{\text{floor}} := L_{\text{outer}} + L_{\text{retention}}$$

External Forces (water/wave pressures):

$$h_{\text{surge}} := 0\text{ft (MSL)} \quad h_{\text{retention}} := 12\text{ft (MSL)} \quad p_{\text{outer}} := 1025 \frac{\text{kg}}{\text{m}^3} \quad p_{\text{retention}} := 1000 \frac{\text{kg}}{\text{m}^3}$$

$$F_{\text{Goda.H}} := 0 \frac{\text{kN}}{\text{m}} \quad p_{\text{Goda.bottom}} := 0 \frac{\text{kN}}{\text{m}^2} \quad (\text{normal conditions: no surge level and significant waves})$$

$$p_{\text{hydro.outer}} := p_{\text{outer}} \cdot g \cdot [h_{\text{surge}} - (h_{\text{bottom}} - t_{\text{floor}})] = 116.4 \frac{\text{kN}}{\text{m}^2}$$

$$p_{\text{hydro.retention}} := p_{\text{retention}} \cdot g \cdot [h_{\text{retention}} - (h_{\text{bottom}} - t_{\text{floor}})] = 149.5 \frac{\text{kN}}{\text{m}^2}$$

$$H_1 := F_{\text{Goda.H}} \cdot w_{\text{span}} = 0 \text{ N}$$

$$H_2 := \left[\frac{1}{2} \rho_{\text{outer}} \cdot g \cdot [h_{\text{surge}} - (h_{\text{bottom}} - t_{\text{floor}})]^2 \right] \cdot (w_{\text{span}} + 2 \cdot t_{\text{wall}}) = 4.73 \times 10^7 \text{ N}$$

$$H_3 := \left[\frac{1}{2} \rho_{\text{retention}} \cdot g \cdot [h_{\text{retention}} - (h_{\text{bottom}} - t_{\text{floor}})]^2 \right] \cdot (w_{\text{span}} + 2 \cdot t_{\text{wall}}) = 7.98 \times 10^7 \text{ N}$$

$$V_1 := \rho_{\text{outer}} \cdot g \cdot (h_{\text{surge}} - h_{\text{bottom}}) \cdot L_{\text{outer}} \cdot w_{\text{span}} = 1.4 \times 10^8 \text{ N}$$

$$V_2 := \rho_{\text{retention}} \cdot g \cdot (h_{\text{retention}} - h_{\text{bottom}}) \cdot L_{\text{retention}} \cdot w_{\text{span}} = 6.12 \times 10^7 \text{ N}$$

$$V_3 := M_{\text{gate}} \cdot g + 2 \cdot M_{\text{tower}} \cdot g = 9.56 \times 10^7 \text{ N}$$

$$V_4 := \rho_{\text{concrete}} \cdot [2 \cdot t_{\text{wall}} \cdot (h_{\text{pier}} - h_{\text{bottom}}) + b_{\text{floor}} \cdot t_{\text{floor}}] \cdot L_{\text{floor}} = 6.23 \times 10^8 \text{ N}$$

$$V_5 := \rho_{\text{hydro.outer}} \cdot L_{\text{floor}} \cdot b_{\text{floor}} = 4.1 \times 10^8 \text{ N}$$

$$V_6 := \frac{1}{2} \cdot (\rho_{\text{hydro.retention}} - \rho_{\text{hydro.outer}}) \cdot L_{\text{floor}} \cdot b_{\text{floor}} = 5.82 \times 10^7 \text{ N}$$

$$\Sigma V := V_1 + V_2 + V_3 + V_4 - V_5 - V_6 = 4.51 \times 10^8 \text{ N}$$

$$\Sigma H := -H_1 - H_2 + H_3 = 3.26 \times 10^7 \text{ N}$$

unity check: $\phi := 25^\circ$ $\text{delta}(\delta) := 0.8\phi$ $\tan(\text{delta}(\delta)) = 0.36$

$$\frac{\Sigma V \cdot \tan(\text{delta}(\delta))}{\Sigma H} = 5.05 > 1.0$$

Lever arm

$$a_{H1} := 0 \text{ m}$$

$$a_{H2} := \left(\frac{1}{3} \right) \cdot [h_{\text{surge}} - (h_{\text{bottom}} - t_{\text{floor}})] = 3.86 \text{ m}$$

$$a_{H3} := \left(\frac{1}{3} \right) \cdot [h_{\text{retention}} - (h_{\text{bottom}} - t_{\text{floor}})] = 5.08 \text{ m}$$

$$a_{V1} := \left(\frac{L_{\text{floor}}}{2} \right) - \frac{1}{2} \cdot L_{\text{outer}} = 5.33 \text{ m}$$

$$a_{V2} := \left(\frac{L_{\text{floor}}}{2} \right) - \frac{1}{2} \cdot L_{\text{retention}} = 19.81 \text{ m}$$

$$a_{V3} := \left(\frac{L_{\text{floor}}}{2} \right) - L_{\text{retention}} = 14.48 \text{ m}$$

$$a_{V4} := 0 \text{ m}$$

$$a_{V5} := 0 \text{ m}$$

$$a_{V6} := \frac{L_{\text{floor}}}{6} = 8.38 \text{ m}$$

$$\Sigma M_H := M_{H1} + M_{H2} - M_{H3}$$

$$\Sigma M_V := -M_{V1} + M_{V2} + M_{V3} + M_{V4} + M_{V5} + M_{V6}$$

$$\text{check: eccentricity} := \frac{\Sigma M_H + \Sigma M_V}{\Sigma V} = 4.69 \text{ m} < \frac{L_{\text{floor}}}{6} = 8.38 \text{ m}$$

check on maximum soil stresses:

$$\sigma_{\text{com}} := \frac{\Sigma V}{b_{\text{floor}} \cdot L_{\text{floor}}} + \frac{\Sigma M_H + \Sigma M_V}{\frac{1}{6} \cdot b_{\text{floor}} \cdot L_{\text{floor}}^2} = 199.7 \frac{\text{kN}}{\text{m}^2} < 300 \frac{\text{kN}}{\text{m}^2}$$

Moment

$$M_{H1} := a_{H1} \cdot H_1 = 0 \text{ kN}\cdot\text{m}$$

$$M_{H2} := a_{H2} \cdot H_2 = 1.82 \times 10^5 \text{ kN}\cdot\text{m}$$

$$M_{H3} := a_{H3} \cdot H_3 = 4.06 \times 10^5 \text{ kN}\cdot\text{m}$$

$$M_{V1} := a_{V1} \cdot V_1 = 7.46 \times 10^5 \text{ kN}\cdot\text{m}$$

$$M_{V2} := a_{V2} \cdot V_2 = 1.21 \times 10^6 \text{ kN}\cdot\text{m}$$

$$M_{V3} := a_{V3} \cdot V_3 = 1.38 \times 10^6 \text{ kN}\cdot\text{m}$$

$$M_{V4} := a_{V4} \cdot V_4 = 0 \text{ kN}\cdot\text{m}$$

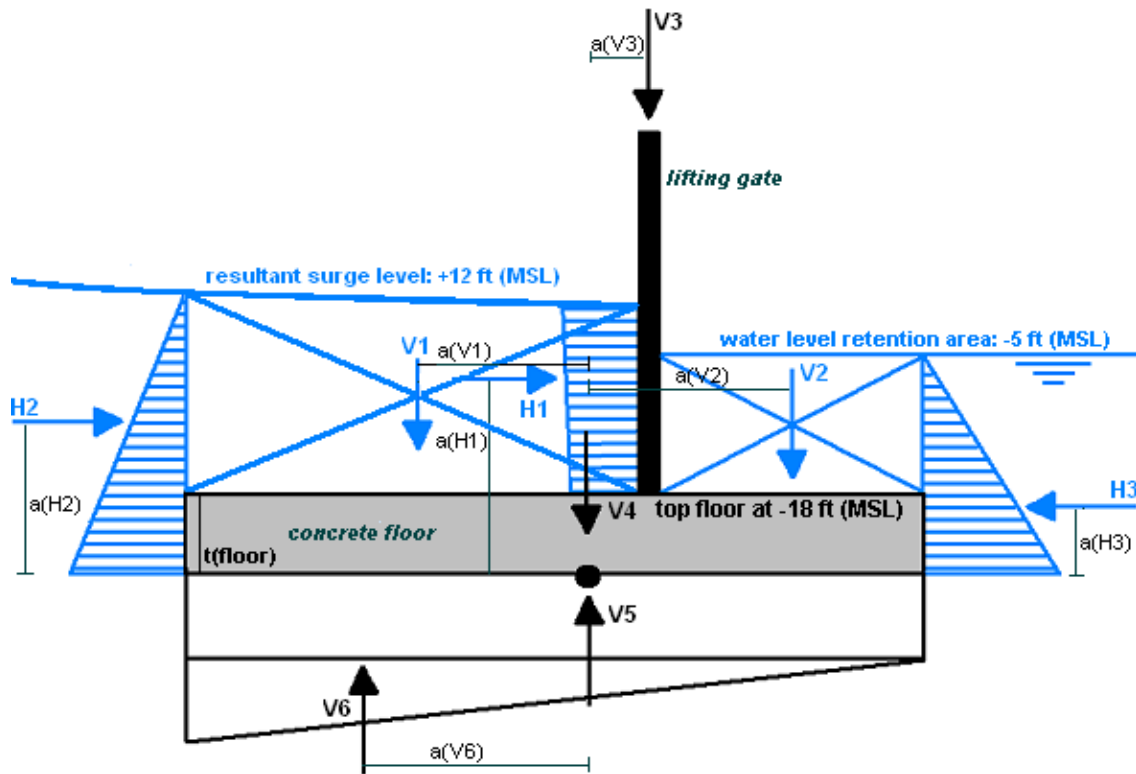
$$M_{V5} := a_{V5} \cdot V_5 = 0 \text{ kN}\cdot\text{m}$$

$$M_{V6} := a_{V6} \cdot V_6 = 4.88 \times 10^5 \text{ kN}\cdot\text{m}$$

$$e_H := \frac{\Sigma M_H}{\Sigma H} = -6.85 \text{ m}$$

$$e_V := \frac{\Sigma M_V}{\Sigma V} = 5.18 \text{ m}$$

H.4.3 Maximum surge level and maximum wave conditions in combination with the occurrence of a wave low



Data:

$$h_{\text{bottom}} := -18\text{ft (MSL)} \quad h_{\text{sill}} := h_{\text{bottom}}$$

$$\text{soil characteristics: MSL -8 to -25 = clay (interdistributary): } p_{\text{wet,ci}} := 15 \cdot \frac{\text{kN}}{\text{m}^3} \text{ and } \phi_{\text{ci}} := 22.5^\circ$$

$$\text{MSL -25 to -45 = clay (pro-delta): } p_{\text{wet,pd}} := 18 \cdot \frac{\text{kN}}{\text{m}^3} \text{ and } \phi_{\text{cpd}} := 25.0^\circ$$

Dimensions barrier:

$$h_{\text{pier}} := 30\text{ft (MSL)} \quad h_{\text{tower}} := 180\text{ft (MSL)} \quad M_{\text{tower}} := 4500 \cdot 10^3 \text{kg} \quad p_{\text{concrete}} := 24 \frac{\text{kN}}{\text{m}^3}$$

$$w_{\text{span}} := 210\text{ft} \quad M_{\text{gate}} := 750 \cdot 10^3 \text{kg}$$

$$t_{\text{wall}} := 10\text{ft} \quad t_{\text{floor}} := 20\text{ft} \quad b_{\text{floor}} := w_{\text{span}} + 2 \cdot t_{\text{wall}}$$

$$L_{\text{outer}} := 130\text{ft} \quad L_{\text{retention}} := 35\text{ft} \quad L_{\text{floor}} := L_{\text{outer}} + L_{\text{retention}}$$

External Forces (water/wave pressures):

$$h_{\text{surge}} := 12\text{ft (MSL)} \quad h_{\text{retention}} := -5\text{ft (MSL)} \quad p_{\text{outer}} := 1025 \frac{\text{kg}}{\text{m}^3} \quad p_{\text{retention}} := 1000 \frac{\text{kg}}{\text{m}^3}$$

$$F_{\text{Goda,H}} := 1159 \frac{\text{kN}}{\text{m}} \quad p_{\text{Goda,bottom}} := 85.6 \frac{\text{kN}}{\text{m}^2}$$

$$p_{\text{hydro,outer}} := p_{\text{outer}} \cdot g \cdot [h_{\text{surge}} - (h_{\text{bottom}} - t_{\text{floor}})] = 153.2 \frac{\text{kN}}{\text{m}^2}$$

$$p_{\text{hydro,retention}} := p_{\text{retention}} \cdot g \cdot [h_{\text{retention}} - (h_{\text{bottom}} - t_{\text{floor}})] = 98.6 \frac{\text{kN}}{\text{m}^2}$$

$$H_1 := F_{\text{Goda.H}} \cdot w_{\text{span}} = 7.42 \times 10^7 \text{ N}$$

$$H_2 := \left[\frac{1}{2} p_{\text{outer}} \cdot g \cdot [h_{\text{surge}} - (h_{\text{bottom}} - t_{\text{floor}})]^2 \right] \cdot (w_{\text{span}} + 2 \cdot t_{\text{wall}}) = 8.18 \times 10^7 \text{ N}$$

$$H_3 := \left[\frac{1}{2} p_{\text{retention}} \cdot g \cdot [h_{\text{retention}} - (h_{\text{bottom}} - t_{\text{floor}})]^2 \right] \cdot (w_{\text{span}} + 2 \cdot t_{\text{wall}}) = 3.48 \times 10^7 \text{ N}$$

$$V_1 := p_{\text{outer}} \cdot g \cdot (h_{\text{surge}} - h_{\text{bottom}}) \cdot L_{\text{outer}} \cdot w_{\text{span}} = 2.33 \times 10^8 \text{ N}$$

$$V_2 := p_{\text{retention}} \cdot g \cdot (h_{\text{retention}} - h_{\text{bottom}}) \cdot L_{\text{retention}} \cdot w_{\text{span}} = 2.65 \times 10^7 \text{ N}$$

$$V_3 := M_{\text{gate}} \cdot g + 2 \cdot M_{\text{tower}} \cdot g = 9.56 \times 10^7 \text{ N}$$

$$V_4 := p_{\text{concrete}} \cdot [2 \cdot t_{\text{wall}} \cdot (h_{\text{pier}} - h_{\text{bottom}}) + b_{\text{floor}} \cdot t_{\text{floor}}] \cdot L_{\text{floor}} = 6.23 \times 10^8 \text{ N}$$

$$V_5 := p_{\text{hydro.retention}} \cdot L_{\text{floor}} \cdot b_{\text{floor}} = 3.48 \times 10^8 \text{ N}$$

$$V_6 := \frac{1}{2} \cdot (p_{\text{hydro.outer}} - p_{\text{hydro.retention}}) \cdot L_{\text{floor}} \cdot b_{\text{floor}} = 9.62 \times 10^7 \text{ N}$$

$$\Sigma V := V_1 + V_2 + V_3 + V_4 - V_5 - V_6 = 5.35 \times 10^8 \text{ N} \quad \Sigma H := H_1 + H_2 - H_3 = 1.21 \times 10^8 \text{ N}$$

$$\text{unity check: } \phi := 25^\circ \quad \text{delta}(\delta) := 0.8\phi \quad \tan(\text{delta}(\delta)) = 0.36$$

$$\frac{\Sigma V \cdot \tan(\text{delta}(\delta))}{\Sigma H} = 1.61 > 1.0$$

Lever arm

$$a_{H1} := 6.83 \text{ m} + t_{\text{floor}} = 12.93 \text{ m}$$

$$a_{H2} := \left(\frac{1}{3} \right) \cdot [h_{\text{surge}} - (h_{\text{bottom}} - t_{\text{floor}})] = 5.08 \text{ m}$$

$$a_{H3} := \left(\frac{1}{3} \right) \cdot [h_{\text{retention}} - (h_{\text{bottom}} - t_{\text{floor}})] = 3.35 \text{ m}$$

$$a_{V1} := \left(\frac{L_{\text{floor}}}{2} \right) - \frac{1}{2} \cdot L_{\text{outer}} = 5.33 \text{ m}$$

$$a_{V2} := \left(\frac{L_{\text{floor}}}{2} \right) - \frac{1}{2} \cdot L_{\text{retention}} = 19.81 \text{ m}$$

$$a_{V3} := \left(\frac{L_{\text{floor}}}{2} \right) - L_{\text{retention}} = 14.48 \text{ m}$$

$$a_{V4} := 0 \text{ m}$$

$$a_{V5} := 0 \text{ m}$$

$$a_{V6} := \frac{L_{\text{floor}}}{6} = 8.38 \text{ m}$$

$$\Sigma M_H := M_{H1} + M_{H2} - M_{H3}$$

$$\Sigma M_V := -M_{V1} + M_{V2} + M_{V3} + M_{V4} + M_{V5} + M_{V6}$$

$$\text{check: eccentricity} := \frac{\Sigma M_H + \Sigma M_V}{\Sigma V} = 5.11 \text{ m} < \frac{L_{\text{floor}}}{6} = 8.38 \text{ m}$$

check on maximum soil stresses:

$$\sigma_{\text{com}} := \frac{\Sigma V}{b_{\text{floor}} \cdot L_{\text{floor}}} + \frac{\Sigma M_H + \Sigma M_V}{\frac{1}{6} \cdot b_{\text{floor}} \cdot L_{\text{floor}}^2} = 244.1 \cdot \frac{\text{kN}}{\text{m}^2} < 300 \cdot \frac{\text{kN}}{\text{m}^2}$$

Moment

$$M_{H1} := a_{H1} \cdot H_1 = 9.59 \times 10^5 \cdot \text{kN} \cdot \text{m}$$

$$M_{H2} := a_{H2} \cdot H_2 = 4.16 \times 10^5 \cdot \text{kN} \cdot \text{m}$$

$$M_{H3} := a_{H3} \cdot H_3 = 1.17 \times 10^5 \cdot \text{kN} \cdot \text{m}$$

$$M_{V1} := a_{V1} \cdot V_1 = 1.24 \times 10^6 \cdot \text{kN} \cdot \text{m}$$

$$M_{V2} := a_{V2} \cdot V_2 = 5.26 \times 10^5 \cdot \text{kN} \cdot \text{m}$$

$$M_{V3} := a_{V3} \cdot V_3 = 1.38 \times 10^6 \cdot \text{kN} \cdot \text{m}$$

$$M_{V4} := a_{V4} \cdot V_4 = 0 \cdot \text{kN} \cdot \text{m}$$

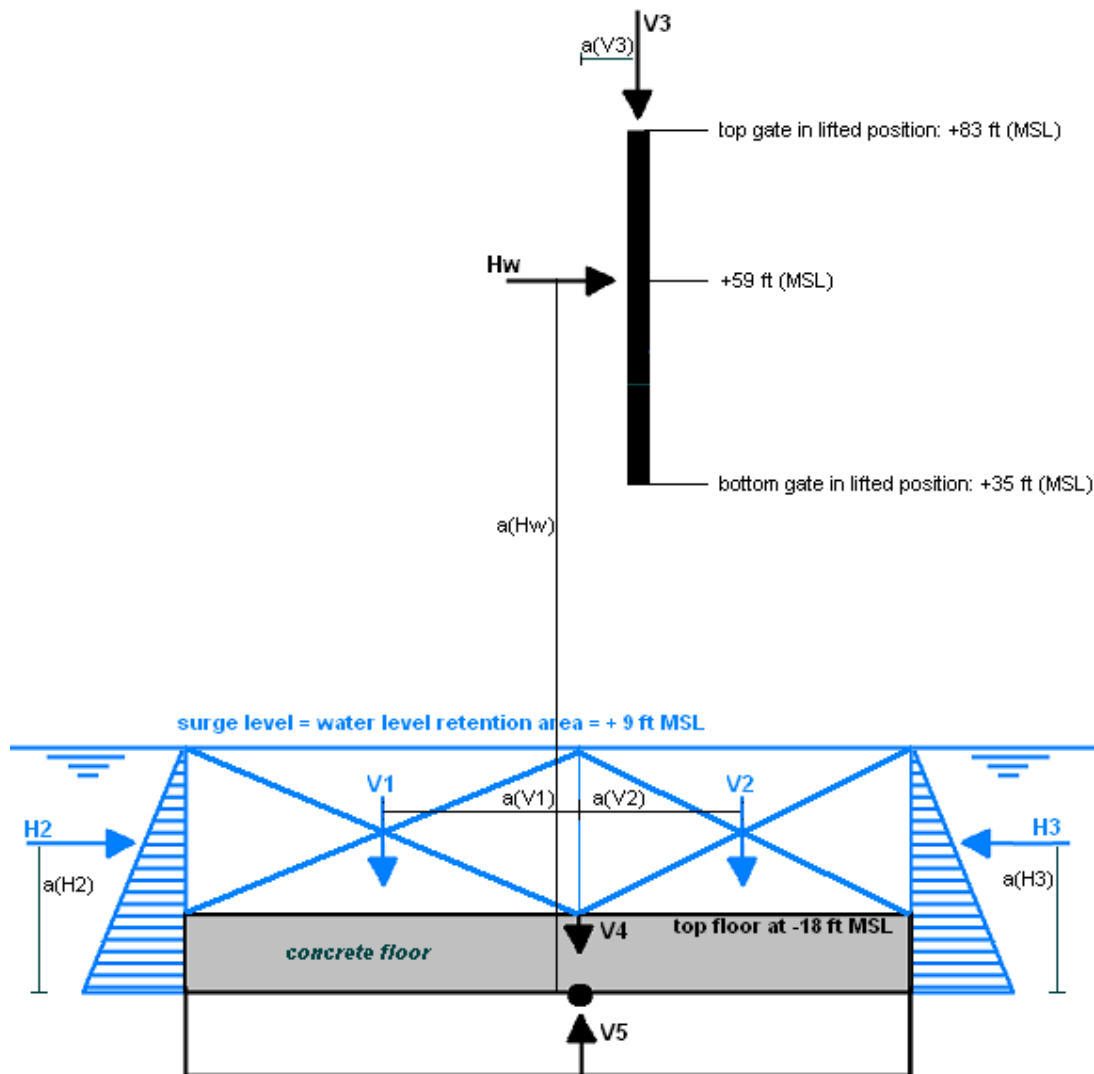
$$M_{V5} := a_{V5} \cdot V_5 = 0 \cdot \text{kN} \cdot \text{m}$$

$$M_{V6} := a_{V6} \cdot V_6 = 8.06 \times 10^5 \cdot \text{kN} \cdot \text{m}$$

$$e_H := \frac{\Sigma M_H}{\Sigma H} = 10.38 \text{ m}$$

$$e_V := \frac{\Sigma M_V}{\Sigma V} = 2.75 \text{ m}$$

H.4.4 Representative wind load on the gate in lifted position



Data:

$$h_{\text{bottom}} := -18 \text{ ft (MSL)} \quad h_{\text{sill}} := h_{\text{bottom}}$$

soil characteristics: MSL -8 to -25 = clay (interdistributary): $p_{\text{wet,ci}} := 15 \cdot \frac{\text{kN}}{\text{m}^3}$ and $\phi_{\text{ci}} := 22.5^\circ$
 MSL -25 to -45 = clay (pro-delta): $p_{\text{wet,pd}} := 18 \cdot \frac{\text{kN}}{\text{m}^3}$ and $\phi_{\text{cpd}} := 25.0^\circ$

Dimensions barrier:

$$h_{\text{pier}} := 30 \text{ ft (MSL)} \quad h_{\text{tower}} := 180 \text{ ft (MSL)} \quad M_{\text{tower}} := 4500 \cdot 10^3 \text{ kg} \quad p_{\text{concrete}} := 24 \frac{\text{kN}}{\text{m}^3}$$

$$w_{\text{span}} := 210 \text{ ft} \quad M_{\text{gate}} := 750 \cdot 10^3 \text{ kg}$$

$$t_{\text{wall}} := 10 \text{ ft} \quad t_{\text{floor}} := 20 \text{ ft} \quad b_{\text{floor}} := w_{\text{span}} + 2 \cdot t_{\text{wall}}$$

$$L_{\text{outer}} := 130 \text{ ft} \quad L_{\text{retention}} := 35 \text{ ft} \quad L_{\text{floor}} := L_{\text{outer}} + L_{\text{retention}}$$

External Forces (water/wave pressures):

$$\begin{aligned}
 h_{\text{surge}} &:= 9\text{ft (MSL)} & h_{\text{retention}} &:= 9\text{ft (MSL)} & P_{\text{outer}} &:= 1025 \frac{\text{kg}}{\text{m}^3} & P_{\text{retention}} &:= 1000 \frac{\text{kg}}{\text{m}^3} \\
 F_{\text{Goda.H}} &:= 0 \frac{\text{kN}}{\text{m}} & P_{\text{Goda.bottom}} &:= 0 \frac{\text{kN}}{\text{m}^2} \\
 P_{\text{hydro.outer}} &:= P_{\text{outer}} \cdot g \cdot [h_{\text{surge}} - (h_{\text{bottom}} - t_{\text{floor}})] = 144 \frac{\text{kN}}{\text{m}^2} \\
 P_{\text{hydro.retention}} &:= P_{\text{retention}} \cdot g \cdot [h_{\text{retention}} - (h_{\text{bottom}} - t_{\text{floor}})] = 140.5 \frac{\text{kN}}{\text{m}^2}
 \end{aligned}$$

Determination of leading wind load

Data:

$$\begin{aligned}
 h_{\text{gate}} &= 14.63\text{ m} & w_{\text{span}} &= 64\text{ m} & A_{\text{gate}} &:= h_{\text{gate}} \cdot w_{\text{span}} = 936.5\text{ m}^2 \\
 P_{\text{air}} &:= 1.25 \frac{\text{kg}}{\text{m}^3} & \text{wind speed: } v_{\text{wind.max}} &:= 27.9 \frac{\text{m}}{\text{s}} \quad (\text{table 6.1: maximum wind speed in normal conditions})
 \end{aligned}$$

Static response: $q_{\text{wind.static}} = \frac{1}{2} \cdot P_{\text{air}} \cdot v_{\text{wind.max}}^2 \cdot (1 + 2 \cdot d \cdot l)$

turbulence intensity: $l := 0.25$ (typical value)

$d = \sqrt{2 \cdot \ln(T_{\text{wind}} \cdot f_0)}$ in which: $T_{\text{wind}} := 3600\text{ s}$ (duration of the wind, set on 1 hour)

$f_0 := 0.13\text{ Hz}$ (central frequency, typical value)

$d := \sqrt{2 \cdot \ln(T_{\text{wind}} \cdot f_0)} = 3.51$

$q_{\text{wind.static}} := \frac{1}{2} \cdot P_{\text{air}} \cdot v_{\text{wind.max}}^2 \cdot (1 + 2 \cdot d \cdot l) = 1.34 \times 10^3 \frac{\text{N}}{\text{m}^2}$

$F_{\text{static.max}} := q_{\text{wind.static}} \cdot A_{\text{gate}} = 1254.4\text{ kN}$

Dynamic response: $q_{\text{wind.dynamic}} = \frac{1}{2} \cdot P_{\text{air}} \cdot v_{\text{wind.max}}^2 \cdot \left[1 + 2 \cdot d \cdot l \cdot \sqrt{1 + \frac{\pi}{4 \cdot \zeta_{\text{steel}}} \cdot \frac{f \cdot S_c(f)}{\sigma^2(v)}} \right]$

damping coefficient for steel: $\zeta_{\text{steel}} = 0.015$ (typical value)

$\frac{f \cdot S_c(f)}{\sigma^2(v)} = \frac{2 \cdot x^2}{3 \cdot (1 + x^2)^{\frac{4}{3}}}$ in which f is the natural frequency of the gate. +

$m_{\text{total.upper.position}} := m_{\text{gate}} + m_{\text{additional}} = 7.88 \times 10^5\text{ kg}$ $k_{\text{gate.total}} := 1 \cdot 10^6 \frac{\text{N}}{\text{m}}$ (assumed values, to be checked)

$f_{\text{natural}} := \frac{1}{2 \cdot \pi} \cdot \sqrt{\frac{k_{\text{gate.total}}}{m_{\text{total.upper.position}}}} = 0.18 \frac{1}{\text{s}}$

$x = \frac{f \cdot L}{v}$ $L_{\text{wind.gust}} := 1200\text{ m}$ (typical value)

$x := \frac{f_{\text{natural}} \cdot L_{\text{wind.gust}}}{v_{\text{wind.max}}} = 7.71$ $\frac{2 \cdot x^2}{3 \cdot (1 + x^2)^{\frac{4}{3}}} = 0.17$

$q_{\text{wind.dynamic}} := \frac{1}{2} \cdot P_{\text{air}} \cdot v_{\text{wind.max}}^2 \cdot \left[1 + 2 \cdot d \cdot l \cdot \sqrt{1 + \frac{\pi}{4 \cdot \zeta_{\text{steel}}} \cdot \frac{2 \cdot x^2}{3 \cdot (1 + x^2)^{\frac{4}{3}}}} \right] = 3149.3 \frac{\text{N}}{\text{m}^2}$

$F_{\text{dynamic.max}} := q_{\text{wind.dynamic}} \cdot A_{\text{gate}} = 2949.2\text{ kN}$

$\text{Factor}_{\text{dynamic|static}} := \frac{F_{\text{dynamic.max}}}{F_{\text{static.max}}} = 2.35$

$$H_1 := 0 \text{ N}$$

$$H_2 := \left[\frac{1}{2} \rho_{\text{outer}} \cdot g \cdot [h_{\text{surge}} - (h_{\text{bottom}} - t_{\text{floor}})]^2 \right] \cdot (w_{\text{span}} + 2 \cdot t_{\text{wall}}) = 7.23 \times 10^7 \text{ N}$$

$$H_3 := \left[\frac{1}{2} \rho_{\text{retention}} \cdot g \cdot [h_{\text{retention}} - (h_{\text{bottom}} - t_{\text{floor}})]^2 \right] \cdot (w_{\text{span}} + 2 \cdot t_{\text{wall}}) = 7.05 \times 10^7 \text{ N}$$

$$\text{Additional wind load: } H_w := 2950 \cdot \text{kN} = 2.95 \times 10^6 \text{ N}$$

$$V_1 := \rho_{\text{outer}} \cdot g \cdot (h_{\text{surge}} - h_{\text{bottom}}) \cdot L_{\text{outer}} \cdot w_{\text{span}} = 2.1 \times 10^8 \text{ N}$$

$$V_2 := \rho_{\text{retention}} \cdot g \cdot (h_{\text{retention}} - h_{\text{bottom}}) \cdot L_{\text{retention}} \cdot w_{\text{span}} = 5.51 \times 10^7 \text{ N}$$

$$V_3 := M_{\text{gate}} \cdot g + 2 \cdot M_{\text{tower}} \cdot g = 9.56 \times 10^7 \text{ N}$$

$$V_4 := \rho_{\text{concrete}} \cdot [2 \cdot t_{\text{wall}} \cdot (h_{\text{pier}} - h_{\text{bottom}}) + b_{\text{floor}} \cdot t_{\text{floor}}] \cdot L_{\text{floor}} = 6.23 \times 10^8 \text{ N}$$

$$V_5 := \rho_{\text{hydro.retention}} \cdot L_{\text{floor}} \cdot b_{\text{floor}} = 4.95 \times 10^8 \text{ N}$$

$$V_6 := \frac{1}{2} \cdot (\rho_{\text{hydro.outer}} - \rho_{\text{hydro.retention}}) \cdot L_{\text{floor}} \cdot b_{\text{floor}} = 6.19 \times 10^6 \text{ N}$$

$$\Sigma V := V_1 + V_2 + V_3 + V_4 - V_5 - V_6 = 4.82 \times 10^8 \text{ N}$$

$$\Sigma H := H_1 + H_2 - H_3 + H_w = 4.71 \times 10^6 \text{ N}$$

$$\text{unity check: } \phi := 25^\circ \quad \text{delta}(\delta) := 0.8\phi \quad \tan(\text{delta}(\delta)) = 0.36$$

$$\frac{\Sigma V \cdot \tan(\text{delta}(\delta))}{\Sigma H} = 37.26 > 1.0$$

Lever arm

$$a_{H1} := 0 \text{ m}$$

$$a_{H2} := \left(\frac{1}{3} \right) \cdot [h_{\text{surge}} - (h_{\text{bottom}} - t_{\text{floor}})] = 4.78 \text{ m}$$

$$a_{H3} := \left(\frac{1}{3} \right) \cdot [h_{\text{retention}} - (h_{\text{bottom}} - t_{\text{floor}})] = 4.78 \text{ m}$$

$$a_{Hw} := 59 \text{ ft} - (h_{\text{bottom}} - t_{\text{floor}}) = 29.57 \text{ m}$$

$$a_{V1} := \left(\frac{L_{\text{floor}}}{2} \right) - \frac{1}{2} \cdot L_{\text{outer}} = 5.33 \text{ m}$$

$$a_{V2} := \left(\frac{L_{\text{floor}}}{2} \right) - \frac{1}{2} \cdot L_{\text{retention}} = 19.81 \text{ m}$$

$$a_{V3} := \left(\frac{L_{\text{floor}}}{2} \right) - L_{\text{retention}} = 14.48 \text{ m}$$

$$a_{V4} := 0 \text{ m}$$

$$a_{V5} := 0 \text{ m}$$

$$a_{V6} := \frac{L_{\text{floor}}}{6} = 8.38 \text{ m}$$

Moment

$$M_{H1} := a_{H1} \cdot H_1 = 0 \text{ kN}\cdot\text{m}$$

$$M_{H2} := a_{H2} \cdot H_2 = 3.45 \times 10^5 \text{ kN}\cdot\text{m}$$

$$M_{H3} := a_{H3} \cdot H_3 = 3.37 \times 10^5 \text{ kN}\cdot\text{m}$$

$$M_{Hw} := a_{Hw} \cdot H_w = 8.72 \times 10^4 \text{ kN}\cdot\text{m}$$

$$M_{V1} := a_{V1} \cdot V_1 = 1.12 \times 10^6 \text{ kN}\cdot\text{m}$$

$$M_{V2} := a_{V2} \cdot V_2 = 1.09 \times 10^6 \text{ kN}\cdot\text{m}$$

$$M_{V3} := a_{V3} \cdot V_3 = 1.38 \times 10^6 \text{ kN}\cdot\text{m}$$

$$M_{V4} := a_{V4} \cdot V_4 = 0 \text{ kN}\cdot\text{m}$$

$$M_{V5} := a_{V5} \cdot V_5 = 0 \text{ kN}\cdot\text{m}$$

$$M_{V6} := a_{V6} \cdot V_6 = 5.19 \times 10^4 \text{ kN}\cdot\text{m}$$

$$\Sigma M_H := M_{H1} + M_{H2} - M_{H3} + M_{Hw}$$

$$e_H := \frac{\Sigma M_H}{\Sigma H} = 20.29 \text{ m}$$

$$\Sigma M_V := -M_{V1} + M_{V2} + M_{V3} + M_{V4} + M_{V5} + M_{V6}$$

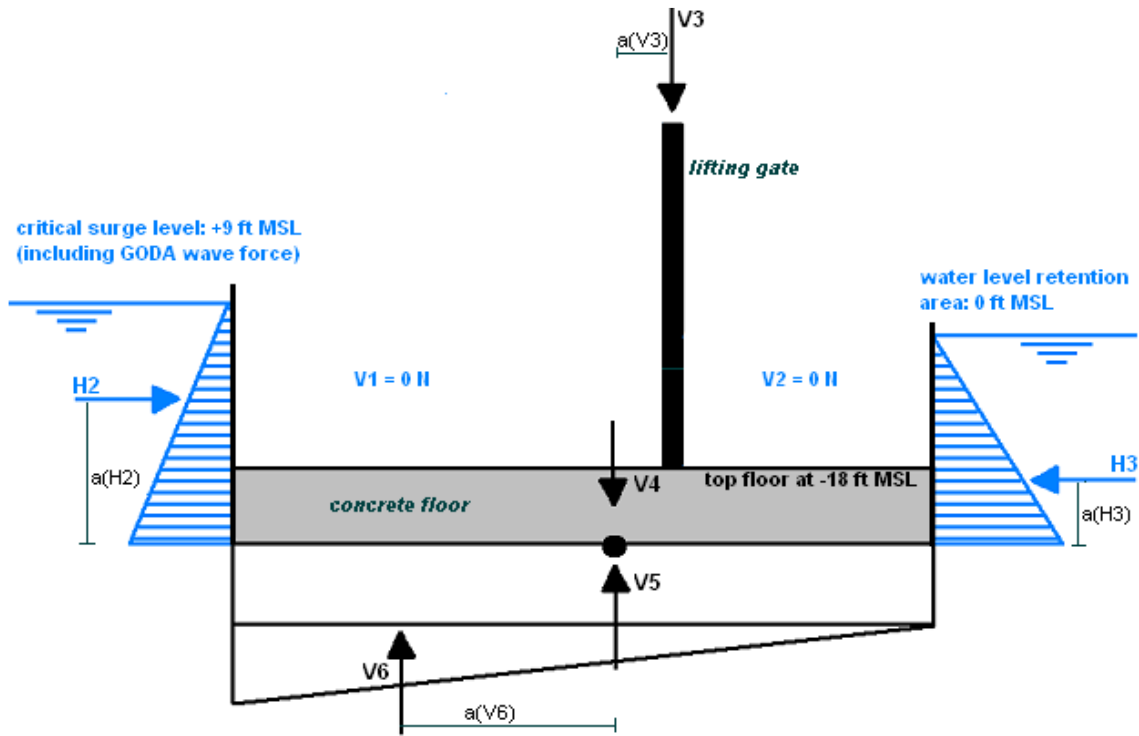
$$e_V := \frac{\Sigma M_V}{\Sigma V} = 2.92 \text{ m}$$

$$\text{check: eccentricity} := \frac{\Sigma M_H + \Sigma M_V}{\Sigma V} = 3.12 \text{ m} < \frac{L_{\text{floor}}}{6} = 8.38 \text{ m}$$

check on maximum soil stresses:

$$\sigma_{\text{com}} := \frac{\Sigma V}{b_{\text{floor}} \cdot L_{\text{floor}}} + \frac{\Sigma M_H + \Sigma M_V}{\frac{1}{6} \cdot b_{\text{floor}} \cdot L_{\text{floor}}^2} = 187.8 \frac{\text{kN}}{\text{m}^2} < 300 \frac{\text{kN}}{\text{m}^2}$$

H.4.5 Severe conditions during temporary closure of the substructure for maintenance



Data:

$$h_{\text{bottom}} := -18 \text{ft (MSL)} \quad h_{\text{sill}} := h_{\text{bottom}}$$

soil characteristics: MSL -8 to -25 = clay (interdistributary): $\rho_{\text{wet,ci}} := 15 \frac{\text{kN}}{\text{m}^3}$ and $\phi_{\text{ci}} := 22.5^\circ$
 MSL -25 to -45 = clay (pro-delta): $\rho_{\text{wet,pd}} := 18 \frac{\text{kN}}{\text{m}^3}$ and $\phi_{\text{cpd}} := 25.0^\circ$

Dimensions barrier:

$$h_{\text{pier}} := 30 \text{ft (MSL)} \quad h_{\text{tower}} := 180 \text{ft (MSL)} \quad M_{\text{tower}} := 4500 \cdot 10^3 \text{kg} \quad \rho_{\text{concrete}} := 24 \frac{\text{kN}}{\text{m}^3}$$

$$w_{\text{span}} := 210 \text{ft} \quad M_{\text{gate}} := 750 \cdot 10^3 \text{kg}$$

$$t_{\text{wall}} := 10 \text{ft} \quad t_{\text{floor}} := 20 \text{ft} \quad b_{\text{floor}} := w_{\text{span}} + 2 \cdot t_{\text{wall}}$$

$$L_{\text{outer}} := 130 \text{ft} \quad L_{\text{retention}} := 35 \text{ft} \quad L_{\text{floor}} := L_{\text{outer}} + L_{\text{retention}}$$

External Forces (water/wave pressures):

$$h_{\text{surge}} := 9 \text{ft (MSL)} \quad h_{\text{retention}} := 0 \text{ft (MSL)} \quad \rho_{\text{outer}} := 1025 \frac{\text{kg}}{\text{m}^3} \quad \rho_{\text{retention}} := 1000 \frac{\text{kg}}{\text{m}^3}$$

$$F_{\text{Goda,H}} := 225 \frac{\text{kN}}{\text{m}} \quad \rho_{\text{Goda,bottom}} := 19.2 \frac{\text{kN}}{\text{m}^2} \quad \text{assumed wave conditions: } H_s = 12/3 = 4 \text{ft}$$

$$\rho_{\text{hydro,outer}} := \rho_{\text{outer}} \cdot g \cdot [h_{\text{surge}} - (h_{\text{bottom}} - t_{\text{floor}})] = 144 \frac{\text{kN}}{\text{m}^2} \quad T_p = 14/2 = 7 \text{sec}$$

$$\rho_{\text{hydro,retention}} := \rho_{\text{retention}} \cdot g \cdot [h_{\text{retention}} - (h_{\text{bottom}} - t_{\text{floor}})] = 113.6 \frac{\text{kN}}{\text{m}^2}$$

$$H_1 := F_{\text{Goda.H}} \cdot w_{\text{span}} = 1.44 \times 10^7 \text{ N}$$

$$H_2 := \left[\frac{1}{2} \rho_{\text{outer}} \cdot g \cdot [h_{\text{surge}} - (h_{\text{bottom}} - t_{\text{floor}})]^2 \right] \cdot (w_{\text{span}} + 2 \cdot t_{\text{wall}}) = 7.23 \times 10^7 \text{ N}$$

$$H_3 := \left[\frac{1}{2} \rho_{\text{retention}} \cdot g \cdot [h_{\text{retention}} - (h_{\text{bottom}} - t_{\text{floor}})]^2 \right] \cdot (w_{\text{span}} + 2 \cdot t_{\text{wall}}) = 4.61 \times 10^7 \text{ N}$$

$$V_1 := 0 \text{ N}$$

$$V_2 := 0 \text{ N}$$

$$V_3 := M_{\text{gate}} \cdot g + 2 \cdot M_{\text{tower}} \cdot g = 9.56 \times 10^7 \text{ N}$$

$$V_4 := \rho_{\text{concrete}} \cdot [2 \cdot t_{\text{wall}} \cdot (h_{\text{pier}} - h_{\text{bottom}}) + b_{\text{floor}} \cdot t_{\text{floor}}] \cdot L_{\text{floor}} = 6.23 \times 10^8 \text{ N}$$

$$V_5 := \rho_{\text{hydro.retention}} \cdot L_{\text{floor}} \cdot b_{\text{floor}} = 4 \times 10^8 \text{ N}$$

$$V_6 := \frac{1}{2} \cdot (\rho_{\text{hydro.outer}} - \rho_{\text{hydro.retention}}) \cdot L_{\text{floor}} \cdot b_{\text{floor}} = 5.36 \times 10^7 \text{ N}$$

$$\Sigma V := V_1 + V_2 + V_3 + V_4 - V_5 - V_6 = 2.65 \times 10^8 \text{ N} \quad \Sigma H := H_1 + H_2 - H_3 = 4.06 \times 10^7 \text{ N}$$

$$\text{unity check: } \phi = 25^\circ \quad \text{delta}(\delta) = 0.8\phi \quad \tan(\text{delta}(\delta)) = 0.36$$

$$\frac{\Sigma V \cdot \tan(\text{delta}(\delta))}{\Sigma H} = 2.38 > 1.0$$

Lever arm

$$a_{H1} := 5.38 \text{ m} + t_{\text{floor}} = 11.48 \text{ m}$$

$$a_{H2} := \left(\frac{1}{3} \right) \cdot [h_{\text{surge}} - (h_{\text{bottom}} - t_{\text{floor}})] = 4.78 \text{ m}$$

$$a_{H3} := \left(\frac{1}{3} \right) \cdot [h_{\text{retention}} - (h_{\text{bottom}} - t_{\text{floor}})] = 3.86 \text{ m}$$

$$a_{V1} := 0 \text{ m}$$

$$a_{V2} := 0 \text{ m}$$

$$a_{V3} := \left(\frac{L_{\text{floor}}}{2} \right) - L_{\text{retention}} = 14.48 \text{ m}$$

$$a_{V4} := 0 \text{ m}$$

$$a_{V5} := 0 \text{ m}$$

$$a_{V6} := \frac{L_{\text{floor}}}{6} = 8.38 \text{ m}$$

Moment

$$M_{H1} := a_{H1} \cdot H_1 = 1.65 \times 10^5 \text{ kN}\cdot\text{m}$$

$$M_{H2} := a_{H2} \cdot H_2 = 3.45 \times 10^5 \text{ kN}\cdot\text{m}$$

$$M_{H3} := a_{H3} \cdot H_3 = 1.78 \times 10^5 \text{ kN}\cdot\text{m}$$

$$M_{V1} := a_{V1} \cdot V_1 = 0 \text{ kN}\cdot\text{m}$$

$$M_{V2} := a_{V2} \cdot V_2 = 0 \text{ kN}\cdot\text{m}$$

$$M_{V3} := a_{V3} \cdot V_3 = 1.38 \times 10^6 \text{ kN}\cdot\text{m}$$

$$M_{V4} := a_{V4} \cdot V_4 = 0 \text{ kN}\cdot\text{m}$$

$$M_{V5} := a_{V5} \cdot V_5 = 0 \text{ kN}\cdot\text{m}$$

$$M_{V6} := a_{V6} \cdot V_6 = 4.49 \times 10^5 \text{ kN}\cdot\text{m}$$

$$\Sigma M_H := M_{H1} + M_{H2} - M_{H3}$$

$$e_H := \frac{\Sigma M_H}{\Sigma H} = 8.19 \text{ m}$$

$$\Sigma M_V := -M_{V1} + M_{V2} + M_{V3} + M_{V4} + M_{V5} + M_{V6}$$

$$e_V := \frac{\Sigma M_V}{\Sigma V} = 6.92 \text{ m}$$

$$\text{check: eccentricity} := \frac{\Sigma M_H + \Sigma M_V}{\Sigma V} = 8.17 \text{ m} < \frac{L_{\text{floor}}}{6} = 8.38 \text{ m}$$

check on maximum soil stresses:

$$\sigma_{\text{com}} := \frac{\Sigma V}{b_{\text{floor}} \cdot L_{\text{floor}}} + \frac{\Sigma M_H + \Sigma M_V}{\frac{1}{6} \cdot b_{\text{floor}} \cdot L_{\text{floor}}^2} = 148.5 \frac{\text{kN}}{\text{m}^2} < 300 \frac{\text{kN}}{\text{m}^2}$$

H.4.6 Ship collision: indicative calculation to estimate order of magnitude and expected influence

Design vessel: $L_V := 300\text{ft}$ $B_V := 105\text{ft}$ $D_V := 15\text{ft}$

Assumed vessel speed and angle of impact (normal moving vessel subjected to wind load):

$$v_V := 2 \frac{\text{m}}{\text{s}} \quad \phi := 15^\circ \quad \rho_W := 1000 \frac{\text{kg}}{\text{m}^3}$$

$$\text{Design kinetic energy of the moving vessel: } E_{\text{kin.design}} = \frac{1}{2} \cdot m_V \cdot v_V^2 \cdot C_E \cdot C_M \cdot C_S \cdot C_C$$

- Mass of the vessel, equal to the water displacement: $m_V = \rho_W \cdot L_V \cdot B_V \cdot D_V \cdot C_B$

$$C_B := 0.9 \text{ (pushed convoy)} \quad m_V := \rho_W \cdot L_V \cdot B_V \cdot D_V \cdot C_B = 1.204 \times 10^7 \text{ kg}$$

- Eccentricity factor: $C_E = \frac{K_V^2 + K_V^2 \cdot \cos(\phi)^2}{K_V^2 + R_V^2}$ in which:

$$\text{radius of gyration of the vessel: } K_V := (0.19 \cdot C_B + 0.11) \cdot L_V = 25.7 \text{ m}$$

$$\text{distance of point of contact to the center of mass: } R_V := 0.35 \cdot L_V = 32 \text{ m}$$

$$C_E := \frac{K_V^2 + K_V^2 \cdot \cos(\phi)^2}{K_V^2 + R_V^2} = 0.76$$

- Virtual mass factor: $C_M := 1 + 2 \cdot \frac{D_V}{B_V} = 1.29$

- Softness factor: $C_S := 1.0$

- Cushion factor: $C_C := 1.0$

$$E_{\text{kin.design}} := \frac{1}{2} \cdot m_V \cdot v_V^2 \cdot C_E \cdot C_M \cdot C_S \cdot C_C = 2.346 \times 10^4 \cdot \text{kN} \cdot \text{m}$$

H.5 Retaining wall – optimum front plate thickness, stiffeners and cross beams

H.5.1 Front plate

yield point S355: $f_{y,d} := 355 \frac{\text{N}}{\text{mm}^2}$

representative field width: $b_{qp} := 1\text{m}$

MatrixFrame: $M_{p,max} := 26.21\text{kN}\cdot\text{m}$ and $V_{p,max} := 150.21\text{kN}$
 $N_{p,max} := 5000\text{kN}$ (assumed at 10% of resultant normal force in front chord)

The plate section is loaded by a combination of a bending moment, normal force and shear force. The equivalent stress should be equal or less than the yield point:

$$\sigma_{eq} = \sqrt{\sigma_{y,s,d}^2 + 3\tau_{yz,s,d}^2} \leq f_{y,d}$$

$$\sigma_{y,s,d} = \frac{M_{p,max}}{W_p} + \frac{N_{p,max}}{b_{qp} \cdot t_p} \quad \text{with: } W_p = \frac{1}{6} \cdot b_{qp} \cdot t_p^2$$

$$\tau_{yz,s,d} = \frac{3}{2} \frac{V_{p,max}}{b_{qp} \cdot t_p} \quad (\text{standard equation for the maximum shear stress in a rectangular cross-section})$$

$$\sigma_{eq,s,d}(t_p) := f_{y,d}$$

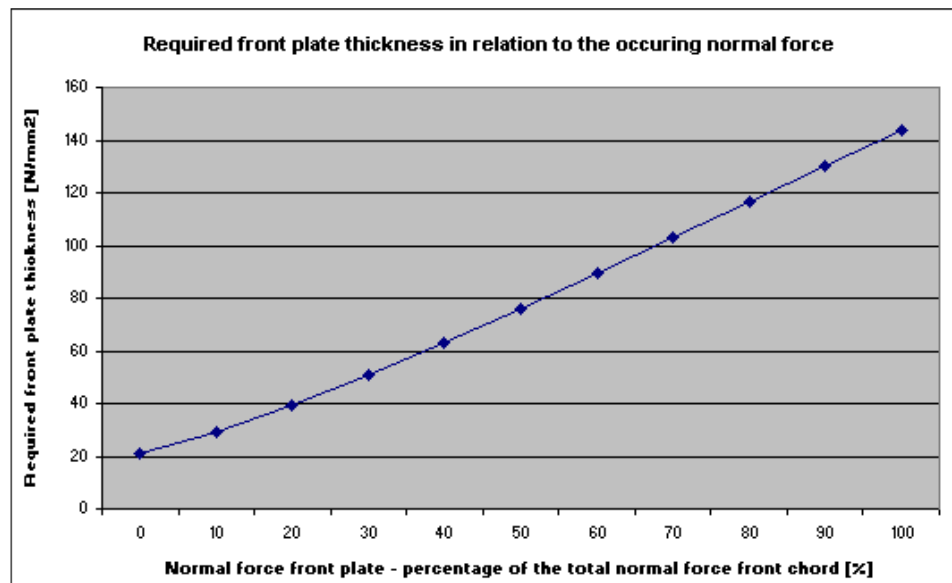
Guess value: $t_p := 25\text{mm}$

Given

$$\sigma_{eq,s,d}(t_p) = \sqrt{\left(\frac{M_{p,max}}{\frac{1}{6} \cdot b_{qp} \cdot t_p^2} + \frac{N_{p,max}}{b_{qp} \cdot t_p} \right)^2 + 3 \cdot \left(\frac{3}{2} \frac{V_{p,max}}{b_{qp} \cdot t_p} \right)^2}$$

Find(t_p) = 29.2 mm

Dependency of the front plate thickness on the occurring normal force



H.5.2 Method of separation of components

Longitudinal stiffener

yield point S355: $f_{y,d} := 355 \frac{\text{N}}{\text{mm}^2}$

MatrixFrame: mutual distance maximum moment maximum shear force
(Appendix I.5.1) $\Delta x = 1.0 \text{ m}$ $M_{\Delta x1} := 26.21 \text{ kN}\cdot\text{m}$ $V_{\Delta x1} := 150.21 \text{ kN}$

thus $\Delta x := 2 \cdot \text{m}$ $M_{s,\text{max}} := M_{\Delta x1} \left(\frac{\Delta x}{1.0 \cdot \text{m}} \right)^2 = 104.84 \cdot \text{kN}\cdot\text{m}$
 $V_{s,\text{max}} := V_{\Delta x1} \cdot \left(\frac{\Delta x}{1.0 \cdot \text{m}} \right) = 300.42 \cdot \text{kN}$

The leading cross-section is subjected to a combination of a bending moment and a shear force. The equivalent stress should be equal or less than the yield point:

$$\sigma_{\text{eq}} = \sqrt{\sigma_{y,d}^2 + 3\tau_{v,d}^2} \leq f_{y,d}$$

To find the actual profile, an iterative calculation has to be performed containing the following steps:

1. Assume IPE-profile by calculating minimum section factor: $W_{\text{min}} := \frac{M_{s,\text{max}}}{f_{y,d}} = 2.95 \times 10^5 \cdot \text{mm}^3$

IPE 300 $h_p := 300 \text{ mm}$ $t_w := 7.1 \text{ mm}$ $I_{zz} := 8356 \cdot 10^4 \text{ mm}^4$
 $b_p := 150 \text{ mm}$ $t_f := 10.7 \text{ mm}$ $W_{z,\text{el}} := 557 \cdot 10^3 \text{ mm}^3$

2. Determine influence of the shear force: $\tau = \frac{V_{s,\text{max}} \cdot S_z^a}{t_w \cdot I_{zz}} \leq \frac{f_{y,d}}{\sqrt{3}}$

$$S_z := b_p \cdot t_f \left(\frac{h_p - t_f}{2} \right) + t_w \cdot \frac{1}{2} \left(\frac{h_p}{2} - t_f \right)^2 = 3.01 \times 10^5 \cdot \text{mm}^3$$

$$\tau_d := \frac{V_{s,\text{max}} \cdot S_z}{t_w \cdot I_{zz}} = 152.4 \cdot \frac{\text{N}}{\text{mm}^2} < \frac{f_{y,d}}{\sqrt{3}} = 205 \cdot \frac{\text{N}}{\text{mm}^2}$$

4. Check the equivalent stress:

$$\sigma_{\text{eq},s,d} := \sqrt{\left(\frac{M_{s,\text{max}}}{W_{z,\text{el}}} \right)^2 + 3 \cdot \tau_d^2} = 324.3 \cdot \frac{\text{N}}{\text{mm}^2} < f_{y,d} = 355 \cdot \frac{\text{N}}{\text{mm}^2}$$

Results:

	Profile	A_{IPE}	$\sigma_{\text{eq},s,d}$	W_{max} (MatrixFrame)
	[]	[mm ²]	[N/mm ²]	[mm]
$\Delta L = 1.0 \text{ m}$	<i>IPE 180</i>	$23.9 \cdot 10^2$	349.4	0.6
$\Delta L = 2.0 \text{ m}$	<i>IPE 300</i>	$53.8 \cdot 10^2$	324.3	1.5
$\Delta L = 3.0 \text{ m}$	<i>IPE 400</i>	$84.5 \cdot 10^2$	317.3	2.7
$\Delta L = 4.0 \text{ m}$	<i>IPE 500</i>	$116 \cdot 10^2$	311.5	4.1

Cross beam

yield point S355: $f_{y,d} := 355 \frac{\text{N}}{\text{mm}^2}$

<u>MatrixFrame:</u> (Appendix I.5.2)	mutual distance $\Delta x = 1.0 \text{ m}$	maximum moment $M_{\Delta x1} := 760.32 \text{ kN}\cdot\text{m}$	maximum shear force $V_{\Delta x1} := 711.52 \text{ kN}$
---	---	---	---

thus: $\Delta x := 2 \cdot \text{m}$

$$M_{\text{cb,max}} := M_{\Delta x1} \left(\frac{\Delta x}{1.0 \cdot \text{m}} \right) = 1.521 \times 10^3 \cdot \text{kN}\cdot\text{m}$$

$$V_{\text{cb,max}} := V_{\Delta x1} \left(\frac{\Delta x}{1.0 \cdot \text{m}} \right) = 1.423 \times 10^3 \cdot \text{kN}$$

The leading cross-section is subjected to a combination of a bending moment and a shear force. The equivalent stress should be equal or less than the yield point:

$$\sigma_{\text{eq}} = \sqrt{\sigma_{M_{y,d}}^2 + 3\tau_{V_d}^2} \leq f_{y,d}$$

To find the actual profile, an iterative calculation has to be performed containing the following steps:

1. Assume HEA-profile (standard IPE-profile not sufficient): $W_{\text{min}} := \frac{M_{\text{cb,max}}}{f_{y,d}} = 4.28 \times 10^6 \cdot \text{mm}^3$

HE700A $h_p := 690 \text{ mm}$ $b_p := 300 \text{ mm}$ $t_w := 14.5 \text{ mm}$ $t_f := 27 \text{ mm}$

$A_{\text{tot}} := 260 \cdot 10^2 \text{ mm}^2$ $I_{zz,HE} := 215300 \cdot 10^4 \cdot \text{mm}^4$ $W_{z,el} := 6241 \cdot 10^3 \text{ mm}^3$

2. Determine influence of the shear force: $\tau = \frac{V_{g,\text{max}} \cdot S_z^a}{t_w \cdot I_{zz}} \leq \frac{f_{y,d}}{\sqrt{3}}$

$$S_z := b_p \cdot t_f \left(\frac{h_p - t_f}{2} \right) + t_w \cdot \frac{1}{2} \left(\frac{h_p}{2} - t_f \right)^2 = 3.42 \times 10^6 \cdot \text{mm}^3$$

$$\tau_d := \frac{V_{\text{cb,max}} \cdot S_z}{t_w \cdot I_{zz,HE}} = 155.8 \cdot \frac{\text{N}}{\text{mm}^2} < \frac{f_{y,d}}{\sqrt{3}} = 205 \cdot \frac{\text{N}}{\text{mm}^2}$$

4. Check the equivalent stress:

$$\sigma_{\text{eq,s,d}} := \sqrt{\left(\frac{M_{\text{cb,max}}}{W_{z,el}} \right)^2 + 3 \cdot \tau_d^2} = 363.6 \cdot \frac{\text{N}}{\text{mm}^2} < f_{y,d} = 355 \cdot \frac{\text{N}}{\text{mm}^2}$$

Not sufficient!
thus HE800A

H.5.3 Method of equivalent cross-section

Longitudinal stiffener

yield point S355: $f_{y,d} := 355 \frac{\text{N}}{\text{mm}^2}$

<u>MatrixFrame:</u>	mutual distance	maximum moment	maximum shear force
(Appendix I.5.1)	$\Delta x = 1.0 \text{ m}$	$M_{\Delta x1} := 26.21 \text{ kN}\cdot\text{m}$	$V_{\Delta x1} := 150.21 \text{ kN}$

thus $\Delta x := 2 \cdot \text{m}$ $M_{s,max} := M_{\Delta x1} \left(\frac{\Delta x}{1.0 \cdot \text{m}} \right)^2 = 104.84 \text{ kN}\cdot\text{m}$

$$V_{s,max} := V_{\Delta x1} \cdot \left(\frac{\Delta x}{1.0 \cdot \text{m}} \right) = 300.42 \text{ kN}$$

$$N_{s,max} := \frac{5000 \text{ kN}}{2} = 2.5 \times 10^6 \text{ N} \quad (\text{assumed at 10\% of resultant normal force in front chord, divided over 2 stiffeners})$$

The leading cross-section is subjected to a combination of a bending moment, normal force and a shear force. The equivalent tension should be equal or less than the yield point:

$$\sigma_{eq} = \sqrt{\sigma_{My,d}^2 + 3\tau_{Vd}^2} \leq f_{y,d}$$

To find the actual profile, an iterative calculation has to be performed containing the following steps:

1. Assume IPE-profile by calculating minimum section factor: $W_{min} := \frac{M_{s,max}}{f_{y,d}} = 2.95 \times 10^5 \cdot \text{mm}^3$

IPE 240 $h_p := 240 \text{ mm}$ $b_p := 120 \text{ mm}$ $t_w := 6.2 \text{ mm}$ $t_f := 9.8 \text{ mm}$

$$A_{tot} := 39.1 \cdot 10^2 \text{ mm}^2 \quad I_{zz, IPE} := 3892 \cdot 10^4 \text{ mm}^4 \quad W_{z,el} := 324 \cdot 10^3 \text{ mm}^3$$

$$t_{plate} := 30 \text{ mm} \quad \Delta x_{stiffener} := 1 \text{ m} = 1 \times 10^3 \cdot \text{mm}$$

2. Determine the center of gravity and moment of inertia of the equivalent cross-section:

center of gravity

part	A_i	z_{ci}
1 (front plate)	$A_1 := t_{plate} \cdot \Delta x_{stiffener} = 3 \times 10^4 \cdot \text{mm}^2$	$z_{c1} := \frac{t_{plate}}{2} = 15 \cdot \text{mm}$
2 (IPE - profile)	$A_2 := A_{tot} = 3.91 \times 10^3 \cdot \text{mm}^2$	$z_{c2} := t_{plate} + \frac{h_p}{2} = 150 \cdot \text{mm}$

$$\Sigma A := A_1 + A_2 = 3.39 \times 10^4 \cdot \text{mm}^2$$

$$\Sigma S_{zci} := A_1 \cdot z_{c1} + A_2 \cdot z_{c2} = 1.04 \times 10^6 \cdot \text{mm}^3 \quad z_c := \frac{\Sigma S_{zci}}{\Sigma A} = 30.57 \cdot \text{mm}$$

equivalent moment of inertia:

$$I_{zz,eq} = \Sigma I_{zz,eigen} + \Sigma I_{zz,steiner} \quad \text{with: } I_{zz,steiner,i} = A_i \cdot (\Delta z_{ci})^2$$

part moment of inertia

1 $I_{zz,eigen,1} := \frac{1}{12} \cdot \Delta x_{stiffener} \cdot t_{plate}^3 = 2.25 \times 10^6 \cdot \text{mm}^4$

$$I_{zz,steiner,1} := A_1 \cdot (z_c - z_{c1})^2 = 7.269 \times 10^6 \cdot \text{mm}^4$$

2 $I_{zz,eigen,2} := I_{zz, IPE} = 3.892 \times 10^7 \cdot \text{mm}^4$

$$I_{zz,steiner,2} := A_2 \cdot (z_c - z_{c2})^2 = 5.577 \times 10^7 \cdot \text{mm}^4$$

$$I_{zz,eq} := I_{zz,eigen,1} + I_{zz,steiner,1} + I_{zz,eigen,2} + I_{zz,steiner,2} = 1.042 \times 10^8 \cdot \text{mm}^4$$

3. Determine the stress due to the bending moment: $\sigma_{y,d} = \frac{M_{s,max} \cdot e_{max}}{I_{zz,eq}} + \frac{N_{s,max}}{\Sigma A}$

$$M_{s,max} = 104.84 \cdot \text{kN} \cdot \text{m} \quad e_{max} := (t_{plate} + h_p) - z_c = 239.4 \cdot \text{mm}$$

$$\sigma_{y,d} := \frac{M_{s,max} \cdot e_{max}}{I_{zz,eq}} + \frac{N_{s,max}}{\Sigma A} = 314.6 \cdot \frac{\text{N}}{\text{mm}^2}$$

4. Determine influence of the shear force: $\tau = \frac{V_{g,max} \cdot S_z^a}{b \cdot I_{zz}} \leq \frac{f_{y,d}}{\sqrt{3}}$

$$V_{s,max} = 300.42 \cdot \text{kN}$$

$$\Delta x = 1.0 \text{ m} \quad b_1 := \Delta x_{stiffener} \quad S_{zc1} := (z_c \cdot \Delta x_{stiffener}) \cdot \frac{1}{2} \cdot z_c = 4.67 \times 10^5 \cdot \text{mm}^3$$

$$\Delta x = 2.0 \text{ m} \quad b_2 := b_p = 120 \cdot \text{mm} \quad \text{always check the center of gravity: influences both } S_z \text{ and } b!$$

$$S_{zc2} := (t_{plate} \cdot \Delta x_{stiffener}) \cdot (z_c - z_{c1}) + \frac{1}{2} \cdot b_p \cdot (z_c - t_{plate})^2 = 4.67 \times 10^5 \cdot \text{mm}^3$$

$$\Delta x = 3.0 \text{ m} \quad b_3 := t_w = 6.2 \cdot \text{mm}$$

$$S_{zc3} := b_p \cdot t_f \cdot \left(t_{plate} + h_p - \frac{t_f}{2} - z_c \right) + \frac{1}{2} \cdot (t_{plate} + h_p - t_f - z_c)^2 \cdot t_w = 4.39 \times 10^5 \cdot \text{mm}^3$$

$$\Delta x = 4.0 \text{ m} \quad b_4 := t_w = 6.2 \cdot \text{mm}$$

$$S_{zc4} := b_p \cdot t_f \cdot \left(t_{plate} + h_p - \frac{t_f}{2} - z_c \right) + \frac{1}{2} \cdot (t_{plate} + h_p - t_f - z_c)^2 \cdot t_w = 4.39 \times 10^5 \cdot \text{mm}^3$$

$$\text{variable:} \quad S_z := S_{zc2} \quad b := b_2$$

$$\tau_d := \frac{V_{s,max} \cdot S_z}{b \cdot I_{zz,eq}} = 11.2 \cdot \frac{\text{N}}{\text{mm}^2} < \frac{f_{y,d}}{\sqrt{3}} = 205 \cdot \frac{\text{N}}{\text{mm}^2}$$

5. Check the equivalent stress:

$$\sigma_{eq,s,d} := \sqrt{\sigma_{y,d}^2 + 3 \cdot \tau_d^2} = 315.2 \cdot \frac{\text{N}}{\text{mm}^2} < f_{y,d} = 355 \cdot \frac{\text{N}}{\text{mm}^2}$$

Results

	IPE	z_c	$I_{zz,eq}$	S_z	b	$\sigma_{eq,s,d}$
	[-]	[mm]	[mm ⁴]	[mm ³]	[mm]	[N/mm ²]
$\Delta x = 1.0 \text{ m}$	140	19.41	$1.89 \cdot 10^7$	$1.88 \cdot 10^5$	$\Delta x_{stiffener}$	287.9
$\Delta x = 2.0 \text{ m}$	240	30.57	$1.04 \cdot 10^8$	$4.67 \cdot 10^5$	b_p	315.2
$\Delta x = 3.0 \text{ m}$	400	62.25	$5.38 \cdot 10^8$	$1.42 \cdot 10^6$	t_w	329.0
$\Delta x = 4.0 \text{ m}$	500	88.89	$1.07 \cdot 10^9$	$2.31 \cdot 10^6$	t_w	320.0

As Δx increases to 3 m or more, the influence of the front plate diminishes and no benefit is gained anymore by using the equivalent cross-section method over the separation method!

Cross beam

yield point S355: $f_{y,d} := 355 \frac{\text{N}}{\text{mm}^2}$

<u>MatrixFrame:</u>	mutual distance	maximum moment	maximum shear force
(Appendix I.5.2)	$\Delta x = 1.0 \text{ m}$	$M_{\Delta x1} := 760.32 \text{ kN}\cdot\text{m}$	$V_{\Delta x1} := 711.52 \text{ kN}$

thus: $\Delta x := 2 \cdot \text{m}$

$$M_{\text{cb,max}} := M_{\Delta x1} \left(\frac{\Delta x}{1.0 \cdot \text{m}} \right) = 1.521 \times 10^3 \cdot \text{kN}\cdot\text{m}$$

$$V_{\text{cb,max}} := V_{\Delta x1} \left(\frac{\Delta x}{1.0 \cdot \text{m}} \right) = 1.423 \times 10^3 \cdot \text{kN}$$

The leading cross-section is subjected to a combination of a bending moment and a shear force. The equivalent tension should be equal or less than the yield point:

$$\sigma_{\text{eq}} = \sqrt{\sigma_{M_{y,d}}^2 + 3\tau_{V_d}^2} \leq f_{y,d}$$

To find the actual profile, an iterative calculation has to be performed containing the following steps:

1. Assume HEA-profile (standard IPE-profile not sufficient): $W_{\text{min}} := \frac{M_{\text{cb,max}}}{f_{y,d}} = 4.28 \times 10^6 \cdot \text{mm}^3$

HE700A $h_p := 690 \text{ mm}$ $b_p := 300 \text{ mm}$ $t_w := 14.5 \text{ mm}$ $t_f := 27.0 \text{ mm}$

$A_{\text{tot}} := 260 \cdot 10^2 \text{ mm}^2$ $I_{\text{zz,HE}} := 215300 \cdot 10^4 \cdot \text{mm}^4$ $W_{\text{z,el}} := 6241 \cdot 10^3 \text{ mm}^3$

$t_{\text{plate}} := 30 \text{ mm}$ $\Delta x = 2 \text{ m}$

2. Determine the center of gravity and moment of inertia of the equivalent cross-section:

center of gravity

part	A_i	z_{ci}
1 (front plate)	$A_1 := t_{\text{plate}} \cdot \Delta x = 6 \times 10^4 \cdot \text{mm}^2$	$z_{c1} := \frac{t_{\text{plate}}}{2} = 15 \cdot \text{mm}$
2 (IPE - profile)	$A_2 := A_{\text{tot}} = 2.6 \times 10^4 \cdot \text{mm}^2$	$z_{c2} := t_{\text{plate}} + \frac{h_p}{2} = 375 \cdot \text{mm}$

$\Sigma A := A_1 + A_2 = 8.6 \times 10^4 \cdot \text{mm}^2$

$\Sigma S_{zci} := A_1 \cdot z_{c1} + A_2 \cdot z_{c2} = 1.07 \times 10^7 \cdot \text{mm}^3$ $z_c := \frac{\Sigma S_{zci}}{\Sigma A} = 123.84 \cdot \text{mm}$

equivalent moment of inertia:

$I_{\text{zz,eq}} = \Sigma I_{\text{zz,eigen}} + \Sigma I_{\text{zz,steiner}}$ with: $I_{\text{zz,steiner},i} = A_i \cdot (\Delta z_{ci})^2$

part moment of inertia

1 $I_{\text{zz,eigen},1} := \frac{1}{12} \cdot \Delta x \cdot t_{\text{plate}}^3 = 4.5 \times 10^6 \cdot \text{mm}^4$

$I_{\text{zz,steiner},1} := A_1 \cdot (z_c - z_{c1})^2 = 7.107 \times 10^8 \cdot \text{mm}^4$

2 $I_{\text{zz,eigen},2} := I_{\text{zz,HE}} = 2.153 \times 10^9 \cdot \text{mm}^4$

$I_{\text{zz,steiner},2} := A_2 \cdot (z_c - z_{c2})^2 = 1.64 \times 10^9 \cdot \text{mm}^4$

$I_{\text{zz,eq}} := I_{\text{zz,eigen},1} + I_{\text{zz,steiner},1} + I_{\text{zz,eigen},2} + I_{\text{zz,steiner},2} = 4.51 \times 10^9 \cdot \text{mm}^4$

3. Determine the stress due to the bending moment: $\sigma_{y,d} = \frac{M_{cb,max} \cdot e_{max}}{I_{zz,eq}}$

$$M_{cb,max} = 1.52 \times 10^3 \cdot \text{kN} \cdot \text{m} \quad e_{max} := (t_{plate} + h_p) - z_c = 596.2 \cdot \text{mm}$$

$$\sigma_{y,d} := \frac{M_{cb,max} \cdot e_{max}}{I_{zz,eq}} = 201.1 \cdot \frac{\text{N}}{\text{mm}^2}$$

4. Determine influence of the shear force: $\tau = \frac{V_{g,max} \cdot S_z^a}{b \cdot I_{zz}} \leq \frac{f_{y,d}}{\sqrt{3}}$

$$V_{cb,max} = 1.42 \times 10^3 \cdot \text{kN}$$

$$\Delta x = 1.0 \text{ m} \quad b_1 := \Delta x \quad S_{zc1} := (z_c \cdot \Delta x) \cdot \frac{1}{2} \cdot z_c = 1.53 \times 10^7 \cdot \text{mm}^3 \quad \text{always check the center of gravity: influences both } S_z \text{ and } b!$$

$$\Delta x > 1.0 \text{ m} \quad b_2 := t_w = 14.5 \cdot \text{mm}$$

$$S_{zc2,upper} := A_1 \cdot (z_c - z_{c1}) + b_p \cdot t_f \left[z_c - \left(t_{plate} + \frac{t_f}{2} \right) \right] + \frac{1}{2} \cdot t_w \left[z_c - \left(t_{plate} + t_f \right) \right]^2 = 7.21 \times 10^6 \cdot \text{mm}^3$$

$$S_{zc2,lower} := b_p \cdot t_f \left(t_{plate} + h_p - \frac{t_f}{2} - z_c \right) + \frac{1}{2} \left(t_{plate} + h_p - t_f - z_c \right)^2 \cdot t_w = 7.07 \times 10^6 \cdot \text{mm}^3$$

$$\text{variable:} \quad S_z := S_{zc2,upper} \quad b := b_2$$

$$\tau_d := \frac{V_{cb,max} \cdot S_z}{b \cdot I_{zz,eq}} = 157 \cdot \frac{\text{N}}{\text{mm}^2} < \frac{f_{y,d}}{\sqrt{3}} = 205 \cdot \frac{\text{N}}{\text{mm}^2}$$

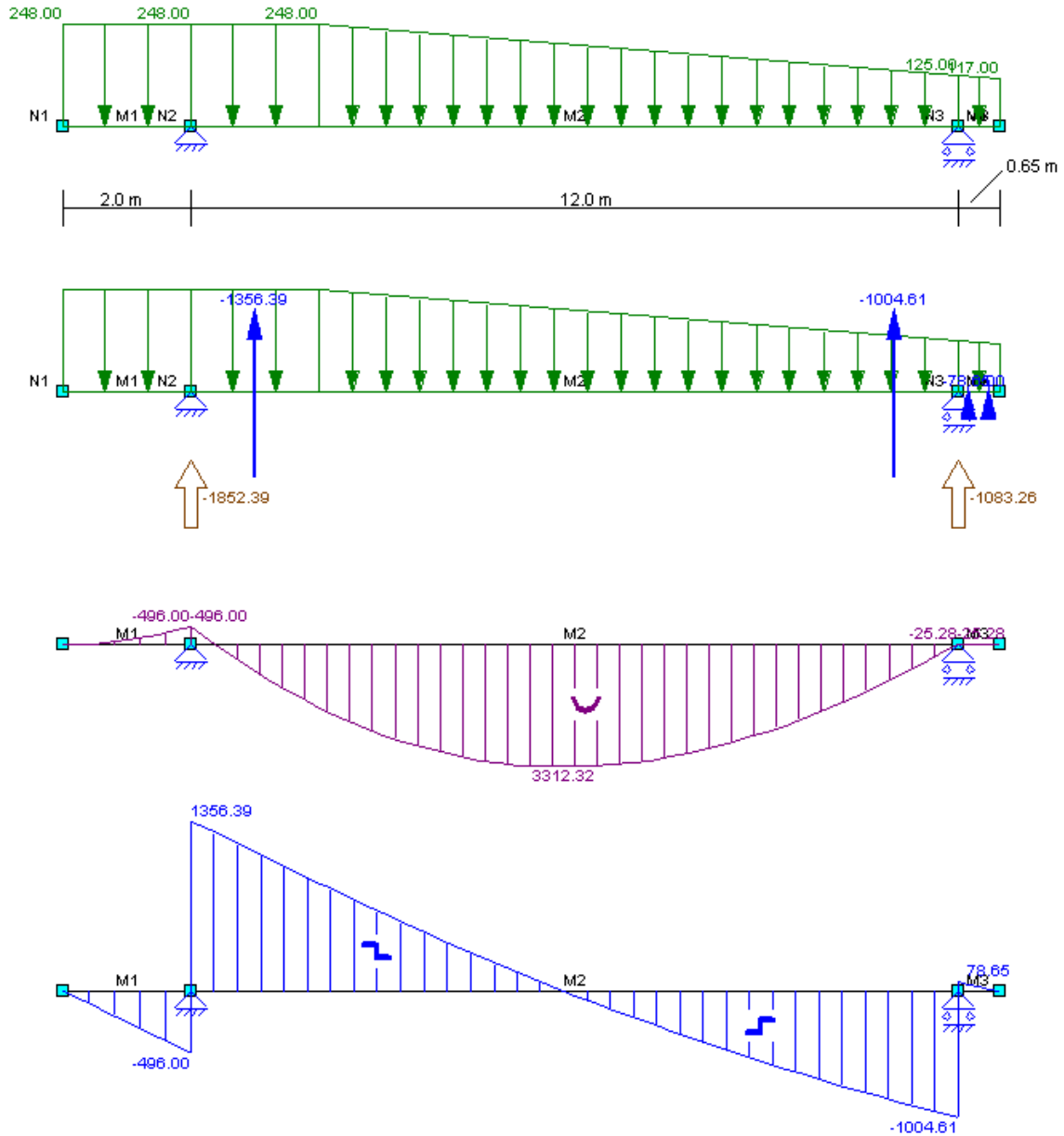
5. Check the equivalent stress:

$$\sigma_{eq,s,d} := \sqrt{\sigma_{y,d}^2 + 3 \cdot \tau_d^2} = 338.2 \cdot \frac{\text{N}}{\text{mm}^2} < f_{y,d} = 355 \cdot \frac{\text{N}}{\text{mm}^2}$$

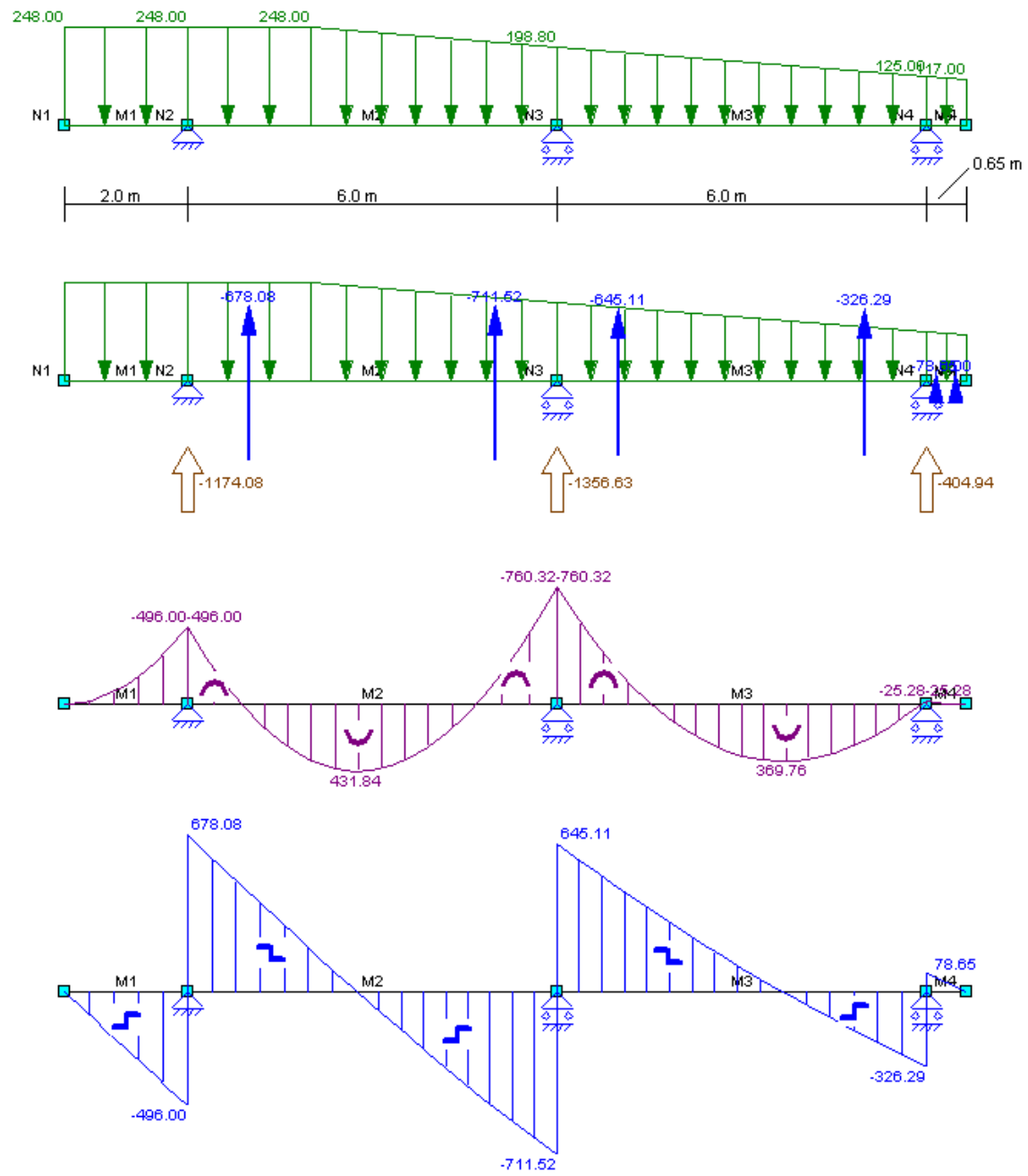
APPENDIX I – MatrixFrame Results

I.1 Cross beam – optimum number of supports

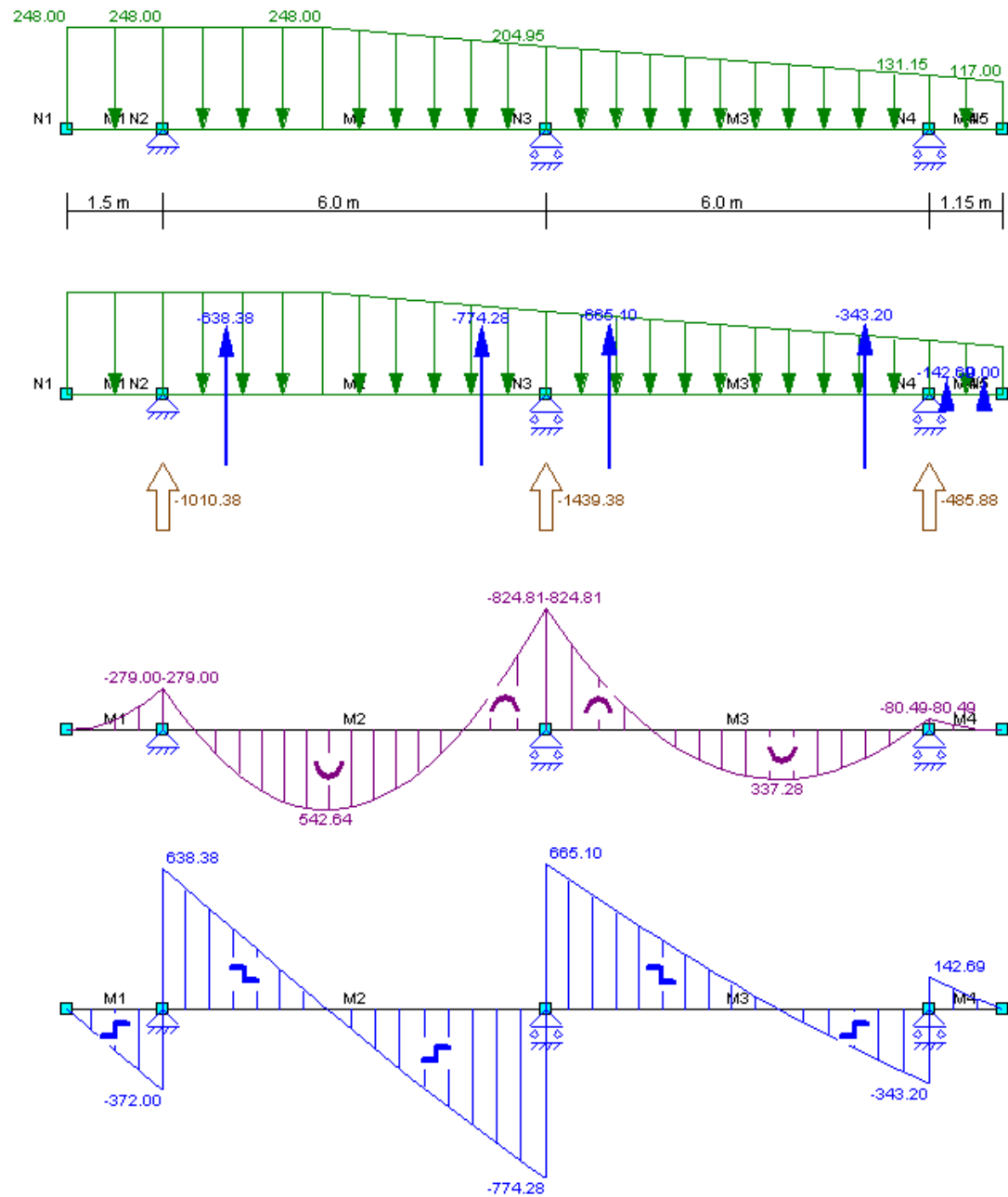
I.1.1 Cross beam at two supports with field lengths: 2.0 / 12.0 / 0.65 [m]



I.1.2 Cross beam at three supports with field lengths: 2.0 / 6.0 / 6.0 / 0.65 [m]

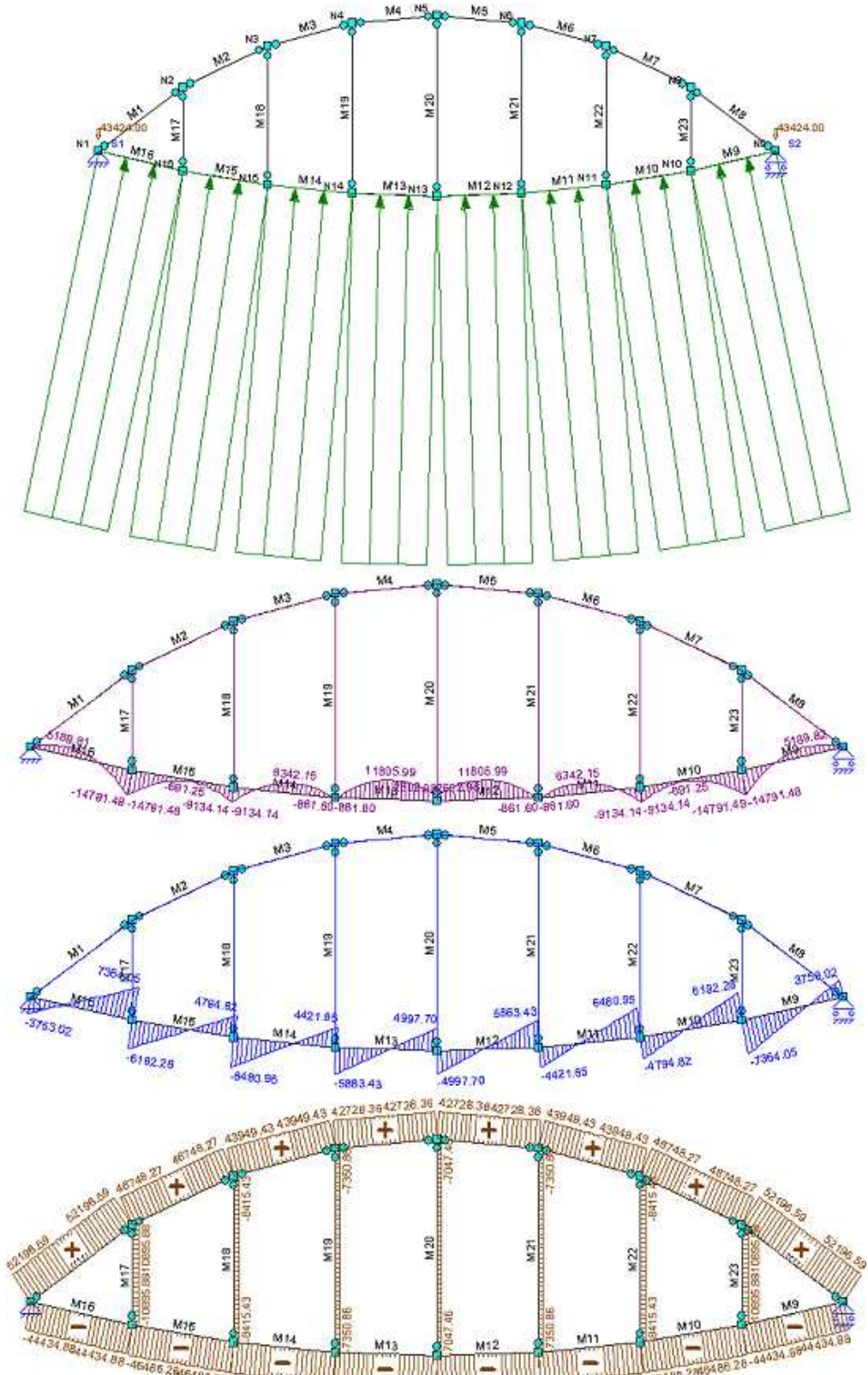


I.1.3 Cross beam at three supports with field lengths: 1.5 / 6.0 / 6.0 / 1.15 [m]

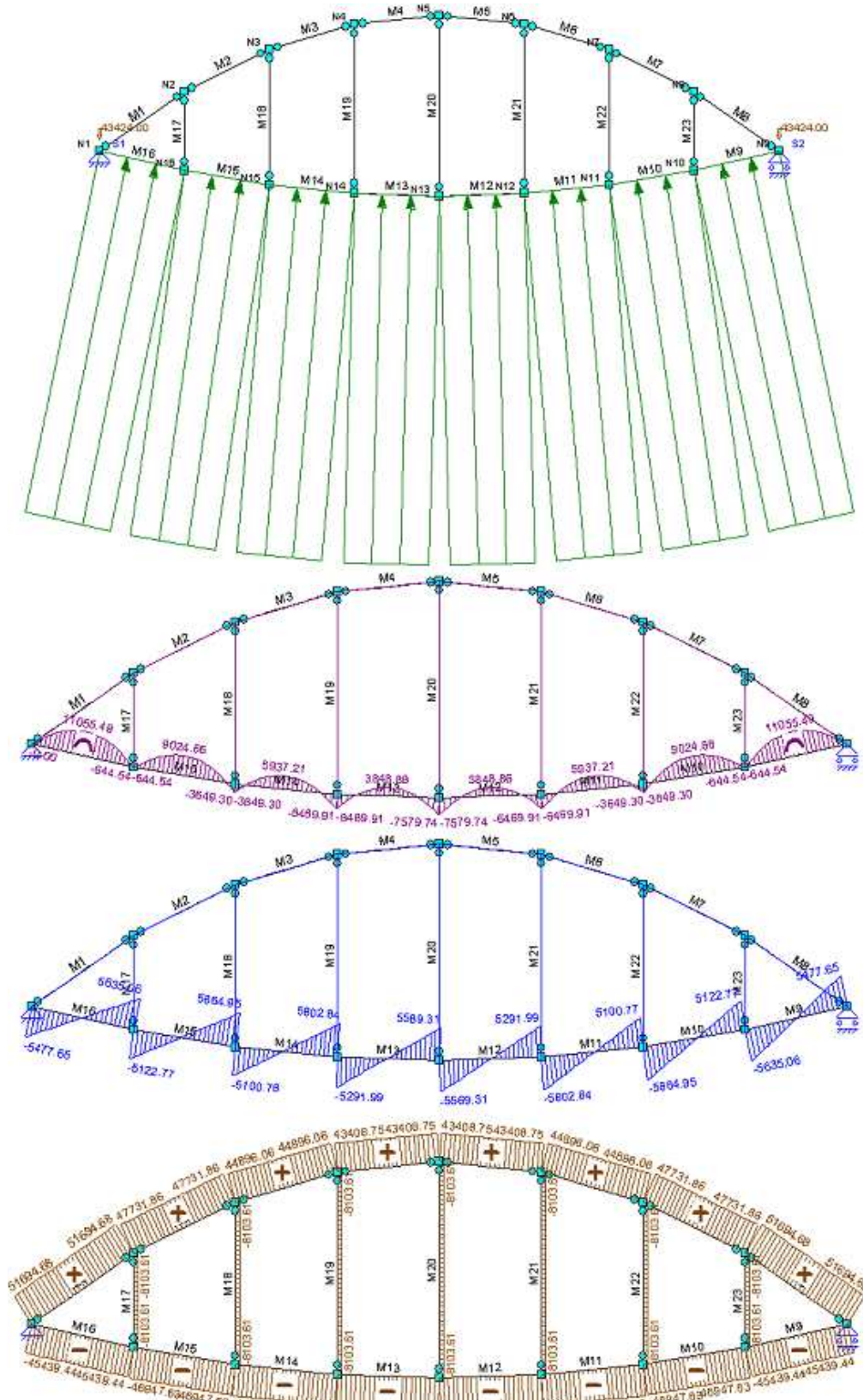


1.2 Lens-shaped barrier section, *hinged joints* – optimum gate curvature and optimum pitch ratio

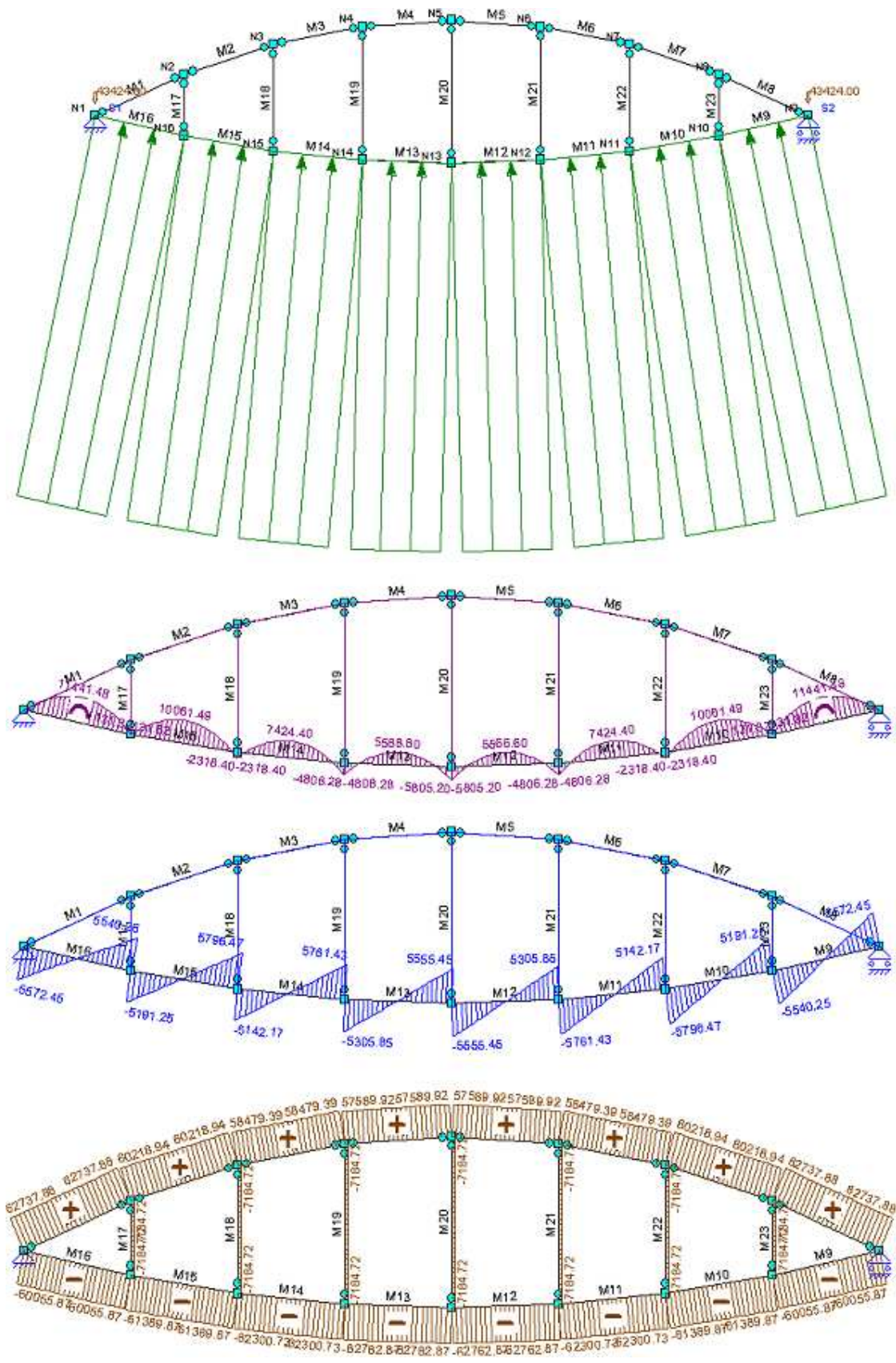
1.2.1 Circular configuration, hinged ($q = 1357 \text{ kN/m}$) – wall arch pitch = 4.0 m, rear chord pitch = 12.0 m



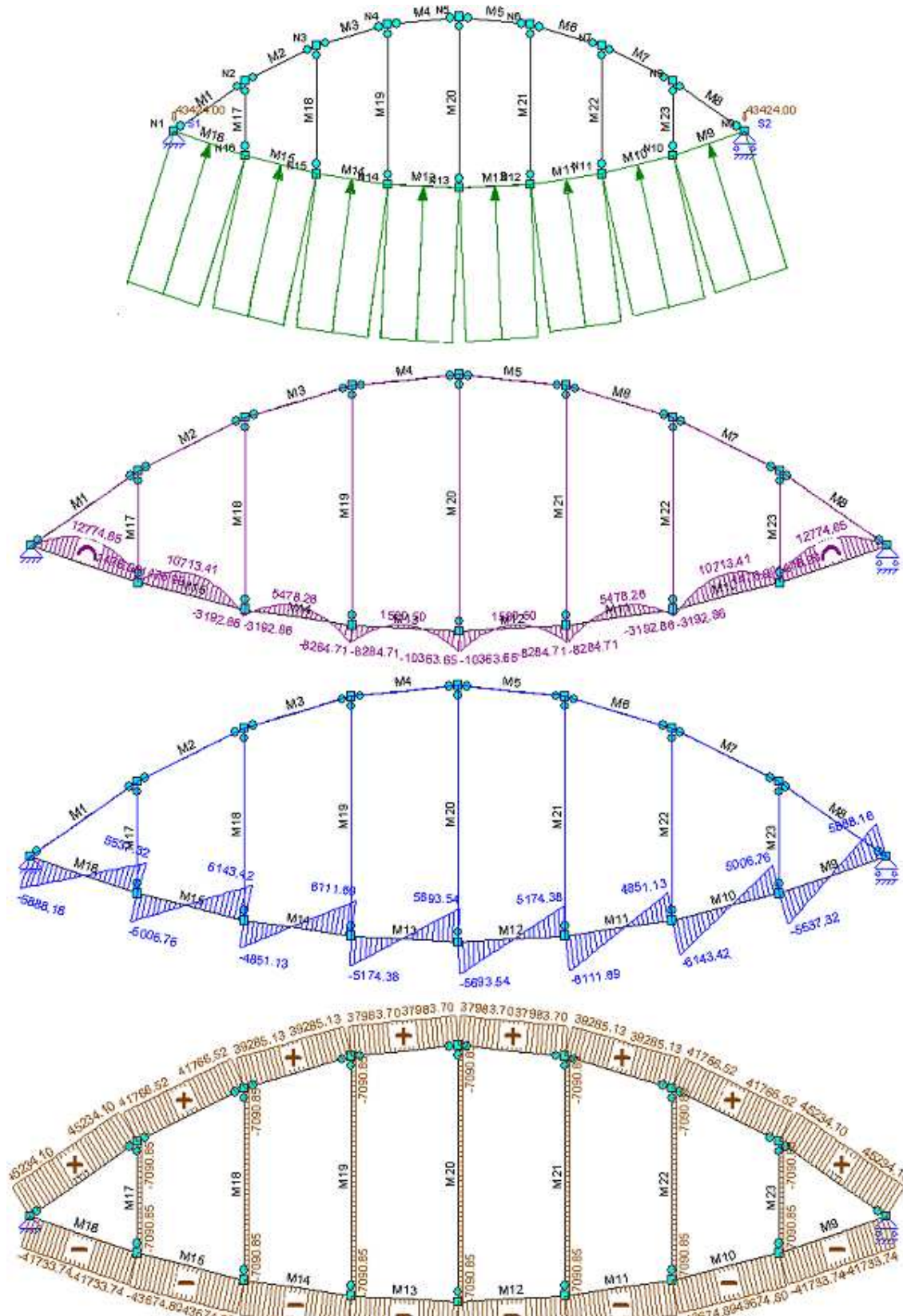
I.2.2 Parabolic configuration, hinged ($q = 1357 \text{ kN/m}$) – wall arch pitch = 4.0 m, rear chord pitch = 12.0 m



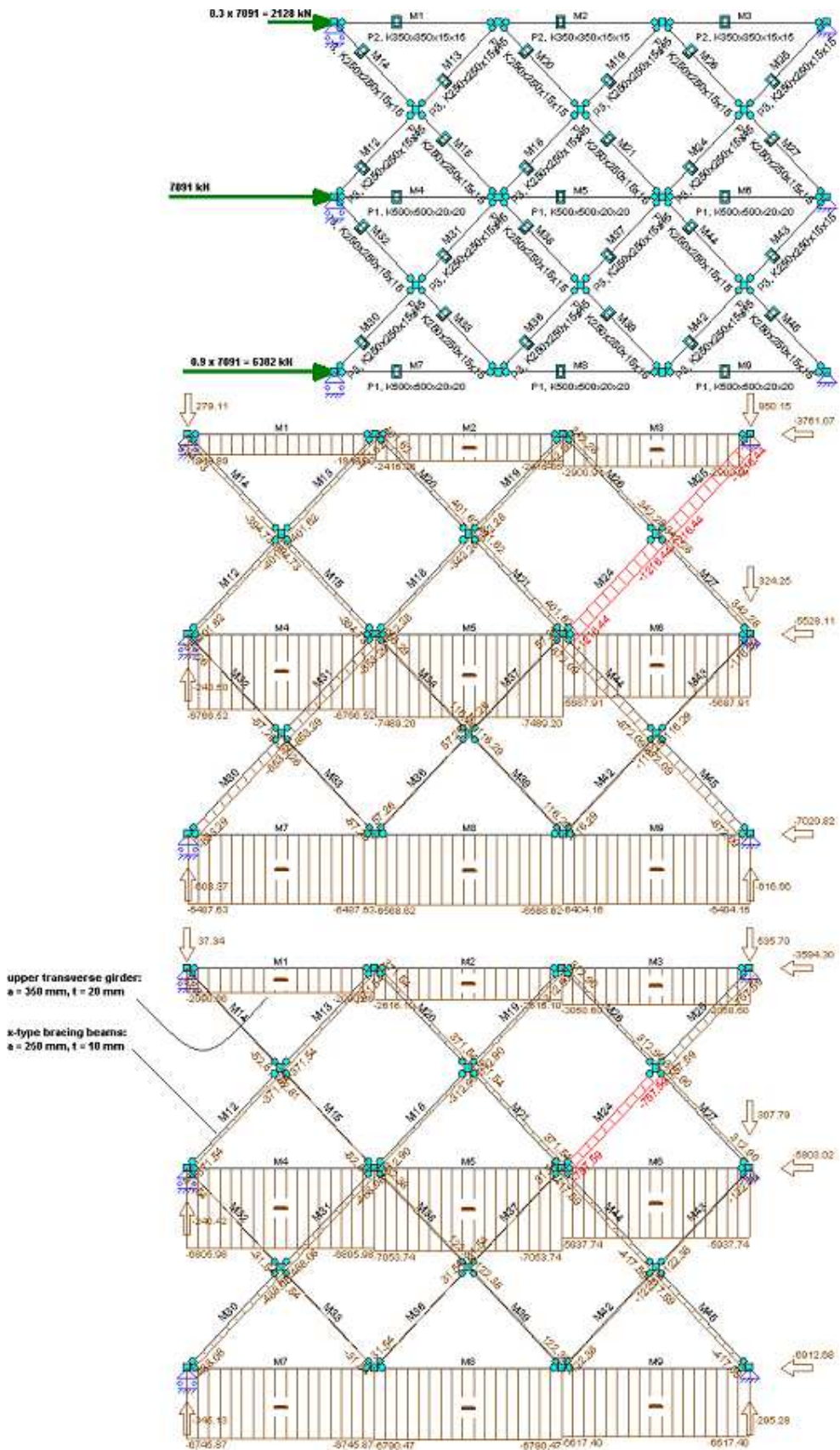
I.2.3 Parabolic configuration, hinged ($q = 1357 \text{ kN/m}$) – wall arch pitch = 4.0 m, rear chord pitch = 8.0 m



I.2.4 Parabolic configuration, hinged ($q = 1357 \text{ kN/m}$) – wall arch pitch = 6.0 m, rear chord pitch = 12.0 m

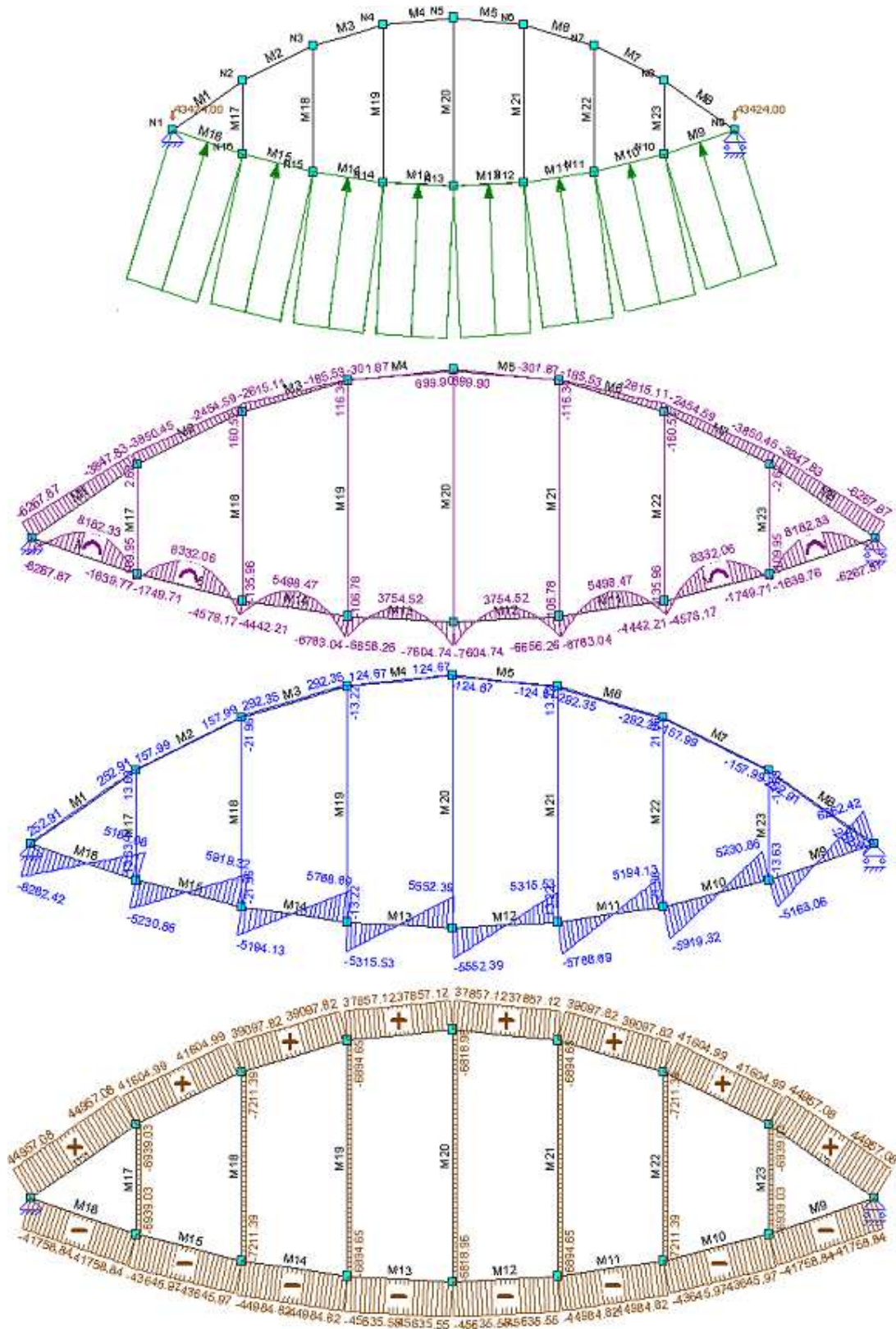


1.2.5 Predetermined configuration, hinged ($q = 1357 \text{ kN/m}$) – Transverse girders and x-bracing system

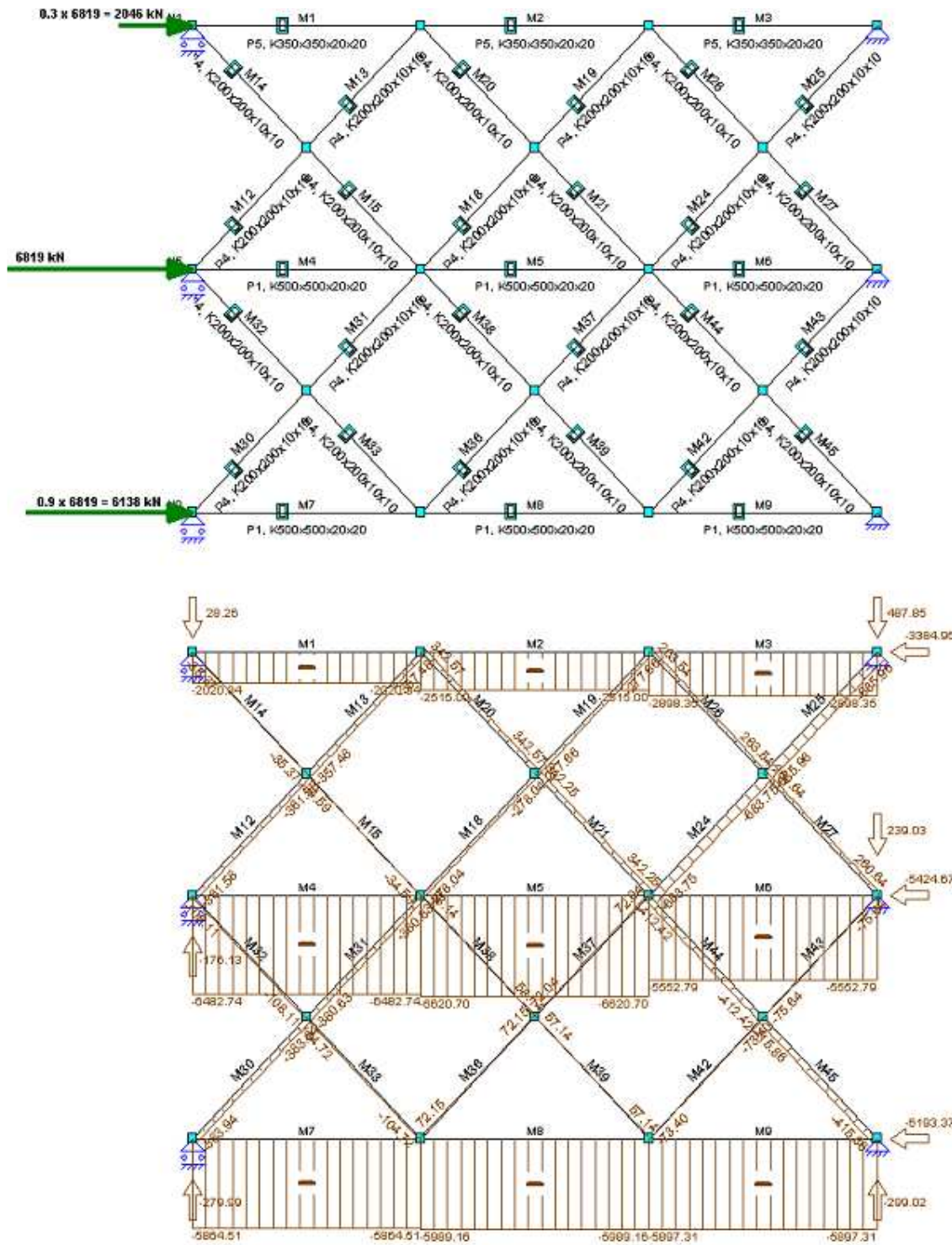


I.3 Lens-shaped barrier section with *clamped joints* – optimum development of member forces

I.3.1 Parabolic configuration, clamped ($q = 1357 \text{ kN/m}$) – wall arch pitch = 6.0 m, rear chord pitch = 12.0 m

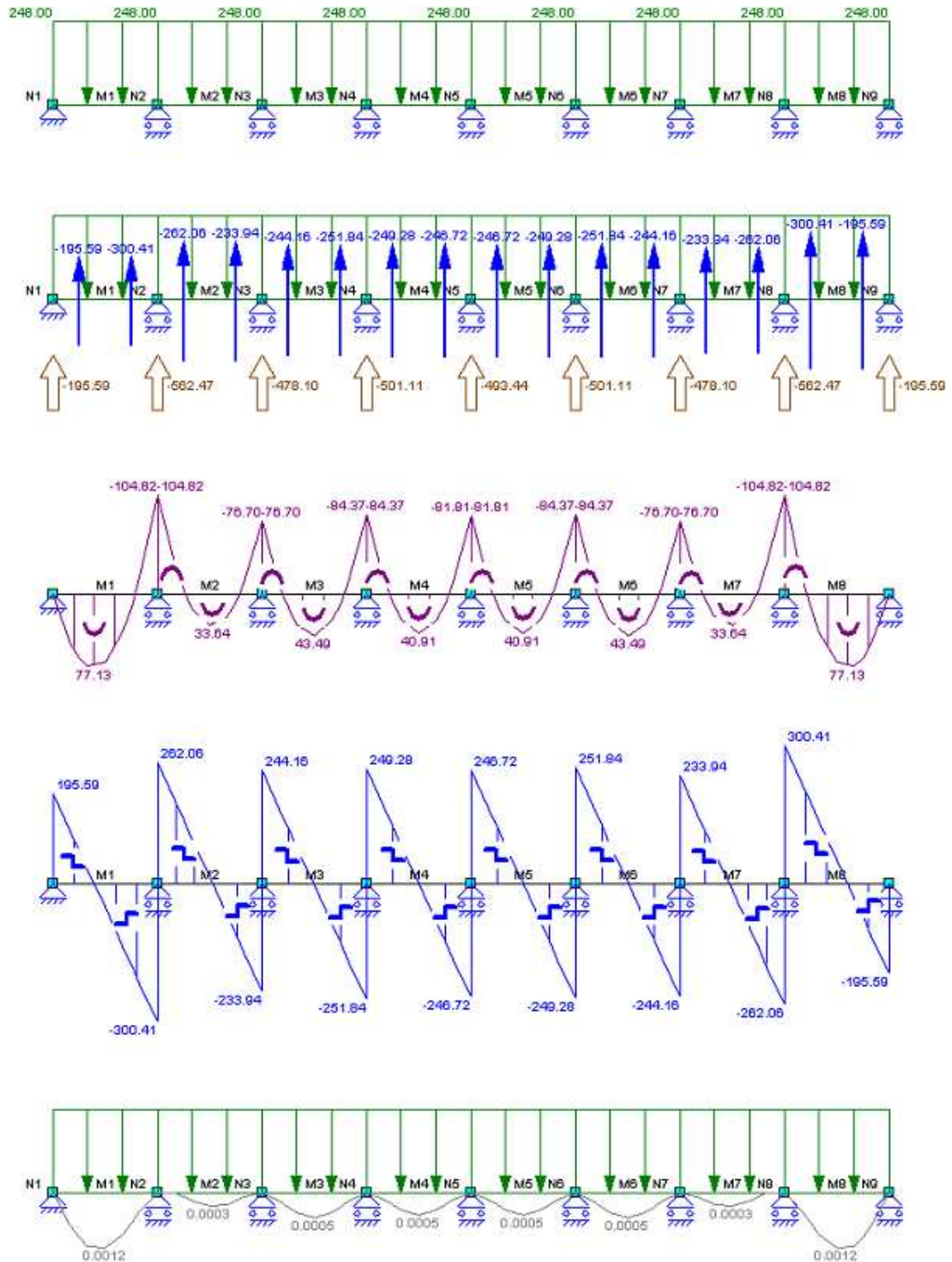


I.3.2 Predetermined configuration, clamped ($q = 1357 \text{ kN/m}$) – transverse girders and x-type bracing system



I.5 Retaining wall – optimum front plate thickness – longitudinal stiffeners and cross beams

I.5.1 Longitudinal stiffener



1.5.2 Cross beam

